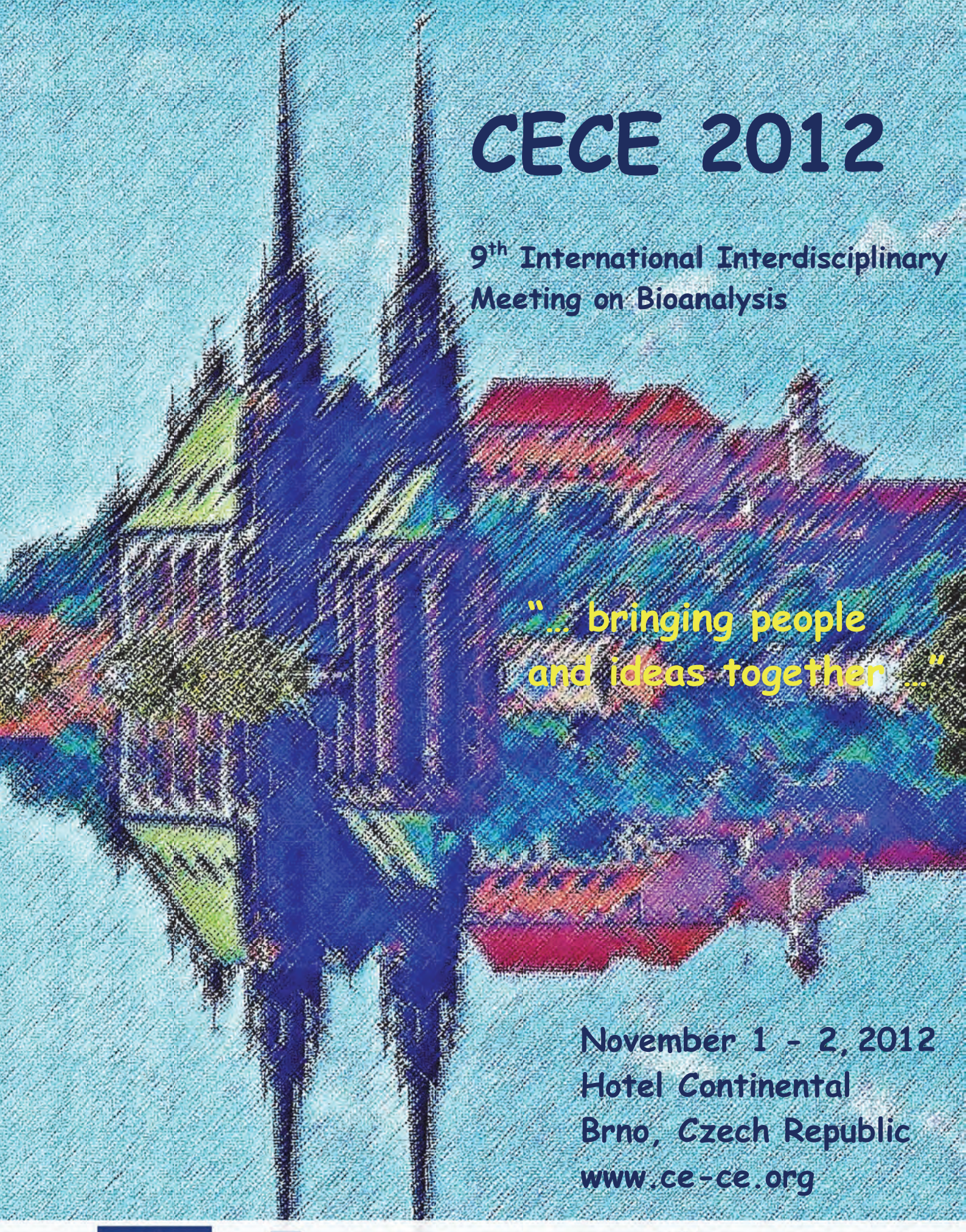

CECE 2012

9th International Interdisciplinary Meeting on Bioanalysis

"... bringing people and ideas together ..."

November 1 - 2, 2012
Hotel Continental
Brno, Czech Republic
www.ce-ce.org

SEVENTH FRAMEWORK PROGRAMME

CEITEC
Central European Institute of Technology
BRNO | CZECH REPUBLIC

UNIVERSITAS MASARYKIANA BRUNENSIS

iac brno

ISBN: 978-80-904959-1-3

Proceedings Editors: František Foret, Jana Křenková, Andras Guttman[*], Karel Klepárník and Petr Boček

Institute of Analytical Chemistry AS CR, v. v. i., Veveří 97, 602 00 Brno

[*] Fullbright Scholar at IACH, Brno - Northeastern University, Boston, MA, USA and Debrecen University, Hungary

Organized by:

- Institute of Analytical Chemistry AS CR, v. v. i., Veveří 97, 602 00 Brno
- Masaryk University, Žerotínovo nám. 9, 601 77 Brno
- CEITEC – Central European Institute of Technology, c/o Masaryk University, Žerotínovo nám. 9, 601 77 Brno
- Supported by the EU Seventh Framework Programme under the "Capacities" specific programme (Contract No. 286154 – SYLICA)

Organizing committee: František Foret, Jana Křenková, Karel Klepárník, Iveta Drobníková, Monika Staňková. Webmaster: František Matulík

Find the meeting history and more at www.ce-ce.org

Foreword

Welcome to CECE 2012. This is the 9th CECE in a row and, in a unique sense, a different one. Besides, the two days with invited lectures and poster sessions we have added an extra day for oral presentations of young scientists – graduate students and postdocs. For completeness we also include the programme of the young scientists section (CECE Junior) in these proceedings. Additionally, this year the meeting is free of charge thanks to the financial support by the EU Seventh Framework Programme under the "Capacities" specific programme (Contract No. 286154 - SYLICA). Of course our original goal of “bringing together scientists who may not meet at specialized meetings, promote informal communication of researchers from different disciplines and map the current status of the fields shaping the bioanalytical science” remains intact. The organizers want to thank the invited speakers and all the participants and hope that you will enjoy the scientific presentations as well as personal contacts and informal discussions.

Franta Foret

Brno, October 18, 2012

Program - CECE Junior 2012

Wednesday, October 31

9:00 - 9:05
Introduction to CECE Junior – Frantisek Foret

9:05 – 9:35 **Opening invited lecture**
Wolfgang Thormann
University of Bern, Bern, Switzerland
ENANTIOSELECTIVE CAPILLARY ELECTROPHORESIS FOR DRUG METABOLISM STUDIES IN VIVO AND IN VITRO

9:35 –9:50
Zdeňka Jarolímová[a], Přemysl Lubal[a,b], Viktor Kanický[a,b]
[a] Department of Chemistry, Faculty of Science, Masaryk University, Kotlářská 2, Brno
[b] Central European Institute of Technology (CEITEC), Masaryk University, Kamenice 5, Brno
CITP IN CLINICAL ANALYSIS

9:50 – 10:05
Jindra Musilová, Zdeněk Glatz
Department of Biochemistry, Faculty of Science and CEITEC – Central European Institute of Technology, Masaryk University, Kamenice 5, 625 00 Brno, Czech Republic
METABOLOMICS: NUCLEOTIDE AND COENZYME DETERMINATION IN CELLS BY CAPILLARY ELECTROPHORESIS

10:05 – 10:20
Antonín Bednařík[a], Pavel Kuba[b], Pavel Houška[b], Iva Tomalová[a], Eugene Moskovets[c], Jan Preisler[a]
[a] Central European Institute of Technology/Department of Chemistry, Masaryk University, Kamenice 5, 62500 Brno-Bohunice, Czech Republic
[b] Faculty of Mechanical Engineering, Brno University of Technology, Brno, Czech Republic
[c] MassTech, Inc. 6992 Columbia Gateway Drive, Suite #160, Columbia, MD 21046, USA
SPEEDING UP MASS SPECTROMETRY IMAGING WITH FAST PRECISION MIRROR SCANNING

10:20 – 10:40 **Coffee break**

10:40 – 10:55
Jan Partyka, František Foret
Institute of Analytical Chemistry of the AS CR, v.v.i., Veveri 97, 602 00 Brno, Czech Republic
CAPILLARY ELECTROPHORESIS WITH CONTACTLESS CONDUCTIVITY DETECTION OF CATIONIC-DERIVATIZED OLIGOSACCHARIDES

10:55 – 11:10
Radim Knob[a,b], Michael C. Breadmore[a], Rosanne Guijt[c], Jan Petr[b], Mirek Macka[a]
[a] Australian Centre for Research on Separation Science (ACROSS) and School of Chemistry, University of Tasmania, Private Bag 75, Hobart, TAS 7001, Australia

[b] Regional Centre of Advanced Technologies and Materials, Dept. Anal. Chem., Faculty of Science, Palacký University in Olomouc, 17. Listopadu 12, Olomouc, Czech Republic, CZ-77146
[c] Australian Centre for Research on Separation Science (ACROSS) and School of Pharmacy, University of Tasmania, Private Bag 26, Hobart, TAS 7001, Australia
CONTROL OF THE POLYMERIZATION TOWARDS POROUS LAYER OPEN TUBULAR CAPILLARY COLUMNS

11:10 – 11:25
Karina Romanova, Petr Císař, Dalibor Štys
Faculty of Fisheries and Protection of Waters, School of Complex Systems, University of South Bohemia, Zámek 136, 373 33 Nové Hrady, Czech Republic
LIVING CELLS STATE TRAJECTORY IN TIME-LAPSE MICROSCOPY

11:25 – 11:40
Ákos Szekrényes[a], Jana Krenkova[b], Zsolt Keresztessy[c], Frantisek Foret[b], András Guttman[a]
[a] Horváth Laboratory of Biosepartion Sciences, Research Center for Molecular Medicine, University of Debrecen, Nagyerdei krt. 98, 4032 Debrecen, Hungary
[b] Institute of Analytical Chemistry of the Academy of Sciences of the Czech Republic, v. v. i, Veveri 97, 602 00 Brno, Czech Republic
[c] Debrecen Clinical Genomics Center, Department of Biochemistry and Molecular Biology, Medical and Health Sciences Center, University of Debrecen, Nagyerdei krt. 98, 4032 Debrecen, Hungary
ORIENTED IMMOBILIZATION OF PNGASE F ON A POROUS POLYMER MONOLITH FOR RAPID N-GLYCAN RELEASE

11:40 – 11:55
Roman Bleha[a], Lucie Kucelová[b], Ján Brindza[b], Andriy Synytsya[a]
[a] Department of Carbohydrates and Cereals, ICT Prague, Technická 5, 166 28 Prague 6, Czech Republic
[b] Institute of Biodiversity Conservation and Biosafety, Faculty of Agrobiology and Food Resources, Slovak University of Agriculture, Tr. A. Hlinku 2, 949 76 Nitra, Slovak republic
SPECTROSCOPIC DISCRIMINATION OF BEE POLLEN AND HONEYCOMB POLLEN SAMPLES

12:00-14:00 **Lunch and poster presentations**

14:00 – 14:15
Martin Beneš, Jana Svobodová, Vlastimil Hruška, Iva Zusková, Bohuslav Gaš
Department of Physical and Macromolecular Chemistry, Faculty of Science, Charles University in Prague, Prague, Czech Republic
PREDICTION OF ELECTROMIGRATION DISPERSION IN ELECTROPHORETICAL SYSTEMS WITH COMPLEXATION AGENTS

14:15 – 14:30
Jana Svobodová[a], Martin Beneš[a], Pavel Dubský[a], Gyula Vigh[b], Bohuslav Gaš[a]
[a] Charles University in Prague, Faculty of Science, Department of Physical and Macromolecular Chemistry, Hlavova 8, Prague, Czech Republic
[b] Department of Chemistry, Texas A&M University, College Station, Texas, USA
UNFORESEEN PHENOMENA IN CHIRAL SEPARATIONS IN CAPILLARY ELECTROPHORESIS

14:30 – 14:45

Jan Soukup, Pavel Jandera
Department of Analytical Chemistry, Studentská 95, 532 10 Pardubice, Czech Republic

CHEMICALLY MODIFIED C SILICA-BASED COLUMNS: UNIVERSAL STATIONARY PHASES FOR HPLC SEPARATIONS

14:45 – 15:00

Anna Zhyrova, Dalibor Štys, Petr Císař and Tomáš Náhlík
School of Complex Systems, University of South Bohemia, Zámek 136, 373 33 Nové Hrady, Czech Republic

BELOUSOV-ZHABOTINSKY REACTION AS A GENERAL MODEL FOR THE DESCRIPTION OF COMPLEX SELF-ORGANIZING SYSTEMS

15:00 – 15:15

Zdeňka Šťastná[a,b], Statis Pataridis[a], Pavla Sedláková[a], Ivan Mikšík[a]
[a] Institute of Physiology, Academy of Sciences of the Czech Republic, v.v.i.,Vídeňská 1083, 142 20 Prague, Czech Republic
[b] Department of Analytic Chemistry, Faculty of Chemical Technology, University of Pardubice, Studentská 573, 532 10 Pardubice, Czech Republic

ANALYSIS OF NON-ENZYMATIC POSTTRANSLATIONAL MODIFICATED (GLYCATED) ALBUMIN BY NANO-LC/MS/MS

15:15 – 15:30

Filip Duša[a,b], Karel Šlais[a]
[a] Institute of Analytical Chemistry of the ASCR, v.v. i., Veveří 97, Brno, 602 00, Czech Republic
[b] Department of Biochemistry, Faculty of Science and CEITEC, Masaryk University, Kamenice 5, Brno, 625 00, Czech Republic

MICROPREPARATIVE SOLUTION ISOELECTRIC FOCUSING OF PEPTIDES AND PROTEINS IN NONWOVEN STRIP

15:30 – 15:45

Rudolf Kupcik[a], Pavel Rehulka[b], Barbora Jankovicova[a], Zuzana Svobodova[a], Lenka Hernychova[b,c], Jana Klimentova[b], Jiri Stulik[b], Zuzana Bilkova[a]
[a] Department of Biological and Biochemical Sciences, University of Pardubice, Studentska 573, 532 10 Pardubice, Czech Republic
[b] Institute of Molecular Pathology, Faculty of Military Health Sciences, University of Defense, Trebesska 1575, 500 01 Hradec Kralove, Czech Republic
[c] Regional Centre for Applied Molecular Oncology, Masaryk Memorial Cancer Institute, Zluty kopec 7, 656 53 Brno, Czech Republic

MICROCHIP ISOLATION COMBINED WITH MS-IDENTIFICATION OF PHOSPHOPROTEINS FROM FRANCISELLA TULARENSIS

15:45 – 16:00

Pavel Podešva, František Foret
Institute of Analytical Chemistry, Veveri 97, 902 00 Brno, Czech Republic

THIN METAL FILMS IN RESISTIVITY-BASED CHEMICAL SENSING

16:00 – 16:15
Ludovit Schreiber, Radoslav Halko, Milan Hutta, Anna Kabzanová, Soňa Lopuchová
Prírodovedecká fakulta UK, Katedra analytickej chémie, Mlynská dolina, 842 15 Bratislava
ULTRA FAST HPLC METHOD FOR TADALAFIL ACCORDING TO PH.EUR. VALIDATION CRITERIA AND IDENTIFICATION OF IMPURITIES USING ACCURATE MASS MS

16:15 **Closing remarks**

Program - CECE 2012

Thursday, November 1

9:08 – 9:15 **Opening remarks**

9:15 – 9:45
Roman A. Zubarev, Karolinska Institutet, Stockholm, Sweden
Identifying and quantifying 10,000 proteins in 10 hours – feasible, possible, done?

9:45 - 10:15
Ales Svatos, Max Planck Institute for Chemical Ecology, Jena, Germany
Laser assisted mass spectrometric imaging of plants, insects, and bacteria.

10:15 – 10:45 **Coffee break**

10:45 – 11:15
Christian Neusüß, Aalen University, Aalen, Germany
CE-ESI TOF MS for the analysis of intact proteins: recent progress and the application towards the differentiation of various EPO preparations.

11:15- 11:45
Vincenzo Cucinotta, University of Catania, Catania
Optimisation in the chiral and achiral separation of a multicomponent sample in electrokinetic chromatography: methodology development.

11:45 - 12:15
Mikhel Kaljurand, Tallin University of Technology, Tallinn, Estonia
Capillary electrophoresis (CE) as a promising technology for field and point-of-care (POC) instruments.

12:15 – 14:15 **Lunch break – poster session**

14:15 – 14:45
Hervé Cottet, Université de Montpellier, France
Study of antibacterial activity by capillary electrokinetic separation methods.

14:45 – 15:15
François de l'Escaille, Analis R&D, Suarlée, Belgium
Application of capillary electrophoresis in optimization and control of fermentation and cell culture.

15:15 – 15:45
Pier Giorgio Righetti, Politecnico di Milano, Milano, Italy
Mark Twain: how to fathom the depth of your pet proteome.

16:10 - **City walk with invited speakers**

19:00 - **Conference dinner with traditional Moravian music - Hotel Continental**

Friday, November 2

9:00 – 9:30
Petr Cigler, Institute of Organic Chemistry and Biochemistry, Prague, CR
Photoluminiscent diamond nanoparticles – new diagnostic and visualization probes.

9:30 – 10:00
Marek Minarik, Genomac International, Prague, CR
Applying CE and microchip CE to molecular cancer analysis: From research to clinical utility.

10:00 – 10:30
Andras Guttman, Northeastern University, Boston, USA
New advances in capillary electrophoresis of therapeutic antibodies.

10:30 – 11:00 **Coffee break**

11:00 – 11:30
Guillaume Mottet, Institut Curie, Paris, France
3D chip for low cost cell analysis.

11:30 - 12:00
Zuzana Bilkova, University of Pardubice, CR
Magnetic beads-based microfluidic systems - the past and the future.

12:00 – 14:00 **Lunch break – poster session**

14:00 – 14:30
Staffan Nilsson, Pure & Applied Biochemistry LTH, Lund University, Sweden
Open Chip SAW-MALDI MS Sample Handling.

14:30 – 15:00
Tomas Adam, University of Olomouc, CR
Diagnosing inherited metabolic disorders by metabolomic tools.

15:00 – 15:30
Michal Roth, Institute of Analytical Chemistry, Brno, CR
Sub-, near- and supercritical water in analytical separations and instrumentation development.

15:30 - 16:00
Miroslav Fojta, Institute of Biophysics, Brno, CR
Redox Labelling of Nucleic Acids for Electrochemical DNA Sensing.

16:00 **Closing remarks**

About the Invited Speakers

Wolfgang Thormann earned his Ph.D. in 1981 from the University of Bern, Switzerland, was postdoctoral fellow at the University of Arizona (USA) and at Deakin University (Australia), and became research associate professor at the Center for Separation Science, University of Arizona (USA) in 1985. In 1988 he joined the Department of Clinical Pharmacology, University of Bern (Switzerland) and became the head of the departmental analytical service laboratory. After the closure of the Department of Clinical Pharmacology in 2011, his laboratories became the Clinical Pharmacology Laboratory of the Institute for Infectious Diseases (University of Bern). The Thormann research group specializes in the exploration, development and application of novel approaches in analytical and preparative free fluid electrophoresis. It develops new diagnostic tools based on capillary electrophoresis for analysis of drugs, metabolites and endogenous compounds in body fluids and tissues. Major activities include the determination of the stereoselectivity in drug metabolism and the monitoring of alcohol markers. Other activities focus on the elucidation of the fundamentals of electrokinetic mass transport and separation in free fluids using dynamic computer simulation and experimental validation on analytical and preparative instruments. Wolfgang Thormann is author and co-author of more than 250 publications and is co-author of Mosher et al., The Dynamics of Electrophoresis (VCH, Weinheim, 1992).

Roman Zubarev has received PhD in Ion Physics from the Uppsala University, Sweden, in 1997. After postdoc training in Fred W. McLafferty's group at the Cornell University in USA, he became associate professor at the Chemistry Department in Odense, Denmark. In 2002 Dr. Zubarev came back to Uppsala as professor of proteomics. In 2009 he has moved to Karolinska Institutet in Stockholm, taking a professorship in medicinal proteomics. Dr. Zubarev has pioneered electron capture dissociation and related fragmentation techniques. For his contribution to mass spectrometry he has been awarded by the Carl Brunnee award (IMSC, 2006) and Biemann medal (ASMS, 2007). Dr. Zubarev has published more than 180 peer-reviewed papers, and has several patents. He is a Treasurer of HUPO.

Aleš Svatoš

Current Research Interests:

Mass spectrometry, natural product identification, proteomics, microfluidics, organic chemistry

Interdisciplinary Affiliation; Chemical ecology, sexual communication of insects, biosynthesis

Education:

Dipl. ing. and PhD (CSc) from Institute of Chemical Technology, (VSCHT) Prague, Czech Republic

Professional Career:

since 2002 Max Planck Institute for Chemical Ecology, Jena, Germany, Mass Spectrometry Group leader (C3)
1986-2001 Institute of Organic Chemistry and Biochemistry (IOCB), Prague
1997 Bonn University (AvH, Prof. Boland)
1991-1993 Postdoctoral fellowships Cornell University (Prof. Meinwald)

Administrative Experience:

2000-2002 Scientific council of UOCHB Prague, The Czech Republic (Head)
2001-recent: Scientific council of VSCHT Prague, The Czech Republic (Member)
Referee for ca 10 journals (Science Communications, Nature Chemical Biology, PNAS, J. Proteome Res., Proteomics, Plant Physiology, Phytochemistry, Electrophoresis, J. Chem. Ecol, Analytical Chemistry, RCM)

Honours and Awards:

Alexander von Humboldt Forschungsstipendium 1997
Alexander von Humboldt / CSIR India Research Award 2009

Christian Neusüß

since 2009	Dean of the master course „Analytical and Bioanalytical Chemistry“ at University of Aalen
since 2006	Professor for General and Analytical Chemistry at University of Aalen
2001 - 2006	Scientist at Bruker Daltonik GmbH: Application and method development for Electrospray-Mass Spectrometry in coupling with microscale separation techniques.
1996 - 2001	Scientist at the „Institut für Troposphärenforschung" in Leipzig. Ph.D. (August 2000): Chemical characterization of size-segregated atmospheric aerosol particles (University of Leipzig)
1989 - 1996	Study chemistry in Heidelberg (Diploma 1996) and Bergen (Norway)

Full Professor of Analytical Chemistry from 1994, **Vincenzo Cucinotta** has carried out his academic activity for the most at the University of Catania, Italy.

He started its activity of scientific research in the field of the thermal analysis, and then its scientific interests were directed towards the equilibria in solution, especially through the use of potentiometry, a subject which has occupied him for a long time. Due to his inorganic formation, the systems involved were mainly metal complexes, their formation and stability in solution. However, soon it was clear that the subject of molecular recognition could not be neglected even for systems apparently simple, like in the formation of mixed ligand complexes. With the choice to investigate in the field of cyclodextrins, the molecular recognition became a main subject of interest, and the involvement in NMR and in optical spectroscopy as optimal techniques for this kind of research, became more and more important. Cyclodextrins thus implied the use of new techniques. Furthermore, in order to study their interaction with metal ions, it was soon clear the necessity to have the availability of derivatives, often new, as well as that these derivatives were not commercially available. In the rare cases where they were already been synthesised, nonetheless the commercially available products were simply mixtures of many different pure compounds, differing one another both in the degree of substitution and in their relative position (regioisomerism). However, potentiometric investigation requires the use of one and very pure compound. This forced us to also become synthetic chemists in carbohydrate chemistry.

From the beginning of the new millennium, both being an analytical chemist and being involved in the most important class of selectors used in capillary electrophoresis, lead his scientific activity towards this technique, also by using mass spectrometry as detecting technique. His previous scientific experience permits him to have an original approach in this field. The use of techniques like electrokinetic chromatography and ligand exchange capillary electrophoresis has benefited both from the expertise in equilibria solution studies and in the preparation and use of cyclodextrin derivatives. The former aspect is important in predicting the species present in order to optimise the separation performance, the latter aspect permits him to carry out chiral separations with high selectivity, by exploiting the chiral selectivity of cyclodextrin derivatives. The novelty of this approach was also synthesised by the expression “rational approach to separation science”.

As a milestone in his involvement in capillary electrophoresis, he had the opportunity to organise, as chairman, the most important and long-aged scientific meeting specifically devoted to this technique in 2008 in his town, Catania, “ITP2008”.

He is author of more than one hundred papers, the most of them ISI, and he is reviewer for several prestigious scientific journals.

Mihkel Kaljurand is professor and director of the Institute of Chemistry which is based in the Tallinn University of Technology, Tallinn, Estonia. Prior to joining to Tallinn University of Technology, Prof. Kaljurand served as the senior researcher at Estonian Academy of Sciences, where he also received his candidate of chemistry degree in 1979 (Leningrad University) and doctor of sciences degree (Moscow Institute of Physical Chemistry) in 1991. He has worked with a number of public organizations in his research endeavors, including NASA and Southern Illinois University (Carbondale IL, USA).

Mihkel Kaljurand has been awarded Estonian Science Prize (twice)

and he has been awarded fellowships by the Fulbright Visiting Scholar Program (y. 2002) and the National Research Council Research Associateship Program (y. 1995-1996). His teaching interests and experience are in the areas of analytical chemistry. He has written extensively on chemometrics, instrumental analysis and separation science. Dr. Kaljurand's current research focuses on automatization and miniaturization of capillary electrophoresis and on green analytical chemistry.

After graduating from the Ecole Supérieure de Physique et Chimie Industrielles de Paris (ESPCI ParisTech, France), **Hervé Cottet** completed his PhD in analytical chemistry in 1999 at the Ecole Nationale Supérieure de Chimie de Paris (*ENSCP*, ParisTech, France) under the supervision of Prof. Pierre Gareil. He worked on Capillary Electrophoresis (CE) of synthetic polymers and polyelectrolytes. After a one year post-doc at the Technical University of Eindhoven (the Netherlands), where he investigated the use of non-aqueous solvents in CE, he joined the University of Montpellier in 2000 as assistant professor. In 2007, he obtained a full professor position at the Max Mousseron Biomolecules Institute in Montpellier. His current research work concentrates at the interface between separation sciences and biology (structure-activity correlations, study of biomolecules interactions, antibacterial activity, bacteria analysis). He is developing CE methodologies (free solution and gel-based separations, frontal analysis, isotachophoresis, isoelectric focusing, 2D-separations, electrophoretic mobility modeling) and Taylor Dispersion Analysis for the characterization of (bio)polymers, dendrimers, polyelectrolytes, nanoparticles and bacteria. In 2006, he awarded the price from the Analytical chemistry Division of the French Chemical Society. In 2011, he has been nominated as a junior member of the Institut Universitaire de France (IUF). He is the author of more than 70 peer-reviewed articles in the field of analytical chemistry and polymer sciences.

François de l'Escaille joined Analis in 1985 and in 2001 the research and development division of Analis. Actually he holds the position of Business Development and R&D Manager. He is responsible for new applications and new markets. Main interests is capillary electrophoresis applications in order to develop kits for In Vitro Diagnostics, Pharmaceutical analysis, Food analysis, Chemical analysis, etc… He is an active member of CASSS as associated director and Committee member of CE Pharm. He is also corporate representative at IFCC and active is several working groups on standardization. In Belgium he is active in BioWin the Health Cluster in Wallonia and board member of the Wal-DX working group.

Before this position he held several positions in Analis as sales person and product management. Previous jobs include position at Baxter, Miles-Ames, FMC and Beiersdorf, where he gained experience in the field of Diagnostics, Medical device, Medical consumer good and Food Processing.

François de l'Escaille holds a degree of Master in Bioengineering and Master of Industrial Management from the University of Louvain n Belgium (1977 and 1978) and Master in

Biomedical Engineering (1981). He is author and co-author of several articles on capillary electrophoresis.

Pier Giorgio Righetti earned his Ph. D. in Organic Chemistry from the University of Pavia in 1965. He then spent 3 years as a Post. Doc. at MIT and 1 year at Harvard (Cambridge, Mass, USA). He is full professor of Proteomics at the Milan's Polytechnic.

He is in the Editorial Board of Electrophoresis, J. of Chromatography A, J. Proteomics, BioTechniques, Proteomics, Proteomics Clinical Applications. He has co-authored the book Hamdan M., Righetti P.G.: Proteomics Today Wiley-VCH, Hoboken, 2005, and published >540 scientific articles.

He has developed isoelectric focusing in immobilized pH gradients, multicompartment electrolyzers with isoelectric membranes, membrane-trapped enzyme reactors, temperature-programmed capillary electrophoresis and combinatorial peptide ligand libraries for detection of the low-abundance proteome.

On 540 articles reviewed by the Web of Knowledge (Thomson Reuters), Righetti scores 14.000 citations, with an average of 26 citations/article and with a H-index of 54. Only in the last six years he has received citations ranging from 1000 to 1200 per year.

He has won the CaSSS (California Separation Science Society) award (October 2006), at that time in its 12th edition, and the Csaba Horvath Medal award, presented on April 15, 2008 by the Connecticut Separation Science Council (Yale University). In 2011, he has been nominated honorary member of the Spanish proteomics society and in 2012 he has won the Beckman award and medal granted in February at the Geneva MSB meeting.

Petr Cígler

Education:

MSc. Faculty of Science, Charles University in Prague (Inorganic Chemistry)

Ph.D. Institute of Chemical Technology in Prague, Czech Republic (Analytical Chemistry)

Stays:

2004-2005 Department of Analytical Chemistry, Chemo- and Biosensors, University of Regensburg, Germany

2007 Laboratoire de Chimie Organo-Minérale, Université Louis Pasteur, Strasburg, France

2008-2009 The Scripps Research Institute, La Jolla, U.S.A. (postdoctoral stay in laboratory of Prof. M.G. Finn)

Current employment:

2009 Researcher at Institute of Organic Chemistry and Biochemistry AS CR, v.v.i.

Selected awards:

2006 Sanofi-Aventis Prize for Pharmacy (under the auspices of Professor Jean-Marie Lehn)

2008 Unipetrol Prize for thesis “Novel Approaches to Analysis and Resistance of HIV Protease”
2011 Carl and Gerty Cori Prize for Chemistry (Sigma-Aldrich)
2011 Alfred Bader Prize for Bioorganic and Bioinorganic Chemistry
2012 Scopus Awards (1st place)
2012 The Price of The Learned Society of the Czech Republic for pedagogues
Co-author of 28 articles in peer-reviewed journals, 6 patents, 3 chapters in monographs and 66 conference contributions

Research Focus:
Functional protein and inorganic nanoparticles, their preparation and surface modifications. Construction of nanosensors and bionanosensors for recognition and determination of biologically interesting analytes. Multimodal in vivo analysis. Self-assembly and aggregation of molecules; molecular recognition. Design and synthesis of enzyme inhibitors. Exoskeletaly substituted carboranes and metallacarboranes.

Marek Minarik received his Ph.D. in bioanalytical chemistry from the Northeastern University in Boston in 2001 with Barry Karger at the Barnett Institute. The topic of his Ph.D. thesis was development of capillary-array electrophoresis instrumentation for micropreparative bioanalysis. Between 2000 and 2002 worked in R&D at Molecular-Dynamics (later Amersham Biosciences) in Sunnyvale, CA developing applications for clinical and forensic DNA testing.Currently a co-founder and president of Genomac in Prague, Czech Republic a biotech and private genomic research center. His main area of research interest is in development of tools and technologies for genomic analyses with emphasis on clinical applications in the field of complex diseases including solid cancers, cardiovascular and neuropsychiatric disorders.
Author of over 50 scientific papers and 4 issued patents (3 US, 1 International).

Andras Guttman graduated from the University of Veszprem (Hungary) in chemical engineering, where he also received his doctoral degree in 1981. From 1981-87 he worked as an assistant professor at the Semmelweis University (Hungary) and from 1987-1989 joined the Barnett Institute (Boston) as a postdoctoral fellow. He started his industrial career in 1990 by joining Beckman Instruments as a principal scientist and developed the replaceable gel technology for capillary electrophoresis, which gel was used later to sequence the Human genome. In 1996 he became Vice President of Research in a San Diego startup company Genetic Biosystems. From 199-2004 Dr Guttman lead the microfluidics development a group at the Torrey Mesa Research Institute (San Diego). In 2004 he received the Marie Curie Chair Professorship of the European Commission and established the Horvath Laboratory of Bioseparation Sciences in Innsbruck (Austria) and worked on proteomics and glycomics based biomarker discovery. Prof Guttman moved back to the US in 2008 to become a professor at the Barnett Institute (Boston), but residing in San Diego (CA). He has contributed more than 205 scientific publications, 32 book

chapters, edited several textbooks and holds 19 patents. Dr Guttman is a board member of CASSS and on the editorial panels of numerous leading international scientific journals, such as Analytical Chemistry, Journal of Chromatography and Electrophoresis. He has received numerous recognitions such as the Analytical Chemistry Award of the Hungarian Chemical Society in 2000, elected as an external member of the Hungarian Academy of Sciences in 2004 and became a Fulbright Scholar in 2012.

Guillaume Mottet received his PhD in physics at Ecole Normal Supérieur de Cachan (France) in 2009. The topic of his PhD was the conception of a bio-microsystem for the fusion of cancer cells and dendritic cells. This system was based on dielectrophoresis and electrofusion. He followed with postdoctoral fellowship in Institut Curie. His current research focuses on developing bio-chip based on microfluidic for cancer diagnostic.

Zuzana Bilkova has graduated in Molecular Biology and Genetics, Charles University, Prague, Czech Republic; she got her Ph.D. in Analytical chemistry (spec. Immunochemistry) in 2000 from the Faculty of Chemical Technology, University of Pardubice. Till now she acts as associate professor of analytical chemistry and from 2005 she has been named as a head of Department of Biological and Biochemical Sciences. Department provides the academic background for the education and practical preparation of students for analysis of biological materials, specialists in diagnostic assays in medicine. Dr. Bilkova is the guarantor of the lectures Immunochemistry, Immunoanalytical methods and Clinical immunology. She is in charge of immunochemistry research group specialized in analytical and separation methods based on molecular recognition and affinity interaction, largely combined with magnetic micro- or nanoparticles as a solid phase. Her scientific expertise can be summarized: immunochemistry, bioaffinity chromatography, and structural analysis of clinically relevant biomarkers. She is a member of many scientific and advisory boards. Up to the present days she has published more than 50 papers in scientific journals and gave more than 30 lectures at symposiums and conferences.

Staffan Nilsson
Professor, Lecturer Center for Chemistry and Chemical Engineering Pure & Applied Biochemistry, LTH, Lund, Sweden - *since 2007*

Main scientific achievements
Purification of biological active membrane-protein 1988; HPLC Protein G 1987; TLAC of protein (pregnancy test) 1992; Real-Time Fluorescence Imaging of CE-separations 1995; Protein based Monolith CEC enantioseparation 1995; MIP based Monolith CEC enantioseparation 1997; “Wall-less” test tubes for CE 1998; Airborne Cell analysis 2000; MIP nanoparticle PSP-CEC enantioseparation 2000; Ultrasonic trapping in CE 2001; NP-PSP-CEC-ESI/MS 2002; Airborne Chemistry-Protein Crystallisation 2003; Airborne Chemistry X-ray Scattering 2003; \Nano-Spray ESI MS CEC/CE 2004; Levitated droplet dye laser 2006; NACE of EtOH Markers 2008; Monoclonal nanoparticle PSP-MIP-CEC 2008; Airborne Cell-Cell communication 2009; Chip-PSP-CEC 2010; Open Chip SAW-MALDI MS Sample Handling 2012.

Tomáš Adam currently holds the position of Head of Department of Clinical Biochemistry at Faculty Hospital in Olomouc. He graduated from the Faculty of Natural Sciences of Palacky University in Olomouc in 1989. He obtained his Ph.D. in biochemistry in 1999 and received an Associate Professorship in medical genetics in 2005.
He is a founder of the Laboratory of Inherited Metabolic Disorders at Palacky University and University Hospital in Olomouc which currently serves as diagnostic center and newborn screening center for Moravia region. His research activity focuses on nucleotide metabolism, biomedical application of separation technologies and most recent scientific work is directed to metabolomics. His bibliography includes over 60 original papers and review articles and also chapters in books. He has successfully supervised many Ph.D. students and presented multiple lectures at international conferences. He is a regular active member of a number of international scientific societies.

Michal Roth received his M.Sc. in physical chemistry from the Masaryk University in Brno and Ph.D. in analytical chemistry from the Czechoslovak Academy of Sciences. In the Institute of Analytical Chemistry of the Czechoslovak Academy of Sciences, he was engaged consecutively in trace analysis and thermodynamic measurements by gas chromatography. During his postdoctoral stay in the laboratory of Prof. Miloš Novotný (Department of Chemistry, Indiana University, Bloomington) he became interested in the use of supercritical fluids in analytical chemistry and, later on, in the applications of high-temperature, high-pressure compressed liquids. M. Roth is author or co-author of 70 papers in international peer-reviewed journals and about 80 contributions to international conferences on analytical separation methods and chemical

thermodynamics. He was a visiting scientist at the University of Patras (Greece), Ruhr-Universität Bochum (Germany), Kangwon National University (Republic of Korea) and Georgia Institute of Technology (USA). Currently, his interests fall into a cross-disciplinary field between separation methods of analytical chemistry and chemical engineering thermodynamics, including measurement and modeling of solubilities of nonvolatile organics in pressurized hot water and studies of solute–ionic liquid–carbon dioxide systems employing capillary column supercritical fluid chromatography. The most recent activities of his group involve an intense co-operation with other groups in the Institute on the use of near- and supercritical water in the development of silica- and glass-based devices for analytical separation methods.

Miroslav Fojta (born 1967) studied biochemistry at the Charles University in Prague and earned his PhD (1995) in biophysics at the Institute of Biophysics (IBP), Academy of Sciences of the Czech Republic in Brno with Prof. E. Paleček. At the IBP he obtained also his postdoctoral training. He started his independent research at the IBP at the end of 1990s and became the head of the Department of Biophysical Chemistry and Molecular Oncology from 2005. In the same year he finished his habilitation at the Masaryk University in Brno where he teaches as an external Associate Professor. In 2011 he joined the Centre for Structural Biology at CEITEC MU as a research group leader. Miroslav Fojta is a recipient of the Wichterle Premium and the Prize of the Learned Society of the Czech Republic. His expertise includes electrochemistry of nucleic acids, chemical modification of biopolymers and its application in analysis of nucleotide sequences, DNA damage and protein-DNA interactions.

Abstracts of Oral Presentations – CECE Junior

ELECTROPHORETICALLY MEDIATED MICROANALYSIS FOR CHARACTERIZATION OF THE ENANTIOSELECTIVE CYP3A4 CATALYZED N-DEMETHYLATION OF KETAMINE

Hiu Ying Kwan, Wolfgang Thormann

Clinical Pharmacology Laboratory, Institute for Infectious Diseases, University of Bern, Murtenstrasse 35, CH-3010 Bern, Switzerland

ABSTRACT

An electrophoretically mediated microanalysis method was developed to investigate the stereoselectivity of the CYP3A4 mediated N-demethylation of ketamine. Ketamine was incubated on-line in a 50 µm id bare fused-silica capillary together with human CYP3A4 Supersomes using a pH 7.4 phosphate buffer at 37°C. A plug of reactants containing racemic ketamine and the NADPH regenerating system including all required co-factors for the enzymatic reaction was injected, followed by a plug of the metabolizing enzyme CYP3A4. These two plugs were bracketed by plugs of incubation buffer to ensure proper conditions for the enzymatic reaction. The rest of the capillary was filled with a pH 2.5 running buffer comprising 50 mM Tris and phosphoric acid with highly sulfated γ-cyclodextrin (2%) as chiral selector. Reaction was enhanced by applying a voltage of -10 kV for 10 s. After incubation at 37 °C without power application, the capillary was cooled to 25°C followed by application of -10 kV for the separation and detection of the formed enantiomers of norketamine. Elucidated kinetic values were found to be comparable to those obtained from an off-line assay of a previous study.

Keywords: Electrophoretically mediated microanalysis, electrokinetic chiral separation

1 INTRODUCTION

Enantioselective capillary electrophoresis is a well established and attractive methodology. Due to high resolution, short analysis time and low consumption of chemicals and solvents, it is applied to assess the stereoselective metabolism of a drug and to characterize enzymatic metabolic pathways *in vitro* [1]. The enzymatic reaction, often followed by an extraction, is typically carried out in a vial prior to the capillary electrophoresis analysis of the products. In recent years, enzymatic metabolic reactions of drugs were also performed in the capillary with subsequent analysis of the formed products [2], an approach which is known as electrophoretically mediated microanalysis (EMMA). In this study, an EMMA method was developed to investigate the stereoselectivity of the CYP3A4 mediated N-demethylation of ketamine to norketamine. Ketamine is a chiral phencyclidine used as an anesthetic drug for short term surgical interventions and in subanesthetic doses for postoperative pain relief. It is known from a previous study that norketamine is not metabolized by CYP3A4 [3]. Thus, quantification of norketamine formation was possible via incubation of norketamine (10-160 µM per enantiomer) instead of ketamine and otherwise identical conditions. Norketamine formation rates were fitted to the Michaelis-Menten model and the elucidated values for V_{max} and K_m were compared to those obtained from the off-line assay of a previous study [4]. The data obtained revealed that CYP3A4 N-demethylation of ketamine occurs in a stereoselective manner [5].

2 MATERIAL AND METHODS

A Proteome Lab PA 800 instrument (Beckman Coulter, Fullerton, CA, USA) equipped with a 50 μm id fused-silica capillary (Polymicro Technologies, Phoenix, AZ, USA) of 44 cm total length (effective length of 34 cm) was used. Ketamine was incubated on-line in a 50 μm ID bare fused-silica capillary together with human CYP3A4 Supersomes using a 100 mM phosphate buffer (pH 7.4) at 37°C. A plug of about 14 nL volume containing racemic ketamine and the NADPH regenerating system including all co-factors for the enzymatic reaction was injected (plug N+S in panel A of Fig. 1), followed by an equally sized plug of the enzyme CYP3A4 (500 nM) (plug E in panel A of Fig. 1). The two plugs were bracketed by plugs of incubation buffer (IB in Fig. 1A) to ensure proper conditions for the enzymatic reaction. The rest of the capillary was filled with a pH 2.5 running buffer (RB in Fig. 1A) comprising 50 mM Tris, phosphoric acid and 2 % w/v of highly sulfated γ-cyclodextrin (Beckman Coulter). Mixing of reaction plugs was enhanced via application of -10 kV for 10 s. After incubation at 37 °C without power application, the capillary was cooled to 25 °C within 3 min followed by application of - 10 kV for the separation and detection of the norketamine enantiomers at 195 nm.

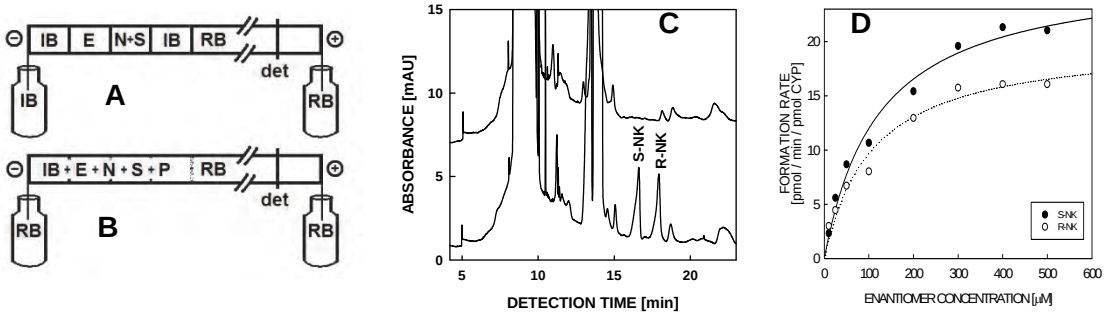

Fig.1: Enzymatic N-demethylation of ketamine to norketamine (NK) in the EMMA format (panel A) with subsequent enantioselective electrophoretic analysis of the formed products (panel B). The electroperograms in panel C were obtained with a 30 min zero-potential amplification time for experiments in presence (lower graph) and absence (upper graph) of racemic ketamine. For data obtained after 8 min zero-potential amplification, the determined norketamine formation rates were fitted to the Michaelis-Menten model (panel D). For details refer to [5].

3 RESULTS AND DISCUSSION

In the EMMA format, norketamine formation rates could be determined with an 8 min zero-potential amplification (Fig. 1D) and the elucidated values for V_{max} and K_m were found to be comparable to those obtained from the off-line assay of a previous study [4,5]. The EMMA based study revealed that the metabolism of ketamine via CYP3A4 is stereoselective (Fig. 1D). To our knowledge, this is the first study using EMMA to assess the kinetics of enantioselective drug metabolism mediated by a CYP450 enzyme. Further work should be addressed to shorten the analysis time, to understand the contribution of electrophoretic transport to plug mixing and to include an internal standard such that the EMMA method can be further improved and widely applied to assess enzymatic activity in a fast, low-cost and automated way.

ACKNOWLEDGEMENTS

This work was supported by the Swiss NSF.

LITERATURE

[1.] Caslavska, J., Thormann, W., J. Chromatogr. A 2011, 1218, 588-601.

[2.] Fan, Y., Scriba, G.K.E., J. Pharm. Biomed. Anal. 2010, 53, 1076-1090.

[3.] Portmann, S., Kwan, H.Y., Theurillat, R., et al., J. Chromatogr. A 2010, 1217, 7942-7948.
[4.] Kwan, H.Y., Thormann, W., Electrophoresis 2011, 32, 2738-2745.
[5.] Kwan, H.Y., Thormann, W., Electrophoresis 2012, 33, in press.

CITP IN CLINICAL ANALYSIS

Zdeňka Jarolímová[a], Přemysl Lubal [a, b], Viktor Kanický[a,b]

[a] *Department of Chemistry, Faculty of Science, Masaryk University, Kotlářská 2, Brno, CZ*
[b] *Central European Institute of Technology (CEITEC), Masaryk University, Kamenice 5, Brno, CZ*

ABSTRACT

A method for the analysis of renal stones by capillary isotachophoresis (CITP) with conductometric detection was developed when the qualitative and quantitative analysis of organic compounds (urate, oxalate) and inorganic ions (phosphate, Ca^{2+}, Mg^{2+}, Na^{+}, NH_4^{+}) species commonly present in mixed renal stones in three separate steps can be carried out with limits of detection about 10 µmol.L^{-1}. The developed method was validated by the analysis of real samples and can also be employed for the determination of the above mentioned analytes in some other samples (bones, teeth) concerning apatite biominerals (fluoro-, carbonate-, chloro-apatite). In addition, this method can be used also for the analysis of biofluids (urine).

Keywords: capillary isotachophoresis, clinical analysis, biominerals

1 INTRODUCTION

In recent years many studies have been devoted to the determination of individual elements in human tissues since many health problems are caused by their lack or excess. One of these diseases is urolithiasis - crystalline particles (kidney or urinary stones) are formed in a renal parenchyma or urinary tract [1]. Urolithiasis occurs in patients regardless of gender, age or location [1]. The main components of kidney stones are: hydrates of calcium oxalate ($Ca(COO)_2.nH_2O$, n = 1 for whewellite, n = 2 for weddelite), calcium phosphates ($Ca_x(PO_4)_y$) and some of its forms – hydroxylapatite (HA), brushite, dahlite, etc.; magnesium phosphates ($Mg_x(PO_4)_y$) mostly in struvite, newberyite and a mixture of Mg(II) and Ca(II) salts as whitlockite; uric acid and their sodium and ammonium salts and cystine and xanthine in small amounts [1].
Classical methods of chemical analysis used in the past for the classification and analysis of kidney stones are time-consuming and yielding not sufficiently accurate results [2] and therefore at present the advanced instrumental techniques (e.g. IR and Raman spectrometry [2], polarization and scanning electron microscopy [2], synchrotron radiation X-ray microtomography, laser induced breakdown spectroscopy, atomic absorption and inductively coupled plasma (ICP) spectrometry with optical and mass spectrometry detection) are employed since obtain the information on major, minor and trace level elemental/compound composition but some of them can also enable spatial analysis with structure determination. Separation techniques are recommended for their analysis due to the ionic character of the analytes present in urine [3]. In this work, the analytical capillary isotachophoresis (CTIP) was used for the study of the composition of renal stones by simultaneous determination of

anionic/cationic species of both an inorganic and organic nature. So far, only one preliminary study describing anionic ITP analysis of model binary mixtures of calcium oxalate/calcium phosphate or calcium oxalate/uric acid has been described [4] and no other paper dealing with the complete ITP analysis of renal stones by this technique. The method was also tested for analysis of organic acids in plants serving as signaling molecules.

2 MATERIALS AND METHODS

An isotachophoretic analyzer EA 102 (Villa Labeco, Spišská Nová Ves, Slovakia) with a contact conductomectric detector was used for the separation and determination of analytes in analytical column of diameter 0.3 mm and length 200 mm. The separation was carried out at a constant driving current of 100 µA for cationic system, 80 µA for the determination of oxalate and phosphate, and 70 µA for determination of uric acid. In order to improve sensitivity and limits of detection, the current was reduced for all systems to 50 µA prior to detection. The analysis was repeated at least 2-times to get the representative results.
The following chemicals were used: hydrochloric acid (J.T.Baker), disodium tetraborate (TB) by Lachema, Czech Republic, sulphuric acid (Merck, Germany), while L-histidine, hexanoic acid (HEX),hydroxylapatite, uric acid, ammonium chloride, 1,3-bis[tris(hydroxymethyl)methylamino]propane (BTP) were purchased from Sigma-Aldrich, (USA) and calcium oxalate monohydrate, magnesium and calcium chloride, hydroxyethylcellulose and imidazole were obtained from Fluka (Switzerland). The chemical compounds used in this study were of the highest purity and were used as received. Deionized water was used from Milli-Q RG (Millipore Corp., USA). The aqueous solutions used for uric acid analysis were prepared from carbon dioxide-free water in order to eliminate the bicarbonate zone during ITP analysis. Carbon dioxide-free water was prepared from redistilled water saturated by argon. Uroliths were collected and provided by prof. Petr Martinec (Institute of Geonics, Czech Academy of Sciences, v. v. i, Ostrava, Czech Republic).

3 RESULTS AND DISCUSION

The sample dissolution procedure is based on experiments when artificial model samples as binary/ternary mixtures of the most abundant compounds in the examined urolith specimens, i.e. hydroxylapatite, calcium oxalate, and uric acid, were subjected to dissolution experiments carried out with selected reagents (HCl, $HClO_4$, H_2SO_4, citric acid, EDTA, NaOH, KOH, tetrabutylammonium hydroxide) to design the optimum dissolution procedure. Moderately elevated temperatures (~50-60 °C) proved to be insufficient for the complete sample dissolution and therefore the reaction mixture was kept at boiling point under reflux. Selection of a suitable dissolving agent was based on the optimization of LE/TE composition [4-6].

Table 1: Operational systems employed in ITP analysis.

Parameters	Cationic analysis	Anionic analysis	
System Nr.	1	2	3
Leading	7.5 mmol/L	10 mmol/L Cl^-	
Electrolyte	H_2SO_4		
Terminating	10 mmol/L BTP	10 mmol/L HEX	5 mmol/L TB
Electrolyte			
Counter Ion	SO_4^{2-}	L-histidine	Imidazole
pH	2.1	5.5	7.2
Additive		0.1% HEC	

A known amount (~15 mg) of material was taken from the homogenized kidney stone powder for analysis. This subsample was transferred into a boiling flask and treated according to Flow Chart in 1 ml of 1-M NaOH for uric-acid determination or in 1 ml of 1-M HCl for the

determination of other compounds. The resulting solution containing usually a small undissolved residue was diluted with 15-20 ml of distilled water and subjected to boiling under reflux to dissolve the remaining solids. Then the clear solution was transferred into a 25-ml volumetric flask and filled up to the mark with distilled water. In the case of cationic analysis, the acidic samples were neutralized to pH 6-8 by the addition of a BTP solution. The determination of urolith constituents cannot be carried out simultaneously due to different ionic nature of the analytes. Therefore, the ITP analysis was divided into three steps (see experimental conditions in detail in Table 1):

i) determination of anionic species ($C_2O_4^{2-}$, HPO_4^{2-});
ii) determination of organic compounds (urate);
iii) determination of cationic species (Ca^{2+}, Mg^{2+} , Na^{+}, NH_4^{+}).

The analytical properties of developed method for all analytes of interest are given in Table 2.

Table 2: The analytical properties of applied ITP analytical method.

Analyte	RSH [d]	Sensitivity (Zone Length/c) s/mM	LOD [e] (μmol/L)	Dynamic Linear Range (mM)	Intra-assay [f] RSD, %
NH_4^{+} [a]	0.304(3)	428(19)	40	0.04-0.20	2.9
Na^{+} [a]	0.481(3)	441(24)	25	0.025-0.15	3.1
Ca^{2+} [a]	0.594(3)	164(4)	16	0.016-0.27	4.4
Mg^{2+} [a]	0.625(3)	245(3)	13	0.013-0.20	3.7
$Oxalate^{2-}$ [b]	0.125(2)	51.3(2)	13	0.013-0.50	2.1
$Phosphate^{3-}$ [b]	0.691(4)	150(1)	25	0.025-0.50	2.5
$Urate^{-}$ [c]	0.271(5)	124.0(8)	17	0.017-0.35	1.5
$Xanthate^{-}$ c	0.354(7)	153(3)	14	0.014-0.27	1.0

a) system 1; b) system 2; c) system 3

d) "Relative Step Height" (RSH) is a qualitative parameter of the substance in the system defined as $RSH_X = \frac{h_X - h_L}{h_T - h_L}$, where h_X is the height of analyte, h_L is the height of leading electrolyte and h_T is the height of terminating electrolyte

e) the limit of detection (LOD) was calculated as 3×sy,x / slope of calibration plot

f) repeated measurement, n = 15

Examples of analysis of samples are given in Fig. 1. All the results of analysis were correlated with values obtained by ICP-MS and elemental analysis taken from [7] (see Fig. 2). The linear plot Y = 1.01(4)×X, where X and Y are values found by the proposed ITP and used ICP-MS analytical method, demonstrates no systematic error in determination of all analytes within a broad concentration range. The RSD for repeated measurements does not exceed 5% for quantitative analysis.

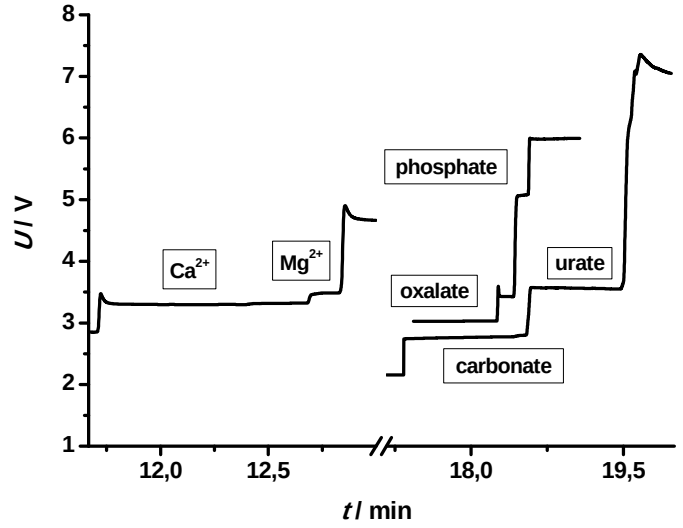

Fig. 1: Example of analysis of renal stone (Ca^{2+}/Mg^{2+} Nr. 1, phosphate/oxalate Nr. 2, urate Nr. 3.

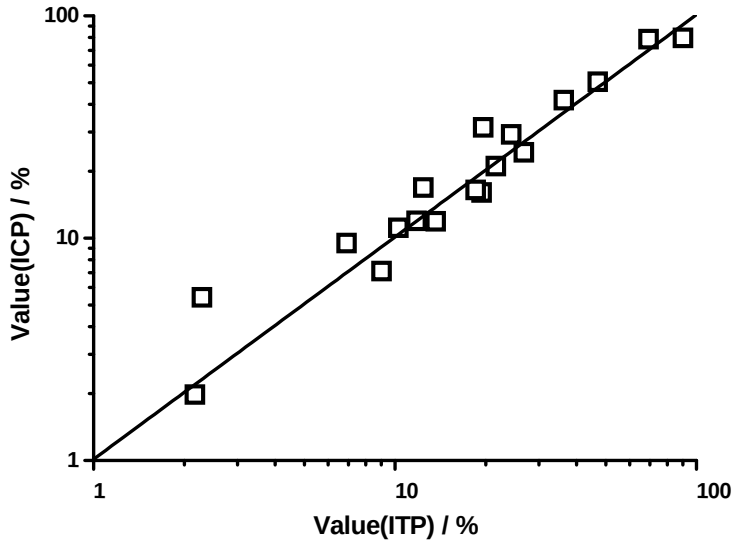

Fig. 2: Comparison of all results obtained by ITP method and elemental analysis for the determination of ions in urinary stones.

4 CONCLUSIONS

The work describes the development and validation of the ITP procedure suitable for the analysis of urinary calculi. This method was optimized for sample treatment as well as for ITP analysis. The procedure can be used for qualitative analysis (uroliths classification) and quantitative determination of Ca^{2+}, Mg^{2+}, Na^{+}, NH_4^{+}, $C_2O_4^{2-}$, PO_4^{3-}, urate ions in renal stones. In addition, this procedure can be applied to the analysis of mixtures of inorganic ions and/or organic compounds of a similar chemical nature in other biominerals (e.g. teeth, bones) and biofluids (urine) concerning K^{+}, CO_3^{2-}, F^{-} and citrate ions. The robust method is fast (total time of ITP analysis is about 1 hour) and cheaper when compared with other analytical techniques (ICP-MS, ion chromatography, CZE).

ACKNOWLEDGEMENTS

The work was supported by Ministry of Education of the Czech Republic (projects KONTAKT ME09065 a LC06035) and Grant Agency of the Czech Republic (project 203/09/1394). We would like to thank prof. Petr Martinec, who provided us with the urolith samples for analysis and Dr. Jiří Machát who carried out elemental analysis.

LITERATURE

[1.] Königsberger, E., Königsberger, L.C. (Eds.), *Biomineralization: Medical Aspects of Solubility*, Wiley, New York 2006.
[2.] Schubert, G., *Urological Research* 2006, *34*, 146-150.
[3.] Muńoz, J.A., López-Mesas, M., Valiente, M., *Talanta* 2010, 81, 392-397.
[4.] Bruchelt, G., Oberritter, H., Schmidt, K.H., *Isotachophoretic analysis of urinary calculi*, in Holloway C.J. (Ed.), *Analytical and preparative isotachophoresis*, de Gruyter , Berlin, New York 1984.
[5.] Yagi, T., Kojima, K., Nariai, H., Motooka, I., *Bulletin of Chemical Society of Japan* 1982, *55*, 1831-1833.
[6.] Verheggen, Th., Mikkers, P., Everaerts, F., *Journal of Chromatography* 1980, *182*, 317-324.
[7.] Benová, D., *Diploma Thesis*, Masaryk University, Brno 2009.

METABOLOMICS: NUCLEOTIDE AND COENZYME DETERMINATION IN CELLS BY CAPILLARY ELECTROPHORESIS

Jindra Musilová, Zdeněk Glatz

Department of Biochemistry, Faculty of Science and CEITEC – Central European Institute of Technology, Masaryk University, Kamenice 5, 625 00 Brno, Czech Republic

ABSTRACT

Capillary electrophoresis (CE) is popular and suitable method for the metabolome analysis particularly due to high-efficient separations of a diverse range of chemical compounds, short analysis times and low sample volume requirements. New separation conditions for selective and rapid determination of 17 energetically important metabolites by CE were optimized. Applicability of this new method to real samples was demonstrated on bacterium *P. denitrificans* and stem cells extracts.

Keywords: metabolomics, capillary electrophoresis

1 INTRODUCTION

Metabolomics includes approaches to analyze the metabolome by the help of different analytical techniques. The whole process of metabolite determination can be simply divided into three steps: a) inactivation of metabolism in cells, b) extraction of metabolites from cells and c) there measurements. The preparation procedures before measurement are often source of variability in the analysis. Metabolome studies aim to relate metabolite levels with the response of biological systems to a genetic or environmental changes [1.] therefore high-rapid quenching of all biochemical processes and high-efficient metabolite release from biological sample is demanded. Nucleotides and coenzymes are central energetic metabolites in complex metabolic network. Their determination is thus important because their pool characterizes the energetic state of the cell under a variety of physiological conditions during cell growth. Numerous method for nucleotide and coenzyme determination in biological samples have been developed, high-performance liquid chromatography (HPLC) predominates in biochemical practice but CE has its position in this field.

2 EXPERIMENTAL

2.1 CE instrumentation and conditions

All experiments were performed on the Agilent ^{3D}CE System 7100 equipped with a diode array UV-VIS detector and data software ^{3D}CE ChemStation. Metabolite samples were dissolved in deionised water, injected by pressure of 35 mbar for 25 s into the uncoated fused-silica capillary (75 µm id × 375 µm od; effective length: 86.5 cm) and detected at 260, 280 and 340 nm.

2.2 Preparation of cell extracts

The nucleotides from bacterial and stem cells were extracted three times by 50 % ACN and spun down [2.] All three supernatants combined into a final extract were evaporated by vacuum concentrator. The solid was dissolved in deionized water and subsequently filtered through Ultrafree MC/PLCC Milipore 5 kDa ultrafilter to remove proteins and other debris.

3 RESULTS

The separation conditions were optimized with aspect to different composition and pH of separation buffer and temperature of capillary. The optimal separation was achieved in 150 mM glycine buffer (pH 9.45) by using voltage 30 kV (positive polarity) and temperature of capillary 25 °C (Fig. 1). Resulting method showed RSD (n = 10) in the range from 0.4 to 0.7 % for migration time and from 3.9 to 4.4 % for relative peak area of metabolites with the exception for NADPH (6.2 %).

The optimized methodology was applied on the cell extract of bacterium *Paracoccus denitrificans* where 11 metabolites were unequivocal determined and stem cell extract where 10 metabolites were determined.

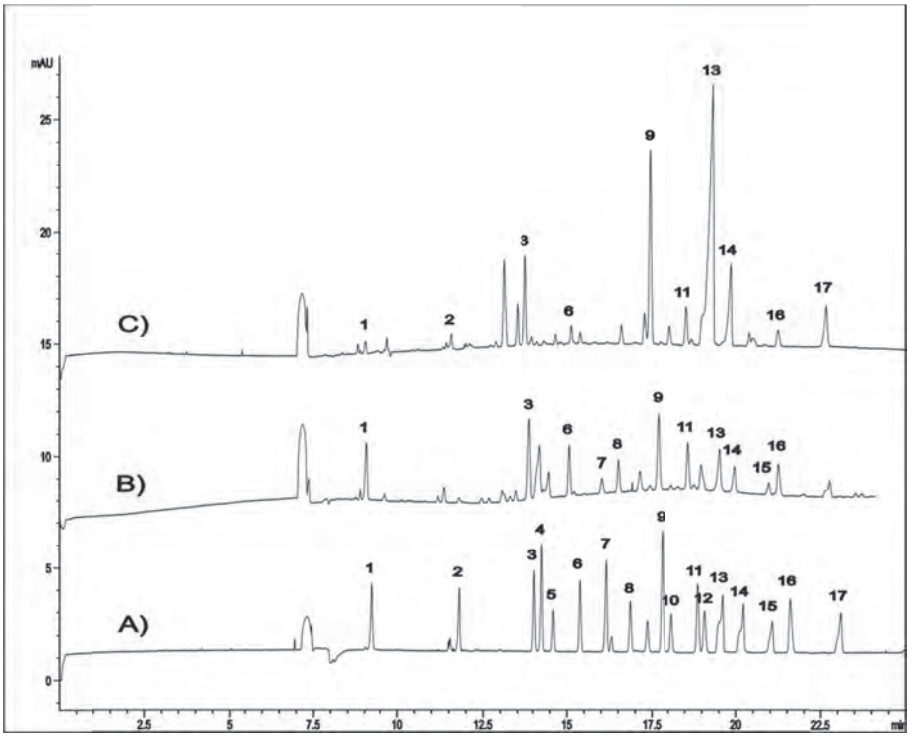

Fig. 1. : A) Electroforeogram of standard mixture, B) bacterium Paracoccus denitrificans and C) stem cell extract; NAD^+ (1), NADH (2), AMP (3), $NADP^+$ (4), CMP (5), GMP (6), Acetyl CoA (7), UMP (8), ADP (9), NADPH (10), GDP (11), CDP (12), ATP (13), GTP (14), CTP (15), UDP (16), UTP (17).

ACKNOWLEDGEMENTS

This work was supported by grants P206/11/0009 and P206/12/G014 from Grant Agency of Czech Republic.

LITERATURE

[1.] Villas-Bôas, S. G., Roessner, U., Hansen, M. A. E., Smedsgaard, J., Nielsen, J. (Ed.), Metabolome Analysis: An Introduction, John Wiley & Sons, Inc., Hoboken, New Jersey 2007.
[2.] Kimbal, E., Rabinowitz, J. D., Anal. Biochem. 2006, 358, 273–280.

SPEEDING UP MASS SPECTROMETRY IMAGING WITH FAST PRECISION MIRROR SCANNING

Antonín Bednařík[a], Pavel Kuba[b], Pavel Houška[b], Iva Tomalová[a], Eugene Moskovets[c], Jan Preisler[a]

[a] *Central European Institute of Technology/Department of Chemistry, Masaryk University, Kamenice 5, 62500 Brno-Bohunice, Czech Republic, 175475@mail.muni.cz*
[b] *Faculty of Mechanical Engineering, Brno University of Technology, Brno, Czech Republic*
[c] *MassTech, Inc. 6992 Columbia Gateway Drive, Suite #160, Columbia, MD 21046, USA*

ABSTRACT

MALDI mass spectrometry imaging (MALDI MSI) is one of the most rapidly evolving techniques in the field of mass spectrometry. This technique holds a great potential in biomarker discovery, drug distribution analysis and in biosciences generally. Hand in hand with new and more demanding applications a need of new high-throughput instrumentation arises. Though a 1 kHz lasers generation of mass spectrometers brought significant decrease of MSI time, a single high resolution image (10 000 pixels) acquisition can still consume many hours. Here we introduce an incorporation of a high speed scanning mirror redirecting the desorbing laser as a possible way to increase the MSI performance.

Keywords: mass spectrometry imaging

1 INTRODUCTION

During past decade the MALDI MSI of biological tissues took an influential place among imaging techniques. One of the key aspects of MALDI MSI is the speed of image acquisition. A high resolution MS image requires collecting of average mass spectra from 10 000 or more spots (pixels) across the sample. The total MSI analysis involves the data acquisition by defined number of laser shots at a given frequency, data processing and sample target translation to the next pixel. This task sequence is repeated N times, where N is the number of pixels in the final image. For one pixel, the cycle time T_{cycle} can be defined. T_{cycle} involves spectra acquisition time T_{acq}, data processing time T_{proc} and sample target translation time T_{trans}.

$$T_{cycle} = T_{acq} + T_{proc} + T_{trans}$$

The total MSI time could be written as:

$$T_{total} = N.T_{cycle}$$

Data acquisition of 100 laser shots with 2 kHz laser would be 50 ms. Data processing time is the smallest contribution to the cycle time, it ranges from 10 to 20 ms. The stage translation time could last over 100 ms, depending on the distance between two pixels and, as the slowest step, becomes the limiting factor for of the overall MSI analysis. The novel approach in the moving forward to the next pixel implements the redirecting of the desorbing laser beam on sub-millisecond scale by a fast scanning mirror. Thus, the major component, T_{trans}, is replaced by negligible time T_{scan}. Hence, the time necessary to obtain the MS image is significantly decreased.

2 METHODS

2.1 Prototype mass spectrometer

Prototype axial high-throughput mass spectrometer features 2.5 m long flight tube, 20-cm cubic 6-way cross chamber with ion source and ion deflectors, a laboratory-built circuitry for delayed-extraction and ion mirror (ABI 4700). The 20-cm cubic ion source chamber with three large UV-transparent windows allows easy modifications of the experimental arrangement as well as direct visual inspection of samples. Two turbomolecular pumps, Turbovac TW700 and Turbovac TW300 (Leybold Vacuum) are used to evacuate the system. A 355 nm 200 Hz - 10 kHz diode-pumped frequency-tripled Nd:YAG laser (DTL-374QT Laser system; Lasers Innovations) serves for desorption and ionization. Energy of laser radiation is 7.5 μJ/pulse at the 2 kHz repetition rate. The vacuum-compatible x-y stages can move the MALDI plate holder at speeds up to 5 mm/sec, with a declared positioning accuracy 3 microns. Finally, a high speed 2 GS/s digitizer/averager (AP 200, Acqiris) is used for data acquisition and accumulation. The resolution of the instrument in the linear mode is 4 000, in the reflector mode it reaches 15 000.

2.2 Fast precision scanning mirror

The prototype special feature is incorporation of the fast precision scanning mirror (6810P; Cambridge Technology), which is capable of redirecting desorption laser beam on a sub-millisecond time scale. With a proper optical design, the scanning mirror can move the laser beam few millimeters across the sample. Due to the large size of the ion source optics, mass resolution should not deteriorate considerably during the beam travel.[1,2] In the MSI mode the mirror scanning can be used to substitute the horizontal stage translation (x-axis) at a limited range. Tiny (< 3 mm wide) sample areas can be mapped simply by combination of x-axis mirror scanning and y-axis stage movements. Larger sample areas can be stitched together from smaller scanned segments. Furthermore, the fast scanning mirror may also serve as an optical shutter and the laser pulse train does not have to be interrupted during the stage translation.

2.4 Chemicals

The four model peptides, namely bradykinin, angiotensin I, renin, adrenocorticotropic hormone (ACTH) fragment 19-38 and α-Cyano-4-hydroxycinnamic *acid* (*CHCA*) matrix were purchased from Sigma-Aldrich. For deposition of model sample, the solution containing 60:40 acetonitrile:water, 6 mg/ml CHCA; 0.2 % trifluoroacetic acid (TFA), 1 μM bradykinin, 1 μM angiotensin I, 2 μM renin and 5 μM ACTH was prepared.

2.5 Sample deposition

Model sample mixture was deposited on MALDI targets by micropipette, later by common MSI deposition techniques, piezo-nanospotting and airbrush coating. For piezo-nanospotting deposition, the drop-on-demand dispenser MJ-ABP-01 with 50 μm orifice (MicroFab Technologies Inc.) was used. Well defined matrix spots with fine homogeneity of crystals

were obtained. Airbrush deposition was carried out by Infinity airbrush (Harder & Steenbeck Airbrush) with 0.15 mm orifice. The 100 µl of the liquid was sprayed on the MALDI plate from distance 5 to 10 cm with outflow 85 µl per minute under working pressure 3 bar.

3 EXPERIMENTAL

3.1 Speeding up MALDI MS Imaging

The MSI speeds of commercial time-of-flight (TOF) mass spectrometer (AutoFlex™ Speed, Bruker Daltonics) and that of our laboratory-built TOF prototype were compared. MSI maps consisting from 10 000 pixels (step 100 µm) were recorded on the both instruments. The total MSI times were recorded and are shown in Table 1.

Table 1: MSI time comparison of AutoFlex™ Speed (Bruker Daltonics) and our prototype

Device/Mode	**Desorbing laser frequency f (kHz)**	***Translation time*** T_{trans} ***(ms)***	***Acquisition time*** T_{acq} ***(ms)***	**Processing time** T_{proc} ***(ms)***	**One pixel time** T_{cycle} ***(ms)***	***Total MSI time*** T_{total} **(min)**
AutoFlex Speed/x-y stages MSI	1	-	-	-	750	**~ 125**
Prototype/ x-y stages MSI	1	95	100	10	206	**34.5**
Prototype/Mirror scanning MSI	1	220	100	10	130	**21.9**
Prototype/Mirror scanning MSI	2	220	51	10	83.5	**13.1**

3.2 Instrumental arrangement and quality of the MS images

Mirror scanning was performed in two arrangements, scanning through grids of ion extraction optics and scanning from the side. Scanning through the grids was found to produce significant image distortions, when the laser hits the grid wires during the scanning. Hence, the scanning from a side was used in further experiments including the acquisition of images showed in Fig. 1. The maximum mirror scan range, which allowed the imaging without significant decrease of the ion signal, was found to be 3 and 1.5 mm in the linear and reflector modes, respectively. Fig. 1 a) shows the sprayed model sample and the imaged area of 1 cm^2 divided into 100 x 100 raster (100 µm step). Fig. 1 b) is the MS image of CHCA matrix recorded in the linear mode, stitched from 2-mm mirror scan segments. Fig. 1 c) shows the same sample area recorded in the reflector mode, stitched from 1-mm mirror scan segments. Relatively higher ion intensity fluctuations across the scan were observed in the reflector mode.

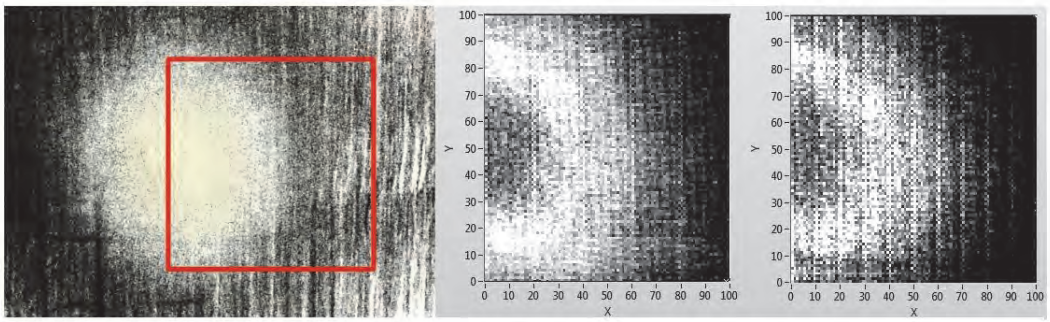

Fig. 1: a) Visual image of the model sample showing distribution of CHCA matrix crystals, b) MS image of CHCA matrix, linear mode, c) MS image of CHCA matrix, reflector mode

4 CONCLUSIONS

A high-throughput axial mass spectrometer prototype with a fast precision scanning mirror was constructed and its MS imaging capabilities were tested with model peptide samples. Fast and precise mirror scanning can substitute for a stage movement within the ranges of 3 or 1.5 mm in the linear or reflector modes without a significant ion signal intensity decrease. Larger sample areas can be easily mapped by image stitching from smaller segments using combined movement of the mirror and the horizontal translational stage. Significant decrease of the MSI time was achieved by implementation of the mirror scanning compared to the classical imaging relying on mere sample target translation. A map consisting of 10 000 pixels was recorded in 13.1 minutes, an order of magnitude faster in comparison with the commercial instrument.

ACKNOWLEDGEMENTS

This work was supported by Czech Science Foundation (P206/10/J012) and CEITEC - Central European Institute of Technology (CZ.1.05/1.1.00/02.0068)

LITERATURE

[1.] Preisler, J.; Hu, P.; Rejtar, T.; Moskovets, E.; Karger, B. L., *Analytical Chemistry* **2002,** *74* (1), 17-25.

[2.] Moskovets, E., Preisler, J., Chen, H. S., Rejtar, T., Andreev, V., Karger, B. L., *Analytical Chemistry* **2006**, 78, 912-919.

CAPILLARY ELECTROPHORESIS WITH CONTACTLESS CONDUCTIVITY DETECTION OF CATIONIC-DERIVATIZED OLIGOSACCHARIDES

Jan Partyka, František Foret

Institute of Analytical Chemistry of the AS CR, v.v.i., Veveri 97, 602 00 Brno, Czech Republic, partyka@iach.cz

ABSTRACT

In this work, derivatization of oligosaccharides by reductive amination with quaternary ammonium label was studied for electrophoretic preconcentration and separation with

contactless conductivity detection (C4D). (2-aminoethyl)-trimethylammonium chloride (AETMA) which has one permanent positive charge was selecvted as a cationic label. The labeled oligosaccharides were separated by capillary zone electrophoretic (CZE) and transient isotachophoretic-electrophoretic (t-ITP/CZE) modes.

Keywords: oligosaccharide; conductivity detection; (2-aminoethyl)trimethylammonium chloride

1 INTRODUCTION

Glycosylation is the most frequent post-translation modification of proteins. Glycans are commonly analyzed by mass spectrometry but the glycan analysis is often complicated by too complex matrix and it usually requires a separation step such as chromatography or capillary electrophoresis. The glycans and oligosaccharides are difficult detect with optical detectors because of absence of a chromophore or fluorophore in their molecule. For this reason derivatization step with optically active label is necessary. In addition, thanks to derivatization the oligosaccharides obtain also charged group(s) improving their separation by electrophoretic techniques. In this study we have investigated derivatization of oligosaccharides by AETMA for CE and future CE ESI/MS analysis. This label has one permanent positive charge allowing the separation of oligosaccharides as cations in 100 mM acetic acid at low pH value. Thanks to this approach the application in CE ESI/MS is possible. The quaternary label is not detectable by UV or LIF detectors therefore we used conductivity detection which proved to be very sensitive with detection sensitivity in low nanomolar concentration range.

2 CZE SEPARATION OF DERIVATIZED OLIGOSACCHARIDES

The samples including dextran ladder, isomaltotriose, maltopentaose, maltoheptaose, 6´-sialyl-D-lactose and glycans from ribonuclease B were derivatized by protocol described by Unterieser and Mischnick [1.]. Shortly, the oligosaccharide was derivatized by reductive amination in methanolic solution with acetic acid. The AETMA and reductive reagent 2-picoline borane were added with various concentrations (2-10 times higher than concentration of oligosaccharide). These derivatized oligosaccharides were separated as cations by CZE in polyvinylalcohol (PVA)-coated capillary (Fig. 1.). Formic acid and acetic acid (100 mM) were used as background electrolyte (BGE) because of future connection with ESI/MS. Since the AETMA label contains a quaternary amine group, the derivatized oligosaccharides have positive charge at any pH of the separation buffer and can be easily separated by CE. Moreover, 6´-sialyl-D-lactose, which has negatively charged sialic acid, migrated as cation in mixture with dextran ladder. Thanks to low pH value of BGE the ionization of sialic group was strongly suppressed allowing its detection as a cation. The partial negative charge on the molecule with m.w. = 718.72 Da shifted its migration close to the 13 glucose units species in the dextran ladder with m.w. = 2342.02 Da. This shift in the electrophoretic mobility is a clear indicator of the partial negative charge due to the presence of sialic acid.

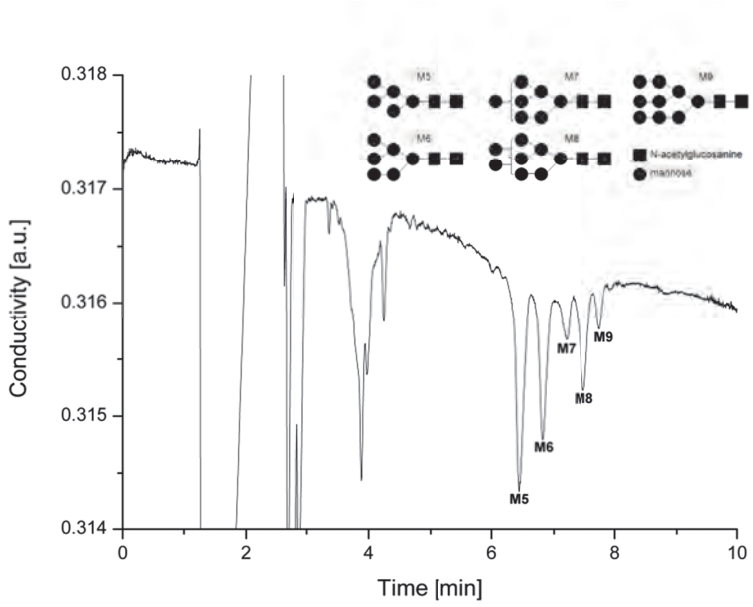

Fig. 1. : Electrophoretic separation of AETMA labeled glycans released from ribonuclease B. The sample was separated by t-ITP/CZE mode. Separation conditions: 25/30 cm PVA-coated capillary, voltage 10 kV, BGE: 100 mM acetic acid (pH=2.9). Injection conditions: Δh = 10 cm, t = 60 sec. a.u. – arbitrary units.

3 TRANSIENT ITP-PRECONCENTRATION OF DERIVATIZED OLIGOSACCHARIDES

We have also tested on-column preconcentration based on isotachophoretic principle. The AETMA-derivatized oligosaccharides were dissolved in 10 mM ammonium acetate solution. Ammonium ions had the highest mobility in t-ITP/CZE system and served as the leading zone. Acetic acid (100 mM, pH=2.9) was chosen as BGE and served as terminating electrolyte during the preconcentration step. The PVA-coated capillary was initially filled by 100 mM acetic acid. Upon pressure injection of a long sample (up to 70% length of the separation capillary) the AETMA-derivatized oligosaccharides were initially focused into a narrow zone by transient ITP followed by relaxation into the zone electrophoretic separation mode. Over 2 orders of magnitude improvement of the sensitivity was achieved for AETMA-derivatized isomaltotriose, maltopentaose and maltoheptaose by this approach with the initial 5.10^{-8} M sample concentration. Moreover, the separation of 25 peaks of dextran ladder was realized in less than 15 min with baseline resolution.

ACKNOWLEDGEMENTS

Support from the Grant Agency of the Czech Republic (P301/11/2055 and P206/12/G014) and the institutional funding RVO: 68081715 is greatly acknowledged.

LITERATURE

[1.] Unterieser, I. and Mischnick, P., *Carbohydrate Research* 2011, *346*, 68-75.
[2.] Partyka J. and Foret, F., *Journal of Chromatography A* 2012, in press.

CONTROL OF THE POLYMERIZATION TOWARDS POROUS LAYER OPEN TUBULAR CAPILLARY COLUMNS

Radim Knob[a,b], Michael C. Breadmore[a], Rosanne Guijt[c], Jan Petr[b], Mirek Macka[a]

[a] *Australian Centre for Research on Separation Science (ACROSS) and School of Chemistry, University of Tasmania, Private Bag 75, Hobart, TAS 7001, Australia*
[b] *Regional Centre of Advanced Technologies and Materials, Dept. Anal. Chem., Faculty of Science, Palacký University in Olomouc, 17. Listopadu 12, Olomouc, Czech Republic, CZ-77146*
[c] *Australian Centre for Research on Separation Science (ACROSS) and School of Pharmacy, University of Tasmania, Private Bag 26, Hobart, TAS 7001, Australia*
rknob@seznam.cz

ABSTRACT

A novel method for the preparation of monolithic porous layer open tubular (PLOT) columns in fused silica capillaries is presented. In the first experiments, light attenuation by a UV absorbing compound in the polymerization mixture was tested. In another approach, the capillary was first flushed by polymerization mixture followed by a solvent not containing the monomers. However, no useful results were obtained in both cases. When the polymerization mixture at the centre of the capillary was removed with an immiscible liquid (FC-770), a thin layer of polymer monolith was formed. The flushing with FC-770 leaves only a thin film of the polymerization mixture wetting the capillary wall. Subsequent UV initiated polymerization of this film results in PLOT columns with a thin layer of poly(glycidyl methacrylate-*co*-ethyleneglycol dimethacrylate) at the wall of a fused silica capillary.

Keywords: monolith, porous layer open tubular, polymerization

1 INTRODUCTION

Capillary columns utilizing a layer of a stationary phase at the capillary wall were introduced by Golay [1] to gas chromatography and were further tested in liquid chromatography (LC) [2,3]. Due to slow mass transfer between mobile and stationary phases, capillaries with very narrow diameters were suggested to provide improvements over packed columns. However, low mass loadability on thin films limited detection limits and the preparation of such columns lacked reproducibility. In order to overcome the drawbacks, porous layer open tubular (PLOT) columns were developed. The porous properties of the material increase surface area, thus increase sample loading capacity and minimize the issue of the slow mass transfer. In last two decades, monolithic stationary phases underwent a rapid development, the simplicity of the preparation and the ability of tailoring the surface properties attracted attention of many research groups. Monolithic PLOT capillary columns could be prepared using both thermal and UV initiation. The polymerization process has to be controlled in order to provide a homogeneous layer of the monolith. It can be done by reducing the monomer content in the polymerization mixture [7,8] or by limiting the amount of initiator transformed into radicals. UV-initiated polymerization together with rotating the capillary under the light source was introduced by Eeltink *et.al.* [9]. Evanescent wave-initiated photopolymerization [10] was utilized for the fabrication of a short PLOT column which was used as an enzymatic microreactor. Nesterenko *et al.* [10] utilized a moving UV source along the capillary. The approach was modified by Collins *et al.* [11] who dragged the capillary through a UV chamber of UV LEDs.In this work, we present an approach for preparation of thin layer PLOT monolith capillaries. The polymerization mixture is physically restricted at the capillary wall where the polymerization can only occur. A fully-fluorinated immiscible liquid, FC-770, was used to

remove the monolith precursor mixture from the capillary leaving a thin layer held to the wall which is subsequently polymerized by UV light.

2 FABRICATION

2.1 Light attenuation

Our first approach to develop a more robust fabrication process to form a PLOT monolith was through restricting the amount of light that could penetrate the capillary by adding a UV absorbing compound into the polymerization mixture. Its attenuation of the light intensity towards the centre of the capillary should limit the polymerization process to the surface of the capillary where the light intensity is the highest. Despite some successful preliminary attempts, this approach lacked the necessary robustness as it resulted in the formation of a monolith with irregular thickness around the circumference and length of the capillary.

2.2 Monomer free solvents

An alternative solution with a potential to limit the location of monolith growth at the capillary wall is by removing the polymerization mixture from the middle (central part) of the capillary with a liquid phase that does not contain the monomers. A number of pure solvents such as 1-dodecanol, 1-decanol, and cyclohexanol were tested to remove the polymerization mixture from the middle of the capillary. However as these solvents are partially miscible with the polymerization mixture, no satisfactory results were obtained. Therefore, we used a fully fluorinated solvent FC-770 with significantly different physico-chemical properties from the polymerization mixture resulting in immiscibility and differences in wettability of the capillary surface between the two liquid phases.

2.3 PLOT preparation

In our experiments, we used the polymerization mixture according to Deverell et al. [13]. The mixture composed of 0.93 g cyclohexanol, 1.4 g 1-dodecanol, 0.4 g of ethylene dimethacrylate (EDMA) and 0.6 g of glycidyl methacrylate (GMA). Phenylbis(2,4,6-trimethylbenzoyl)phosphine oxide (10 mg, 1% (w/w) with respect to the monomers) was added to the mixture as a photoinitiator. The resultant mixture was sonicated for 10 min and purged with nitrogen for further 10 min. A PTFE coated fused silica capillary previously modified with γ-MAPS was first flushed with the polymerization mixture and then flushed with FC-770. The capillary was irradiated under 360 nm UV-LED array. The capillary was then washed with methanol.

The prepared capillaries were characterized by scanning electron microscopy (SEM). An image showing a homogeneous thin monolith layer is shown in Figure 1A and a detailed view of the capillary wall is presented in Figure 1B.

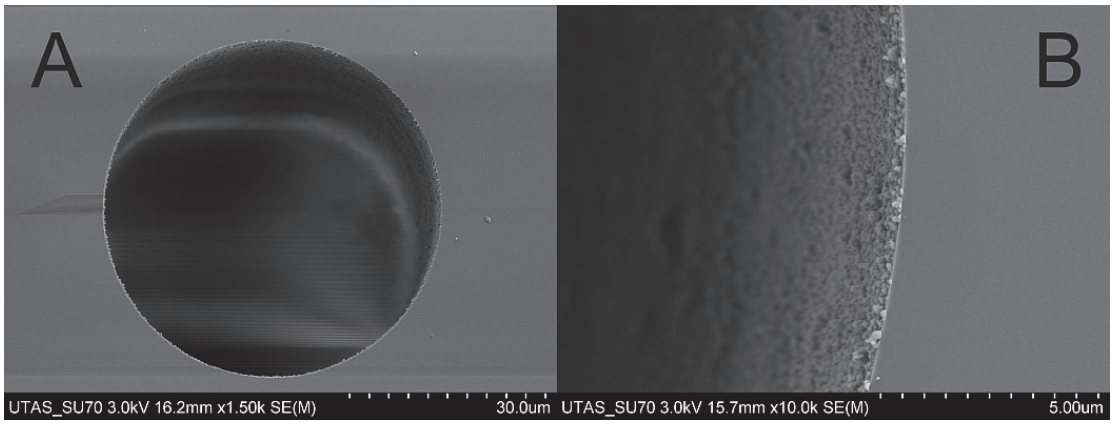

Fig. 1. SEM images of PLOT monolith capillary (A) and a detailed view on the capillary wall (B).

3 CONCLUSIONS

We present another approach for preparation of thin layer PLOT monolith in fused silica capillaries. It is based on the use of an immiscible liquid, FC-770, to force the polymerization mixture into a thin film wetting the capillary wall. This approach overcomes frequently reported difficulties with control of the PLOT monolith thickness and homogeneity and does not require any costly instrumentation or complex experimental design.

The prepared thin layer PLOT poly(GMA-*co*-EDMA) monolith was is aimed to be functionalized with quaternary ammonia functional groups and to be used for separation of selected inorganic anions. This novel approach to preparation of PLOT monolithic capillary columns can be applied to a wide range of monolith formulations and with the variety of post polymerization reactions and used for various applications.

ACKNOWLEDGEMENTS

R. Knob and J. Petr acknowledge support from Operational Program Research and Development for Innovations - European Regional Development Fund (project CZ.1.05/2.1.00/03.0058) and Program Education for Competitiveness - European Social Fund (project CZ.1.07/2.3.00/20.0018). M.C. Breadmore acknowledges receipt of an ARC QEII Fellow from the Australian Research Council (DP0984745). M. Macka acknowledges UTAS New Stars start-up grant. The authors would like to thank Dr. Karsten Gömann (Central Science Laboratory, University of Tasmania) for assistance with the SEM images.

LITERATURE

[1.] Golay, M.J.E in *Gas Chromatography*, Coates, V. J., et al., Academic Press: New York, 1958.
[2.] Knox, J.H., Gilbert, M.T., J. Chromatogr. 1979, 186, 405-418.
[3.] Gulochon, G., Anal. Chem. 1981, 53, 1318-1325.
[4.] Eeltink, S. , Svec, F., Electrophoresis, 2007, 28, 137-147.
[5.] Svec, F., J. Chromatogr. A, 2010, 1217, 902-924.
[6.] Arrua, R. D., Talebi, M., Causon, T.J., Hilder, E.F., Anal. Chim. Acta, 2012, 738, 1-12.
[7.] Yue, G., Luo, Q., Zhang, J., Wu, S.-L., Karger, B.L., Anal. Chem, 2007, 79, 938-946.
[8.] Rosberg, M., Wilson, S.R., Greibrokk, T., Lundanes, E., J. Chromatogr. A, 2010, 1217, 2782-2786.
[9.] Eeltink, S., Svec, F., Frechet, J.M.J., Electrophoresis, 2006, 27, 4249-4256.
[10.] Abele, S., Smejkal, P., Yavorska, O., Foret, F., Macka, M., Analyst, 2010, 135, 477-481.
[11.] Nesterenko, E., Yavorska, O., Macka, M., Yavorsky, A., Paull, B., Anal. Methods, 2011, 3, 537-543.
[12.] Collins, D. A., Nesterenko, E.P., Brabazon, D., Paull, B., Anal. Chem., 2012, 84, 3465-3472.
[13.] Deverell, J.A., Rodemann, T., Smith, J.A., Canty, A.J., Guijt, R.M., Sens Actuators B Chem., 2011, 155, 388-396.

LIVING CELLS STATE TRAJECTORY IN TIME-LAPSE MICROSCOPY

Karina Romanova, Petr Císař, Dalibor Štys

Faculty of Fisheries and Protection of Waters, School of Complex Systems, University of South Bohemia, Zámek 136, 373 33 Nové Hrady, Czech Republic, romanova@frov.jcu.cz

ABSTRACT

Tissue cells exhibit fascinating properties: they synthetize a huge variety of chemicals, gather and process information about their surroundings, communicate, move across environments or change their biochemical composition. Advances in microscopy and culturing techniques made possible to see the cells in action. The most visually interesting events in the life of a cell occur when it divides. Imaging of living cells and tissue is now common in many fields of the life and physical sciences. Time-lapse microscopy makes link of initial cell cycle position with final.

We extracted the region of the cell in order to analyze information about the cell state from spatial structure of observed objects. For maximization of information gain we calculated the point information gain entropy density (PIE/points, Stys et al. 2011). We determine the information contribution of each data point to the object by calculation of difference in Renyi entropy between datasets containing and excluding the examined data point. This procedure we perform for representative set of alpha coefficients and obtain a set of point information gains (PIG). Sum of PIG values for certain alpha is the appropriate PIE/points. Set of PIE/points is a point in the tentative phase space which is unique for each image.

Using statistical procedure of Principal Component Analysis (PCA) and Clustering Analysis we were able to separate the state space in regions occupied by similar images (Stys et al. 2012). The sequence of regions is an objectively determined cell state trajectory, which are stable for certain period of time. For the cell cycle, we found that regions in the cell state space may be identified with known terminology, i.e. we were able to find cell state corresponding to each of the clusters. Such detailed analysis is extremely computationally intensive; however, it might be of high value for rapid diagnostics in medicine, biotechnology and any other discipline utilizing cell biology results.

Keywords: cells state trajectory, information Entropy, Renyi entropy.

1 INTRODUCTION

Imaging of living cells and tissue is now common in many fields of the life and physical sciences. Time-lapse microscopy can be described as the repeated collection of a region of view from a microscope at discrete time intervals. This unit describes the implementation of time-lapse microscopy to link initial cell cycle position with final. It is crucial when performing such experiments that cell viability is at the forefront of any measurement to ensure that the physiological and biological processes that are under investigation are not altered in any way. Many cells and tissues are not normally exposed to light during their life cycle, so it is important for microscopy applications to minimize light exposure, which can cause phototoxicity [1].

The dynamics comprise changes of the shape of the interior objects of the cell (nucleus, organells), changes of the cell volumetric shape (we can see only the projection to the 2D space) and change of the color of the pixels corresponding to the celll interior. If we want to build the analysis of cell behavior for this cell discription we have to have a method for automatic features extraction. The reason for development of an automatic method is that it is simply impossible to objectively describe all the features manually due to time and precision requirements. There are two main groups of objects description from the image: shape oriented and image oriented parametrization. The common problem of an automatic

processing of mammalian time-lapse images is specific properties of the images. Such images have low background objects and object-object contrast, a highly flexible shape of the cell, dynamic image changes in a cell interior. These properties make the automatic feature extraction very difficult.

To successfully image cellular processes in living cells, the cells must be kept in an environment that does not induce stress responses, which can alter the cellular processes of interest. Some of the key factors to consider are the type of culture medium and its contents, and the temperature of the sample, which must be kept stable at 37°C for mammalian cells. Moreover, the pH of the sample must be maintained at a physiological level and evaporation of the medium must be minimized to avoid changes in osmolarity [1].

2 METHOD

The method is based on the calculation of Point Information Gain and Point Information Gain Entropy (PIE) to information of the whole image. For maximal information gain from images we used information entropy based on Rényi equation [2]:

$$H_\alpha(X) = \frac{1}{1-\alpha}\log\left(\sum_{i=1}^{n} p_i^\alpha\right)$$

p_i are probabilities of occurrence at i-th position in the phase space and α is a parameter which reflects the deformation of the distribution.

There is only one parameter α of the transformation which can be defined by a user. The parameter is used for highlighting the specific part of information in the original image and supression of the rest of information [3].

After all, we obtain a complex system in the 39-dimensional space (13 variations of α parameter in 3 different color filters). The best solution while working with such a system was to carry out further processing of the data with the Principal Component Analysis (PCA) - a method that allows not only to reduce the dimensionality of space to 5-dimensional, but also transform a set of our data in accordance with the theory we use. Special arrangement of the data-points in the space of PCA-components creates the state trajectory of the cell cycle.

3 CELL STATE TRAJECTORY

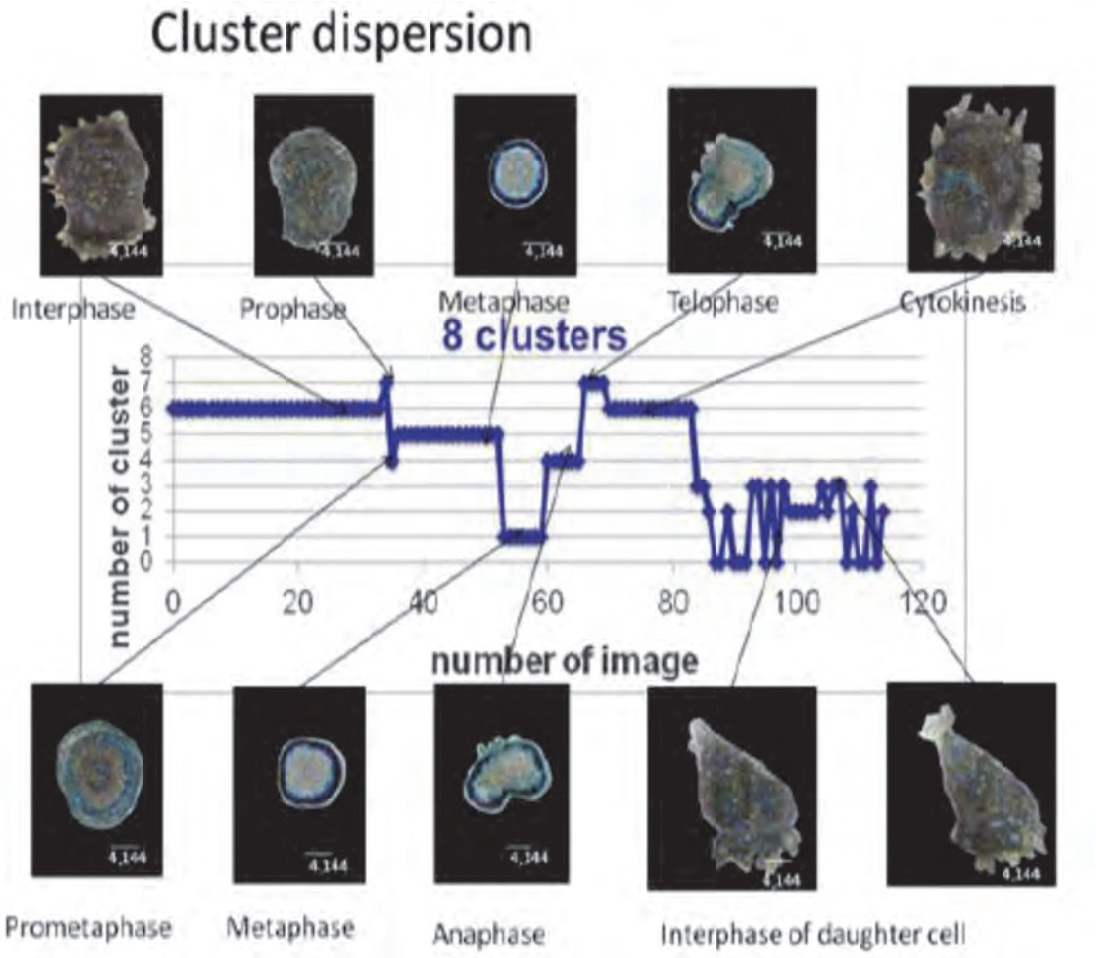

Fig.1 : Trajectory of a cell states. Each of the clusters corresponds to states of cell cycle.

LITERATURE

[1.] Melanie M. Frigault, Judith Lacoste, *J Cell Sci,* 2009,122, 753-767.

[2.] Rényi, A., 1961. On measures of information and entropy. In: Proceedings of the 4th Berkeley Symposium on Mathematics, Statistics and Probability 1960. pp. 547–561.

[3.] Urban J., Vanek J., Stys D.: Proc. of Pattern Recognition and Information Processing, 2009, pp. 183 – 187.

ORIENTED IMMOBILIZATION OF PNGASE F ON A POROUS POLYMER MONOLITH FOR RAPID N-GLYCAN RELEASE

Ákos Szekrényes[a], Jana Krenkova[b], Zsolt Keresztessy[c], Frantisek Foret[b], András Guttman[a]

[a] *Horváth Laboratory of Biosepartion Sciences, Research Center for Molecular Medicine, University of Debrecen, Nagyerdei krt. 98, 4032 Debrecen, Hungary,* akos.szekrenyes@gmail.com

[b] *Institute of Analytical Chemistry of the Academy of Sciences of the Czech Republic, v. v. i, Veveri 97, 602 00 Brno, Czech Republic*

[c] *Debrecen Clinical Genomics Center, Department of Biochemistry and Molecular Biology, Medical and Health Sciences Center, University of Debrecen, Nagyerdei krt. 98, 4032 Debrecen, Hungary*

ABSTRACT

We demonstrate a simple and rapid method for the oriented immobilization of peptide-*N*4-(*N*-acetyl-glucosaminyl) asparagine amidase F (PNGase F) on a porous polymer monolith. The oriented immobilization is based on the affinity of glutathione-S-transferase (GST) tagged PNGase F towards glutathione modified monolith prepared in the capillary format. This approach allows the oriented and easily replaceable immobilization of PNGase F for rapid and efficient release of N-linked glycans. The reactor was tested by deglycosylation of several native glycoproteins such as ribonuclease B, fetuin or human immunoglobulin G. The proteins were effectively deglycosylated in several minutes and the released N-linked glycans were analyzed using off-line MALDI/MS or CE/LIF.

Keywords: PNGase F, oriented immobilization, monolith

1 INTRODUCTION

Rapid analysis of protein linked glycans is of great importance in the biopharmaceutical development and quality control due the growing number of recombinant protein drugs. Over one-third of the currently marketed therapeutic proteins are being glycosylated and these glycosylation is forcefully affecting their immunogenic and pharmacokinetic properties as well as their folding, neutralization, and stability [1].

The initial step of the N-glycosylation analysis is the complete release of N-linked glycans from proteins of interest. This process commonly involves enzymatic digestion using PNGase that cleaves the bond between asparagine and innermost *N*-acetyl-D-glucosamine residue of N-glycans. The digestion is usually performed using the soluble enzyme and requires long incubation time (overnight digestion). Recently several techniques have been applied to reduce the digestion time such as microwave irradiation [2] or pressure cycling technology [3]. However, one of the most promising approaches is the immobilization of PNGase F on the solid support such as monolithic materials [4, 5].

In this work we report the oriented immobilization of PNGase F on the methacrylate based monolith prepared in the capillary format. The developed immobilized PNGase F monolithic reactor was tested by treatment of several model glycoproteins followed by off-line MALDI/MS and CE/LIF analysis of released N-linked glycans.

2 ORIENTED IMMOBILIZATION OF PNGASE F

The poly(glycidyl methacrylate-co-ethylene dimethacrylate) monolithic column was prepared in a 250 µm ID fused silica capillary by thermally initiated radical polymerization [6]. The monolithic column was treated with aqueous ammonia solution and then functionalized with

succinimidyl-6-[(iodoacetyl)amino]hexanoate to enable the coupling of glutathione via sulfhydryl functionalities in the following step. The scheme of preparation of glutathione modified monolithic column is shown in Fig. 1. In the final step, a solution of GST tagged PNGase F was flushed through the glutathione modified column resulting in the oriented immobilization of PNGase F via a GST tag.

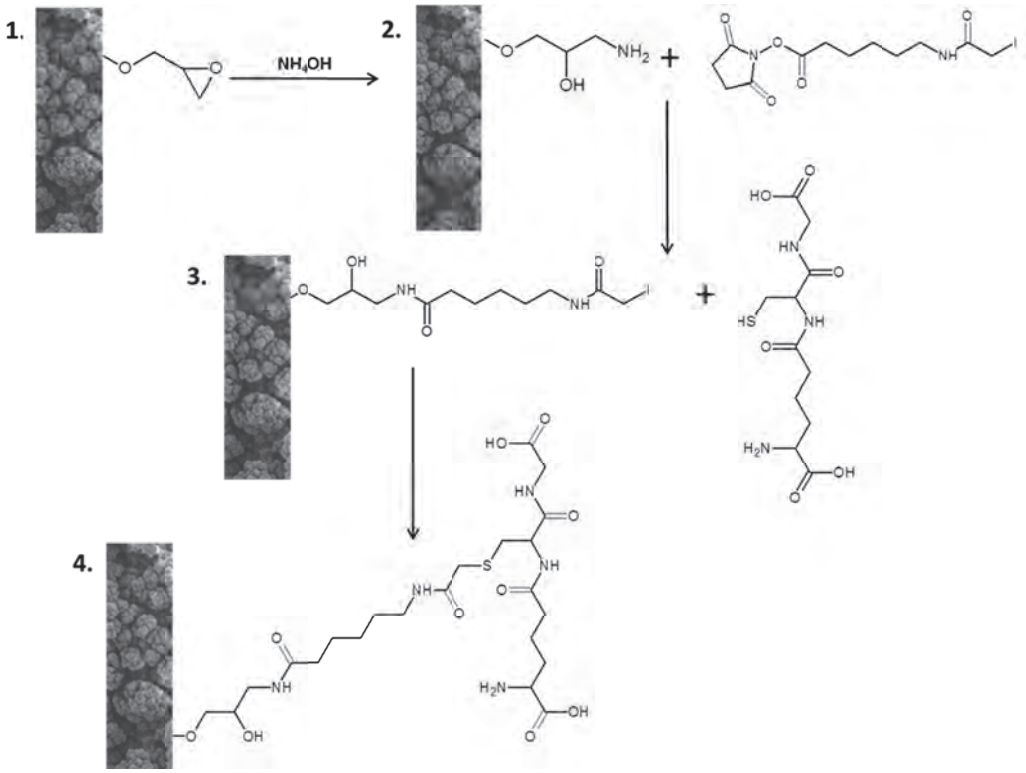

Fig. 1. Preparation of the glutathione modified monolithic column.

3 GLYCAN RELEASE USING THE PNGASE F MONOLITHIC REACTOR

The efficiency of the developed PNGase F monolithic reactor was characterized by deglycosylation of ribonuclease b (containing high mannose structures), human serum immunoglobulin G (containing complex type structures) and calf serum fetuin (highly sialylated structures) as model glycoproteins. The deglycosylation was performed in 5 mmol/L sodium carbonate buffer, pH 7.0 containing 10% (v/v) acetonitrile at room temperature. The solution of native ribonuclease B (1 mg/mL), fetuin (1 mg/mL) or human immunoglobulin G (2.5 mg/mL) was flushed through the 10 cm long reactor at various flow rates corresponding to deglycosylation times of several minutes. The proteins were removed from the collected N-linked glycans using 10kDa MWCO Nanosep micro-filter units (Millipore). The N-linked glycans were analyzed by MALDI-TOF/MS (4700 MALDI-TOF/TOF Proteomic Analyzer, Applied Biosystems) or labeled with 8-aminopyrene-1,3,6-trisulfonic acid (APTS) before CE/LIF analysis. The APTS labeled glycans were purified using a ProZyme APTS clean up module in order to remove the excess of the fluorescent dye. CE/LIF analysis was carried out in a Beckman P/ACE MDQ instrument (50 µm ID CHO coated capillary, 50.2 cm effective length, 500 V/cm field strength).

Fig. 2 shows the electrophoretic analysis of APTS labeled N-linked glycans released from human immunoglobulin G using the PNGase F monolithic reactor. The complete deglycosylation was obtained in 6 min using the monolithic reactor. Similar results were

obtained for treatment of ribonuclease B or fetuin with the optimal deglycosylation time of 3 min.

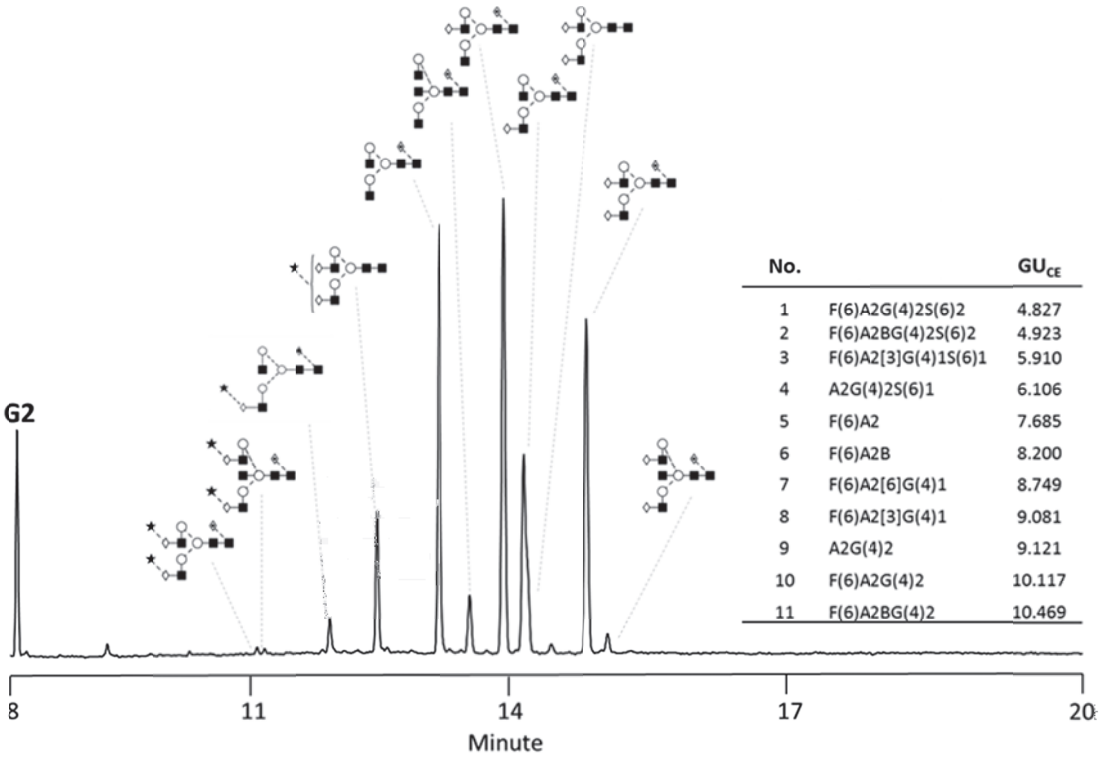

Fig. 2. CE/LIF analysis of APTS labeled N-linked glycans released from immunoglobulin G using the PNGase F monolithic reactor.

The oriented immobilization was also compared with the non-oriented coupling of PNGase F molecule via epoxide functionalities of the generic poly(glycidyl methacrylate-co-ethylene dimethacrylate) monolith. The PNGase F reactor prepared by the non-oriented approach showed significantly lower deglycosylation efficiency as tested by treatment of ribonuclease B. In summary, we have prepared the highly effective PNGase F reactor via oriented immobilization that enables the efficient and rapid release of N-linked glycans from various glycoproteins.

ACKNOWLEDGEMENTS

This project was supported by the OTKA grant # K-81839 of the Hungarian Research Council and also funded from from the SoMoPro programme. Research leading to these results has received a financial contribution from the European Community within the Seventh Framework Programme (FP/2007-2013) under Grant Agreement No. 229603. The research was also co-financed by the South Moravian Region and the EU Seventh Framework Programme under the "Capacities" specific programme (Contract No. 286154 – SYLICA).

LITERATURE

[1.] Walsh, G.; Jefferis, J., *Nature. Biotechnology* 2006, *24*, 1241–1252.
[2.] Zhou, H., Briscoe, A. C., Froehlich, J. W., Lee, R. S., *Analytical Biochemistry* 2012, *427*, 33-35.
[3.] Szabo, Z., Guttman, A., Karger, B. L., *Analytical Chemistry* 2010, *82*, 2588-2593.
[4.] Palm, A. K., Novotny, M. V., *Rapid Communications in Mass Spectrometry* 2005, *19*, 1730-1738.
[5.] Krenkova, J., Lacher, N. A., Svec, F., *Journal of Chromatography A* 2009, *1216*, 3252-3259.
[6.] Krenkova, J., Lacher, N. A., Svec, F., *Analytical Chemistry* 2009, *81*, 2004-2012.

SPECTROSCOPIC DISCRIMINATION OF BEE POLLEN AND HONEYCOMB POLLEN SAMPLES

Roman Bleha [a], Lucie Kucelová [b], Ján Brindza [b], Andriy Synytsya [a]

[a] *Department of Carbohydrates and Cereals, ICT Prague, Technická 5, 166 28 Prague 6, Czech Republic* Roman.Bleha@vscht.cz

[b] *Institute of Biodiversity Conservation and Biosafety, Faculty of Agrobiology and Food Resources, Slovak University of Agriculture, Tr. A. Hlinku 2, 949 76 Nitra, Slovak Republic*

ABSTRACT

Bee pollen is a perspective product of beekeeping successfully used as food supplements. Bee pollen and honeycomb pollen (perga) are sources of many biologically active and nutritive compounds. Discrimination of these materials according to their botanic origin is necessary to evaluate their quality and possible applications. Diffuse reflectance VIS spectroscopy was applied to analysis of 7 samples of monofloral bee pollen and 2 samples of honeycomb pollen of unknown origin. The spectra were used for calculation of CIE Lab colour parameters. Classification of the samples was based on multivariate analysis of the spectra. CIE Lab diagram, HCA dendrogram and PCA score plot led to separation of the samples according to their difference in pigmentation. FTIR spectra of the samples illustrate differences in composition and heterogeneity of some bee pollens. Microscopic image analysis of pollen granules demonstrated evident variability in size, morphology and colour depending on the botanical origin. Differently coloured granules or pollen grains on their surface may be explained by some heterogeneity in botanical composition. Spectroscopic (Vis, FTIR) and microscopic methods confirmed to be effective screening method for pollen analysis.

Keywords: bee and honeycomb pollen, morphology, colour, discrimination analysis, diffuse reflectance VIS spectroscopy, FTIR, microscopic image analysis

1 INTRODUCTION

Bee pollen and honeycomb pollen (perga) are important beekeeping products. They are mixtures of flower pollen grains and nectar with bee excreta; the latter one underwent fermentation inside honeycombs. There bee products are characterised as the source of many bioactive and nutrient compounds, i.e., free amino acids, proteins, fats, fatty acids, mono- and polysaccharides, antioxidants, vitamins, pigments, etc. Monofloral bee pollens of specific botanical origin should have similar chemical composition. By contrast, polyfloral samples containing pollen material from different sources commonly have variable composition depending of the ratio between the botanical sources. It is important to identify bee pollen and honeycomb pollen samples, discriminate them from each other and evaluate their origin and composition. Diffuse reflectance Vis and FTIR spectroscopy has been earlier applied to discrimination of bee pollens based on colour and chemical composition [1] and in analysis of sunflower pollen grains and bee pollen [2]. These methods do not need complex sample preparation and thus exclude destructive factors like chemical and thermal degradation, migration of components during extraction and purification etc. Microscopic image analysis possesses information about the size, morphology and colour of bee pollen granules and thus could be also used for discrimination of bee pollens. The aim of this work is evaluation of these methods for analysis of bee pollen and honeycomb pollen samples.

2 EXPERIMENTAL

2.1 Samples

Samples of bee and honeycomb pollen of different botanical origin were obtained from various localities of Slovak Republic (Fig. 1). Sample specification is summarised in Table 1.

Table 1: Specification of bee pollen and honeycomb pollen samples

Samples	Botanical origin
bee pollen	sunflower (*Heliathus annuus L.*)
	black locust (*Robinia pseudacacia*)
	rape (*Brassica napus L. var. napus*)
	opium poppy (*Papaver somniferum*)
	lacy phacelia (*Phacelia tanacetifolia*)
	white clover (*Trifolium repens* L.)
	willow general (*Salix caprea*)
honeycomb pollen	unknown (2 samples – perga, perga amorpha)

Fig. 1. : Samples of bee pollen and honeycomb pollen (perga).

2.2 FTIR spectroscopy

FTIR absorption spectra (range 400–4000 cm^{-1}, 64 scans, resolution 2 cm^{-1}) were recorded on FTIR spectrometer Nicolet 6700 (Thermo Scientific, USA) in KBr tablets. All the spectra were exported to Origin 6.0 (Microcal Origin, USA) software for further processing (smoothing, baseline correction) and preparation of the graphs.

2.3 Diffuse reflectance Vis spectroscopy

Diffuse reflectance Vis spectra (range 380–800 nm, 10 scans, slot width 4 nm, speed of scanning 240 nm min^{-1}, data interval 2 nm) were recorded on double beam UV-Vis spectrophotometer UV4 (UNICAM, Great Britain) using diffuse reflectance accessory (Labsphere, USA) and Vision 3.0 software (UNICAM, Great Britain). All the spectra were exported to a spreadsheet format for further processing (smoothing, baseline correction) using software Origin 6.0 (Microcal Origin, USA) and Excel 2007 (Microsoft, USA).

2.4 Microscopic image analysis

Microscopic image analysis of 7 monofloral bee pollens (granules) was made using light microscopes. Image analysis of bee pollen and flower samples was performed at the Institute of Physics and Measurement Technology (ICT Prague), laboratory of image analysis. Microscope Nicon Eclipse (Nicon, Japan) and Zeiss stereomicroscope (Zeiss, Federal Republic of Germany), which are equipped with digital cameras, digital images were prepared masks and pollen grains.

3 RESULTS AND DISCUSSION

Normalised diffuse reflectance Vis spectra of bee and honeycomb pollen samples are shown at Fig. 2. Spectral differences reflect some variability in the composition of these pollens. The spectra have broad absorption bands, which have positions depending on the botanical origin of corresponding pollens and the composition and structure of the chromophors. The absorption peak of sunflower bee pollen at 480 nm belongs to carotenoids, and the peak of lacy phacelia bee pollen has the main part between 550–600 nm that belongs to blue flavonoids. In some bee and honeycomb pollens, however, these two classes of pigments can be present together.

Table 2: SIE Lab parameters for bee pollen and honeycomb pollen samples

Samples	L*	a*	b*
sunflower bee pollen	92.01	2.59	1.38
black locust bee pollen	93.61	1.52	2.68
rape bee pollen	93.46	1.28	2.12
opium poppy bee pollen	91.88	1.01	-0.08
lacy phacelia bee pollen	90.57	-0.10	-2.88
white clover bee pollen	91.56	1.09	0.08
willow general bee pollen	92.43	1.20	1.61
honeycomb pollen (perga)	92.09	1.63	1,32
honeycomb pollen (perga amorpha)	92.64	1.06	1.27

CIE Lab hue diagram for the samples is shown in Fig. 3. The CIE Lab parameters calculated from the diffuse reflectance Vis spectra are summarised in Table 2. The plot {a*, b*} demonstrates the discrimination of the pollen samples according to their colour. The basic colours are yellow and yellowish orange, and the main cluster is situated in the area of yellow-orange hues. However, some samples have different colours: reddish orange (sunflower), brownish (white clover, opium poppy) and even blue (lacy phacelia). The L* values of pollen samples (90.6 – 93.6 %) describe the brightness of measured samples dividing them from light to dark. The samples of honeycomb pollen (perga, perga amorpha) showed significant differences in the spectra and in the colour parameters that can be explained by dissimilar botanical origin.

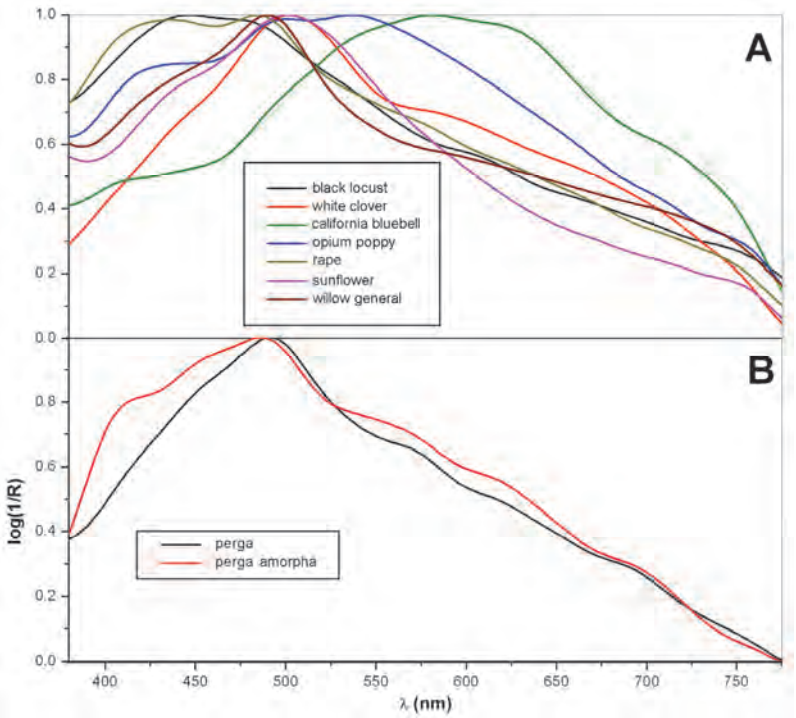

Fig. 2. : Normalised diffuse reflectance Vis spectra of bee pollen (A) and honeycomb pollen (B) samples.

FTIR spectra of bee and honeycomb pollen samples are shown in Fig. 4. Spectral differences reflect variability in the composition of pollen samples as well as of bee pollen granules of the same origin. Band assignment is complicated because of overlapping. Strong absorption in the regions of 3500–3100 cm^{-1} (OH stretching), 3100–2800 cm^{-1} (CH stretching), 1800–1500 cm^{-1} (C=O and C=C stretching) and 1200–950 cm^{-1} (CO and CC stretching) are characteristic for main constituent biopolymers (proteins, polysaccharides). The shoulders near 3200 cm^{-1} (amide A) and 3100 cm^{-1} (amide B) as well as intense peaks at 1660 cm^{-1} (amide I) and 1545 cm^{-1} (amide II) confirmed the presence of proteins [3]. The bands at 781, 818, 870, 1059 a 1151 cm^{-1} are typical for amorphous fructose originated from nectar [4].

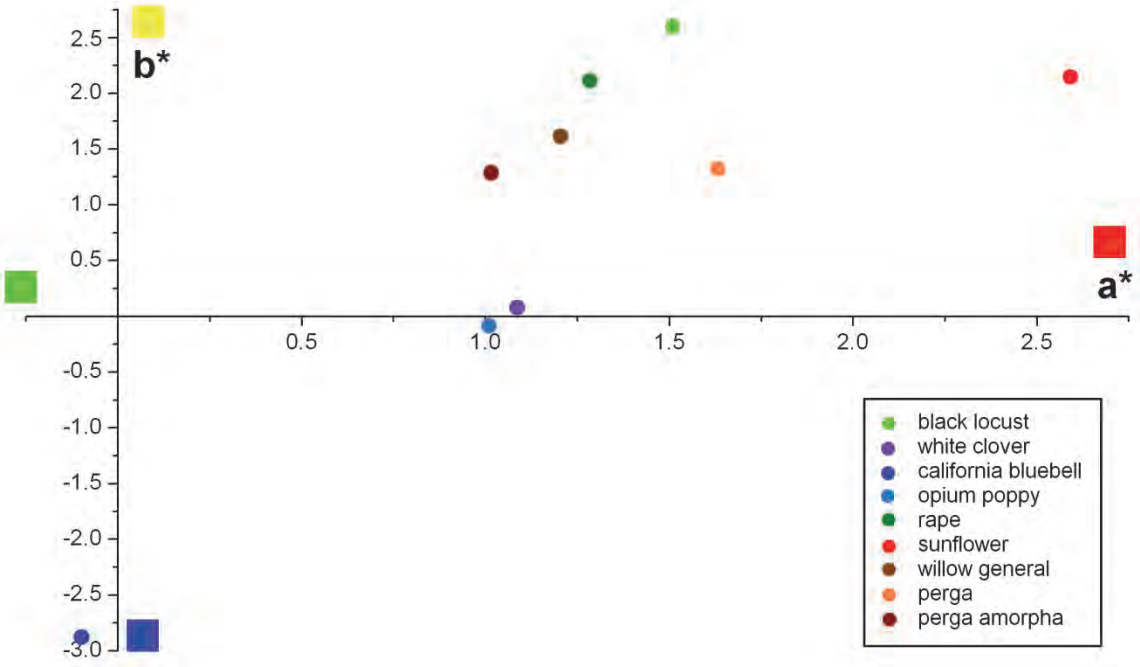

Fig. 3. : CIE Lab hue diagram for bee pollen and honeycomb pollen samples.

Microscopic images of selected bee pollen granules are shown in Fig. 5. The samples demonstrated evident variability in colour depending on the botanical origin. Differently coloured granules or pollen grains on their surface may be explained by some heterogeneity in botanical composition. There is an evident difference in colour and morphology between the granules of the same botanical origin. For example, the colour of opium poppy bee pollen granules varied from yellow to redish brown; the shape and size of the granules varied as well. Similarly, bee pollen samples originated from sunflower and willow general and other sources demonstrate high morphological and colour variability. The differences in colour of monofloral bee pollens can be explained by variable pigment composition and distribution during the maturation of pollen grains. However, the presence of admixtures from other botanical sources is also possible.

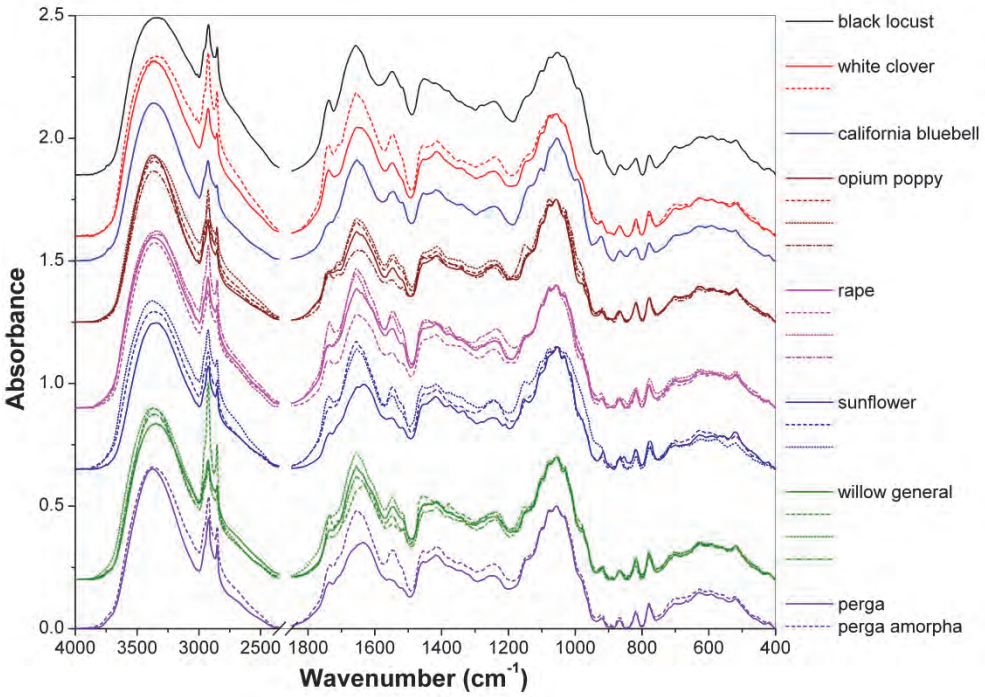

Fig. 4. : FTIR spectra of bee pollen and honeycomb pollen samples: variability for bee pollen granules.

4 CONCLUSIONS

Spectroscopic (FTIR, diffuse reflectance Vis) and microscopic methods are sensitive to structure and composition of bee pollen and honeycomb pollen samples. FTIR confirmed the presence of proteins, polysaccharides and nectar fructose in bee pollen. Diffuse reflectance Vis spectra and CIE L*a*b* parameters calculated from these spectra was used for discrimination of the samples according to their colour. Microscopic image analysis and FTIR confirmed marked variability in composition of bee pollen samples that correlated with colour variability.

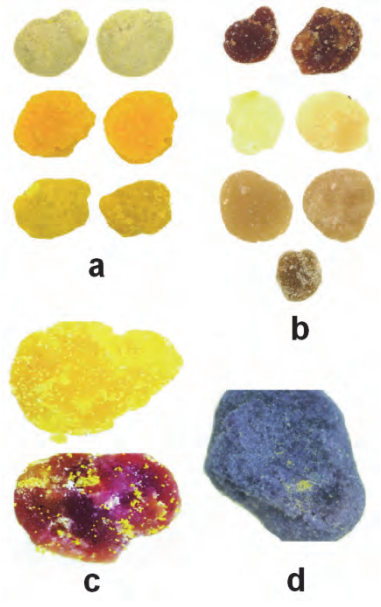

Fig. 5. : Microscopic images of bee pollen granules: a – willow general, b – opium poppy, c – sunflower, d – california bluebell).

ACKNOWLEDGEMENTS

This work was supported by the Ministry of Education, Youth and Sport of the Czech Republic (projects No CEZ: MSM6046137305)

LITERATURE

[1.] Synytsya, An., Synytsya, Al., Bleha, R., Gróf, J., *et al*., *Potravinárstvo* 2010, *4* (special issue), 236-245.
[2.] Synytsya, An., Synytsya, Al., Bleha, R., Brindza, J., *et al*., (2011) *Potravinárstvo* 2011, *5* (special issue), 308-313.
[3.] Barth, A. *Biochimica et Biophysica Acta* 2007, *1767*, 1073-1101.
[4.] Ibrahim, M., Alaam, M., El-Haes, H., Jalbout, A. F., et al., *Eclétic Química* (São Paulo) 2006, *31*, 15-21.

PREDICTION OF ELECTROMIGRATION DISPERSION IN ELECTROPHORETICAL SYSTEMS WITH COMPLEXATION AGENTS

Martin Beneš, Jana Svobodová, Vlastimil Hruška, Iva Zusková, Bohuslav Gaš

Department of Physical and Macromolecular Chemistry, Faculty of Science, Charles University in Prague, Prague, Czech Republic, benes2@natur.cuni.cz

ABSTRACT

Electromigration dispersion (EMD) is a common problem in the electromigration separation methods. The dispersion of the analyte peak can significantly lower the resolution or even disable the separation. There are several computational programs enabling the prediction of EMD in non-complexing separation systems, but the model for systems with complexation agents is still missing.
Therefore, we present the complete theory of EMD in electrophoretical systems with fully charged analytes and neutral complexation agents. This theory was implemented into the newest version of our simulation program PeakMaster 5.3. Thus, we are able to calculate the relative velocity slope S_x, which is usually used as a measure of EMD. The established theory was tested by both experiments and simulations, which were performed by our simulation program Simul 5 Complex, using 3 different chiral separation systems. The values of relative velocity slopes were calculated from both experimental and simulated data and compared with those predicted by PeakMaster 5.3 Complex. The perfect agreement of the data was achieved. The obtained results were also used to explain the development of EMD in systems with complexing agents. As a result, we propose a way to avoid EMD, get sharp and symmetrical analyte peaks, and thus, maximize resolution.

Keywords: Electrophoresis, Complex-forming equilibria, PeakMaster 5.3 Complex

1 INTRODUCTION

The quantities $S_{EMD,A}$ (nonlinear mobility slope of the analyte zone) and S_X (relative velocity slope) were chosen as the most suitable parameters to compare the extent of electromigration dispersion in systems that contained a complex-forming agent. $S_{EMD,A}$ can be calculated from the experimental or simulated data according to Eq.1,

$$S_{\mathrm{EMD,A}} = \frac{u_{\mathrm{MAX,A}} - u_{\mathrm{eff,A}}}{c_{\mathrm{A}}}$$

where $u_{MAX,A}$ is the mobility of an analyte determined from the peak maximum, $u_{eff,A}$ is the effective mobility of the analyte determined from the peak center at infinitely low analyte concentration (determined by fitting the peak with the HVL function[1]) and c_A is the actual analyte concentration in sample zone. Since the analyte concentration in the sample zone is influenced by both diffusion and electromigration dispersion, its value is changing during each experimental and simulated run. That is why we roughly approximate this concentration by the actual analyte concentration at the apex of the analyte peak.
S_X can be calculated from $S_{EMD,A}$ according to Eq.2,

$$S_X = \frac{1}{2}\frac{S_{EMD,A}\kappa_0}{\mu_{eff,A}}$$

where κ_0 is the conductivity of the BGE.

The mathematical model of electromigration dispersion in electrophoretic systems that contain a neutral complexing agent and a strong electrolyte analyte [2] was implemented in the last version of PeakMaster 5.3 [3]. PeakMaster 5.3 Complex yields the values for both $S_{EMD,A}$ and S_X of the analyte. The necessary input data are the experimental conditions, the constituent parameters (dissociation constant, limiting mobility) and the complexation parameters (complexation constant and mobility of the complex). The new version of PeakMaster 5.3 Complex is also able to plot the dependence of $S_{EMD,A}$ or S_X on the cyclodextrin concentration, which can be advantageously used to choose the best separation conditions that maintain electromigration dispersion low and yield sharp, narrow analyte peaks while using the minimum concentration of the complexing agent.
The established theory as well as the new version of PeakMaster 5.3 Complex were verified experimentally and by simulations using the simulation program Simul 5 Complex [4]. The experimental separation systems used for the verification process differed in the choice of the neutral complexing agent, while the same analyte R-flurbiprofen (fully charged at the actual pH of the BGE and at the actual ionic strength of the BGE having an effective mobility in the non-complexing environment equal to -19.81×10^{-9} $m^2V^{-1}s^{-1}$) was used. The neutral complexing agents were selected to provide different complexation constants with the R-flurbiprofen analyte. The complexation constants and the mobilities of the complexes were determined by affinity capillary electrophoresis (ACE) experiments [5].The resulting complexation parameters are summarized in Table 1.

Table 1: Complexation constants and mobilities of the complexes. Analyte: R-flurbiprofen (mobility of the free analyte at the actual ionic strength u_A^0 = 19.81×10^{-9} $m^2V^{-1}s^{-1}$, limiting mobility 24.5×10^{-9} $m^2V^{-1}s^{-1}$). Complexing agent – Example 1: heptakis(2,6-di-*O*-methyl)-β-cyclodextrin, Example 2: heptakis(2,3,6-tri-*O*-methyl)-β-cyclodextrin.

	Example 1	Example 2
K / mol^{-1} dm^3	4 800	552
u_X / 10^{-9} $m^2V^{-1}s^{-1}$	7.54	6.5

The complexation constants and the complex mobilities were used as the input data for the simulations of the experimental runs. Finally, the $S_{EMD,A}$ and S_X values of the analyte were calculated for each experimental and simulated run according to the Eqs. (1) and (2) and compared with those calculated by PeakMaster 5.3 Complex.

2 COMPARISON OF EMD PREDICTED BY PEAKMASTER WITH THE SIMULATED AND THE EXPERIMENTALLY OBTAINED DATA

c/mM	0	0.1	0.2	0.5	2	10	100		0	0.1	0.2	0.5	2	10	100
	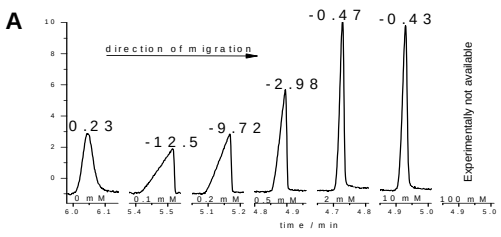								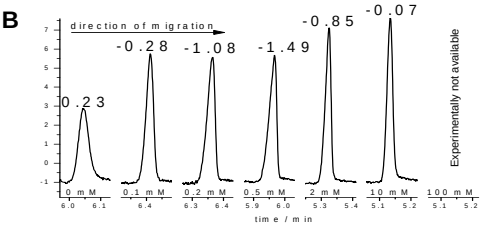						
	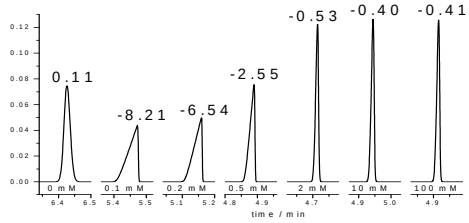								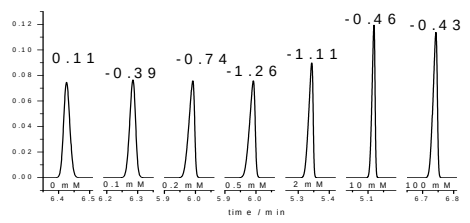						
$S_{EMD,A}$	0.11	-9.25	-7.02	-2.64	-0.51	-0.41	-0.41		0.11	-0.39	-0.74	-1.26	-1.11	-0.46	-0.43

Fig. 1: Comparison of the experimental (upper panels) and simulated (lower panels) electropherograms for A: Example 1, B: Example 2 and values calculated by PeakMaster 5.3 Complex.

The experimental analyte peaks and those simulated by Simul 5 Complex are shown in Figure 1. They are in almost perfect agreement as regards position, peak shape and amplitude. Values of $S_{EMD,A}$ and S_X were calculated using PeakMaster 5.3 Complex with the implemented complexation mode as well as from the experimental and the simulated detector traces. The $S_{EMD,A}$ and S_X values obtained by PeakMaster 5.3 Complex agree very well with those calculated from the simulated electropherograms for all three chiral selector systems. Though the values determined from the experimental electropherograms slightly differ from the values obtained by either PeakMaster 5.3 or the simulations, they follow the same trends. The differences between the experimental and the simulated/calculated data can be explained by realizing that the exact concentration of the analyte in the analyte zone is not known in the experiments and it can only be roughly approximated from the simulations as described above.

3 INFLUENCE OF COMPLEXATION ON EMD

In Example 1 the complexation constant is very high. The corresponding experimental and simulated analyte peak shapes are shown in Figure 1A. Obviously, the peak shape changes significantly with the cyclodextrin concentration. In the cyclodextrin-free BGE, the analyte peak has an almost Gaussian profile. However, at a chiral selector concentration of 0.1 mM, the analyte peak is suddenly significantly influenced by electromigration dispersion. Thus, the resulting analyte peak is small and strongly tailing. Interestingly, by increasing the concentration of the cyclodextrin in the BGE the value of $S_{EMD,A}$ decreases: at a cyclodextrin concentration of 2 mM and higher, the analyte peaks become almost Gaussian again. At low cyclodextrin concentration, the amount of cyclodextrin present is not sufficient to “saturate” the complexation of the analyte with the cyclodextrin. The mole fraction of the complexed analyte strongly depends on the analyte concentration in the sample zone, and electromigration dispersion occurs. At – and above – 2 mM cyclodextrin concentration almost all analyte is complexed and the degree of complexation depends only slightly on the

concentration of analyte and electromigration dispersion is avoided. Obviously, observed EMD is result of complexation.

In Example 2, the complexation constant is about nine-times lower than in Example 1 (see Table 1). As shown in Figure 1B, the analyte peaks have almost Gaussian profiles, independently on the cyclodextrin concentration. Because of the low complexation constant, the mole fraction of the complexed analyte depends only slightly on the analyte concentration in a sample zone and causes insignificant EMD. The other result arising from the lower complexation constant value is that full complexation is achieved at a much higher cyclodextrin concentration, thus, the complexation contribution plays role over a wider cyclodextrin concentration range.

4 INFLUENCE OF THE COMPLEXATION CONSTANT AND THE MOBILITY OF THE COMPLEX ON EMD

The $S_{EMD,A}$ values are plotted in Figure 2A as a function of the concentration of the neutral complexing agent using the same complexation constant and free analyte mobility values (K = 4000 (mol dm^{-3})$^{-1}$, $u_A^0 = 19.81\times10^{-9}$ m^{2}V^{-1}s^{-1}), but five different mobilities of the complexed forms ranging from a high mobility of $u_X = 19.8\times10^{-9}$ m^{2}V^{-1}s^{-1} to a low mobility of $u_X = 1\times10^{-9}$ m^{2}V^{-1}s^{-1}. For each set of parameter combinations, the $S_{EMD,A}$ values go through a minimum as the cyclodextrin concentration is increased. The minima become sharper, their depth increases and the limiting $S_{EMD,A}$ values (observed at very high cyclodextrin concentrations) remain farther away from zero as the difference between u_A^0 and u_X increases from 0 to 18×10^{-9} m^{2}V^{-1}s^{-1}, leading to increased EMD and worsened peak shape across the entire cyclodextrin concentration range. However, the minima occur at the same cyclodextrin concentr ation irrespectively of the magnitude of the difference between u_A^0 and u_X.

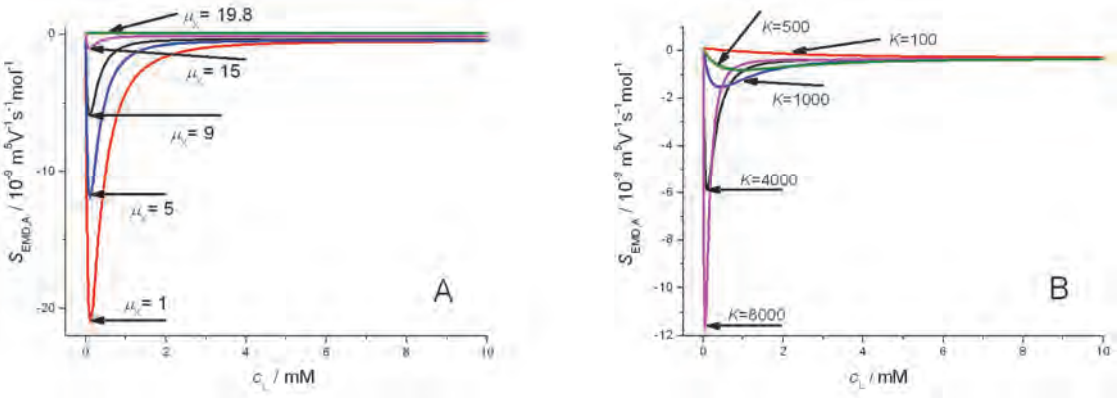

Fig. 2: Theoretical dependences of $S_{EMD,A}$ on cyclodextrin concentration in BGE for analyte R-flurbiprofen and different theoretical complexation agents. A) Complexation parameters: u_X= 1, 5, 9, 15 and 19.8×10^{-9} m^{2}V^{-1}s^{-1}, K = 4000 mol dm^{-3}. The curves are marked by the value of mobility of complex. B) Complexation parameters: $u_X=9\times10^{-9}$ m^{2}V^{-1}s^{-1}, K = 100, 500, 1000, 4000 and 8000 mol dm^{-3}. The curves are marked by the value of complexation constant.

The $S_{EMD,A}$ values are plotted in Figure 2B as a function of the cyclodextrin concentration using the same complex mobility and free analyte mobility values ($u_X= 8.82\times10^{-9}$ m^{2}V^{-1}s^{-1}, $u_A^0= 19.8\times10^{-9}$ m^{2}V^{-1}s^{-1}), but five different complexation constants ranging from a low K = 100 (mol dm^{-3})$^{-1}$ to a high K = 8000 (mol dm^{-3})$^{-1}$. Again, for each set of parameter combinations, the $S_{EMD,A}$ values go through a minimum as the cyclodextrin concentration is increased. As the K values increase from 500 to 8000 (mol dm^{-3})$^{-1}$ the minima occur at lower cyclodextrin concentrations, become sharper, their depth increases, and approach their limiting $S_{EMD,A}$ values (i.e., those observed at very high cyclodextrin concentrations) sooner (at lower

cyclodextrin concentrations). This means that though EMD is increased and peak shape is worsened as *K* becomes larger, the complexation induced distortion persists over a narrower cyclodextrin concentration range.

ACKNOWLEDGEMENTS

The Grant agency of Charles University, grant no. 323611, Grant Agency of the Czech Republic, grant No. P205/11/J043 and No. P208/10/0353 and the Ministry of Education, Youth and Sports of the Czech Republic, project Kontakt LH11018 are gratefully acknowledged for the financial support.

LITERATURE

[1.] Haarhoff, P.C., van der Linde, H.J., *Anal. Chem.,* 1966*, 38,* 573

[2.] Hruska, V., Svobodova, J., Benes, M., Gas, B., J. Chromatogr. A, 2012, http://dx.doi.org/10.1016/j.chroma.2012.06.086

[3.] Riesova, M., Hruska, V., Gas, B., *Electrophoresis,* 2012*, 33,* 931

[4.] Svobodova, J., Benes, M., Hruska, V., Uselova, K., Gas, B., *Electrophoresis*, 2012, *33*, 948

[5.] Rundlett, K.L., Armstrong, D.W., *Electrophoresis*, 2001, *22*, 1419

UNFORSEEN PHENOMENA IN CHIRAL SEPARATIONS IN CAPILLARY ELECTROPHORESIS

Jana Svobodová[a], Martin Beneš[a], Pavel Dubský[a], Gyula Vigh[b], Bohuslav Gaš[a]

[a] *Charles University in Prague, Faculty of Science, Department of Physical and Macromolecular Chemistry, Hlavova 8, Prague, Czech Republic, svobod.j@seznam.cz*

[b] *Department of Chemistry, Texas A&M University, College Station, Texas, USA*

ABSTRACT

Capillary electrophoresis is widely used separation technique, which is very well described theoretically. Existing theoretical models offer deep insight into electrophoretical separation and enable to predict the results of separation, and thus, to propose the best separation conditions. Recently, our group presented the complete theoretical model of electromigration for separation systems with complexation agents, which was implemented into our simulation program Simul 5 Complex. In this paper Simul 5 is verified for separation systems with weak electrolyte analytes and neutral chiral selectors. The simultaneous effect of complexation and dissociation is in the scope of interest. The results of the simulations are compared with theoretical predictions and experimental data found in literature. Very good capability of the model to predict otherwise unexpected phenomena such as electromigration dispersion or reversal of migration order of enantiomers is demonstrated.

Keywords: Capillary Zone Electrophoresis, Chiral Separations, Cyclodextrin

1 INTRODUCTION

Capillary zone electrophoresis (CZE) became a widely used technique for the separation of enantiomers because a wide variety of chiral selectors (most often cyclodextrins, CDs) can be applied to achieve fast separations. In 1992 Wren and Rowe derived an expression for effective mobility of enantiomer complexing with chiral selector[1]. Later Rawjee *et al.*

expressed the effective mobility as function of two variables, the pH and the chiral selector concentration of the BGE [2,3]. Simultaneously, they proposed selectivity[2,3] and resolution[4,5] as suitable object functions for optimization of separation conditions. However, the authors admit that numerical simulation is necessary to predict correctly the shape of analyte peaks, which might be influenced by nonlinear phenomena such as electromigration dispersion. Recently, the complete model of electromigration for separation systems with complexation agents was derived by Hruska *et al.*[6]. This model is applicable for any number of BGE constituents and analytes in any dissociation state, one ligand in any charge state. Stoichiometry 1:1 is assumed. It was implemented into our simulation program Simul 5 Complex, which enables to predict the results of chiral separation. Very good agreement between theoretical predictions and experiments was shown as regards positions, shapes and amplitudes of analyte peaks[7]. Simul 5 was shown to be powerful tool to predict and explain different phenomena connected with chiral separation in CE.

2 THEORY

Taking into account simultaneous acid-base and complexation equilibria following reaction scheme can be proposed for weak acid HA (whose enantiomers are HR or HS) (see Fig. 1). Individual equilibria are characterized by corresponding complexation constants. Based on this reaction scheme Rawjee and Vigh derived the expression for mobility of weak acid as function on concentration of chiral selector and oxonium cations as shown below[2,3]. u_A is the mobility of free analyte and u_{ACD} is mobility of the analyte-cyclodextrin complex. To find the optimal separation conditions authors utilized selectivity $A_{R/S}$ as suitable object function. Selectivity is defined as the ratio of effective mobilities of individual enantiomers.

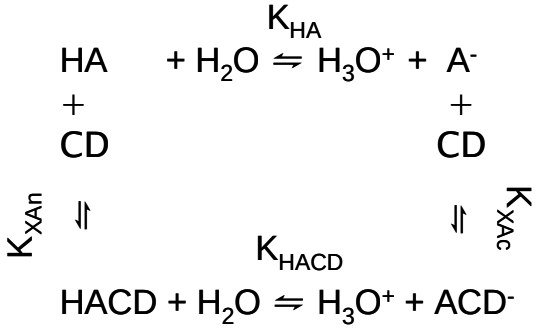

$$u_A^{eff} = u_A \frac{1 + \frac{u_{ACD}}{u_A} K_{XAc}[CD]}{1 + K_{XAc}[CD] + \frac{[H_3O^+]}{K_{HA}}(1 + K_{XAn}[CD])}$$

Fig. 1.: Reaction scheme for simultaneous dissociation and complexation of weak acid HA and cyclodextrin CD.

3 RESULTS AND DISCUSSION

Different separation systems were selected for evaluation of the established theoretical model. These separation systems differed in the choice of chiral selector, analyte and in complexation strength. The analytes were selected to cover all I (ibuprofen), II (model analyte), III (homatropine, dipeptide Ala-Tyr) type enantiomers according to Rawjee and Vigh discrimination[2,3], β-cyclodextrin was utilized as suitable chiral selector. Complexation parameters, which are necessary for simulations as well as for theoretical predictions, were found in literature[4,8].

The potentially best separation conditions were selected based on the 3D dependence of selectivity on cyclodextrin concentration and pH (as shown in **Fig. 2.**) and simulations were performed at these conditions. Very good agreement between selectivity values calculated theoretically and from simulated electrophoregrams was obtained. We were able to confirm the results of Rawjee, Staerk and Vigh[2] that Type I enantiomers, which differ only in complexation constants of not-dissociated form, can be separated only at the pH close to pKa at relatively low concentration of chiral selector. Simul 5 Complex is also able to cover the reversal of electromigration order with changing pH or concentration of complexation agent (see **Fig.3.**).

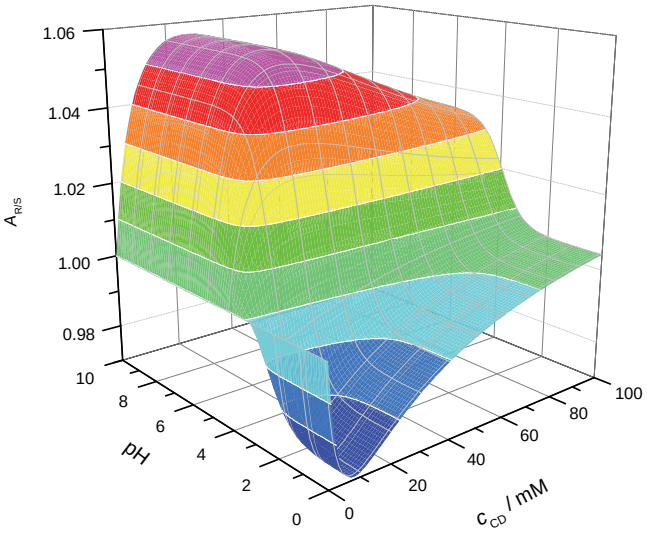

Fig. 2.: The 3D dependence of selectivity on concentration of cyclodextrin and pH of background electrolyte for analyte Ala-Tyr and β-cyclodextrin

Moreover, simulations were able to cover also additional phenomena as correct peak shape. The example of simulated electrophoregrams is demonstrated in Fig. 3. for analyte Ala-Tyr. Although the 3D dependence of selectivity on cyclodextrin concentration (see Fig. 2.) and pH suggests very good separation at pH 4.51, no separation was achieved at these conditions due to the strong electromigration dispersion of enantiomer peaks. Optimal separation was achieved at low pH and low concentration of cyclodextrin. Almost symmetrical peak shapes were obtained at these conditions, while at higher concentration of cyclodextrin and the same pH peaks were distorted by electromigration dispersion and not separated anymore. These results confirm the experimental observations obtained by Hammitzsch-Wiedemann and Scriba [8].

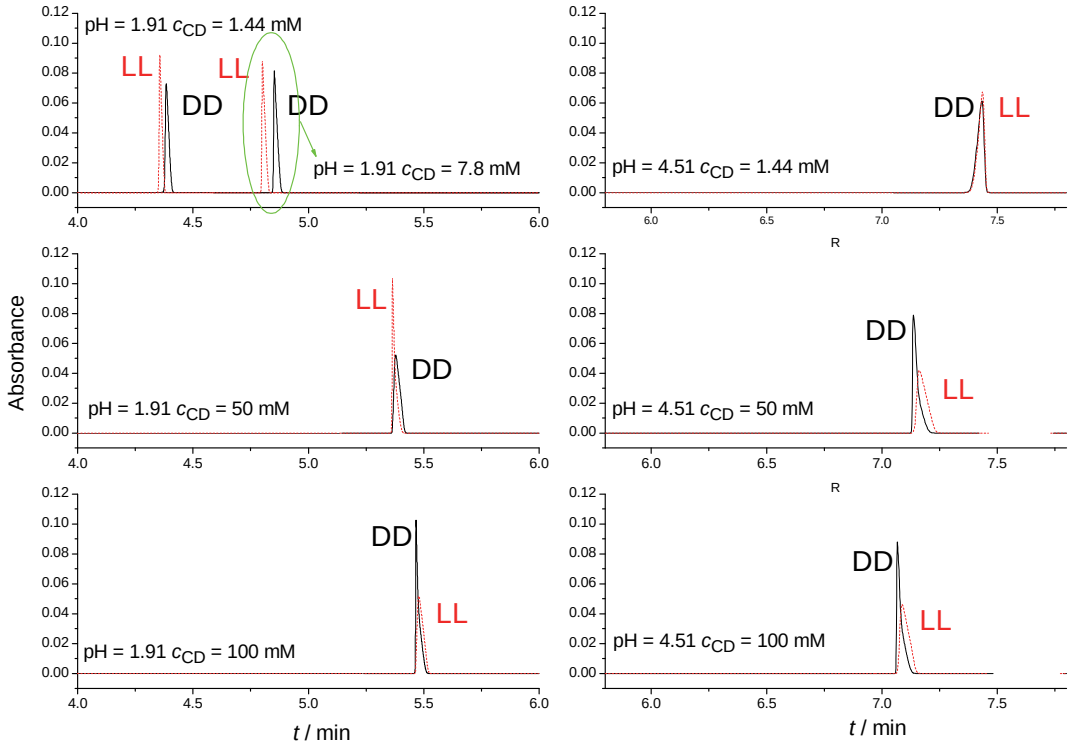

Fig.3.: Simulated electropherograms for enantiomers of dipeptide Ala-Tyr complexing with β-cyclodextrin. Individual electrophoregrams are designated by pH and cyclodextrin concentration. Solid black line: DD enantiomer; Red dashed line: LL enantiomer.

Simultaneously, we were able to show other unexpected phenomena that mobility of analyte can increase, decrease or be independent on concentration of neutral complexation agent. The increasing mobility of enantiomers with concentration of β-cyclodextrin is demonstrated in **Fig. 3**. at pH 4.51. This unforeseen phenomenon was further verified theoretically. If the condition $K_{XAc}|u_{ACD}| > K_{XAn}|u_A|$ is fulfilled, the certain pH exists, at which mobility of analyte does not depend on concentration of complexation agent. This pH can be calculated theoretically as shown in this equation.

$$pH = pK_A - \log\left(\frac{K_{XAc}|u_{ACD}| - K_{XAn}|u_A|}{K_{XAc}(|u_A| - |u_{ACD}|)}\right)$$

3 CONCLUSION

Simul 5 Complex was shown to be powerful tool to predict the results of chiral separation and to find optimal separation conditions. Very good agreement between theoretical and experimental results was obtained. Simultaneously, simulations showed otherwise unpredictable phenomena as electromigration order reversal of enantiomer peaks or influence of electromigration dispersion on separation. Electromigration dispersion caused by complexation might significantly disturb chiral separation.

ACKNOWLEDGEMENTS

The support by the Grant Agency of the Czech Republic, grant no. 203/08/1428 and grant no. P206/12/P630, Grant Agency of Charles University, grant no. 323611, project Kontakt LH11018 and the long-term research plan of the Ministry of Education of the

Czech Republic (MSM0021620857), as well as the TAMU Gradipore Chair in Separation Science Endowment are gratefully acknowledged.

LITERATURE

[1.] Wren, S. A. C., Rowe, R. C., J Chromatogr. A 1992, 603, 235-241.
[2.] Rawjee, Y. Y., Staerk, D. U., Vigh, G., J Chromatogr. 1993, 635, 291-306.
[3.] Rawjee, Y. Y., Williams, R. L., Vigh, G., J Chromatogr. A 1993, 652, 233-245.
[4.] Rawjee, Y. Y., Williams, R. L., Vigh, G, J Chromatogr A 1994, 680, 599-607.
[5.] Rawjee, Y. Y., Vigh, G., Anal Chem 1994, 66, 619-627.
[6.] Hruska, V., Benes, M., Svobodova, J., Zuskova, I., Gas B, Electrophoresis 2012, 33, 938-947.
[7.] Svobodova, J., Benes, M., Hruska, V., Uselova, K., Gas B, Electrophoresis 2012, 33, 948-957.
[8.] Hammitzsch-Wiedemann, M., Scriba G. K. E., Anal Chem 2009, 81, 8765-8773.

CHEMICALLY MODIFIED C SILICA-BASED COLUMNS: UNIVERSAL STATIONARY PHASES FOR HPLC SEPARATIONS

Jan Soukup, Pavel Jandera

Department of Analytical Chemistry, Studentská 95, 532 10 Pardubice, Czech Republic,
jan.soukup@upce.cz

ABSTRACT

We tested the retention of phenolic acids in full mobile phase (acetonitrile/water containing buffer) composition range on two chemically modified hydrosilated (C silica-based) columns in order to show versatility of those stationary phases. Cogent UDC cholesterol™ and Cogent bidentate C18™ columns show significant dual reversed-phase/normal-phase retention behavior, hence those stationary phases can be used both in aqueous normal-phase (ANP) and in reversed-phase (RP) modes. The effect of the aqueous acetate buffer concentration on retention factors of phenolic acids over the full mobile phase composition range, including both ANP and RP mechanisms, can be described by a four-parameter equation for dual-retention mechanism.

Keywords: C silica-based stationary phases, aqueous normal-phase LC, dual retention mechanism.

1 INTRODUCTION

The aqueous normal-phase LC mode (ANPLC) (sometimes called “Hydrophilic Liquid Chromatography”, HILIC) uses polar stationary phases in combination with mobile phases containing high concentrations of organic solvents (usually acetonitrile) in water, often with a buffer additive [1]. In the past years, ANP technique has attracted attention as perspective complementary alternative to reversed-phase HPLC for separations of polar compounds, which still represent challenging problem [2-4]. Particularly interesting are HILIC applications for the analysis of small polar compounds [5,6].

C silica (hydrosilated silica gel) was introduced many years ago. However, its interesting chromatographic properties have only recently found increasing use. The hydrosilation process changes significantly the properties of the silica gel surface by substituting up to 95% of original silanol (Si–O–H) groups from the surface of the adsorbent by less polar silica hydride (Si–H) groups [7]. C silica-based material is suitable for normal phase liquid

chromatography with organic mobile phases, but its main application range lies in aqueous normal phase liquid chromatography [8]. The un-modified silica hydride shows very low hydrophobicity hence very low retention under reversed-phase conditions [9]. A suitable chemical modification of silica hydride, e.g. depositing of carbon on the surface (diamond hydride), or the attachment of non-polar ligands, such as C18, C8 or cholesteryl providing selective properties for separation of polar compounds, enhances the hydrophobicity of the stationary phase, which leads to significant increase of the retention in highly aqueous mobile phases.

In normal-phase chromatography (NP), the retention increases with increasing sample polarity. The mobile phase affects significantly the retention in LC and in classical non-aqueous adsorption NP chromatography the retention decreases as the concentration of a polar solvent with high elution strength increases in binary organic mobile phases. Likely, at high concentrations of the organic solvent in the HILIC mobile phase range, the retention on polar stationary phases decreases at increasing concentration of water as the more polar solvent in aqueous–organic mobile phases. On the same polar column, the retention may decrease for more polar samples and at increasing concentrations of organic solvent in highly aqueous binary mobile phases, showing typical RP behavior. Consequently, the graphs displaying the effects of the composition of aqueous–organic mobile phases on the retention show characteristic “U shape”. Assuming additivity of the HILIC and RP contributions to the retention, the effect of the volume fraction of water (or of an aqueous buffer), φ_{H2O}, on the retention factors, k, in the full composition range of aqueous–organic mobile phases can be described by Eq. (1):

$$\log k = a_2 + m_{RP} \cdot \varphi_{H2O} - m_{HILIC} \cdot \log(1 + b \cdot \varphi_{H2O}) \qquad (1)$$

The parameter m_{HILIC} characterizes the effect of the aqueous component on the rate of decreasing HILIC contribution to the retention in highly organic mobile phases, while the parameter m_{RP} describes its effect on the rate of increasing contribution of the RP mechanism to the retention in the aqueous-rich mobile phases; a_2 is an empirical constant and has no exact physical meaning and the parameter b is the correction term for limited HILIC retention in mobile phases with very low concentrations of water.

2 EXPERIMENTAL

All the experiments were measured using an HPLC setup including a high pressure pump (ECOM, Prague, Czech Republic) connected with a variable UV detector from the same manufacturer. The columns were placed in a thermostatted column compartment and the detection wavelength was set to 275 nm, the UV absorption maximum for flavones.

2.1 Materials and Reagents

The characteristics of the Cogent C silica columns (all from MicroSolv, Eatontown, NJ, USA), are listed in **Table 1**.

Table 1: Characteristics of Cogent C silica columns.

Column	*L* [mm]	*Id* [mm]	V_M [mL]	t_{MAX} [°C]	ε_T	*pH range*
Cogent UDC cholesterol™	75	4.6	0.80	100	0.64	2.0 – 8.0
Cogent Bidentate C18™	75	4.6	0.80	100	0.64	2.0 – 9.2

Table 2: List of phenolic the acid standards.

Phenolic acid	Number	Abbreviation	Purity [%]	Mr [g/mol]
salicylic	1	SAL	98	138.13
coumaric	2	COU	98	164.17
p-hydroxybenzoic	3	PHB	99	138.12
ferulic	4	FER	98	194.20
vanillic	5	VAN	97	168.16
sinapic	6	SIN	98	224.23
syringic	7	SYR	98	198.19
4-hydroxyphenylacetic	8	HPA	98	152.16
protokatechuic	9	PRO	98	154.13
caffeic	10	CAF	97	180.17
gallic	11	GAL	98	170.00
chlorogenic	12	CLG	97	354.34

The standards of phenolic acids (**Table 2**) were purchased from Sigma–Aldrich in the best available purity. Acetonitrile (LiChrosolv grade), ammonium acetate and formic acid (both reagent grade) were obtained from Merck, Darmstadt, Germany. Water was purified using a Milli-Q water purification system (Millipore, Bedford, MA, USA).

2.2 Methods

The mobile phases were prepared by mixing appropriate volumes of 10 mmol/L solution of ammonium acetate (with pH adjusted to 3.26 by formic acid) in water with 10 mmol/L solution of ammonium acetate in acetonitrile. The stock solutions of flavonoid standards were prepared in 95% aqueous acetonitrile and working solutions were obtained by diluting the stock solutions in the mobile phase. The column hold-up volume, V_M, was determined as the elution volume of toluene in the pure acetonitrile as the mobile phase. Before each new series of experiments, the columns were equilibrated by flushing with 20 column hold-up volumes of the fresh mobile phase and the separation temperature was adjusted. The retention times, t_R, were measured over the full composition range of the mobile phases containing 10 mmol/L ammonium acetate in aqueous acetonitrile. The measurements were repeated in triplicate and arithmetic means of the experimental retention times, t_R, and the appropriate column hold-up time, t_M, were used to calculate the retention factors, $k = t_R/t_M - 1$. The Adstat 1.25 software (Trilobyte Statistical Software, Pardubice, Czech Republic) was utilized for the determination of the parameters of Eq. (1) by non-linear regression of the experimental data sets.

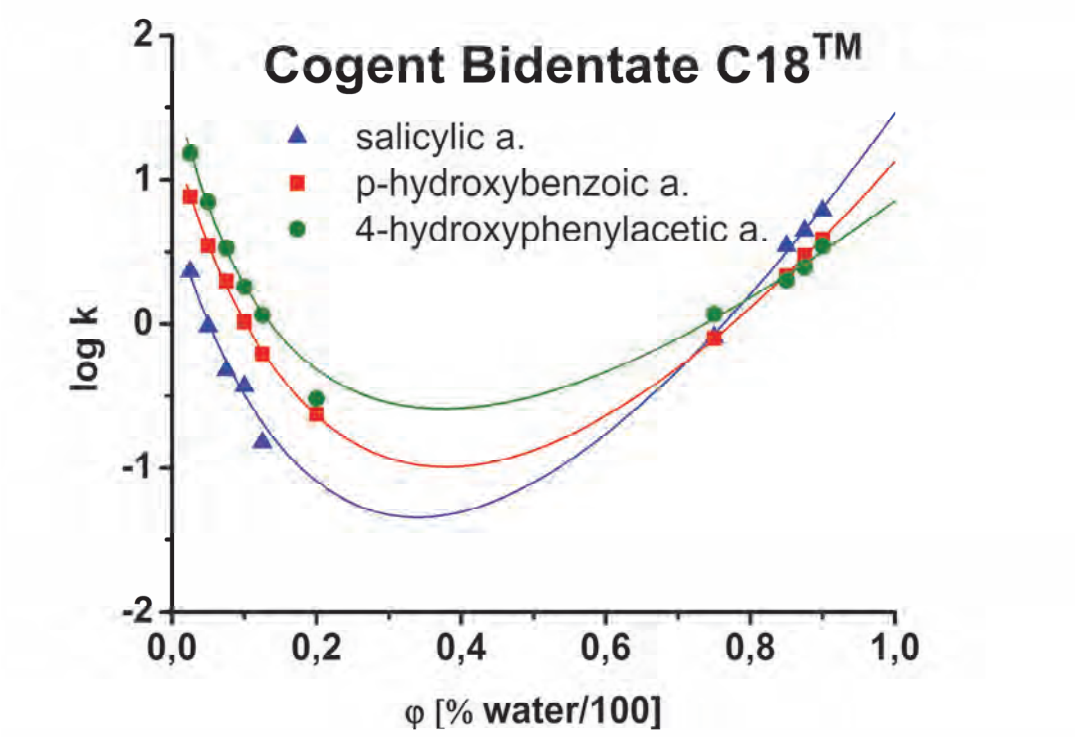

Fig. 1.: Effects of the volume fraction of aqueous buffer (10 mM ammonium acetate, pH 3.26), φ (10^{-2} vol.%), on the retention factors, k, of phenolic acids. Temperature 40 ◦C; flow rate, F_m = 0.5 mL·min^{-1}; sample volume 10 µL. Points: experimental data, lines: best-fit plots of Eq. (1).

3 RESULTS AND DISCUSION

Both tested columns can be used for aqueous normal-phase (ANP) separations of less polar phenolic acids with a single phenolic –OH group in mobile phases containing more than 85% acetonitrile. Protocatechuic, caffeic, gallic and chlorogenic acids with 2 or 3 phenolic groups (Nos. 9, 10, 11 and 12 in Fig. 2) are too strongly retained in the HILIC mode and show very asymmetric peaks. The peak symmetry did not improve significantly when changing the pH of the mobile phase, or when varying the ammonium acetate buffer ionic strength in between 5 mmol/L and 20 mmol/L. We used the columns also at the upper temperature limits indicated in the manufacturer's literature and we did not observe any separation deterioration over the two-months working period.

The hydrosilated silica modified with non-polar ligands has more hydrophobic surface and consequently significantly enhanced retention in the RP mode. We observed that the retention factors, k, of all phenolic acids increase at decreasing concentration of the aqueous ammonium acetate buffer in the organic-rich ANP mobile phases and increase in highly aqueous mobile phases (RP mode) and that the experimental data show characteristic U-shape plots of retention factors versus the concentration of aqueous buffer in the mobile phase, φ, on two modified hydrosilated silica columns: C18 bidentate and UDC cholesterol. As shown in example in (**Fig. 1**), phenolic acids are retained on the bidentate column in highly aqueous (RP mode) and even in highly organic (ANP mode) mobile phases; hence those two different modes can be used to separate the phenolic acids. Cholesterol column tested shows identical behavior as bidentate column but provides better resolution and selectivity in ANP and also in RP mode which document chromatograms in **Fig. 2**.

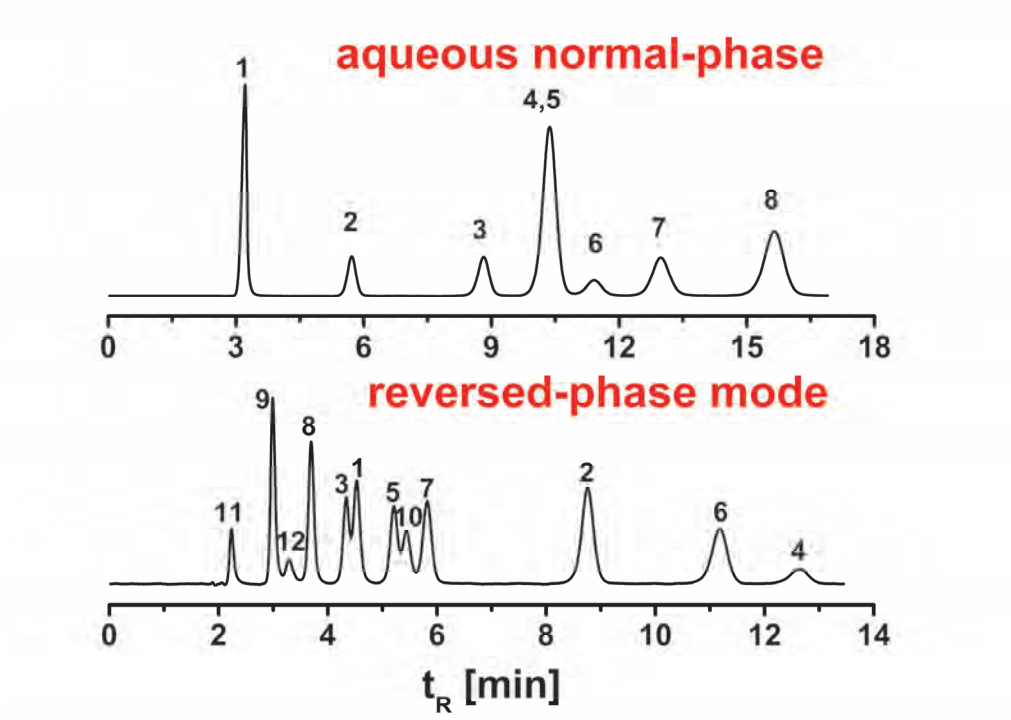

Fig. 2.: Separations of the phenolic acids in the ANP and RP modes on cholesterol column. Experimental Conditions: ANP mobile phase – 10 mM ammonium acetate in 5/95 water/acetonitrile (water acidified with formic acid to pH 3.26), RP mobile phase – 10 mM ammonium acetate in 85/15 water/acetonitrile (water acidified with formic acid to pH 3.26) Temperature 40°C; flow rate, F_m = 0.5 mL·min^{-1}; sample volume 10 µL. Numbers in chromatograms belong to phenolic acids in **Table 2**.

The four-parameter Eq. (1) fits the experimental retention data over the broad composition range of the mobile phase, including the low φ HILIC range and the high φ RP range (full lines in Fig. 1). **Table 3** lists the best-fit parameters a, m_{HILIC}, m_{RP} and b of Eq. (2). High values of the multiple correlation coefficients, R^2, and relatively low standard deviations of the parameters demonstrate good validity of Eq. (1) to describe the dual HILIC/RP retention model for phenolic acids on hydrosilated silica columns.

Table 2: Best-fit parameters a, m_{RP}, m_{HILIC} and b of Eq. (1) on hydrosilated columns. R^2: multiple correlation coefficients. The abbreviations of phenolic acids are as in Fig. 2.

Cogent UDC cholesterol™						Cogent bidentate C18™				
Phen. acid	a_2	m_{RP}	m_{HILIC}	b	R^2	a_2	m_{RP}	m_{HILIC}	b	R^2
SAL	3.46	8.33	5.73	78.42	98.83	0.72	13.12	18.35	3.72	99.24
COU	1.14	6.94	6.15	11.42	97.55	1.01	10.15	19.27	3.14	99.22
PHB	2.05	7.10	6.68	17.32	98.43	1.28	11.14	16.01	4.09	99.81
FER	2.12	7.29	6.24	18.82	98.31	1.26	23.86	57.72	1.51	99.94
VAN	2.09	6.30	5.75	20.00	98.66	1.30	13.31	22.29	2.96	99.90
SIN	1.97	8.33	7.82	12.56	98.14	1.30	29.86	88.07	11.35	99.96
SYR	2.01	7.62	7.70	12.40	98.56	1.47	18.40	37.26	2.11	99.92
HPA	2.31	6.63	6.87	15.59	99.04	1.71	6.43	7.10	9.61	99.43

ACKNOWLEDGEMENTS

This work was financially supported by the project Enhancement of R&D Pools of Excellence at the University of Pardubice reg. Nr. CZ.1.07/2.3.00/30.0021.

LITERATURE

[1.] Alpert, A.J., *Journal of Chromatography* 1990, *449*, 177-196.
[2.] Hemström, P., Irgum, K., *Journal of Separation Science* 2006, *29*, 1784-1821.
[3.] Jandera, P., *Journal of Separation Science* 2008, *31*, 1421-1437.
[4.] Jandera, P., Analitica Chimica Acta 2011, *692*, 1-25.
[5.] Soukup, J., Jandera, P., *Journal of Chromatography A* 2012, *1245*, 98–108.
[6.] Soukup, J., Jandera, P., *Journal of Chromatography A* 2012, *1228*, 125–134.
[7.] Sandoval, J.E., Pesek, J.J., *Analytical Chemistry* 1989, *61*, 2067-2075.
[8.] Pesek, J.J., Matyska, M.T., *Journal of Separation Science* 2009, *32*, 3999-4011.
[9.] Molikova, M., Jandera, P., *Journal of Separation Science* 2010, *33*, 453-463.

BELOUSOV-ZHABOTINSKY REACTION AS A GENERAL MODEL FOR THE DESCRIPTION OF COMPLEX SELF-ORGANIZING SYSTEMS

Anna Zhyrova, Dalibor Štys, Petr Císař and Tomáš Náhlík

School of Complex Systems, University of South Bohemia, Zámek 136, 373 33 Nové Hrady, Czech Republic, zhyrova@frov.jcu.cz

ABSTRACT

All biological systems ranging from organized herds to colonies of individual cells represent the self-organizing (SO) systems. Studying and modeling of these systems will allow us to predict their future behavior and interaction with other systems. In the selection of the appropriate model is more than half of successful for development of a new method analysis of complex systems whose behavior is difficult to predict the long-time evolution period. As a basic model of intra-cellular (or intra-organelles) pattern formation was chosen Belousov-Zhabotinsky (BZ) reaction. The general goal of the work is to collect data which would allow us to compare it with an available simplified model of the reaction. There are a few models; neither of them predicts the experimentally detectable behavior. This is always composed of observed sequence of states stable for certain period of time. The sequence of states is regular; the time of transitions between the states as well as concrete shape of travelling waves is sensitively dependent on initial conditions. We have performed a representative series of analyses in several different geometries and created a state trajectory using several selected image identifiers (point information gain entropy density – PIE/points). The PIE/point values define an approximate state space which may be analyzed using multivariate analysis. We will show how the multivariate analysis may be used for construction of tentative model and possible variables and coordinates in the internal phase space of the system. In this paper we provide results of this analysis.

Keywords: information entropy, state trajectory

1 ADVANTAGES OF BELOUSOV-ZHABOTINSKY REACTION MODEL

The Belousov- Zhabotinsky (BZ) reaction is used as example of self-organizing system which is easily and intelligibly observable and experimentally accessible. The BZ reaction was devised as a primitive model of citric acid cycle. To the surprise of the authors, it brought

about the phenomenon of chemical clock (in mixed systems) or spontaneous pattern formation (in still compartments). Most BZ reactions are homogeneous. The BZ reaction makes it possible to observe development of complex patterns in time and space by naked eye on a very convenient human time scale of dozens of seconds and space scale of several millimeters. The BZ reaction can generate up to several thousand oscillatory cycles in a closed system [1], which permits studying chemical waves and patterns without constant replenishment of reactants. Unlikely, for example, living cells, the self-organization in the Belousov-Zhabotinsky reaction (as well as in other chemical clocks) is expressed macroscopically and in two dimensions. When performed in a thin – few centimeters thick – layer, it creates easily observable travelling waves which may be captured by ordinary color camera and analyzed. The analysis does not require elaborate reconstruction of series of 3D images as in the case of bird flocks or fish schools or organ behavior. Moreover, the experimenter in case of chemical clock has full control of mechanical constraints imposed on the system.

This approach allows us to discourse whether the developed method is sensitive to changes in the shape and size of the investigated objects and how well the resulting model describes the internal changes in the self-organizing properties. The forms for the reaction are selected in accordance with existing geometry in developing cell shapes – rectangular (parenchymal cells), triangular (neurons of the cerebral cortex are predominantly pyramidal form), square (form of the Archaea bacteria subgroup - *Haloquadratum walsbyi*, some of the prokaryotes cells), etc. States in the course of the reaction may be identified in all cases when the geometry of the experimental vessel allows creation of travelling waves.

2 METHOD OF ANALYSIS

The first step of construction state trajectory of this reaction was plotting red vs. green vs. blue channel gained from photos. This 3D plot shows that individual attractors may be discriminated and that many state trajectories may be constructed but this needs some image processing method. To achieve these goals, we used the same method what were used for cells processing – then Rényi entropy calculation and the State trajectory construction.

$I_\alpha(r) = \frac{1}{\alpha-1} log \sum_i p_i^\alpha$ α is called Rényi entropy coefficient and ρ_i are probabilities of occurrence of

given intensity for given point x, y coordinate of camera pixel at given α in the image without and with the examined point

The colour channels and different Rényi entropy coefficients may be combined to best discriminate individual states [2, 3].

Information entropy can be computed from the *whole* image or just from selected part of it. Selected part of image obtained as *cross* of pixel's row and column (center pixel is counted only once). In such way we decrease the "probability" of remove pixel value (information are weighted by probabilities).

Without having certain knowledge about the characters of the processes probability density function and guided by the laws of the central limit theorem, we have chosen the principal component analysis (PCA) supported by the Unscrasmbler 10.X as the method of multivariate analysis for our system proceeding.

3 STATE TRAJECTORY CONSTRUCTION

The principal components are best approximation to internal orthogonal coordinates in state space approximate to stochastic (macroscopic) variables of which each has normal distribution.

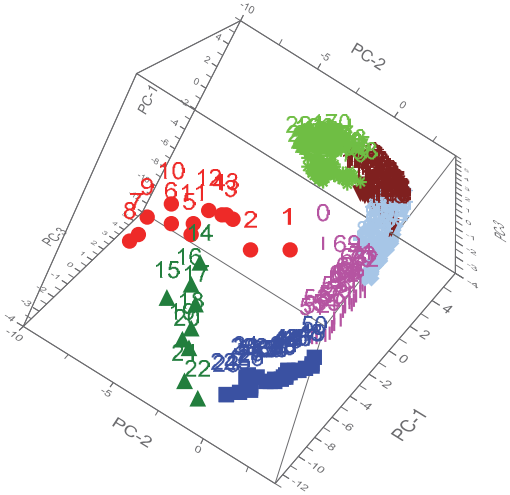

Fig. 1. Special arrangement of the scores of the data in the 3D space creates the state trajectory of the BZ reaction. All data divided on the clusters depend on the value of the PCA-components. As can be noticed all data are well separated into individual clusters and each cluster represents a certain phase of the reaction – formation firs of color spots, grooving these spots into a series of expanding concentric rings, waves disappearance by the end of the reaction.

States in the course of the reaction may be identified in all cases when the geometry of the experimental vessel allows creation of travelling waves. The identification of the internal coordinate system is main task of experimentation and development [4].

States in the course of the reaction may be identified in all cases when the geometry of the experimental vessel allows creation of travelling waves. The identification of the internal coordinate system is still matter of experimentation and development and the state of the art is critically reported.

LITERATURE

[1.] Belousov B., Biophysics, 1959, 9, 306 – 311
[2.] Urban J., Vanék J., Stys D., Proc. of Pattern Recognition and Information Processing, 2009, 283-287
[3.] Stys, D., Vanek, J., Nahlik, T., Urban, J., Cisar P., Mol. BioSyst., 2011, 7, 2824-2833
[4.] Stys D., Jizba P., Papacek S., Nahlik T., and Cisar P., IWSOS 2012, LCNS 7166, 2012, 36-47

ANALYSIS OF NON-ENZYMATIC POSTTRANSLATIONAL MODIFICATED (GLYCATED) ALBUMIN BY NANO-LC/MS/MS

Zdeňka Šťastná[a,b], Statis Pataridis[a], Pavla Sedláková[a], Ivan Mikšík[a]

[a] *Institute of Physiology, Academy of Sciences of the Czech Republic, v.v.i.,Vídeňská 1083, 142 20 Prague, Czech Republic, miksik@biomed.cas.cz*

[b] *Department of Analytic Chemistry, Faculty of Chemical Technology, University of Pardubice, Studentská 573, 532 10 Pardubice, Czech Republic*

ABSTRACT

Posttranslational modifications of proteins are important reactions, which significantly affect the function of proteins in the organism. In principle, they can be divided into enzymatic and non-enzymatic modifications. Non-enzymatic reactions include glycation (earlier called nonezymatic glycosylation), which plays an important role in the development of chronic complications of diabetes mellitus, uremia, in the process of aging and degeneration of the brain.

This work deals with the study of glycated albumins (human serum albumin and bovine serum albumin). Methodologically we used nano-liquid chromatography coupled to Q-TOF mass spectrometer. *In vitro* modified proteins were cleavaged by trypsin and arising peptides were separated on C18 nano column with trap-column. Peptides and their modifications were analysed by high-resolution Q-TOF mass spectrometer MaXis with precision determination of mass below 2 ppm.

We found some modifications of proteins. Besides well known carboxymethyllysine new ones were determined – create mass shift 78, 132 and 218. Origin of these modifications is discussed and possible structure is presented. All found modifications were allocated to the structure of proteins and reactivity to various oxo-compounds was also examined.

Keywords: non-enzymatic glycation, serum albumin

1 INTRODUCTION

In non-enzymatic glycation of proteins free amino groups of peptides/proteins react with carbonyl groups of reducing sugars without the catalytic action of enzymes. This reaction was firstly described by Louis Maillard [1], who observed browning of protein in their heating with sugars, and in his honor it is called Maillard reaction. Initially it appeared, that this reaction is relevant only in food chemistry, but in 1971 it was found, that glycation takes place in every living organism [2], especially if concentration of sugar in blood is increased. The non-enzymatic glycation takes place in three steps, which may be called initiation, propagation and termination, analogous to chain radical reactions.

In the first step the so-called early glycation products are formed. It involves condensation of reducing sugars (mainly glucose, but also ribose, fructose, pentose, galactose, mannose, ascorbate and xylulose) with ε-amino group of lysine residue (eventually amino group of terminal amino acid or of arginine) and the formation of unstable Schiff base, which rapidly rearranges to a much stable ketoamine called Amadori product [3]. The variables, that regulate it *in vivo*, are a concentration of reducing sugar and protein, a half-life of protein, a free amino group reactivity and a permeability of cell walls for sugars. *In vivo* conditions Amadori product reaches equilibrium in approximately 15-20 days and it accumulates in both the long- and short-lived protein [4]. During the propagation the Amadori products are resolved to carbonyl compounds (glyoxal, methylglyoxal, deoxyglukoson), which are highly reactive and can again react with free amino groups of proteins, thus promoting a non-enzymatic glycation. In the last step the above-mentioned propagators react with free amino groups and by oxidation, dehydration and cyclising reactions form advanced glycation end

products (called AGEs). These products are thermodynamically stable and terminate glycation non-enzymatic reaction [5].
Amount of AGEs in the body reflects the equilibrium between their formation and catabolism (degradation in the tissues, renal excretion). A high content of AGEs forms in diabetic patients and their excretion is insufficient in patients with renal failure. In both groups, therefore there is accumulation of AGEs in plasma, which leads to the production of toxic substances, interaction with the basal membrane and bonds to lipoproteins and collagen (common long-lived protein). Pathological formation of cross linkages caused by AGEs leads to increased stiffness matrix proteins, limiting their functionality and increases its resistance to proteolytic enzymes [6].
Serum albumin is produced in hepatocytes and it is the most abundant protein in blood plasma (constituting 55-65% of all plasma proteins). However, in plasma is only approximately 42% of albumin, the rest can be found in the tissues (mainly subcutaneous tissue and muscles) and a small amount penetrates the blood-brain barrier into the cerebrospinal fluid. Albumin is a soluble protein with ellipsoidal shape (in contrast to other plasma proteins which are glycoproteins). It consists of a single polypeptide chain comprising of 585 amino acids. It contains 17 disulfide bridges. Protease enzymes break down this protein into three domains with different functions. The half-life of albumin is about 20 days, and then it is reduced by the endothelium of blood capillaries. A small amount of albumin penetrates into urine or it is lost by diffusion into the alimentary canal.
Albumin is a transport protein of thyroid hormones (thyroxine, triiodothyronine), non-esterified fatty acids, unconjugated bilirubin, hem, steroid substances, plasma tryptophan and some minerals (such as calcium, magnesium and zinc). Furthermore, it binds a large part of drugs (such as penicillin, digoxin and salicylates). Another important function of albumin arises from its high plasma concentrations (35-53 g/l) and a relatively low molecular weight (68 kDa). Albumin participates in the maintenance of plasma oncotic pressure (more than 75%).

2 MATERIALS AND METHODS

2.1 Sample preparation

Bovine serum albumin (BSA) or human serum albumin (HSA) were dissolved in phosphate buffer (0.2 mol/l NaH_2PO_4; pH 7.4) to a final concentration of 1 mg/ml. These solutions were incubated (at 37 °C, 7 days) with ribose (0.1 mol/l in the final solution). BSA and HSA control samples were prepared in a similar way, only without added ribose. Due to the contamination which could occur during incubation, sodium azide and a thin layer of toluene were added to each sample. Dialysis followed after incubation and lasted 24 hours.
A 0.5 ml of buffer pH 8.4 (6 mol/l guanidine HCl; 1.2 mol/l Tris-HCl; 2.5 mmol/l Na_2EDTA) was added to a 5 mg lyophilized sample of BSA and HSA. Reduction of disulfide bridges was performed by adding 25 μl of 1 mol/l dithiothreitol. Samples were incubated for 30 minutes at 65 °C. The subsequent carboxymethylation of cysteine took place using 60 μl of 1 mol/l iodoacetic acid (incubation at room temperature, 40 minutes in the dark). This reaction was stopped by adding 15 μl of 1 mol/l dithiothreitol.
BSA and HSA samples were desalted in Econo-Pac 10 DG columns (Bio-Rad Laboratories, Hercules, CA, USA) and lyophilized. Desalted samples were diluted to the concentration 5 mg/ml with 20 mmol/l ammonium bicarbonate buffer (pH 7.8) and treated with trypsin (1:50 enzyme:substrate ratio). Incubation was done at 37°C for 24 hours. Blank samples were prepared by incubating the enzyme solution alone under identical conditions.

2.2 Analysis of tryptic digests with LC-MS/MS

For analyses, the samples were diluted 100 times and 5 μL of the sample were injected. The nano-HPLC apparatus used for protein digests analysis was a Proxeon Easy-nLC (Proxeon, Odense, Denmark) coupled to a maXis Q-TOF (quadrupole – time of flight) mass

spectrometer with ultrahigh resolution (Bruker Daltonics, Bremen, Germany) by nanoelectrosprayer. The nLC-MS/MS instruments were controlled with the software packages HyStar 3.2 and micrOTOF-control 3.0. The data were collected and manipulated with the software packages ProteinScape 3.0 and DataAnalysis 4.0 (Bruker Daltonics).

A 5 μl of the peptide mixture were injected into a NS-AC-11-C18 Biosphere C18 column (particle size: 5 μm, pore size: 12 nm, length: 150 mm, inner diameter: 75 μm), with a NS-MP-10 Biosphere C18 precolumn (particle size: 5 μm, pore size: 12 nm, length: 20 mm, inner diameter: 100 μm), both manufactured by NanoSeparations (Nieuwkoop, Netherlands).

The separation of peptides was achieved via a linear gradient between mobile phase A (water) and B (acetonitrile), both containing 0.1 % (v/v) formic acid. Separation was started by running the system with 5 % mobile phase B, followed by gradient elution to 30 % B at 70 min. The next step was gradient elution to 50 % B in 10 min., and then a gradient to 100 % B in 8 min. Finally, the column was eluted with 100 % B for 2 min. Equlibration before the next run was achieved by washing the column with 5 % mobile phase B for 10 min. The flow rate was 0.25 μL min and the column was held at ambient temperature (25 °C).

On-line nano-electrospray ionization (easy nano-ESI) in positive mode was used. The ESI voltage was set at +4.5 kV, scan time 1.3 Hz. Operating conditions: drying gas (N_2), 1 L/min; drying gas temperature, 160 °C; nebulizer pressure, 0.4 bar. Experiments were performed by scanning from 100 to 2200 m/z. The reference ion used (internal mass lock) was a monocharged ion of $C_{24}H_{19}F_{36}N_3O_6P_3$ (m/z 1221.9906). Mass spectra corresponding to each signal from the total ion current chromatogram were averaged, enabling an accurate molecular mass determination. All LC-MS and LC-MS/MS analyses were done in duplicates.

2.3 Statistical evaluation of MS data for scheduled precursor list generation

The profile MS chromatograms were measured for 5 non-glycated (control) and 5 glycated samples of BSA and HSA. The data sets were then statistically evaluated in ProfileAnalysis software and scheduled precursor lists for all ion increases were created. The scheduled precursor lists were then used to measure MS/MS spectra of these particular ions. The resulting MS/MS data were then searched for possible known modifications which were described previously by others.

Several good quality spectra that had not been assigned to any particular peptide during the first database search for known modifications were then evaluated manually for the mass increase. The new mass increases found were then added to a Mascot server and a new search on the same data was performed to find other possible modification sites.

2.4 Database searching

Data were processed using ProteinScape software. Proteins were identified by correlating tandem mass spectra of BSA and HSA samples to the IPI bovine and IPI human databases, respectively, using the MASCOT searching engine (www.matrixscience.com).

3 RESULTS AND DISCUSSION

In this work high resolution tandem mass spectrometry was successfully applied for study of peptide/protein modifications caused by glycation, in our case monotopic modifications of lysine. Using the high resolution MS and MS/MS spectra it was found that the lysine in VTKC*C*TESLVNR peptide (C* indicates carboxymethyl cysteine) has been carboxymethylated (ΔM: 58.001). However, three other mass increases ΔM: 78.010, 132.038 and 218.074 were also found. The first one can be assigned to a formula C_5H_2O (a modification most probably derived from pyrraline). Pyrraline has been known for a long time to occur in proteins glycated by glucose. It is therefore very likely, that a glycation with ribose (pentose) will result in a similar structure with only five carbon atoms (Fig. 1A) missing one CH_2OH group. The second modification with ΔM: 132.04 can be assigned to another

pyrraline-derived structure (Fig. 1B) having a molecular formula $C_5H_8O_4$. As for the last ΔM: 218.074, the possible molecular formulas include among others $C_{16}H_{10}O$ and $C_9H_{14}O_6$ with very similar theoretical ΔM making it impossible to propose a structure.

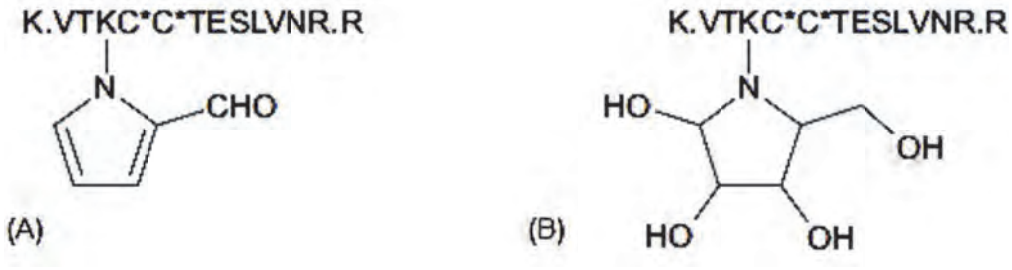

Fig.1.: Schematic draws of proposed structures of VTKC*C*TESLVNR peptide modified with pyrraline-derived advanced glycation products (A) C_5H_2O, ΔM=78.010 and (B) $C_5H_8O_4$, ΔM=132.038. Please note that N in cyclic structure originates from lysine (K) in ppeptide structure.

The new molecular formulas were added as new variable modifications into search by Mascot server and a new search was performed to see whether there are other modified sites within BSA molecule. We have found that the peptide KVPQVSTPTLVEVSR has also been modified by the same types of modifications.
In order to verify the above mentioned results, we have also glycated human serum albumin in addition to BSA. The comparison of results for BSA and HSA samples is presented in Table 1 and 2.
Finally, raw profile MS spectra were manually searched for these modifications. We have found that in some cases the signal was too low for the ions to be fragmented, yet, we have found the exact masses for all newly discovered modifications (see the results in Table 2 with Mascot score ”N/A”).

Table 1: Glycation sites and related peptides and modifications found in a glycated bovine serum albumin. **K** indicates modified lysine, C* indicates carboxymethyl cysteine, CML indicates carboxymethyl lysine.

Location	Peptide	m/z	z	Modification of lysine			Mascot Score
				ΔM observed [Da]	Δm/z [ppm]	Mol. formula	
K: 498	K.VT**K**C*C*TESLVNR.R	516.2345	3+	78.01026	-0,20	C_5H_2O	59.8
		763.8432	2+	58.00099	-2.94	CML	73.4
		509.5646	3+	58.00056	-3.22	CML	47.5
		534.2436	3+	132.0376	-2.93	$C_5H_8O_4$	59.4
		562.9224	3+	218.0740	N/A	unknown	59.6
K: 437	R.**K**VPQVSTPTLVEVSR.S	620.0094	3+	218.0743	N/A	unknown	68.4
		573.3203	3+	78.00659	-2.10	C_5H_2O	58.4
		591.3311	3+	132.0394	-1.64	$C_5H_8O_4$	64.5
		566.6517	3+	58.00115	-2.54	CML	50.3
K: 463	R.C*C*T**K**PESER.M	416.1621	3+	78.00920	-1.09	C_5H_2O	44.4

Table 2: Glycation sites and related peptides and modifications found in a glycated human serum albumin. **K** indicates modified lysine, C* indicates carboxymethyl cysteine, CML indicates carboxymethyl lysine.

Location	Peptide	m/z	z	Modification of lysine			Mascot Score
				ΔM observed [Da]	Δm/z [ppm]	Mol. formula	
K: 499	R.VT**K**C*C*TESLVNR.R	509.5649	3+	58.00146	-2.63	CML	64.7
		516.2334	3+	78.00696	-2.33	C_5H_2O	48.9
		562.9226	3+	218.0746	N/A	unknown	44.8
		763.8434	2+	58.00139	-2.68	CML	N/A
		534.2433	3+	132.0367	-3.49	$C_5H_8O_4$	N/A
K: 438	K.**K**VPQVSTPTLVEVSR.N	573.3210	3+	78.00905	-0.88	C_5H_2O	51.9
		620.0093	3+	218.0740	N/A	unknown	N/A
		566.6518	3+	58.00145	-2.37	CML	N/A
		591.3309	3+	132.0388	-1.98	$C_5H_8O_4$	N/A

4 CONCLUSIONS

The glycation of albumins with ribose leads to a series of advanced glycation end products (AGE). To date, only a limited amount of AGEs has been described. In this study we have used high resolution MS and MS/MS spectrometry to identify three new mass increases belonging to new AGEs and we have also proposed molecular formulas for two of these new modifications.

The first one with ΔM: +78.010 can be attributed to a molecular formula C_5H_2O and has a structure similar to a pyrraline, a glucose derived AGE. The second modification with ΔM: +132.038 has a proposed molecular formula $C_5H_8O_4$. There was also one additional mass increase (ΔM: +218.074) of an unknown structure.

We have demonstrated that there are two lysine locations within the albumin sequence that are prone to glycation. These sites are often modified by series of different AGEs which indicates that they are highly reactive. For BSA, these lysines are at positions 437 and 498 (for HSA, the positions are: 438 and 499).

ACKNOWLEDGEMENTS

This work was supported by the Czech Science Foundation (Grants Nos. P206/12/0453 and 203/08/1428), the Academy of Sciences of the Czech Republic, Research Project AV0Z50110509 and support for long-term conceptual development of research organization RVO:67985823, which is gratefully acknowledged.

LITERATURE

[1.] Maillard, L.C. *C.R.*, *Seances Acad. Sci.* 1912, *154*, 66.
[2.] Trivelli, L.A., Ranney, H.M., Lai, H.T., *N. Engl. J. Med.* 1971, *284*, 353-357.
[3.] Watkins, N.G., Thorpe, S.R., Baynes, J.W., *J. Biol. Chem.* 1985, *260*, 10626-10636.
[4.] Lapolla, A., Traldi, P., Fedele, D,. *Clinical Biochemistry* 2005, *38*, 103-115.
[5.] Ahmed, N., Argirov, O.K., Minhas, H.S., Cordeiro, C.A.A., Thornalley, P.J., *Biochem. J.* 2002, *364*, 1-14.
[6.] Paul, R.G., Bailey, A.J., *Int. J. Biochem. Cell. Biol.* 1999, *31*, 653-660.

MICROPREPARATIVE SOLUTION ISOELECTRIC FOCUSING OF PEPTIDES AND PROTEINS IN NONWOVEN STRIP

Filip Duša [a,b], Karel Šlais [a]

[a] *Institute of Analytical Chemistry of the ASCR, v.v. i., Veveří 97, Brno, 602 00, Czech Republic*
[b] *Department of Biochemistry, Faculty of Science and CEITEC, Masaryk University, Kamenice 5, Brno, 625 00, Czech Republic*

ABSTRACT

Recently we devised a new instrument for micropreparative analysis [1]. It is based on solution phase isoelectric focusing (sIEF) performed in a narrow channel (approximately 2 – 4 mm wide) with a strip of nonwoven fabric serving as the analysis bed. The strip can be precut before an analysis to make harvesting of fractions easier. Isoelectric focusing is driven by a programmable electrophoretic power supply. Progress of analysis is monitored by addition of colored isoelectric point (*pI)* markers. Usually sIEF runs are performed overnight. Evaporation of water is one of crucial features of analysis and it forces free liquid to shrink into the nonwoven fabric strip. Moreover, water evaporation increases liquid viscosity by altering ethylene glycol/water ratio. Fractions can be harvested simply by collecting and washing precut segments after the sIEF run. In this paper we used sIEF device for purification of caseinomacropeptide (CMP) from crude whey. Obtained fractions were further analyzed by HPLC. From acquired data a plot with chromatograms of all fractions was constructed to show purification profile of CMP. We proved that the new instrument is capable of quantitative purification of CMP complex from a globulin fraction.

Keywords: isoelectric focusing, preparative, whey

1 INTRODUCTION

Isoelectric focusing is suitable and broadly used method for protein purification and separation. There are several sIEF devices based on following designs: multicompartment, off-gel and continuous flow. Here, we present a new device [1] based on nonwoven strip. Sweet whey is rich in proteins including CMP which is valuable dietary supplement [2]. Next to CMP, α-lactalbumin and β-lactoglobulin are the most abundant proteins in whey and thus two major contaminants. Concerning above mentioned proteins/peptides we found in literature their *pI*s to be 3.15 – 4.15, 4.2 – 4.5 and 5.13 respectively [3, 4]. With knowledge of these isoelectric points we purified CMP from crude whey using our new sIEF device.

2 EXPERIMENTAL

2.1 Device description

Isoelectric focusing device consist of a plastic trough with a pre-cut nonwoven fabric strip on the bottom. On Figure 1 you can see design and operational protocol of IEF device. The figure is divided into parts designated with letters and arranged alphabetically to describe workflow. Top view of the solution phase IEF device based on segmented nonwoven fabric strip can be seen on Figure 1A. The plastic trough is clipped to a base with a pair of wires which serves as electrodes. The end of the anode is made of a carbon rod. Separation space is defined by the dimensions of strip which can be optionally precut into segments. Plastic cover foil serves both as a contamination protection and as a retarder of evaporation.

2.2 sIEF operation protocol

Running solution was prepared from: 0.375 ml of 1 % solution of dried whey, 0.05 ml of stock solution of colored *pI* markers, 0.1 ml ethylene glycol, 0.05 ml butan-1-ol, 0.025 ml 0.1 mol·l^{-1} 1 imidazolyl-acetic acid and 0.1 ml of 0.1 mol·l^{-1} Tris. On figure 1B you can see detail of pipetting running solution onto the strip which soaks up along the whole strip (Figure 1C). Cover foil is placed over the strip (Figure 1D), power is turned on (Figure 1E) and separation is done. After finished IEF, fractions are harvested by picking up the segments (Figure 1F), fixing the segments into pipette tips (Figure 1G) and washing out the fractions into micro test tubes (Figure 1H).

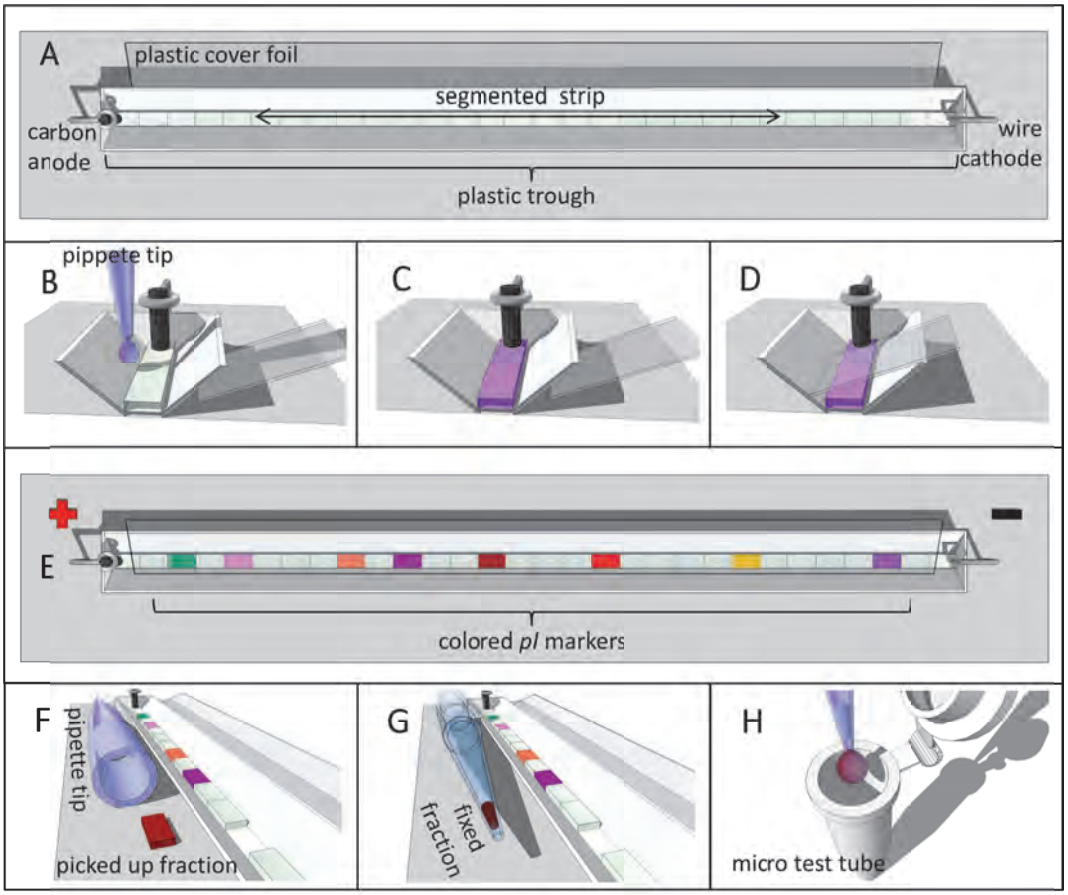

Fig. 1: sIEF operation protocol

2.3 Reversed-phase liquid chromatography

Subsequently, fractions are subjected to reversed-phase liquid chromatography (RPLC). All chromatographic separations were performed using the Agilent 1200 Series chromatographic. The separations were performed on the microbore Poroshell 300SB-C18 column (5 µm particle size, 1 × 75 mm, Agilent Technologies) equipped with the C18 cartridge guard. Linear gradient from 5 to 80% (v/v) of acetonitrile with 0.1 % of trifluoracetic acid over 30 min was used for separation. The elution was run at the flow rate of 20 µl·min^{-1} and 70 °C. The detection was performed at 214 nm and 280 nm using the diode-array detector.

3 RESULTS AND DISSCUSION

Chromatograms obtained from RPLC analysis were processed into one plot where concentration profiles of the three most abundant proteins/peptides in whey can be seen (Figure 2). IEF fractions in the figure are numbered from anodic to cathodic side, meaning the

fraction number one is the most acidic fraction. On Figure 2 one can easily recognize that CMP (designated with gray rectangle) was almost quantitatively separated from α-lactalbumin and β-lactoglobulin (traces of α-lactalbumin left in the first four fractions). Straight line of chromatograms of fractions six, seven and eight is due to utilizing imidazolyl-acetic (*pI* 4.8) acid as *pI* spacer between the three mentioned proteins/peptides. Although common way of CMP purification is ultrafiltration, we proved that our sIEF device can be used as alternative and provide CMP of high purity.

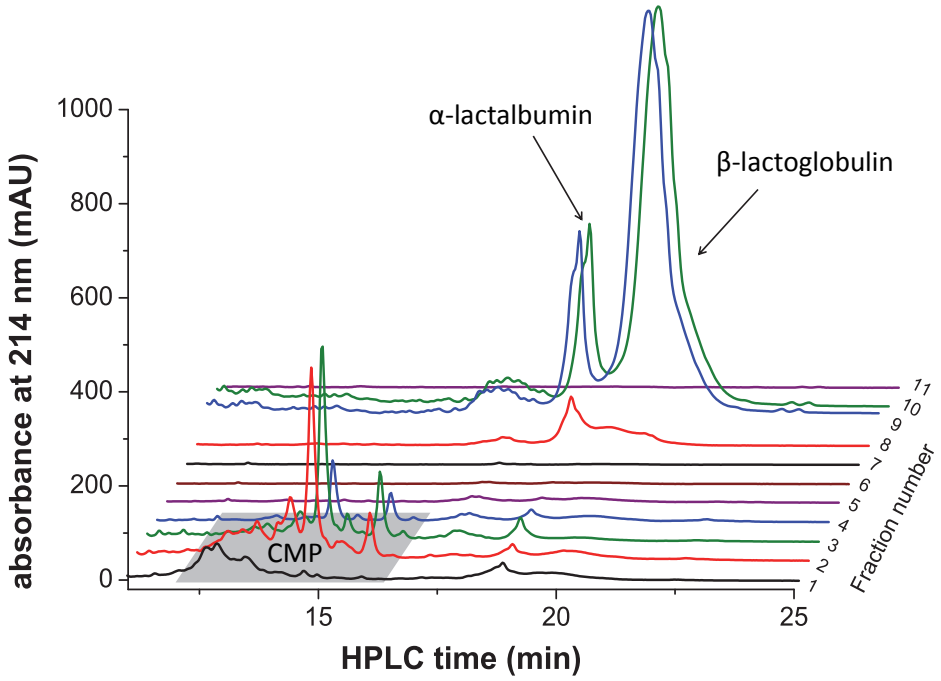

Fig. 2: Chromatograms from HPLC analysis of sIEF fractions.

ACKNOWLEDGEMENTS

This work was supported by the Ministry of the Interior of the Czech Republic (Project No. VG20102015023), by the Ministry of Education, Youth and Sports of the Czech Republic by OPVK grant No. CZ.1.07/2.3.00/20.0182 Vytvoření multidisciplinárního výzkumného a vzdělávacího centra bioanalytických technologií (BBC) and by the Academy of Sciences of the Czech Republic (Institutional Research Plan RVO: 68081715).

LITERATURE

[1.] Šlais. PV 2012-100

[2.] Madureira, A. R., Tavares, T., Gomes, A. M. P., Pintado, M. E., Malcata, F. X., Journal of Dairy Science 2010, 93, 437-455.

[3.] Farrell, H. M., Jimenez-Flores, R., Bleck, G. T., Brown, E. M., Butler, J. E., Creamer, L. K., Hicks, C. L., Hollar, C. M., Ng-Kwai-Hang, K. F., Swaisgood, H. E., Journal of Dairy Science 2004, 87, 1641-1674.

[4.] Kreuss, M., Strixner, T., Kulozik, U., Food Hydrocolloids 2009, 23, 1818-1826.

MICROCHIP ISOLATION COMBINED WITH MS-IDENTIFICATION OF PHOSPHOPROTEINS FROM *FRANCISELLA TULARENSIS*

Rudolf Kupcik[a], Pavel Rehulka[b], Barbora Jankovicova[a], Zuzana Svobodova[a], Lenka Hernychova[b,c], Jana Klimentova[b], Jiri Stulik[b], Zuzana Bilkova[a]

[a] *Department of Biological and Biochemical Sciences, University of Pardubice, Studentska 573, 532 10 Pardubice, Czech Republic*
[b] *Institute of Molecular Pathology, Faculty of Military Health Sciences, University of Defense, Trebesska 1575, 500 01 Hradec Kralove, Czech Republic*
[c] *Regional Centre for Applied Molecular Oncology, Masaryk Memorial Cancer Institute, Zluty kopec 7, 656 53 Brno, Czech Republic*

ABSTRACT

Posttranslational modifications of proteins, such as phosphorylation, play a key role in many biological processes. Due to low abundances phosphoproteins digested into peptides typically require isolation and preconcentration before MS analysis. For these purposes we developed new methodical approach based on phosphopeptides enrichment by magnetic TiO_2 particles in microfluidic chip. Enriched phosphopeptides were subsequently fractionated by microcolumn RP-LC using gradient elution and offline application to MALDI plate. For confirmation of phosphorylation MS and MS/MS analysis was followed by on-plate dephosphorylation by alkaline phosphatase. The obtained spectra were compared before and after dephosphorylation, which enhanced the probability of a correct identification. This procedure was applied firstly to tryptic digest of alpha-casein and then to digest of *Francisella tularensis* subsp. *holarctica* strain FSC200 (FTH FSC200) lysate. Finally bacterial phosphoproteins were identified using database searching and manual evaluation.

Keywords: microfluidics, phosphoproteins, *Francisella tularensis*

1 INTRODUCTION

Protein phosphorylation is one of the most frequent and the most important reversible posttranslational modifications in organism. It plays role in many cellular processes such as proliferation, division, differentiation of cells, signal transduction, gene expression and metabolism.[1] To understand these biological processes at the molecular level the identification and characterization of the phosphoproteins is required. However phosphopeptides are present at low abundance in the proteolytic digest, so the ion signals of phosphopeptides are seriously suppressed by the signal of abundant nonphosphorylated peptides.[2] In prokaryotic species number of phosphorylatred proteins is much lower than in eukaryotes.[3] Due to this fact the selective enrichment of phosphopeptides before analysis by mass spectrometry is necessary. Numerous methods have been already developed for this enrichment, including immunoprecipitation[4], immobilized metal ion affinity chromatography (IMAC)[5] or metal oxide affinity chromatography (MOAC) using TiO_2[6] or ZrO_2[7] etc.

Highly sensitive mass spectrometric methods are often applied for proper detection and characterization of phosphorylation sites of phosphoproteins. Neutral loss scan with MS/MS, which is used for identification of precursor ions displaying this signature loss, is example of such approach. However, this method is time-consuming and reduced in sensitivity.[2] On the other hand we can use comparison of spectra before and after dephosphorylation for verification of phosphate group presence.

Francisella tularensis, the Gram-negative facultative intracellular bacterium, that causes a serious infectious disease tularemia, is considered to be a potential bioterrorism agent. Protein phosphorylation is often directly involved in virulence of bacterial pathogens.[8] Here we present efficient procedure for specific isolation of phosphopeptides from bacterial lysate

using TiO_2 magnetic nanoparticles in microchip, followed by microcolumn RP-LC separation and MALDI-TOF MS analysis, which can help to basic understanding of key virulence factors and the infection strategy employed by *Francisella tularensis* that is still limited.[9]

2 EXPERIMENTAL PROCEDURES

2.1 Digestion of proteins

Alpha-casein dissolved in 50 mM ammonium bicarbonate was denaturated with dithiotreitol (DTT), alkylated by iodoacetamide (IA) and treated with sequencing grade modified trypsin (1%, w/w) for 18 hours at 37°C. Lysate of FTH FSC200 was diluted with 50 mM ammonium bicarbonate (50%, v/v) and denatured by heating at 90°C for 20 minutes. Reductive alkylation (using DTT and IA) and digestion with grade modified trypsin (1%, w/w) for 18 hours at 37°C followed.

2.2 Isolation of phosphorylated peptides using TiO_2 nanoparticles

TiO_2 nanoparticles (MagPrep® TiO_2, 100-200 nm, Merck, Darmstadt, Germany) were used for isolation of phosphorylated peptides from the mixture of peptides obtained by digestion. Nonspecific binding of nonphosphorylated peptides was reduced by adding of 2,5-dihydroxybenzoic acid (DHB)[6] into the loading solution contained 80% acetonitrile (ACN) and 0.1% trifluoracetic acid (TFA). A 0.5% ammonia solution was used for elution of selectively bound phosphorylated peptides. For optimization of enrichment procedure, tryptic digest of alpha-casein was used. After optimization procedure was applied for enrichment of phosphopeptides from FTH FSC200 lysate. All isolation steps were carried out in microfluidic device (microfluidic Chipshop, Jena, Germany) by using preparative microchip with 120 µl. This microchip was fabricated from Topas (Cyclic Olefin Copolymer).

2.3 Fractionation of isolated peptides by microcolumn RP-LC

Elution fractions collected within the enrichment were fractionated by microcolumn RP-LC. Teflon column (25 mm long, 0.25 mm I.D.) was filled with Ascentis® Express Peptide ES C18 particles (2.7 µm). Peptides were loaded in 2 % ACN and 0.1 % TFA. After loading, peptides were separated with gradient of ACN (2-25 %) contained 0.1 % TFA. Microfractions were continually spotted to 24 MALDI targets per 0.75 µl. After this, 0.5 µl of MALDI matrix was added to each spot and analysis by MALDI-TOF MS was done.

2.4 Dephosphorylation of peptides

Dephosphorylation of phosphopetides was carried out directly on MALDI plate.[10] by applying of 1 µl of 10 mM ammonium bicarbonate with 0.14 U of alkaline phosphatase on each spot. Plate was incubated for 30 minutes at room temperature. Finally spots were washed with 5 % TFA and analyzed by MALDI-TOF MS again.

2.5 MALDI-TOF MS

MS analysis was performed using a 4800 Proteomics Analyzer MALDI-TOF/TOF instrument (Applied Biosystems, Framingham, USA). All spectra were measured in positive reflector mode. DHB (5 mg/ml of 50 % ACN, 0.1 % TFA and 2 % phosphoric acid) for analysis of alpha-casein digest and α-cyano-4-hydroxycinnamic acid (CHCA, 5 mg/ml of 50 % ACN and 0.1 % TFA) for analysis of digest from FTH FSC200 lysate were used as MALDI matrix respectively.

3 RESULTS AND DISCUSSION

Initial optimization of the enrichment procedure was performed using tryptic fragments originating from alpha-casein. For this procedure 200 pmol of peptide mixture and only 20 mg/ml of DHB in loading solution for nonspecific biding reduction were used. The results confirmed the assumptions of successful isolation of phosphopeptides.

For specific isolation and identification of bacterial phosphopeptides 227 µl of FTH FSC200 cytosol lysate containing 3.5 mg of protein material was used. For reduction of nonspecific binding 200 mg/ml of DHB was used. Two phosphopeptides from FTH FSC200 were identified after fractionation by microcolumn RP-LC and comparison of MS and MS/MS spectra before and after dephosphorylation. The first one has sequence: Ac–HNFATQDATHGN**S**LSHR and originating from 50S ribosomal protein L3 (*Fig. 1*). The second one is: Ac–HLLVQ**S**ESECQQIKK and originating from peptidyl-propyl cis-trans isomerase (*Fig. 2*). Both were acetylated on terminal histidin. Several other phosphopeptides were found, but they could not be identified, because their fragmentation spectra were poor.

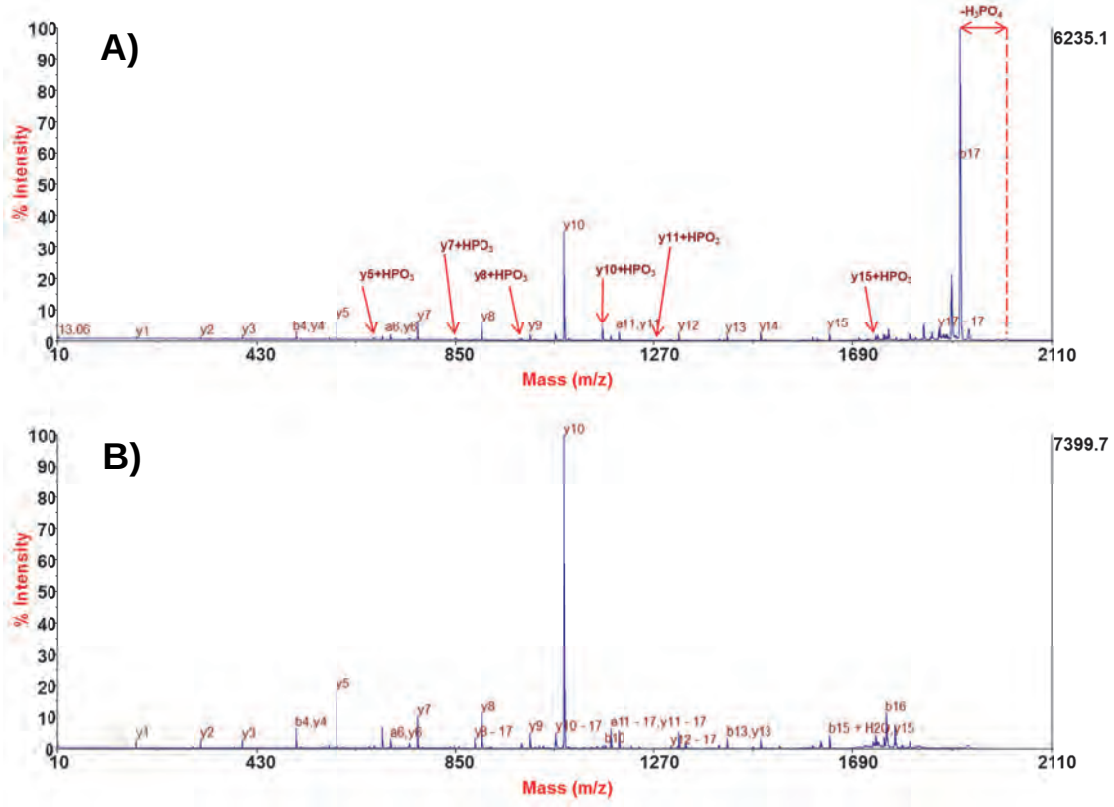

Fig. 1. : MALDI-TOF/TOF mass spectra of peptide from 50S ribosomal protein L3 (FTH FSC200) for the precursor ions (A) Ac–HNFATQDATHGN**S**LSHR, 2014.88 Da, and (B) its dephosphorylated form Ac–HNFATQDATHGNSLSHR 1934.90 Da. Phosphorylated fragments are marked red.

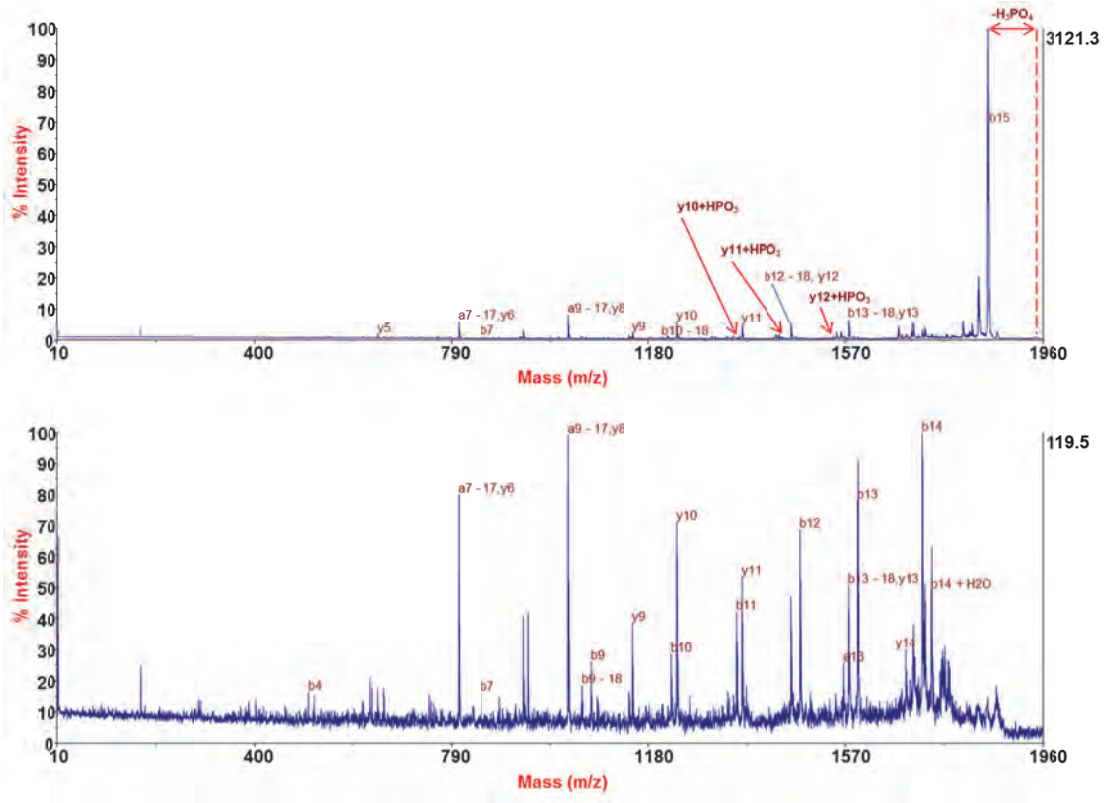

Fig. 2. : MALDI-TOF/TOF mass spectra of peptide from peptidyl-propyl cis-trans isomerase (FTH FSC200) for the precursor ions (A) Ac–HLLVQ**S**ESECQQIKK, 1948.94 Da, and (B) its dephosphorylated form Ac–HLLVQSESECQQIKK, 1868.98 Da. Phosphorylated fragments are marked red.

4 CONCLUSION

Whereas in bacteria number of phosphorylated proteins in time is low, isolation method as we used must be very effective. Using described approach we successfully isolated and identified phosphopeptides from *Francisella tularensis* subsp. *holarctica* strain FSC200 and confirmed usability of dephosphorylation for characterization of phosphorylation site. In next studies functional analysis of phosphorylated proteins and comparison of phosphorylation among different strains of *Francisella tularensis* will be performed.

ACKNOWLEDGEMENTS

This work was supported by the Czech Science Foundation (GA203/09/0857), EU project NADINE (No. 246513), project SGFCHT 07/2012, a long-term organization development plan no. 1011 from the Faculty of Military Health Sciences, University of Defence, Czech Republic, project „Strengthening of the excellent teams at the University of Pardubice“, No. CZ.1.07/2.3.00/30.0021 (co-financed by the European Social Fund and State Budget of Czech Republic) and project RECAMO, CZ.1.05/2.1.00/03.0101 (co-financed by the the European Regional Development Fund and the State Budget of the Czech Republic).

LITERATURE

[1.] Halada, P., Chemicke Listy 2005, 99, 922-929.

[2.] Sun, S., Ma, H., Han, G., Wu, R., Zou, H., Liu, Y., Rapid Communications in Mass Spectrometry 2011, 25, 1862-1868.

[3.] Gnad, F., Forner, F., Zielinska, D. F., Birney, E., Gunawardena, J., Mann, M., Molecular & Cellular Proteomics 2010, 9, 2642-2653.
[4.] Rush, J., Moritz, A., Lee, K. A., Guo, A., Goss, V. L., Spek, E. J., Zhang, H., Zha, X.M., Polakiewicz, R. D., Comb, M. J., Nature Biotechnology 2005, 23, 94-101.
[5.] Zhou, W., Merrick, B. A., Khaledi, M. G., Tomer, K.B., Journal of The American Society for Mass Spectrometry 2000, 11, 273-282.
[6.] Larsen, M. R., Thingholm, T. E., Jensen O. N., Roepstorff, P., Jorgensen, T. J. D., Molecular & Cellular Proteomics 2005, 4, 873-886.
[7.] Gates, M. B., Tomer, K. B., Deterding, L. J., Journal of The American Society for Mass Spectrometry 2010, 21, 1649-1659.
[8.] Misra, S. K., Milohanic, E., Ake, F., Mijakovic, I., Deutscher, J., Monnet, V., Henry, C., Proteomics 2011, 11, 4155-4165.
[9.] Hrstka, R., Stulik, J., Vojtesek, B., Microbes and Infection 2005, 7, 619-625.
[10.] Torres, M. P., Thapar, R., Marzluff, W. F., Borchers, CH. H., Journal of Proteome Research 2005, 4, 1628-1635.

THIN METAL FILMS IN RESISTIVITY-BASED CHEMICAL SENSING

Pavel Podešva, František Foret

Institute of Analytical Chemistry, Veveri 97, 902 00 Brno, Czech Republic
podesva@iach.cz

ABSTRACT

Measurement of basic electric properties (current, voltage, resistance) is the most frequent technique in practically all scientific disciplines. Direct electric measurements are simple, precise and provide very large dynamic range. Since the related equipment is simple and inexpensive sensors based on electric measurements are very attractive for many applications in chemistry, environmental sciences or medicine. In this work, we present resistivity sensor for direct measurement of thiols in liquid samples.

Keywords: chemiresistor, glutathione, adsorbtion

1 INTRODUCTION

Chemiresistor is a sensor, changing its resistivity with change of adjacent chemical environment [1, 2]. In this work we use gold thin film sensor [3] interacting with thiols in liquid phase. When thiolated molecules adsorb on the gold surface, building a self-assembled monolayer [4, 5], a covalent bond between the sulphur and gold atom with 50% of C-C bond strength is established [6]. Covalently attached gold atoms do not participate on electric conduction anymore, thus increasing the resistivity of the thin metal layer. When the gold layer is sufficiently thin (<80nm), this effect becomes very strong and the difference between clear and completely saturated surface can be represented by shift in resistance of up to 5%. [7].

1.1 Instrumentation

The device was constructed as a microfluidic apparatus with four sensing elements arranged in the Wheatstone bridge to exclude influence of the temperature coefficient of resistivity. In ideal case, when the bridge is balanced, the voltage between the sensing nodes is zero. Only one element was used at a time. Sample was fed into the channels by quartz capillaries. The

chip consisted of two parts – glass plate with sensors and PDMS part with channels bonded together with the aid of plasma activation. We tested dynamic range of the device by aliquote series of thiolated and non-thiolated compounds. The chosen thiolated compounds were the glutathione and cysteine. Tripeptide Gly-Pro-Glu and β-alanine were used as the non-thiolated counterparts because of their structural similarity.

2 RESULTS

During the experiments we have found, that the sensor is capable to measure in concentration range of 7 orders of magnitude. After each measurement the sensor was regenerated by series of voltage pulses. This device allows performing inexpensive, robust, relatively fast and simple analyses of thiols or traping of thiols and releasing them for for further analyses. This will be described in a following study.

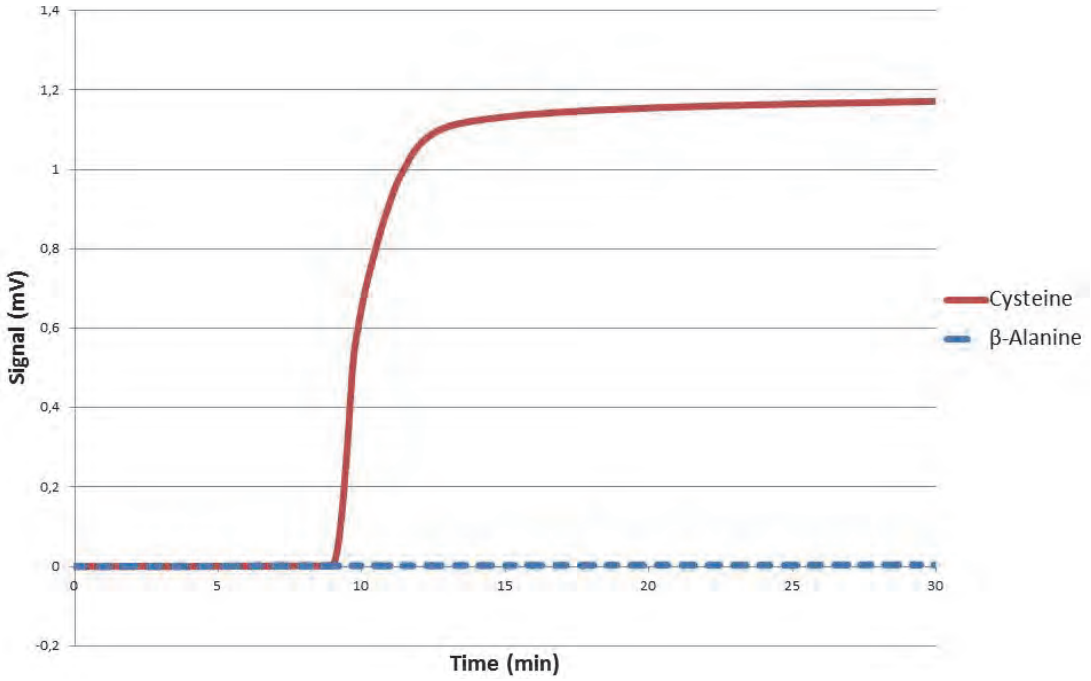

Fig. 1. Comparsion between chip response to 1mM β-alanine and 1mM cysteine.

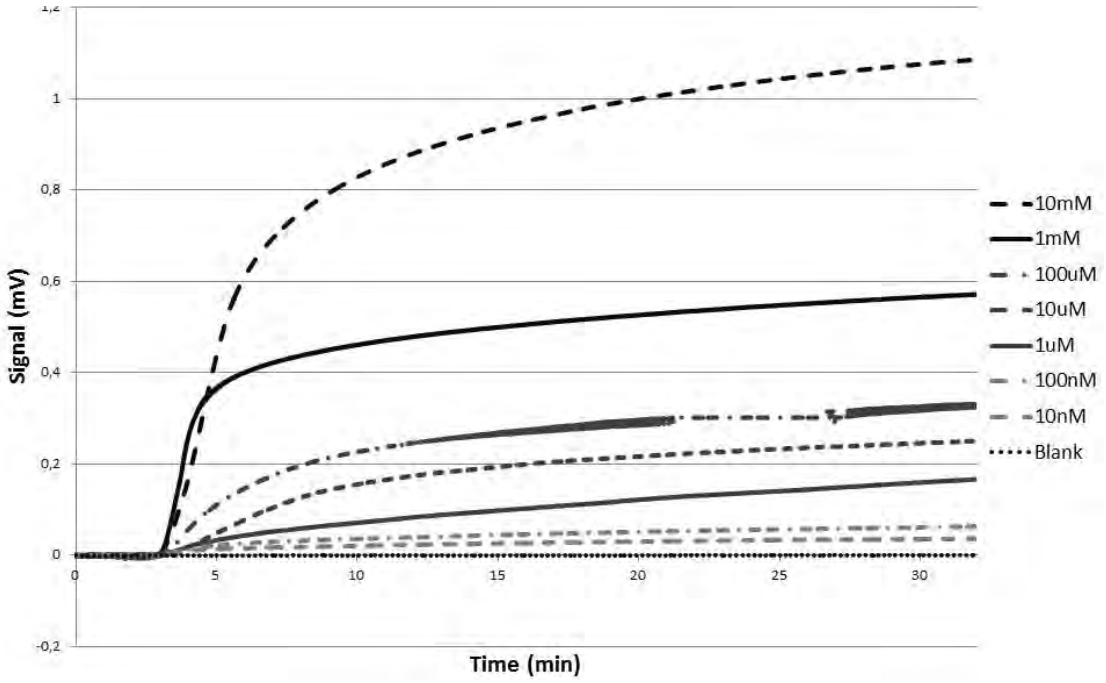

Fig. 2. Comparsion of chip response to Glutathione aliquote series in range 10 nM to 10 mM.

ACKNOWLEDGEMENTS

Financial support from the Grant Agency of the Czech Republic (P301/11/2055 and P206/12/G014) and the institutional support RVO: 68081715 is acknowledged. Special thanks to Dr. Milos Klima klima@sci.muni.cz for help with plasma activation.

LITERATURE

[1.] Podesva, P.; Foret, F., Thin Metal Films in Resistivity-based Chemical Sensing (review) *Current analytical chemistry* 2012, *submitted*.

[2.] Tucceri, R., A review about the surface resistance technique in electrochemistry. *Surface Science Reports* 2004, *56* (3-4), 85-157.

[3.] Tellier, C. R., Thin Metal Film Sensors. *Active and Passive Electronic Components* 1985, *12* (1), 9-32.

[4.] Flynn, N. T.; Tran, T. N. T.; Cima, M. J.; Langer, R., Long-Term Stability of Self-Assembled Monolayers in Biological Media. *Langmuir* 2003, *19* (26), 10909-10915.

[5.] Schonenberger, C.; Jorritsma, J.; Sondaghuethorst, J. A. M.; Fokkink, L. G. J., Domain-Structure of Self-Assembled Alkanethiol Monolayers on Gold. *Journal of Physical Chemistry* 1995, *99* (10), 3259-3271.

[6.] Fried, G. A.; Zhang, Y. M.; Bohn, P. W., Effect of molecular adsorption at the liquid-metal interface on electronic conductivity: the role of surface morphology. *Thin Solid Films* 2001, *401* (1-2), 171-178.

[7.] Riu, J.; Maroto, A.; Rius, F. X., Nanosensors in environmental analysis. *Talanta* 2006, *69* (2), 288-301.

ULTRA FAST HPLC METHOD FOR TADALAFIL ACCORDING TO PH.EUR. VALIDATION CRITERIA AND IDENTIFICATION OF IMPURITIES USING ACCURATE MASS MS

Ludovit Schreiber, Radoslav Halko, Milan Hutta, Anna Kabzanová, Soňa Lopuchová

Prírodovedecká Fakulta UK, Katedra analytickej chémie, Mlynská dolina, 842 15 Bratislava
schreiber@fns.uniba.sk

ABSTRACT

Erectile dysfunction (ED), inability to achieve a penile erection sufficient for satisfactory sexual performance is estimated to affect many men worldwide. ED is more common in advanced age and related to hypertension or diabetes mellitus or use of certain pharmacological agents e.g. antihypertensive. ED has been treated by the drugs that inhibit the enzyme phosphodiesterase type 5 (PDE5) activities. Tadalafil is a selective phosphodiesterase type 5 inhibitor, which is used to treat mild to severe ED in man. Drug testing is an integral part of pharmaceutical analysis and routine quality control monitoring of drug. Standard analytical method for Tadalafil impurities determination according to European Pharmacopoeia takes more than 60 minutes of HPLC analysis time. The speed and economic analysis is becoming increasingly important in many application areas of HPLC including pharmaceutical analysis in order to increase throughput and reduce costs. The latest UHPLC instrumentation and stationary phases chemistry allows to successfully reduce analysis time, increase detection and quantification limits. Ultrafast, robust and reliable 6 minutes HPLC method was developed and validated according to European Medicines Agency recommendations for validation of analytical methods. Known Tadalafil impurities were identified using accurate mass TOF instrument and qualified with novel metabolite ID software.

ACKNOWLEDGEMENTS

This work was generously supported by the grant of Scientific Grant Agency of the Ministry of ducation of Slovak Republic and the Academy of Sciences - project VEGA 1/1349/12 and the grant of Slovak Research and Development Agency - project APVV-0583-11. This work is partially outcome of the project VVCE-0070-07 of Slovak Research and Development Agency solved in the period 2008-2011 and Hermes Labsystems Slovakia and Zentiva a.s. Hlohovec.

Invited Speakers Abstracts

ELECTROPHORETICALLY MEDIATED MICROANALYSIS FOR CHARACTERIZATION OF THE ENANTIOSELECTIVE CYP3A4 CATALYZED N-DEMETHYLATION OF KETAMINE

Hiu Ying Kwan, **Wolfgang Thormann**

Clinical Pharmacology Laboratory, Institute for Infectious Diseases, University of Bern, Murtenstrasse 35, CH-3010 Bern, Switzerland

ABSTRACT

An electrophoretically mediated microanalysis method was developed to investigate the stereoselectivity of the CYP3A4 mediated N-demethylation of ketamine. Ketamine was incubated on-line in a 50 µm id bare fused-silica capillary together with human CYP3A4 Supersomes using a pH 7.4 phosphate buffer at 37°C. A plug of reactants containing racemic ketamine and the NADPH regenerating system including all required co-factors for the enzymatic reaction was injected, followed by a plug of the metabolizing enzyme CYP3A4. These two plugs were bracketed by plugs of incubation buffer to ensure proper conditions for the enzymatic reaction. The rest of the capillary was filled with a pH 2.5 running buffer comprising 50 mM Tris and phosphoric acid with highly sulfated γ-cyclodextrin (2%) as chiral selector. Reaction was enhanced by applying a voltage of -10 kV for 10 s. After incubation at 37 °C without power application, the capillary was cooled to 25°C followed by application of -10 kV for the separation and detection of the formed enantiomers of norketamine. Elucidated kinetic values were found to be comparable to those obtained from an off-line assay of a previous study.

Keywords: Electrophoretically mediated microanalysis, electrokinetic chiral separation.

1 INTRODUCTION

Enantioselective capillary electrophoresis is a well established and attractive methodology. Due to high resolution, short analysis time and low consumption of chemicals and solvents, it is applied to assess the stereoselective metabolism of a drug and to characterize enzymatic metabolic pathways *in vitro* [1]. The enzymatic reaction, often followed by an extraction, is typically carried out in a vial prior to the capillary electrophoresis analysis of the products. In recent years, enzymatic metabolic reactions of drugs were also performed in the capillary with subsequent analysis of the formed products [2], an approach which is known as electrophoretically mediated microanalysis (EMMA). In this study, an EMMA method was developed to investigate the stereoselectivity of the CYP3A4 mediated N-demethylation of ketamine to norketamine. Ketamine is a chiral phencyclidine used as an anesthetic drug for short term surgical interventions and in subanesthetic doses for postoperative pain relief. It is known from a previous study that norketamine is not metabolized by CYP3A4 [3]. Thus, quantification of norketamine formation was possible via incubation of norketamine (10-160 µM per enantiomer) instead of ketamine and otherwise identical conditions. Norketamine formation rates were fitted to the Michaelis-Menten model and the elucidated values for V_{max} and K_m were compared to those obtained from the off-line assay of a previous study [4]. The

data obtained revealed that CYP3A4 N-demethylation of ketamine occurs in a stereoselective manner [5].

2 MATERIAL AND METHODS

A Proteome Lab PA 800 instrument (Beckman Coulter, Fullerton, CA, USA) equipped with a 50 μm id fused-silica capillary (Polymicro Technologies, Phoenix, AZ, USA) of 44 cm total length (effective length of 34 cm) was used. Ketamine was incubated on-line in a 50 μm ID bare fused-silica capillary together with human CYP3A4 Supersomes using a 100 mM phosphate buffer (pH 7.4) at 37°C. A plug of about 14 nL volume containing racemic ketamine and the NADPH regenerating system including all co-factors for the enzymatic reaction was injected (plug N+S in panel A of Fig. 1), followed by an equally sized plug of the enzyme CYP3A4 (500 nM) (plug E in panel A of Fig. 1). The two plugs were bracketed by plugs of incubation buffer (IB in Fig. 1A) to ensure proper conditions for the enzymatic reaction. The rest of the capillary was filled with a pH 2.5 running buffer (RB in Fig. 1A) comprising 50 mM Tris, phosphoric acid and 2 % w/v of highly sulfated γ-cyclodextrin (Beckman Coulter). Mixing of reaction plugs was enhanced via application of -10 kV for 10 s. After an incubation at 37 °C without power application, the capillary was cooled to 25 °C within 3 min followed by application of - 10 kV for the separation and detection of the norketamine enantiomers at 195 nm.

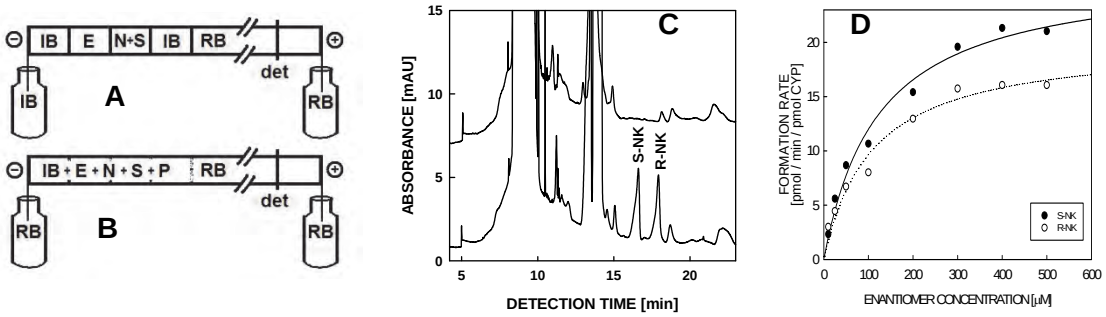

Fig.1: Enzymatic N-demethylation of ketamine to norketamine (NK) in the EMMA format (panel A) with subsequent enantioselective electrophoretic analysis of the formed products (panel B). The electroperograms in panel C were obtained with a 30 min zero-potential amplification time for experiments in presence (lower graph) and absence (upper graph) of racemic ketamine. For data obtained after 8 min zero-potential amplification, the determined norketamine formation rates were fitted to the Michaelis-Menten model (panel D). For details refer to [5].

3 RESULTS AND DISCUSSION

In the EMMA format, norketamine formation rates could be determined with an 8 min zero-potential amplification (Fig. 1D) and the elucidated values for V_{max} and K_m were found to be comparable to those obtained from the off-line assay of a previous study [4,5]. The EMMA based study revealed that the metabolism of ketamine via CYP3A4 is stereoselective (Fig. 1D). To our knowledge, this is the first study using EMMA to assess the kinetics of enantioselective drug metabolism mediated by a CYP450 enzyme. Further work should be addressed to shorten the analysis time, to understand the contribution of electrophoretic transport to plug mixing and to include an internal standard such that the EMMA method can be further improved and widely applied to assess enzymatic activity in a fast, low-cost and automated way.

ACKNOWLEDGEMENTS

This work was supported by the Swiss NSF.

LITERATURE

[1] Caslavska, J., Thormann, W., J. Chromatogr. A 2011, 1218, 588-601.
[2] Fan, Y., Scriba, G.K.E., J. Pharm. Biomed. Anal. 2010, 53, 1076-1090.
[3] Portmann, S., Kwan, H.Y., Theurillat, R., et al., J. Chromatogr. A 2010, 1217, 7942-7948.
[4] Kwan, H.Y., Thormann, W., Electrophoresis 2011, 32, 2738-2745.
[5] Kwan, H.Y., Thormann, W., Electrophoresis 2012, 33, in press.

IDENTIFYING AND QUANTIFYING 10,000 PROTEINS IN 10 HOURS – FEASIBLE, POSSIBLE, DONE?

Konstantin Chingin[a], Juan Astorga-Wells[a,b], Mohammad Pirmoradian Najafabadi[a,b], Harshavardhan Budamgunta[a],Thorleif Lavold[b], and **Roman A. Zubarev**[a,c]

[a] *Physiological Chemistry I, Department of Medical Biochemistry and Biophysics, Karolinska Institutet, SE-17 177 Stockholm, Sweden*
[b] *Biomotif AB, Stockholm, Sweden*
[c] *Science for Life Laboratory, Stockholm, Sweden*

It took proteomics more than 15 years from its inception to reach the bottom of the proteome – that is, to observe whole or almost whole expressed proteome (≥10,000 proteins). The very few reports on this achievement published so far have exercised little restrain on the amount of used material, labor or instrumental cost. Despite the recent advances in mass spectrometric instrumentation, it is clear that routine application of the whole-proteome analysis will require development of instruments and methods going far beyond the current state of the art. In particular, the very large dynamic range of cellular proteome – some seven orders of magnitude – by almost 1000 times exceeds the dynamic range of the most advanced proteomics instruments. Traditionally, dealing with this problem requires extensive separation of proteins and peptides before the LC/MS analysis, which is one of the limitations of the whole proteomics as it is currently practiced. The task is therefore to reduce the pre-LC/MS separation to a bare minimum. In principle, a well-designed LC/MS experiment can analyze over 1000 unique proteins per hour of LC gradient. Therefore, aiming at detecting and quantifying 10,000 proteins in 10 h is a realistic (although at the moment of writing this abstract not yet reached) goal.

In our laboratory, we pursue three independent approaches, each of which should in principle be capable of delivering the desired number of proteins within given time limits. One of them is using a novel device for fractionation of peptides in ESI-friendly solution by their pI values [1]. This and other two approaches will be described; their relative advantages will be discussed, and the most recent results presented.

LITERATURE

[1.] Chingin, K.; Astorga-Wells, J.; Pirmoradian Najafabadi, M.; Lavold, T.; Zubarev, R. A. Separation of polypeptides by isoelectric point focusing in electrospray-friendly solution using multiple-junction capillary fractionator, Anal. Chem., in press.

LASER ASSISTED MASS SPECTROMETRIC IMAGING OF PLANTS, INSECTS, AND BACTERIA

Aleš Svatoš[a], Filip Kaftan[b], Vladimír Vrkoslav[b], Josef Cvačka[b], Dirk Hörscher[c], Hans Peter Saluz[d]

[a] Mass spectrometry/Proteomics research Group, Max Planck Institute for Chemical Ecology, Hans-Knöll-Straße 8, D-07745 Jena, Germany
[b] Institute of Organic Chemistry and Biochemistry, Academy of Science of the Czech Republic, v. v. i., Flemingovo nám. 2, CZ-166 10 Prague 6, Czech Republic
[c] Department of Entomology Max Planck Institute for Chemical Ecology, Hans-Knöll-Straße 8, D-07745 Jena, Germany
[d] Department of Cell and Molecular Biology, Leibniz Institute for Natural Product Research and Infection Biology – Hans Knöll Institute, Beutenbergstr. 11a, 07745 Jena, Germany
svatos@ice.mpg.de

ABSTRACT

Matrix-assisted laser desorption/ionization (MALDI) mass spectrometry imaging (MSI) has recently found frequent application in mapping the distribution of small molecules in numerous biological samples or tissues. The data obtained using MSI have been used to follow or explain important biological processes or to rationalize previous biological observations. But because many experiments have been performed on a qualitative level, no data have been obtained regarding the concentration of imaged compounds in the samples. Here we offer a reasonably simple method to fill this gap.

We developed and optimized protocols for sample preparation for MSI experiments either using laser desorption/ionization (LDI) of matrix-assisted desorption/ionization (MALDI) for ionization of metabolites from surfaces. In one case quantification of glucosinolates on *Arabidopsis thaliana* leaves was successfully implemented.

Using developed set of methods we can perform qualitative and quantitative MSI of surface – accruing metabolites ranging from neutral and polar lipids, phenolics, phytoallexins. Obtained distribution maps were correlated with biological activity of visualized compounds and in many cases these MSI maps strongly support proposed biological hypothesis.

Modern MSI methods are ready to contribute to surface chemistry analysis and addressing pending biological questions on spatial distributions of chemical signals.

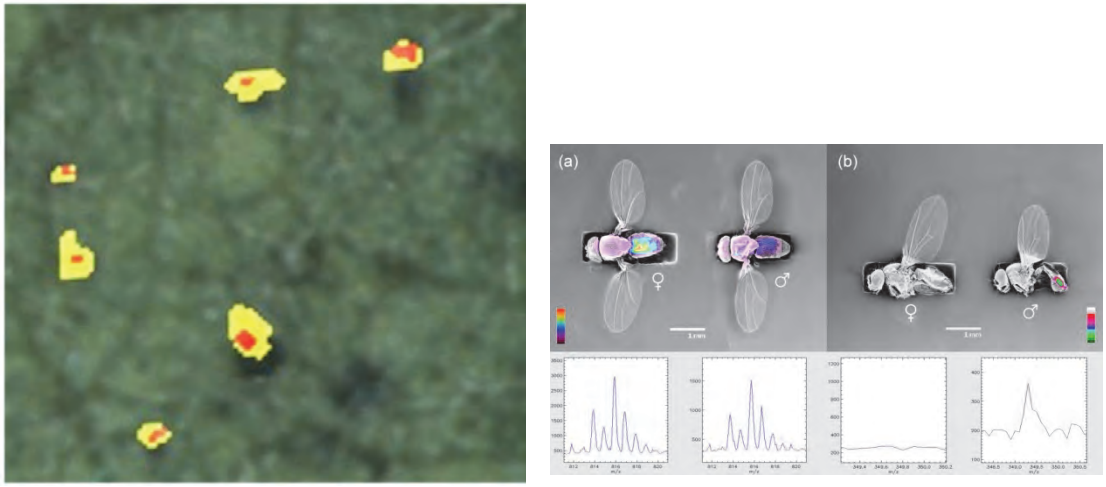

Fig. 1. LDI-MSI of cotton leaves and fruit flies surfaces. Pigment gland of leaves are co-localized with areas of gossypol high concentrations (in red/yellow color). TGA and cVA (male) were detected on the fly body.

ACKNOWLEDGEMENTS

Financial supports from Max Planck and Leibniz Societies are cordially acknowledged.

LITERATURE

[1.] Svatos, A Mass spectrometric imaging of small molecules. *Trends Biotechnol.* **2010**, *28*, 425-43.

[2.] Hölscher, D., Shroff, R., Knop, K., Gottschaldt, M., Crecelius, A., Schneider, B., Heckel, D. G., Schubert, U. S., Svatos, A. Matrix-free UV-laser desorption/ionization (LDI) mass spectrometric imaging at the single-cell level: Distribution of secondary metabolites of *Arabidopsis thaliana* and *Hypericum* species. *Plant J.* **2009**, 60, 907-918.

[3.] Vrkoslav, V.; Muck, A.; Cvačka, J.; Svatoš, A. *J. Am. Soc. Mass. Spectrom.* **2010,** *21*, 220-231.

CE-ESI TOF MS FOR THE ANALYSIS OF INTACT PROTEINS: RECENT PROGRESS AND THE APPLICATION TOWARDS THE DIFFERENTIATION OF VARIOUS EPO PREPARATIONS

Christian Neusüß, Angelina Taichrib, Markus Pioch

Aalen University, Beethovenstr. 1, D-73431 Aalen, Germany
christian.neusuess@htwaalen.de

ABSTRACT

CE/MS is gaining importance as an analytical technique especially for the identification and characterization of intact proteins. A CE/MS method has been optimized with respect to the general application for small intact protein analysis in biopharmaceutical applications. Various capillary coating procedures have been compared for a range of different small proteins as well as erythropoietin glycoforms. A commercial soluble acrylamide-based coating results in efficient and reproducible separation (migration times mean RSD = 1.4%; peak areas mean RSD = 12.3%) using an optimized rinsing and re-coating procedure [1]. Separation efficiency in the context of various coatings will be discussed in detail based on calculations of corrected mobilities of the proteins.

The optimized method has been validated with respect to major parameters. An extensive principal component analysis revealed that the presented method is robust and useful for the relative quantitation of proteins and protein isoforms. In this way the presented method will contribute to the improved characterization of a large variety of intact proteins in the biomedical and pharmaceutical area and will enable the differentiation of different preparations including possible counterfeits.

Keywords: CZE-MS, intact proteins

1 METHODS

A CE experiments were performed on a HP ^{3D}CE (Agilent Technologies, Waldbronn, Germany) using capillaries with an ID of 50 µm and a length of approximately 60 cm. The coating solutions used were UltraTrol™ low normal (LN) and UltraTrol™ high reversed (HR) (both derivatized polyacrylamide, Target Discovery, Palo Alto, CA, USA) and 0.1 mg/mL N,N-dimethylacrylamide-ethylpyrrolidine metacrylate copolymer in water (hereafter termed “copolymer” – lab prepared and kindly provided by A. Cifuentes, Spain). Permanently coated capillaries (Guarant™ from Alcor BioSeparations, Palo Alto, CA, USA, and polyacrylamide (PAA) coated capillaries from WICOM, Heppenheim, Germany) were conditioned only with

water. The trimethoxysilylpropyl(polyethylenimine) coating (PEI, Gelest Inc., Morrisville, PA, USA) was prepared according to the US Patent 6,923,895 B2, applying one layer. BGE consisted of 0.5 mol/L or 1mol/L acetic acid.
The CE-MS coupling was carried out via electrospray ionisation (ESI) using a commercial CE-ESI-MS interface (Agilent Technologies, Waldbronn, Germany) which has a triple-tube-design. A co-axial sheath liquid (SL) flow, typically composed of water and 2-propanol (1:1 v/v) with an addition of 1% HAc, was provided during analyses at a flow rate of 3 µL/min.
A micrOTOFQ quadrupole time-of-flight mass spectrometer controlled by micrOTOFcontrol software (Bruker Daltonik GmbH, Bremen, Germany) was used. The ESI sprayer was grounded while the transfer capillary was kept at a constant voltage of -4500 V (positive ion polarity mode). The nebulizer gas (nitrogen) pressure was set to 0.2 bar. The ion optics were optimized to the highest possible intensity in the mass range of m/z 700 – 3000.

2 COMPARISON OF VARIOUS COATINGS FOR THE ANALYSIS OF INTACT PROTEINS BY CE-MS

Different neutral and cationig coatings were tested both for a set of standard proteins and the separation of glycoforms of recombinant human erythropoietin. The results are shown in Fig. 1.

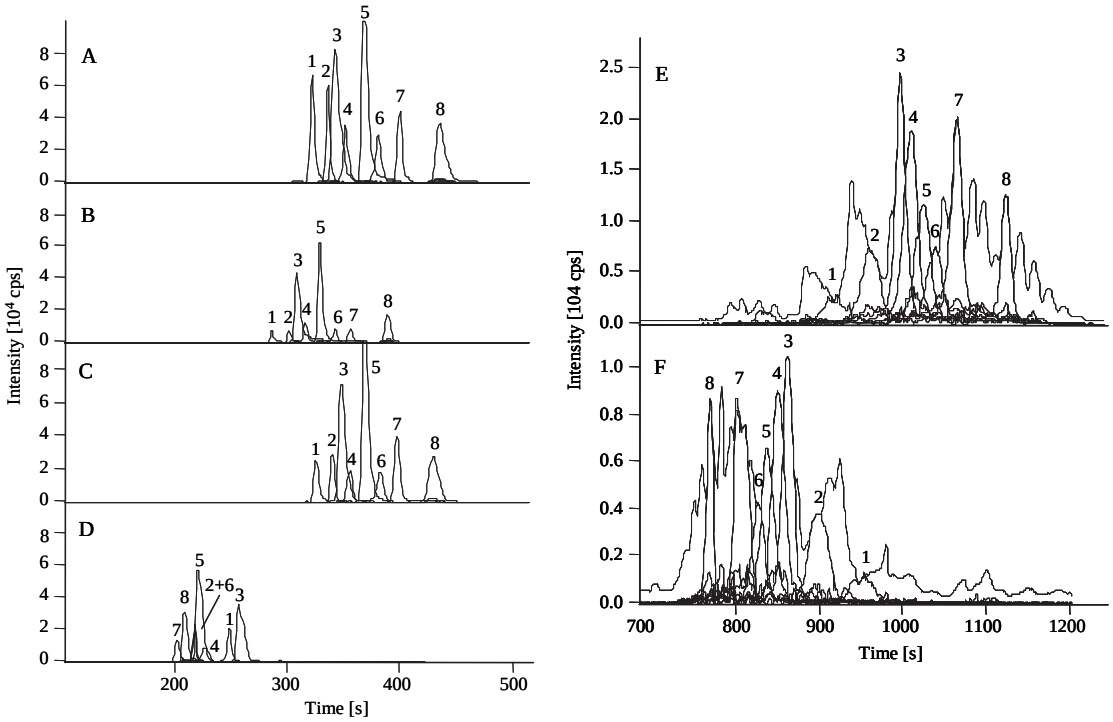

Fig. 1: Separation of model proteins lysozyme (1), β-lactoglobulin A (2), cytochrome c (3), RNase A (4), myoglobin (5), RNase B (6), trypsin inhibitor (7), and carbonic anhydrase (8) in different coated capillaries: A. LN, B. permanent PAA, C. Guarant™, D. PEI coating. Separation of rhEPO on a LN (E) and a HR (F) coated capillary. The dotted lines represent the base peak electropherograms, while the solid lines show the ion traces of some selected EPO glycoforms.

2 DIFFERENTIATION OF EPO PREPARATIONS BASED ON GLYCOFORM DISTRIBUTION

Based on the distribution of major glycoforms taking sialilation, antennarity, and acetylation into account various preparations of EPO were compared. Using Principal Component

Analysis all preparations, including those with small differences (different batches) could be differentiated based on the first three PCs. As an example the score plot of PC1 versus PC2 for 14 preparations is shown in Fig. 2. The overlaying groups are separated in the third dimension (PC1-PC3).

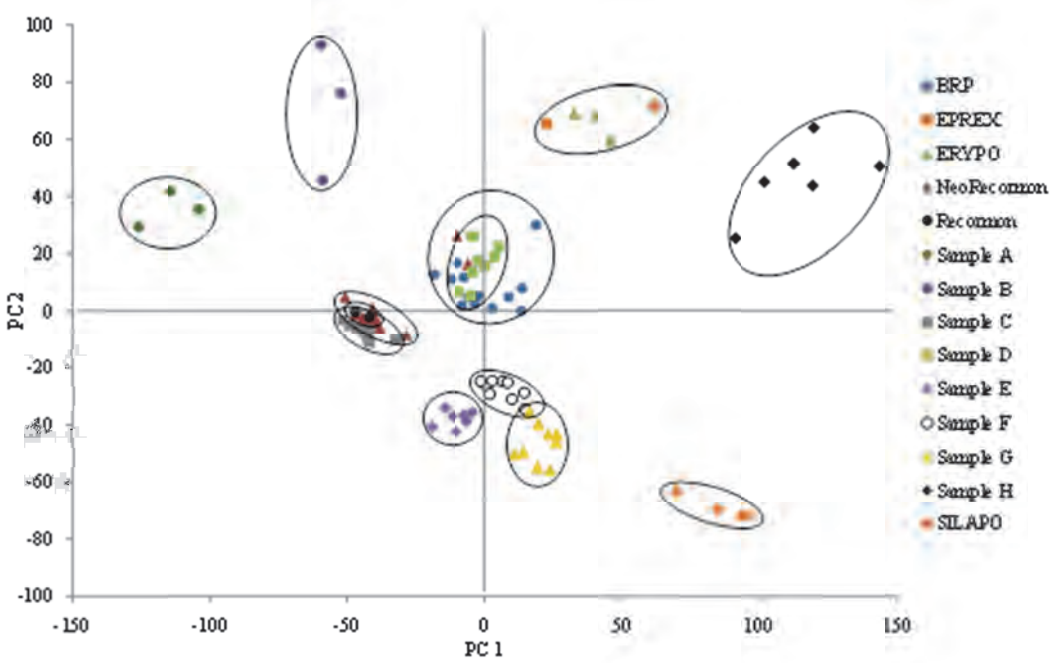

Fig. 2: Score plot for PC1 and PC2 of the PCA on the different EPO preparations.

3 CONCLUSIONS

CE-MS is an information rich technique for the analysis of intact protein. The presented method is fast, robust and reliable. Thus, detailed characterization of complex (glycol)proteins are possible enabling the straightforward optimization of biopharmaceuticals as well as the detection of counterfeits.

ACKNOWLEDGEMENTS

The authors would like to thank V. Dolník for kindly providing the Guarant™ capillary and A. Cifuentes for kindly providing the N,N-dimethylacrylamide-ethylpyrrolidine metacrylate copolymer. J. Sommer is acknowledged for his help on the EOF measurements. The authors acknowledge financial support in the course of the announcement "Sicherung der Warenketten" of the Federal Ministry of Education and Research (BMBF) within the scope of the program "Forschung für die zivile Sicherheit" of the Federal Government.

LITERATURE

[1.] Angelina Taichrib, Markus Pioch, Christian Neusüß, *Electrophoresis* 2012*, 33,* 1356–1366.

[2.] Angelina Taichrib, Markus Pioch, Christian Neusüß, *Anal Bioanal Chem*, 2012, *403*, 797–805.

OPTIMISATION IN THE CHIRAL AND ACHIRAL SEPARATION OF A MULTICOMPONENT SAMPLE IN ELECTROKINETIC CHROMATOGRAPHY: METHODOLOGY DEVELOPMENT

Alessandro Giuffrida, Marianna Messina, Annalinda Contino, **Vincenzo Cucinotta**

Department of Chemical Sciences, University of Catania, viale A. Doria 6, 95125 Catania, Italy
ecucinotta@unict.it

ABSTRACT

A set of ten different enantiomeric pairs of dansyl-derivatives of α-amino acids were contemporarily separated in electrokinetic chromatography, by the use as selector of a cyclodextrin derivative synthesised in our laboratory through an accurate strategy of choice of the experimental conditions. As a part of this strategy, we have developed a procedure of identification of the single peaks in the electropherograms called LACI (lastly added component identification).

Keywords: chiral separations, electrokinetic chromatography, amino acids

1 INTRODUCTION

Cyclodextrins are natural cyclic oligosaccharides, that, owing to their molecular recognition ability and to their chirality, represent one of the most important class of chiral receptors [1]. Their peculiar properties have been much exploited in separation science, and particularly in capillary electrophoresis [2-5]. However, in this technique, a strong limit is represented by their electrical neutrality, which excludes their use for the separation of neutral analytes. Also as concerns charged analytes, there is no doubt that the presence of a charge in the selector molecule makes easier the separation, particularly between enantiomers, by increasing the difference of electrophoretic mobility between the free and the complexed analyte. In a series of papers [6-10], we have described the application of cyclodextrins derivatives of different kind, synthesised in our laboratory, to chiral separations in capillary electrophoresis (CE). All of them include a moiety with acid-base properties, which thus can become charged in the function of the pH value. Beside other kind of derivatives obtained by fluorescein isothiocyanate derivatisation, recently investigated by some of us [11-13], we have dedicated much attention to the dansyl derivatives of amino acids (DNS-AAs) [14-17], a class of chiral analytes which has been much studied in literature [18-20]. The chiral selectors that we used represent different kind of cyclodextrin derivatives. Beside a monoderivative on primary position, the 6-Mono-deoxy-(2-aminoethylamino)-β-CD (CDen) [21], and a γ-cyclodextrin derivatized on a secondary position, the 3-deoxy-3-amino-2(S),3(R)-γ-cyclodextrin (GCD3AM) [22], three selectors are hemispherodextrins [15,17,23], a class of cyclodextrin derivatives specifically designed in our laboratory, and characterised by the presence, in addition to the well known cyclodextrin cavity, of a bridge between two opposite position of the primary rim. If we look at the resolution values obtained in the separation between the members of enantiomeric pairs of DNS-AAs, also in the presence of very low concentration of chiral selector (in some cases nearly equal to the concentration of the analytes), we see how effective are these molecules for the chiral separation of this class of analytes.

As a further step in this project, we thought to tackle the problem of the contemporary separation of the investigated enantiomeric pairs. From the preliminary experiments, it was soon clear that it was a quite difficult task. Thus, we have decided to proceed by developing a specific methodology, and here, we report the results obtained in the separation of ten enantiomeric pairs of DNS-AAs out of the eleven shown in Fig. 1 using as chiral selectors

both GCD3AM [16] (without the serine pair) and the 6A,6D-dideoxy-6A,6D-N-[6,6'-di-(β-alanylamido)]-6,6'-dideoxy-α,α'-trehalose]-β-CD (THALAH) [15] (without the threonine pair), also shown in Fig. 1.

2 EXPERIMENTAL

2.1 Materials

The syntheses of GCD3AM [22] and of THALAH [15] have been previously reported. Dns-amino acids were obtained from Fluka, Sigma–Aldrich, Buchs, Switzerland.

2.2 Measurements

CE measurements were carried out on a Beckman P/ACE MDQ equipped with a diode array detector. An uncoated fused-silica capillary (Beckman, 61.0 cm total lenght, 51.0 cm effective lenght, 75 μm i.d.) was held at a constant temperature of 25 °C. The system operated at a variable voltage varying in the 20 - 30 kV range. BGEs for the separation experiments were prepared by dissolving CD derivatives (1.5-3mM) in 20mM of ammonium acetate at pH=6.8. The sample solutions (0.03mM in each racemate) were obtained by dissolving the analites in Milli-Q water. The samples were hydrodynamically injected at 0.6 psi for 8 s. Before each experiment, the capillary was flushed (pressure of 20 psi) with 100mM of NaOH, 20mM of CH3COONH4, and the BGE used in separation.

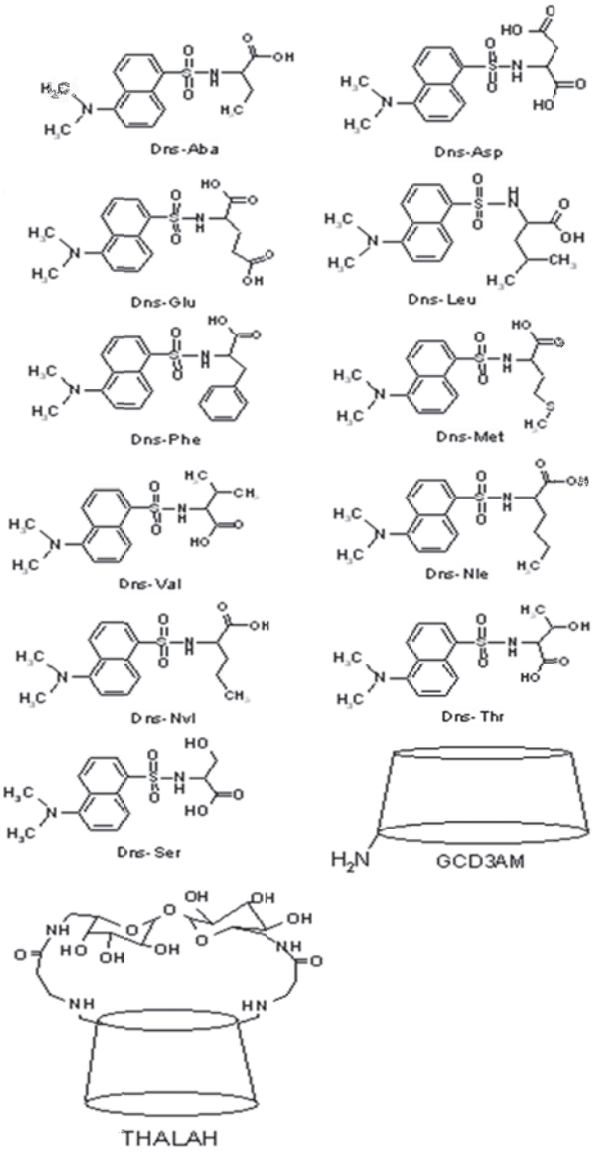

Fig. 1. Schematic structures of the studied analytes and selectors.

3 RESULTS AND DISCUSSION

We will discuss the influence of three different parameters on the separations of the enantiomeric pairs of DNS-AAs reported in Fig.1, using as selector THALAH, and then we will show the method for identifying the single analytes which we have developed, using as an example the system with GCDAM3 as selector.

3.1 Varying the pH value of the BGE

First of all, we should recall the acid-base properties both of the selector and of the analytes. All the data were directly determined by following the variation of the electrophoretic mobility in the function of the BGE pH. The selector, in the absence of metal ions, behaves as a diamine, thus undergoing a double protonation (log K_1 = 7.7; log K_2 = 5.2, values determined elsewhere [2]).

After dansylation, the amino acid has a carboxylic group, while the primary amino group is substituted by the tertiary amino group of the naphthyl ring, whose basicity is very low (log K < 3.5). The protonation values of the carboxylate are much higher than in the parent amino acid (log K is about 4.1). It should be recalled that the derivatives of glutamic and aspartic acid are exceptions, due to the presence of a second carboxylate group (log K_1 > 5.5 ; log K_2 < 3.5).
As a test of the utility of the electrophoretic data in order to follow the protonation of the components of the investigated system, let us consider the electrophoretic mobilities of our analytes at two different pH values, which we have reported in Table 1. It is readily apparent that at alkaline pH the mobilities for aspartate and glutamate derivatives are far higher than for all the other analytes, due to their double negative charge, compared with one negative charge for all the other analytes. Going to pH = 4.7, while the two dianionic species undergo a partial protonation, becoming monoanionic, the other analytes slightly decrease the absolute value of their mobility, thus showing that the protonation in their cases is only started, and the anion is still the main species. These protonation data are important for two different reasons. One reason is that the electrostatic interaction between analyte and selector gives a significant contribution to the effectiveness of the separation, as easily shown in the separation of the DNS-AAs with GCD3AM [3], carried out at three different pH values. The influence of the selector on the increase of the mobilities of the analytes was maximum in the case of pH = 6.8, where almost all the selector is cationic and the analytes are almost completely deprotonated (though, obviously, in the cases of aspartate and glutamate the species will be dianionic). The second reason is that at pH values near to the log K values, the influence of the pH on both the formation degrees of the species and consequently on the observed mobility values of the analytes is very strong. When we investigate the systems with the contemporary presence of an enantiomeric pair of DNS-AA and THALAH, we readily realise that, in order to optimise the separation process, due to the overlapping between the pH ranges of protonation of analyte and selector, we are forced to carry out the experiments at a pH value of compromise, where both of them undergo a strong variation of their protonation degree. Due to the presence of different species for each component, we have the contemporary formation of different complexes, on varying the specific species involved. This prevents us from obtaining a straightforward correlation between the measured electrophoretic mobility and the equilibria data concerning the formation of the complexes even in the simplest case of the presence of one enantiomeric pair. Experimental data confirm this thesis, no further suggestion can be obtained by these experiments in order to optimise the pH where to carry out the multicomponent separation. Thus, we have chosen the pH value for the separation only on the basis of the values of protonation constants. The value of 5.1 is sufficiently high to have the analytes almost completely anionic and it is sufficiently low to have still more than 50% of the selector deprotonated.

Table 1. Mobility values (10^{-9} $m^2V^{-1}s^{-1}$) corrected for EOF, at two different pH values for the free analytes. **DNS-AAs**

	μ_{corr}	
	pH=4.7	pH=9.3
dns-asp	-17.53	-27.44
dns-met	-12.92	-14.55
dns-glu	-16.23	-26.80
dns-ser	-13.04	-16.02
dns-aba	-12.3	-15.58
dns-val	-11.58	14.94
dns-leu	-12.00	-14.46
dns-nrv	-12.2	-15.00
dns-nrl	-12.24	-14.73
dns-phe	-11.59	-14.87

3.2 Varying the electric field

The increase of the electric field influences the separation by two distinct effects. The former effect is due to the narrowing of the peaks, and the second is the decrease in the migration times, due to the increase of both the electrosmotic flow (EOF) and the electrophoretic mobility. Since the efficiency depends in an opposite way by both these factors, the result will depend on the prevailing effect. In our case, the increase of electric field gave rise to a parallel increase in efficiency and correspondingly in resolution, and thus we have chosen the highest investigated voltage value (30 KV).

3.3 Varying the selector concentration

This parameter is perhaps the most difficult to optimise. This mainly depends on the difficulty to transfer the information that we can obtain by the study of a single enantiomeric pair to the case of the multicomponent sample. What occurs is that any analyte perturbs the equilibria concerning all the other analytes through the use of the selector for the equilibrium of formation of its own complex, and thus reducing the available concentration of selector for all the other analytes. This means that any investigation, even the most accurate, concerning the specific analyte enantiomeric pair, gives very poor information for the case of interest of contemporary separation of many enantiomeric pairs. Thus, we have simply decided to vary the selector concentration in order to verify what value would assure the highest number of resolved peaks. By this quite empiric procedure, whose results are reported in Fig. 2, we have succeeded to resolve all the peaks (20 peaks can effectively be observed in the corresponding electropherogram), when using 1,8 mM as concentration of THALAH (at a voltage of 30KV and a pH of 5.1, values chosen as described in the previous sections).

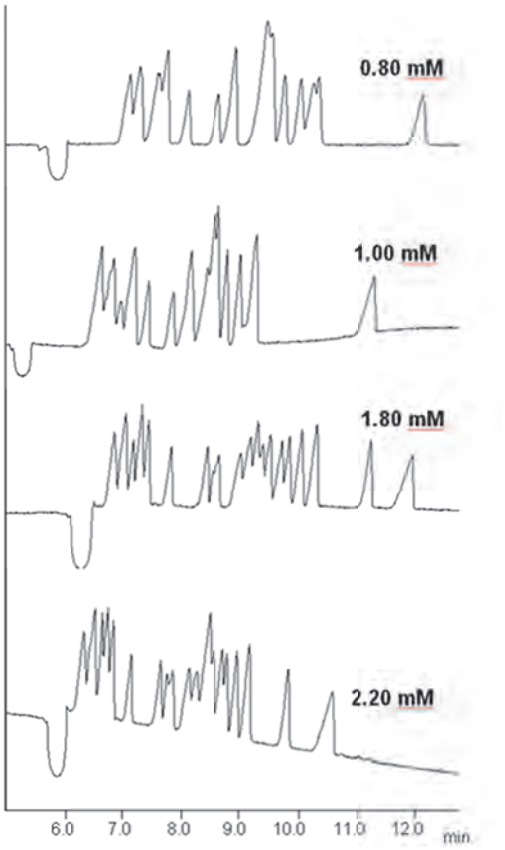

Fig. 2. Electropherograms of the multicomponent system at different concentrations of THALAH (pH = 5.1, ΔV = 30 KV.

3.4 Identifying the single analytes (LACI)

This procedure can be easily understood by showing the electropherograms reported in Fig. 3. It shows the addition in successive steps of each enantiomeric pair in the chosen experimental conditions of pH, selector concentration and electric field. In this case, as said before, we used as selector GCDAM3, its concentration was 1.8 mM, the pH was 6.8 (by ammonium acetate), and the applied voltage 20 KV.
The identification of each analyte was obtained by looking at the new peaks appearing in the electropherograms after the addition of the concerned enantiomeric pair.

As concerns the identification of the specific enantiomer for each amino acid pair, and thus of the enantiomer migration order (EMO), we have exploited the data elsewhere obtained [16], where the identification was carried out by adding an excess of the L-enantiomer to differentiate it from the D-enantiomer. The visual inspection of the electropherograms, while confirming that the addition of new analytes influences the equilibria concerning the analytes already present in the sample, as shown by the slight variation in the peaks due to other analytes, removes any possible doubt about their identification. We call this procedure "lastly added component identification" (LACI).

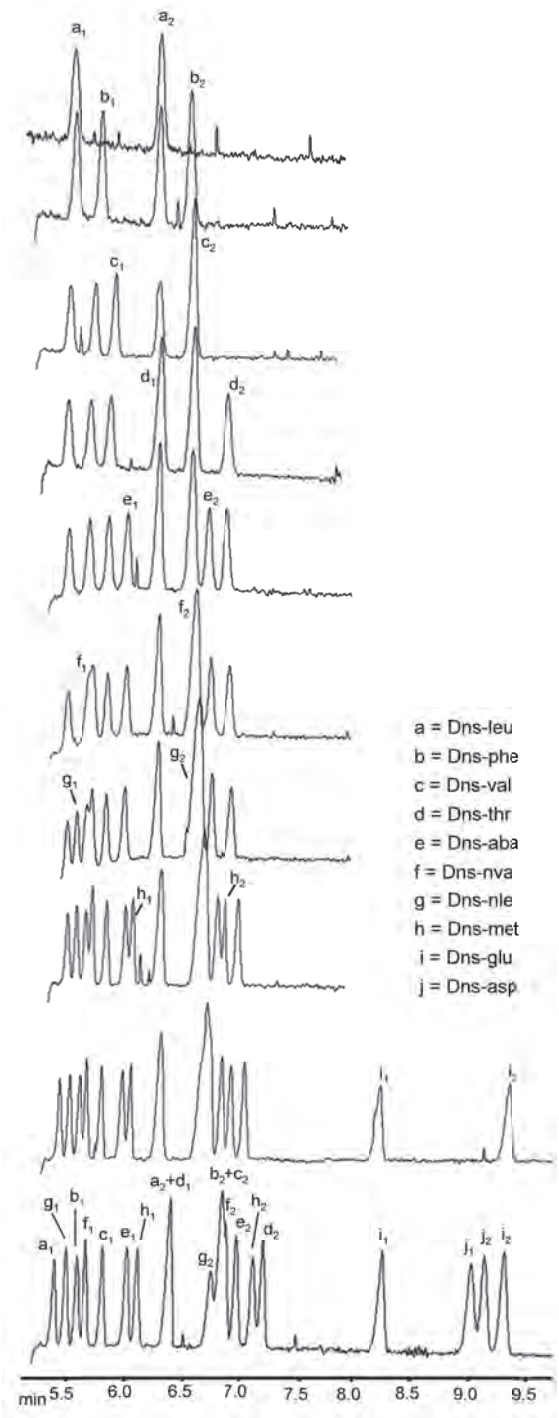

Fig. 3. Electropherograms showing the LACI procedure in the presence of GCD3AM (pH = 6.8, ΔV = 20 KV).

4 CONCLUDING REMARKS

The challenge to separate many enantiomeric pairs of similar analytes was tackled by a complex strategy involving the variation of different experimental parameters.

In order to identify the single analytes one by one, a procedure was developed which we call LACI. Further applications of the present methodology will be carried out in order to further optimise the separation, also for new systems.

LITERATURE

[1.] Szejtli, J. *Chem. Rev.* 1998*, 98*, 1743–1753.

[2.] Juvancz, Z., R. Bodane, Kendrovics, R., Ivayi, R., Szente, L., *Electrophoresis* 2008, *29*, 1701-1712.

[3.] Tang, W., Ng, S.,C., *J. Sep. Sci*., 2008, *31,* 3246-3256.

[4.] Fanali, S., *Electrophoresis,* 2009, *30,* S203-S210.

[5.] Scriba, G., K., E., *J. Sep. Sci.,* 2008, *31,* 1991-1999.

[6.] Cucinotta, V., Giuffrida, A., Grasso, G., Maccarrone, G., Vecchio, G., *Analyst*, 2003**,** *128,* 134-136.

[7.] Cucinotta, V., Giuffrida, A., La Mendola, D., Maccarrone, et al. *J.Chromatogr. B*, 2004, *800,* 127-133.

[8.] Cucinotta, V., Giuffrida, A., Maccarrone, G., Messina, M., et al., *J.Pharm.Biomed.Anal.,* 2005, *37*, 1009-1014.

[9.] Cucinotta, V., Giuffrida, A., Maccarrone, G., Messina, M., et al., *Dalton Trans.*, 2005, 2731-2736.

[10.] Cucinotta, V., Giuffrida, A., Maccarrone, G., Messina, M., Vecchio, G., *Electrophoresis,* 2006, *27*, 1471–1480.

[11.] Giuffrida, A., Leon, C., Garcia-Canas, V., Cucinotta, V., Cifuentes, A., *Electrophoresis*, 2009, *30*, 1734-1742.

[12.] Giuffrida, A., Tabera, L., Gonzales, R., Cucinotta, V., Cifuentes, A., *J. Chromatogr. B*, 2008, *875,* 243–247.

[13.] Giuffrida, A., Caruso, R., Messina, M., Maccarrone, G., et al., *J. Chromatogr. A.,* 2012, in press.
[14.] Cucinotta, V., Giuffrida, A., Grasso, G., Maccarrone, G., et al., *J. Chromatogr. A*, 2007, *1155*, 172-179.
[15.] Cucinotta, V., Giuffrida, A., Maccarrone, G., Messina, M., et al., *Electrophoresis*, 2007, *28*, 2580-2588.
[16.] Giuffrida, A., Contino, A., Maccarrone, G., Messina, M., Cucinotta, V., *J. Chromatogr. A,* 2009, *1216*, 3678-3686.
[17.] Cucinotta, V., Giuffrida, A., Grasso, G., Maccarrone, et al., *J. Sep. Sci.* 2011, *34*, 70-76.
[18.] Sanchez-Hernandez, L., Castro-Puyana, M., Marina, M., L., Crego, A., L., *Electrophoresis*, 2012, *33*, 228-242.
[19.] Kitagawa, K., Otsuka, K., *J. Chromatogr. B*, 2011, *879,* 3078-3086.
[20.] Schmid, M., G., Gübitz, G., *Anal. Bioanal. Chem*. 2011, *400* , 2305–2316.
[21.] Bonomo, R.,P., Cucinotta, V., D'Alessandro, F., Impellizzeri, G., et al., *J.Incl.Phenomena*, 1993, *15,* 167-180.
[22.] Contino, A., Cucinotta, V., Giuffrida, A., Maccarrone, G., Messina, M., et al., *Tetrahedron Lett*., 2008, *49,* 4765-4767.
[23.] Cucinotta, V., Grasso, G., Vecchio, G., *J. Incl. Phen. Mol. Rec.* 1998, *31*, 43–55.
[24.] Cucinotta, V., Contino, A., Giuffrida, A., Maccarrone, G., Messina, M., *J. Chromatogr. A*, 2010, *1217,* 953-967.
[25.] Giuffrida, A., Contino, A., Maccarrone, G., Messina, M., Cucinotta, V., *Electrophoresis* 2011, *32*, 1176-1181.

CAPILLARY ELECTROPHORESIS (CE) AS A PROMISING TECHNOLOGY FOR FIELD AND POINT-OF-CARE (POC) INSTRUMENTS

Mihkel Kaljurand

Institute of Chemistry, Tallinn University of Technology, Akadeemia tee 15, Tallinn, Estonia
mihkel@chemnet.ee

CE was very actively studied at the beginning of the 1990s, but its development has stagnated in recent years. We need new ideas to develop further this not fully acknowledged field. Surprisingly, CE has received little recognition as a promising technology for field and POC analysis. Field analytical chemistry and *in situ* analysis at POC are growing trends that have the potential to liberate the analyst from tedious and inconvenient sample treatment.
As stated by Ryvolova et al. [1] capillary-based systems have certain unmatched advantages (compared to chip-based miniaturized CE), especially in the relative simplicity of the regular cylindrical geometry of the CE capillary, maximal volume-to-surface ratio, no need to design and to fabricate a chip, low costs of capillary compared to chip, and better performance with some detection techniques.
We will describe a new portable CE instrument design based a contactless conductivity detector (CCD). The device is intrinsically small in size, and many interesting analytes can be detected with a CCD. It performs adequately, is able to work in harsh environments with a minimal number of failures, and is easy to maintain and operate. Appropriate sampling methods have been developed for such instruments: surface wipe sampling and soil extraction. The instrument has been used for determination of environmental pollutants, of genuine chemical warfare agents and residues after explosions.
An automated fraction collection interface was developed for coupling portable CE with MALDI-MS. This fraction collection approach is based on the electrowetting on dielectric (EWOD) phenomenon performed on a digital microfluidic (DMF) board [2]. For situations in which the amount of sample is limited, an advanced sampling method based on DMF will be presented [3].

Keywords: capillary electrophoresis; point of care analysis; digital microfluidics

LITERATURE

[1.] Ryvolova, M., Preisler, J., Brabazon, D., Macka, M., Trends Anal. Chem. 2010, 29, 339-353.
[2.] Gorbatsova, J., Borissova, M., Kaljurand, M., ELECTROPHORESIS 2012, 33, 2682–2688.
[3.] Gorbatsova, J., Jaanus, M., Kaljurand, M., Anal. Chem. 2009, 81, 8590–8595.

STUDY OF ANTIBACTERIAL ACTIVITY BY CAPILLARY ELECTROKINETIC SEPARATION METHODS

Hervé Cottet[a], Farid Oukacine[a,b], Nicolas Sisavath[a], Delphine Destoumieux-Garzón[c], David M. Goodall[d], Laurent Garrelly[b]

[a] *Institut des Biomolécules Max Mousseron (UMR 5247 CNRS, Université de Montpellier 1, Université de Montpellier 2), place Eugène Bataillon CC 1706, 34095 Montpellier Cedex 5, France.* hcottet@univ-montp2.fr
[b] *COLCOM SARL, Cap Alpha Avenue de l'Europe, Clapiers 34940 Montpellier, France*
[c] *Laboratoire Ecologie des Systèmes Marins Côtiers (UMR 5119 CNRS, Université Montpellier 2, IRD, Ifremer and Université Montpellier 1), 34095 Montpellier, France*
[d] *Paraytec Ltd, York House, Outgang Lane, Osbaldwick, York YO19 5UP, United Kingdom*

ABSTRACT

The excessive use of antimicrobials both in humans and animal husbandry has led to emergence of bacterial strains which are resistant to a range of antimicrobials, including first-choice agents for the treatment of humans [1]. Thus, the emergence of resistance to antibacterials requires the search for new anti-infective compounds and rapid identification of their antibacterial efficiencies.

Different methodologies based on capillary electrophoresis (CE) are proposed to study the antibacterial activity and the interactions between antibacterial compounds and bacteria. The possible antibacterial activity of cationic molecules on bacteria (Gram-positive and Gram-negative) can be studied by detecting the bacteria before, during and after their meeting with the cationic antibacterial compound. For that, a UV area imaging detector having two loops and three detection windows was used with a 95 cm × 100 μm i.d. capillary. In the antibacterial assay, the bacteria (negatively charged) and the cationic molecules were injected separately from each end of the capillary [2]. The bacteria were mobilized by anionic ITP mode [3] while cationic molecules migrate in the opposite direction in conditions close to CZE. The assay was used to study the antibacterial activity of the second generation of dendrigraft poly-*L*-lysines (DGL) on *Micrococcus luteus* and *Erwinia carotovora*. The results obtained showed a fast bacteriolytic activity against *Micrococcus luteus* and a strong interaction with *E. carotovora*. Stoechiometry and affinity constant of the interaction between DGL and *E. carotovora* were also studied by electrokinetic separation techniques, leading to quantitative data at a molecular level. Since dendrigraft poly-*L*-lysines are non-immunogenic and with low toxicity, this new class of dendritic biomacromolecules is very promising for antibacterial applications.

Keywords: Capillary electrophoresis, bacteria, antibacterial activity

1 EXPERIMENTAL SECTION

1.1 Capillary electrophoresis with multiple UV detection points for antibacterial assay

CE experiments were carried out with a 3D-CE instrument (Agilent technologies system, Waldbronn, Germany) equipped with a diode array detector. Separation capillaries prepared from bare silica tubing were purchased from Composite Metal Services (Shipley, UK). The temperature of the capillary cassette was maintained constant at 25 °C. Leading electrolyte (LE) was composed of 4.5 mM Tris + 50 mM boric acid + 3.31 mM HCl. Terminating electrolyte (TE) was of 13.6 mM Tris + 150 mM boric acid. The pH values of leading and terminating electrolytes are respectively 7.28 and 7.94. Between each run, the capillary was washed with LE for 10 min. Immediately prior to the injection, the bacteria samples were vortexed during 1.5 min to avoid bacteria sedimentation in the vial. UV detection at three independent windows in a looped capillary was carried out with an ActiPix D100 UV area imaging detector (Paraytec, York, UK). The light source was a pulsed xenon lamp and the selected wavelengths were 280 and 214 nm using filters with 20 nm bandpass (full width at half-maximum). The sample rate used for acquisition was 20 Hz and the detector constant time was 0.1 s.

1.2 Hydroxypropyl cellulose coating

The hydroxypropyl cellulose (HPC) coated capillaries were prepared by dissolving the HPC polymer (M_w 10^5 g mol^{-1}) at room temperature in water to a final concentration of 5% (w/w). The 1 m length capillary columns were filled with the polymer solution using a syringe pump (KDS100, Holliston, USA) for 30 min, and the excess of polymer solution was removed using N_2 gas at 0.4 bar. The HPC polymer layer was immobilized by heating the capillary in a GC oven (GC-14A, Shimadzu, France) at 60 °C for 10 min and using a linear ramp from 60 °C to 140 °C at 5 °C/min, and finally 140 °C for 20 min, keeping N_2 pressure at 0.4 bar. Before use, the coated capillaries were rinsed with water for 10 min. At the end of each day, the HPC coated capillary was flushed with water for 10 min and with air for 5 min.

2 RESULTS AND DISCUSSION

Fig. 1 gives a schematic outline of the methodology implemented for the antibacterial assay. Bacteria sample was injected at the cathodic end of the capillary and the cationic molecule was injected at the anodic end of the capillary. This allows monitoring the electrophoretic profile of the bacteria plug before, during and after the meeting with the cationic compound. In this methodology, the bacteria plug moves under anionic ITP conditions, allowing the bacteria zone to keep focused, whilst the cationic compound is displaced under nearly zone conditions since LE and TE are both based on Tris cation.

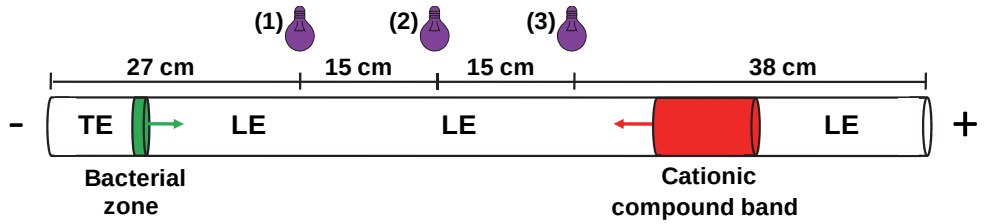

Fig. 1: Schematic representation of the methodology used to study the antibacterial activity of cationic compounds. Adapted from [2].

Fig. 2 displays the antibacterial assay between a dendrigraft poly-*L*-lysine of second generation (G2) and *Micrococcus luteus* (Gram +) using the principle described in Fig. 1. It can be noticed that the signal of *Micrococcus luteus* completely disappeared after contact with the G2 band (see trace 1 vs trace 3 at both 214 and 280 nm). Note that the wavelength at 280 nm is specific to the detection of the bacteria, while both G2 and bacteria were detected at 214 nm. These results clearly demonstrate the antibacterial (lysis) activity of G2 toward *Micrococcus luteus*. The same methodology was applied toward another bacterial strain (*E. carotovora*, Gram -) and demonstrated the adsorption of G2 onto the surface of the bacteria without any lysis of the bacterial membrane.

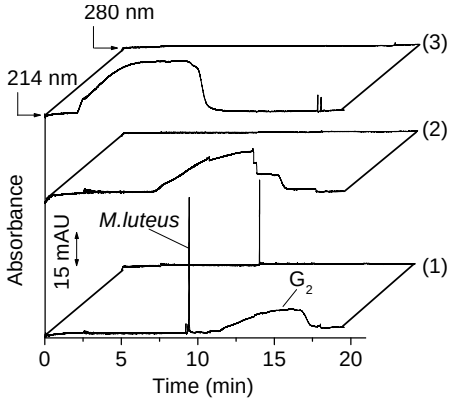

Fig. 2: Electropherograms obtained for the meeting beetween G2 (cationic compound) and *M. luteus* in a single capillary with three independent windows (1), (2) and (3) as indicated in Figure 1 and two wavelengths (214 nm and 280 nm). Adapted from [2].

More recently, we investigated to possibility to get quantitative figures of merit on the bacteria/antibacterial interactions by CE techniques. Namely, stoichiometry and association constants were determined using electrokinetic supercharging to quantify the free concentration of antibacterial compound in different bacteria/antibacterial mixtures. Isotherms of adsorption were plotted giving access to valuable informations on the interaction at a molecular level.

3 CONCLUSION

Different CE modes (CZE, ITP, electrokinetic supercharging, CIEF) coupled to single or multi-points detectors can be used to investigate antibacterial activity and, more generally, interactions between bacteria and antibacterial compounds. Such methodologies may contribute to investigate the correlation between the structure / characteristics of the antibacterial compounds and its antibacterial (lysis) activity.

ACKNOWLEDGEMENTS

H.C. gratefully acknowledges the supports from the Institut Universitaire de France and from the Région Languedoc-Roussillon for the fellowship "Chercheurs d'Avenir". We also thank COLCOM for funding PhD fellowship for F. O., the ANR Dendrimat (grant reference ANR-096MAPR-0022-03) and Yorkshire Forward for support through a Development Grant to Paraytec Ltd (grant reference YHF/02803/RD09).

LITERATURE

[1.] World Health Organization. Report No. WHO /EMC/ZOO/97.4 Press: Berlin, Germany, 1997.

[2.] Oukacine, F.; Romestand, B.; Goodall, D., M.; Massiera, G.; Garrelly, L.; Cottet, H. Anal. Chem., 2012, 84, 3302–3310.

[3.] Oukacine, F.; Garrelly, L.; Romestand, B.; Goodall, D.M.; Zou, T.; Cottet, H. Anal. Chem., 2011, 83, 1571-1578.

APPLICATION OF CAPILLARY ELECTROPHORESIS IN OPTIMIZATION AND CONTROL OF FERMENTATION AND CELL CULTURE

François de l'Escaille, Jean-Bernard Falmagne

Analis R&D, Rue de Néverlée 11, 5020 Suarlée, Belgium
fde@analis.be

ABSTRACT

It is well known that Capillary Electrophoresis allows fast separation of analytes with a minimum of sample preparation. The technique is also known to be very flexible allowing analysis of small molecules as well as big proteins. To illustrate this we will present recent work done on follow-up of cell culture.
The performance of fermentation and cell culture are critical to the quality and consistency of production of therapeutic products. Besides temperature, pH and dissolved oxygen, it is important to follow the nutrients and the metabolites.
Most of the nutriments and metabolites consist of inorganic ions, carbohydrates, alditols, alcohols, organic acids, and amino acids. They are polar and ionized, but they lack a chromophore.
Analis R&D have developed several methods and applications for analysis anions, organic acids, cations, carbohydrates and proteins, so that it is interesting to verify the application of those methods for the follow-up of fermentation and cell culture.

Keywords: organic acid, carbohydrate, cell-culture

1 METHODS

1.1 Indirect UV Detection

Most available capillary electrophoresis, such the Beckman PA 800 *plus* instruments are equipped with UV or LIF detection systems. To be able to detect analytes having no chromophore an indirect UV detection system is used. For indirect UV detection the background electrolyte contains a UV absorbing component, called *"probe".* The analyte will displace this probe and a negative peak will be recorded. This method is used to measure anions, organic acids but also cations and aliphatic amines.

1.2 Photoreaction induced UV Detection

Glycans and carbohydrates are usually labeled with APTS, via reductive amination in the presence of an acid catalyst. Rovio [1, 2] found that at high pH, in the presence of NaOH and under the influence of low UV [3] a photo oxidation takes places generating an intermediate product that absorb at 270 nm. This method allows detection of reducing and non-reducing carbohydrates as well detection of polyols.
A variety of monosaccharide's (such as arabinose, glucose, mannose, galactose, fructose, fucose…); disaccharides (such as saccharose, maltose, lactose…); amino glycan's (such as N-Acetyl-Glucosamine who co-migrate with Galactose, N-Acetyl-Galactosamine,…) polyols (such as sorbitol, maltitol,…) may be analysed.

2 ANALYSIS OF CELL-CULTURE SUPERNATANS

We obtained samples from a company making mAb for diagnostic purpose. mAb were grown in RPMI media and in IMDM media. Samples were collected on day 0, 1, 2, 3, 4 and day 7, but also the supernatant at the end of the fermentation and after process concentration.

Methods were adapted to obtain short analysis time, such as less than 4 minutes for carbohydrates, 7 minutes for organic acids, 5 minutes for cations and 6 minutes for proteins.

3 CONCLUSION

Capillary Electrophoresis, using existing methods and kits and with a minimum of sample preparation, mostly dilution of the sample; is able to follow several parameters during fermentation process. It can not only identify the analyte of interest, but can monitor other parameters to trace when a problem occur.

LITERATURE

[1.] Stella Rovio, Jari Yli-Kauhaluoma, and Heli Sirén (2007). Determination of neutral carbohydrates by CZE with direct UV detection. Electrophoresis 28, 3129 -3135.

[2.] Stella Rovio, Helena Simolin, Krista Koljonen, and Heli Sirén (2008). Determination of monosaccharide composition in plant fiber materials by capillary zone electrophoresis. J. Chromatogr. A 1185, 139 – 144

[3.] Cédric Sarazin, Nathalie Delaunay, Christine Costanza, Véronique Eudes, Jean-Maurice Mallet, and Pierre Gareil (2011). New avenue for mid UV-range detection of underivatized carbohydrates and aminoacids in capillary electrophoresis. Anal. Chem.83, 7381-7387.

MARK TWAIN: HOW TO FATHOM THE DEPTH OF YOUR PET PROTEOME

Pier Giorgio Righetti, Elisa Fasoli and Alfonsina D'Amato

Department of Chemistry, Materials and Chemical Engineering "Giulio Natta", Politecnico di Milano, Via Mancinelli 7, 20131 Milano, Italy

ABSTRACT

The present lecture will highlight recent progresses in the technique of combinatorial peptide ligand libraries (CPPL), a methodology that has much to offer for the detection of low- to very-low abundance proteins in any proteome. In particular, advances in exploration of the urinary, plasma and tissue proteomes are discussed and evaluated. It will be shown that when treating biological fluids, such as plasma, with CPLLs, the detection sensitivity, which in the control only reaches 10 ng/mL, can be enhanced to as high as 10 pg/mL, with an increment of sensitivity of three orders of magnitude. Exploring such extreme low concentration intervals will allow access to those most sought after biomarkers that so far have been much elusive. Even in tissue proteome extracts, up to the present not analyzed via CPLLs, massively overloading the CPLL beads will allow exploration of very low-abundance proteins in presence of a set of highly abundant tissue proteins. The possibility of using CPLLs as a two-dimensional pre-fractionation of any proteome is also evaluated: on the charge axis, CPLL capture can be implemented at no less than three different pH values (4.0, 7.2 and 9.3), thus permitting a capture of proteinaceous analytes bearing a net positive or net negative charge, respectively. When capture is performed in absence of salts or at high levels of salts, one can favour capture of hydrophilic vs. hydrophobic proteins, respectively. This would thus be a genuine 2D protocol, working on orthogonal separation principles (charge vs. hydrophobicity). As the horizon of CPLLs is expanding and its use is exponentially growing, we expect major breakthroughs in, e.g., biomarker discovery, a field that as suffered a decade of failures.

PHOTOLUMINISCENT DIAMOND NANOPARTICLES – NEW DIAGNOSTIC AND VISUALIZATION PROBES

Petr Cígler

Institute of organic chemistry and biochemistry, Academy of Sciences of the Czech Republic, Flemingovo nam. 2, 166 10 Prague 6, Czech Republic
cigler@uochb.cas.cz

ABSTRACT

Fluorescence from NV-centers embedded in diamond lattice is extremely photostable and it finds vast field of applications in optical microscopy, intracellular particle tracking, high-resolution magnetometry, and quantum information applications. By decreasing the size of bulk diamond crystals to nanodimensions, many chemical features of the material, as well as the fluorescence properties, change. In the talk, selected problems connected with surface modification of nanosized diamond crystals, attachment of chemical sensing architectures to them and their colloidal stability will be addressed. Fluorescent nanodiamonds modified by proper functional structures will be shown as unique unbleachable nanoprobes for construction of future sensors useful in biological and medicinal applications.

APPLYING CE AND MICROCHIP CE TO MOLECULAR CANCER ANALYSIS: FROM RESEARCH TO CLINICAL UTILITY

Marek Minarik

Genomac Research Institute, Prague, Czech Republic

ABSTRACT

Decisions in clinical oncology are glowingly relying on modern tools and technologies coming from genome research. Currently, several treatment options are available to most patients suffering from common forms of solid cancers (e.g.colorectal, lung, pancreas ...). The clinical decision is taken based on the extent of the tumor defined by TNM (tumor, nodes, metastasis) or other types of staging. The treatment options usually include surgical removal of tumorous tissue, irradiation of the tumor, pharmacological chemotherapy or a combination thereof. Assessment of the disease prognosis is often the key component in the decision process. A number of molecular aberrations found in cancerous tissue such as DNA mutations, gene amplifications or DNA hypermethylation may be utilized as biomarkers defining the disease prognosis. At the same time such molecular markers may also be used to predict the likelihood of a positive response towards a specific pharmacological therapy used to treat the tumor. The presentation will demonstrate use of CE and chip CE in analysis of various molecular cancer genetic and epigenetic markers and its application in rational therapy selection, monitoring of the disease progression and assessment of its survival prognosis.

ACKNOWLEDGEMENT

Supported by IGA grant NT13638.

NEW ADVANCES IN CAPILLARY ELECTROPHORESIS OF THERAPEUTIC ANTIBODIES

András Guttman, Akos Szekrenyes, Csaba Varadi and Marta Kerekgyarto

Horvath Laboratory of Bioseparation Sciences, University of Debrecen, Hungary

ABSTRACT

The emerging bioindustrial sector requires novel bioanalytical methods to address the challenging regulatory aspects entailing comprehensive characterization of biopharmaceuticals by sensitive and high resolution bioanalytical techniques. During the development phase rapid assessment of product purity and quantification is necessary. In addition, quite a few other critical features should be analyzed, among them glycosylation is being one of the most important (including microheterogeneity and site specificity). The analytical needs depend on the actual application in hand, but high throughput is usually a prerequisite during clone selection, while high sensitivity is important during product release, especially revealing the presence of immunogenic epitopes. Capillary electrophoresis is representing a well-established and widely used protein analysis technique in the biotechnology industry. In CGE format it is readily applicable for rapid purity assessment and subunit characterization of IgG molecules including detection of non-glycosylated heavy chains (NGHC) and separation of possible subunit variations such as truncated light chains (Pre-LC) or alternative splice variants. Ultrasensitive techniques are required for rapid analysis of possible immunogenic residues, such as galactose-α-1,3-galactose or N-glycolylneureminic acid on therapeutic antibodies expressed in murine or CHO cell lines. Capillary electrophoresis in conjunction with exoglycosidase digestion is a sensitive method for full structural elucidation of IgG glycans containing such immunogenic epitopes. This presentation will discuss the latest advances in the field of CE based analysis of therapeutic antibodies. Particular respect will be paid to clone selection and product characterization using CE-SDS and CE based glycosylation analysis.

3D CHIP FOR LOW COST CELL ANALYSIS

Guillaume Mottet[a], Karla Perez-Toralla[a], Ezgi Tulukcuoglu[a], Jerome Champ[a], Irena Draskovic[b], Stephanie Descroix[a], Laurent Malaquin[a], Jean Louis Viovy[a]

[a] *Institut Curie, Centre de Recherche UMR 168, Paris, France*
[b] *Institut Curie, Centre de Recherche UMR 3244, Paris, France*

ABSTRACT

We present a low cost chip with 3D microchambers for the capture and analysis of cells. The use of such device with simple design, small footprint and reduced volume allows the implementation of standard biological protocols in chip for clinical diagnosis applications.
Slide preparation of immobilized cells or tissue is a key to many cytological analyses. One must control the spreading of cells from a clinical sample in order to achieve a high density and homogenous distribution of cells on a limited surface. Our main motivation was to implement a simple and effective microfluidic design in order to collect cells in specific 3D chambers prior further proteomic or genomic analysis. The thickness of the capture chamber

(height=350 µm) is ten times bigger than that of the inlet and outlet channels (height=30µm). Flow velocity will thus abruptly decrease at the entrance of the chamber (Figure 2). Cells driven by the laminar flow will decelerate in the chamber, settle down and attach to the lower surface. The microchannel walls were previously treated with a solution of Poly-L-lysine that enhances the attachment of cells to solid surfaces via electrostatic interactions. This surface treatment has proven to be robust since cells once attached to the surface resist even at high flow rates (several rinsing steps). This way, we were able to obtain a single layer of cells with a high density and homogenous distribution in a specific area of the chip (no cells were observed outside the capture chambers) (Figure 3). This technique has already proven its efficiency in 2D extruded chips [1]. In such configuration however the reduction of the flow velocity is usually induced by the enlargement of the channels, which causes a significant decrease of cells density and impedes spreading homogeneity. Flow distribution structures can be used to compensate for the latter but they require complex designs and induce a progressive slow down of cells which favour their adhesion before entrance in the capture area. Using a 3D structure yields an abrupt slowdown which limits this problem. It also simplifies the design and reduces the chip foot print. The microfabrication of such designs is now made very easy by the manufacturing of aluminum master mold through micro-milling technology and the replication of the structures using hot-embossing techniques (Figure 1). The chips are made with Cyclo Olefin Copolymer material [2], Fig 3.
To validate our system we implemented a Fluorescence in Situ Hybridization (FISH) analysis. FISH is a FDA approved diagnostic technique, based on fluorescent DNA probes that hybridize to the targeted gene. It provides quantitative information about gene and chromosome aberrations at the single cell level [3]. In conventional protocols, however, it requires a long and fastidious process; in particular the temperature control is crucial. Figure 4 shows FISH results inside the microfluidic chamber. A quite uniform distribution of cells is achieved, improving cell morphology and FISH analysis. We are now working on the automation of the system in order to have a complete platform to analyze relevant clinical samples.

LITERATURE

[1.] "Controlled deposition of cells in sealed microfluidics using flow velocity boundaries," R. D. Lovchik, F. Bianco, M. Matteoli and E. Delamarche, Lab on a Chip, 9, 1395 (2009).

[2.] “Fabrication of thermoplastics chips through lamination based techniques” S. Miserere, G. Mottet, V. Taniga, S. Descroix, J-L. Viovy and L. Malaquin, Lab on a Chip,12, (2012).

[3.] “Her-2/neu gene amplification characterized by fluorescence in situ hybridization: poor prognosis in node-negative breast carcinomas”, M.Press et al., J Clin Oncol, 15, (1997).

MAGNETIC BEADS-BASED MICROFLUIDIC SYSTEMS: THE PAST AND THE FUTURE

Zuzana Bilkova, Zuzana Svobodova

Department of Biological and Biochemical Sciences, Faculty of Chemical Technology, University of Pardubice, Studentska St. 573, 532 10 Pardubice, Czech Republic

Zuzana.Bilkova@upce.cz

ABSTRACT

In recent years, nanotechnologies have greatly impacted biotechnological research and analytical technologies for genomics, proteomics, clinical diagnostics, cell-based assays,

disease screening and drug discovery. Many of such applications have potential to bring the analysis closer to patient to evaluate immediately level of certain biomarkers [1]. Special devices enabling such analysis are called micro-total analysis systems (μ-TAS), lab-on-chips (LOC), point of care devices (POCT) or biomicrodevices [2]. Development of such microfluidic system requires complex knowledge of physics, microfabrication techniques and surface chemistry, moreover methods for analysis of biological material and medical background. Interestingly, in last two decades, microfluidic devices based on affinity magnetic separations using magnetic micro/nanoparticles were developed and successfully applied in all aforementioned fields of bioanalysis [3].

The magnetic particles have most frequently spherical monodisperse shape and are made magnetisable and/or superparamagnetic, meaning they are only magnetic in a magnetic field. Employing magnetic beads in microfluidic devices brings broad range of advantage. Analytical system which comprises of magnetic particles and flow injection system are characterized by outstanding repeatability and reproducibility. Extremely high specific surface of integrated nano(micro)particles (high surface-to-volume ratio) leads to a smaller diffusion distance, shorter analysis time and thus time-to-result. Increased sensitivity and specificity of the analysis enables to detect extremely rare analytes occurring in highly complex heterogeneous biological material with no need of sample pretreatment. Above all, magnetic-field based analytical steps opened widespread opportunities not only for diagnostics but also for biocatalysis and biotechnology. Beads-based immunoassays (e.g. particle capture ELISA) [4], bead-based microfluidic enzyme catalysis [5] or self-assembled beads-based channels for cell sorting [6], bead-based DNA in-microchip analysis [7], multiplex assays (e.g. Luminex), digital microfluidic platform (DMF) [8], droplet microfluidics [9] and biobarcoded magnetic beads assays [10] are selected examples documenting the strength of this arrangement.

Keywords: magnetic beads, μ-TAS, bioanalysis

ACKNOWLEDGEMENTS

The work leading to this invention has received funding from the Czech Science Foundation (GA203/09/0857), the European Community´s 7th FP (2007-2013) under grant agreements n° 228980 (CAMINEMS) and n°246513 (NADINE).

LITERATURE

[1.] Derveaux, S., Stubbe, B.G., Braeckmans, K., et. al., Analytical and Bioanalytical Chemistry 2008, 391(7), 2453-2467.
[2.] Chin, C.D., Linder, V. and Sia, S.K., Lab Chip 2012, 12(12), 2118-2134.
[3.] Gijs, M., LaCharme, F. and Lehmann, U., Chemical Reviews 2010, 110(3), 1518-1563.
[4.] Sista, R.S., Eckhardt, A.E., Srinivasan, V., Pollack, M.G., et.al., Lab on a Chip 2008, 8(12), 2188-2196.
[5.] Slovakova, M., Minc, N., Bilkova, Z., Smadja, C., et. al., Lab Chip 2009, 5(9), 935-942.
[6.] Saliba, A., Saias, L., Psychari, E., Minc, N., et. al., PNAS 2010, 107(33), 14524-14529.
[7.] Lien, K., Liu, C., Lin, Y., Kuo, P., et. al., Microfluidics and Nanofluidics 2009, (4), 539-555.
[8.] Sista, R., Hua, Z., Thwar, P., Sudarsan, A., et. al., Lab Chip 2008, 8(12), 2091-2104.
[9.] Teh, S., Lin, R., Hung, L. and Lee, A.P., Lab Chip 2008, 8(2), 198-220.
[10.] Lee, H., Kim, J., Kim, H., et. al., Nat Mater 2010, 9(9), pp. 745-749.

OPEN CHIP SAW-MALDI MS SAMPLE HANDLING

Loreta Bllaci[a], Alexander Jönsson[a], Sven Kjellström[b], Sandra Lemos[c], Lena Eliasson[d],James R. Friend[e], Leslie Y. Yeo[e] and **Staffan Nilsson**[a]

[a] *Pure & Applied Biochemistry LTH, Lund University, Sweden*
[b] *Department of Biochemistry and Structural Biology, Lund University, Sweden*
[c] *Department of Biochemistry I - Ruhr University, Bochum, Germany*
[d] *Clinical Sciences Malmö CRC, Entr 72, building 91, level 11, Univeristyhospital Malmö, Sweden*
[e] *RMIT University, GPO Box 2476,Melbourne VIC 3001, Australia*

ABSTRACT

SAW atomizer has been interfaced with MALDI MS for fast analysis of small volumes (< 1µL) sampled in a membrane. SAW propagate through and underneath the membrane and atomize the liquid bound sample into 2-10 µm diameter aerosol which is subsequently deposited on a MALDI plate for further analysis. Fast peptide profiling of *islets of Langerhans* and bio fluid (saliva, tear film) has been achieved. MALID MS of a single beta cells and a single islet using the acousitic levitation technique leads to a wall less analysis with low contamination and high sensitivity.

Keywords: SAW, Acoustic levitation, Airborne

1 INTRODUCTION

An open microfluidic device for handling of small volumes (< 1 µL), has been interfaced to MALDI MS [1]. Surface Acoustic Wave (SAW) atomizer consist of a piezoelectric material with two single-phase unidirectional transducers (SPUDTs) electrodes driven at 30 MHz [2-4]. High energy SAW generates small aerosols (2-10 µm diameter) from a deposited droplet over 15 seconds. No molecular damage has been shown via SDS-PAGE [3]. SAW propagate and atomize the membrane-bound liquid sample. The membrane aids sample pre-purification, by entrapping impurities within the membrane fibers. SAWs self-pumping effect, generates direct sample transportation to the MALDI plate and avoids the risk of clogging; often a problem of closed microfluidic devices. SAW atomizer is here used primarily in rapid metabolic screening of islet of Langerhans endocrine cell clusters involved in the pathogenesis of T2D. However due to the membrane format which favors non-invasive sampling and the instant, non-chemical extraction, the atomizer has been used in rapid body fluid protein/peptide profiling (saliva, gingival fluid, tear film). Minimal sample requirements, fast and easy operation, makes SAW an attractive tool in future diagnostics. Single/few cell analysis, in the context of T2D molecular studies, has also been performed in “wall-less test tube” via the acoustic levitation technique [5, 6]. With such approach, it is possible to handle small volumes without any adsorption to walls or related contamination. Flow-through droplet dispensers are used to deliver stimulators/inhibitors to the cells within the levitated droplet. Protein/peptide data from single β-cell and single islet and has been achieved by the combination of the airborne system and MALDI MS.

2 EXPERIMENTAL

Freshly prepared islet(s) were pipetted on a piece of membrane, placed on the atomizer and supplemented with buffer (30 mM glucose) bound to the membrane. Acetylcholine (100 µM) was then applied and allowed to stimulate the resting islet for 5 minutes. Following the islet stimulation, SAWs were generated. The resulting aerosol, rich in islet's cell relesates, was collected on the MALDI plate (Figure 1). The alpha-cyano-4-hydroxycinnamic acid matrix (CHCA), applied on the same membrane, was SAW-extracted and deposited on the plate in a similar fashion. The described procedure developed by us, which was essential in qualitative spectra acquisition, is also refereed as *SAW-deposition*. After each experiment, the piezoelectric substrate was cleaned with acetone, isopropanol and rinsed with milliQ water as described by Ho[4]. Single β-cell within a levitated droplet (500 pL, 5mM glucose Hepes buffer) were stimulated for 5 min with 5µM acetylcholine that was delivered to the droplet via a piezoelectric dispenser [5]. All samples were collected to a MALDI plate prepared with a crystal layer of CHCA and allowed to crystallise.

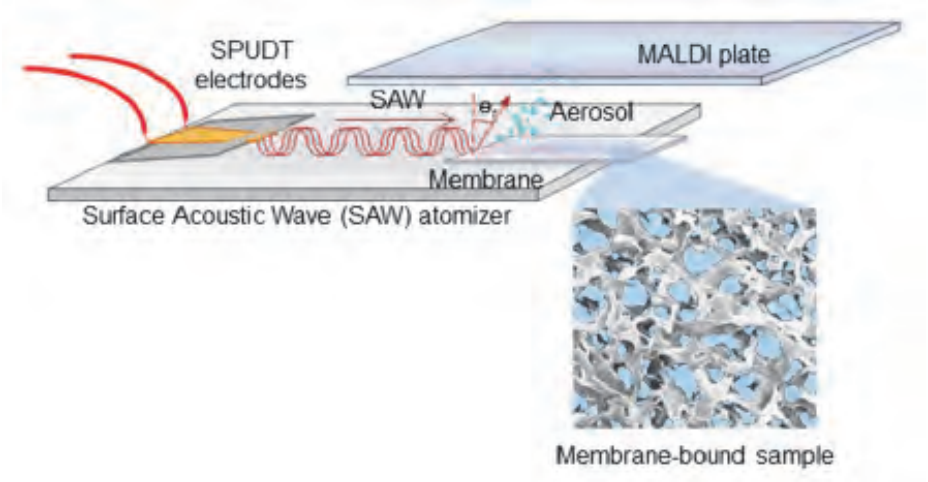

Fig. 1. (A) The SAW atomizer's working principle and experimental setup. The atomizer consists of a piezoelectric material with two SPUDT electrodes which generate unidirectional Rayleigh-wave SAW that propagate towards and underneath the sample. High energy SAWs drives liquid atomization even when the liquid is previously sampled on a membrane. The resulting aerosols are collected on a MALDI plate for MS analysis.

3 RESULTS

Fast MALDI MS spectra generated from stimulated, intact islets of healthy mice are shown in Figure 2A. As expected, high glucose concentrations (30 mM glucose) in combination with acetylcholine (100 µM) has triggered β-cells to release insulin and other co-secreted molecules. A weak peak corresponding to the suppressed glucagon release from α-cells is also indicated in the spectra. The acquisition of qualitative spectra, characterized by high S/N values, reproducibility and a LOD of less than 100 attomole, are attributed to the novel way of SAW based sample-matrix deposition procedure— an essential step of MALDI analysis. Rapid MALDI MS peptide profiling of biofluid (saliva, gingival fluid, tear film) sampled and preserved on a membrane has been also achieved. Figure 2B shows the tear film acquired spectra, sampled on a membrane and air-dried prior to analysis and Figure 2C shows the spectra acquired from the saliva sampled in the same way. MALDI MS spectra acquired from a levitated single β-cell (Fig. 2D), induced (5 mM glucose, 5µM acetylcholine) for 6 minutes are characterised by strong signals of insulin, C-peptide and amylin.

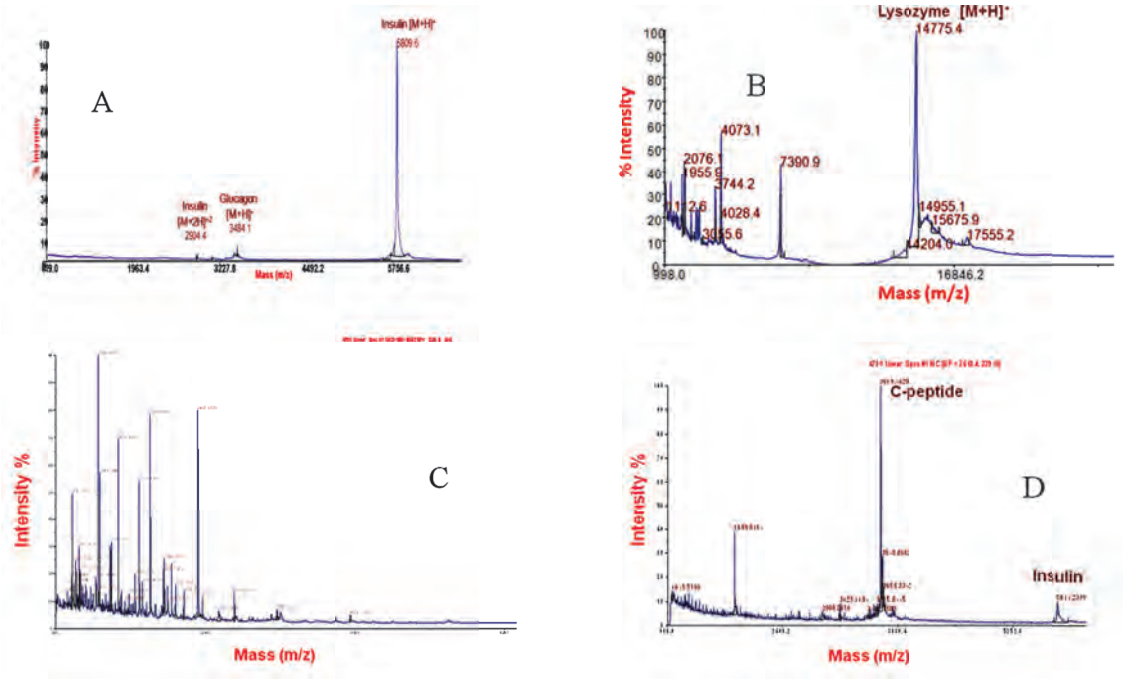

Fig. 2. (A) Acquired spectra from islets in 30 mM glucose HEPES, 100 µM acetylcholine using the SAW-deposition. (B) Tear film SAW-MALDI of membrane dried tear film, Lysozyme labelled(14.7 kDa). (C) SAW-MALDI of saliva, on dried membrane, using ascorbic acid to break down mucins, (D) Single β-cell MALDI MS, stimulated in the acoustic levitator.

4 CONCLUSION

The combination of two airborne analytical systems, the acoustic levitation and SAW-atomizer, with MALD MS has been achieved. The acoustic levitation shows an outstanding sensitivity (20-80 attomole) in protein analysis released from single β-cell. However, single islet analysis has also been done using the SAW atomizer—a fast and easy sample handling tool for MALDI MS. Acetylcholine-stimulated islets relesates, sampled on a membrane, were extracted via SAW and detected with MALDI MS. Since the sample here is minimally chemically pretreated the risk of MALDI artefacts is considerably reduced. The reproducibility, and sensitivity (less than 100 attomole) of SAW-MALDI is mainly attributed the newly developed SAW-based sample-matrix deposition method. Besides performing an instant non-chemical, membrane purification/extraction of the sample, the chip reduces the use of vials, containers and related analysis cost. The membrane format of the SAWs operation allow for non-invasive sampling of small volumes biofluid (less than 1 µL) and related MS-based diagnostication.

LITERATURE

[1.] Bllaci, L., Kjellström, S., Eliasson, L., Friends, J.R., Yeo, L. Y., Nilsson, S., *Fast SAW-MALDI MS of Cell Response for Type 2 Diabetes Studies.* 2012: p. (Submitted).

[2.] Qi, A., Yeo, L. Y., Friend, J. R., *Interfacial Destabilization and Atomization Driven by Surface Acoustic Waves.* Phys Fluids, 2008. 20(074103): p. 14.

[3.] Qi, A.Y., L., Friend, J., Ho, J. , *The extraction of liquid, protein molecules and yeast cell's from paper through surface acoustic wave atomization.* Lab Chip, 2009. 10: p. 470-476.

[4.] Ho, J.T., M. K.;Go, D. B.;Yeo, L. Y.;Friend, J. R.;Chang, H.-C. , *Paper-Based Microfluidic Surface Acoustic Wave Sample Delivery and Ionization Source for Rapid and Sensitive Ambient Mass Spectrometry.* Anal. Chem. , 2011. 83: p. 260–3266.

[5.] Lemos, S.G., N., Degerman, E., Eliasson, L., Bllaci, L., Nilsson, S. , *Interfacing Airborne Cell Chemistry with MALDI-TOF-MS* 2012: p. (Submitted).

[6.] Santesson, S., Degerman, E., Rorsman, P., Johansson, T., Lemos, S., Nilsson, S., *Cell-cell communication Between Adipocytes and Pancreatic Beta-cells in Acoustically Levitated Droplets.* Integrative Biology 2009. 1: p. 595-601.

DIAGNOSING OF INHERITED METABOLIC DISORDERS BY METABOLOMIC TOOLS – AN UNTARGETED APPROACH APPLIED TO MEDIUM CHAIN ACYL-COA DEHYDROGENASE DEFICIENCY

Lukáš Najdek[a], David Friedecký[a], Hana Janečková[a], Kateřina Mičová[a], Iveta Fikarová[a], Helene Podmore[b], Garry Woffendin[b], **Tomáš Adam**[a]

[a] *Laboratory of Metabolomics, Laboratory of Inherited Metabolic Disorders and Institute of Molecular and Translational medicine, University Hospital and Palacky University in Olomouc, Hněvotínská 5, 775 15 Olomouc, Czech Republic*
[b] *Thermo Fisher Scientific, Stafford House, Boundary Way, HP2 7GE Hemel Hempstead, United Kingdom*

ABSTRACT

Inherited metabolic defects are disorders caused by enzyme deficiencies and medium chain acyl-CoA dehydrogenase deficiency (MCADD) is one of the best understood defects. We report here the use of untargeted metabolomic approach consisting of liquid chromatography coupled with exact mass spectrometry. For data processing (chromatogram alignment, peak identification and statistics) XCMS Online (The Scripps Research Institute, CA, USA) was used. Approximately 600 features were detected per sample. The most influential compounds which separate patients from controls were hexanoyl-, octanoyl-, decanoylcarnitines. Besides of these well known biomarkers two atypical phospholipids showed p-values less than 0.01. With this approach we were able to discriminate all patients with MCADD from healthy controls. Untargeted approach is suitable for identification of MCADD patients and potentially for other inherited metabolic disorders and also for the detection of new potential biomarkers.

1 INTRODUCTION

1.1 Inherited metabolic disorders and MCADD

Inborn errors of metabolism are a large group of defects comprising hundreds of diseases. The typical common pathobiochemical sign is an accumulation of enzyme substrate in body fluids. Identification and quantification of these compounds is the key to the diagnosing of metabolic disorders.

Medium chain acyl-CoA-dehydrogenase (MCADD OMIM #201450) is one of the most common inherited metabolic disorders with incidence in Caucasian population from 1:10000 to 1:27000 newborns, depending on the region. The enzyme (EC 1.3.99.3) is responsible for metabolisation of acyl-carnitines with moiety of 6-10 carbon long. Patients with this disorder can suffer from various symptoms from hypoglycemia to acute encephalopathy triggered by e.g. common infectious disease. Almost half of the patients die within first episode. The condition is screened in neonates in majority of developed countries.

1.2 Metabolomics

Metabolomics is a scientific branch studying collection of low molecular weight compounds (metabolites) in a biological system – cell, organ or organism – which are products of

biological processes. We can distinguish two different ways of metabolomic analyses: targeted and untargeted approach. In targeted metabolomics we are looking for specific (pre-defined) metabolites in the samples by liquid chromatography – tandem mass spectrometry. The advantage of this approach is sensitivity and that we can be sure about the identity of the metabolites we work with, but we are blind to the rest of the compounds in the sample. On the other hand, in untargeted metabolomics we are looking at all metabolites at once (usually by liquid chromatography – exact mass spectrometry), but the disadvantage is that the identification is not always straightforward. Usually you can compare measured exact mass spectra (or MS^n spectra) with metabolomic databases (HMDB, MetLin, etc.). If you are not able the get a match in the databases another option is a comparison with data that you acquire by measuring of standards if available. Otherwise structure can be solved by designing fragmentation patterns in commercial software (e.g. Mass Frontier) and then combining predicted patterns with MS^n data.

2 EXPERIMENTAL

Dry blood spots (3 mm disc) of controls (n=5) and patients (n=5) were extracted by methanol and water in ratio 1:1 (200 uL). Supernatants were centrifuged and analysed by modified LC-MS method previously published [1] (LC: Luna NH2, 2x150 mm, MP: 20 mM ammonium acetate (pH 9.45) and acetonitrile, 35 min, injection: 1 uL) with detection by exact mass instrument Orbitrap Elite (Thermo Scientific). Orbitrap operated in full scan mode (240000 resolution) within range of 70 - 900 m/z. Polarity was set to positive mode. Data were processed by XCMS Online software (The Scripps Research Institute, CA, USA) and statistical computing was done with built in parameters in XCMS Online software.

3 RESULTS & DISCUSSION

Typical analysis contained approximately 600 features which were used for statistical evaluation. Principal component analysis showed good separation of patient samples from healthy controls (**Fig.1**). Our exact mass data of patient samples showed increased levels of previously known acylcarnitines (hexanoyl-, octanoyl-, decanoyl- carnitines) and also not so far identified abnormal levels of two atypical phospholipids. These phospholipids contained fatty acyl fragment in *sn*-2 position with an odd number of carbon and ω-terminal carboxylate. There are two provisional theoretical explanations for the increase presence of the newly identified phospholipids. First, they can be products of oxidative stress known to affect MCADD deficient cells [2, 3]. Second mechanism can be direct synthesis from accumulated fatty acids through Kennedy pathway [4] after previous omega-oxidation (known to be increased in beta-oxidation defects [5]).

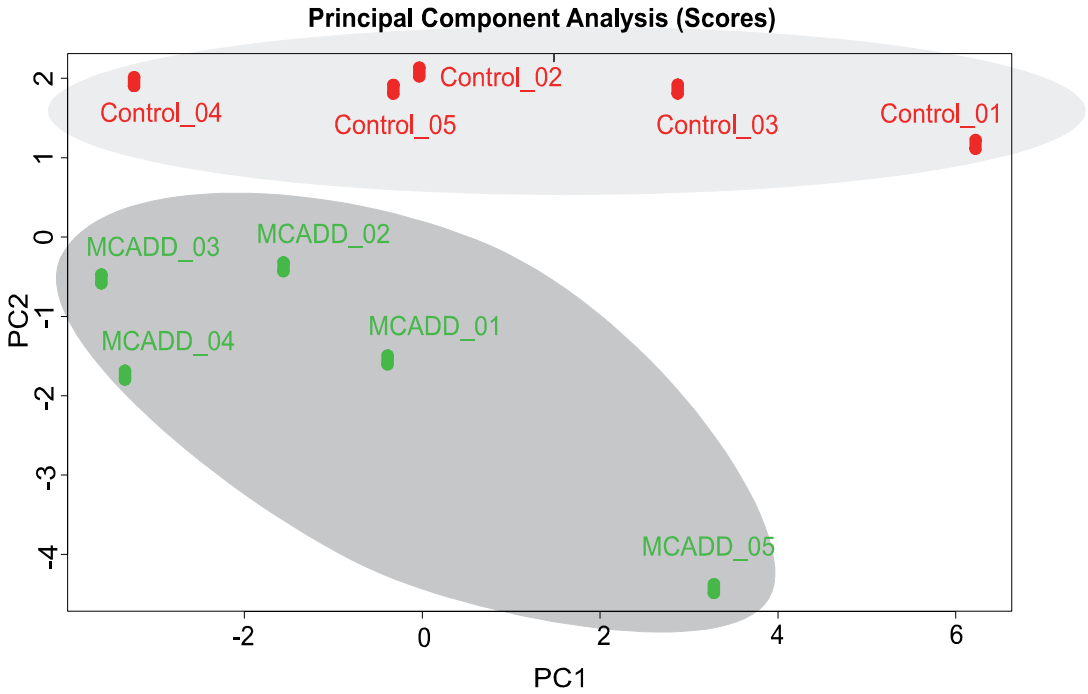

Fig. 1: Principal component analysis of exact mass data. MCADD patients (marked green; n=5) and healthy controls (marked red; n=5).

4 CONCLUSION

We used untargeted metabolomic approach with statistical evaluation to identify MCADD patients. All control and patient samples were separated from each other in principal component analysis, showing that untargeted approach is suitable for identification of inborn errors of metabolism. We found potential new phospholipid markers for MCADD. Confirmation of the findings on larger groups of patients and controls using targeted analysis together with elucidation of biochemical mechanisms is our next goal and it need further research.

ACKNOWLEDGEMENT

Supported by grants IGA MZCR NT12218, and LF U 2012-016. The infrastructural part of this project (Institute of Molecular and Translational Medicine) was supported from the Operational programme Research and Development for Innovations (project CZ.1.05/2.1.00/01.0030).

LITERATURE

[1.] Bajad, S. U. *et al.* Separation and quantitation of water soluble cellular metabolites by hydrophilic interaction chromatography-tandem mass spectrometry. *J Chromatogr A* 1125, 76-88, doi:S0021-9673(06)00993-9 [pii]10.1016/j.chroma.2006.05.019 (2006).

[2.] Scaini, G. *et al.* Toxicity of octanoate and decanoate in rat peripheral tissues: evidence of bioenergetic dysfunction and oxidative damage induction in liver and skeletal muscle. *Molecular and Cellular Biochemistry* 361, 329-335, doi:DOI 10.1007/s11010-011-1119-4 (2012).

[3.] Schuck, P. F. *et al.* Medium-chain fatty acids accumulating in MCAD deficiency elicit lipid and protein oxidative damage and decrease non-enzymatic antioxidant defenses in rat brain. *Neurochem Int* 54, 519-525, doi:DOI 10.1016/j.neuint.2009.02.009 (2009).

[4.] Kennedy, E. P. The Biological Synthesis of Phospholipids. *Can J Biochem Phys* 34, 334-348 (1956).

[5.] Wanders, R. J. A., Komen, J. & Kemp, S. Fatty acid omega-oxidation as a rescue pathway for fatty acid oxidation disorders in humans. *Febs J* 278, 182-194, doi:DOI 10.1111/j.1742-4658.2010.07947.x (2011).

SUB-, NEAR- AND SUPERCRITICAL WATER IN ANALYTICAL SEPARATIONS AND INSTRUMENTATION DEVELOPMENT

Pavel Karásek, Lenka Šťavíková, Barbora Hohnová, Josef Planeta, Dana Moravcová, Marie Horká, Karel Šlais, **Michal Roth**

Institute of Analytical Chemistry of the ASCR, v. v. i., Veveří 97, 602 00 Brno, Czech Republic
roth@iach.cz

ABSTRACT

Apart from being the greenest of all solvents, water is also the most tuneable solvent in the sense of property variations that can result from proper adjustments of operating temperature and pressure. Although most applications of water as a solvent in analytical chemistry operate between room temperature and the normal boiling point, there are multiple uses of high-temperature water in analytical chemistry as well. In this contribution, several applications of subcritical, near-critical and supercritical water in analytical separations and technologies are discussed, as developed or under development in the authors' institution.

Keywords: pressurized hot water extraction, monolithic silica column, tapered capillary

1 WATER PROPERTIES

By varying the operating temperature and pressure, the solvating properties of water can be tuned to cover a much wider range than those of any other single-component solvent. **Table 1** illustrates the relevant properties of water at ambient conditions and in an arbitrary supercritical state. Both relative permittivity and solubility parameter of water in the supercritical state are lower than those of *n*-pentane at room temperature, indicating a relatively nonpolar character of supercritical water. In any property shown in **Table 1**, intermittent values between the two limits are accessible through adjustments of temperature and pressure, thus providing water with an extreme degree of tunability of its solvent properties. High temperature certainly makes supercritical water a hostile medium to most substances relevant to bioanalysis; despite that, however, high temperature water can still be at least indirectly useful in bio-related analytical separations as shown in the few examples to follow.

Table 1. Water property variations with temperature and pressure

T / °C	*P* / MPa	solubility parameter / $(J.cm^{-3})^{1/2}$	relative permittivity	ion product / $(mol.kg^{-1})^2$
25	0.1	47.9	78.4	1.01×10^{-14}
500	30	5.96	1.68	1.19×10^{-21}

2 EXAMPLE APPLICATIONS OF HIGH-TEMPERATURE WATER

2.1 Pressurized hot water as extraction solvent for unstable analytes

Wine production industries generate large amounts of waste including grape skins; in red wine varieties such as St. Laurent or Alibernet, the waste skins contain valuable 3-O-monoglucoside anthocyanins that can serve as natural colorants and/or antioxidants for functional food formulations. Extraction of the anthocyanins from waste skins is therefore of great interest and, with prospective application of the extracts in food industry, water seems an obvious extraction solvent of choice. However, as with all other temperature- and/or hydrolysis-sensitive compounds, the optimum temperature for extraction of anthocyanins

(**Fig. 1**) is a trade-off between the need to enhance the yield of target compounds and the need to avoid their degradation during extraction with hot water [1.].

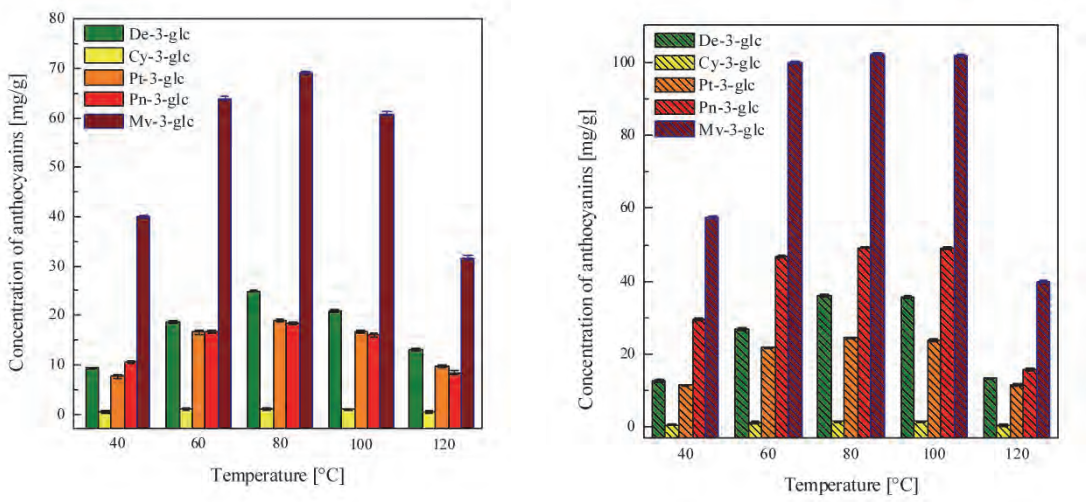

Fig. 1: Concentrations of 3-O-monoglucoside anthocyanins in aqueous extracts of grape skins of St. Laurent (left) and Alibernet (right) varieties as functions of the extraction temperature. Symbol key: De = delphinidin, Cy = cyanidin, Pt = petunidin, Pn = peonidin, Mv = malvidin.

2.2 Pressurized hot water as extraction solvent for stable analytes

With the rising production, use and disposal rate of electronic communication devices such as smartphones and tablets, questions may arise regarding the environmental fate, impact and possible health effects of the individual chemicals employed in production of the devices. One of the key properties for assessment of the environmental impact is the aqueous solubility of the substance in question. **Fig. 2** shows the aqueous solubilities of several aromatic compounds with large π-electron systems that have been used as hole transport materials in organic light emitting diode (OLED) displays. The measurement method consisted of generating saturated aqueous solution of the target analyte by slowly passing water through a packed bed of the solid analyte, transferring the analyte from the aqueous medium to an organic solvent, and HPLC analysis of the organic phase. The solubilities had to be measured [2.] at elevated temperatures up to 260 °C. To keep water in the liquid state, the operating pressure was maintained within the range 5–7 MPa. Extrapolation of the high-temperature data to provide aqueous solubilities at 25 °C yields gross, semi-quantitative estimates of room-temperature solubilities, indicating that the solubility at 25 °C of any OLED-related compound studied here should be less than 2×10^{-11} g / 1 kg of water. Hopefully, therefore, these substances do not impose any immediate environmental concern.

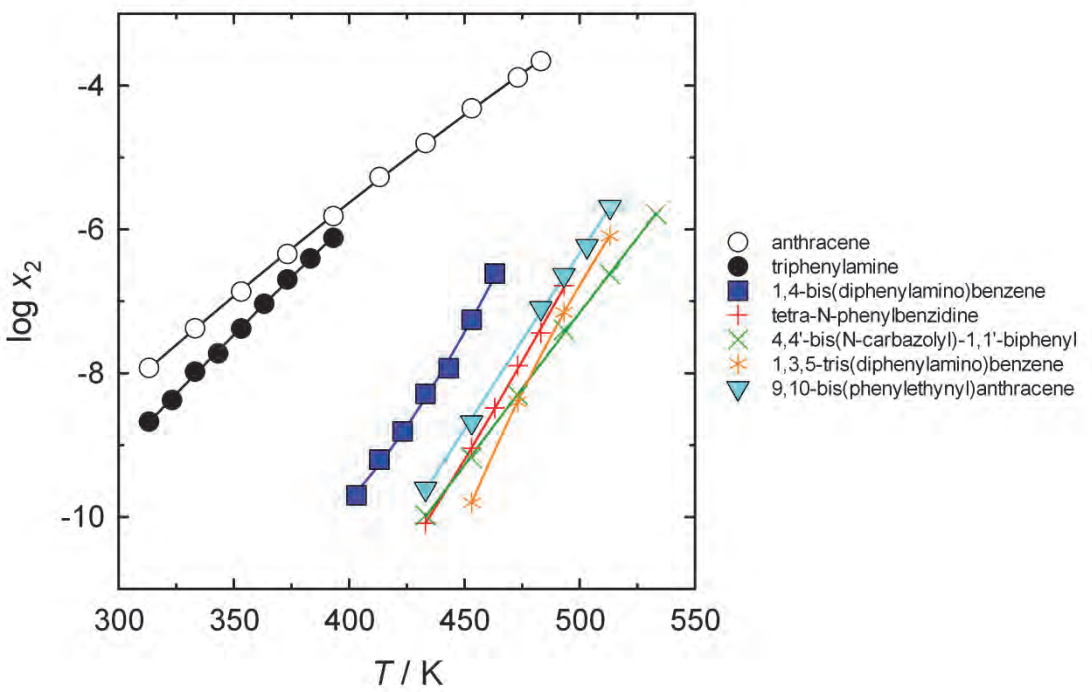

Fig. 2: Solubilities (equilibrium mole fractions) of selected hole transport materials and reference solutes in pressurized hot water. Pressure range was 5–7 MPa.

2.3 Supercritical water in surface treatment of constant-diameter fused silica capillaries

Since their introduction as column material for capillary gas chromatography [3.], fused-silica capillaries have become reliable workhorses in both chromatographic and electromigration techniques of analytical separations. Depending on the particular application of the capillary, it is very often necessary to modify the chemistry and/or roughness of the inner surface. Because near-critical water dissolves both quartz [4.] and fused silica [5.], it can be used to roughen the inner surfaces of fused silica capillaries [6.]. Moreover, unlike all other agents used previously for the purpose, water has the significant virtue in that it cannot pollute the treated surface with any heteroatoms that may be difficult to remove and/or highly undesirable in the intended application of the treated capillary. Since the polyimide coating of the capillary can withstand a short-term exposure to high temperature (~450 °C), near-critical water appears to provide a useful agent for roughening the inner surfaces of fused silica capillaries prior to preparation of monolithic silica columns as shown in **Fig. 3** [6.]. Under certain experimental conditions [7.], the conventional way of pre-treatment of the capillary surface may suffer from imperfect bonding between the silica monolith and the capillary wall, leading to formation of by-pass channels for the mobile phase between the monolith and the wall. Sometimes, the mobile phase pressure can even eject the silica monolith out of the column. The rough surface of the capillary that results from treatment with near- or supercritical water may help to keep the silica monolith in place.

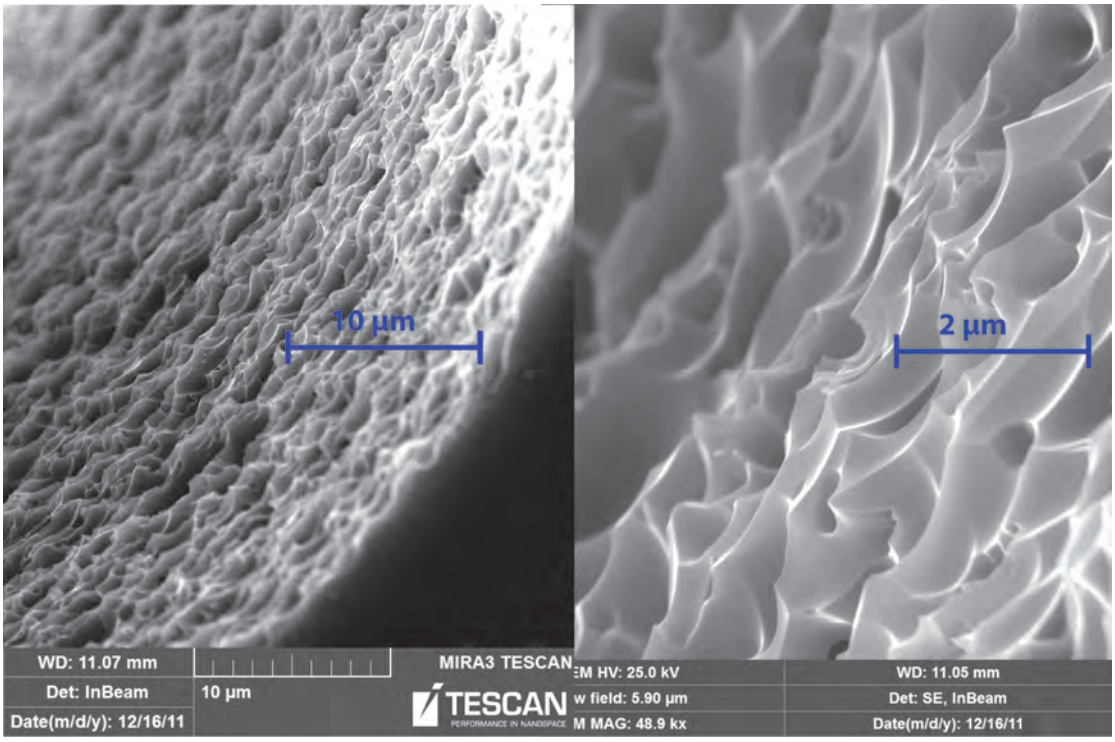

Fig. 3: Effect of treatment of 100 µm i.d. fused silica capillary with supercritical water in semi-dynamic mode. Experimental conditions: 400 °C, 32 MPa, 20 replacements of supercritical water.

2.4 Supercritical water in preparation of tapered fused silica capillaries

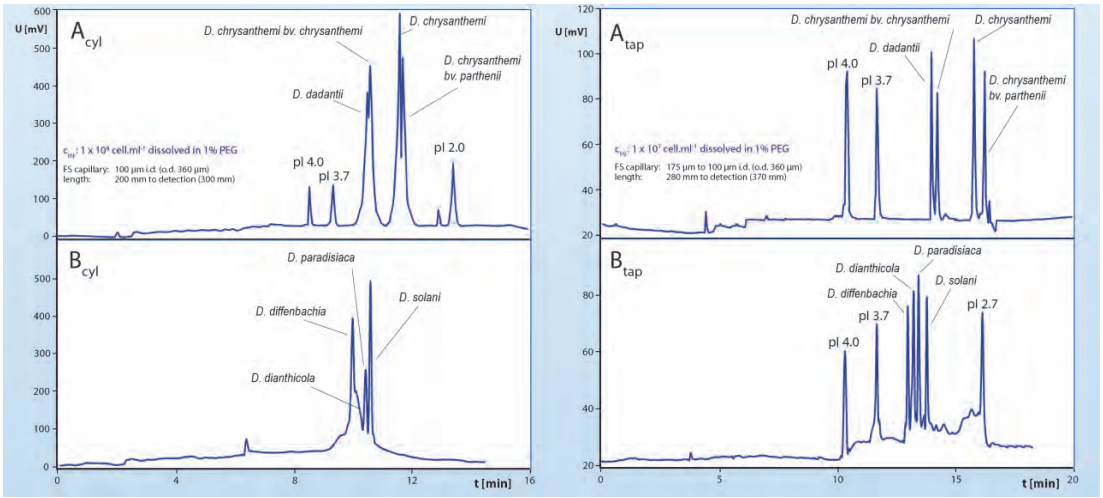

Fig. 4: Resolution of several *Dickeya* bacterium species with similar isoelectric points by capillary isoelectric focusing in 2.0–4.0 pH gradient employing cylindrical (left) and tapered (right) capillary.

Depending on the flow mode of supercritical water through the treated capillary, the capillary may either remain cylindrical after the treatment (Sect. 2.3.) or it may be turned into a capillary with a long, bubble-like cavity from which a conical (tapered) section can be cut out

[6.]. Previous theoretical considerations [8.] have indicated that the use of a tapered capillary may enhance the resolution of amfolytes by capillary isoelectric focusing as compared to the resolution obtained in a cylindrical capillary. **Fig. 4** suggests that the resolution enhancement is really the case even when the longitudinal profile of the capillary employed did not quite match the optimum profile predicted by the theory.

3 CONCLUSION

Although near- and supercritical water is a reactive and aggressive medium, it can still be indirectly useful even for bioanalytical separations. Among the topics discussed in this contribution, the most promising directions capitalize on the ability of supercritical water to solubilize fused silica. Therefore, supercritical water can be used for reproducible preparation of tapered capillaries to enhance the resolution of amfolytes by capillary isoelectric focusing, and also for the inner surface treatment of fused silica capillaries prior to preparation of monolithic silica columns for applications in HPLC.

ACKNOWLEDGEMENTS

We thank the Czech Science Foundation (Projects P206/11/0138, P503/11/P523 and P106/12/0522), the Ministry of Interior of the Czech Republic (Projects VG20102015023 and VG20112015021) and the Academy of Sciences of the Czech Republic (Institutional Support RVO:68081715) for funding of this work.

LITERATURE

[1.] Šťavíková, L., Polovka, M., Hohnová, B., Karásek, P., Roth, M., *Talanta* 2011, *85*, 2233-2240.

[2.] Karásek, P., Hohnová, B., Planeta, J., Šťavíková, L., Roth, M., *Chemosphere*, submitted (Ms. No. CHEM26623).

[3.] Dandeneau, R. D., Zerenner, E. H., *Journal of High Resolution Chromatography & Chromatography Communications* 1979, *2*, 351-356.

[4.] Anderson, G. M., Burnham, C. W., *American Journal of Science* 1965, *263*, 494-511.

[5.] Fournier, R. O., Rowe, J. J., *American Mineralogist* 1977, *62*, 1052-1056.

[6.] Karásek, P., Planeta, J., Roth, M., *Analytical Chemistry*, submitted (Ms. No. ac-2012-02849q).

[7.] Planeta, J., Moravcová, D., Roth, M., Karásek, P., Kahle, V., *Journal of Chromatography A* 2010, *1217*, 5737-5740.

[8.] Šlais, K., *Journal of Microcolumn Separations* 1995, 7, 127-135.

REDOX LABELING OF NUCLEIC ACIDS FOR ELECTROCHEMICAL DNA SENSING

Miroslav Fojta

Institute of Biophysics ASCR v.v.i., Královopolská 135, CZ-612 65 Brno, Czech Republic; Central European Institute of Technology, Masaryk University, Kamenice 753/5, CZ-625 00 Brno, Czech Republic

fojta@ibp.cz

ABSTRACT

DNA exhibits intrinsic electrochemical activity due to electrochemically reducible or oxidizable nucleobases and displays characteristic adsorption/desorption behavior at mercury or amalgam electrodes. Label-free electrochemical DNA analysis is thus in principle possible and it has been utilized in various applications such as detecting DNA damage. Nevertheless,

in sequence-specific DNA sensing, typing of single-nucleotide polymorphisms (SNP) etc., utilization of electroactive labels appears to be advantageous. In this contribution, several examples of using redox-active DNA tags in electrochemical DNA sensing is presented.

1 INTRODUCTION

Nucleic acids (NA) exhibit electrochemical activity due to electrochemical reducibility or oxidizability of the nucleic acids constituents [1]. This intrinsic NA electroactivity as well as chracteristic surface activity have been utilized in a number of label-free NA assays (see Table I for examples). At the mercury and some amalgam electrodes, both redox and tensammetric responses of the NAs are strongly sensitive to the accessibility of nucleobase residues, providing information about DNA structure. Despite generally less pronounced structure sensitivity of NA oxidation signals measured at the carbon electrodes, oxidation of guanine represents the most popular way to label-free NA electrochemical analysis. Many electrochemical sensing systems have been proposed to detect DNA hybridization – forming duplex DNA of two complementary single strands, of which one is specifically designed as a probe to detect the complementary target strand featuring the analyte. It seems that a more reliable distinction among the probe/target/hybrid duplex DNA, and particularly recognition of single nucleotide substitutions in the target DNA, can be attained through application of redox active labels rather than through label-free DNA electrochemistry [2].

2 NUCLEIC ACIDS LABELING WITH OXOOSMIUM COMPLEXES

Incorporation of oxoosmium tags into nucleic acids can be attained through the reaction of osmium tetroxide complexes (Os(VIII),L) with pyrimidine (predominantly thymine) nucleobases, or via the reaction of osmate(VI) complexes (Os(VI),L) with terminal ribose residues in ribonucleotides. Modification of base-unpaired thymines within oligo- and polynucleotide chains under physiological conditions and distinct electrochemical properties of the Os,L-labeled DNA render the Os(VIII),L reagents useful for various modes of electrochemical DNA sensing [3]. Electrochemical studies of the oxoosmium-modified DNAs with mercury-based electrodes revealed three reversible faradaic processes within potential region between 0.0 and -1.0 V, and a process involving catalytic hydrogen evolution around -1.2 V. At carbon or gold electrodes, the reversible faradaic signals due to the Os,L DNA adducts can be observed. A strategy employing reporter probes (RP) labeled with the osmium tags has been developed to analyze DNA sequences via molecular hybridization and more recently also to monitor DNA-protein interactions. Moreover, some of the the oxoosmium reagents (such as Os(VIII),bipy, where bipy stands for 2,2'-bipyridine) have successfully been applied to detect DNA damage and thymine residues within single base mismatches [3].

Table 1. Examples of label-free and label-based electrochemical DNA assays

Purpose	Label (indicator)	Electrode material	Molecular principle	Source of the signal
DNA damage	label-free	mercury, amalgam	strand breakage and/or enzymatic DNA digestion, double-helix unwinding at the electrode	adsorption /desorption of DNA
	label free	carbon	damage to an electroactive nucleobase (usually guanine)	usually guanine oxidation
	Os,bipy	carbon	enzymatic DNA digestion combined with selective chemical modification of ssDNA	redox of Os,bipy/DNA adducts
DNA hybridization	label-free	carbon, ITO	double helix formation of complementary strands, differing in guanine content	guanine oxidation
	label-free	carbon, gold	double helix formation of complementary strands; distinction between ss and ds DNA by negative charge density	EIS with anionic depolarizer
	labeled reporter probes: Os(VIII),L, ferrocene	carbon, gold	double helix formation between a ss target and labeled complementary probe	redox of covalently bound tags
DNA minisequen-cing; SNP typing	labeled dNTP: ferrocene, nitrophenyl, [Os(bpy)3]2+	carbon, gold	site-specific incorporation of labeled nucleotides	redox of covalently bound tags

(Techniques reviewed in 1-4)

3 ENZYMATIC INCORPORATION OF LABELLED NUCLEOTIDES

Labeled DNAs can be prepared enzymatically via incorporation of modified nucleotides using DNA polymerases or terminal deoxynucleotidyl transferases (TdT) [4] and deoxynucleotide triphosphates (dNTPs) bearing suitable redox tags. The palette of available labeled dNTPs is being continuously expanded owing to progress in the methodology of synthesis of base-modified dNTPs, involving C7-substitutions of 7-deazapurines, C8-substitutions of purines and C5-substitutions of pyrimidines [4]. Several electroactive DNA tags (such as ferrocene, nitro- and aminophenyl, [M(bpy)3]3+/2+ complexes of Ru or Os, anthraquinone etc.) producing specific electrochemical signals due to their reversible or irreversible reduction or oxidation at different potentials have been applied. Diversity in electrochemical properties of these labels offers their facile distinction from one another, as well as from intrinsic DNA responses related to reduction or oxidation of natural nucleobases. Simple nucleobase analogues, such as 7-deazapurines (commercially available as dNTPs), are applicable as specific electroactive tags as well since these bases exhibit substantially lower overpotentials of electrochemical oxidation, compared to their natural counterparts [5]. The enzymatic DNA

labelling strategy has been applied in a number of biological applications, including DNA hybridization, PCR monitoring, SNP typing and DNA-protein interaction studies.

ACKNOWLEDGEMENT

Financial support from The Czech Science Foundation GACR (project P206/12/G151) and GA ASCR (IAA400040901) is gratefully acknowledged.

LITERATURE

[1.] Paleček E., Bartošík M.: *Chem Rev* 2012 *112*, 3427–3481.
[2.] Fojta, M, Havran, L, Pivonkova, H, Horakova, P, Hocek, M. *Curr Org Chem* 2011, *15*, 2936-2949.
[3.] Fojta, M.; Kostecka, P.; Pivonkova, H.; Horakova, P.; Havran, L*. Curr Anal Chem*, 2011, *7*, 35-50.
[4.] Hocek M., Fojta M. *Chem. Soc. Rev*. 2011, *40*, 5802-5814
[5.] Pivonkova, H.; Horakova, P.; Fojtova, M.; Fojta, M*.: Anal. Chem*. 2010, *82*, 6807-6813

Abstracts of Poster Presentations

P01 METHOD DEVELOPMENT OF AMINO ACIDS PROFILING FOR PYRIDOXIN DEPENDENT EPILEPTIC SEIZURES DIAGNOSIS

Andrea Cela, Ales Madr, Jindra Musilova, Marta Zeisbergerova, Zdenek Glatz

Department of Biochemistry, Faculty of Science and CEITEC, Masaryk University, Kamenice 5, 625 00 Brno, Czech Republic
glatz@chemi.muni.cz

ABSTRACT

Metabolic disorders associated with epileptic seizures can be resolved by the monitoring of α-aminoadipic acid semialdehyde, piperideine-6-carboxylate and pipecolic acid levels in plasma, urine or cerebrospinal fluid. Some epileptic seizures are related to a deficiency of enzymes involved in the amino acids metabolism and elevated levels of prolin and of the other amino acids can be observed. As a result, amino acid profiling can be used for diagnostic purposes. Method development of amino acid profiling of human sera using capillary electrophoresis coupled with in-house-assembled capacitively coupled contactless conductivity detection was performed and concluded in background electrolyte composed of 8 % (v/v) acetic acid and 0.1 % (m/m) hydroxyethyl-cellulose, cassette temperature 30 °C, separation voltage +30 kV, capillary made of bare fused silica of 80.0 cm total length and 50 μm of inner diameter. Human sera was got rid of proteins by acetonitrile precipitation in 1:1 volume ratio and the supernatant was then directly introduced into capillary by a 50 mbar pressure gradient for 12 seconds.

Keywords: pyridoxin dependent epilepsy, amino acids profiling, capillary electrophoresis

1 INTRODUCTION

Some epileptic seizures are related to metabolic disorders affecting availability of pyridoxal-phosphate (PLP). It can be caused by either increasing the PLP utilization/inactivation, or by reduction of PLP synthesis. The first case is called *pyridoxine dependent epilepsy* (PDE) and is treatable by high doses of pyridoxine. The second case is called *pyridoxal-phosphate dependent epilepsy* (PPDE) which is treatable by high PLP doses [1].

PDE is associated with mutations in ALDH7A1 or ALDH4A1 genes. ALDH7A1 gene encodes an enzyme α-aminoadipic acid semialdehyde (α-AASA) dehydrogenase (antiquitin) involved in the pipecolic acid (PA) pathway of the lysine metabolism. Piperideine-6-carboxylate (P6C) is a cyclic Schiff base of α-AASA. Deficiency of antiquitin causes accumulation of P6C which inactivates PLP by undergoing Knoevenagel reaction. ALDH4A1 gene encodes an enzyme pyrroline-5-carboxylate (P5C) dehydrogenase. It catalyzes conversion of P5C to glutamic acid in the proline metabolism. Deficiency of P5C dehydrogenase causes P5C accumulation. P5C inactivates PLP by undergoing Knoevenagel reaction. Patients suffering from PDE have elevated levels of α-AASA, P6C and PA as well as glycine and proline in urine, plasma and cerebrospinal fluid (CSF) [2].

PPDE is related to pyridoxamine 5'-phosphate oxidase deficiency which converts pyridoxine and pyridoxamine to PLP. PLP acts in amino acids and neurotransmitter metabolisms.

PDE and PPDE can be revealed by a molecular analysis of the respective genes, by a determination of the reliable biomarkers using high-performance liquid chromatography [2-3]

and by the amino acid profiling using capillary electrophoresis (CE) where the most valid are levels of glycine, proline and hydroxyproline.
CE is a powerful analytical technique offering high separation efficiency. It is suitable for the determination of the amino acids in biological fluids such as plasma, urine and CSF. All amino acids can be detected in their native form using capacitively coupled contactless conductivity detector (C^4D), which enables also detection of analytes, when strongly absorbing organic solvents are used as background electrolytes (BGEs) in CE [4].

2 EXPERIMENTAL

2.1 Material and methods

There were utilized Agilent G7100A CE System (Agilent Technologies, Santa Clara, CA, USA) equipped with in-house-assembled C^4D. C^4D was derived from the one presented by Gas *et al.* [5] with operational frequency 2.46 MHz. Data acquisition and integration was performed by Agilent ChemStation software.
Separations were carried on bare fused silica capillaries (CM Scientific, Silsden, UK) of inner diameter 50 µm, outer diameter 375 µm and total length 80.0 cm. Effective length (*i.e.* from sample introduction end to C^4D cell) was 65.6 cm.
All chemicals were of analytical grade purity. Stock solutions of the amino acids were of 20 mM concentration and were stored in a refrigerator. Stock solution of 1 % (m/m) hydroxyethyl-cellulose (HEC) was prepared by stirring the solution overnight and stored at a room temperature. BGE was prepared by mixing the appropriate volume of an acetic acid (HAc) and the stock solution of HEC giving final concentration of HAc and HEC, 6-20 % (v/v) and 0.1 % (m/m), respectively. BGE was filtered using syringe membrane filter devices with 0.45 µm pores and degassed in an ultrasonic bath for 10 minutes.

2.2 Sample treatment

For the method development there were used lyophilized human sera purchased from Sigma-Aldrich. Sera were reconstituted in Milli-Q water (Millipore Corporation, Billerica, MA, USA) and aliquots were stored frozen at -70 °C. Aliquots were tempered at 25 °C prior to sample treatment step. It included simple protein precipitation by an addition of acetonitrile in the volume ratio 1:1. Mixture was thoroughly stirred and the supernatant was collected after 10 minutes of centrifugation at 10 000×g. The supernatant was enriched by the addition of 250 µM of creatinine (CR), glycine (Gly), L-prolin (Pro) and *trans*-4-hydroxy-L-proline (OH-Pro) and final dilution of sera was 2.1 times.

2.3 Method development

Initial separation conditions were based on the paper by Coufal *et al.* [4]. These were tested many times on different biological samples [6-8] with slight changes in concentrations of HAc and in the replacement of HEC by other hydrophilic polymers. The polymer acts as electroosmotic flow suppressor and improves precision in migration times between runs [4].

3 RESULTS

3.1 Effect of acetic acid concentration on selectivity

Firstly, there were tested HAc concentrations in range of 10-20 % (v/v). Lower concentrations of HAc showed to be more suitable for sera analyses, thus final optimization of HAc concentration was made in range of 6-11 % (v/v) by 1 % increment. There was selected 8 % (v/v) HAc for further optimization steps based on resolution and baseline stability criteria.

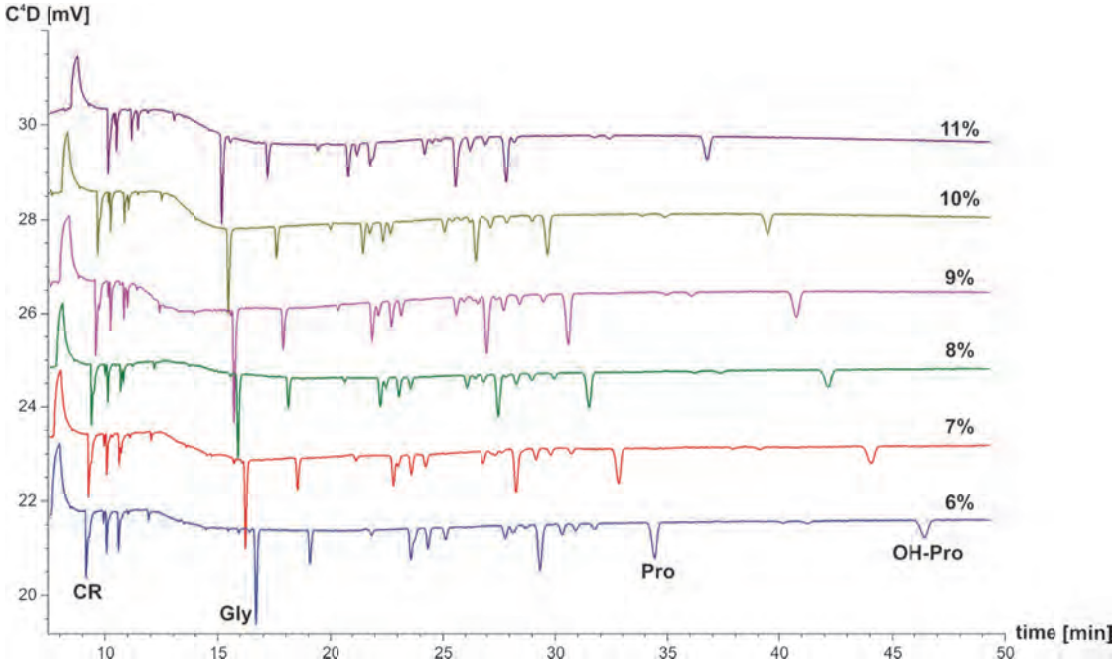

Fig. 1: Effect of HAc on selectivity. There was studied influence of HAc concentration in the range of 6-11 % (v/v) on selectivity in the analysis of the human sera sample. The human sera were diluted twice in acetonitrile in order to precipitate protein, centrifuged for 10 minutes at 10 000×g and the supernatant was introduced into capillary by the 50 mbar pressure gradient for 12 seconds. Capillary was made of bare fused silica with inner diameter 50 µm, total and effective lengths were 80.0 cm and 65.6 cm, respectively. Separation voltage was +30 kV, cassette temperature was 25 °C. Sample was spiked by 250 µM of CR, Gly, Pro and OH-Pro.

3.2 Effect of temperature on separation

Temperature can affect dissociation equilibria of analytes, *i.e.* effective mobilities as well, thus resolution between peaks of the analytes can be altered. There were examined effects of the temperature on the resolution in the range of 15-45°C concerning baseline resolution of CR, Gly, Pro and OH-Pro. There was chosen 30 °C because of the total separation time is for 5 minutes shorter with insignificant changes in the resolutions in comparison with the separation at 25°C.

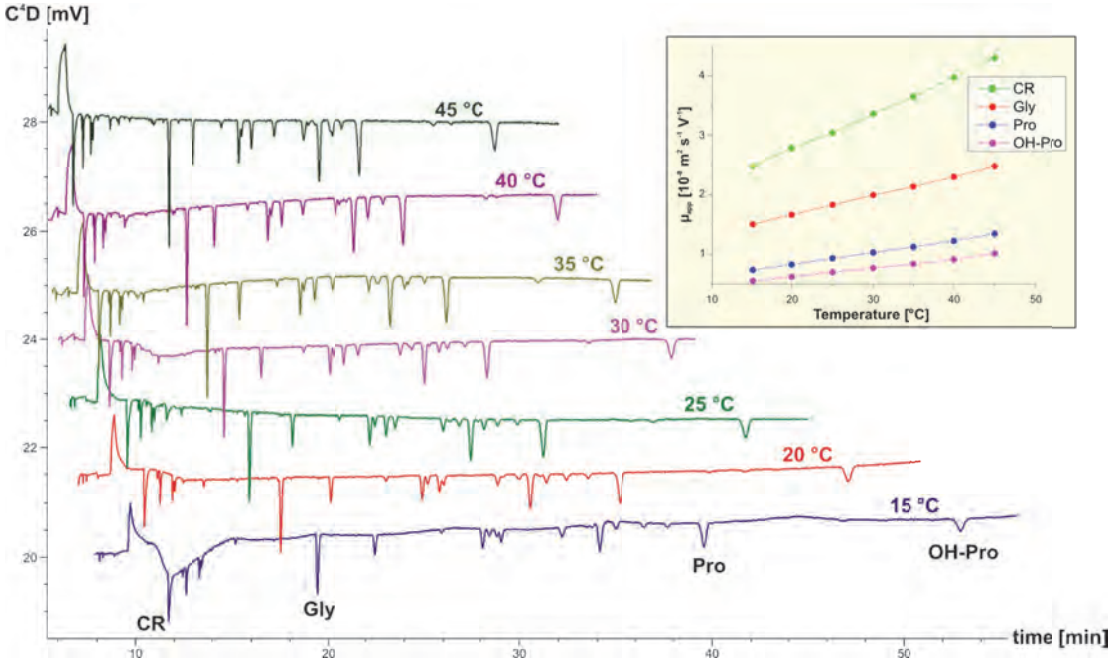

Fig. 2: Effect of temperature on separation of the human sera. The embedded graph shows the dependence of the effective mobility of selected analytes on the temperature. There was studied influence of the temperature in the range of 15-45°C on the resolution in the analysis of the human sera sample. The human sera were diluted twice in acetonitrile in order to precipitate protein, centrifuged for 10 minutes at 10 000×g and the supernatant was introduced into capillary by the 50 mbar pressure gradient for 12 seconds. Capillary was made of bare fused silica with inner diameter 50 μm, total and effective lengths were 80.0 cm and 65.6 cm, respectively. BGE was composed of 8 % (v/v) HAc and 0.1 % (m/m) HEC. Separation voltage was +30 kV. Sample was spiked by 250 μM of CR, Gly, Pro and OH-Pro.

4 CONCLUSION

Method development for the amino acids profiling based on CE coupled with C^4D was presented. Final conditions include BGE consisting of 8 % (v/v) HAc and 0.1 % (m/m) HEC, cassette temperature 30 °C, separation voltage +30 kV, capillary made of bare fused silica of 80.0 cm total length and 50 μm of inner diameter and sample introduction into capillary by the 50 mbar pressure gradient for 12 seconds.

ACKNOWLEDGEMENTS

Financial supports granted by the Czech Science Foundation are highly acknowledged (Projects P206/11/0009 and P206/12/G014).

LITERATURE

[1.] Plecko, B., Stockler, S., *Canadian Journal of Neurological Sciences* 2009, *36*, 73-77.
[2.] Mills, P.B., Footitt, E.J., Mills, K.A., Tuschl, K., *et al., Brain* 2010, *133*, 2148-2159.
[3.] Sadilkova, K., Gospe Jr., S.M., Hahn, S.H., *Journal of Neuroscience Methods* 2009, *184*, 136-141.
[4.] Coufal, P., Zuska, J., van de Goor, T., Smith, V., *et al., Electrophoresis* 2003, *24*, 671-677.
[5.] Gas, B., Zuska, J., Coufal, P., van de Goor, T., *Electrophoresis* 2002, *23*, 3520-3527.
[6.] Samcova, E., Tuma, P., *Electroanalysis* 2006, *18*, 152-157.
[7.] Tuma, P., Samcova, E., Duska, F., *Journal of Separation Science,* 2008, *31*, 2260-2264.
[8.] Tuma, P., Malkova, K., Samcova, E., Stulik, K., *Journal of Separation Science,* 2010, *33*, 2394-2401.

P02 DIFFERENCES IN FINGERPRINTS OF BIOFILM-POSITIVE AND BIOFILM-NEGATIVE *CANDIDA* STRAINS EXPLOITABLE FOR CLINICAL PRACTICE

Marie Vykydalová[a,b], Marie Horká[a], Jiří Šalplachta[a], Filip Růžička[c], Vladislav Kahle[a]

[a] *Institute of Analytical Chemistry of the ASCR, v. v. i., Veveří 97, 602 00 Brno, Czech Republic.*
vykydalova@iach.cz
[b] *Department of Biochemistry, Faculty of Science, Masaryk University Brno, Kotlářská 267/2, 611 37 Brno, Czech Republic*
[c] *Department of Microbiology, Faculty of Medicine, Masaryk University, Pekařská 53, 602 00 Brno, Czech Republic*

ABSTRACT

Phenotypically indistinguishable strains *Candida parapsilosis* and *Candida metapsilosis* can form strongly adhesive biofilm layers. Biofilm-positive forms are clinical important and can cause recurrent and invasive candidiasis, especially in immune-compromised patient. Typically, biofilm grows on catheters and implanted devices. On the other hand, biofilm-negative *Candida parapsilosis* is typically a commensal of human skin of healthy people.
In this study, we have presented differences in fingerprints of *Candida parapsilosis* and *Candida metapsilosis* as well as their biofilm-positive and biofilm-negative forms. Fingerprints of yeasts were obtained by sodium dodecyl sulfate polyacrylamide gel electrophoresis, capillary isoelectric focusing, and matrix-assisted laser desorption/ionization time-of-flight mass spectrometry. Samples for analyses were prepared by treatment of yeasts by boiling water or ethanol. Fingerprints of tested yeasts cells have differed in all cases. This knowledge can be used for obtaining rapid and simple method which distinguishes above mentioned yeasts in standard biochemical laboratories.

Keywords: *Candida*, biofilm, fingerprint

1 INTRODUCTION

Candida parapsilosis is the second most commonly isolated *Candida* species from blood cultures. The incidence of infections caused by this pathogen has dramatically increased during last few years. It is most frequently isolated from skin and is deemed as a part of normal microflora. But also it is important nosocomial pathogen [1.]. *Candida parapsilosis* was divided into three closely related distinct species: *Candida parapsilosis, Candida metapsilosis* and *Candida orthopsilosis* [2.]. These yeasts can exist either as biofilm-positive, (+), they form adhesive biofilm layer, or as biofilm-negative, (-), form.
Rapid identification and differentiation of yeasts as well as their biofilm-positive and biofilm-negative forms is necessary for successful treatment and survival of the patients. Molecular biological methods as polymerase chain reaction (PCR) [3.] and enzyme-linked immuno-sorbent assay (ELISA) can be used for differentiation of members of this group but these techniques have several disadvantages. They are time-consuming, expensive and they are not parts of standard laboratories.
Earlier reports have revealed the possibility of application of electrophoretic separation techniques, capillary isoelectric focusing (CIEF), and capillary zone electrophoresis (CZE) as well as matrix-assisted laser desorption/ionization time-of-flight mass spectrometry (MALDI-TOF MS) for differentiation of *Candida* strains [4.-6.].
In this paper, treated yeasts cells (supernatnts, pellets, and whole cells) were investigated using SDS-PAGE for supernatants, CIEF for pellets and MALDI-TOF MS for whole cells.

2 MATERIAL AND METHODS

2.1 Preparation of sample

All the strains examined in this study were clinical strains obtained from Masaryk University and St. Anna University Hospital (Brno, Czech Republic).

2.1.1 Supernatants

Yeasts (±100 mg) from one dish of medium were put to 500 µL of boiling water where they were retained for 1 hour. After these procedures the suspensions were centrifuged at 6100 × g for 15 min. The supernatants were dosed onto SDS-PAGE gel. Pellets remaining in vials after removing of the supernatant were used for next analysis (see section 2.1.2).

2.1.2 Pellets

Pellets obtained by treatment of yeasts cells by boiling water or 70% EtOH (pellets were prepared by the same way as pellets obtained by treatment yeasts by boiling water) were resuspended in water (8×10^7 cells in 1 mL), centrifuged 6100× g for 15 min. and injected together with p*I* marker into the capillary.

2.1.3 Whole cells

Twenty microliters of particular yeast suspension was mixed with 20 mL of sinapinic acid (SA) solution (16 mL^{-1} in acetonitrile/0.1% trifluoroacetic acid, 3 : 2, v/v) just before mass spectrometric analysis.

2.2 Instrumentation

2.2.1 SDS-PAGE

Precipitated proteins obtained after evaporation of supernatants were dissolved in 100 µL of sample buffer (0.5M Tris–HCl, pH 6.8, 2% (w/v) SDS, 26% (v/v) glycerol, 5% (v/v) β-mercaptoethanol, 0.01% (w/v) bromophenol blue). 20 µL of samples were dosed into gel 4–20% Mini-PROTEAN® TGX™ Precast Gel. Analysis was performed on Mini-PROTEAN 3 Cell (Bio-Rad, Hercules, CA, USA). Constant voltage of 160 V was used to run the gel. Protein visualization was performed with CBB G-250 in accordance with manufacturer's manual.

2.2.2 CIEF

UV detection and pH gradients 2.0-5.0 and 5.0-7.5 were carried out for CIEF. Procedure and conditions were described in previous work [8.].

2.2.3 MALDI-TOF MS

MALDI-TOF MS experiments were performed on 4700 Proteomics Analyzer (Applied Biosystems) in linear positive ion mode, 3,5-dimethoxy-4-hydroxycinnamic acid (sinapinic acid) was used as a matrix. Experimental conditions are described in detail elsewhere [7.].

3 RESULTS

The experiments were repeated three-times for each monitored strain as well as their forms and culture-to-culture and strain-to-strain reproducibility was verified.

3.1 SDS-PAGE

Wide-range gradient gel from 14.2 to 200.0 kDa for SDS-PAGE analysis was used in order to catch most proteins from the supernatants obtained using boiling water. Pictures of SDS-

PAGE gel is shown in Fig. 1. Significant differences in present bands are observed in fingerprints of all tested samples yeasts almost in the whole range of molecular weights, 14.2-119.0 kDa. Sharp protein bands are found in lower mass region 14.2-36.0 kDa. Other differences are observed in mass region from 55.0 to 119.0 kDa. *C. parapsilosis* and *C. metapsilosis* as well as their biofilm-positive and biofilm-negative forms could be easily distinguished using this technique.

3.2 CIEF

Pictures of CIEF fingerprints are shown in Fig. 2. Significant differences in present peaks are observed in fingerprints of all tested samples biofilm-positive yeasts. Fingerprints of yeasts treatment by boiling water are similar but p*I* individual peaks have different value. On the other hand, fingerprints of yeasts treatment by 70 % (v/v) EtOH are different in number of peaks as well as value of p*I.* Also these techniques could be differentiating *C.parapsilosis* and *C.metapsilosis*.

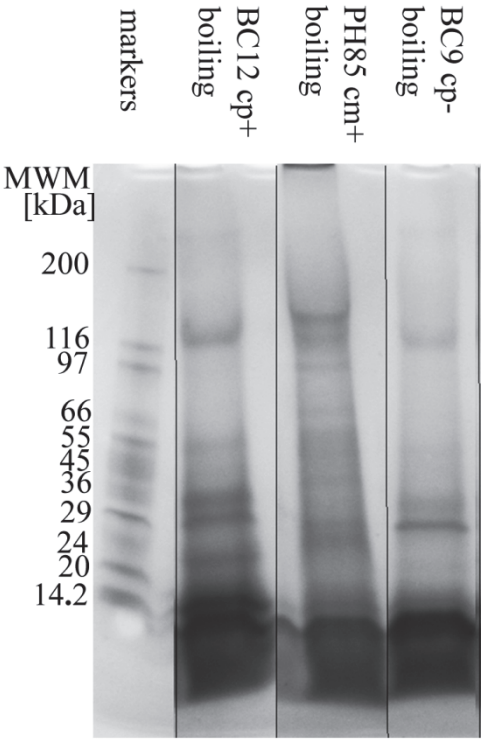

Fig. 1.: Comparison of SDS-PAGE fingerprints of supernatant of treatedyeasts *C. parapsilosis*and *C. metapsilosis*and their biofilm-positive (cp+, strains BC12, PH85) and biofilm-negative (cp-, strain BC9) forms.

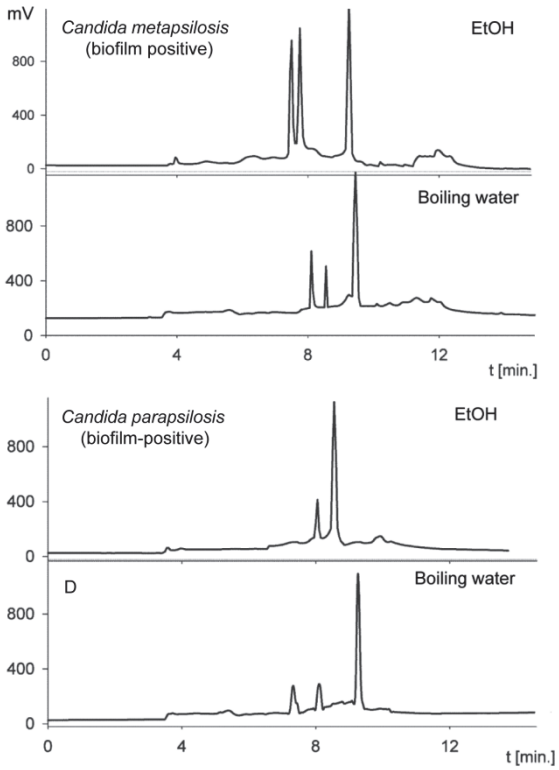

Fig. 2: Comparsion of CIEF fingerprints of pellet of *C. parapsiolosis and C. metapsilosis* in the pH gradient 2-5 with UV detection.

3.3 MALDI-TOF MS

Fingerprints obtained using MALDI-TOF MS are shown in Fig. 3. Obtained data have revealed that *C. parapsilosis* and *C. metapsilosis* differ distinctively from each other mainly in the 2200-7000 m/z range. Furthermore, biofilm-negative and biofilm-positive strains can be

also distinguished based on MALDI fingerprints of cellular suspension as results from the measured data. Biofilm-negative and biofilm-positive strains of both *C. parapsilosis* and *C. metapsilosis* differ in the range of m/z 2200-6000 and 7000-14000. MALDI-TOF MS seems to be an efficient and reliable tool able to differentiate between C. ''psilosis'' species as well as between biofilm-negative and biofilm-positive forms within a species.

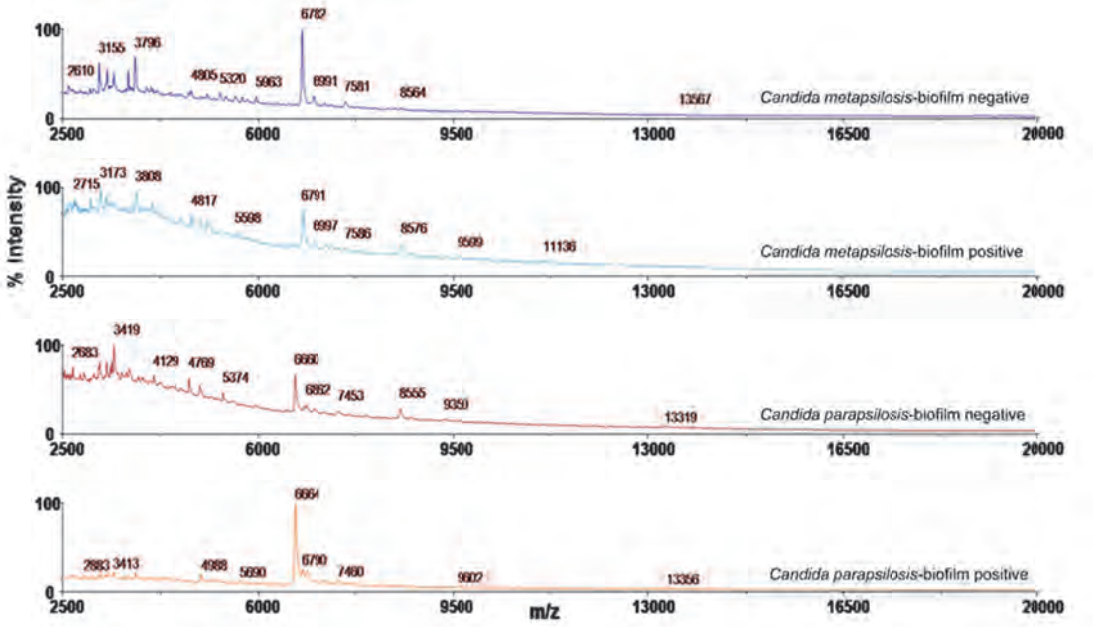

Fig. 3.: MALDI-TOF mass spectra obtained from cellular suspensions of biofilm-negative and biofilm-positive strains of *C. metapsilosis* and *C. parapsilosis*, respectively.

ACKNOWLEDGEMENTS

This work was supported by the grant of the Ministry of the Interior of the Czech Republic No. VG20112015021 and with institutional support RVO: 68081715, and by the Ministry of Education Youth and Sports of the CR - project Development of Multidisciplinary Research and Educational Centrum for Bioanalytical Technologies No.CZ.1.07/2.3.00/20.0182.

LITERATURE

[1.] Růžička, F., Holá, V., Votava, M., Tejkalová, R., *Folia Microbiologica* 2007, *52*, 209-214.

[2.] Tavanti, A., Davidson, A. D., Gow, N. A. R., Maiden. M.C. J., *et al.*, *Journal of Clinical Microbiology* 2005, *43*, 284-292.

[3.] Dendis, M., Horváth, R., Michálek, J., Růžička, F., *et al*., *Clinical Microbiology and Infection* 2003, *9*, 1191-1202.

[4.] Horká, M., Růžička, F., Holá, V., Šlais, K., *Electrophores* 2009, *30*, 2134-2141.

[5.] Horká, M., Růžička, F., Kubesová, A., Němcová, *et al*., *Journal of Chromatography A* 2011, *1218*, 3900-3907.

[6.] Růžička, F., Horká, M., Holá, M., Kubesová, *et al*., *Journal of Microbiological Methods* 2010, *80*, 299-301.

[7.] Kubesová, A., Šalplachta, J., Horká, M., Růžička, F., Šlais, K. *Analyst* 2012, *137*, 1937-1943.

[8.] Horká, M., Kubíček, O., Růžička, F., Holá, V., *et al.*, *Journal of Chromatography A* 2007, *1155*, 164-171.

P03 NANO COLUMN GRADIENT SEPARATIONS: IMPLEMENTATION OF SIMPLE SPLITLESS GRADIENT GENERATOR WITH INTEGRATED SAMPLE DELIVERY

Jozef Šesták[a,b], Filip Duša[a,c], Dana Moravcová[a], Vladislav Kahle[a]

[a] *Institute of Analytical Chemistry of the ASCR, v. v. i., Veveří 97, 602 00 Brno, Czech Republic, sestak@iach.cz*
[b] *Faculty of chemistry, Brno University of Technology, Purkyňova 464/118, 612 00, Brno, Czech Republic*
[c] *Department of Biochemistry, Faculty of Science, Masaryk University, Kotlářská 2, 611 37 Brno, Czech Republic*

ABSTRACT

Automated liquid chromatographic system based on simple splitless gradient generation principle and with integrated sample delivery has been assembled and tested. Gradient generator was represented by 100-µl glass microsyringe held in inclined position and operated by programmable OEM syringe pump. Continuous gradients of mobile phase were created in the syringe barrel by successive sucking of adequate volume of four mobile phases with gradually decreasing acetonitrile concentration and due to turbulent mixing at the syringe needle-barrel boundary. Fluids were delivered through ten port selector valve. Syringe needle was connected to the central port of the selector valve via short piece of the fused silica capillary which also served as an injection loop. System performance was evaluated using test mixture of six alkylphenones as well as tryptic digest of bovine serum albumin. Good values of relative standard deviation of retention times and sample injection volumes were received (RSD < 0.3 % and RSD < 5 % respectively).

Keywords: Splitless gradient; Nano column; BSA

1 INTRODUCTION

Benefits of gradient elution and reduced column diameter in liquid chromatography have been well documented elsewhere [1-4]. High mass sensitivity of nano columns, flow rate compatibility with electrospray, and opportunity to separate analytes of wide range of polarity by gradient elution is attractive for many researchers going about biologic samples these days. Employing nano columns on standard HPLC gradient instrumentation is not effective due to splitting of major part of mobile phase and large gradient delay volume. However, repeatable generation of splitless mobile phase gradient for micro and nano columns at the flow rates below 1 µl·min^{-1} is not an easy task. Commercial systems have been placed on the market not long ago. They are robust but they are bulky and expensive too. Simple and easily modifiable system may be adequate substitute for such complex and expensive instrumentation and may serve well in certain sectors (e. g. basic research, education). Thus, we have recently published a simple laboratory set-up for peptide pre-concentration and separation by gradient elution [5] and now we have developed an automated splitless gradient liquid chromatographic system for the gradient elution in micro and nano columns with the low backpressure.

2 DESCRIPTION OF SPLITLESS GRADIENT CHROMATOGRAPHIC SYSTEM

2.1 Gradient generator

Gradient generator was represented by glass microsyringe held in inclined position. Pressure resistance of glass syringes up to 50 bars is sufficient when the columns with a low

backpressure are used. If portion of low eluting mobile phase is sucked into the syringe initially filled with strong eluting mobile phase a sigmoidal gradient with prolonged linear mid part is formed due to turbulences occurring in the place of sudden change of the tubing diameter (syringe needle-barrel boundary) [6, 7]. Maximum volume of sigmoidal gradient generated this way is limited and relatively small. Gradient volume is expanded when adequate volumes of three or four mobile phases with gradually decreasing acetonitrile concentration are successively sucked into the syringe. It is essential that the syringe is in an inclined position under the angle of 20° with the needle pointing downwards. The heavier water-rich part of the mobile phase is then located in the lower part of the syringe barrel.

2.2 Instrument function

Chromatographic system consists of the NE-500 OEM programmable syringe pump (1) equipped with 100-µl glass microsyringe (2) (SGE Analytical Science, Victoria, Australia) and ten port selector valve C55-1340 I (3). Experimental design is depicted in **Fig. 1**. Hydraulic connections were performed using fused silica capillaries (MicroQuartz, Munich, Germany). Syringe needle was connected to the central port of the selector valve via short piece of the fused silica capillary (100 mm × 180 µm i. d, 360 µm o. d.) which also served as an injection loop (5). The first four ports served as inlets for ACN-water mobile phases with gradually decreasing acetonitrile concentration (6-9). The fifth port served as the sample (10) inlet and the sixth one was connected to the separation column (11). The seventh port served as a path to the waste (12) while remaining ports stayed unoccupied.

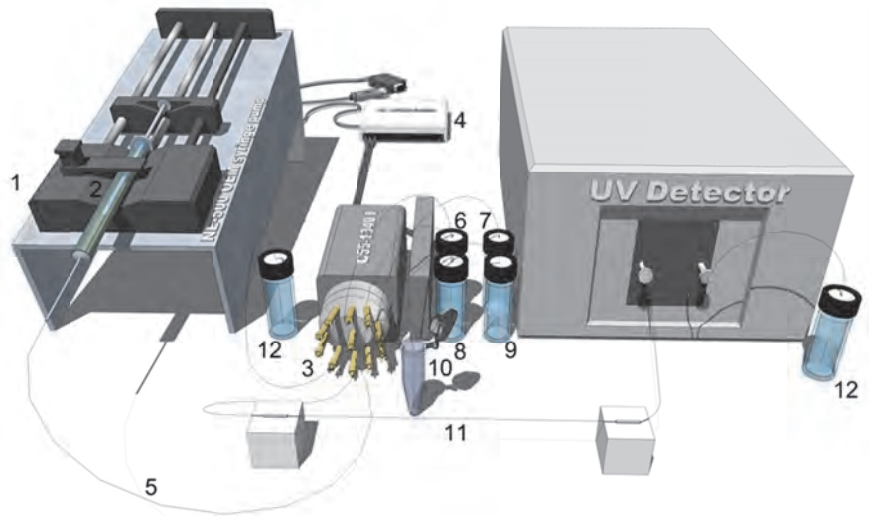

Fig. 1.: Instrument design. (1) Programmable syringe pump, (2) Glass syringe, (3) Ten port selector valve, (4) NI-USB 6009 data acquisition device, (5) Sample loop, (6-9) Mobile phases, (10) Sample, (11) Separation column, (12) Waste.

Controlling software for syringe pump operation and stream selection was programmed in LabVIEW development environment (National Instruments, Austin, TX). First of all the syringe was filled with the lowest eluting mobile phase and adequate volume was pushed through the column to re-equilibrate it. Remaining volume of the syringe was drained into waste. Remains of previous mobile phase were wash out from the syringe by repeated sucking and pushing of adequate volume of the final mobile phase into the waste. Then the adequate volumes of the four mobile phases with gradually decreasing acetonitrile concentration were sucked into the syringe. The flow path was then changed and desirable volume of a sample was sucked into the sample loop. After the flow path had switched to the column, the analysis began.

3 PERFORMANCE OF SPLITLESS GRADIENT CHROMATOGRAPHIC SYSTEM

Gradients of different steepness were created by successive sucking of adequate volumes of 5, 30, 55, and 80 % v/v solution of acetonitrile (marked by 20 mg·l^{-1} of uracil) in water. Absorbance of uracil was measured by Agilent VWD SL+ detector (G1314E, Agilent Technologies, Santa Clara, CA) equipped by a nano cell (SunChrom, Friedrichsdorf, Germany) with effective optical path of 0.17 mm. Gradient capabilities of suggested system are illustrated in **Fig. 2**.

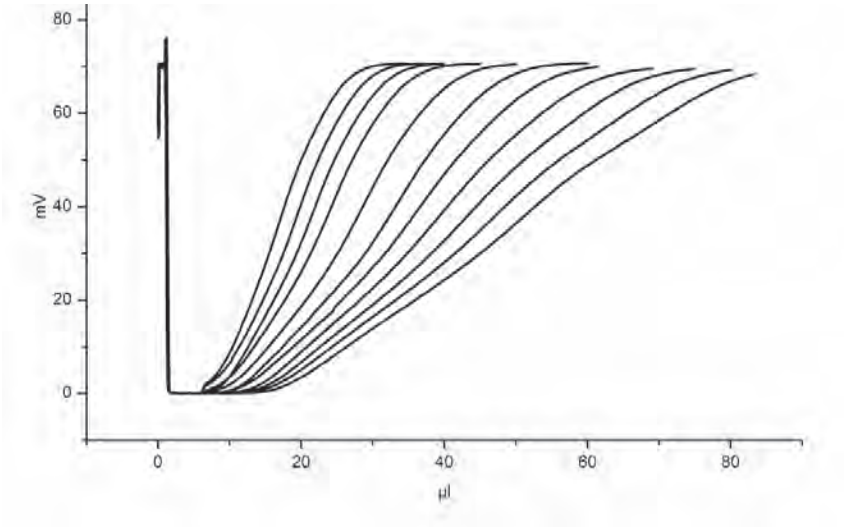

Fig. 2.: Gradient profiles created by sucking of gradually increasing volumes of 5, 30, 55, and 80 % v/v solution of acetonitrile in water (100% acetonitrile contained 20 mg·l^{-1} of uracil). Gradient delivered at the flow rate of 1 µl·min^{-1}. Gradient trace detected at 254 nm.

To determine a repeatability of sample delivery a mixture of six alkylphenones in the range from 0.1 µl to 3 µl was injected using the principles of on-column focusing [8]. Relative standard deviations of peak areas were about 5 % and less. A solution of BSA tryptic digest was then injected and analyzed to demonstrate suitability of chromatographic system to perform gradient elution of proteomic samples. Overlaid chromatograms are shown in **Fig. 3**. Relative standard deviations of the retention times (n = 8) of ten highest peaks were from 0.17 to 0.30 %.

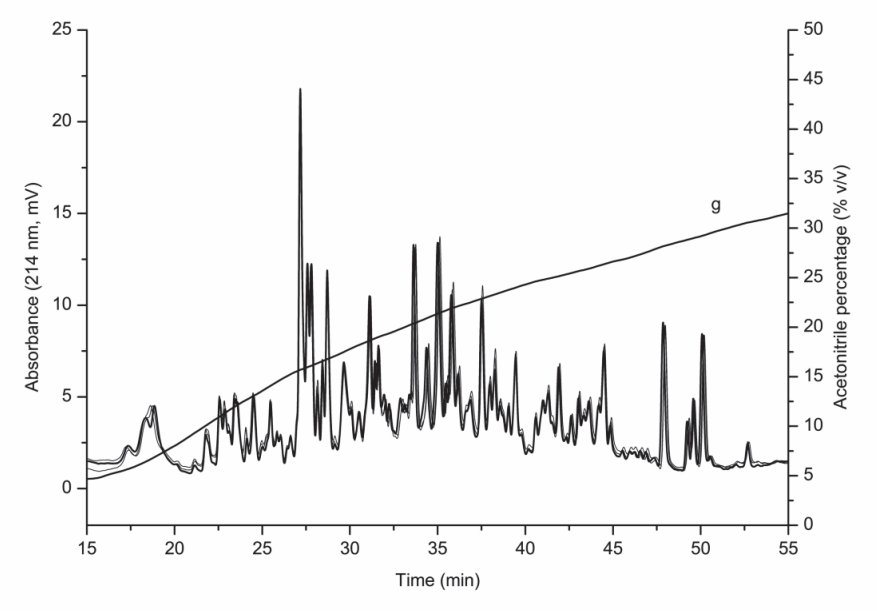

Fig. 3.: Gradient separation of BSA tryptic digest – overlaid chromatograms of three successive runs. g = gradient track; Sample: 0.5 µl 1 $g \cdot l^{-1}$. Column: Chromolith CapRod RP-18e 150 mm × 0.1 mm. Mobile phase gradient formed by successive sucking of 15, 20, 20, and 20 µl of 5, 30, 55, and 80 % v/v, respectively, solution of acetonitrile in water (each contained 0.1 % v/v of TFA). Mobile phase flow rate: 0.5 $\mu l \cdot min^{-1}$. Temperature: 25 °C.

ACKNOWLEDGEMENTS

This work was supported by the Ministry of the Interior of the Czech Republic (Project No. VG20112015021 and Project No. VG20102015023) and by the Academy of Sciences of the Czech Republic (Institutional support RVO: 68081715).

LITERATURE

[1] Jandera, P., Churacek, J., Gradient Elution in Column Liquid Chromatography: Theory and Practice, Elsevier, New York 1985.

[2] Snyder, L. R., Dolan, J. W., High-performance Gradient Elution: The Practical Application of the Linear Solvent Strenght Model, Wiley, Hoboken 2007.

[3] Kucera, P., Microcolumn high-performance liquid chromatography, Elsevier, New York 1984.

[4] Krejci, M., Trace analysis with microcolumn liquid chromatography, Marcel Dekker, New York 1992.

[5] Moravcova, D., Kahle, V., Rehulkova, H., Chmelik, J., Rehulka, P., J. Chromatogr. A 2009, 1216, 3629-3636.

[6] Que, A.H., Kahle, V., Novotny, M.V., J. Microcolumn. Sep. 2000, 12, 1-5.

[7] Kahle, V., Vazlerova, M., Welsch, T., J. Chromatogr. A 2003, 990, 3-9.

[8] Ling, B. L., Baeyens, W., Dewaele, C., J. Microcolumn. Sep. 1992, 14, 17-22.

P04 MICROPREPARATIVE SOLUTION ISOELECTRIC FOCUSING OF PEPTIDES AND PROTEINS IN NONWOVEN STRIP

Filip Duša[a,b], Karel Šlais[a]

[a] *Institute of Analytical Chemistry of the ASCR, v.v. i., Veveří 97, Brno, 602 00, Czech Republic*
[b] *Department of Biochemistry, Faculty of Science and CEITEC, Masaryk University, Kamenice 5, Brno, 625 00, Czech Republic*

ABSTRACT

Recently we devised a new instrument for micropreparative analysis [1]. It is based on solution phase isoelectric focusing (sIEF) performed in a narrow channel (approximately 2 – 4 mm wide) with a strip of nonwoven fabric serving as the analysis bed. The strip can be precut before an analysis to make harvesting of fractions easier. Isoelectric focusing is driven by a programmable electrophoretic power supply. Progress of analysis is monitored by addition of colored isoelectric point (*pI)* markers. Usually sIEF runs are performed overnight. Evaporation of water is one of crucial features of analysis and it forces free liquid to shrink into the nonwoven fabric strip. Moreover, water evaporation increases liquid viscosity by altering ethylene glycol/water ratio. Fractions can be harvested simply by collecting and washing precut segments after the sIEF run. In this paper we used sIEF device for purification of caseinomacropeptide (CMP) from crude whey. Obtained fractions were further analyzed by HPLC. From acquired data a plot with chromatograms of all fractions was constructed to show purification profile of CMP. We proved that the new instrument is capable of quantitative purification of CMP complex from a globulin fraction.

Keywords: isoelectric focusing, preparative, whey

1 INTRODUCTION

Isoelectric focusing is suitable and broadly used method for protein purification and separation. There are several sIEF devices based on following designs: multicompartment, off-gel and continuous flow. Here, we present a new device [1] based on nonwoven strip. Sweet whey is rich in proteins including CMP which is valuable dietary supplement [2]. Next to CMP, α-lactalbumin and β-lactoglobulin are the most abundant proteins in whey and thus two major contaminants. Concerning above mentioned proteins/peptides we found in literature their *pI*s to be 3.15 – 4.15, 4.2 – 4.5 and 5.13 respectively [3, 4]. With knowledge of these isoelectric points we purified CMP from crude whey using our new sIEF device.

2 EXPERIMENTAL

2.1 Device description

Isoelectric focusing device consist of a plastic trough with a pre-cut nonwoven fabric strip on the bottom. On Figure 1 you can see design and operational protocol of IEF device. The figure is divided into parts designated with letters and arranged alphabetically to describe workflow. Top view of the solution phase IEF device based on segmented nonwoven fabric strip can be seen on Figure 1A. The plastic trough is clipped to a base with a pair of wires which serves as electrodes. The end of the anode is made of a carbon rod. Separation space is defined by the dimensions of strip which can be optionally precut into segments. Plastic cover foil serves both as a contamination protection and as a retarder of evaporation.

2.2 sIEF operation protocol

Running solution was prepared from: 0.375 ml of 1 % solution of dried whey, 0.05 ml of stock solution of colored *pI* markers, 0.1 ml ethylene glycol, 0.05 ml butan-1-ol, 0.025 ml 0.1 mol·l^{-1} 1 imidazolyl-acetic acid and 0.1 ml of 0.1 mol·l^{-1} Tris. On figure 1B you can see detail of pipetting running solution onto the strip which soaks up along the whole strip (Figure 1C). Cover foil is placed over the strip (Figure 1D), power is turned on (Figure 1E) and separation is done. After finished IEF, fractions are harvested by picking up the segments (Figure 1F), fixing the segments into pipette tips (Figure 1G) and washing out the fractions into micro test tubes (Figure 1H).

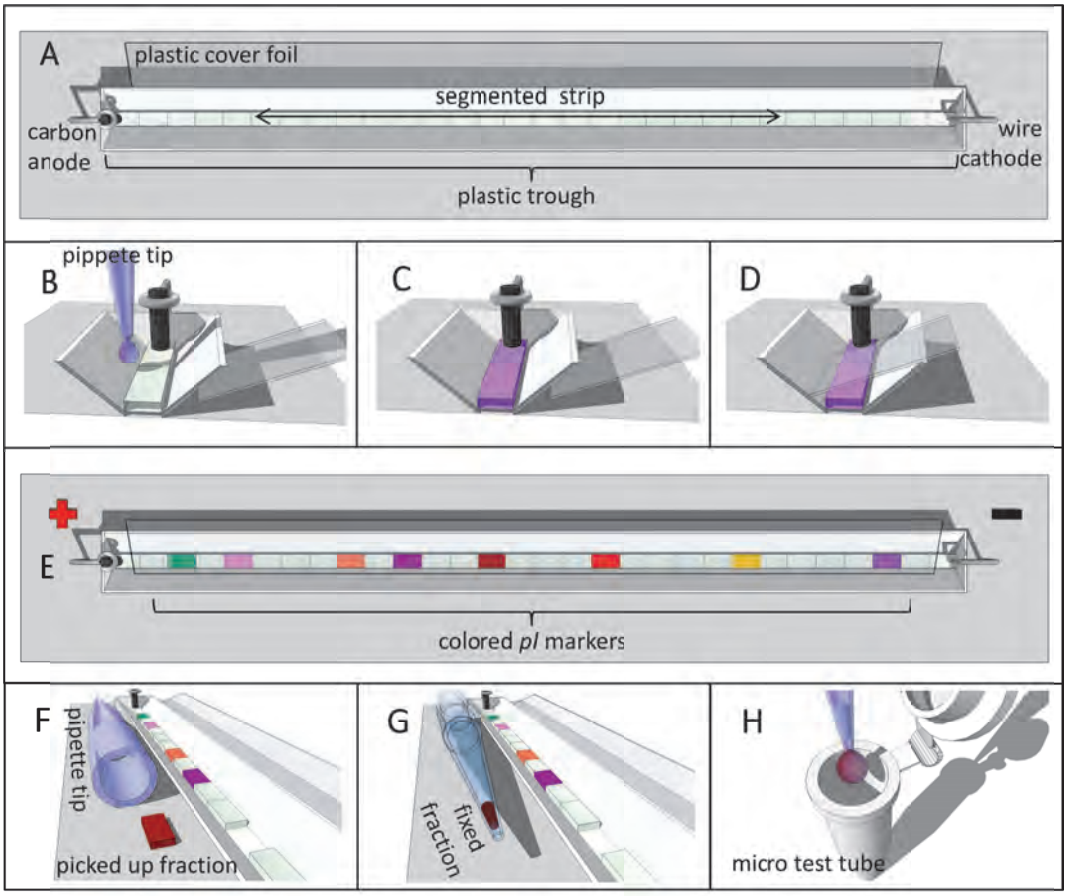

Figure 1: sIEF operation protocol.

2.3 Reversed-phase liquid chromatography

Subsequently, fractions are subjected to reversed-phase liquid chromatography (RPLC). All chromatographic separations were performed using the Agilent 1200 Series chromatographic. The separations were performed on the microbore Poroshell 300SB-C18 column (5 µm particle size, 1 × 75 mm, Agilent Technologies) equipped with the C18 cartridge guard. Linear gradient from 5 to 80% (v/v) of acetonitrile with 0.1 % of trifluoracetic acid over 30 min was used for separation. The elution was run at the flow rate of 20 µl·min^{-1} and 70 °C. The detection was performed at 214 nm and 280 nm using the diode-array detector.

3 RESULTS AND DISSCUSION

Chromatograms obtained from RPLC analysis were processed into one plot where concentration profiles of the three most abundant proteins/peptides in whey can be seen

(Figure 2). IEF fractions in the figure are numbered from anodic to cathodic side, meaning the fraction number one is the most acidic fraction. On Figure 2 one can easily recognize that CMP (designated with gray rectangle) was almost quantitatively separated from α-lactalbumin and β-lactoglobulin (traces of α-lactalbumin left in the first four fractions). Straight line of chromatograms of fractions six, seven and eight is due to utilizing imidazolyl-acetic (*pI* 4.8) acid as *pI* spacer between the three mentioned proteins/peptides. Although common way of CMP purification is ultrafiltration, we proved that our sIEF device can be used as alternative and provide CMP of high purity.

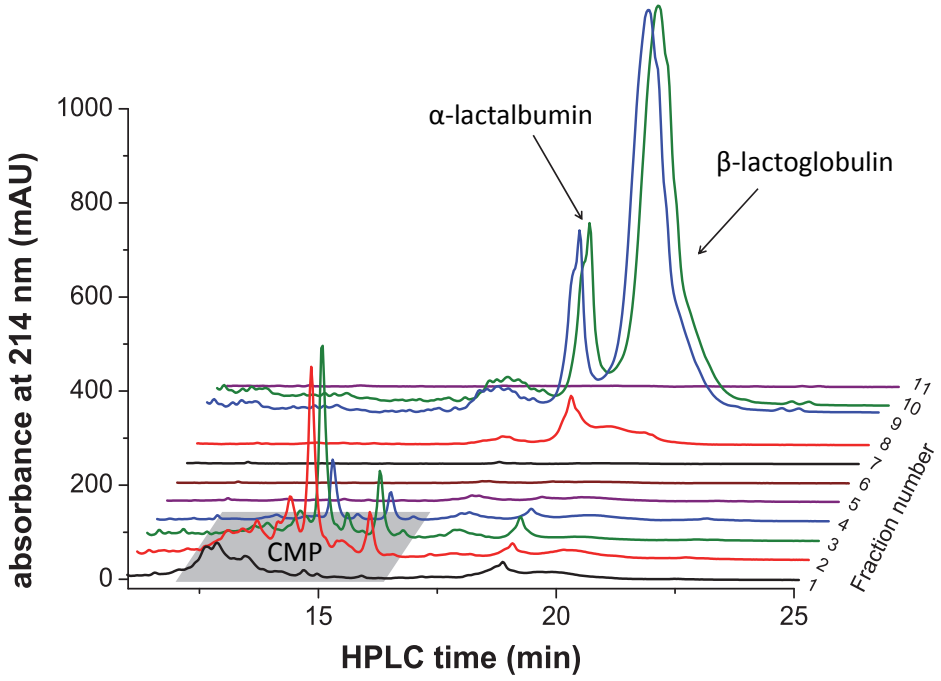

Figure 2: Chromatograms from HPLC analysis of sIEF fractions.

ACKNOWLEDGEMENTS

This work was supported by the Ministry of the Interior of the Czech Republic (Project No. VG20102015023), by the Ministry of Education, Youth and Sports of the Czech Republic by OPVK grant No. CZ.1.07/2.3.00/20.0182 Vytvoření multidisciplinárního výzkumného a vzdělávacího centra bioanalytických technologií (BBC) and by the Academy of Sciences of the Czech Republic (Institutional Research Plan RVO: 68081715).

LITERATURE

[1.] Šlais. PV 2012-100

[2.] Madureira, A. R., Tavares, T., Gomes, A. M. P., Pintado, M. E., Malcata, F. X., Journal of Dairy Science 2010, 93, 437-455.

[3.] Farrell, H. M., Jimenez-Flores, R., Bleck, G. T., Brown, E. M., Butler, J. E., Creamer, L. K., Hicks, C. L., Hollar, C. M., Ng-Kwai-Hang, K. F., Swaisgood, H. E., Journal of Dairy Science 2004, 87, 1641-1674.

[4.] Kreuss, M., Strixner, T., Kulozik, U., Food Hydrocolloids 2009, 23, 1818-1826.

P05 POTENTIAL OF EXHALED BREATH CONDENSATE ANALYSIS IN POINT OF CARE DIGNOSTICS

Petr Kubáň[a], Eeva-Gerda Kobrin[b], Mihkel Kaljurand[b]

[a] *Group of Bioanalytical Instrumentation, CEITEC MU, Veveri 97, 602 00, Brno, Czech Republic, petr.kuban@ceitec.muni.cz*
[b] *Institute of Chemistry, Tallinn University of Technology, Akadeemia tee 15, 12618 Tallinn, Estonia*

ABSTRACT

Exhaled breath condensate has been analyzed for its ionic content by capillary electrophoresis with capacitively coupled contactless conductometric detection. Two devices for exhaled breath condensate collection were compared. These include a tube-in-tube cooled sampler and a simple zip-lock bag. The devices allow collection of small volumes (100-200 µL) of exhaled breath condensate in less than 2 min. A method for quick (less than 3 min) simultaneous determination of inorganic cations, inorganic anions and organic anions from the samples using dual-opposite end injection principle with a short fused silica capillary (35 cm, 50 µm i.d.) was optimized with final background electrolyte composition of 20 mM 2-(N-morpholino)ethanesulfonic acid, 20 mM L-histidine, 30 µM cetyltrimethylammonium bromide and 2 mM 18-crown-6 was used. It has been shown that changes of nitrite could be observed in acute inflammation of upper airways and in person with diagnosed mild chronic obstructive pulmonary disease, while the changes of other ions could also be observed.

Keywords: Exhaled breath condensate, capillary electrophoresis, point of care diagnostics.

1 INTRODUCTION

It has been long known that changes of chemical composition in tissues and biological fluids may be indicative of processes occurring in the organism, including an ongoing disease, previous intake of drugs of abuse or signaling other physiological conditions. Analysis of these markers in biological fluids is most commonly performed after so called “invasive” sampling (such as venipuncture during the blood sampling, lumbar puncture to sample cerebrospinal fluid from the spinal column or biopsy for identification and analysis of suspect tissues). On contrary, “non-invasive“ sampling represents an appealing alternative, because it causes minimum stress to the organism and can be easily obtained even far from medical facilities and by non-trained personnel. In particular, non-invasive sampling is attractive in the field of medical prevention, screening, diagnostics and therapy of diseases at an early stage. Unfortunately, in current medical and clinical practice, non-invasive sampling is not very common as there is a lack of approved non-invasive sampling techniques and corresponding analytical methods. This applies for instance for the analysis of exhaled breath condensate (EBC). EBC is the liquid obtained upon cooling and condensation of exhaled air. Exhaled breath is saturated with water vapors that will condensate by breathing through a cooling or freezing system. Although the condensate consists mostly of water vapor, it also contains aerosol particles or respiratory fluid droplets. The aerosolized particles contribute to the non-volatile EBC constituents, such as inorganic ions, small organic molecules and proteins. The analysis of EBC may offer a simple way of monitoring of various diseases related (but not limited) to the function of lung and respiratory tract [1]. EBC sampling consists of simple breathing into a specially designed device: commercially available devices can be used, such as bench top EcoScreen [2] or portable Rtube [3], but home made devices typically perform similarly to the commercial ones. One disadvantage of home made devices is that they are not portable and may require rather bulky accessories. Another significant problem with conventional EBC sampling is the required sample volume which is typically

several milliliters with sampling times between 10 and 60 minutes. The large sample volume requirement depends mainly on the subsequent analytical method used. In this contribution we show that CE with contactless conductivity detection (C4D) can be used for analysis of ionic content of EBC that is collected with very simple collection devices. We employ an optimized separation system with dual-opposite end injection and C4D detection for analysis of anions and cations in EBC simultaneously in less than 3 min. Practical example of EBC analysis by CE-C4D include screening of inorganic nitrogen reactive species during acute and chronic airway inflammation. The promising results obtained underscore the diagnostic potential of CE-C4D combined with non-invasive EBC sampling.

2 RESULTS AND DISCUSSION

2.1 Samplers for EBC collection, comparison of tube-in-tube and bag-type of samplers

Two types of EBC collection devices were used and tested. They are depicted in Figure 1. The EBC collection device is depicted in Figure 1A. It was constructed with maximum simplicity and minimal cost using commonly available laboratory consumables from a 50 mL polypropylene (PP) tube with skirted base and a and a 5 mL PP pipette tip. The PP tube was filled with DI water to provide the cooling of the pipette tip walls upon freezing. The simplest possible devices consisted of a LD-PE bag purchased in local store (Fig 1B). The bags were rinsed with DI water and dried prior use.

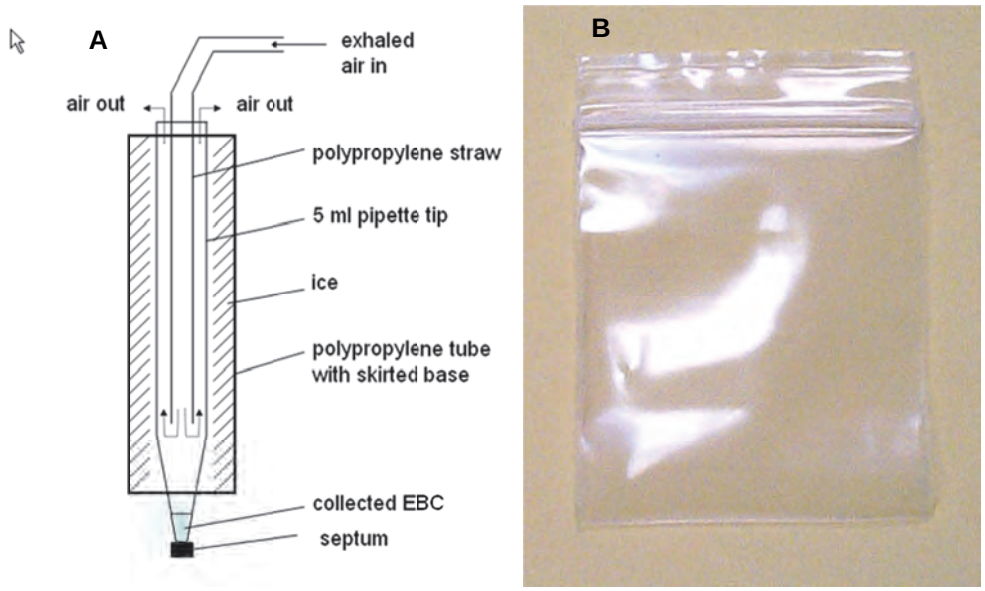

Fig. 1. Schematic of an in-house constructed tube-in-tube EBC collection device (A) and LD-PE zip-lock bag (B) used in the studies.

2.2 Electrophoretic system

A purpose-built CE instrument with C4D detector [4] was employed for all electrophoretic separations. The separation voltage of - 18 kV was provided by a high voltage power supply unit (Spellman CZE2000R Start Spellman, Pulborough, UK). The separation capillaries used were fused-silica capillaries (50 µm I.D., 375 µm O.D., 35 cm total length, Polymicro Technologies, Phoenix, AZ, USA). All CE experiments were performed at ambient temperature. Injection of standard solutions and EBC samples was carried out hydrodynamically by immersing the injection capillary end into a sample vial and elevating it

to a height of 10 cm for a specified time interval. Dual opposite end injection (DOEI) was accomplished by injecting the sample from both capillary ends.

2.3 Comparison of tube-in-tube and bag sampler for anion screening

The samplers were used in an initial suitability study to compare their performance. The test consisted of 2 minute breathing through the straw into the sampling device (A) or directly into the LD-PE bag (B). The collected liquid was subsequently analyzed by CE for anionic content. The results revealed that the data traces are very similar. Although the tube-in-tube sampling device is preferred because the collection efficiency was about 4-fold more efficient, the LD-PE bag can be used in remote or as an emergency sampler. It can eventually be tight sealed and send to the laboratory for analysis by regular mail.

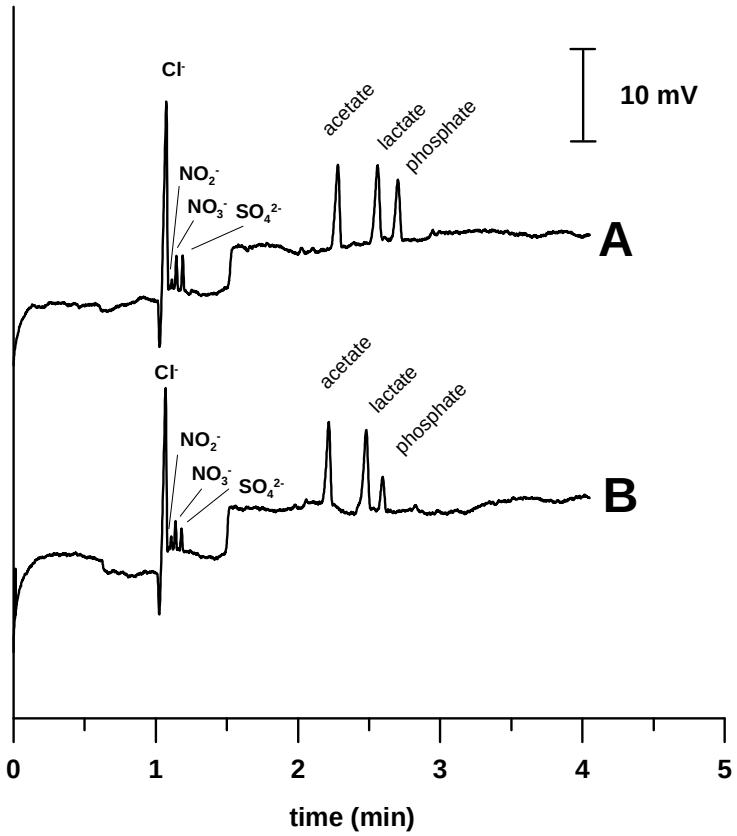

Fig. 2. Comparison of sampling devices: (A) tube-in-tube sampler, (B) zip-lock bag. CE conditions: -18kV, contactless conductivity detection. 20s HD injection from 10 cm.

2.4 Simultaneous separation of ions in EBC

The optimization of the separation conditions for simultaneous separation of anions and cations typically includes individual separations of both groups injected from opposite capillary ends, with the detection cell positioned at different positions along the separation capillary. The separation can be achieved by injecting the sample from both ends with a time delay, as demonstrated by Kubáň and Karlberg [5]. Two injection sequences are possible to achieve full separation of all ions. In the first one, the cations are injected first from cathodic capillary end and high voltage is applied for 25 s, followed by the injection of anions. By delaying the injection of anions by 25 s, the cations are separated first, followed by the anions

without any overlap. Conversely, by reversing the injection order and injecting anions first and applying the high voltage for 55 s before the cations are injected, the cations can be “fitted” to migrate between the formate and acetate peak. The possible separation scenarios are depicted in Figure 3.

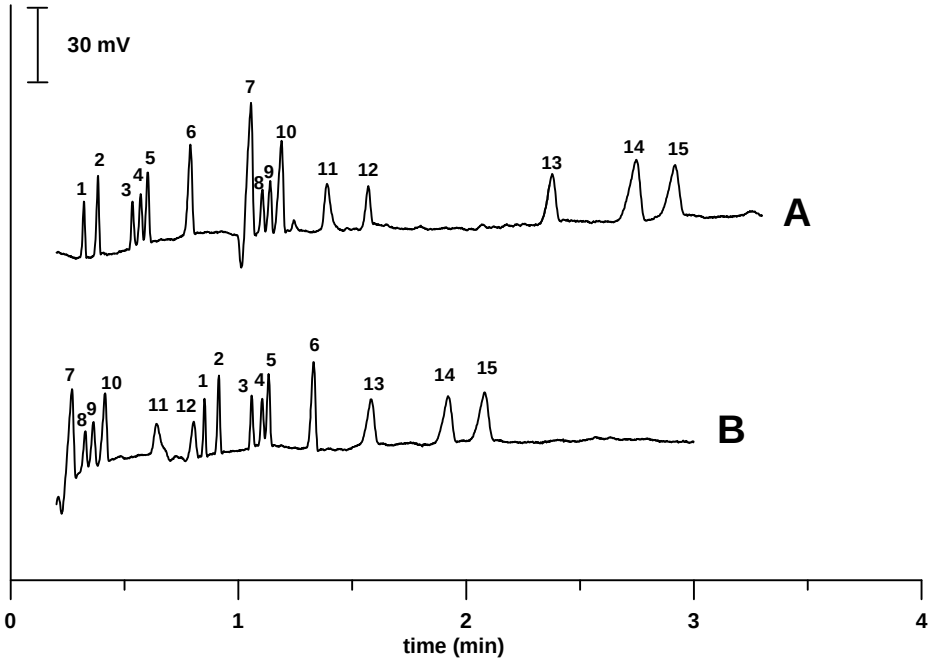

Fig. 3. Simultaneous separation of anions and cations using different injection sequences. (A)-timely displaced injections of cations (20s, HD injection from 10 cm), HV application 25s, followed by anions (20s, HD injection from 10 cm). (B)-timely displaced injections of anions (20s, HD injection from 10 cm), HV application 55s, followed by cations (20s, HD injection from 10 cm). Inlays: Example of simulated migration times vs. detector position (15 cm from anodic side). (A)-delayed injection of anions by 25 s, (B)-delayed injection of cations by 55s. CE conditions: -18kV, contactless conductivity detection. Peaks: (1)-NH_4^+, (2)-K^+, (3)-Ca^{2+}, (4)-Na^+, (5)-Mg^{2+}, (6)-Li^+, (7)-Cl^-, (8)-NO_2^-, (9)-NO_3^-, (10)-SO_4^{2-}, (11)-SCN^-, (12)-formate, (13)-acetate, (14)-lactate, (15)-phosphate.

2.5 Analysis of real samples

In an initial study (not shown here) we have analyzed 75 samples of healthy, non-smoker, population for the ionic content of EBC as a possible screening method to recognize and monitor respiratory tract inflammation or other (chronic) respiratory disease. It has been shown in several studies that increased levels of nitrogen-reactive species can be found in EBC of persons with serious lung condition. In here, we present some first promising results. Figure 4, trace A, shows an example of a simultaneous separation of anions and cations in EBC sample from a healthy volunteer with no record of any respiratory disease. The trace B shows an electropherogram of the same person during an acute infection of upper respiratory tract with serious cough, elevated temperature and other symptoms of common cold. The trace C in the same Figure, shows an electropherogram of a person with a diagnosed mild form of chronic obstructive pulmonary disease (COPD). The traces A, B and C look very similar, except that significantly elevated level of nitrite can be found in both traces B (nitrite: 7.3±0.5 µM) and C (nitrite: 9.6±0.8 µM). When comparing the traces A and B, the nitrite concentration is significantly higher in B than the level of nitrite before the acute respiratory tract inflammation and is about twice as high as the average nitrite concentration determined during the initial screening study of healthy volunteers. In trace C, except nitrite, elevated nitrate, sulphate and lactate were also observed. Whether these observations are related to

COPD and the acute inflammation would require a much more through and detailed study which is currently under way.

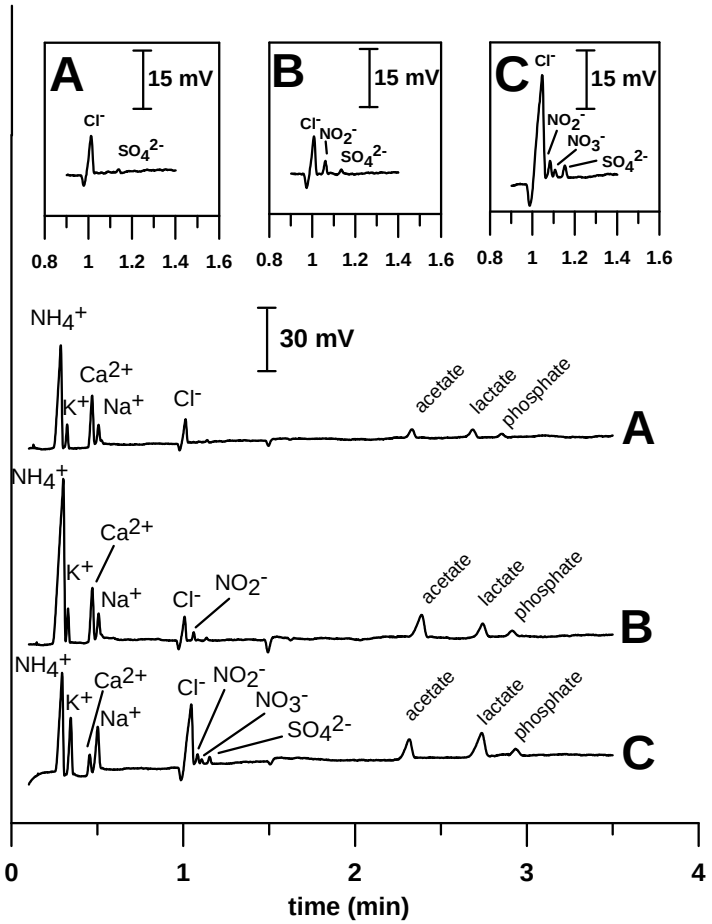

Fig. 4. Analysis of EBC. Electropherogram of simultaneous determination of anions and cations in: (A) - a healthy male, 38 years old, (B)- the same person as in (A) suffering from acute cold and serious cough, (C) – female, 67 years old, diagnosed with mild form of COPD. CE conditions are the same as in Figure 3A, except injection times: cations: 10s, anions 20s.

3 CONCLUSIONS

It has been demonstrated that capillary electrophoresis with C4D using DOEI can be used to rapidly analyze both inorganic cations and inorganic and organic anions present in EBC. The EBC sampling relies on a simple, inexpensive in-house made device that can be constructed in any analytical laboratory. The collection time is significantly reduced; typically 1-2 min is sufficient to collect 100-200 µL of EBC sample for CE analysis. It has been shown that changes of nitrite could be observed during acute inflammation of upper airways and in EBC of a person with diagnosed mild COPD, while the changes of other ions were also observed. Whether this method could possibly be used as a simple, non-invasive, point of care screening tool would however require deeper clinical study.

ACKNOWLEDGEMENTS

The financial funding from the European Union's Seventh Framework Programme under grant agreement no. 229830 IC-UP2 is acknowledged.

LITERATURE

[1.] S. Kharitonov, P.J. Barnes, Am. J. Respir. Crit. Care Med. 163 (2001) 1693-1722.
[2.] http://www.filt.de/
[3.] http://www.rtube.com/
[4.] L. Zhang, S.S. Khaloo, P. Kubáň, P.C. Hauser, Meas. Sci. Technol. 17 (2006) 3317-3322.
[5.] P. Kubáň, B. Karlberg, Anal. Chem. 70 (1998) 360-365.

P06 SEASONAL VARIATIONS OF METALS AND IONS IN PM1 AEROSOL IN BRNO AND ŠLAPANICE

Pavel Mikuška[a], Kamil Křůmal[a], Martin Vojtěšek[a], Nela Kubátková[a,b], Zbyněk Večeřa[a]

[a] *Institute of Analytical Chemistry, Academy of Sciences of the Czech Republic, v.v.i., Veveří 97, 602 00 Brno, Czech Republic, mikuska@iach.cz*
[b] *Faculty of Chemistry, Brno University of Technology, Purkyňova 464/118, 612 00 Brno, Czech Republic*

ABSTRACT

Submicron aerosol particles in the size fraction PM1 were collected in Brno and Šlapanice in winter and summer of 2009 and 2010. The aerosols were analysed for content of selected metals and ions.

Local traffic in summer and coal and wood combustion during household heating in winter were identified as the main emission sources of aerosols in both towns. Secondary aerosol components formed a significant part of aerosol during the whole year.

Keywords: PM1 aerosols, metals, ions

1 INTRODUCTION

Epidemiological studies [1-3] have suggested a statistical association between health effects and ambient fine particle concentrations, especially the submicron fraction (PM1) that can penetrate deep into the alveolar region of the lungs. Chemical composition of PM2.5 and PM10 is subject of many studies, however, relatively little attention has so far been paid to PM1 aerosols. Determination of their composition is essential to understand their properties and reactivity and hence their environmental and health effects [4].

2 EXPERIMENTS

Aerosol particles in the size fraction PM1 were collected in Brno at balcony on the first floor of the Institute of Analytical Chemistry faced to Veveří Street while the collection of aerosols in Šlapanice was performed in the garden of a family house (Fig. 1). Aerosols in the size fraction PM1 were sampled every day for 24-hours over one week in winter and summer of 2009 and 2010. A total number of 56 filters (28 samples from Brno and 28 samples from Šlapanice) were collected.

The aerosols were collected using a high-volume sampler (DHA-80, Digitel, 30 m^3 h^{-1}) on cellulose-nitrate filters (150 mm diameter, 3 µm, Sartorius). In parallel, the aerosols were sampled on 47 mm Teflon filters (Zefluor, 1 µm, PALL Corporation) using a low-volume sampler (1 m^3 h^{-1}), consisting of a NILU filter unit (type 9633) and a Teflon coated aluminium cyclone inlet (URG-2000-30EH). To avoid interferences of gaseous pollutants (NH_3, NO_2, HNO_3, HONO, SO_2, O_3, HCl, VOCs, …), an annular diffusion denuder [5] was placed between

the cyclone and the NILU filter unit. During passing of air through the denuder, the gaseous interferences were efficiently removed by their collection onto a solid absorbing layer (i.e., mixture of Na_2SO_3 and activated charcoal) while aerosols passed through the denuder without any change.

Mass concentrations of collected aerosols were determined by weighing filters, using a microbalance (±1 µg; M5P, Sartorius). Filters were equilibrated before weighing for 48 hours in air-conditioned room under constant conditions (temperature 20 ± 1 °C, relative humidity 50 ± 3 %).

Exposed cellulose-nitrate filters with collected aerosols were digested in nitric acid at microwave device UniClever (Plazmatronika) and extracts were analysed for 15 selected metals (Al, K, Ca, Fe, Mn, Zn, Cu, Pd, Cd, Ba, As, Pb, V, Ni, Sb) employing an ICP-MS (7500 CE, Agilent).

Exposed teflon filters were extracted with deionized water under ultrasonic agitation and extracts were analysed using an ion chromatography (ICS-2100, Dionex) for the content of 6 anions (nitrate, sulfate, nitrite, fluoride, chloride, oxalate) and 5 cations (NH_4^+, Na^+, K^+, Ca^{2+}, Mg^{2+}).

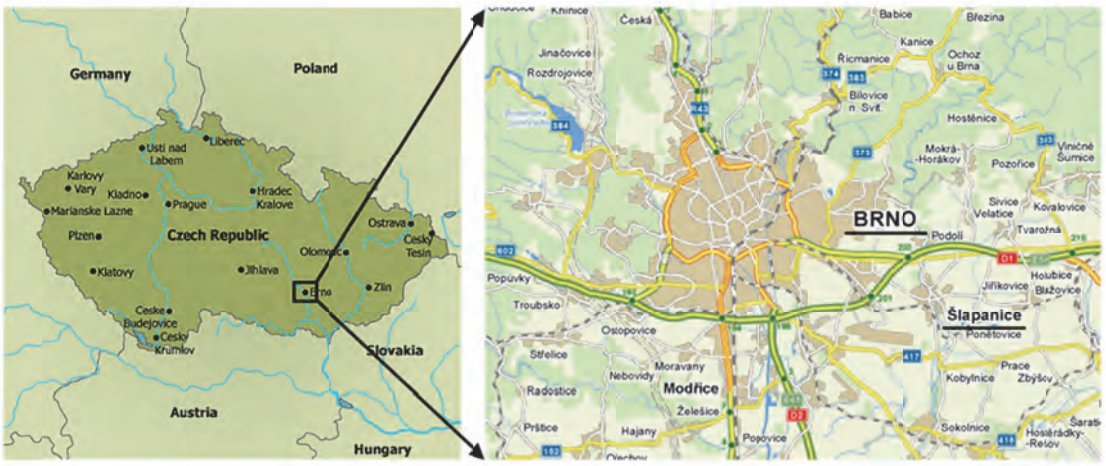

Fig. 1: Location of Brno and Šlapanice in the Czech Republic.

3 RESULTS AND DISCUSSION

Brno represents a big city with 370 000 inhabitants while Šlapanice is a small town with 6 000 inhabitants.

Mean mass concentrations of PM1 aerosols in winter were higher than those during summer campaigns both in Brno and Šlapanice. During the same seasons, mass concentrations of PM1 aerosols at both localities were comparable.

Metals and especially ions formed in winter season significant part of mass of PM1 aerosols (metals 1.7-4.9%, ions 7.1-41.5%) while in summer their contribution to PM1 was much smaller (metals 0.9-1.8%, ions 3.9-25.1%).

The concentrations of metals were, in general, in winter higher than in summer. In winter period, the concentrations of metals in Šlapanice were higher than those in Brno whereas summer concentrations of metals at both localities were comparable. The highest winter concentrations were found for lead and potassium originated from combustion of wood and coal while in summer, lead, potassium, calcium, barium, aluminium, zinc and iron were prevailing metals (Fig. 2). Higher concentrations of K, Pb, Zn, Ni, Cu, As, V and Cd in winter than those in summer indicate combustion of wood, coal and oil as their main winter source in

PM1 aerosols. In summer, exhaust from vehicles appeared to be the major source of metals in aerosols.

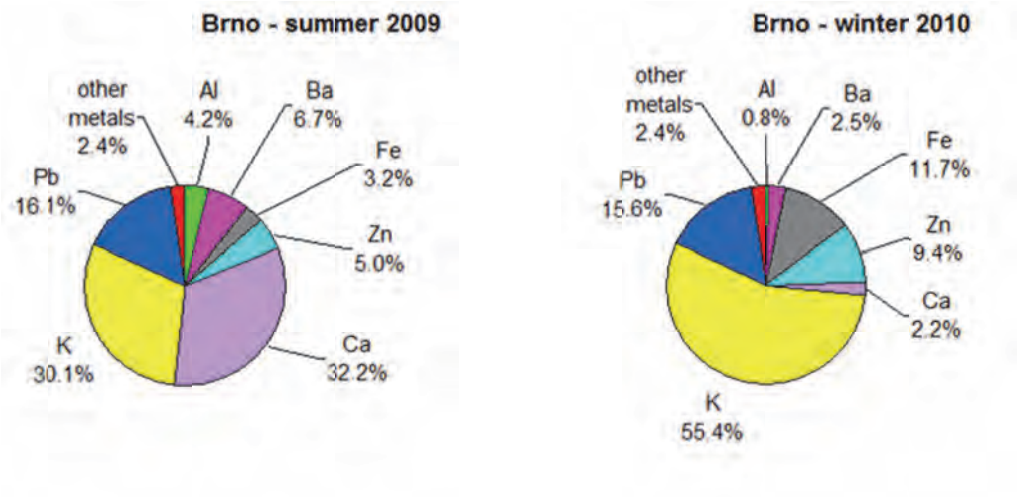

Fig. 2: Relative contribution of analysed metals to the total metal content in PM1 aerosols during campaign in summer 2009 and winter 2010 in Brno.
other metals: Cd, Mn, As, Sb, Cu, V, Ni

Secondary components, sulfate, nitrate and ammonium prevail among particulate ions forming 84-98% of total concentration of analysed ions (Fig. 3). Sulfate and nitrate were predominant anion species contributing 84-98% of total anion concentration. Significant seasonal variability was observed for nitrate. In winter, nitrate contributed by 51-74% to total anion content while summer contribution of nitrate decreased to 10-23%. Lower summer concentrations of nitrate result from volatilization of NH_4NO_3 and from higher sampling losses of nitrate at higher temperatures [6]. Sulfate showed different seasonal trend, its winter contribution to total anion concentration of 18-33% increased to 67-79% in summer.

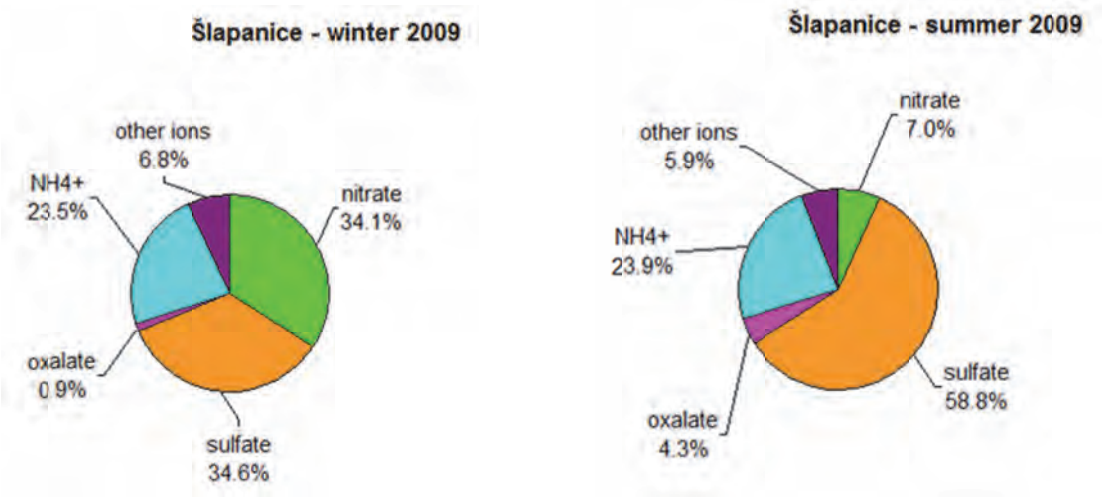

Fig. 3: Relative contribution of analysed ions to the total ion content in PM1 aerosols during summer and winter campaign 2009 in Šlapanice.
other ions: fluoride, chloride, nitrite, Na^+, Ca^{2+}, Mg^{2+}, K^+

ACKNOWLEDGEMENTS

This work was supported by Institute of Analytical Chemistry of ASCR under an Institutional support RVO:68081715, by Grant Agency of the CR under grant No. P503/11/2315 and by Ministry of the Environment of the Czech Republic under grant No. SP/1a3/148/08.

LITERATURE

[1] Schwartz, J., Dockery, D.W. and Neas, L.M., *Journal of Air, Waste and Management Association* 1996, *46*, 927–939.
[2] Pope III, C.A*., Aerosol Science and Technology* 2000, *32*, 4–14.
[3] Brunekreef, B. and Holgate, S.T., *Lancet* 2001, *360*, 1233-1242.
[4] Singh, R., Sharma, B.S. and Chalka, S.N., *Environmental Monitoring and Assessment* 2010, *168*, 195–203.
[5] Mikuška, P., Večeřa, Z., Bartošíková, A. and Maenhaut, W., *Analytica Chimica Acta* 2012, *714*, 68-75.
[6] Wang, Y., Zhuang, G., Zhang, X., Huang, K., Xu, Ch., Tang, A. and Chen, J., An, Z., *Atmospheric Environment* 2006, *40*, 2935–2952.

P07 METHOD FOR ON-LINE PRE-CONCENTRATION AND ANALYSIS OF HEAVY METALS USING LIGAND STEP GRADIENT FOCUSING IN COMBINATION WITH ITP

Eliška Glovinová, Jan Pospíchal

Department of Chemistry and Biochemistry, Faculty of Agronomy, Mendel University, Zemědělská 1, 61300 Brno, Czech Republic

ABSTRACT

A capillary electrophoretic method for the pre-concentration of metals based on selective focusing of metal chelates with subsequent on-line ITP analysis was developed and verified. The selected ions of metals were subjected to pre-concentration from the mixture and analysed. Focusing of the metals was carried out in a ligand step gradient, which was created by the addition of a convenient ligand agent to the regular stationary pH step gradient.

Keywords: pre-concentration, heavy metals, ligand step gradient focusing

1 INTRODUCTION

To reach higher sensitivity in metal analysis we developed convenient sample pre-concentration method which was on-line combined with common analytical ITP. Developed pre-concentration method is based on the principle of stationary neutralization reaction boundary-NRB and its combination with ligand - chelating agents. A stationary ligand step gradient – LSG [1] boundary is created in the column with two adjacent electrolytes branches of different chelating power and pH, see Fig.1. In acid phase, metal and metal complexes are positively charged and forced migrate to the LSG boundary, in the alkaline phase, the complexes are negatively charged and again migrate towards LSG-boundary. A steady state zone of concentrated metal complexes is created. Focused zones are then mobilized and analyzed by ITP. Presence of sample metal ions in one electrolyte /dosing elektrolyte-DE/ during the focusing causes a time dependent accumulation of the metals.

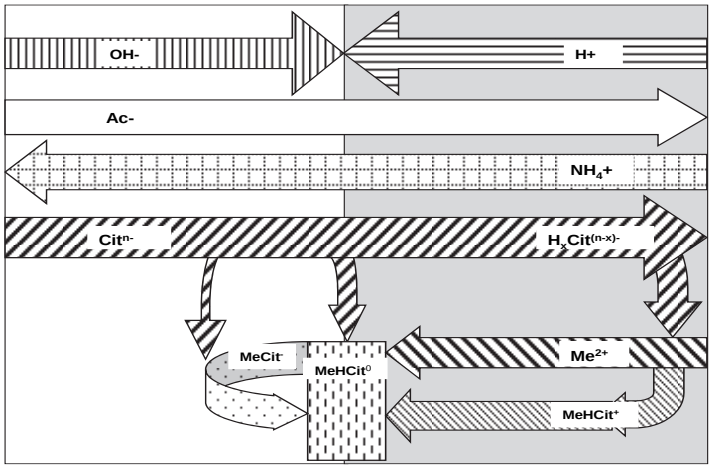

Fig. 1. The scheme of the flows in the ligand step gradient (LSG) boundary. Hydroxyl and oxonium ions are neutralized on the boundary; ammonium, acetate, and citrate ligand ions cross the boundary; metal ions are continuously dosed from the acid electrolyte; metal complexes are focused on the boundary.

2 EXPERIMENTAL

2.1 Apparatus

The commercially available isotachophoretic apparatus (CS Isotachophoretic Analyzer, Villa Labeco, Slovak Republic) in the column-coupling configuration equipped with conductivity detection in the pre-separation and analytical column was used.

2.2 Electrolytes

Alkaline primary (focusing) electrolyte: LE/PE: 0.01M NH_4Ac + 0.01M NH_4OH + 0.002M ammonium citrate + 1% polyethyleneglycole, pH=9.24.
Acidic dosing (focusing) electrolyte: DE: 0.01M HAc + 0.01M NH_4Ac + 0.1% Tritone X100+sample metals, pH 4.75.
ITP analytical electrolyte: LE: 0.02M NH_4Ac + 0.1M HAc + 0.002M ammonium citrate, 0.1% Tritone X100, pH=4.00, TE: 0.03M HAc.

2.3 Procedure

The column is filled with proper electrolytes see Fig.2. The anodic terminating chamber is filled with the acidic dosing electrolyte /DE/, the separation column and the proper (cathodic) electrolyte chamber is filled with primary alkaline electrolyte /PE/, the analytical capillary and the corresponding (cathodic) electrolyte chamber is filled with the leading electrolyte /LE/.
By switching on the driving current, a sharp LSG boundary is created in the column in between dosing and primary electrolyte and continuous dosing procedure starts. Metal cations and positively charged metal citrate complexes are driven from the acidic dosing electrolyte to the LSG boundary, where are focused. After accumulation of sufficient amount of metals for the analysis, a dosing electrolyte in the terminating electrolyte /TE/ chamber is changed for the terminating which causes mobilization. The focused zones of non charged metal citrate complexes are acidified; they gain a positive charge or break down, releasing

free metal cations, and migrate to the second analytical column. Here are analyzed by ITP in the leading electrolyte, and detected.

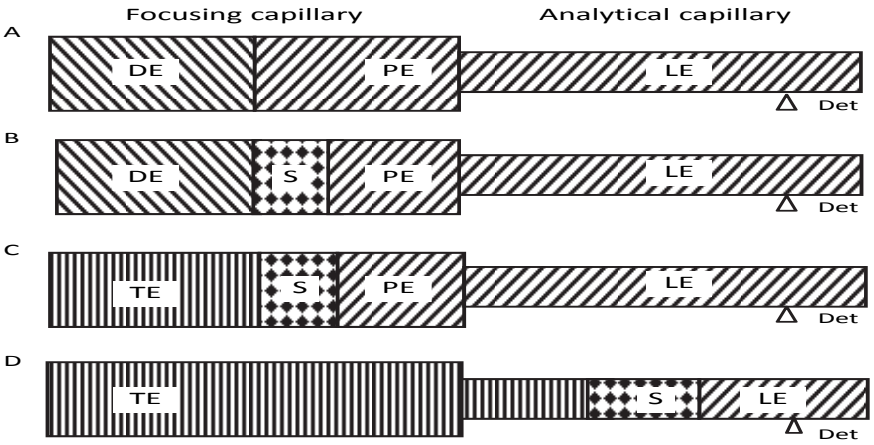

Fig. 2 The scheme of the analytical procedure. (A) Column prepared for the analysis, filled with PE and DE electrolytes; (B) Continuous dosing procedure; (C) Mobilizing procedure: DE replaced with TE; (D) Detection procedure: ITP analysis in the analytical column.

3 RESULTS

For experimental verification, an equimolar mixture of nine metals Na^{+}, Ca^{2+}, Mg^{2+}, Mn^{2+}, Cd^{2+}, Zn^{2+}, Ni^{2+}, Pb^{2+}, Cu^{2+} ($2x10^{-6}$M each – 20% of cLOD) was focused, analytical records are shown on Fig. 3. A time dependence of the zone length of each metal as a function of time was plotted. The dependence is fairly linear for all metals, Ca b[0]4,9 b[1]4,56 r2 0,9989; Mg b[0] 0,8 b[1] 2,82 r2 0,9999;Mn b[0] 1,1 b[1] 2,74 r2 0,9989;Cd b[0] 1 b[1]2,82 r20,9931;Zn b[0] 0,7 b[1] 2,8 r2 0,9894;Ni b[0]1,7 b[1] 1,94 r2 0,9958;Pb b[0]1,4 b[1] 2,1 r2 0,9993;Cu b[0] 0,6 b[1] 0,78 r2 0,9825, with except of sodium, which is not focused on the LSG boundary.

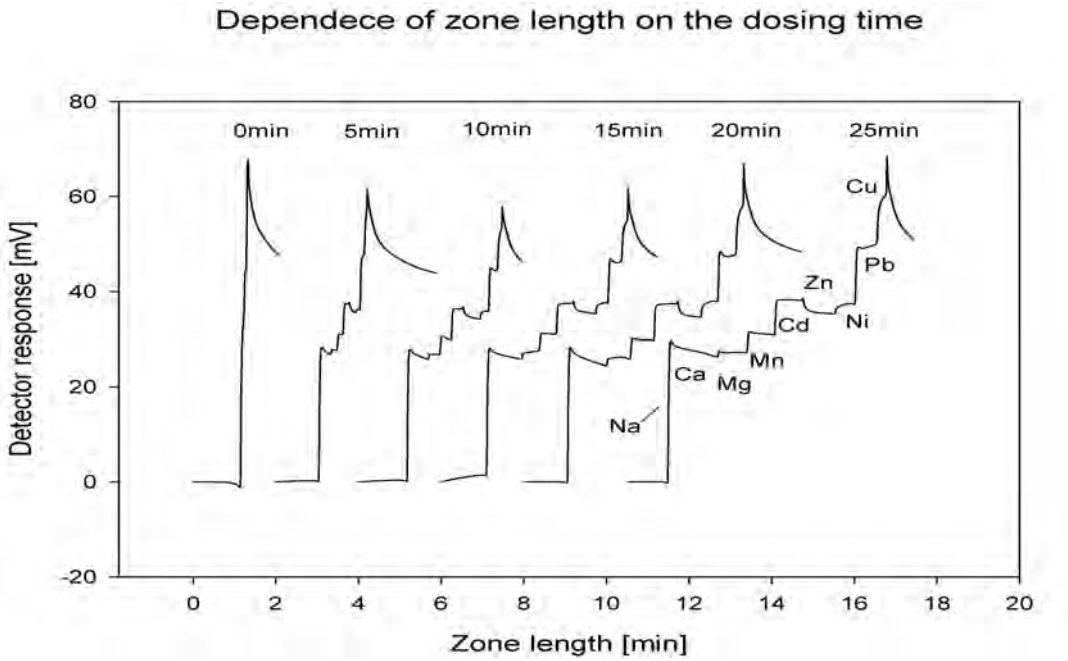

Fig. 3. Dependence of zone length on the dosing time for the mixture of metals of 2.10^{-6} $mol.dm^{-3}$ each.

4 CONCLUSION

Metal complexes were pre-concentrated, focused and analyzed using the combination of ligand step gradient focusing method with subsequent mobilization and on-line ITP analysis. A continuous dosing technique was used for the lowering the detection limit ca. two orders of magnitude, with acceptable dosing time of 25 min. Using citrate as a complexing agent yields in selective removing of alkali metals /e.g. Na/ from the sample mixture.

ACKNOWLEDGEMENTS

This work was supported by the Grant Agency of the Czech Republic, Grant No. 206/10/1219.

LITERATURE

[1.] E. Sisperova, E.Glovinova, J.Budilova and J.Pospichal, J. Chromatogr.A. 1281 (2011) p. 3105.

P08 A SIMPLE SAMPLE PRETREATMENT DEVICE WITH SUPPORTED LIQUID MEMBRANE FOR DIRECT INJECTION OF UNTREATED BODY FLUIDS AND IN-LINE COUPLING TO A COMMERCIAL CAPILLARY ELECTROPHORESIS INSTRUMENT

Pavla Pantůčková, Pavel Kubáň, Petr Boček

Institute of Analytical Chemistry of the Academy of Sciences of the Czech Republic, v. v. i., Veveří 97, CZ-60200 Brno, Czech Republic, pantuckova@iach.cz

ABSTRACT

A simple sample pretreatment device employing extractions across supported liquid membranes (SLMs) was designed for in-line coupling to a commercial CE instrument. The device can be easily assembled/disassembled and SLMs can be replaced after each extraction thus minimizing sample carry-over, avoiding tedious SLM regeneration and reducing total pretreatment time and costs. The pretreatment device consisted of two polypropylene conical units interspaced with a planar SLM, which was impregnated with 1-ethyl-2-nitrobenzene. The two units separated by the SLM were pressed against each other and filled with 40 µL of donor (untreated body fluid) and acceptor (deionized water) solutions. The pretreatment device was placed into conventional CE where it is supported by a soft spring. During the injection step, the soft spring is pressed down and both provides contact of the capillary with SLM and prevents the rupture of SLM. Position of separation capillary injection end and high voltage electrode was optimized in order to ensure efficient injection of pretreated body fluids. Three basic drugs (nortriptyline, haloperidol and loperamide) in donor solutions were selectively transported across the SLM within 10 min and were injected to the separation capillary directly from the SLM surface. The basic drugs were determined in a background electrolyte solution consisting of 15 mM Na_2HPO_4 and 40 mM H_3PO_4 at pH 2.7. The method showed good repeatability of peak areas (3.8 – 11.0%) and migration times (less then 1.4%), linear relationship over two orders of magnitude (r^2 = 0.990 – 1.000) and limits of detection between 12 and 100 µg/L in standard solutions, human urine and human serum samples.

Keywords: biological samples, capillary electrophoresis, supported liquid membranes

1 INTRODUCTION

CE analysis of samples with complex matrix, e. g., human body fluids, requires nearly always efficient and selective sample pretreatment procedure [1,2]. Of course, on-line and/or in-line procedures are always advantageous. In recent years, supported liquid membranes (SLMs) opened new direction in the field of sample pretreatment prior to analysis by a suitable analytical separation method (like HPLC and CE) [3,4,5]. In this work, a new SLM-based pretreatment device is described for in-line coupling to CE. The system is compatible with the injection system of commercial CE instrument (P/ACE 5000, Beckman Instruments). Its performance is exemplified by direct injection of human body fluids, where some selected drugs, i. e., nortriptyline, haloperidol and loperamide were analysed.

2 SAMPLE PRETREATMENT DEVICE AND ITS OPERATION

A sample pretreatment device, which is compatible with injection system of Beckman P/ACE CE instruments, is depicted in Figure 1. A photograph showing the uncapped sample vial with the pretreatment device accommodated in the spring is shown in Figure 1C.

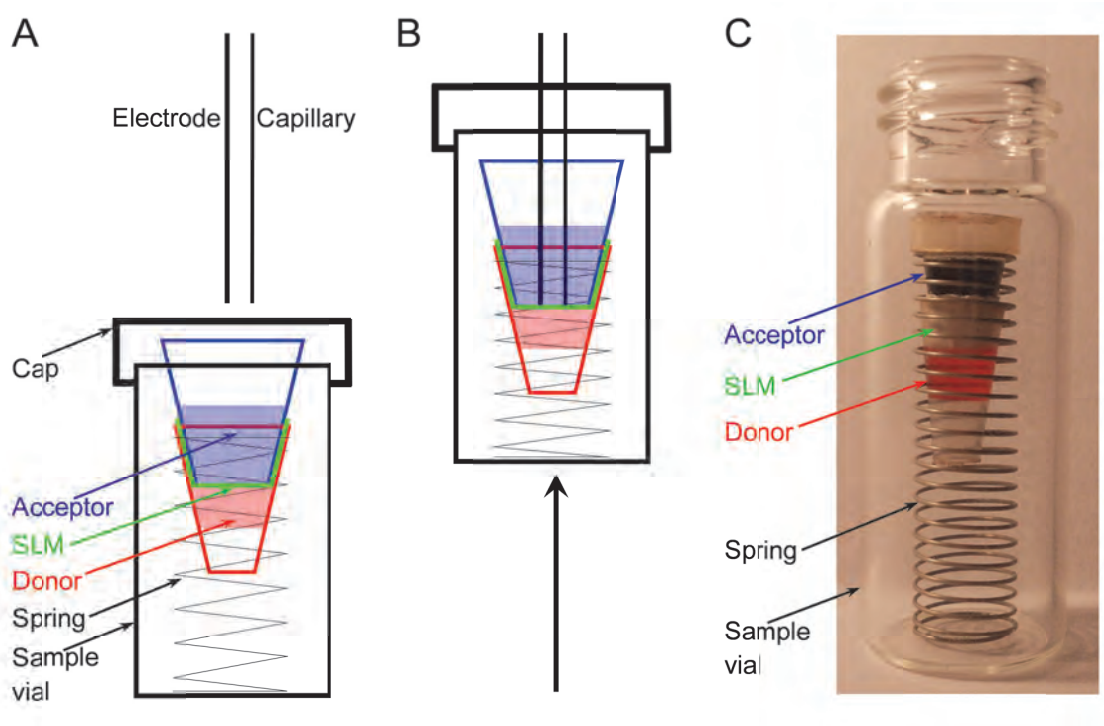

Fig. 1. Sample pretreatment device for in-line coupling to a commercial CE instrument. (A) sample vial before sample injection, (B) sample vial during injection of the pretreated sample (separation capillary and high voltage electrode are in contact with SLM), (C) a photograph of the sample vial with the assembled sample pretreatment device; the acceptor unit is partly hidden by the SLM.

Untreated and undiluted body fluids are filled into the donor unit of the pretreatment device and injections are performed directly from the SLM surface in the acceptor unit, which is filled with deionized water. Total volumes of organic solvents and donor and acceptor solutions per analysis are in low µL range. BGE solution consisting of 15 mM Na_2HPO_4 and 40 mM H_3PO_4 at pH 2.7 was used for the CE-UV determination of nortriptyline, haloperidol and loperamide. The injection end of the separation capillary had to be positioned as close to the SLM as

possible to ensure the highest analyte concentration transfer. The position of the separation capillary injection end and of the high voltage electrode had to be optimized, as well. Optimum injection was obtained for the set-up using identical height of capillary injection end and high voltage electrode tip (see Figure 1 A and B). The differences in extraction efficiencies of the compounds were observed and they depended also on the type of donor matrix. The reason is that the facilitated transfer of ionic substances across liquid membranes is a complex mechanism, which consists of a diffusion process across an aqueous diffusion film, a fast interfacial chemical reaction, and a diffusion across the membrane itself [6, 7]. pH gradients offered no advantage over the simplest possible model where deionized water-based solutions are used on both sides of the SLM. For this reason, standard donor solutions were prepared in deionized water (with NaCl addition), body fluids were used untreated, and deionized water was used as acceptor solution in all subsequent measurements. SLMs were prepared by impregnating the polypropylene membrane with 6 µL of 1-ethyl-2-nitrobenzene.

3 RESULTS

Transfer of the analytes across the SLM was comparable for standard solution and serum. An increased transfer of analytes was observed for urine, see Fig. 2.

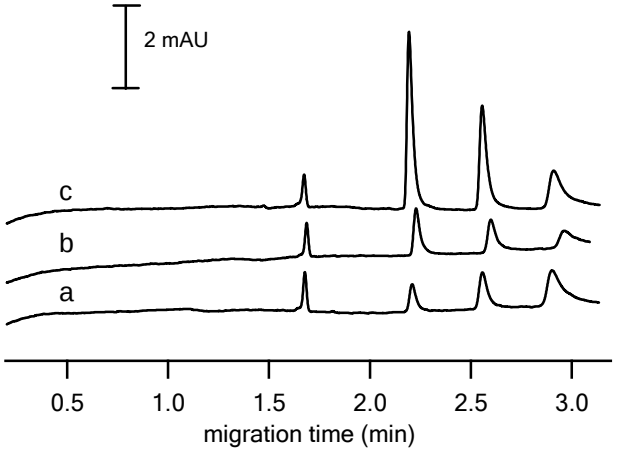

Fig. 2. CE records of the solutions spiked with selected basic drugs (1 mg·L^{-1}) measured after sample pretreatment for 10 min: (a) spiked standard solution of 150 mM NaCl, (b) spiked human serum, (c) spiked human urine. CE conditions: BGE solution, 15 mM Na_2HPO_4 and 40 mM H_3PO_4 at pH 2.7; voltage, + 10 kV; injection, 5 sec at 0.5 psi. SLM conditions: organic solvent, 1-ethyl-2-nitrobenzene; acceptor, deionized water.

Repeatability, expressed as RSD values of peak areas, was within the range 3.8 – 11.0%, and recoveries ranged between 19% and 137%. LODs, defined as 3 S/N ratio, were between 12 and 100 µg.L^{-1}. The presented approach enables use of disposable SLMs, simplifies manipulation with the pretreatment device, accelerates the extraction process and significantly reduces volumes of extracted body fluids.

4 CONCLUSIONS

A simple device compatible with the injection system of a commercial CE instrument was developed for direct injection and CE-UV analysis of model basic drugs in untreated body fluids. The analytical method is rapid and cost-effective, uses only µL volumes of organic solvents and biological samples, acceptor solution consists of sole deionized water and no handling of biological samples, other than pipetting into the pretreatment device, is required.

The pretreatment device can be simply assembled/disassembled and SLMs can be replaced in a user-friendly manner after each sample pretreatment. The presented sample pretreatment device might be readily extended to other existing CE instruments.

ACKNOWLEDGEMENTS

The authors gratefully acknowledge financial support from the Academy of Sciences of the Czech Republic (Institutional Support RVO:68081715) and from the Grant Agency of the Czech Republic (Grant No. P206/10/1219).

LITERATURE

[1.] Gebauer, P., Křivánková, L., Pantůčková, P., Boček, P., Thormann, W., *Electrophoresis* 2000, *21*, 2797-2808.
[2.] Křivánková, L., Gebauer, P., Pantůčková, P., Boček, P., *Electrophoresis* 2002, *23*, 1833-1843.
[3.] J.Y. Lee, H.K. Lee, K.E. Rasmussen, S. Pedersen-Bjergaard, *Anal. Chim. Acta* 2008, *624,* 253-268.
[4.] Kubáň, P., Boček, P., *J. Chromatogr. A* 2012, *1234*, 2-8.
[5.] Kubáň, P., Kiplagat, I. K., Boček, P., *Electrophoresis* 2012, in press: DOI
[6.] Danesi, P. R., Horwitz, E. P., Rickert, P. G., *J. Phys. Chem*. 1983, *87*, 4708-4715.
[7.] Danesi, P. R., *Separ. Sci. Technol.* 1984, *19*, 857-894.

P09 A SENSITIVE GRADIENT LIQUID CHROMATOGRAPHY METHOD FOR ANALYSIS AMINO ACIDS IN DEGRADATION PRODUCTS OF HUMIC SUBSTANCES

Natália Bielčíková, Róbert Góra, Milan Hutta, Simona Čurmová

Department of Analytical Chemistry, Faculty of Natural Sciences, University Comenius in Bratislava, Mlynska Dolina CH-2, SK-84215 Bratislava, Slovakia; masarykova@fns.uniba.sk

ABSTRACT

The aim of this work is development of liquid chromatographic method for the separation and determination of amino acids (AA) in degradation products of humic acids (HA) isolated from peat and soil. Analyzed HA samples were decomposed by hydrolysis with 6 $mol.l^{-1}$ hydrochloric acid at 110°C. Degradation products of HA were derivatized by diethyl ethoxymethylenemalonate (DEEMM). Monolithic type chromatography column Chromolith performance RP-18e 100-4.6 with same type guard column was used for the separation of mixture of amino acid standards and samples of HA hydrolysates. Following chromatographic conditions were employed: gradient elution by mixing 20 $mmol.l^{-1}$ trifluoroacetic acid solution (pH 5.0) (A) and methanol (B) at flow rate 1 $ml.min^{-1}$ and 10 µl sample solution was injected to chromatographic system. Under these chromatographic conditions, separation of nineteen derivatized AA was achieved in 30 min.

Keywords: Amino acids, Humic acid, Diethyl ethoxymethylenemalonate.

1 INTRODUCTION

Humic substances (HS) are complex macromolecular substances that are widely distributed in the environment and in natural waters, soils, sediments and represent a significant proportion of the organic carbon in the environment[1]. HS are probably formed from association of various components in the (bio) chemical degradation of plant and animal

waste and synthetic microbial activity (amino acid, lignin, pectins and carbohydrates). HS isolated from soils and sediments can be divided on the basis of solubility in dilute solutions of acids and bases to three fractions: humic acids (HA), fulvic acid (FA) and humin[2].
Soil humic acids (HA) are mixture of natural organic compounds containing more aromatic structures and carboxyl groups, such as fulvic acids[3]. Given that free amino acids (AA) are quickly decomposed by microbes, most AA is present in the soil in a bound form such as huminopeptide structural units and usually bound to the central core of FA and HA, which protects them from rapid degradation by microorganisms[4].
Combination of reverse-phase high-performance liquid chromatography (RP-HPLC) with pre-column derivatization - enables analysis of AA using fluorimetric or spectrophotometric detection in the UV and VIS spectrum. Used derivatization reagents for the analysis of amino acids should meet the following conditions[5]:
reagent must be able to respond to all AA and the primary and the secondary amino group
derivatization must be reproducible
derivatized AA must be stable
The most frequently used derivation reagent are: aminoquinolyl-6-N-hydroxysuccinimidyl carbamate (AQC)[6], dansyl chloride (Dans-Cl)[7], o-phtalaldehyde (OPA)[8], phenylisothiocyanate (PITC)[9], 4-Nitrophenyl isothiocyanate (NPITC)[10], 9-fluorenylmethyl chloroformate (FMOC)[11] and diethyl ethoxymethylenemalonate (DEEMM)[12].
The present work deals with the analysis of amino acids in degradation products humic acids by the method of liquid chromatography using pre-column derivatization with DEEMM.

2 EXPERIMENTAL

2.1 Chemicals

HPLC-grade methanol 99% for LC, trifluoroacetic acid 99% (TFA) onto prep mobile phase and hydrochloride acid 33% (HCl) required for acidic hydrolysis of HA samples were obtained from Merck (Darmstadt, Germany). Amino acid standards (l-glutamine, l-cysteine, l-proline, l-tryptophan, l-tyrosine, l-histidine, l-leucine, l-isoleucine, l-phenylalanine, l-alanine, l-aspartic acid, l-arginine, l-asparagine, glycine, l-serine, l-valine, l-methionine, l-threonine, l-lysine, and l-glutamic acid) were purchased from Merck (Darmstadt, Germany), Derivatization agent diethyl ethoxymethylenemalonate, sodiumtetraborate were purchased from Sigma Aldrich co. (St. Louis, MO, USA) Water for gradient HPLC was prepared by Labconco Pro-PS unit (Labconco, Kansas City, U.S.A) and purified by Millipore Simplicity system (Molsheim, France).

2.2 Equipment

HPLC system LaChrom Merck - Hitachi (Merck, Darmstadt, Germany) was consisting from pump L-7100 provided by quarternary low-pressure gradient, autosampler L-7200, column oven L-7300, diode-array detector L-7450A, fluorescence detector L-7480, interface D-7000, PC data station with software HSM ver.3.1 and on-line four channel solvent degasser L-7612. Chromatographic analysis was performed using an analytical column Chromolith performance RP-18e (100×4.6 mm) with guard column (Chromolith Guard Cartridges RP-18e 5×4.6 mm).

2.3 LC/UV analysis

HPLC conditions were as follows: mobile phase A: buffer solution (pH = 5; 20 mmol.l^{-1} trifluoroacetic acid); mobile phase B: methanol. Gradient program was as follows: 0–9 min, 15%; 9–21 min, 15-50%; 21–26 min, 50%; 26–30 min, 80% B. The eluent flow rate was 1 ml.min^{-1}, the column oven was maintained at 35 °C and 10 µl of the sample was injected. The UV detection wavelength was 280 nm and 254 nm.

3 RESULTS AND DISCUSSIONS

Based on information from perused literature[4] and according to the nature and structure of the humic matter, we choose 20 proteinogenic AA, which could be, very likely present, in degradation products of HA isolated from soil or peat. In actual design methods gradient RP-HPLC we used in addition to the knowledge gained from the literature and from our past experience in the analysis of complex mixtures, such as amino acids, including extracts from the roots of maize[13] and commercial plant with a high content of humic substances[14]. Onto derivatization of amino acid standards and samples of hydrolysates with AA content, we preferred reagent DEEMM mainly due to its excellent properties. Among those certainly is formation of thermodynamically and kinetically stable products with a characteristic spectrum band at 280 nm, which is an important prerequisite for the design of robust RP-HPLC method using spectrophotometric detection.

In the introductory part of the work, we focus on optimizing conditions for the separation of amino acids, depending on the composition of the mobile phase. Based on our preliminary measurements, and the results[14,15] published so far a trifluoroacetic acid (TFA) was chosen as an inorganic (aqueous) mobile phase, due to its advantageous properties and the potential possibility of using MS detection in the future[16]. At the beginning, we have focused on the influence of pH of the mobile phase (TFA ranging pH from 3.00 to 7.00) to separation process. Obtained results showed that the optimum pH buffer TFA in the mobile phase for the separation of a standard AA and AA present in the samples of HA hydrolysates at pH = 5.00. In the following step, we focused to study the impact of the ionic strength of aqueous constituent of mobile phase to separation of AA using monolithic type column Chromolith Performance RP-18e (100x4.6 mm) and for the other measurements we choose TFA concentration of 20 mmol.l^{-1}.

In Fig. 1 is illustrated typical chromatographic profile of derivatization agent DEEMM at 254 and 280 nm. As from figure result, DEEMM has a relatively high response at a wavelength of 254 nm and offers total of 5 system peaks, on the other hand the response DEEMM at a wavelength of 280 nm, we was used in the determination of AA, shows only one peak with relatively low response beside to responses of DEEMM derivatized AA, for which the wavelength 280 nm are specific and characteristic.

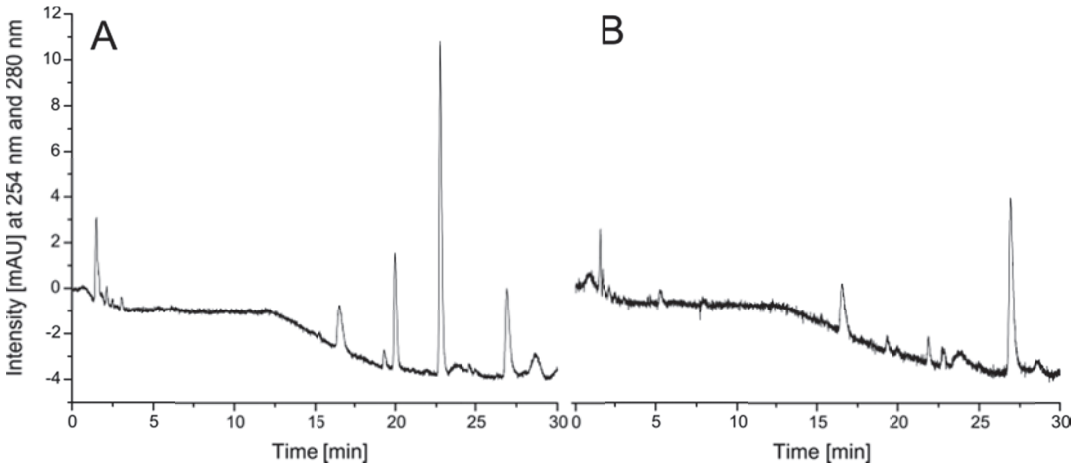

Fig. 1. : Chromatography DEEMM record at 254 (A) and 280 nm (B). Separation conditions: Gradient elution with mixing 20 mmol l^{-1} TFA at pH 5.0 (A) and methanol (B), injection volume 10µl, column temperature 35 ° C, flow rate of 1 ml.min^{-1}.

Typical chromatogram of AA standards and sample of hydrolysates of HA isolated from peat are presented in Fig. 2. In both analyzed samples of degradation products of humic acids

(isolated from soil and peat) were found majority of proteogenic AA. Glycine, Aspartic acid, Threonine and Alanine were the most prevalent AA in analyzed samples.

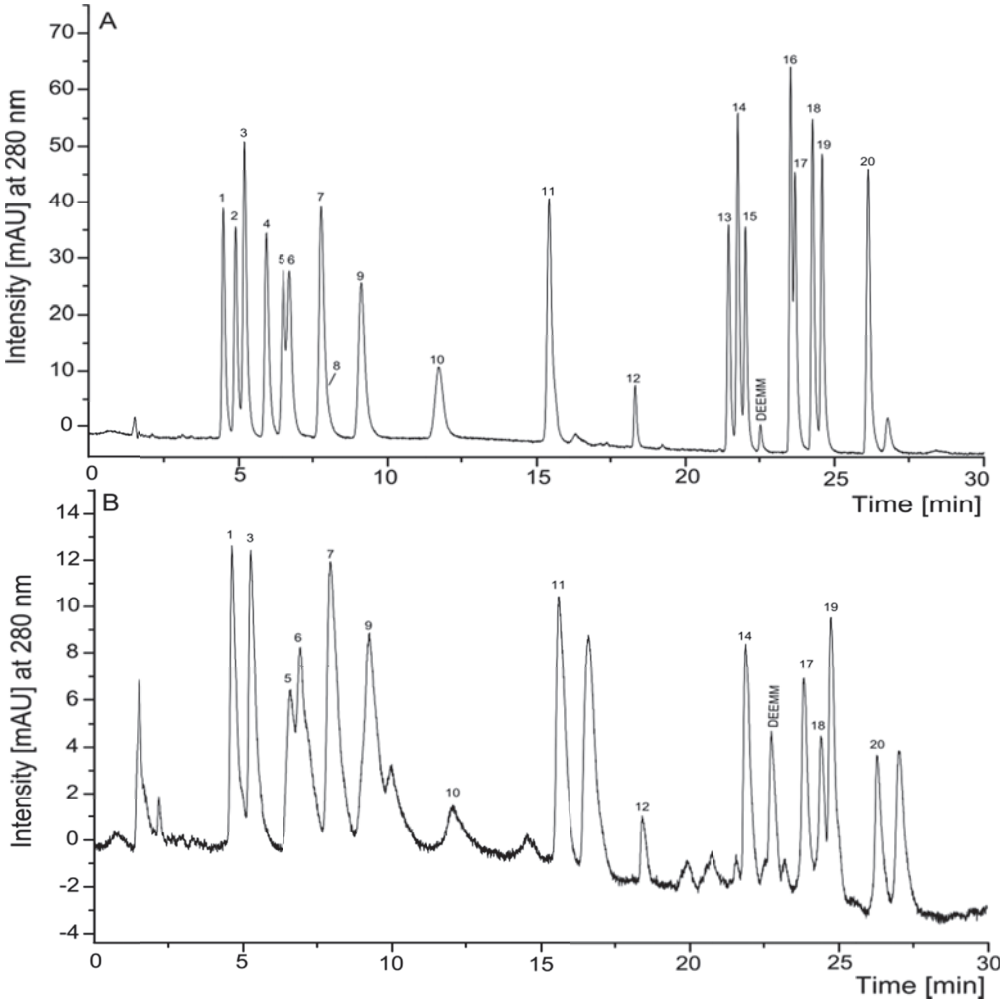

Fig. 2. : Typical chromatograms of (a) AA standard solution and (b) AA content in the samples of hydrolysates of HA isolated from peat (locality Cérová) obtained at 280 nm). Peak identification: 1–aspartic acid, 2–asparagine, 3–serine, 4–glutamine, 5–glutamic acid, 6–histidine, 7–glycine, 8–proline, 9–threonine, 10–arginine, 11–alanine, 12–tyrosine, 13–methionine, 14–valine, 15–tryptophan, 16–cysteine, 17–phenylalanine, 18–isoleucine, 19–leucine, 20–lysine.

4 CONCLUSION

Described method was successfully applied to determination of the amino acid composition in degradation products of selected of humic acid samples from different origin. Both analysed samples of humic acids indicated higher abundance of amino acids. Glycine (in samples isolated from peat), Aspartic acid (in samples isolated from soil), Threonine and Alanine were the major AA in samples of degradation products of selected of humic acid.

ACKNOWLEDGEMENTS

This work was generously supported by the grant of Scientific Grant Agency of the Ministry of Education of Slovak Republic and the Academy of Sciences - project VEGA 1/1349/12 and the grant of Slovak Research and Development Agency - project APVV-

0583-11. This work is partially outcome of the project APVV-0595-07 of Slovak Research and Development Agency solved in the period 2008-2011.

LITERATURE

[1.] Choudhry, G.G., in Hutzinger O. Ed., The Handbook of Environmental Chemistry Vol. 1., Part C., The Natural environment and the biogeochemical cycles, p. 1. Springer Verlag, Heidelberg, 1989.
[2.] Wu, C. F., Evans, D. R., Dillon, J. P., *Anal. Chim. Acta* 2002, *464*, 47-55.
[3.] Hutta, M., Góra, R., Halko, R., Chalányová, M., *J. Chromatogr. A* 2011, 1218, 8946-8957.
[4.] Szajdak, L., Jezierski, A., Cabrera, M. L., *Org. Geochem.* 2003, *34*, 693-700.
[5.] Oravec, P., Podhradský, D., *J. Biochem. Biophys. Methods* 1995, *30*, 145-152.
[6.] Hou, S., He, H., Zhang, W., Xie, H., Zhang, X., *Talanta* 2009, 80, 440-447.
[7.] Negro, A., Garbisa, S., Gotte, L., Spina, M., *Anal Biochem.* 1987, 160, 39-46.
[8.] Cotte, F. J., Casabianca, H., Giroud, B., Albert, M., Lheritier, J., Loustalot-Grenier, F. M., *Anal. Bioanal. Chem.* 2004, 378, 1342-1350.
[9.] Brashy-El, M. A., Ghannam-Al, M. S., *Analyst* 1997, 122, 147-150.
[10.] Cohen, A. S., *J. Chromatogr. A* 1990, 512, 283.
[11.] Jámbor, A., Perl, M. I., *J. Chromatogr. A* 2009, 1216, 3064-3077.
[12.] Hermosín, I., Chicón, M. R., Cabezudo, D., *Food Chem.* 2003, *83*, 263-268.
[13.] Hutta, M., Chalányová, M., Góra, R.: In: Proc. 11th Int. Symposium, Advances and applications of chromattography in industry, August 27-31, 2001, Bratislava, Slovak Republic. ISSN 1335-8413, Slovak University of Technology in Bratislava, 2001.
[14.] Masaryková, N., Góra, R., Hutta, M., In: Student Research Conference PriF UK 2011, 27. April 2011, Bratislava, Slovak Republic ISBN 970-80-223-3013-8, Comenius University in Bratislava, 2011.
[15.] Masaryková N., Góra R., Hutta M.: In: Proc. 7th ISC Modern Analytical Chemistry, September 29-30, 2011, Prague, Czech Republic ISBN 978-80-7444-010-6, Charles University in Prague, 2011.
[16.] Liu, Y., Miao, Z., Lakshmanan, R., *et al., Int. J. Mass. Spectrom.* 2012, 325-327, 161-166.

P10 PROTEOMIC EVALUATION OF MCF-7 HUMAN BREAST CANCER CELLS AFTER TREATMENT WITH RETINOIC ACID ISOMERS: PRELIMINARY INSIGHTS

Dana Flodrová[a], Dagmar Benkovská[a, b], Dana Macejová[c], Lucia Bialešová[c], Július Brtko[c], Janette Bobálová[a]

[a] *Institute of Analytical Chemistry of the ASCR, v. v. i., Veveří 97, 602 00 Brno, Czech Republic, bobalova@iach.cz*
[b] *Brno University of Technology, Faculty of Chemistry, Purkyňova 118, 612 00 Brno, Czech Republic*
[c] *Institute of Experimental Endocrinology, SAS, Vlárska 3, 833 06 Bratislava, Slovak Republic*

ABSTRACT

The specific aim of this work was exploration of molecular mechanisms in relation to therapy of human breast cancer. One of the efficient strategies to battle cancer is biomarker identification as an important tool in early cancer diagnosis and advisable treatment. Retinoids have been regarded as important therapeutic agents for many types of cancers, including human breast. The effects of 9-*cis* retinoic acid and all-*trans* retinoic acid in human MCF-7 breast cancer line have been investigated. The total cell proteins were extracted utilizing a commercially RIPA buffer (Radio-Immunoprecipitation Assay) and separated on 1D sodium dodecyl sulfate polyacrylamide gel electrophoresis (1D SDS-PAGE). The proteins

were subsequently in-gel digested by trypsin and identified by matrix assisted laser desorption ionization technique with time of flight mass analyzer (MALDI-TOF/TOF).

Keywords: retinoids, breast cancer, proteomic analysis

1 INTRODUCTION

Retinoids belong to a large family of natural and synthetic compounds related to vitamin A that are known to have therapeutic effects due to their antiproliferative and apoptosis-inducing action. In addition, they are successfully used for the treatment of acute promyelocytic leukemia as well as for selected skin diseases and are promising anti-cancer drugs for another types of cancer [1]. The pleiotropic activities of retinoids are mediated by two basic types of nuclear receptors belonging to the nuclear receptor superfamily: all-*trans*-RA receptors (RARα, RARβ and RARγ) and retinoid X receptors (RXRα, RXRβ and RXRγ) as retinoid-inducible transcription factors [2]. Retinoids inhibit carcinogenesis, and suppress tumour growth and invasion in a variety of tissues. To determine the proteins affected by the presence of the retinoic acid isomers, we used 1D SDS-PAGE-based bottom-up proteomics strategy for the study of the proteome of MCF-7 breast cancer cell line, which was chosen as an experimental model. MCF-7 cells are useful for *in vitro* breast cancer studies because the cell line has retained several great characteristics particular to the mammary epithelium.

At present, proteomics is one of the essential trends in biological science and it can be defined as the systematic analysis of the proteome [3]. Moreover, comparative proteomics offers a dynamic view of the proteome including the qualitative and quantitative changes of proteins [4].

2 EXPERIMENTAL

2.1 Cell culture

The human breast cancer MCF-7 cell line was grown and passaged routinely as monolayer cultures. For experiments the cells were used at passage 10-30. Cells were seeded in Petri dishes in Dulbecco´s modified Eagle´s medium (DMEM) supplemented with 10% fetal bovine serum (FBS), antibiotics (penicillin, streptomycin, gentamicin) and cultured in humidified atmosphere of 5 % CO_2 and 95 % air at 37°C. The cells were treated either with the 10^{-6}M 9-*cis* retinoic acid (9cRA) or 10^{-6}M all-*trans* retinoic acid (ATRA) and also with their combination for 48 h. Compounds at selected concentration were dissolved in ethanol and then added into medium. Control cells were incubated with particular concentration of ethanol. After incubation cells were washed twice with ice-colled PBS. The cell lysis was made according to an instruction manual from the RIPA (Radio-Immunoprecipitation Assay) Buffer by Sigma. The cell lysates were stored at –70 °C for further use.

2.2 1D SDS-PAGE

Before gel electrophoresis, the Laemmli sample buffer (62.5 mM Tris-HCl, pH 6.8, 2 % SDS, 25 % glycerol, 0.01 % Bromophenol Blue, 5 % β-mercaptoethanol) was added to cell lysis in ratio 1:1. After briefly being boiled (10 min, 95°C) in a water bath, 13 µL of each sample was applied onto the 12 % SDS gel. Separation was performed at constant voltage 140 V. The visualization was carried out using Coomassie Brilliant Blue G-250 dye.

2.3 In-gel digestion

Stained protein spots were excised from the gel and digested (after reduction with 10 mM dithiothreitol and subsequent alkylation with 55 mM iodoacetamide) with trypsin (digestion buffer: 50 mM NH_4HCO_3, 5 mM $CaCl_2$, 12.5 ng/µl of enzyme) overnight at 37 °C. The resulting tryptic peptides were extracted from the gel by three changes of 0.1% trifluoroacetic

acid (TFA) and acetonitrile (1:1, v/v). Combined extracts were finally dried in the Speed-Vac centrifuge. For mass spectrometric analyses the dried extract was dissolved in 10 µl of 0.1% TFA and purified by ZipTip C_{18} (Millipore).

2.4 Mass spectrometry and database searching

A solution of α-cyano-4-hydroxycinnamic acid (8 mg/mL in acetonitrile/0.1% TFA, 1:1, v/v) for dried-droplet preparation was used for both MS and MS/MS analysis of peptides. MALDI MS experiments in positive ion reflectron mode were performed on AB SCIEX TOF/TOF™ 5800 System (AB SCIEX, Framingham, MA, USA) equipped with a 1 kHz Nd:YAG laser. Acquired mass spectra were processed using 4000 Series Explorer software and the data were submitted to the Mascot database searching. Protein identifications were assigned using the NCBInr database with taxonomy restriction to Homo sapiens.

3 RESULTS AND DISCUSSION

MCF-7 cells (**Fig. 1**) were incubated with 9cRA, ATRA and with their combination for 48 h in order to investigate changes in protein expression during the cell cycle. Total proteins were extracted by RIPA buffer and separated by 1D SDS-PAGE. Several bands were detected in the gel. **Fig. 2** shows protein profiles of MCF-7 cell line obtained on the sample before RA derivatives incubation (MCF-7+EtOH), after 9cRA incubation (MCF-7+9cRA), ATRA incubation (MCF-7+ATRA) and finally combination of 9cRA and ATRA incubation (MCF-7+9cRA+ATRA). Although the resolution of protein bands was satisfactory, as can be seen in **Fig. 2**, only minor qualitative (about 70 kDa and 44 kDa) together with some minor quantitative differences were found in the gel of MCF-7 lines. Marked bands of MCF-7 lines (**Fig. 2**) were in-gel digested with trypsin and desalted.

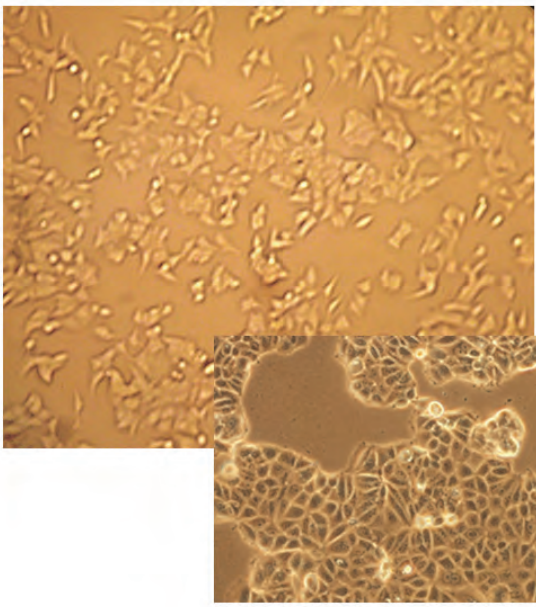

Fig. 1.: Picture of MCF-7 cells.

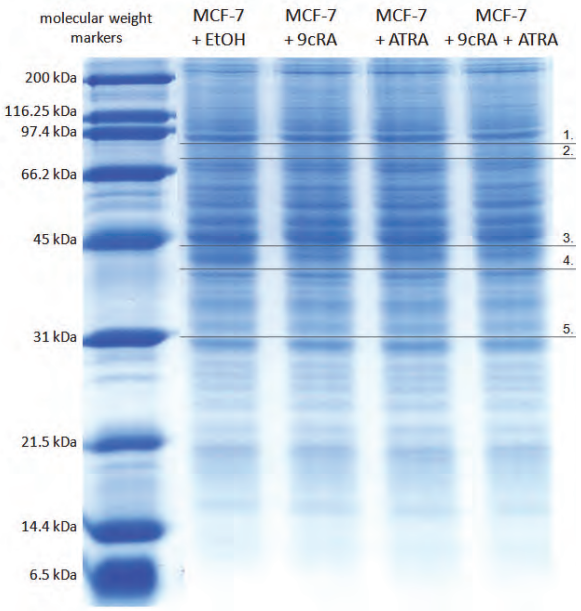

Fig. 2.: SDS-PAGE separation of cell lysis from individual treated groups.

Following this, a MALDI-TOF mass spectrometry analysis was applied to identify proteins in selected bands. Additional MS/MS analysis of individual peptides and database searching resulted in identification of the following proteins summarized in **Table 1**.

We have focused primarily on the proteins that belong to the specific breast cancer biomarkers [5]. Between these important proteins with regard to early cancer detection are mainly heat shock protein HSP 90-beta, or heat shock cognate 71 kDa protein isoform 1. An example of MS and one MS/MS spectra of heat shock protein HSP 90-beta is shown in **Fig. 3.** The amino acid sequence of investigated protein is also shown in **Fig. 3c**.

Table 1: Summary of identified proteins

line	protein	gi number	mass (Da)	peptide matches	coverage (%)	function
1.	heat shock protein HSP 90-beta	gi|20149594	83554	11	17	molecular chaperon, protein binding/folding
	heat shock protein HSP 90-alpha isoform 1	gi|153792590	98670	5	7	molecular chaperon, protein binding/folding
	tumor necrosis factor type 1 receptor associated protein TRAP-1 - human	gi|1082886	75694	1	2	apoptosis process, ATP binding
2.	heat shock cognate 71 kDa protein isoform 1	gi|5729877	71082	6	14	molecular chaperon, protein binding/folding
	chain A, atpase domain of human heat shock 70kDa protein 1	gi|6729803	41973	6	20	molecular chaperon, protein binding/folding
	heat shock 70kDa protein 8 isoform 1 variant	gi|62897129	71083	8	16	molecular chaperon, protein binding/folding
3.	cytokeratin 18 (424 AA)	gi|30311	47305	3	7	structural constituent of cytoskeleton, protein binding
4.	keratin, type I cytoskeletal 19	gi|24234699	44079	5	14	structural constituent of cytoskeleton, protein binding
5.	14-3-3 protein zeta/delta	gi|4507953	27899	3	16	regulation of signaling pathways
	chain A, binary complex of 14-3-3 sigma and P53 Pt387-peptide	gi|291463695	28225	2	8	regulation of signaling pathways

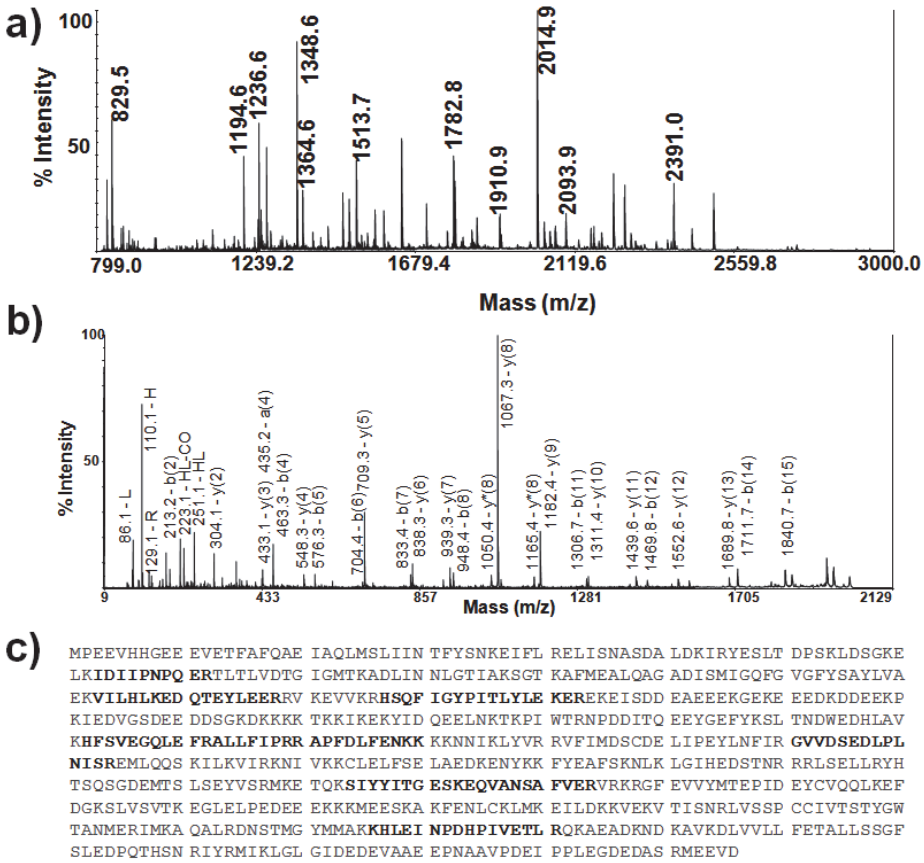

Fig. 3: An example of MS (a), chosen MS/MS fragmentation spectrum of peptide at m/z 2014 (b) and amino acids sequence with marked identified peptides (c) corresponding to heat shock protein HSP 90-beta.

Taken together our results indicate that the applied separation procedure using bottom-up MS based proteomics provides a fast way of fractionation and identification of important proteins and can be used for screening chosen key proteins. Our data offer preliminary information about the representation of proteins under the effects of retinoic acid isomers on MCF-7 cancer line. In forthcoming work we intend to use either the protocol for application of 2D SDS-PAGE or fractionation of proteins by the liquid-phase technique and tandem mass spectrometry to obtain significant changes from treated MCF-7 breast cancer line with two retinoic acid isomers.

ACKNOWLEDGEMENTS

This work was supported by the 7AMB12SK151, APVV-SK-CZ-0211-11, APVV-0160-11, VEGA 2/0008/11 and CEMAN grants, by the project No. CZ.1.07/2.3.00/20.0182 and with institutional support RVO:68081715 from Institute of Analytical Chemistry of the ASCR, v. v. i.

LITERATURE

[1.] Carlberg, C., Saurat, J-H., Siegenthaler, G., *Biochemical Journal* 1993, *295*, 343-346.
[2.] Brtko, J., *Biomedical Papers of the Medical Faculty of the University Palacky Olomouc Czech Republic* 2007, *151*, 187-194.
[3.] Pandey, A., Mann, M., *Nature* 2000, *405*, 837-846.
[4.] Farinha, A.P., Irar, S., de Oliveira, E., Oliveira, M.M., Pages, M., *Proteomics* 2011, *11*, 2389-2405.
[5.] Sarvaiya, H.A., Yoon, J.H., Lazar, I.M., *Rapid Communications in Mass Spectrometry* 2006, *20*, 3039-3055.

P11 PREPARATION OF HYPERCROSSLINKED MONOLITHIC COLUMN FOR SEPARATION OF POLAR COMPOUNS

Veronika Skerikova, Jiri Urban, Pavel Jandera, Magda Stankova

Department of analytical chemistry, Faculty of chemical-technology, University of Pardubice, Studentska 573, 53210 Pardubice, Czech Republic, Jiri.Urban@upce.cz

ABSTRACT

Hypercrosslinking, as a post-polymerization modification, allows preparation of high surface area organic polymer monoliths suitable for fast and efficient separation of small molecules in isocratic mode of capillary liquid chromatography. Infrared spectroscopy has confirmed that not all reactive chloromethyl groups in poly(styrene-co-chloromethyl styrene-co-divinylbenzene) monolithic capillary columns are consumed by hypercrosslinking modification. Remaining reactive chloromethyl groups allow following modification of monolithic surface. We have modified these remaining groups with thermally initiated 4,4′-azobis(4-cyanovaleric acid) initiator to produce activated hypercrosslinked surface. Once activated, almost any functional group can be attached to the hypercrosslinked monolith. We have used zwitterionic N,N-dimethyl-N-methacryloxyethyl-N-(3-sulfopropyl)ammonium betaine monomer to prepare a column allowing separation of polar compounds in hydrophilic interaction chromatography. The surface modification method has been optimized in terms of permeability, efficiency and selectivity of prepared monolithic capillary columns. The optimized column has been used for an isocratic and a gradient separation of proteins and phenolic acids.

Keywords: Organic polymer monoliths, HILIC, Hypercrosslinking

1 INTRODUCTION

1.1 Hydrophilic interaction chromatography

Very polar compounds have in Reversed-phase liquid chromatography (RP-LC) very low retention and their determination is difficult. Hydrophilic Interaction LIquid Chromatography (HILIC) can by alternative to RP-LC separation. The main characteristic of HILIC is combination of polar mobile phase, which is typical for RP-LC, and of polar stationary phase, which is typical for normal phase liquid chromatography (NP-LC) [1, 2]. Very often, zwitterionic stationary phases (with sulfobetaine group) are used in HILIC, because this stationary phase is resistant to high percentage of water in mobile phase.

1.2 Monolithic capillary column

To save the solvent and sample and reduce the waste, capillary monolithic columns whit sulfobetaine stationary phase are alternative to the conventional columns. The key advantages of monolithic columns in the capillary format include the absence of frits necessary to retain the packed bed and a moderate column back pressure at high mobile phase flow-rates [3]. Organic polymer monolithic capillary columns are prepared by in situ polymerization of suitable organic monomers in fused silica capillaries with inner diameters of 0.1 – 0.4 mm. The polymerization reaction mixtures consist of a combination of monomers and cross-linkers, an initiator and a porogen solvent mixture [4 - 9].

1.3 Hypercrosslinked monolithic capillary column

The unfavorable reactivity ratios for monomers lead to porous polymer structures that are amenable to hypercrosslinking. The divinylbenzene polymerizes faster than monovinyl styrene and vinylbenzyl chloride. Thus, remaining monomer mixture becomes significantly

richer in the monovinyl monomers as the polymerization reaction approaches completion and affords only slightly crosslinked chains attached to the surface of highly crosslinked microglobular scaffolds. After solvation with a thermodynamically good solvent, this layer can be crosslinked via the Friedel-Crafts reaction. The polymer chains become fixed in their solvated state during the reaction thus forming pores that persist even after the solvent is removed [10].
The presence of the reactive chloromethyl groups on the surface of the prepared hypercrosslinked monolithic stationary phases eliminates the need to introduce such a group, as in the case of the monolithic materials prepared from the non-functional monomers. Additionally, the large variety of direct reactions allows for a broad range of choices of modification protocols with no or minimal side products; thus, simplifying the overall modification procedure [11-12].

2 EXPERIMENTAL CONDITIONS

Chemicals

All monomers and reagents were purchased from Sigma–Aldrich (Steinheim, Germany; Milwaukee, WI, USA; St. Louis, MO, USA), Fluka (Buchs, Switzerland) and Penta (Chrudim, Czech Republic). Acetonitrile was purchased from LiChrosolv Gradient grade, Merck (Darmstadt, Germany) and methanol from Sigma-Aldrich (Steinheim, Germany). The standards of phenolic compounds, proteins and neurotransmiters were purchased from Fluka (Buchs, Switzerland) and Sigma-Aldrich (St. Louis, MI, USA). Water was deionized and purified in a Milli-Q water purification system (Millipore, Bedford, MA, USA). All standard solutions and HPLC mobile phases were filtered through a 0.22 µm membrane filter (Millipore).

2.2 Instrumentation

A modular micro liquid chromatograph was assembled from two LC10ADvp pumps (Shimadzu, Kyoto, Japan) with a high-pressure gradient controller; a micro valve injector with a 60-nL inner sampling loop (Valco, Houston, USA) controlled using a pneumatic actuator and an electronic time switch for injection of sample volumes a 60 nL; a restrictor capillary inserted as a mobile phase flow splitter before the injector; a variable wavelength LCD 2083 UV detector adapted for capillary electrophoresis with a fused silica capillary flow-through cell, 50 µm id (ECOM, Prague, Czech Republic), operated at 220 nm; and a personal computer with a chromatographic CSW Data Station for Windows, version 1.5 (Data Apex, Prague, Czech Republic). Fused silica capillary monolithic columns were fitted directly into the body of a micro-valve injector on one side and connected to the detector on the other, using zero-volume fittings.

2.3 Column preparation

Before polymerization, the inner wall surface of a polyimide-coated fused silica capillary was modified to improve the adhesion of the monolith bed to the capillary walls, as recommended by *Lee et al.* [13]. Monolithic stationary phases were prepared in silica capillaries by in-situ (co)polymerization of 16% of divinylbenzene, 12% of styrene, 12% of chloromethyl styrene, 41% of 1-dodecanol and 19% of toluene. 2,2´-Azobisisobutyronitrile (AIBN) was used as the initiator of the polymerization reaction (1% w/w, relative to the sum of monomers). The polymerization mixtures were filled into fused silica capillaries with modified internal walls using a micro-syringe. Both ends of the filled capillary were sealed with rubber stoppers and the capillary was placed in a circulated-water thermostat. The polymerization reaction was performed at 70°C for 20 h. Then, both ends of the capillary were cut and the monolithic column was washed with acetonitrile.

2.4 Hypercrosslinking and surface grafting

To prepare hypercrosslinked monolithic capillary column suitable for the separation of low-molecular compounds, a generic monolithic column was connected to the syringe pump and washed at room temperature by flow rate of 0.25 µL.min^{-1} with 1,2-dichlorethane for 2 h, iron trichloride in 1,2-dichlorethane (50 mg/**1** mL) for 2 h, then capillary was sealed with rubber stoppers and placed in a circulated-water thermostat for 2 h at 90°C to perform the hypercrosslinking modification.

Hypercrosslinked monoliths were flushed with water overnight, followed by mixture of triethylamine (TEA) and N,N-dimethylformamide (DMF) (1:3) for 2 h, and 4,4´-azobis(4-cyanovaleric acid) in mixture of TEA and DMF (1:2:6) for 1, 8 or 20 h. Then were columns flushed with 20% w/w [2-(methacryloyloxy)-ethyl]-dimethyl-(3-sulfopropyl)-ammonium hydroxide (MEDSA) in methanol for 2 h, capillary was sealed with rubber stoppers and placed in a circulated-water thermostat for 1, 8 or 24 h at 50, 70 or 90°C to perform the surface modification with grafting of sulfobetaine groups.

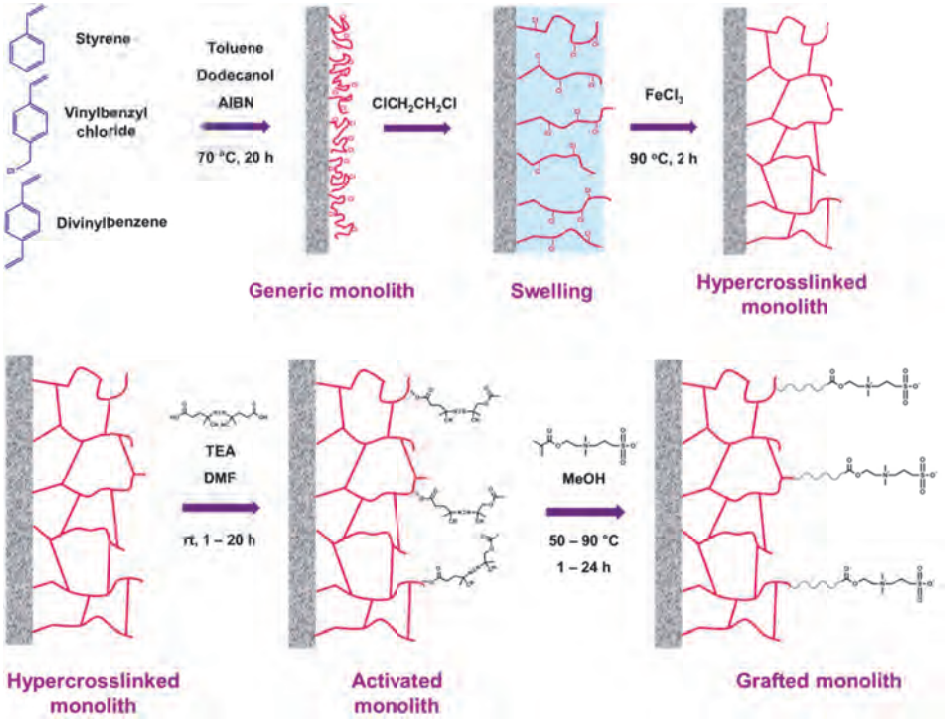

Fig. 1. : Scheme of preparation and post-polymerization modification of monolithic capillary column.

3 RESULTS AND DISCUSSION

3.1 Optimization of column preparation

A design of experiments procedure (Fig. 2.) was used to optimize the preparation of hypercrosslinked columns with variables including time used to activate monolith with 4,4′-azobis(4-cyanovaleric acid) (1, 8, and 20 h), and time (1, 8, and 24 h) and temperature (50, 70, and 90 °C) of grafting of zwitterionic N,N-dimethyl-N-methacryloxyethyl-N-(3-sulfopropyl)ammonium betaine monomer to prepare HILIC column. Optimal conditions involved the activation of the monolithic surface with 4,4′-azobis(4-cyanovaleric acid) for 8 hours, followed by the thermally initiated grafting of MEDSA for 8 hours at 70°C (Column 8/8/70).

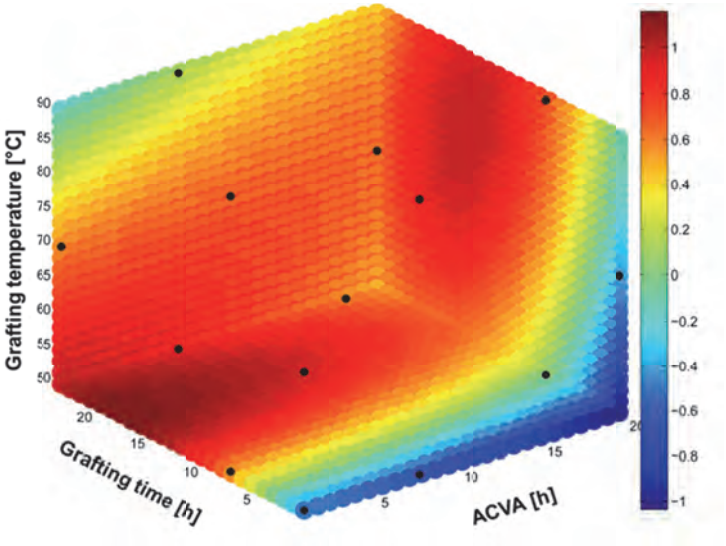

Fig. 2.: Graphical expression of optimized model describing the effect of surface activation, and time and temperature of grafting on the retention of thiourea in 98% aqueous acetonitrile. The black points are original data measured due to the design of experiments. The bar corresponds to the retention of thiourea at constant conditions.

The comparison of the retention of test mixture confirmed successful grafting (Fig. 3.). While there is no retention of polar compounds on the generic and hypercrosslinked monolithic columns, the grafting of the zwitterion monomer on the surface of hypercrosslinked monolith provides columns with high retention of polar thiourea in 98% aqueous acetonitrile.

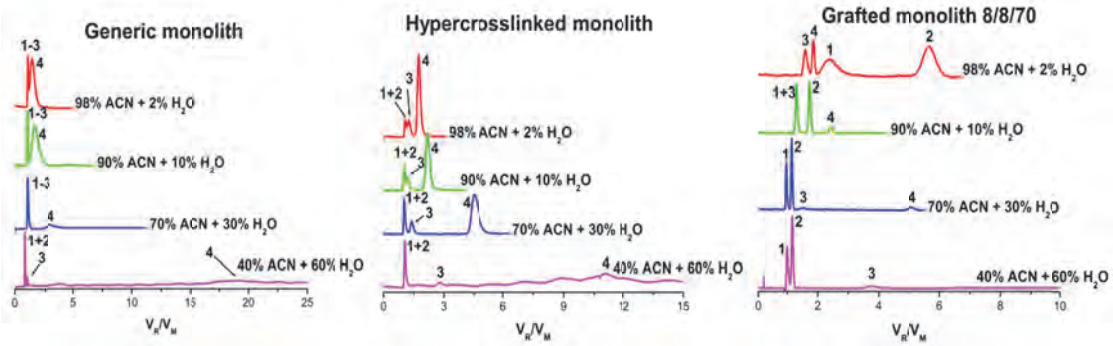

Fig. 3. : Separation of uracil (1), thiourea (2), phenol (3) and toluene (4) on generic, hypercrosslinked and grafted monolith. Mobile phase: aqueous acetonitrile, ambient temperature, UV-detection [214 nm], l = 167 mm, i.d. = 320 µm.

Hypercrosslinked monolithic capillary columns with zwitterion functionality provide dual-retention mechanism including hydrophilic interaction (for mobile phase with less than 20% of water) and reversed-phase retention (for mobile phases with more than 20% of water), which means that the retention of the polar compounds can be tuned by the change in the mobile phase composition.

3.2 Column stability

The repeatability of separation of phenol, toluene and thiourea had to be tested, in order to prove the stability of grafting. Consecutive injections of mixture of standards were carried out and it was observed that the grafted column showed good stability. The elution times remained almost constant over more than 7 500 injections and no compression of stationary phase was observed (Fig. 4.).

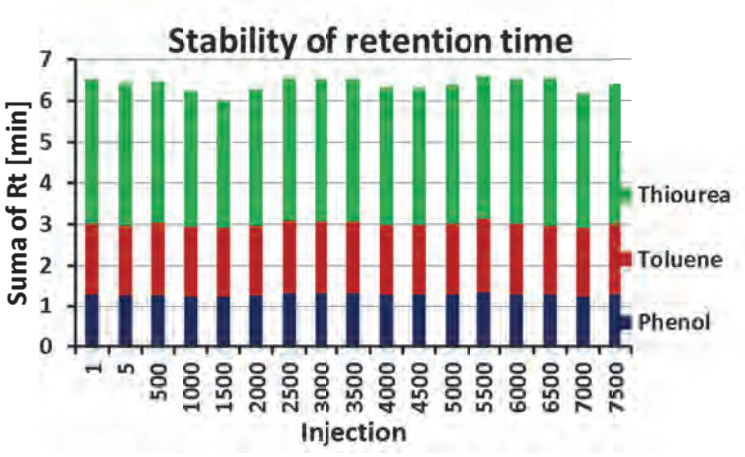

Fig. 4. : Stability of retention times of separated compounds on grafted monolith. Mobile phase: 98% aqueous acetonitrile, F_m: 10 µL.min^{-1}, inj.: 10 nL, ambient temperature, UV-detection [214 nm], l = 155 mm, i.d. = 320 µm.

3.3 Separation of polar compounds

Hypercrosslinked monolithic capillary column with zwitterion functionality was used for the separation of phenolic acids and proteins.

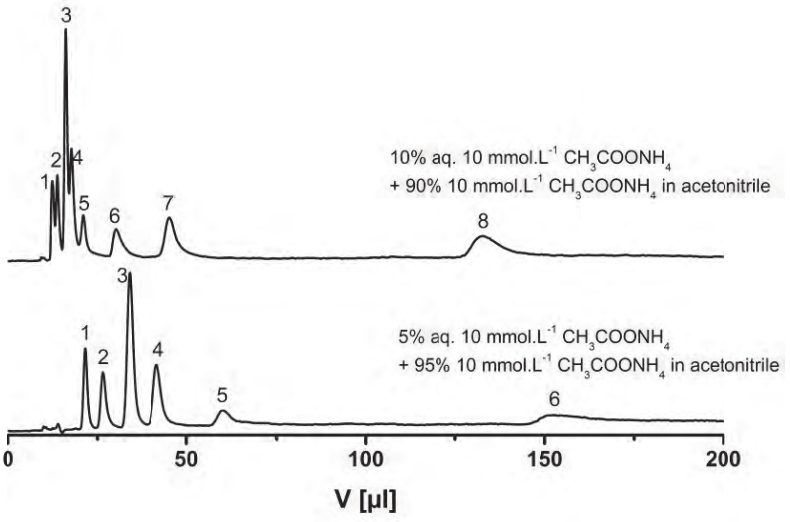

Fig. 5.: Isocratic elution of phenolic acids, 1 – sinapic a., 2 – ferulic a., 3 – syringic a., 4 – vanillic a., 5 – p-hydroxybenzoic a., 6 – caffeic a., 7 – protocatechuic a., 8 – gallic a., on grafted monolithic column 8/8/70. Mobile phase: aqueous 10 mmol.L^{-1} ammonium acetate acidified by formic acid and 10 mmol.L^{-1} ammonium acetate in acetonitrile, ambient temperature, UV-detection [220 nm], l = 279 mm, i.d. = 320 µm, F_m = 7.5 µL.min^{-1}.

Mobile phase for separation of phenolic acids in HILIC-mode consisted of 10 mmol.L^{-1} ammonium acetate in acetonitrile and aqueous 10 mmol.L^{-1} ammonium acetate acidified by formic acid. In mobile phase with 10% of aqueous salt were eight phenolic acids eluted using less than 150 µl of mobile phase and resolution of sinapic acid, ferulic acid, syringic acid and vanillic acid was lower than one. In mobile phase with 5% of aqueous salt solution resolution of first four compounds significantly increased, however the total elution volume also increased. Peaks of more polar compounds were broad and gallic acid was not eluted from the column whatsoever. Due to very high differences in retention of target phenolic acids, gradient elution is recommended to elute all compounds from the column in short time.
Proteins were eluted using aqueous acetonitrile with 0.15% of trifluoroacetic acid. Gradient elution was used in both HILIC- and RP-mode. HILIC provides better resolution of insulin, β-

lactoglobulin and cytochrome C than reversed-phase chromatography. Highly organic mobile phase also allowed, due to low backpressure, use higher flow-rate and decrease total elution time of proteins.

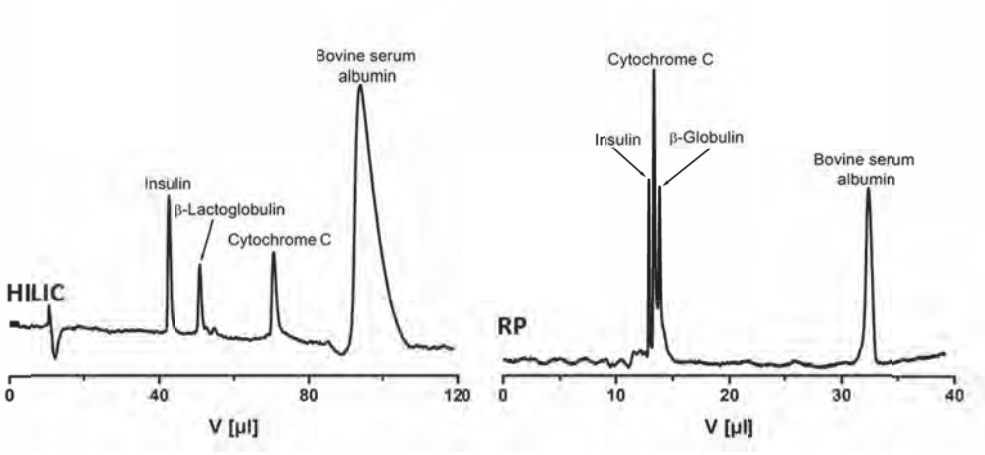

Fig. 6. : Gradient elution of proteins on grafted monolithic column 8/8/70. Mobile phase (A): water with 0.15% TFA, mobile phase (B): acetonitrile with 0.15% TFA, room temperature, UV-detection [214 nm], l = 279 mm, i.d. = 320 µm, HILIC-condition: gradient: 0. min – 90% (B), 15. min – 25% (B), 16. min – 90% (B), F_m = 7.5 µL.min^{-1}, RP-condition: gradient: 0. min – 20% MP(B), 15. min – 90% (B), 20. min – 90% (B), 21. min – 20% (B), F_m = 1.2 µL.min^{-1}.

4 CONCLUSION

Two step surface modification of poly(styrene-co-chloromethyl styrene-co-divinylbenzene) including hypercrosslinging and thermally initiated surface grafting allows preparation of hypercrosslinked monolithic stationary phases suitable for the separation of polar compounds in hydrophilic interaction chromatography. The preparation of columns has been optimized in terms of thiourea retention in 98% aqueous acetonitrile. Optimal conditions involved the activation of the monolithic surface with 4,4′-azobis(4-cyanovaleric acid) for 8 hours, followed by the thermally initiated grafting of MEDSA for 8 hours at 70°C. Prepared grafted polymer monolith columns achieve long column lifetime and good repeatability even after thousands of runs. The optimized column has been applied for separation of mixture of phenolic acids and proteins.

ACKNOWLEDGEMENTS

The financial support of GACR project P206/12/P049 is gratefully acknowledged.

LITERATURE

[1.] Pesek J., Matyska M. T.: *LC GC North America* 2007, *25*, 480.
[2.] http://www.sielc.com/Technology_HILIC.html.
[3.] Asiaie R., Huang X., Farnan D., Horvath C.: *J. Chromatogr. A* 1998, *806*, 251.
[4.] Zou H., Huang X., Ye M., Luo Q.: *J. Chromatogr. A* 2002, *954*, 5.
[5.] Legido-Quigley C., Marlin N.D., Melin V., Manz A., Smith N.W.: *Electrophoresis* 2003, *24*, 917.
[6.] Svec F., Frechet J.M.J.: *Chem. Mater.* 1995, *7*, 707.
[7.] Viklund C., Švec F., Frechet J.M.J., Irgum U.: *Chem. Mater.* 1996, *8*, 744.
[8.] Santora B.P., Gagne M.R., Moloy K.G., Radu N.S.: *Macromolecules* 2001, *34*, 658.
[9.] Svec F., Frechet J.M.J.: *Macromolecules* 1995, *28*, 7580.
[10.] Urban J., Svec F., Fréchet J.M.J., *Anal. Chem.* 2010, *82*, 1621.
[11.] Tripp J.A., Svec F., Fréchet J.M.J., *J. Comb. Chem.* 2001, *3*, 604.
[12.] Urban J., Svec F., Fréchet J.M.J., *J. Chromatogr. A* 2010, *1217*, 8212.
[13.] Lee D., Svec F., Frechet J.M.J.: *J. Chromatogr. A* 2004, *1051*, 53.

P12 RP-HPLC SEPARATION OF THREE SELECTED CHIRAL PESTICIDES USING COLUMN-SWITCHING TECHNIQUES

Mária Chalányová, Ivana Petránová, Veronika Vojtková, Milan Hutta

Department of Analytical Chemistry, Faculty of Natural Sciences, Comenius University, Mlynská dolina CH-2, 842 15 Bratislava, Slovakia

ABSTRACT

The reverse-phase liquid chromatographic chiral separation of three chiral pesticides (permethrin, cypermethrin, epoxiconazole) using the column switching techniques with achiral-chiral column were investigated. As achiral column Silasorb Phenyl and chiral β-cyclodextrin stacionary phase Chiradex was used. The mobile phase consist of methanol and water at flow rate was 0,5 ml. min^{-1} and 1 $ml.min^{-1}$, under isocratic mode. UV detection at 230 nm. The chromatographic parameters capacity factor (k´), separation factor (α) and resolution (R_S) was studied.

In this configuration, the separation conditions were found for epoxiconazole, permethrin enantiomers. Cypermethrin was particialy separated at 7 peaks.

In the future, we would like to expand on the reasearch and analysis of selected drugs and proteins.

Keywords: chiral pesticides, column switching, chiral separation

1 INTRODUCTION

The use of a wide range of chemicals to destroy pests and weeds is an important aspect of agricultural practice. Application of pesticides has resulted in increasing crop yields precious. The expanded use of such pesticides expectedly results in residues in foods, which has led to widespread concern over the potential adverse effects of these chemicals on human health [1]. A pesticides are included among toxic and often volatile substances in the environment [2]. More than 25% of the frequently used pesticides are chiral compounds [3] and consist of two or more enantiomers [4]. It is well known that the enantiomers of a chiral pesticides usually show different bioactivity and toxicity [5]. HPLC separation on chiral stationary phase is a very useful, rapid, non-destructive technique for the analysis of the enantiomers [6].

2 EXPERIMENTAL

2.1 Instrumentation

LC analnysis was carried out by the HPLC system LiChroGraph (Merck – Hitachi, Darmstadt, Germany) consisting of:
L – 6200A Intelligent pump provided by quarternary low-pressure gradient and high-pressure dynamic mixer; L – 4250 UV-VIS detector; 2 manual injection valves (Rheodyne model 7125, 7010, resp.; Cotati, California, U. S. A.); PC-based data acquisition system CSW ver. 1.0, 20-bit A/D converter (Data Apex, Praque, Czech Republic). Column switching techiques required an additional Knauer pump (Berlin, Germany) and Knauer variable wavelenght detector–1000 Berlin, (Germany). Short achiral column Silasorb Fenyl (30x3) mm, 5 µm particals, Tessek, Praha (Czech Republic); Chiral column Chiradex (250x4) mm, 5 µm particals Merck, Darmstadt, (Germany).

2.2 Chemicals and standards

Methanol gradient grade, Merck, Darmstadt, (Germany),
Ultrapure water Simplicity ® UV, (Millipore S.A.S., France)
Epoxconazole 93,5%, Cypermethrin 95,8%, Permethrin 97,3% (Riedel-de Haën, Germany)

2.3 Chromatographic condition

The mobile phase consist of methanol:water (50:50 v/v, 55:45 v/v or 70:30 v/v), flow rate 0,5 ml.min^{-1} and 1ml.min^{-1}, injection volume of standard 20 µl, UV detection at 230 nm.

3 RESULT AND DISCUSION

To study the separation of selected chiral pesticides permethrin, cypermethrin from group of synthetic pyrethroids and epoxiconazole group of triazole pesticides were used reverse-phase liquid chromatography RP-HPLC using a column switching techniques with achiral-chiral column with spectrophotometric detection at 230 nm. As achiral column Silasorb Phenyl was used where concentration of the analyte in the form of narrow zone (focusing) is achieved. In the case of crude extract of real samples clean-up of extract from co-extracted substances of complex matrix is attained. The chromatographic peak width on the second detector was determined the moment of valve switching when the analyte is eluted back-flush techniques from a achiral to chiral column Chiradex. The mobile phase composition for chiral separation of enantiomers for epoxiconazole is methanol:water (50:50, v/v), for permethrin methanol:water (70:30, v/v), for cypermethrin methanol:water (55:45,v/v).

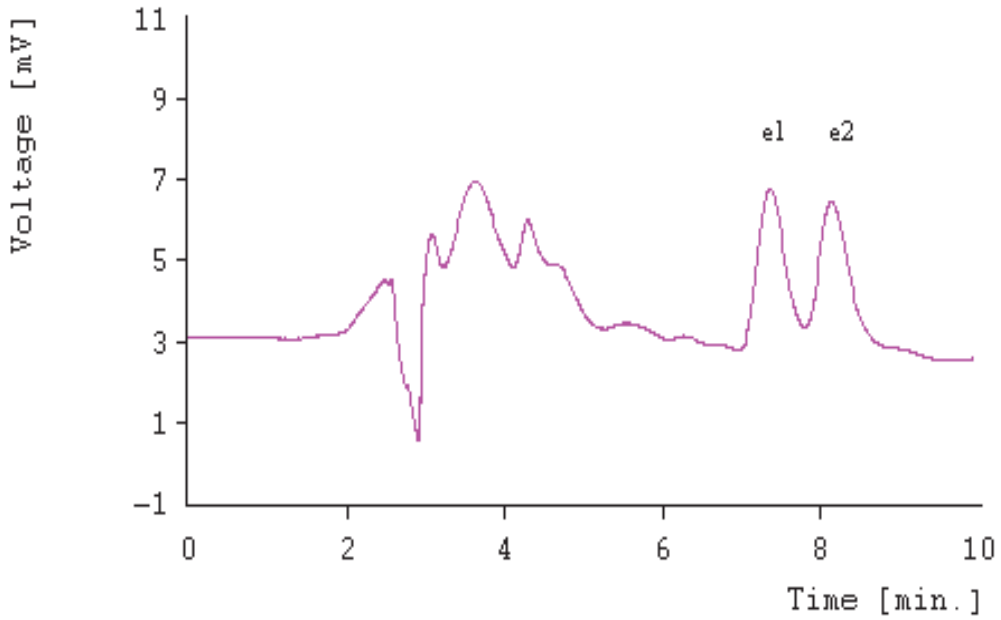

Fig. 1. Enantioseparation of epoxiconazole using column switching techniques with back-flush elution of analyte from achiral to chiral column.
Experimental condition: Chiral column Chiradex: methanol:water (50:50, v/v), 0,5 ml.min^{-1}. UV detection at 230 nm. Abbreviation: **e1, e2** are enantiomers of epoxiconazole.

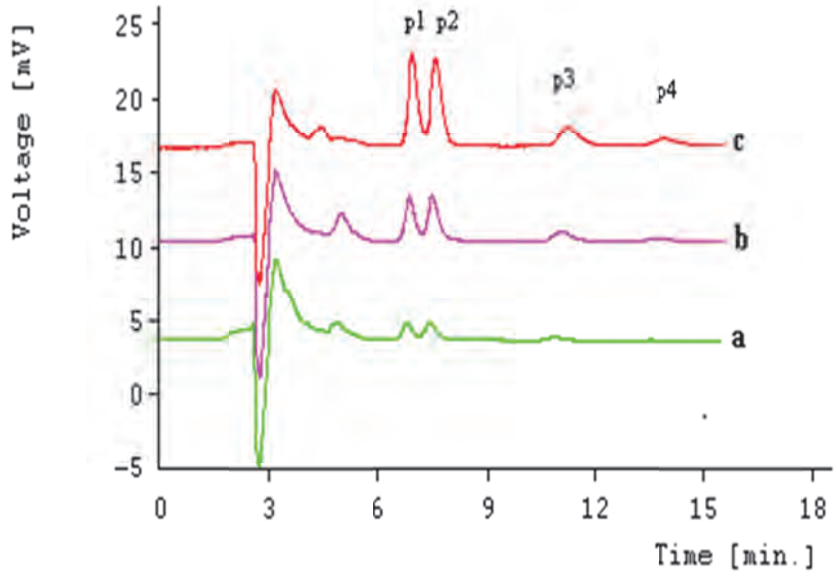

Fig. 2. Enantioseparation of permethrin using column switching techniques with back-flush elution of analyte from achiral to chiral column; concentration of permethrin is **a)** 1 µg.ml^{-1}; **b)** 5,0 µg.ml^{-1}, **c)** 10 µg.ml^{-1}.
Experimental condition: Achiral column Silasorb Phenyl: methanol:water (50:50, v/v), 0,5 ml.min^{-1}. Chiral column Chiradex: methanol:water (70:30, v/v), 1 ml.min^{-1}. UV detection at 230 nm. Abbreviation: **p1-p4** are enantiomers of permethrin.

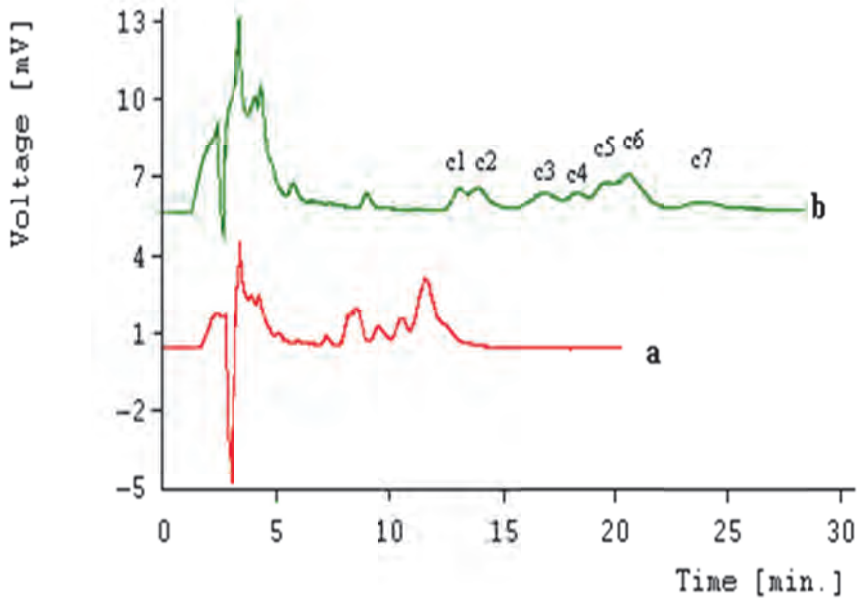

Fig.3. Enantioseparation of cypermethrin using column switching techniques with back-flush elution of analyte from achiral to chiral column.
Experimental condition: Achiral column Silasorb Phenyl: methanol:water (50:50, v/v); 0,5 ml.min^{-1} Chiral column Chiradex: **a)** methanol:water (60:40, v/v), 1 ml.min^{-1} **b)** methanol:water (55:45, v/v), 1 ml.min^{-1}. UV detection at 230 nm. Abbrevation: **c1-c7** are enantioseparation of cypermethrin.

4 CONCLUSION

Enantiomeric separation of chiral pesticides is actual analytical problem. A relatively fast and inexpensive procedure has been developed for the enantiomeric separation of chiral pesticides. Epoxiconazole has one chiral center in the molecule and was separated to two enantiomers. Permethrin contains in its molecule two chiral centers, which are separated into 4 enantiomers. Cypermethrin has three chiral centers in the molecule. Theoretically consists of 8 enantiomers. Cypermethrin is partially separated into seven peaks c1-c7.

ACKNOWLEDGEMENTS

This work was generously supported by the grant of The Agency of the Ministry of Education, Science, Research and Sport of the Slovak Republic for the Structural Funds of EU - project ITMS 26240220034.

LITERATURE

[1.] al-Saleh, IA., Journal of Environmental Pathology, Toxicology and Oncology 1994, *13*, 151-161.
[2.] Fenik, J., Tankiewicz, M., Biziu, M., Trends in Analytical Chemistry 2011, *30,* 814-826.
[3.] Wang, P., Liu, D., Jiang, S., Gu, X., Z. Zhou, Chirality 2007, *19*, 114-119.
[4.] Tian, Q., Lv, CH., Ren, L., Zhou, Z., Chromatographia 2010, *71*, 855-865.
[5.] Tian, Q., Lv, CH., Wang, P., Ren, L., Zhou, Z., Journal of Separation Science 2007, *30*, 310-321.
[6.] Wang, P., Zhou, Z., Jiang, S., Yang, L., Chromatographia 2004, *59*, 625-629.

P13 NEW MODIFICATION OF DIFFUSIVE GRADIENT IN THIN FILM TECHNIQUE (DGT) FOR DETERMINATION OF METALS IN SEDIMENTS

Michaela Gregusova, Bohumil Docekal

Institute of Analytical Chemistry of the ASCR, v.v.i, Veveri 97, CZ-602 00 Brno, Czech Republic, gregusova@iach.cz

ABSTRACT

The diffusive gradient in thin film (DGT) technique has been used for measuring fluxes and concentrations of labile metal species in waters, soils and sediments. The DGT probes offer a number of advantages over other conventional monitoring techniques as grab sampling, by reducing the errors of sample storage and transportation. When DGT probes are exposed to aqueous systems over a certain time, metal species diffuse into the binding gel through the diffusion layer and thus provide time averaged concentrations of metal species in situ. Application of a modified constrained sediment probe with selective resin gel based on Spheron-Oxin® (5 sulphophenyl-azo-8-hydroxyquinoline) ion exchanger for measurement of time averaged concentrations of manganese, iron and uranium in sediment pore water is described. A set of incubation experiments with sediments from selected localities in Czech Republic was designed for studying various aspects of metal removal/release processes, and their results are presented and discussed.

Keywords: DGT, sediment, uranium

1 INTRODUCTION

The diffusive gradient in thin film (DGT) technique has been used for measurement of concentrations and fluxes of labile metal species in environmental systems, in characterization of waters, soils and sediments. When DGT probes are exposed to aquatic systems over a certain time period, metal species diffuse through the well-defined diffusion layer into the binding resin gel and provide in situ time averaged concentrations of mobile metal species [1]. In sediments, the probes disturb local sediment/pore water equilibrium under well-defined conditions, so that the sediment response, metal re-supply fluxes can be monitored in situ [2-3].The scope of the work was to investigate performance of a modified DGT probe for sediment characterization.

2 EXPERIMENTAL

A modified constrained sediment probe [4] packed with agarose based resin and diffusive gels were exposed to uranium spiked sediment core to obtain high resolution profiles of manganese, iron and uranium to show its performance. The diffusive equilibrium in thin films technique (DET) was used to obtain complementary high resolution pore water profiles of total concentrations of dissolved metals species. Sediment sample was homogenized, incubated before and after spiking of sediment core by depleted uranium (DU) standard solution. Segmented sediment DGT and DET probes were deployed in sediment core for one week, and pH and redox potential depth profiles were also measured. Mobile metals species were taken up by the Spheron-Oxin® based resin gel. Metals were eluted from the strips of gels by 1 M nitric acid, and subsequently determined by ICP MS (Agilent 7700 Series).

3 EQUATIONS

Generally, the calculation of the time-averaged DGT concentration C_{DGT} in a mixed aqueous solution is based on the equation [8]:

$$C_{DGT} = M \Delta g / (D\ t\ A)$$

where M is the metal uptake, Δg is the thickness of the diffusion layer, D is the diffusion coefficient of the metal ion in water, t is the deployment time and A is the area of the sampling window.

4 TABLES AND ILLUSTRATIONS

The DGT technique can provide information on geochemical cycling and fluxes of metals. As documented in graph, the modified segmented probe enables to obtain sediment depth profiles of metals with the resolution down to the millimeter level. The depth profile of uranium and iron in sediment obtained by using modified constrained probe is shown in Fig. 1. The amount of accumulated uranium in resin gel strips decreased from 60 ng in water overlaying sediment to 2 ng in the sediment core. As expected, the uranium depth profile displays also significant peak at the spiked sediment horizon of 12 cm, showing the resolution capability of the modified probe.

The redox potential exhibits significant changes to negative values close to the water-sediment interface, and it remains fairly constant in deeper horizons of the sediment core. In addition, iron profile is also given in Fig. 1. The uranium depth profile shows changes in uranium speciation, the reductive immobilization just below the water-sediment interface in accordance to the redox and iron profile. The pH in the overlying water and the upper sediment was close to 7.5, decreasing with depth to a constant value close to 7.2 (data not shown).

These results demonstrate that modified constrained probe is capable of providing valuable information on distribution of metals in sediments and changes in metals speciation

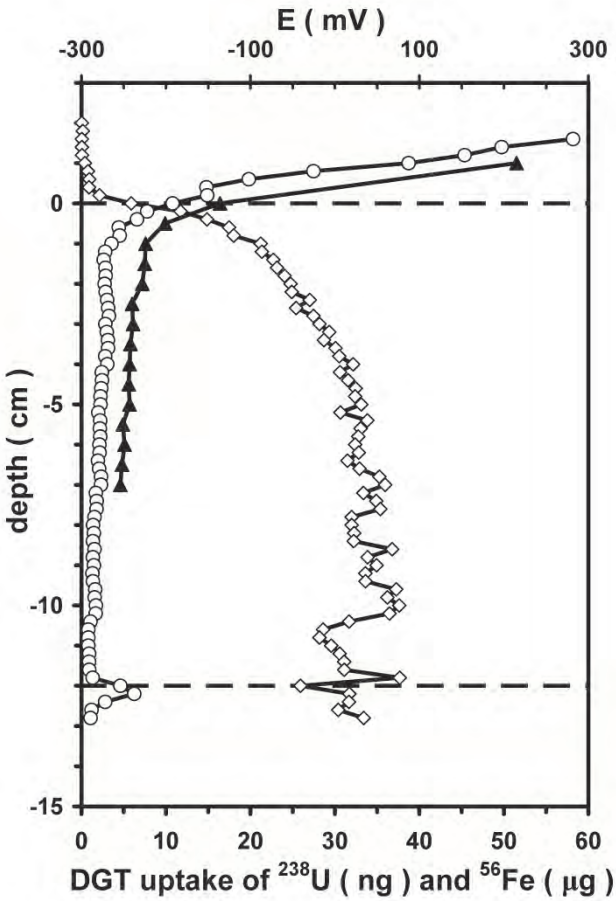

Fig. 1. :.Depth profiles of redox potential (▲), uranium (o) and iron (◊) uptake by resin gel strips in the pore water of the sediment from the Brno reservoir (pH 7.5 - 7.2). In determination of U and Fe, detection limits of 9 pg U and 15 ng Fe were found. Dashed lines in 0 and 12 cm depth horizons represent water-sediment interface and uranium spike, respectively.

ACKNOWLEDGEMENTS

This work was performed within the Institutional support RVO: 68081715, projects P503/10/2002 of the Czech Science Foundation.

LITERATURE

[1.] H.Zhang, W.Davison, Analycital Chemistry 1995, *67*, 3391.

[2.] H.Zhang, W.Davison, B. Knight, S. McGrath, Environmental Science and Technology 1998, *32,* 704.

[3.] M.P.Harper, W.Davison, H.Zhang, W.Tych, Geochimica et Cosmochimica Acta 1998, *62*, 2757.

[4.] B.Dočekal, M.Gregušová, Analyst 2012, *137*, 502.

P14 PROFILING OF SOIL AND PEAT HUMIC SUBSTANCES BY ANION-EXCHANGE CHROMATOGRAPHY

Janka Ráczová, Milan Hutta, Veronika Komorowská

Comenius University in Bratislava, Faculty of Natural Sciences, Department of Analytical Chemistry, Mlynská dolina CH-2, 842 15 Bratislava, Slovak Republic, raczova@fns.uniba.sk

ABSTRACT

A simple anion-exchange liquid chromatographic method has been developed to assay commercial available humic substances and alkaline extracts of various types of soils. The anion-exchange HPLC analysis used short glass column (30x3 mm) filled with Separon HEMA-BIO 1000 sorbent with (diethylamino)ethyl functional groups (60 μm particles) and a mobile phase A constituted of aqueous solution of tetrasodium salt of EDTA (pH 12.0; 5 mmol L^{-1}) and mobile phase B constituted of aqueous solution of tetrasodium salt of EDTA (pH 12.0, 500 mmol L^{-1}). The wavelength of the detection was set to 480 nm (λ_{ex}) and 530 nm (λ_{em}) for humic substances and soils. The proposed method provided an accurate and precise analysis of commercial available humic substances and alkaline extracts of various types of soils.

Keywords: humic substances, EDTA, anion-exchange chromatography

1 INTRODUCTION

In recent years most of the soil and agrochemical scientists have paid serious attention to the research of humus substances (humic, and fulvic acids) and their action on plant growth and development and the direct processes running in soils.

The ecological significance of the biological effects of humic substances becomes more meaningful when we consider the overall impact of these humic materials on the productivity and fertility of soil and water ecosystems. In addition to facilitating the dissolution of most otherwise insoluble metallic salts, humic substances are involved in a variety of reactions in soils, sediments, and water with major nutrients such as ammonia, nitrates phosphates, and silicates. Research indicates that these interactions not only considerably increase the retention and residence time of the nutrients in the growing media, but also enrich and biologically condition the growing media. These interactions and effects together have profound influence on the biological production process [1].

The importance of separation methods in the chemistry of humic substances (HS), including liquid chromatographic (LC) methods is currently stressed by a review article of Hutta et al [2] that reviews advance of the topic since the review of Janoš [3]. Hutta *et.al.* [4] showed the usefulness of stepwise gradient elution in RP-HPLC for characterization of HSs and lignins as a natural precursors of HSs.

In spite of direct evidence for potential of ion-exchange mechanisms, there is lack of articles on this topic. Majority of information related to the ionic properties of humic substances and/or ion-exchange separation mechanisms can be found in literature sources dealing with natural or waste water treatment by use of ion-exchange membranes and their fouling by HSs [5,6]. Therefore we decided to evaluate analytical potential of the application of stepwise gradient [4] in combination with anion-exchange chromatography (IEC) for analysis and characterization of various types of samples in alkaline medium.

We report the verification of separation mechanism in development of a simple IEC assay with diode array UV (DAD) and fluorimetric (FLD) detection for the analysis and characterization of commercially available HAs, various types of organic matter extracted by

alkali solutions from soil samples and several model aromatic acids representing various negative charge characteristics.

2 EXPERIMENTAL

2.1 Chemicals and reagents

All the reagents and model analytes were of analytical-reagent grade unless stated otherwise. Water for gradient HPLC was prepared by Labconco Pro-PS unit (Labconco, Kansas City, USA). Sodium hydroxide (Merck, Darmstadt, Germany) was used for preparation of solutions of humic substances, soils and aromatic acids. Superpure EDTA (Sigma Aldrich, Steinheim, Germany) of was used for preparation of mobile phases.
Commercial humic acid were purchased from Sigma-Aldrich (denoted as ALD) with relative molecular mass 500-1000, according to product catalogue. Humic substance Ecohum (denoted as ECO) was a commercially available fertilizer isolated form peat with ammonia solution at industrial scale. Humic substances Cerová and Suchá Hora (denoted as CER and SH, respectively) were isolated from peat using fractionation procedure recommended by IHSS [7, 8]. The soil samples used in this study were collected from different localities of Slovakia (Gbely, Šajdikové Humence, Senec and Kremnica-Skalka; denoted as GBELY, ŠAJDÍK, SENEC, SKALKA, respectively).

2.2 Instrumentation

Study of retention behavior and selected groups of HS and soils was carried out by the HPLC system Spectra SYSTEM (Thermo Separations Products, USA). An inoLab pH 730 (WTW, Weilheim, Germany) pH meter with combined glass and silver /silver chloride electrode was used throughout, whereby all measurements of pH were carried out with correction to the alkaline error. Extractions of HSs from soils and peat were done by the laboratory shaker KS 125 (IKA Labortechnik, Kunkel, Germany).

2.3 Methods

A compact glass column (30x3 mm) filled with 0.25 g of Separon HEMA-BIO 1000 (diethylamino)ethyl (DEAE) functionalized hydroxyethylmetacrylate (HEMA) sorbent (60 μm particles, Tessek, Prague, Czech Republic) was used for the fractionation of HSs and alkaline soil extracts. The separation conditions for optimal gradient elution of HSs were as follows. Mobile phase A composition was: aqueous solution of sodium salt of EDTA (pH 12.0, 5 mmol L^{-1}). Mobile phase B composition was: aqueous solution of sodium salt of EDTA (pH 12.0, 500 mmol L^{-1}). Gradient program for fractionation of HSs and extracted soil organic matter was set from 0.0 to 1.9 min isocratic 0% B in A than from 2.0 to 3.9 min isocratic 1% B in A and from 4.0 min every 2 min there was isocratic step added by increasing of the content of B in A by a factor of 2 up to the last step increased by 36% ending in 100% B in A, maintained till 30.0 min isocratic 100% B in A, from 30.1 to 33.0 min linear decrease from 100% B in A to 0% B in A and between runs 5 min re-equilibration was maintained. Chromatographic conditions were follows: flow rate 1.0 ml min^{-1}; column oven temperature 40°C; injection volume 25 μl; fluorimetric detection (ex. 480 nm; em. 530 nm).

2.4 Sample preparation

The stock solutions of HSs were prepared daily fresh by dissolution of 3 mg of HS per 1 ml of 0.01 mol L^{-1} NaOH. The extraction procedure was performed in the following way: 1 g of sieved soil sample (15 mesh) was treated with 10 mL of 1.0 mol L^{-1} NaOH solution for 30 minutes. The solid residue was discarded. Prior to analysis the stock solutions and the soil extracts were centrifugated for 15 minutes at 3500 rpm.

3 RESULTS AND DISCUSSION

Humic substances are characterized by high polydispersity of almost all properties, therefore the authors focused to the selection of such a gradient shape which could create distinguishable profiles of HSs in a similar fashion as is created in the RP-HPLC assay [7,8]. The authors stressed, that the stepwise gradient elution mode could be used for distinct features gaining also in anion-exchange chromatography.

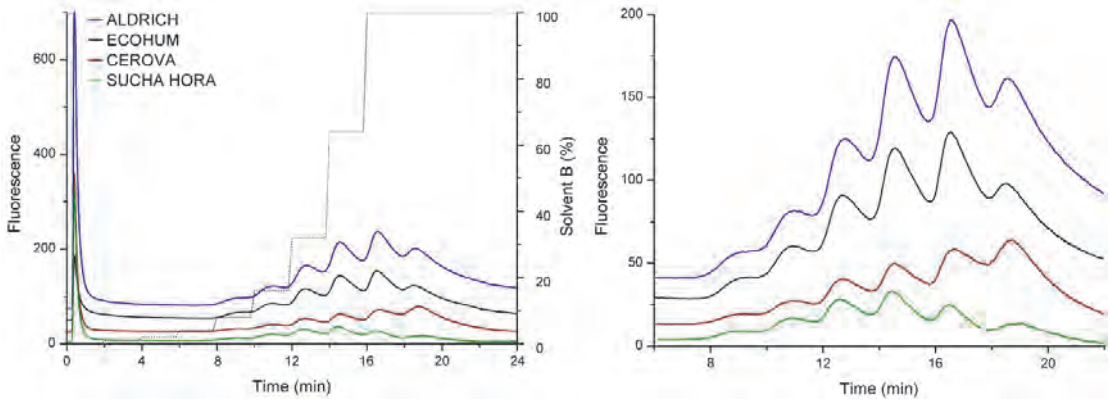

Fig. 1. : Chromatographic profiles of selected humic substances (HA Cerova denoted as CER, HA Aldrich denoted as ALD, HA Ecohum denoted as ECO and HA Sucha Hora denoted as SH). For the other and chromatographic conditions see Section Experimental. Scheme and shape of used stepwise gradient is illustrated on the figure.

Chromatograms of HSs profiling are shown in Figure 1 and they clearly demonstrate ability of devised system to generate characteristic peak-like profiles of HAs of various origin-location as-well-as alkali extracts of soils collected in various localities in Slovakia extracted by 1 mol L^{-1} NaOH containing corresponding HSs (Figure 3). It could be stressed, that the observed profiles are enforced by the step gradient shape. The Figure 1 shows nine-step gradient shape beside the obtained chromatograms. Except the first step, start of every step is overlaps with the valley between two peaks. Thereby, the highest peak is in the profile of ECO, ALD, CER and SH is eluted by 327, 327, 500 and 163 mmol L^{-1} solution of Na_4EDTA, respectively (64, 64, 100 and 32% of mobile phase B in A, respectively).

From the figures also follows, that the proposed chromatographic method is capable to distinguish between the HSs from various origin analogous to the method described in [5] which was based on the hydrophobic interactions. Whereas the profiles of the “standard” HSs are similar the profiles of the alkaline extracts of the soils from localities Gbely and Senec differ in profiles from those of localities Kremnica-Skalka and Šajdíkové Humence. The main observed difference is in the proportion of signals attributed to non-retained or weakly retained HSs (of yellow color – beside fluorescence also absorbing light at 420 nm) eluted by 5 mmol L^{-1} $EDTA^{4-}$ and medium to strongly retained HSs eluted successively by mobile phase containing between 50 mmol L^{-1} and 500 mmol L^{-1} $EDTA^{4-}$ at pH 12.0. Applying the analogy between the types of the analysed soils with the obtained profiles we can conclude, that this method can probably differentiate between non- or weakly retained HAs and strongly retained FAs. This speculation needs further prove by analyzing well-characterized HSs with defined content of HAs and FAs.

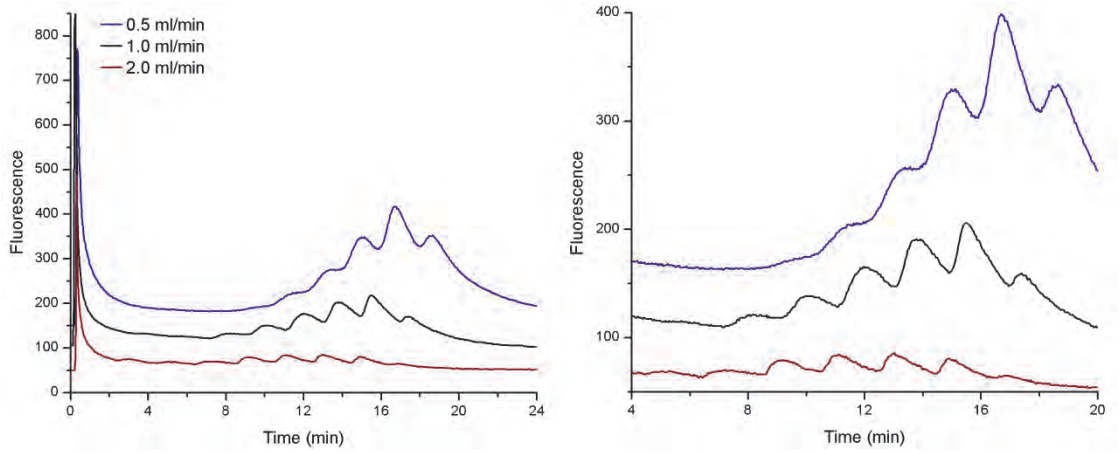

Fig. 2. : Influence of flow rate on chromatographic profiles of humic substance Aldrich. Conditions: Temperature: 40°C, injection volume 25 µl. For the other and chromatographic conditions see Section Experimental.

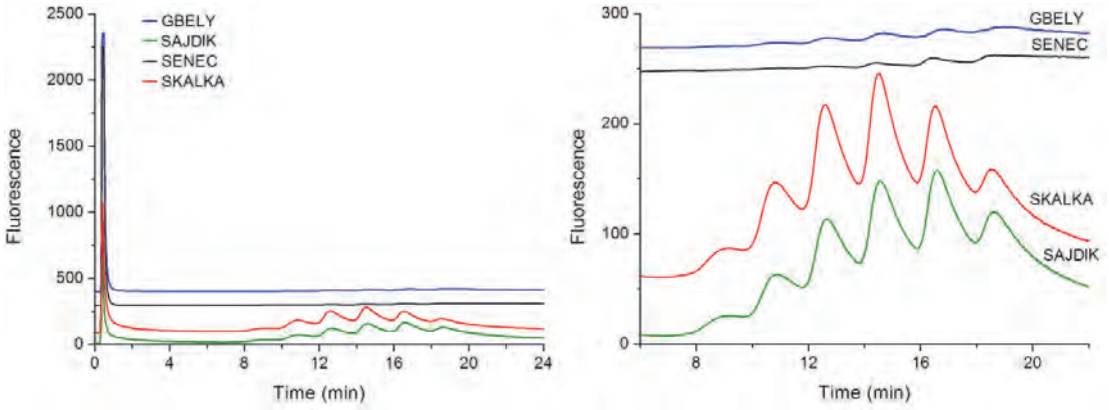

Fig. 3. : Chromatographic profiles of humic substances in extracts of soils from locations of Gbely, Šajdikové Humence, Senec and Kremnica-Skalka (all in Slovak Republic). For the other and chromatographic conditions see Section Experimental.

4 CONCLUSION

The developed anion exchange chromatography allows a relatively simple profiling humic substances and soils alkali extracts. Mobile phase composed of EDTA titrated to pH 12.0 by sodium hydroxide at various concentrations levels with a run time (38 min) and stepwise gradient elution used are advantageous and made the routine humic substances characterization easy. Among the significant advantages of this method are simplicity, sufficient precision ensuring that it is suitable for combinations with other HPLC separation mechanisms (e.g. SEC, RP-HPLC) for comprehensive characterization or fractionation of various types of humic substances and soil extracts.

ACKNOWLEDGEMENTS

This work was generously supported by the grant of The Agency of the Ministry of Education, Science, Research and Sport of the Slovak Republic for the Structural Funds of EU - project ITMS 26240120025.

LITERATURE

[1.] http://www.teravita.com/Technical%20Articles/Ferments%20of%20Humic%20and%20Fulvic%20Acids.htm 10.10. 2012
[2.] Hutta, M., Góra, R., Halko, R., Chalányová, M., *Journal of Chromatography A* 2011, *1218*, 8946-8957.
[3.] Janoš, P., *Journal of Chromatography A* 2003*, 983*, 1-18.
[4.] Hutta, M., Gora, R., *Journal of Chromatography A* 2003*, 1012*, 67-79.
[5.] Lee, H.J., Choi, J.H., Cho, J., Moon, S.H., *Journal of Membrane Science* 2002, *203*, 115-126.
[6.] Lee, H.J., Hong, M.K., Han, S.D., Cho, S.H., Moon, S.H., *Desalination* 2009, *238*, 60-69.
[7.] Kandráč, J., Hutta, M., Foltin, M., *Journal of Radioanalytical and Nuclear Chemistry* 1996, *208*, 577-592.
[8.] Procházková, T., Góra, R., Kandráč , J., Hutta, M., *Journal of Radioanalytical and Nuclear Chemistry* 1998, 229, 61-65.

P15 DETERMINATION OF SELECTED ACIDS IN HUMAN URINE BY COMBINATION OF CAPILLARY ISOTACHOPHORESIS AND CAPILLARY ZONE ELECTROPHORESIS

Michaela Joanidisová, Róbert Bodor, Zdenka Radičová, Marína Rudašová, Marián Masár

Department of Analytical Chemistry, Faculty of Natural Sciences, Comenius University in Bratislava, Mlynská dolina CH2, 842 15 Bratislava, joanidisova@fns.uniba.sk

ABSTRACT

Organic acids, namely furan-2,5-dicarboxylic acid and quinolinic acid, occurring in human urine were analyzed by combination of capillary isotachophoresis (cITP) and capillary zone electrophoresis (CZE) with UV photometric detection. Optimal cITP separation conditions were achieved with a leading electrolyte at pH 3.6 and malate as a terminating anion. CZE separations were carried out at pH 5.7 using malate as the carrier ion. The described method allows direct, rapid and sensitive determinations of the furan-2,5-dicarboxylic and quinolinic acids in human urine without additional sample pretreatment step.

Keywords: isotachophoresis – capillary zone electrophoresis, organic acids, urine

1 INTRODUCTION

Quinolinic acid (QA), a metabolite of tryptophan catabolism, is involved in the pathogenesis of several major inflammatory neurological diseases. In addition, the amount of QA excreted in urine is one of the criteria for vitamin B6 deficiency [1].
Furan-2,5-dicarboxylic acid (FDCA) is a metabolite produced by Aspergillus and possibly other fungal species in gastrointestinal (GI) tract. Clinical significance of their abnormal values indicates dysbiosis [2].
The on-line combination of isotachophoresis (cITP) and capillary zone electrophoresis (CZE) in a column coupling arrangement of the separation unit is a very effective tool for increasing the separation capability and sensitivity of CZE [3]. This work was focused on direct determination QA and FDCA present in complex human urine samples with UV detection. CITP was used as a sample clean-up technique for removing anionic sample macroconstituents and potential interferences.

2 EXPERIMENTAL

2.1 Instrumentation

The cITP-CZE separations were carried out in an electrophoretic analyzer EA-201 assembled with a column coupling configuration of the separation unit. The samples were injected with the aid of a 30 µl internal sample loop of the injection valve. CITP was realized on a FEP capillary with a 90 mm length and a 0.8 mm i.d. An on-column conductivity detector was placed at the end of the cITP capillary. CZE was realized on FEP capillary with a 250 mm length and a 0.3 mm i.d. Photometric UV detector working at a 254 nm wavelength was connected to the CZE capillary via optical fibers. Methylhydroxyethylcellulose (mHEC), added to the leading and background electrolytes, was used as a dynamic coating agent to suppress EOF. The cITP-CZE analyses were carried out in anionic mode of the separation under suppressed hydrodynamic flow conditions. The driving currents applied were 250 and 200 µA for cITP and CZE steps, respectively.

2.2 Chemicals and samples

Chemicals used for the preparations of the electrolyte solutions were obtained from Serva (Heidelberg, Germany), Sigma-Aldrich (St. Louis, MO, USA), Lachema (Brno, Czech Republic) and Merck (Darmstadt, Germany). MHEC 30 000 was obtained from Serva. QA and FDCA of analytical grade were purchased from Sigma-Aldrich.

Water demineralized by a Pro-PS water purification system (Labconco, Kansas City, KS, USA) and kept highly demineralized by a circulation in a Simplicity deionization unit (Millipore, Molsheim, France) was used for the preparation of the electrolyte and sample solutions.

Urine samples, obtained from volunteers, were diluted 10-times with deionized water immediately after the collection and subsequently, filtered through a 1 µm pore size membrane filters (Millipore). The samples prepared in this way were stored in a freezer at -40 °C. Before analysis, samples were melted at a room temperature, diluted and directly injected into the CE equipment.

3 RESULT AND DISCUSSION

Multicomponent samples of biological origin as for example human urine represent a complex matrix with high risk of the peak overlapping in CZE. On-line combination of cITP and CZE offers minimum disturbances coming from the sample matrix due to an effective clean-up effect of cITP and, at the same time, pre-concentration of the analytes injected to the CZE step. Therefore, an optimization of the separation conditions was performed. With respect to acid–base properties of QA (pK_{a1}=2.43, pK_{a2}=4.78) and FDCA (pK_{a1}=2.28), the separations at a low pH were favored. In ITP step, the pH of leading electrolyte (3.6) and terminating ion (malate) were optimized in regard to minimize the number of compounds migrating isotachophoretically. This approach reduced a number of matrix constituents transferable into the CZE step as it prevented ITP migrations of the constituents with pK values higher than that of the terminating constituent.

The composition of background electrolyte was optimized, as well. Terminating ion has been used as a carrier ion in the CZE step. The pH and the ratio of single and double charged counter ions in the background electrolyte were the main parameters influencing the effective mobilities of the separated compounds in CZE stage of cITP-CZE (Fig. 1 and 2). An electropherogram obtained from the cITP-CZE separation of FDCA and QA at different pH (5.4, 5.7 and 6.2) and constant concentration of double charged counter ion (bis tris propane, BTP) and different concentration of single charged counter ion (bis tris, BT) is shown in Fig. 1. The best resolution of FDCA and QA from co-migrating constituents originating from urine was found at pH 5.7.

Very good repeatabilities of total and corrected migration times of different urine and model samples were achieved in cITP-CZE repeated runs. RSD values of total migration time, a sum of the time in cITP and CZE steps, evaluated from 80 measurements of different urine samples with different dilution was 1.5 and 1.2% for FDCA and QA, respectively. The RSD values of corrected migration times of FDCA and QA in CZE step (cITP time subtracted) were 0.4 and 0.9%, respectively (Table 1). Other analytically important parameters of this method are summarized in Table 2. The developed method was verified by the analysis of different urine samples (Fig. 3). The concentrations of FDCA and QA calculated in different urine samples using external calibration and standard addition methods were in a good agreement (Table 3).

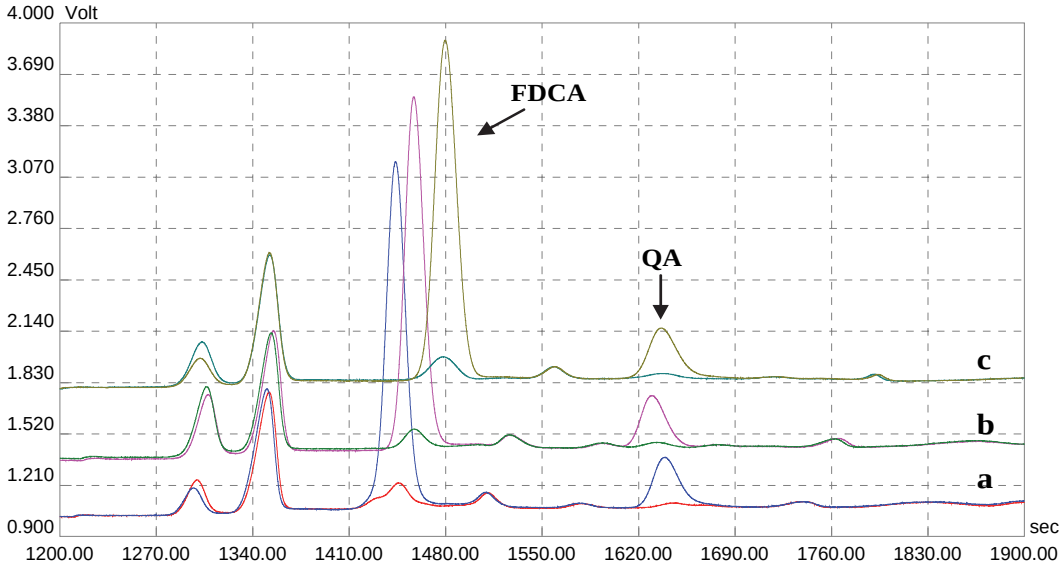

Fig. 1.: CITP-CZE separations of human urine. Separations were performed by using LE solution with pH 3.6 and TE solution with pH 4.1. CZE separations were performed in background electrolyte at pH a) 5.4, b) 5.7 and c) 6.2. Concentration of background anion was constant (50 mM of malate). pH was adjusted by constant concentration of double charged counter ion (BTP) and different concentration of single charged counter ion (BT). Human urine diluted 300-times, and obtained from healthy volunteer and spiked urine sample (5 mM FDCA and QA) was injected.

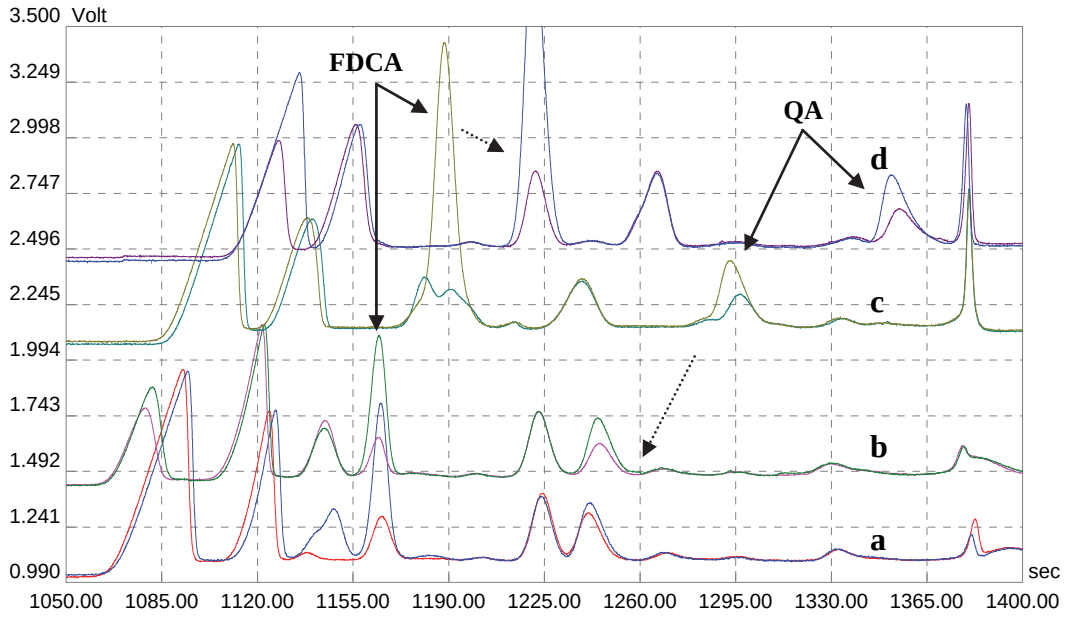

Fig. 2.: CITP-CZE separations of human urine. cITP steps were the same as in Fig. 1. CZE separations were performed in background electrolyte at pH 5.7. Concentration of background anion was constant (25 mM of malate). pH was adjusted by single (BT) and double (BTP) charged counter ions. Concentration of BTP was a) 0, b) 1, c) 7 and d) 15 mM. Human urine diluted 100-times and obtained from healthy volunteer was injected. Urine sample was spiked with a), c) and d) 3 mM FDCA and QA and b) 1 mM FDCA, and 2 mM QA.

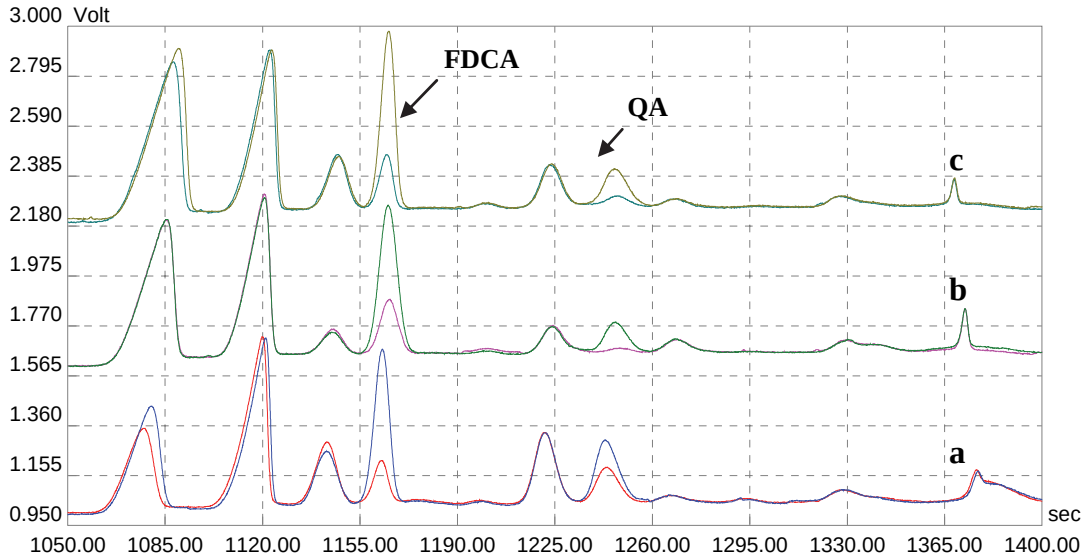

Fig. 3.: CITP-CZE analyses of different human urine. The separations were performed in electrolyte system as in Fig. 2b. Human urine diluted 100-times and spiked (1 mM FDCA, 2 mM QA) urine samples were injected. The samples were obtained from a) volunteer with urinary infection, b) healthy volunteer and c) a volunteer with autism.

Table 1: Repeatabilities of migration times for FDCA and QA

	average t (s)	SD (s)	RSD (%)	average t_{cze} (s)	SD (s)	RSD (%)
FDCA	1155	17.9	1.5	669	2.7	0.4
QA	1237.8	15.3	1.2	751.5	6.6	0.9

The separations were performed in electrolyte system as in Fig. 2b within 7 days. Number of measurements: 80. Samples: urine samples from 3 different volunteers diluted 50- and 100-times, and spiked urine samples, calibration solutions. t - total migration time in cITP-CZE; t_{CZE} - migration time in CZE step (cITP time subtracted).

Table 2: Calibration parameters and LODs for FDCA and QA

analyte	slope (mV s/μM)	intercept (mV s)	R^2	LOD (μM)
FDCA	2996	153	0.9998	0.02
QA	473.1	7.8	0.9995	0.17

Limit of detection (LOD) has been calculated by using method based on 3 times of S/N of the baseline close to the analyte peak. Calibration range: 0.5-5 μM.

Table 3: Contents of FDCA and QA in different human urine samples

urine sample		external calibration		standard addition	
	analyte	c (μM)	mmol/mol creatinine	c (μM)	mmol/mol creatinine
Healthy F=100	**FDCA**	28	1.9	28	**1.9**
	QA	71	4.8	69	**4.6**
Healthy F=50	**FDCA**	26	1.8	29	**2.0**
	QA	64	4.3	69	**4.6**
Urinary infection F=100	**FDCA**	34	1.2	39	**1.3**
	QA	254	8.7	265	**9.0**
Autism F=100	**FDCA**	52	3.5	56	**3.8**
	QA	26	1.8	24	**1.6**

Reference range (in mmol/mol of creatinine): FDCA ≤ 22 and QA 0.6-6.7. c = analyte concentration

4 CONCLUSION

The work was focused on the development of a new method for the determination of FDCA and QA in human urine, organic acids which are important for the diagnosis of certain diseases by on-line combination of cITP and CZE. Suitable separation conditions in both cITP and CZE steps for the resolution of FDCA and QA from other co-migrating constituents present in human urine samples were found. The described method allows direct, rapid and sensitive determination of the FDCA and QA in human urine without other sample pretreatment step.

ACKNOWLEDGEMENTS

This work was generously supported by the grant of The Agency of the Ministry of Education, Science, Research and Sport of the Slovak Republic for the Structural Funds of EU - project ITMS 26240120025.

LITERATURE

[1.] Nawagawa, I., Sasaki A., *Journal of Nutritional Science and Vitaminology* 1997, *23*, 535-548
[2.] Shaw, W., et al., *Clinical Chemistry* 1995, *41*, 1094-1104
[3.] Dankova, M., Strasik S., et al., *Journal of Chromatography A* 2001, *916*, 143-153

P16 MULTIVARIATE STATISTICS FOR THE DIFFERENTIATION OF ERYTHROPOIETIN PREPARATIONS BASED ON INTACT GLYCOFORMS DETERMINED BY CE-MS

Christian Neusüß, Angelina Taichrib, Markus Pioch, Sabine Neuberger

Aalen University, Beethovenstr. 1, D-73431 Aalen, Germany
christian.neususs@htw-aalen.de

ABSTRACT

The comparison of different erythropoietin preparations in the pharmaceutical area gains in importance, due to the increasing number of erythropoietin biosimilars being approved. Since erythropoietin contains three N-glycosylation sites, its natural heterogeneity strongly increases the complexity with respect to the analysis of erythropoietin. The same heterogeneity can however be of potential use to distinguish different erythropoietin preparations, if the analysis method is capable to map the underlying heterogeneity. Here, a previously published method for the analysis of intact proteins by capillary electrophoresis–mass spectrometry [1] was further investigated for the differentiation of various erythropoietin preparations by the use of capillary electrophoresis–mass spectrometry and the subsequent application of multivariate statistics.
Relative peak areas of selected intact erythropoietin isoforms were used as variables in Principal Component Analysis and Hierarchical Agglomerative Clustering. Both of these strategies are suitable for the clear differentiation of all erythropoietin preparations, including marketed products and pre-production preparations, which differ in the manufacturer, the production cell line, and the batch number. In this way, even closely related preparations were distinguished based on the combined information on the sialoform, the antennarity, and the acetylation of the observed isoform.

Keywords: CZE-MS, intact proteins, multivariate statistics

1 METHODS

CE experiments were performed on a HP ^{3D}CE (Agilent Technologies, Waldbronn, Germany) using fused-silica capillaries with an ID of 50 µm and a length of approximately 60 cm. The capillaries were preconditioned, followed by the coating procedure (3 mol/L HCl for 5 min, water for 5 min, coating solution for 5 min, water for 2 min, and background electrolyte for 2 min). The coating solution used was UltraTrol™ low normal (Target Discovery, Palo Alto, CA, USA). The background electrolyte consisted of 1 mol/L acetic acid (HAc). Every five to ten runs recoating needed to be conducted. During the recoating procedure the capillary was removed from the interface to avoid contamination of the electrospray ionization (ESI) source and the mass spectrometer. Prior to injection, the capillary was rinsed for 2 min with

background electrolyte. Then the samples were injected hydrodynamically (100 mbar for 12 or 24 s, respectively). A constant separation voltage of +30 kV was applied.
The CE-MS coupling was carried out via electrospray ionisation (ESI) using a commercial CE-ESI-MS interface (Agilent Technologies, Waldbronn, Germany) with a triple-tube-design. A co-axial sheath liquid (SL) flow, typically composed of water and 2-propanol (50:50) with an addition of 1% HAc, was provided during analyses at a flow rate of 3 µL/min.
A micrOTOFQ quadrupole time-of-flight mass spectrometer controlled by micrOTOFcontrol software program (Bruker Daltonik GmbH, Bremen, Germany) was used. The ESI sprayer was grounded and the transfer capillary was kept at a constant voltage of -4500 V (positive ion polarity mode). The nebulizer gas (nitrogen) pressure was set to 0.2 bar. The ion optics were optimized to the highest possible intensity in the mass range of m/z 700 – 3000.

2 RESULTS AND DISCUSSION

A highly suitable CE-MS method for the extensive characterization of EPO preparations applying a neutral coated capillary has been developed [2]. The method was optimized and validated. This optimized and validated method was applied for the analysis of several marketed and preproduction EPO preparations with differences in the production cell line, the production conditions, and the batch number. 14 different EPO preparations were analyzed repeatedly, resulting in a total of 93 measurements. Examples are presented in Figure 1, showing a large separation between different sialic acid content. Samples with high similarity (e.g. NeoRecormon®, Recormon®) show overall congruence, while large differences to other formulations can be observed.

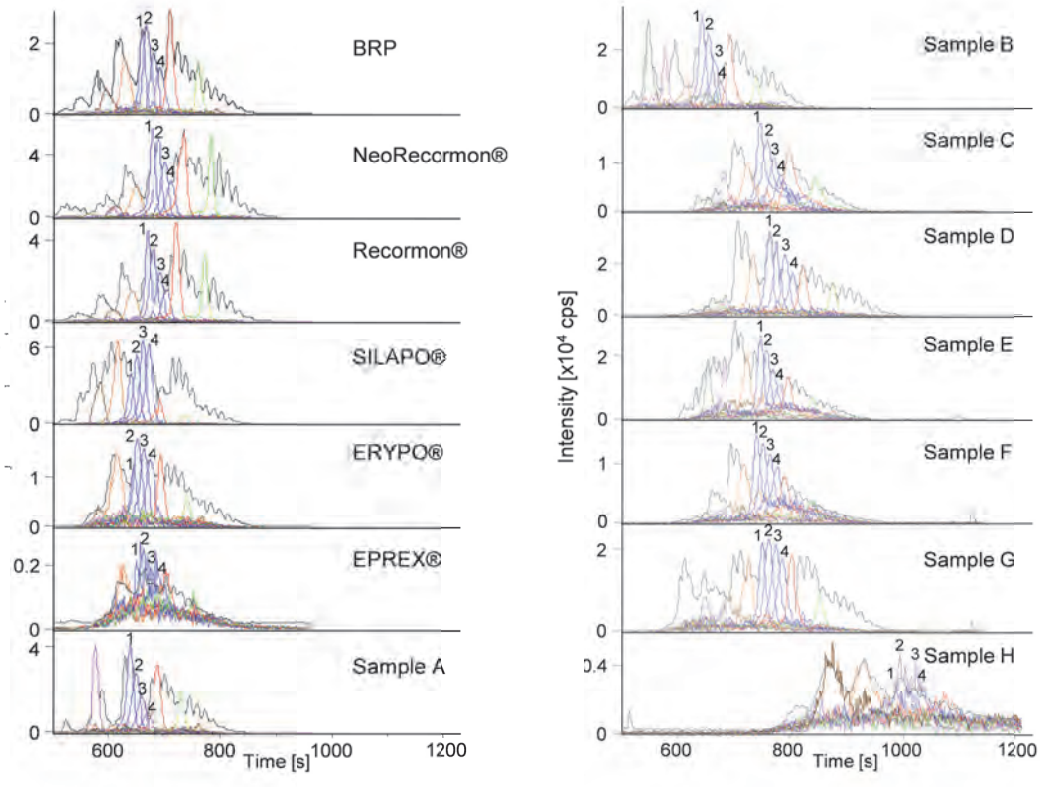

Fig. 1 Separations of the different erythropoietin (EPO). BPE (black) and selected Extraced ion electropherograms (EIE) of various EPO formulations. Peaks with identical color contain the same number of sialic acids.

For the statistical evaluation Principal Component Analysis was used to detect inherent differences in glycosylation patterns. The data matrix was composed of 12 variables and 93 incidents (repeated experiments on 14 different EPO preparations). The variables chosen were EPO isoforms with differences in the glycosylation, acetylation or the number of sialic acids. The high abundance isoform $Hex_{22}HexNAc_{19}Fuc_3SA_{12}$ within each analysis was used for relative peak area calculation. For data processing the data set has been mean centered and normalized prior to PCA. The PCA was done using "The Unscrambler® 7.51" (CAMO Software, Oslo, Norway), resulting in an explained variance of 43% for PC1, 23% for PC2 and 15% for PC3. The results are shown in the score plots in Figs. 2 and 3.

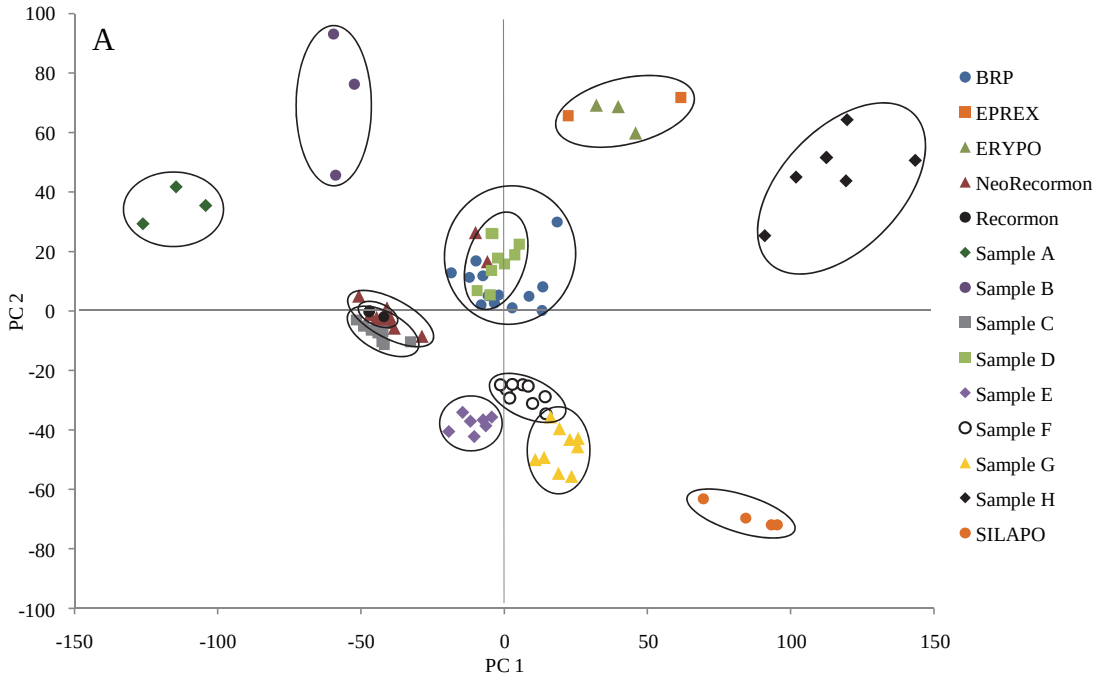

Fig. 2 Score plot (a) for principal component 1 (PC 1) and principal component 2 (PC 2) of the principal component analysis (PCA) on the different EPO preparations.

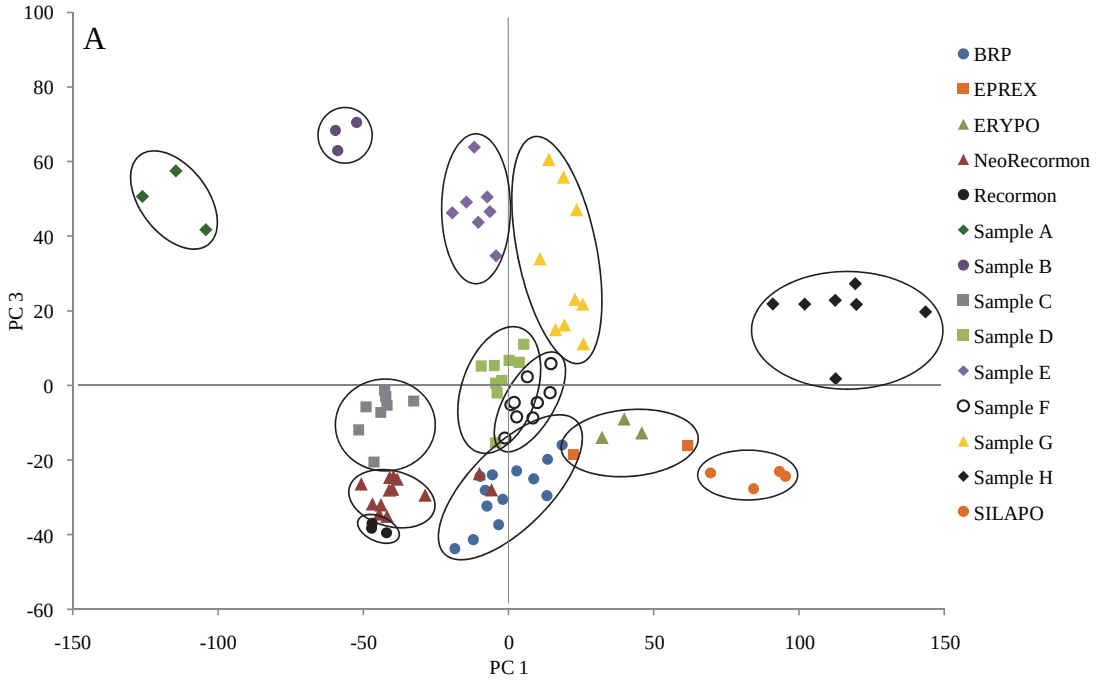

Fig. 3 Score plot (a) for principal component 1 (PC 1) and principal component 3 (PC 3) of the PCA on the different EPO preparations.

The figures show, that most EPO formulations form narrow clusters that are separated from each other. Despite the good separation of the single clusters, few conglomerations can be observed. For example NeoRecormon® is not separated from Recormon®, as these two EPO preparations are known to be the same products with different brand names. Another conglomeration can be observed for BRP and sample D, with BRP showing a higher overall distribution.

These observations demonstrate the restrictions of a PCA considering only two PCs, which, in this case, clarify only about 66 % of the total variance of the multivariate data set. Through incorporation of the PC3 component clusters like BRP can be resolved. In summary, all EPO preparations considered (except EPREX® and ERYPO®) could be distinguished using three PCs, which explained about 80 % of the total variance of the data set.

3 CONCLUSION

The combination of selective analytical techniques and statistical methods is inevitable for the comprehensive and detailed comparison of highly complex biopharmaceuticals due to the high number of isoforms inherent in each EPO preparation. Therefore, PCA was applied to distinguish these preparations on the basis of the relative peak areas of selected EPO isoforms determined by CE-TOF MS. All preparations considered were distinguished using three PCs explaining about 80 % of the total variance of the multivariate data set. A similar clustering was found by hierarchical classification in CA [3].

This strategy is highly suitable for the monitoring of the structural similarity and dissimilarity; hence, this strategy may be applied in quality control, for the detection of counterfeit drugs, for the optimization of the production, and also for the evaluation of biosimilars compared to an innovator biopharmaceutical.

ACKNOWLEDGEMENTS

The authors acknowledge financial support in the course of the announcement "Sicherung der Warenketten" of the Federal Ministry of Education and Research (BMBF) within the scope of the program "Forschung für die zivile Sicherheit" of the Federal Government.

LITERATURE

[1.] Taichrib A, Pelzing M, Pellegrino C, Rossi M, Neusüß C, *J Prot,* 2011, *74*, 958-966
[2.] Taichrib A, Pioch M, Neusüß C, *Electrophoresis* 2012*, 33,* 1356–1366
[3.] Taichrib A, Pioch M, Neusüß C, *Anal Bioanal Chem* , 2012, *403*, 797–805

P17 ANALYSIS OF SPECIFIC METABOLITES FORMED IN RED YEAST CELLS CULTIVATED ON PRETREATED WHEAT STRAW MATERIALS

Siniša Petrik[a], Andrea Hároniková[a], Zsófia Kádár[b], Ivana Márová[a]

[a] *Materials Research Centre, Faculty of Chemistry, Brno University of Technology, Purkynova 118, 612 00 Brno, Czech Republic, xcpetriks@fch.vutbr.cz*
[b] *Department of Chemical and Biochemical Engineering, Center for BioProcess Engineering, Technical University of Denmark, 2800 Kgs. Lyngby, Denmark*

ABSTRACT

Many yeast strains can utilize lignocellulose waste substrates and produce valuable metabolites. In this work hydrothermally pretreated wheat straw was used for production of carotene-enriched biomass by red yeasts *Rhodotorula glutinis, Cystofilobasidium capitatum* and *Sporobolomyces roseus*. To evaluate the convertibility of pretreated wheat straw into ethanol, simultaneous sacharification and fermentation of *S.cerevisiae* was performed under semianaerobic conditions. Analysis of wheat straw fractions was done by HPLC/RI. Analysis and identification of red yeast metabolites was performed by RP-HPLC/PDA/MS (Thermo Finnigan, USA). Samples were filtered through PTFE filters, centrifuged and injected onto Kinetex C18 column (Phenomenex, USA), 2.6 µm, 150 x 4.6 mm with guard column 30 x 4.6 mm. Red yeast strain *S.roseus* produced about 2 mg/g of ergosterol on the filter cake, up to 4 mg/g of ergosterol and 1.5 mg/g of beta-carotene on pretreated wheat straw hydrolysates and also the highest amount of carotenoids and ergosterol on untreated wheat straw. Unusual compounds were found in red yeasts *R. glutinis* and *S. roseus* cultivating on all filter cake samples except on untreated wheat straw sample.

Keywords: carotenoids, ergosterol, wheat straw

1 INTRODUCTION

Lignocellulose waste materials obtained from energy crops, wood and agricultural residues, and from food and feed industry represent the most abundant global source of renewable biomass [1.] Wheat straw, as ubiquitous agricultural waste product all over the World [2.], is one of the most crucial sources for bioethanol production. From a biorefinery perspective, this agricultural waste can also serve as source for production of added value products in an integrated way.

Pretreatment is a requisite step before (bio)processing any lignocellulosics for further purposes in order to increase the digestibility of lignocelluloses structure, by increasing the bioavailability of the carbohydrates (cellulose and hemicellulose) for subsequent bioprocesses [3.] Hydrothermal pretreatment is the first step in the process of converting biomass (i.e. wheat straw) to second generation bioethanol. After hydrothermal pretreatment, enzymes are added to the fibre mass consisting mainly of cellulose and lignin to convert cellulose content to lower carbohydrates to be able to ferment to ethanol in the next step. The liquid fraction of biomass from pretreatment, which contains carbohydrates in polymeric and monomeric forms originating from the breakdown of hemicelluloses at present used as feed, which is considered the most optimal solution. However due to the rich carbohydrate composition, this waste stream has the potential to be used also as a nutrition stress for cultivating red yeast strains, resulting in production of different group of metabolites.

Carotenoids are naturally occurring lipid-soluble pigments, the majority being C_{40} terpenoids. They act as membrane-protective antioxidants that efficiently scavenge $^1O_2$ and peroxyl radicals; their antioxidative efficiency is apparently related to their structure. The most significant part in the molecule is the conjugated double bond system that determines their color and biological action [4.] Other investigated metabolite, ergosterol is one of the most important components in fungal membranes. It is involved in numerous biological functions, such as membrane fluidity regulation, activity and distribution of integral proteins and control of the cellular cycle [5.].

However, the application of chemical synthetic methods to prepare carotenoid/ergosterol compounds as food additives has been strictly regulated in recent years. Therefore, attention is paid to the finding of suitable natural methods for its production. One possibility lies in biotechnological techniques employing the potential of microorganisms that are able to convert various substrates into carotenoid pigments and ergosterol, even if this approach is restricted by a number of useful species and also the carotenoid yield cannot compete with chemical synthesis [6.].

Carotenogenic yeasts are a diverse group of unrelated organisms (mostly *Basidiomycota*), that can be found in soil, fresh and marine water, on plants [7.] Due to ubiquitous and its world-wide distribution in terrestrial, freshwater and marine habitats, they have ability to colonize a large variety of substrates and to assimilate various carbon sources, such as glucose, xylose, cellobiose, sucrose, glycerol, sorbitol, etc. [8.] However, residues from second generation bioethanol production were never involved in such studies. The aim of our research was to investigate hydrothermally pretreated wheat straw as a possible alternative to produce other value added products beside ethanol.

2 MATERIALS AND METHODS

2.1 Strains and cultivation conditions

In this work following carotenogenic yeasts were enrolled into a comparative screening study: *Rhodotorula glutinis* - CCY 20-2-26, *Cystofilobasidium capitatum* - CCY 10-1-1 and *Sporobolomyces roseus* - CCY 19-6-4. All of them were obtained from the Culture Collection of Yeasts (CCY; Institute of Chemistry, Slovak Academy of Sciences, Bratislava, Slovakia). Each red yeast strain was cultivated at the same and optimal growth conditions: aerobically at 28°C, with permanent lighting and shaking the flasks (n= 120 rpm) in two steps. From the agar plate, strains were firstly inoculated into 50 ml of inoculum medium I (INO I, containing (gl^{-1}): glucose, 40 g; $(NH_4)_2SO_4$, 5 g; KH_2PO_4,5 g; $MgSO_4$, 0.34 g; yeast extract,7 g) and cultivated for 24 hours. 25 ml of INO I was then transferred into 125 ml inoculum medium II (INO II, composition was the same as INO I) and cultivated for 24 hours again. 50 ml of INO II was used as a starter culture to inoculate 250 ml of medium for the experiments (production medium). The production medium was composed of (gl^{-1}): glucose, 30 g; $(NH_4)_2SO_4$, 4 g;

KH_2PO_4, 4 g; $MgSO_4$, 0.34. Yeasts cultivations on all types of mediums were performed for 96h, aerobically at 28°C with constant lighting and shaking the Erlemeyer flasks (120rpm).

Fermentation experiments on pretreated wheat straw hydrolysate were performed in two series (A and B). In series A, culture was firstly grown on glucose containing medium with concentration of 40 g/l (INO I and INO II), and the fermentation was carried out on the same medium as inoculum, only glucose was substituted with hydrolysate, 30 g/l. In series B, yeasts were firstly grown on basic glucose medium (INO I), but at the second stage (INO II), hydrolysate was introduced to the medium as a carbon source alongside with glucose at the same weight ratio (50:50). The fermentation was performed on medium containing only hydrolysate (30 g/l), similarly to series A. Control experiments were performed on mediums contained only glucose as a carbon source, 30 g/l.

Carotenogenic (red) yeasts were also cultivated on filter cake (the solid fraction of the pretreated material). Pretreated wheat straw material as a complex carbon source was firstly added in the INO II (20 g/l) together with glucose with the same concentration. Fermentation medium was prepared with only added filter cake instead of glucose; 30 g/l.

The morphological changes of yeasts cells were documented with photomicrographs, using Nikon Microphot-SA microscope (Nikon, Japan) equipped with a UFX-DX metering system.

2.2 Extraction and analysis of yeast metabolites

After cultivation, the culture broths (100 ml) were centrifuged twice (5000 rpm; 10 min) and biomass was collected. Dissintegration of red yeast biomass was made by using a mechanical-chemical disruption method with pestle and mortar and simultaneously addition of 50 ml acetone together with sea sand. The mixture of pigments and other metabolites was liberated from the cell homogenate. After saponification (90°C, 30 min) with 10% ethanolic solution of KOH, carotenoids and other present metabolites were extracted thrice with diethyl ether. Ether extracts were then collected, pre-concentrated and dried under vacuum using rotary evaporator. Later on, the residue was cautiously dissolved in 1 ml of absolute ethanol (UV/VIS grade) and used further for HPLC analysis.

Beta-carotene, as well as ergosterol, extracted from yeast cells were individually identified and quantified by RP-HPLC using PDA detector (Photo Diode Array detector, Surveyor Plus, Thermo Finnigan, USA). Samples were frist filtered through PTFE filters (0.45 mm), then centrifuged and injected directly onto Kinetex C18 column (Phenomenex, USA), 2.6 µm, 150 x 4.6 mm with guard column 30 x 4.6 mm. The used mobile phase was 100% methanol. Isocratic elution was carried out at 45 °C by mobile phase flow rate of 1.0 ml/min. Spectrophotometric detection of carotenoids was achieved at 450 nm, while detection of ergosterol were done at 285 nm. Total carotenoids were calculated and determined approximately as a sum of peaks area of other known carotenoids (torulene, lycopene, torularhodin, phytoene), scanned with PDA detector and evaluated using calibration curve for β-carotene [9.] Data processing of analyses was assessed using Xcalibur 1.3 software (Thermo Finnigan, USA). Beta-carotene as well as ergosterol were quantified using external standards.

3 RESULTS AND DISCUSSION

3.1 Production of yeast metabolites

Biomass production of all three used red yeasts was generally negatively affected during growth in medium containing hydrolysate (Table 1). In control medium the highest biomass production was found in *Cystofilobasidium capitatum* (CC - 16.3 g/l), which decreased by 80 % in medium with hydrolysates. Biomass production was decreased by similar range in all tested strains. However, interestingly, including of adaptation step in series

B led in all samples (1-3) to even lower biomass production when the yeasts were not adapted (series A).

Pigments production was also observed and evaluated in the form of β-carotene and total carotenoids (including β-carotene, torulene, torularhodin, lycopene and phytoene). Growing on all hydrolysates, carotenoids production was significantly decreased using *R. glutinis (RG)* and *C. capitatum (CC)* strains (Table 1). In contrary, wheat straw hydrolysates have shown to be a very good carbon source for carotenoids production in *S. roseus (SR),* especially using hydrolysates obtained at 190°C, where ß-carotene production increased almost three times, while total carotenoids production almost two times without adaptation to the hydrolysate. The maximum concentration was observed in the series A, with production of 1.56 mg/g of biomass of *S.roseus*. Furthermore, good conditions of wheat straw pretreatment on 195°C gives hydrolysates of high quality that, beside very good production of other metabolites, are able to gave satisfactory β-carotene amount. When *S.roseus* were cultivated in medium with no previous adaption to hydrolysates, it was found the concentration of β-carotene 1.22 mg/g of dry biomass. Utilizing hydrolysate, obtained in pretreatment at 200°C, the produced ß-carotene concentration (0.43mg/g) stayed below the value of the control. However the adaptation of the yeast could still further increase to 0.68 mg/g.

Table 1. Biomass and metabolites production using pretreated wheat straw hydrolysates (obtained on 190°C, 195°C and 200°C) for cultivation different carotenogenic yeasts

control	Biomass (g/l)	Ergosterol (mg/g biomass)	β-carotene (µg/g biomass)	Total carotenoids (µg/g biomass)
RG	13.26	0.22	208.48	455.35
CC	16.34	0.14	334.23	531.94
SR	8.26	0.22	531.07	786.34
Sample 1				
RG series A	4.26	0.38	10.71	15.16
RG series B	2.95	0.58	24.65	29.61
CC series A	3.52	0.70	15.16	48.13
CC series B	1.80	1.40	2.04	15.70
SR series A	1.67	1.75	1556.33	1737.34
SR series B	1.17	1.41	194.44	239.72
Sample 2				
RG series A	10.09	0.20	4.44	9.76
RG series B	4.66	0.37	13.73	17.12
CC series A	3.18	0.60	2.84	6.62
CC series B	0.70	3.40	17.51	144.36
SR series A	2.06	1.58	756.23	853.95
SR series B	0.84	4.17	1216.25	1534.73
Sample 3				
RG series A	4.16	0.44	8.58	37.45
RG series B	2.80	0.52	7.81	22.67
CC series A	3.21	0.65	16.63	25.16
CC series B	1.85	0.80	9.92	20.19
SR series A	1.81	1.15	427.95	460.56
SR series B	0.98	1.87	680.06	781.06

3.2 Identification of yeast metabolites

The aim of the study was to investigate the possibility of using hydrothermally pretreated wheat straw as a carbon source for conversion into carotene enriched biomass by red yeast strains. Our study on pigments and sterol production involved not the only the liquid fraction after pretreatment, which is used as a feed now, but also the solid fraction which is used for ethanol production, by applying three different strains (*R. glutinis*, *C. capitatum*, *S. roseus*).

The efficiency of hydrothermal pretreatment was proved by ethanol fermentation studies. The obtained results on ethanol fermentation were similar to obtained by other authors.

β-carotene and total carotenoids production on the solid fraction remained lower compare to control experiments in all cases, although *S. roseus* was still able to produce around 400 µg/g d.m. of ß-carotene growing on filter cakes pretreated without acetic acid. In addition to previously mentioned metabolites, carotenogenic yeasts cultivated on filter cake gave also some unknown compound (assumed to be carotenoids), with characteristic maximum absorption spectra of 296 nm and 306 nm. From chromatograms, it was observed two peaks with that absorption maximum. Those compounds were found in both red yeasts biomass (*S. roseus* and *R. glutinis*) cultivating on all filter cake samples. Only in control medium and sample 7 (wheat straw without hydrothermal pretreatment) was not occurred that specific peak. For cultivating carotenogenic yeasts, using instead of glucose only milled wheat straw, it was obtained characteristic spectra at wavelength 283 nm which correspondent to phytoene. This peak (with absorption maximum of 306 nm) was not also identified in red yeasts biomass when the liquid fraction (hydrolysate) was used as a substrate. It might indicate that the unknown compounds could be degradation products originating from the pretreatment, which should be examined in future studies.

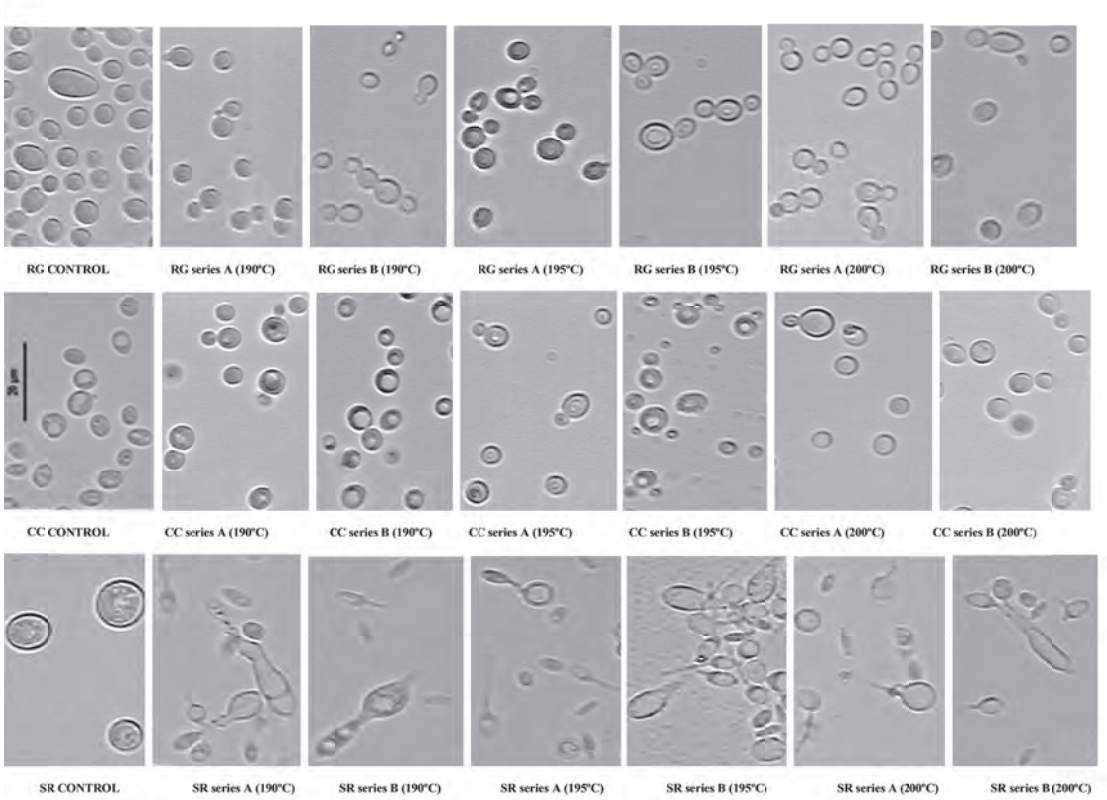

Fig. 1: Microscopic images of carotenogenic yeasts cultivated on wheat straw hydrolysates.

Most carotenoids absorb maximally at three wavelengths, resulting in characteristic three-peak spectra. The greater the number of conjugated double bonds, the higher the λmax values. The two carotenoids that precede ζ-carotene in the desaturation biosynthetic pathway, phytoene (3 conjugated double bonds) and phytofluene (5 conjugated double bonds), are colorless and absorb maximally at 276, 286, and 297 nm and at 331, 348, and 367 nm, respectively, using as a solvent hexane or petroleum ether [10.]. From that point of view and keeping the mind similarity of three-peak spectra, it is exist the possibility that unknown compound (with maximally absorption of 306 nm) could be carotenoid with structure very close to phytoene or some isomer with extra double bond inside the molecule.

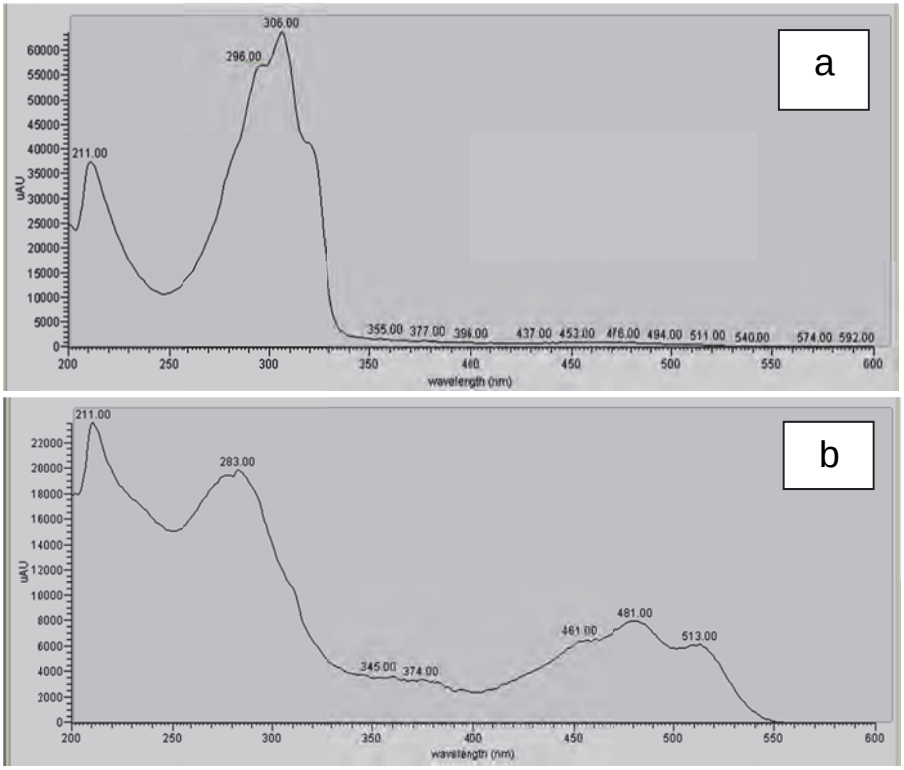

Fig. 2*:* Maximum absorption spectra of unidentified compound (RG, series B, sample 6) - a, and (RG, series B, sample 7) - b

Somehow it can be concluded that complex substrate, such as filter cake, could have some inhibitors with strong influence on enzymatic system in isoprenoid metabolic pathway. Those inhibitors could easily stop the process of isomerisation and further desaturation, accumulating carotenoids with small number of isoprenoid units, such as that with maximum absorption of 306 nm. Respecting that fact, further process of forming colored carotenoids with larger number of conjugate double bond, especially β-carotene, will give small or neglectable amount. Eluting always before, this compound is more polar than β-carotene, using the same reversed mode of separation on the column. Finally, previous statements could give the answer and reason of very low concentration of β-carotene and other “higher carotenoids” using filter cake as a carbon/nitrogen source.

ACKNOWLEDGEMENTS

This work was supported by "Materials Research Centre at FCH BUT" Project No. CZ.1.05/2.1.00/01.0012 from ERDF (European Regional Development Fund), FP7 Framework Programme (PROETHANOL2G, Project no. 251151) and Regional Innovation Strategy 3. of the City of Brno.

LITERATURE

[1.] Lin Y., Tanaka S., *Applied Microbiology and Biotechnology* 2006, *69*, 627-642.
[2.] Kim S, Dale B.E., *Biomass and Bioenergy* 2004, *26*, 361-375.
[3.] Panagiotou G, Olssol L, *Biotechnology and Bioengineering* 2007, *96*, 250-258.
[4.] Sandmann, G., *Archives of Biochemistry and Biophysics* 2011, *385*, 4-12.
[5.] Tan, T., Zhang, M., Gao, H., *Enzyme and Microbial Technology* 2003, *33*, 366-370.
[6.] Libkind, D., van Broock, M.R., *World Journal of Microbiology and Biotechnology* 2006, *22*, 687-692.
[7.] Rosa, C., Peter., G. (Eds.) *Biodiversity and Ecophysiology of Yeasts (The Yeasts Handbook)*, Springer, Berlin, 2005.
[8.] Malisorn, C., Suntornsuk, W., *Bioresource Technology* 2007, *99*, 2281-2287.
[9.] Marova, I, Carnecka, M., Halienova, M., Certik, M., et al., *Journal of Environmental Management* 2012, 95 (S), 338-342.
[10.] Rodriguez-Amaya, D.B., Kimura, M. (Eds.) *Handbook for Carotenoid Analysis,* HarvestPlus, Washington, 2004.

P18 ACHIRAL AND CHIRAL SEPERATIONS OF UNDERIVATIZED AMINOACIDS ON ELECTROPHORETIC CHIP

Katarína Uhlárová, Róbert Bodor, Marián Masár

Comenius University, Faculty of Natural Sciences, Department of Analytical Chemistry, Mlynská Dolina 842 15 Bratislava 4, Slovak Republic
uhlarova@fns.uniba.sk

ABSTRACT

This work deals with achiral and chiral separations of aspartic (Asp) and glutamic acids (Glu) on an electrophoresis chip. In clinical analysis, these amino acids are considered to be the markers of Alzheimer`s and Parkinson`s diseases. Working (suppressed electroosmotic and hydrodynamic flow) and separation conditions for achiral electrolyte system with pH 6.8 were employed. Repeatabilities of migration time for amino acids were evaluated from a series of 6 repeated runs up to 1% RSD while repeatabilities of their corresponding peak areas were less than 5% RSD. Optimized capillary zone electrophoresis (CZE) separation conditions enabled detection of underivatized amino acids at a 200 nmol/l concentration in a 1µl volume of injected sample. In CZE-CZE analysis, cerebrospinal fluid and urine biosamples macroconstituents, such as chloride, sulphate and phosphate, were transferred outside of the separation channel by column switching realized on a column coupling chip. Chiral separations were realized under the same separation conditions using vancomycin as chiral selector.

Keywords: enantiomers, amino acids, chip electrophoresis

1 INTRODUCTION

D, L-enantiomers of amino acids have been found in food and body fluids unbound or bound in proteins [1]. Amino acids are essential in biological processes such as proteosynthesis. The importance of monitoring enantiomeric ratio of these amino acids in biological samples can be demonstrated via example of D-aspartic acid (D-Asp) which has a regulatory function in organ differentiation and in transfer and differentiation of nerve cells in prenatal period [2]. Non-biogenic D-Asp was observed also in human dentine [3, 4], femur [5] and brain tissue [6]. Furthermore, unbound L-glutamic acid (L-Glu) is a neurotransmitter of brain functions

involved in learning and memory related processes. L-Glu together with D-Asp induces acidification of nervous and supportive nervous tissues [7]. In addition these analytes are important in monitoring kidney dysfunction [8], Alzheimer`s and Parkinson`s disease [9, 10] or ageing [3-5].

Since physico-chemical properties of enantiomers are the same there is a demand for such analytical methods offering information about their enantiomeric content. Currently, capillary electrophoresis (CE) along with gas chromatography and high performance liquid chromatography have become a general analytical tool for separation and detection of enantiomers because of small sample volumes, low consumption of solvents, high separation efficiency and short analysis times.

This work deals with the application of electrophoretic principles into miniaturized analytical systems (chips) to achiral separations of Asp and Glu prior to their application to chiral separations. The conductivity detection integrated on electrophoresis chip was used due to the fact that studied amino acids have no chromophore groups.

The optimization of achiral separation conditions for separation of Asp and Glu at the same concentration level as is present in body fluids and the application of the developed CZE method to analysis of real biosamples were performed and followed by chiral separations. A selection of a chiral selector and optimization of chiral separation conditions in order to achieve the best resolution was a crucial issue.

2 MATERIAL AND METHODS

CE separations were performed on a polymethylmetacrylate electrophoresis column coupling (CC) chip (IonChip^{TM} 3.0, Merck, Darmstadt, Germany) with integrated conductivity detection according to the scheme Fig. 1. Separations were realized in anionic mode of separation in hydrodynamically closed system and, at the same time, with electroosmotic flow (EOF) suppressed by adding methyhydroxyethylcellulose (MHEC) to the electrolytes. Model and real samples were injected in diluted carrier electrolyte (10%) for capillary zone electrophoresis (CZE) separations on CC chip in order to eliminate an injection dispersion of 0.9 μl loaded volume. CC chip worked in a single column configuration of the separation channels in CZE separations and in a column switching mode in CZE-CZE separations [11].

Simulated model sample of cerebrospinal fluid (CSF) with high concentrations of potentially interfered anions (chloride, sulphate and phosphate) was prepared. Simulated and real samples were only diluted and filtered through 0.8 μm membrane filter and no other pretreatment or derivatization steps were needed. After collection, urine samples were immediately processed in the laboratory (diluted with deionized water). CSF samples were kindly provided by the 1st Neurology Clinic of Faculty of Medicine, Comenius University in Bratislava.

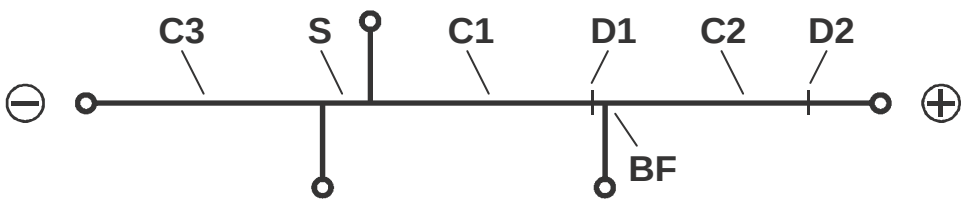

Fig. 1.: Arrangement of the channels on the CC chip. C1, C2 – separation channels, C3 – the third channel, S – sample injection channel, D1, D2 – conductivity sensors in C1 and C2, respectively, BF – bifurcation section.

3 RESULTS AND DISCUSSION

Achiral separation system consisted of N-tris(hydroxymethyl)methyl-2-amino-ethanesulfonate (TES) as carrier ion and organic modifier (methanol) with pH 6.8. Addition of 10% methanol to the TES carrier electrolyte enabled detection of amino acids Asp and Glu in model sample at concentration level close to their limit of quantitation (1µmol/l). Given the 0.9 µl volume of loaded sample, limits of detection (LOD) for Asp and Glu were estimated at 200 nmol/l. Under preferred separation conditions repeatabilities of migration times of studied amino acids were up to 1% RSD, while repeatabilities of their peak areas were less than 5% RSD. Short analysis time, high separation efficiency and linearity of calibration curves in the range 2.5-20 µmol/l were achieved in achiral separation system.

In the context of analysis of simulated and real samples, the presence of macroconstituents at concentration levels from 10^3 to 10^9-times higher than analytes limits their subsequent resolution from these macroconstituents. Using CC technology on the chip, clean-up step of model and real samples prior to separation of amino acids was realized by electrophoretic removal of ionogenic macroconstituents in the first separation channel. Removal of 95% of macroconstituents in model and real sample of CSF by CZE-CZE allowed baseline resolution of Asp and Glu (Fig. 2b). Despite high sample clean-up power of CZE-CZE approach the resolution of Asp and Glu from the matrix of urine was not sufficient. This was probably caused by high content of ionogenic constituents, sulphates and mainly phosphates migrating in the same positions as Asp and Glu (peak overlapping).

Chiral separation system was implemented by adding chiral selector compatible with achiral separation conditions. In order to avoid influencing the resolution power of selector, separations were performed without adding methanol. Chiral selectors, such as native and derivatized cyclodextrins (α-, β-, γ-cyclodextrin, sulphated and hydroxypropyl-β-CD) and macrocyclic antibiotics (vancomycin and teicoplanin) were studied in this respect.

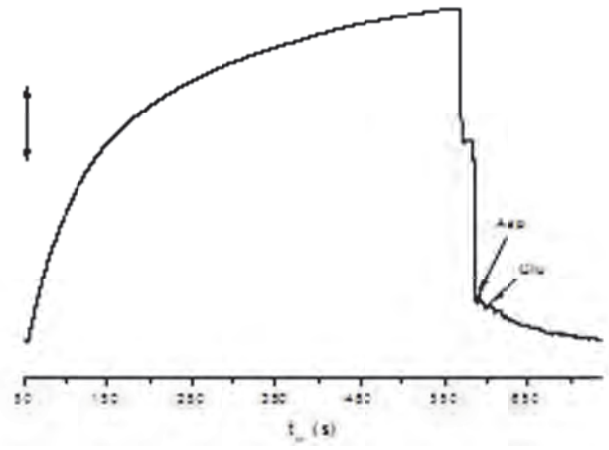

Fig. 2a.: CZE analysis of simulated sample of CSF, an electropherogram from the first detector Sample: 20 µmol/l L-Asp and L-Glu, 347 µmol/l phosphate, 62.5 x 10^3 µmol/l chloride, 2.5 µmol/l fluoride, 14.5 µmol/l bromide, 8.10^{-3} µmol/l iodide; current 20 µA, pH 6.8.

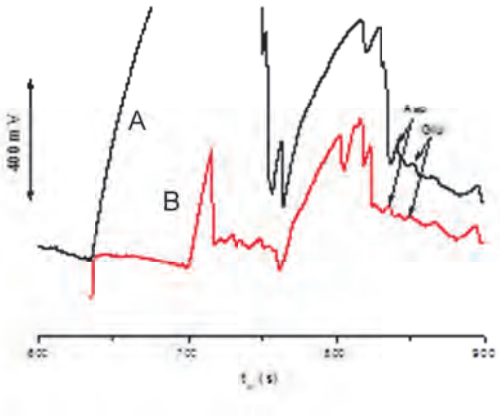

Fig. 2b.: CZE-CZE analysis of simulated sample of CSF, an electropherogram from the second detector. Sample: 20 µmol/l L-Asp and L-Glu, 347 µmol/l, 62.5 x 10^3 µmol/l chloride, 2.5 µmol/l fluoride, 14.5 µmol/l bromide, 8.10^{-3} µmol/l iodide; current 20 µA, pH 6.8; **A)** removal of approx. 95% of matrix constituents; **B)** removal of approx. 99% of matrix constituents.

Native cyclodextrins were appeared as totally inefficient. Sulphated β-CD was able to resolve only D, L-Asp enantiomers. However, high concentration of sulphates in carrier electrolyte caused significant increase of its conductivity and subsequently, led to negative influence on the sensitivity of separation system. Within the group of macrocyclic antibiotics we examined the influence of vancomycin and teicoplanin on enantiomeric resolution of D, L-Asp and D, L-Glu. Bednár et al. [12] used teicoplanin as chiral selector for resolution of studied amino acids. However, under the working and separation conditions employed in this work, teicoplanin added to the carrier electrolyte did not allow resolution of D, L-Asp and D,L-Glu. We found that 5 mmol/l vancomycin present the TES carrier electrolyte at pH 6.8 was effective for enantiomeric resolution of the studied amino acids. The optimized carrier electrolyte was two-times diluted in order to decrease its conductivity while the same concentration of chiral selector was maintained. According to Fig. 3 vancomycin allowed baseline resolution of enantiomers D, L-Glu and partial resolution of D,L-Asp enantiomers.

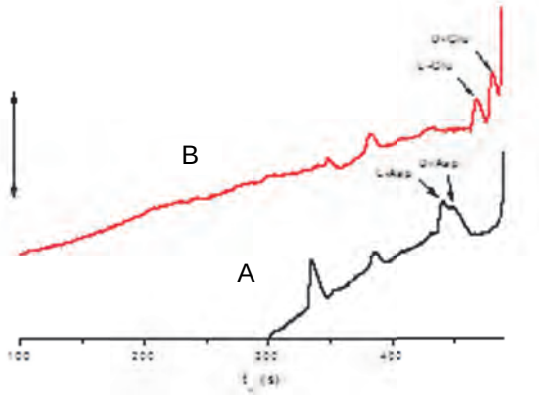

Fig. 3.CZE enantiomeric separation of D,L -Asp a D,L-Glu with addition of 5 mmol/l vancomycin to the TES carrier electrolyte with pH 6.8; an electropherogram from the second detector, current 30 µA, pH 6.8; **A)** 8 µmol/lL-,D-Asp, **B)** 4 µmol/l L-,D-Glu.

4 CONCLUSION

This work dealt with application possibilities of CE on CC chip and integrated conductivity detection in achiral and chiral separations of Asp and Glu in body fluids. CZE separations were performed in a hydrodynamically closed system with suppressed EOF at pH 6.8 in the presence of 10% methanol (organic modifier). Optimized separation conditions enabled to detect studied amino acids on 200 nmol/l concentration levels. CZE-CZE separations of Asp and Glu were performed in CSF and urine samples after electrophoretic removal of ionogenic macroconstituents (chloride, sulphate and phosphate) present in complex matrices on high

concentration levels. D, L-enantiomers of Glu and partially also Asp were resolved in chiral separation media implemented by vancomycin.

ACKNOWLEDGEMENTS

This work was generously supported by the grant awarded by Slovak Research and Development Agency(project APVV-0583-11), the Slovak Grant Agency for Science (VEGA 1/1149/12), Comenius University in Bratislava (UK/119/2012) and the Research & Development Operational Programme funded by the ERDF (CE Green II, 26240120025). This work is partially outcome of the project VVCE-0070-07 of the Slovak Research and Development Agency solved in the period 2008-2011.

LITERATURE

[1.] Tivesten A., Lundqvist A., Folestad S., *Chromatographia* 1997, *44*, 623-633
[2.] Hashimoto A., Kumashiro S., Nishikawa T., Oka T.,et al, *Journal of Neurochemistry*1993, *61*, 348-351
[3.] Helfman P.M., Bada J.L., Shou M.Y., *Gerontology* 1977,*23*, 419-425
[4.] Helfman P.M., Bada J.L., *Nature*1976,*262*, 279-281
[5.] Ohtani S., Matsushima Y., Kobayashi Y., Kishi K., *Journal Of Forensic Sciences* 1998, *43*, 949-953
[6.] Man E.H., Sandhouse M.E., Burg J., Fisher G.H., *Science*1983,*220*, 1407-1408
[7.] Hashimoto A., Oka T., *Progress in. Neurobiology* 1997, *52*, 325353
[8.] Bruckner H., Hausch M., *Journal of Chromatography-Biomedical Applications*1993, *614*, 7-17
[9.] Pines G., Danbolt N.C., Bjoras M., Zhang Y.M., et al., *Nature* 1992, *360*, 464-467
[10.] Kanai Y., Hediger M.A., *Nature* 1992, *360*, 467471
[11.] Kaniansky D., Masár M.,Bodor R., Žúborová M., et al., Electrophoresis 2003, 24, 2208-2227
[12.] Bednar P., Aturky Z., Stransky Z., Fanali S., Electrophoresis 2001, 22, 2129-2135

P19 ANALYSIS OF GFP AND AHP5-GFP FUSION PROTEIN IN THE PLANT EXTRACT USING CE-LIF

Lenka Michalcová[a,b], Radka Dopitová[c], Jan Hejátko[c], Martina Válková[c], Jan Preisler[a,c]

[a] *Department of Chemistry, Faculty of Science and CEITEC, Masaryk University*
[b] *Department of Biochemistry, Faculty of Science and CEITEC, Masaryk University*
[c] *Research group Functional Genomics and Proteomics of Plants, Mendel Centre for Plant Genomics and Proteomics, CEITEC, Masaryk University*

ABSTRACT

We focused on the possibility of determination green fluorescent protein (GFP) and *Arabidopsis* histidine phophotransfer protein 5 fused with GFP (AHP5-GFP) in complex plant samples using capillary electrophoresis with laser-induced fluorescence detection (CE-LIF). The control method is western blotting, where the anti-GFP antibodies enable monitoring the expression level of AHP5-GFP in individual organisms. It was found that CE-LIF is sensitive enough for both proteins. In the future, the developed methods should be used to analyze the phosphorylated and unphosphorylated AHP5-GFP.

Keywords: CE-LIF, GFP

1 INTRODUCTION

The protein AHP5 (*Arabidopsis* histidine phophotransfer protein 5) is a phosphotransmitter of cytokinin signaling pathway in plants. This protein acts as a phosphate transporter between

cytoplasmic membrane and cell nucleus. Protein phosphorylation is located on histidine, which is instable in the acidic environment. Therefore, the sample preparation and separation has to be carried out under conditions in which fosfohistidine is stable.[1]

2 MATERIAL AND METHODS

The suspension culture grown in the dark in MSMO (Murashige and Skoog, modified) medium with 30 g saccharose, kinetin and NAA (1-naphthaleneacetic acid). The cultures were grown in dark at 25°C on a shaker (Multitron II; HT Infors, Switzerland) at 200 rev/min. We harvested two-day of culture, the cells are stored at -80 °C. Suspension culture were homogenized in buffer (50 mM Tris.HCl pH 7.5, 150 mM NaCl, 10 % glycerol, 1 mM DTT, 1 mM EDTA and protease inhibitors). The protein extract was centrifuged twice (12.000 g, 10 min). The supernatant contained the soluble fraction of plant proteins.
Purification with GFP-Trap®_A (ChromoTek, Germany) was performed by commercial protocol.[2] Purification with gel filtration was made on colon Superdex 200 HR 10/30, sample 400 µL, elution was carried by 100 mM Tris pH 8 and was taken fraction of 1.5 mL.
Separations of GFP and GFP tagged proteins were performed on the CE-LIF designed at the Department of Chemistry, MU, Brno. A laser diode (405 nm) was used as the excitacion source. AHP5-GFP fusion protein was expressed in *Arabidopsis thaliana.*

3 RESULT

The limit of detection of GFP was determined 0.01 µg.mL^{-1} (3.7 x 10^{-10} M) using CE-LIF (Fig. 1). The table 1 shows comparison of published *LOD* for GFP. Using western blot (Fig. 2), the lowest detectable GFP concentration was 1.0 µg.mL^{-1}. Hence, CE-LIF is able of detecting about 2 orders lower GFP concentration compared to western blot.

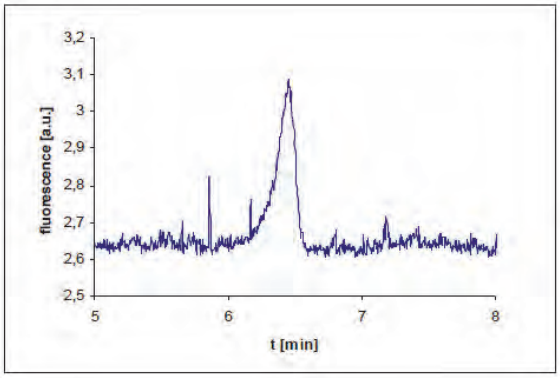

Figure 1: CZE of GFP, c = 0.1 µg.mL^{-1}, BGE 50 mM Tris.HCl buffer with 50 mM NaCl, pH 9, +8 kV, injection at 300 Pa for 5s.

Tab.1: Comparison of published *LOD* for GFP.

LOD [ng.mL^{-1}]	*LOD* [M]	V [nL]	Ref.
90	3.4x10^{-9}	1.9	[3]
0.081	3.0x10^{-12}	17	[4]
-	1.25x10^{-10}	3	[5]
10	3.7x10^{-10}	0.6	this work

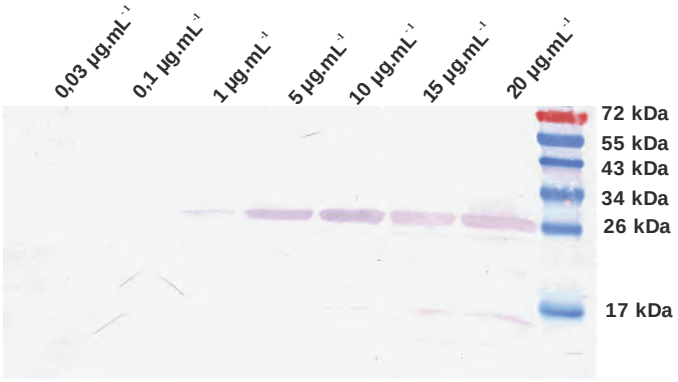

Figure 2: Western blotting of GFP at various concentrations.

The plant extract was purified by two different methods, gel filtration and immunoprecipitation. Typical results are shown in Figs. 3, 4. The concentration of proteins after gel filtration was determined by Bradford method. This method was not used for determination of concentration after immunoprecipitation - due to small volume of sample (~ 50 µL). Therefore the concentration was determined by addition of the GFP standard (Fig. 5). The concentration of protein was estimated as several tenth µg.mL^{-1}.

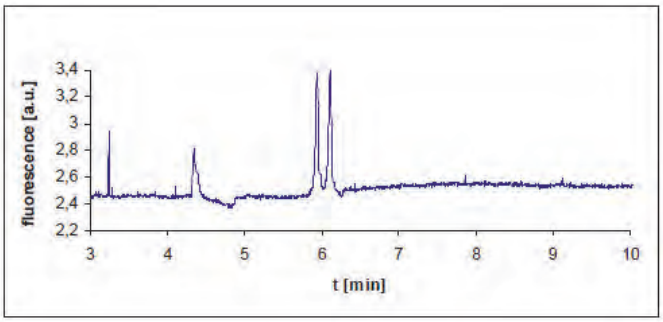

Figure 3: CZE of purified extract after GFP-Trap®_A procedure, BGE 50 mM Tris.HCl buffer with 50 mM NaCl, pH 9, +8 kV, injection at 300 Pa for 5 s.

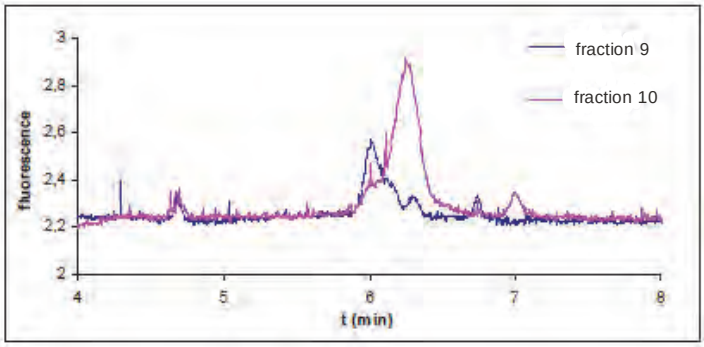

Figure 4: CZE of purified extract after gel filtration procedure, BGE 50 mM Tris.HCl buffer with 50 mM NaCl, pH 9, +8 kV, injection at 300 Pa for 5 s, the concentration of all proteins 5.14 mg.mL^{-1} (fraction 9) and 1.33 mg.mL^{-1} (fraction 10).

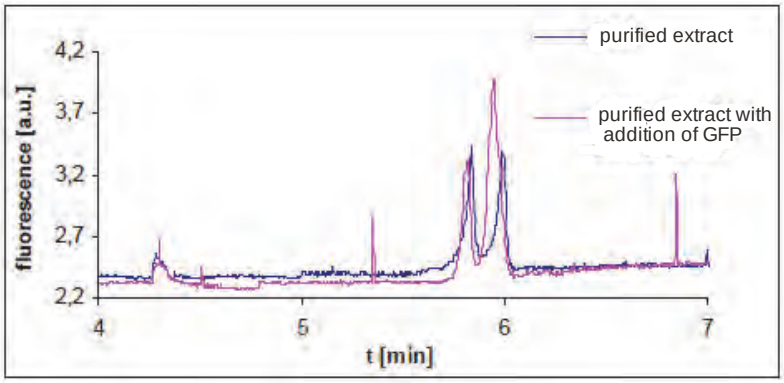

Figure 5: CZE of purified extract after GFP-Trap®_A procedure with addition of standard GFP, BGE 50 mM Tris.HCl buffer with 50 mM NaCl, pH 9, +8 kV, inj. 5 s, 300 Pa.

4 CONCLUSION

In conclusion, CE-LIF proved its sensitivity is sufficient for AHP5-GFP analysis. However, the gel filtration provided very complex sample that cannot be effectively separated by CE-LIF and thus used for the AHP5-GFP determination. In future, using pure AHP5-GFP without the presence of free GFP would be useful to confirm migration properties of AHP5-GFP. A suitable sample purification method, which would maintain the phosphorylated histidine, has to be developed. Separation of phosphorylated and unphosphorylated AHP5-GFP requires suitable and selective purification.

ACKNOWLEDGEMENTS

This work was supported by The Czech Science Foundation (grant no. 203/09/1025 and P206/12/0538), The Ministry of Education, Youth and Sports (MSM0021622415) and the project "CEITEC - Central European Institute of Technology" (CZ.1.05/1.1.00/02.0068) from European Regional Development Fund.

LITERATURE

[1.] To, J. P.; Kieber, J. J., *Trends Plant Sci* 2008, *13* (2), 85-92.
[2.] http://www.chromotek.com/downloads/GFP-Trap_A%20manual.pdf.
[3.] Korf, G. M.; Landers, J. P.; Okane, D. J., *Analytical Biochemistry* 1997, *251* (2), 210-218.
[4.] Craig, D. B.; Wong, J. C. Y.; Dovichi, N. J., *Biomedical Chromatography* 1997, *11* (4), 205-206.
[5.] Zhang, H. F.; Ma, L.; Liu, X.; Lu, Y. T., *Journal of Chromatography B-Analytical Technologies in the Biomedical and Life Sciences* 2004, *804* (2), 413-420.

P20 DGGE ANALYSIS OF ARTIFICIAL *CLOSTRIDIUM* CONSORTIA

Barbora Gregušová, Alena Španová, Bohuslav Rittich

Institute of Food Science and Biotechnology, Faculty of Chemistry, Brno University of Technology, Purkyňova 118, 61200 Brno, Czech Republic
xcgregusovab@fch.vutbr.cz

ABSTRACT

Bacteria of the genus *Clostridium* have biotechnological potential as hydrogen producers, especially when grown in a consortium. In consortia, it is important to examine the species composition. For this purpose, molecular biological methods are used mostly. A very useful tool seems to be PCR-DGGE.
In our work, PCR-DGGE was used to distinguish the co-existing species of *Clostridium* (*C. tyrobutyricum*, *C.butyricum*), both in DNA mixtures of pure cultures and in artificial consortia. We established that it is possible to distinguish the species, if the ratio of DNA in the mixture is 25% or more. When the cells of both species were cultivated in a consortium, *C. tyrobutyricum* dominated in all cases.

Keywords: *Clostridium*, consortia, PCR-DGGE

1 INTRODUCTION

Non-pathogenic *Clostridium* bacteria had been identified as the main species in production of bio-hydrogen by dark fermentation [1]. As hydrogen belongs to the most promising alternatives to fossil fuels [2], its biotechnological production is currently an objective of many studies.
It was reported that microbial consortia produce usually more hydrogen than pure cultures. Moreover, they are able to utilize a broader source of feedstock and to support a wide variety of metabolite activities [3].
It is important to know the bacterial species composition of hydrogen-producing consortia, in order to obtain steady operation. Traditional methods, such as cultivations or biochemical tests, are often not sufficient for identification of environmentally important microorganisms. Because of this, molecular methods based on categorization of bacterial rRNA genes have become popular [4].
PCR-DGGE (polymerase chain reaction-denaturing gradient gel electrophoresis) can be used to study the structure, diversity and evolution of microbial communities from different environments, as well as for identification and typing of microbial entities [5]. It is based on the separation of PCR amplicons of the same size but different sequences.
In this study, DNA mixtures of *Clostridium butyricum* E16A and *Clostridium tyrobutyricum* S5 were prepared in different ratios and analyzed by PCR-DGGE, in order to simulate the clostridial consortia. Furthermore, PCR-DGGE was used for species identification of artificially prepared cell consortia of *C. butyricum* DSM 10702 and *C. tyrobutyricum* DSM 2637^T.

2 AIM OF WORK

The purpose of the current study was to test PCR-DGGE as a tool for species differentiation of *Clostridium* species *C. butyricum* and *C. tyrobutyricum* in microbial consortia.

3 MATERIALS AND METHODS

Clostridium strains used in this study (*C. butyricum* E16A and *C. tyrobutyricum* S5) were isolated from milk and cheese with late-blowing disorders (MILCOM- Dairy Research Institute,Ltd., Tábor, Czech Republic). Control strains (*C. butyricum* DSM 10702, *C.*

tyrobutyricum DSM 2637^T) were obtained from Deutche Sammlung von Mikroorganismen (DSM, Germany). Strains were cultivated anaerobically in Reinforced Clostridium Medium broth (Oxoid 0149, Oxoid – Thermo Fisher Scientific, Hampshire, UK) at 37 °C for 2 days.

To prepare artificial consortia, the cultures of the collection strains (A_{600nm} = 1) were mixed in different ratios (14:1, 2:1, 1:1, 1:2, 1:14) and cultivated together. The consortia were simulated by mixing DNA of the strains in following ratios of *C. tyrobutyricum* S5 to *C. butyricum* E16A – 99:1, 9:1, 3:1, 2:1, 1:1 and vice versa.

Bacterial cultures were centrifuged and sedimented cells were used for DNA isolation by phenol-chloroform method [6]. DNA was amplified by PCR (polymerase chain reaction) using primers Chis150f, ClostIr [4], forward primer containing the GC-clamp. These primers were designed to be genus-specific for *Clostridium*; the length of synthetized PCR products was 540 bp. The composition of PCR mixture was optimized to the final volume 50 µl containing 5 nmol of dNTP, 5 pmol of each primer, 1 U Taq polymerase and 10 ng of DNA matrix.

Amplification program had 30 cycles; each of them consisted of 3 steps: denaturation of DNA at 95 °C for 30 s, primer hybridization at 57 °C for 30 s, synthesis of new DNA strands at 72 °C for 45 s. The initial denaturation was prolonged to 3 min and final extension to 20 min. The PCR products were detected by agarose gel electrophoresis (1.5%) at 80 V for 90 min.

DGGE was performed in INGENYphorU system (Goes, Netherlands) in 6% acrylamide gel with 30-50% denaturing gradient (100% denaturing agent corresponds to 40% formamide and 7 mol l^{-1} urea). The gel was loaded with 20 µl PCR products mixed with 5 µl of loading buffer. Electrophoresis ran in the 0.5×TAE (Tris-acetate-EDTA) buffer at 60 °C and 180 V for 6 hours. Afterwards, the gel was stained by ethidium bromide (1 µg ml^{-1}) and visualized in UV light.

DGGE profiles of PCR-amplified DNA of mixtures were compared with the patterns of the collection strains *C. butyricum* DSM 10702 and *C. tyrobutyricum* DSM 2637^T, in order to identify the species.

4 RESULTS AND DISCUSSION

All cultures were cultivated to the similar absorbance and used for DNA extraction. The concentration and quality of DNA were measured spectrophotometrically. All DNAs were diluted to the concentration 10 ng $µl^{-1}$ and used for the PCR. Agarose gel electrophoresis of PCR products confirmed the presence of the specific PCR product (540 bp) in each sample. The PCR products were loaded on DGGE gel, where the PCR-amplified DNA from the collection strains *C. butyricum* DSM10702 and *C. tyrobutyricum* DSM2637^T were used as the reference.

The results of DGGE analysis of DNA mixtures are shown in **Fig. 4** and in **Table 1**. In lanes 1 and 13, DNA mixture of collection strains was used as the reference. In all other lanes, there is the DNA mixture of the field strains. The method of identifying species by comparing the unknown strains to the collection ones is a cheaper and quite reliable alternative to the sequencing of DGGE bands [5].

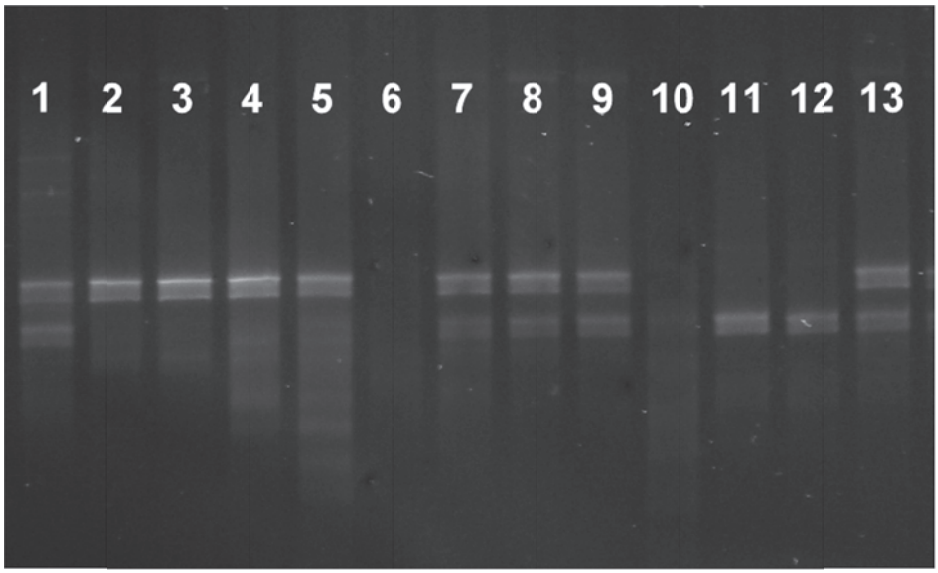

Fig. 4: DGGE analysis of simulated clostridial consortia

Table 1: Results of PCR-DGGE for simulated clostridial consortia

Lane no.	DNA ratio (%) in PCR mixture		DGGE detection of specific band	
	C. butyricum	*C. tyrobutyricum*	*C. butyricum*	*C. tyrobutyricum*
1	50	50	+++	+++
2	0	100	-	+++
3	1	99	-	+++
4	10	90	+/-	+++
5	25	75	+	+++
6	X	X	X	X
7	50	50	++	++
8	67	33	++	++
9	75	25	+++	++
10	90	10	++	-
11	99	1	+++	-
12	100	0	+++	-
13	50	50	+++	+++

+: detection of specific band (the more + signs, the higher intensity) -: specific band not detected

DGGE analysis of the simulated consortia, where the mixtures of DNA of 2 species were used as the template for PCR, revealed that we are able to distinguish both species if there is at least 25% of the species DNA in the mixture. From the intensity of the bands it is possible to estimate which species dominates in the mixture. Therefore, the method can be considered semi-quantitative.

When artificial cell consortia were analyzed, the DGGE profile of all samples showed only one band, namely the specific band for *C. tyrobutyricum*, regardless the initial concentration of *C. butyricum* in the mixture. This means that under tested conditions, *C. tyrobutyricum* grows better than *C. butyricum*. Influence of the cultivation conditions (pH, type of sugar substrate, temperature) on the growth of the strains will be tested, as well as the correlation of the consortium composition and the hydrogen production.

5 CONCLUSION

PCR-DGGE was successfully tested to distinguish co-existing species in the artificially prepared DNA mixtures, as well as in the artificial microbial consortia. The results of this study have shown that PCR-DGGE with the *Clostridium*-specific primers is an effective method for species identification of *C. butyricum* and *C. tyrobutyricum* in mixtures. This tool can be useful for the further research of bio-hydrogen production by *Clostridium*.

ACKNOWLEDGEMENTS

The financial support of the Ministry of Education, Youth and Sports of the Czech Republic, grant No. 2B08070 is gratefully acknowledged.

LITERATURE

[1.] Li, R.Y., T. Zhang a H.H.P. Fang. Bioresource Technology 2011, 102 (18), 8445-8456.
[2.] Das, D., Veziroglu, T. International Journal of Hydrogen Energy 2008, 33, 6046-6057.
[3.] Show, K., Lee, D., Chang, J. Bioresource Technology 2011, 102, 8524-8533.
[4.] Hung, C., Cheng, C., Cheng, L., Liang, C., Lin, C. International Journal of Hydrogen Energy 2008, 33 (5), 1586-1592.
[5.] Ercolini, D. Journal of Microbiological Methods 2004, 56, 297-314.
[6.] Sambrook, J., Russell, D. W. Molecular Cloning: A Laboratory Manual. New York: Cold Spring Harbor Laboratory Press, 2001.

P21 OPTIMIZATION OF MEKC SEPARATION SELECTIVITY OF PHENOLIC COMPOUNDS USING HOMOLOGICAL SERIES OF ANIONIC SURFACTANTS

Jana Váňová, Petr Česla, Jan Fischer, Pavel Jandera

Department of Analytical Chemistry, Faculty of Chemical Technology, University of Pardubice, Studentská 573, 532 10 Pardubice, Czech Republic
Jana.Vanova@student.upce.cz

ABSTRACT

A micellar electrokinetic capillary chromatography method for separation of phenolic acids and flavonoids suitable for application in two-dimensional system in combination with gradient elution reversed-phase liquid chromatography was developed. The influence of type of surfactant on the separation selectivity in background electrolytes with different concentration of acetonitrile was studied. The critical micelle concentration of homological series of sodium alkyl sulfates and migration times of their micelles were determined. The sodium alkyl sulfates with octyl- to octadecyl- alkyl chains were used to achieve the similar time of analysis and similar separation selectivity in background electrolytes with concentration of acetonitrile up to the 20% (v/v).

Keywords: micellar electrokinetic capillary chromatography, separation selectivity, anionic surfactants, critical micelle concentration

1 INTRODUCTION

Micellar electrokinetic capillary chromatography (MEKC) can be used for analysis of large variety of substances in food, pharmaceuticals, environment, cell cultures [1] and biological fluids. Using surfactants, both neutral molecules as well as charged ions can be

separated. MEKC combines advantages of liquid chromatography and capillary electrophoresis. The separation is based on the different distribution coefficient between stationary (pseudostationary phase, respectively) and the aqueous mobile phase [2].

The concentration of surfactant higher than the critical micelle concentration is usually required for the successful MEKC separation, while the type and concentration of surfactant affects the separation selectivity. In present work, we have investigated the effects of the length of alkyl chain in molecules of alkyl sulfates and the concentration of surfactants on separation selectivity of antioxidants in background electrolytes with different concentration of acetonitrile. First, the values of critical micelle concentration in background electrolytes without and with addition of acetonitrile were determined using method based on measurement of current [3] and the method based on a retention model [4]. The migration time of micelles was determined by iterative process [5, 6]. The critical micelle concentrations were determined for alkyl sulfates in water, borate buffer (25 mmol.l^{-1}, pH 9,30) and borate buffer with addition of acetonitrile (5 – 20 %; v/v). Next, the separation of antioxidants was carried out in borate buffer (25 mmol.l^{-1}, pH 9,30) with the 0 – 20 %; v/v of acetonitrile. The concentration of alkyl sulfates was 1,5; 2 and 3 times the critical micelle concentration in the BGE.

2 EXPERIMENTAL

Sodium octyl-, decyl-, dodecyl-, tetradecyl- and octadecyl sulfate, alkylbenzenes (methylbenzene, ethylbenzene, propylbenzene, butylbenzene, pentylbenzene) and selected antioxidants ((-)-epicatechin, (+)-catechin, rutin, hesperetin, naringenin, 4-hydroxyphenylacetic acid, chlorogenic acid, 7-hydroxyflavone, salicylic acid, quercetin, p-hydroxybenzoic acid, caffeic acid, gallic acid, flavone, hesperidin) were obtained from Sigma-Aldrich (Steinheim, Germany). Methanol was from J. T. BAKER (Deventer, Netherlands), toluen was from ACROS (Cell, Belgium) and sodium tetraborate and boric acid were purchased from Fluka (Buchs, Switzerland). Thiourea was from LachNer (Neratovice, Czech Republic). All experiments were carried out using capillary electrophoresis Agilent ^{3D}CE (Palo Alto, CA, USA) in non-coated fused silica capillary (48 cm total length, 40 cm effective length, 50 µm i.d., Agilent) at applied voltage of 20 kV. Detection wavelength was set at 254 nm.

Stock solutions of selected antioxidants were prepared in methanol at concentrations of 0.5 g.l^{-1}. The samples of antioxidants for separation were diluted by water to the concentration of approx. 10 mg.l^{-1}. Separation capillary was preconditioned by flushing with background electrolyte for 2 min prior to the analysis. The samples were injected hydrodynamically by applying pressure of 50 mBar for 5 s at the sample vial inlet.

2.1 Determination of micellar characteristics

Current that passes through the separation capillary is directly proportional to the concentration the surfactant, while the slope of the dependency is different in submicellar and micellar region. The current was measured at 25°C for 5 min. Prior to the each measurement, the capillary was flushed with BGE for 2 min. Dependence of measured current values on the concentration of alkyl sulfate surfactant (Fig. 1) can be fitted by the linear regression using two data sets, one in the concentration range below the critical micelle concentration and second in the micellar region. The critical micelle concentration is determined as the intersection point of both straight lines.

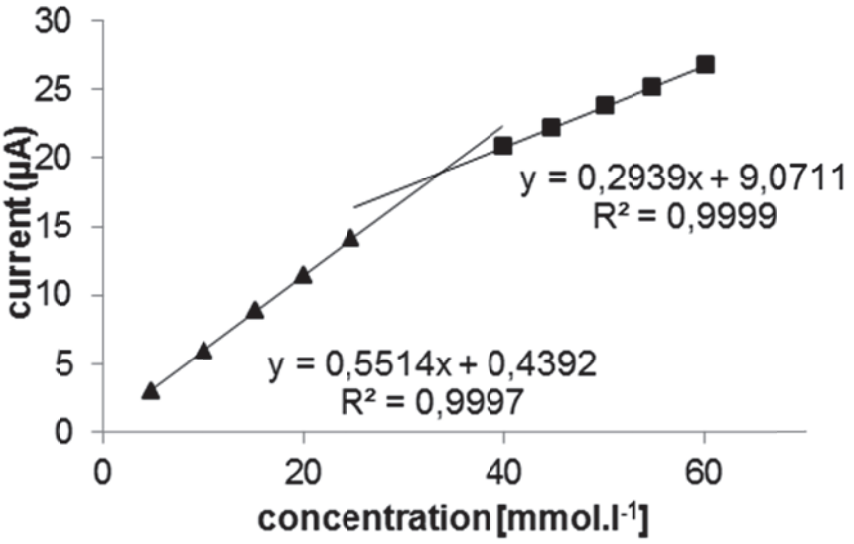

Fig. 1: Dependence of current on the concentration of sodium decyl sulphate in water.

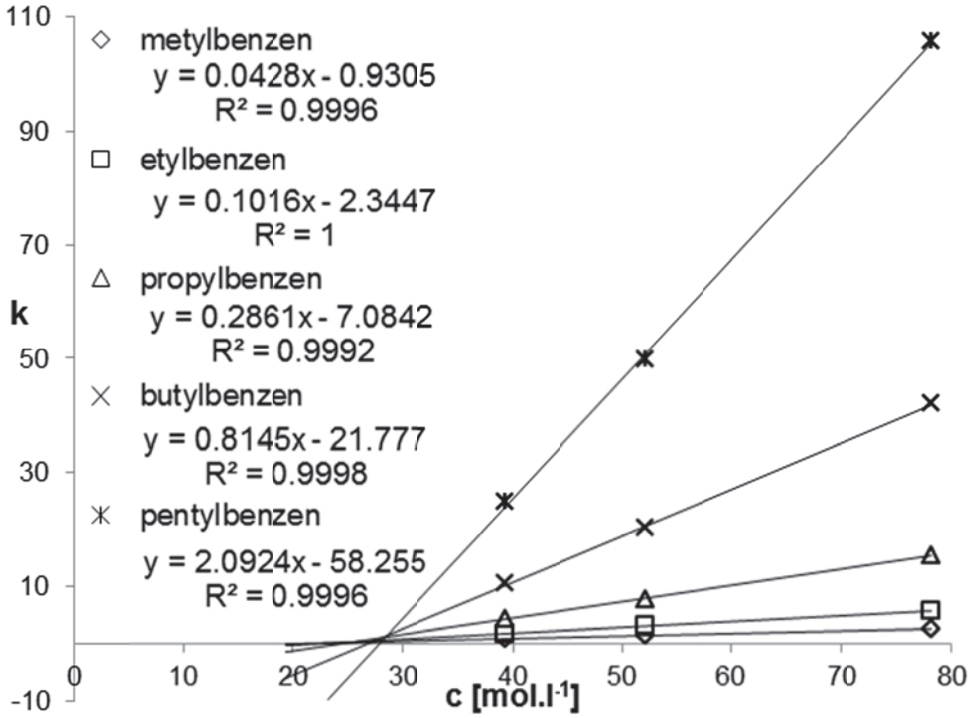

Fig. 2: Dependence of retention factor of alkylbenzenes on concentration of sodium dodecyl sulfate in BGE with 5 % of acetonitrile.

The second approach for determination of critical micelle concentration is based on the retention model. The migration times of alkylbenzenes and thiourea were measured. Retention factors of alkylbenzenes were calculated using migration time of micelles obtained by the iterative process [4]. Dependence of retention factors of alkylbenzenes on concentration of surfactant in solution (shown in Fig. 2) was constructed. Intersection of the straight lines with x-axis corresponds to critical micelle concentration.

The migration time of micelles was the determined using iterative process of migration times of homological series of alkylbenzenes. From the measured values of migration times, t_r, the retention factors, k, were calculated using migration time of micelle, t_{mc} and is migration time of thiourea, t_0, as the marker of electroosmotic flow. In the first step, t_{mc} corresponds to the longest migration time of homologue in alkylbenzene series. Dependence of log k on the number of carbons in alkylbenzenes was constructed using equation:

$$\log k = az + b$$

where z is number of carbons in alkylbenzenes, a and b are constants depending on the type of water phase and micelle phase. The retention factor of the most retained alkylbenzene was calculated and used for recalculation of the new retention time of micelles. The procedure was repeated until the difference between the two calculated values was negligible.

3 TABLES AND ILLUSTRATIONS

The critical micelle concentrations of homological series of sodium alkyl sulfate were determined using two methods. The first method is based on the measurement of current dependence on the concentration of surfactant compound; the second is based on the retention model employing homological series of alkyl benzenes. Measured data show that the critical micelle concentration decreases with increasing number of carbons in alkyl chain (Table 1; Fig. 3). Values of critical micelle concentration of sodium alkyl sulfate increase with increasing concentration acetonitrile in background electrolyte (Table 2).

Table 1: Values of critical micelle concentration [7] and Krafft point [8] of homological series of sodium alkyl sulfates

Surfactant	Critical micelle concentration in water at 25°C [mmol.l^{-1}]	Krafft point [°C]
Sodium decyl sulfate	30	8
Sodium dodecyl sulfate	8,1	16
Sodium tetradecyl sulfate	2,0	36
Sodium hexadecyl sulfate	0,5	44
Sodium octadecyl sulfate	Data not available	56

Table 2: Comparison of the values of critical micelle concentration determined using method based on measurement of current (cmc 1) and method based on a retention model of alkylbenzenes (cmc 2).

Surfactants	Background electrolyte	*cmc* 1 (mmol.l^{-1})	*cmc* 2 (mmol.l^{-1})
Sodium decyl sulphate	Borate buffer, pH 9,30	26,06	24,83
	Borate buffer, pH 9,30 + 5 % acetonitrile	24,02	23,26
	Borate buffer, pH 9,30 + 10 % acetonitrile	26,10	28,45
	Borate buffer, pH 9,30 + 15 % acetonitrile	33,48	36,62
Sodium dodecyl sulphate	Borate buffer, pH 9,30	3,74	3,05
	Borate buffer, pH 9,30 + 10 % acetonitrile	5,98	4,89
	Borate buffer, pH 9,30 + 15 % acetonitrile	7,70	6,49
	Borate buffer, pH 9,30 + 20 % acetonitrile	12,08	9,39

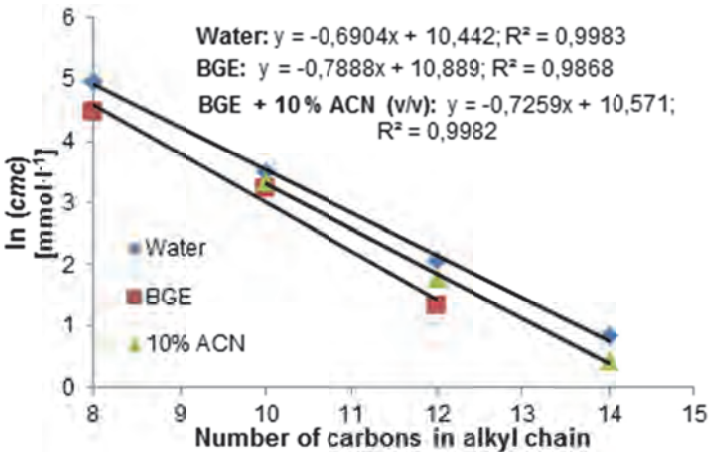

Fig. 3. : Dependency of the logarithm of critical micelle concentration on the number of carbon atoms in the surfactant alkyl chain in water, 25 mmol·l^{-1} borate background electrolyte pH 9,30 and background electrolyte with addition of 10 % of acetonitrile (v/v). Critical micelle concentration was determined by measuring of current in capillary filled with surfactant solutions at 25 °C.

3.1 Application to the separation of antioxidant mixture

Size of migration window between migration time of electroosmotic flow and migration time of micelles was determined. Migration time of electroosmotic flow was detected using thiourea and migration time of micelles was determined using iterative process. Phenolic acids and flavonoids were separated by partitioning between micellar and aqueous phases. The separations in sodium dodecyl sulfate and sodium decyl sulfate as pseudostationary phases are shown in Figs. 4 and 5. The separations with 52,12 mmol.l^{-1} (2x critical micelle concentration) sodium decyl sulfate without acetonitrile in borate buffer and separation with 36,03 mmol.l^{-1} (1,5x critical micelle concetration) sodium decyl sulfate with 5 % (v/v) acetonitrile in background electrolyte yielded approximately the same width of migration window with comparable separation selectivity.

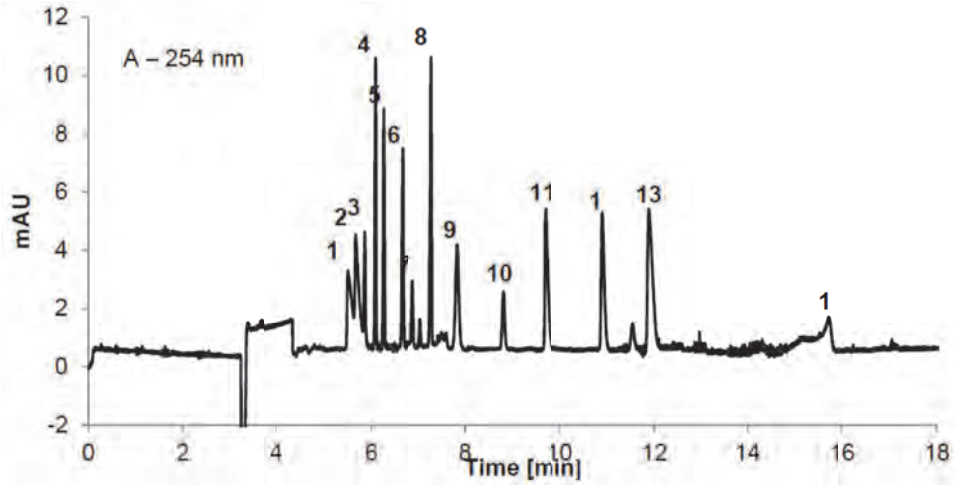

Fig. 4 : Separation of mixture of phenolic acids and flavonoids in 25 mmol·l^{-1} borate background electrolyte pH 9,30 with addition of 52.1 mmol·l^{-1} sodium decyl sulphate (2x *cmc*). Non-coated 48 (40) cm fused silica capillary, 50 μm i.d., applied voltage 20 kV, temperature 25 °C. Analyzed compounds: **1:** (-)-epicatechin, **2:** (+)-catechin, **3:** rutin, **4:** hesperetin, **5:** naringenin, **6:** 4-hydroxyphenylacetic acid, **7:** chlorogenic acid, **8:** 7-hydroxyflavone, **9:** salicylic acid, **10:** quercetin, **11:** p-hydroxybenzoic acid, **12:** caffeic acid, **13:** gallic acid, **14:** flavone.

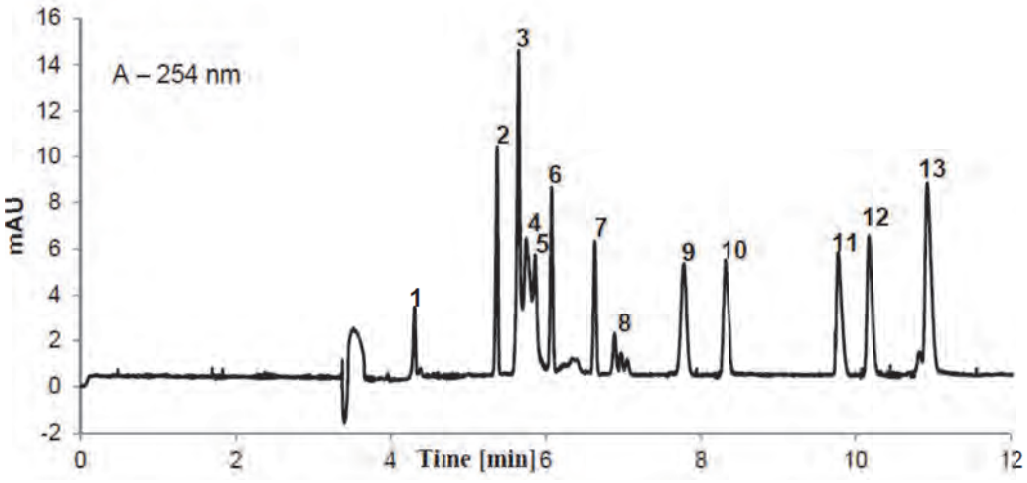

Fig. 5 : Separation of mixture of phenolic acids and flavonoids in 25 mmol·l^{-1} borate background electrolyte pH 9,30 with addition of 8,97 mmol·l^{-1} sodium dodecyl sulphate (1,5x *cmc*) with 10 % (v/v) acetonitrile. Non-coated 48 (40) cm fused silica capillary, 50 μm i.d., applied voltage 20 kV, temperature 25 °C. Analyzed compounds: **1:** hesperidin, **2:** hesperetin, **3:** (-)-epicatechin a 7-hydroxyflavone, **4:** (+)-catechin, **5**: rutin, **6:** naringenin, **7:** 4-hydroxyphenylacetic acid, **8:** chlorogenic acid, **9:** quercetin, **10:** salicylic acid, **11:** p-hydroxybenzoic acid, **12:** caffeic acid, **13:** gallic acid.

4 IMPLICATIONS FOR TWO-DIMENSIONAL LCXMEKC SEPARATIONS

The separation selectivity of phenolic acids and flavonoids and width of the migration time window change in background electrolytes with sodium alkyl sulfate micelles with different length of alkyl chains of tested surfactants and with increasing concentration of acetonitrile in BGE. If the MEKC method is intended for the application in two-dimensional separation system in combination with the gradient reversed-phase liquid chromatography, the increasing concentration of acetonitrile is transferred to the second MEKC separation dimension during the separation [9, 10]. Under steady MEKC conditions, the increasing amount of acetonitrile in the samples in consecutive fractions transferred from LC lead to the change of migration times by shifting the partitioning equilibria towards the less polar aqueous/acetonitrile phase. The shifts can be compensated using changing composition of BGE in MEKC separation step with increasing length of the alkyl chains in surfactant molecules for the compensation of the width of migration time window and the separation selectivity of phenolic acids and flavonoids.

ACKNOWLEDGEMENTS

The financial support by the Czech Science Foundation, project No. 206/12/0398 is gratefully acknowledged.

LITERATURE

[1.] Zhang, J., Chakraborty, U., Foley, J.P., Electrophoresis 2009, 30, 3971-3977.
[2.] Ozaki, H., Ichichara, A., Terabe, S., Journal of chromatography 1995, 709, 3-10.
[3.] Cifuentes, A., Bernal, J. L., Diez-Masa, J. C., Anal. Chem. 1997, 69, 4271.
[4.] Terabe, S., Otsuka, K., Ichikawa, K., Tsuchiya, A., Ando, T., Anal. Chem. 1984, 56, 111.
[5.] Bushey, M. M., Jorgenson, J. W.: Anal. Chem., 1989, 61, 491.
[6.] Bushey, M. M., Jorgenson, J. W.: J. Microcol. Sep., 1989, 1, 125.
[7.] Lebedeva, N. V., Shahine, A., Bales, B. L., J. Phys. Chem. B 2005, 109, 19806 – 19816.
[8.] http://www.nies.go.jp/chiiki1/protoz/toxicity/chemical/anionic.htm, downloaded 3.4.2012.
[9.] Česla, P., Fischer, J., Jandera, P., Electrophoresis 2010, 31, 2200-2210.
[10.] Česla, P., Fischer, J., Jandera, P., Electrophoresis 2012, 33, 2464-2473.

P22 PHOTOLITHOGRAPHIC TECHNIQUE FOR CONTROLLED FABRICATION OF METAL STRUCTURES

Petra Jusková[a], Jitka Hegrová[a], František Foret[a,b]

[a] Institute of Analytical Chemistry of the ASCR, v.v.i.,Veveří 97, 60200 Brno, Czech Republic
[b] CEITEC - Central European Institute of Technology, Masaryk University, Brno, Czech Republic, foret@iach.cz

ABSTRACT

We are describing two strategies for controlled (geometry and dimension) preparation of metal micro-nano structures. Both techniques are based on photolithographic processes with selective pattern transfer.

First technique utilizes agarose gel containing photosensitive silver chloride as the photosensitive layer. Silver structures are formed after irradiation of the gel through the photolithographic mask which defines shape of the resulting structures.

Second approach utilizes photolithographic process to form particles from vacuum deposited thin metal layer deposited over soluble sacrificial layer. Fabrication protocol is adaptable for

different metals and their combinations allowing preparation of monometallic and multimetallic particles.

Keywords: metal microstructures, microfabrication, photolithography

1 INTRODUCTION

Modern analytical detection methods often take advantage of micro/nanoparticles and structures of diverse sizes, geometries and composition. Depending on the specific sensing technique and sample requirements they can be used in variety of bioanalytical formats as quantification tags for optical and electrochemical detection, substrates for multiplexed bioassays, signal transductors [1].

Combination of these micro/nanostructures with magnetic materials opens up another possibility for their controlled assembling and manipulation allowing selection and separation of specifically labeled target cells, cell organelles and biologically active compounds (nucleic acids, proteins, xenobiotics) directly from the crude samples [2]. Magnetic particles of wide diameter range (nanometers to micrometers) with immobilized antibodies and other compounds are commercially available [3]. Combination of their unique features with proper surface modification makes them suitable tool for variety of clinical applications including drug targeting, diagnostics and cancer therapy [4-6].

Selection of the fabrication protocol highly depends on future function of particles; therefore development of the new preparation strategies is of great interest. Current fabrication methods could be sorted into two main categories; top-down and bottom-up techniques. Most of the bottom-up approaches are based on organized assembling of the molecules or colloids [7], when top-down preparation usually exploits some microfabrication technique [8].

Photolithographic technique represents one of the basic microfabrication methods with wide range of applications. In this work, we present two protocols utilizing photolithographic technique for high throughput generation of uniform and well defined metallic structures.

2 FORMATION OF SILVER STRUCTURES WITHIN THE HYDROGEL MATRIX

Hydrogel used as the matrix for creation of structures was prepared from agarose powder SeaPlaque® GTG® Agarose (Lonza Rockland, Inc., Rockland, USA). Solutions of NaCl and $AgNO_3$ were added to the dissolved agarose and immediately formed photosensitive silver chloride. Modified hydrogel was casted between two glass slides with the fixed distance. During exposition, one of the glass slides was replaced with the photolithographic mask. Process resulted in negative latent image in the hydrogel substrate. Development of latent image using hydroquinone based Fomadon LQR developer (mixture: developer/water 1:9) results in visible image made of reduced silver. Remaining portion of silver chloride is removed from the gel using sodium thiosulfate based fixer solution, Fomafix fixer (used in mixture: fixer/water 1:4). Fixer and developer were both obtained from Foma, Hradec Králové, Czech Republic.

We tested several exposure times (3-60 seconds) and different concentrations of agarose hydrogel in the range (1.5 – 4 w %). For further experiments, 5 seconds exposition time was chosen. Longer exposition negatively affects quality of the transferred structures, while shorter exposition was insufficient for complete pattern transfer. Under these conditions, silver layer was formed in ~ 300 μm depth of the 2 milimeter thick hydrogel.

Agarose concentration determines permeability as well as hardness of the prepared hydrogel. We tested several concentrations, where the best results were obtained using ~ 2 % agarose hydrogel. Hydrogel matrix containing silver structures with different shapes is presented on Fig. 1.

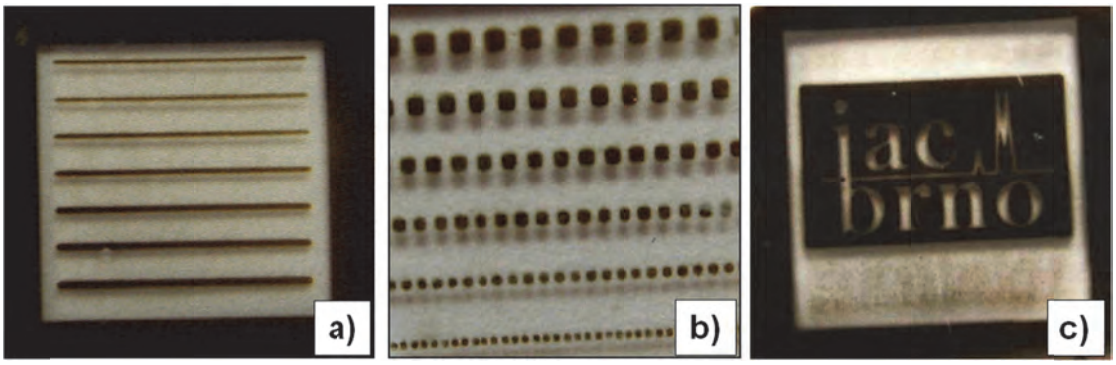

Fig. 1. Silver colloid patterns reduced within the hydrogel matrix: a-b) Lines and squares with height ranged from 0.8 to 0.4 mm. b) Versatility of presenting method is demonstrated on logotype written into the rectangle with dimensions 8.6 mm x 14 mm.

3 PREPARATION OF THE FREE-STANDING METAL PARTICLES

Fabrication protocol starts with deposition of sacrificial – soluble layer onto the glass substrate. This layer was composed of negative photoresist, MaN-420 (Micro resist technology GmbH, Berlin, Germany) mixed with aceton (photoresist/acetone in ratio 1:3). Selected metal was deposited over this layer using a vacuum sputter coater and another layer of positive photoresist Positiv 20 (CRC Industries Europe N. V., Zele, Belgium) was deposited on the top. Desired geometry of the particles was achieved after irradiation and development of the top photoresist layer and etching of the metal portions uncovered in the photolithographic step. Whole process is finished with releasing of particles into suspension by dissolving of the sacrificial layer.

In our work we prepared metal particles with different material composition. Bimetallic particles can allow two different chemistries for further functionalization, in addition utilization of magnetic material like nickel can simplify manipulation with the particles, enabling control over the position and topology of particles within the system. Examples of resulting particles are shown in Fig.2 b and c. Assembling of the magnetic particles under the influence of the magnetic field is depictured on the Fig 2.c.

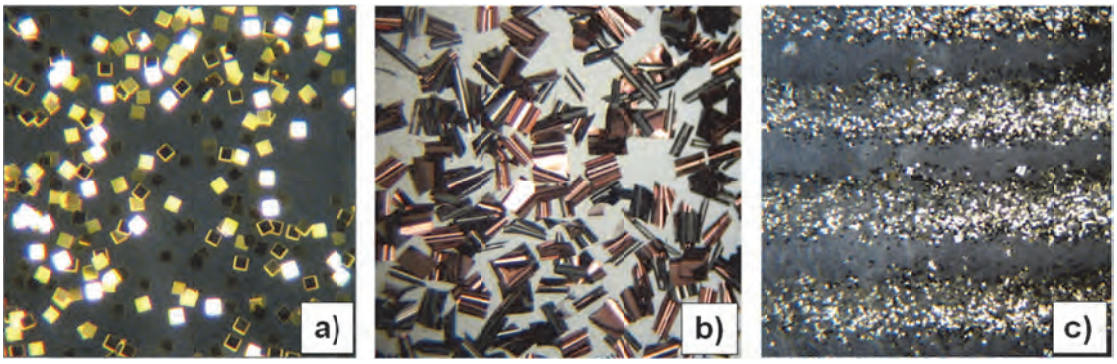

Fig. 2. Thin film metal structures: a) Gold 50 x 50 µm particles with 300 nm thickness. b) Copper-nickel bimetal particles, 100 x 100 µm with thickness of layers: copper (150 nm), nickel (50 nm). c) Assembling of the nickel 50 x 50 µm particles with 300 nm thickness into the lines as a result of the magnetic field.

4 CONCLUSIONS

We described two methods for preparation of the metal structures allowing great control over their size shape and composition.
Selectively reduced metal portions resulting from the first protocol can be used for selective attachment of biomolecules especially in microfluidics where channels with complicated access can be easily modified indirectly by irradiation through photolithographic mask placed on the channel wall. Except silver, there are photographic protocols allowing prepare gold (chrysotype) or iron (cyanotype) and these chemistries could be adapt for our purposes as well.
Second protocol leads to free-standing metal structures with potential application in microfluidics and bioanalysis. Ultra flat and uniform sized particles can be used for signal enhancement and with proper surface modification particles could allow molecule targeting or/and addressable positioning within the microfluidic system.

ACKNOWLEDGEMENTS

Financial support from the Grant Agency of the Czech Republic (P301/11/2055 and P206/12/G014) and the institutional support RVO: 68081715 is acknowledged. Part of the work was realised in CEITEC - Central European Institute of Technology with research infrastructure supported by the project CZ.1.05/1.1.00/02.0068 financed from European Regional Development Fund.

LITERATURE

[1.] Penn, S. G., He, L., Natan, M. J., *Current Opinion in Chemical Biology* 2003, 7, 609-615.
[2.] Boncheva, M., Andreev, S. A., Mahadevan, L., Winkleman, A., et al., *Proceedings of the National Academy of Sciences of the United States of America* 2005, 102, 3924-3929.
[3.] Safarik, I., Safarikova, M., *Journal of Chromatography B* 1999, 722, 33-53.
[4.] Ito, A., Shinkai, M., Honda, H., Kobayashi, T., *Journal of Bioscience and Bioengineering* 2005, 100, 1-11.
[5.] Sun, C., Lee, J. S. H., Zhang, M. Q., *Advanced Drug Delivery Reviews* 2008, 60, 1252-1265.
[6.] El Haj, A. J., Hughes, S., Dobson, J., *Journal of Biomechanics* 2007, 40, S96-S104
[7.] Li, F., Josephson, D. P., Stein, A., *Angewandte Chemie International Edition* 2011, 50: 360–388.
[8.] Merkel, T. J., Herlihy, K. P., Nunes, J., Orgel, R. M., et al., Langmuir, 2010, 26, 13086-13096.

P23 MALDI-TOF MS OF *DICKEYA* AND *PECTOBACTERIUM* SPECIES – CHARACTERIZATION OF PLANT PATHOGENIC BACTERIA

Jiří Šalplachta[a], Anna Kubesová[a], Jaroslav Horký[b], Marie Horká[a]

[a] *Institute of Analytical Chemistry Academy of the ASCR, v. v. i., Veveří 97, 602 00 Brno, Czech Republic, salplachta@iach.cz*
[b] *State Phytosanitary Administration, Division of Diagnostics, Šlechtitelů 23, 77900 Olomouc, Czech Republic*

ABSTRACT

Dickeya and *Pectobacterium* species are known as broad host range phytopathogens. These species are commonly detected using cultural, serological and molecular methods. Although these methods can detect pathogen, they often fail in the case of bacterial characterization. The ability of matrix-assisted laser desorption/ionization time-of-flight mass spectrometry (MALDI-TOF MS) to characterize different *Dickeya* and *Pectobacterium* species was

investigated in the present study. Intact cells of 30 strains of *Dickeya* and *Pectobacterium* species were subjected to MALDI-TOF MS analysis. Our results confirm suitability of suggested analytical procedure for rapid and unambiguous differentiation of *Dickeya* and *Pectobacterium* species based on species specific mass fingerprints.

Keywords: MALDI, bacteria, *Dickeya*

1 INTRODUCTION

Genus *Dickeya* (formerly *Erwinia chrysanthemi*) and genus *Pectobacterium* (formerly a member of the genus *Erwinia*) comprise several bacterial species [1.,2.]. These bacteria are Gram-negative, facultative anaerobic, nonsporing and rod-shaped bacteria that cause diseases on numerous plants worldwide. These bacteria produce cell-wall-degrading enzymes hydrolyzing pectin between individual plant cells, which causes the cells to separate, the state called bacterial soft rot [3.,4.]. The *Dickeya* and *Pectobacterium* species are very important due to their economic impact in agriculture. Since the traditional methods (e.g., PCR, ELISA) often fail in characterization of these species, there is still request for rapid and reliable classification tool [5.,6.]. In this respect, MALDI-TOF MS was used for analysis of intact cells of representative strains of *Dickeya* and *Pectobacterium* species in this study.

2 EXPERIMENTAL

A total of 30 strains of *Dickeya* and *Pectobacterium* species were examined in the present study. These strains were obtained from Division of Diagnostics of the State Phytosanitary Administration (Olomouc, Czech Republic). Cell concentration of all examined bacteria was adjusted to 10^8 cells mL^{-1} for subsequent MS experiments. 3,5-Dimethoxy-4-hydroxycinnamic acid (sinapinic acid) was used as a matrix. Sample preparation is described in detail elsewhere [7.]. All MS experiments were performed on 4700 Proteomics Analyzer (Applied Biosystems, Framingham, MA, USA) equipped with linear detector and a 200 Hz Nd:YAG laser operating at 355 nm. Accelerating voltage was set at 20 kV. Mass spectra were acquired in linear positive ion mode. Recorded mass spectra were processed using Data Explorer (ver. 4.6). Cluster analysis, using STATISTICA (data analysis software system, ver. 10, StatSoft, Inc., www.statsoft.com), was applied to evaluate the obtained MS data and to classify the examined bacteria.

3 RESULTS

The ability of MALDI-TOF MS to characterize different *Dickeya* species was investigated in this study. Traditionally, the first step was optimization of sample preparation including different sample deposition strategies. The best results, in terms of number of observed mass signals, signal-to-noise ratio and reproducibility were achieved by using intact cells and sinapinic acid as a MALDI matrix. An example of MALDI-TOF mass spectra of five selected strains of *Dickeya* and *Pectobacterium* species is displayed in **Fig. 1**. This figure shows characteristic mass fingerprints of the analyzed bacterial strains in the 2000 to 40000 m/z range. Mass signals below m/z 2000 were not taken into consideration with regard to insignificant differences between examined strains. Furthermore, no signal was detected above m/z 40000 in any of recorded mass spectrum. Observed data have revealed that the mass fingerprints are species specific, which allows rapid and reliable characterization of *Dickeya* and *Pectobacterium* species using MALDI-TOF MS.

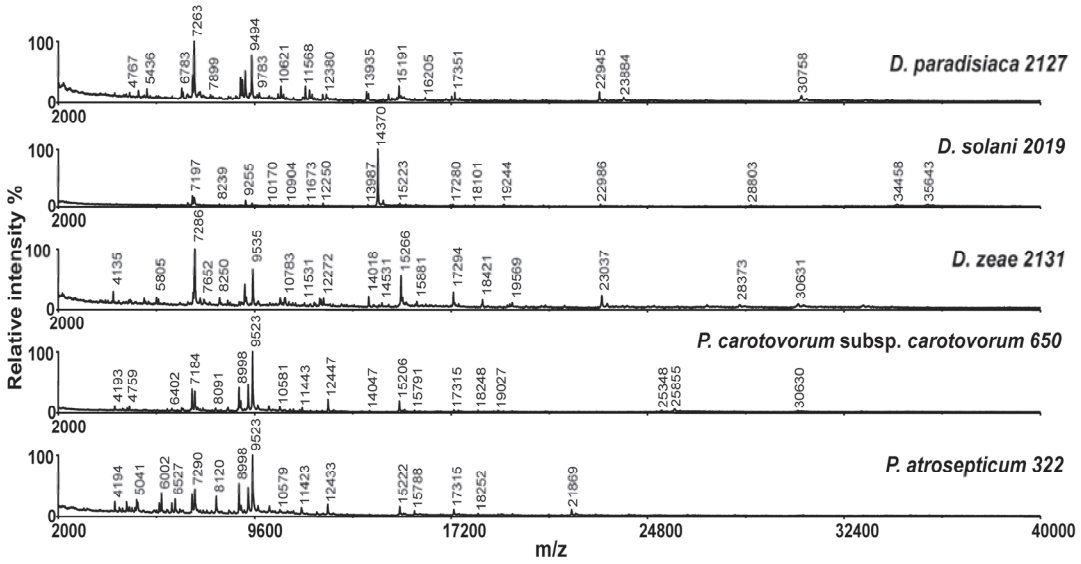

Fig. 1: MALDI-TOF mass spectra of representative strains of different *Dickeya* and *Pectobacterium* species. Mass spectra were acquired in linear positive ion mode, sinapinic acid was used as a matrix.

4 CONCLUSIONS

MALDI-TOF MS was applied to reliable characterization of *Dickeya* and *Pectobacterium* species in this study. Our results confirm suitability of suggested analytical approach for efficient bacterial differentiation of species based on species specific mass fingerprints. MALDI-TOF MS of intact bacterial cells require minimum sample handling and is less time-consuming compared to conventional methods.

ACKNOWLEDGEMENTS

This work was supported by the grant of Ministry of Interior No. VG20102015023, by the Ministry of Education Youth and Sports of the Czech Republic - project Development of Multidisciplinary Research and Educational Centrum for Bioanalytical Technologies No.CZ.1.07/2.3.00/20.0182 and by the institutional support RVO: 68081715.

LITERATURE

[1.] Ma, B., Hibbing, M. E., Kim, H. S., Reedy, R. M., *et al.*, *Phytopathology* 2007, *97*, 1150-1163.
[2.] Toth, I. K., van der Wolf, J. M., Saddler, G., Lojkowska, E., *et al.*, *Plant Pathology* 2011, 60, 385–399.
[3.] Czajkowski, R., Perombelon, M. C. M., van Veen, J. A., der Wolf, J. M., *Plant Pathology* 2011, *60*, 999-1013.
[4.] Barras, F., van Gijsegem, F., Chatterjee, A. K., *Annual Review of Phytopathology* 1994, *32*, 201–34.
[5.] Powney, R., Beer, S. V., Plummer, K., Luck, J., *et al.*, *Australian Plant Pathology* 2011, *40*, 87-97.
[6.] Tsror, L., Erich, O., Hazanovsky, M., Ben, D. B., *et al.*, *Plant Pathology* 2012, *61*, 161-168.
[7.] Horka, M., Kubesova, A., *Salplachta,* J., Zapletalova, E., *et al.*, *Analytica Chimica Acta* 2012, *716*, 155-162.

P24 INVESTIGATION OF PLATINUM-BASED CYTOSTATIC DRUGS INTERACTIONS WITH DNA BY SANGER SEQUENCING

Kristýna Šmerková[a], Simona Dostálová[b], Markéta Ryvolová[a,c], Helena Škutková[b], Vojtěch Adam[a,c], Ivo Provazník[b], René Kizek[a,c]

[a] *Department of Chemistry and Biochemistry, Faculty of Agronomy, Mendel University in Brno, Zemedelska 1, CZ-613 00 Brno, European Union-Czech Republic*
[b] *Department of Biomedical Engineering, Faculty of Electrical Engineering and Communication, Brno University of Technology, Kolejni 4, CZ-612 00 Brno, European Union-Czech Republic*
[c] *Central European Institute of Technology, Brno University of Technology, Technicka 3058/10, CZ-616 00 Brno, European Union-Czech Republic*
kizek@sci.muni.cz

ABSTRACT

Platinum-based cytostatic drugs such as cisplatin, carboplatin and oxaliplatin play an important role in the battle with cancer. The mechanism of their activity is widely studied and the quantification of the drug incorporated in the DNA structure is in the center of attention. In this study we investigated the behavior of the platinum-based cytostatic drug and DNA adducts during the well-established Sanger sequencing method involving capillary electrophoretic (CE) separation. Three selected platinum-based cytostatic drugs (cisplatin, carboplatin and oxaliplatin) were incubated with the DNA fragment (498 bp) to create adducts and subsequently sequenced. It was found that the fluorescence signal provided by fluorescently labeled DNA fragments decreased significantly depending on concentration of the drug. Moreover, even though four types of fluorescently labeled fragments are created during the sequencing reaction prior to the CE separation; similar decrease of the signal was observed in all of the fragment types. This suggests that cytostatic drugs do not influence the CE separation itself but the labeling sequencing reaction. Finally, the difference between three types of the cytostatic drugs was found. It follows from the results that to reach the signal decrease of 75 % compared to the control DNA sample only 0.3 µg/ml of cisplatin is required. On the other hand, 7 and 75 µg/ml of oxaliplatin and carboplatin, respectively are required to reach the same effect. Our hypothesis was verified by electrochemical analysis and the highest amount of platinum was determined in the cisplatinated DNA sample followed by oxaliplatinated and carboplatinated DNA.

Keywords: DNA, cytostatic drugs, DNA sequencing

1 INTRODUCTION

Cancer is the main reason of health problems in developed countries where every fourth death is caused by tumor disease [1]. For tumor therapy the chemotherapeutics including platinum based cytostatic drugs (cisplatin, carboplatin, oxaliplatin) are one of the most commonly used [2]. The biological activity of the first platinum-based cytostatic drug (cispaltin, *cis*-Diamminedichloroplatinum(II)) was discovered by Rosenberg in 1965 [3]. „The second generation“ of platinum cytostatics represented by carboplatin (*cis*diammine-1,1-cyclobutane dicarboxylate) was developed in 80s as a less toxic alternative of cisplatin causing less serious side effects [4]. Cisplatin and carboplatin are effective for therapy of brain, neck, and/or lung cancer; however they have severe toxic and mutagenic effect on both cell and animal model samples. [5, 6]. Both of these cytostatics form same Pt-DNA complexes *in vivo* and it is known that cisplatin is ineffective to call lines resistant to carboplatin and vice versa. Therefore “third generation” – oxaliplatin ((*trans-R,R*)1,2-

iaminocyclohexaneoxalatoplatinum(II)) - was developed in 90s overcoming the resistance [7] and moreover providing lower mutagenity [8].

Sanger sequencing method discovered 35 years ago is based on enzymatic synthesis of DNA fragments with different length [9] and fluorescent labeling of these fragments by dideoxynucleotides with fluorescent tag [10]. Replication of DNA is running until the labeled dideoxynucleotide is incorporated which stops the following elongation of the chain [11]. These fragments are subsequently electrophoreticaly separated and fluorescently detected. Sanger method is due to its accuracy and efficiency still the golden standard in genome research [12].

The analysis of Pt-DNA adducts is routinely performed by electrochemical methods [13, 14], however the application of sequencing reaction combined with capillary electrophoresis represents an alternative method for quantification of platinum-based cytostatic drug intercalated in the DNA structure.

2 EXPERIMENTAL SECTION

2.1 DNA fragment amplification and isolation

For amplification *Taq* PCR kit and DNA isolated from bacteriophage *λ* (New England BioLabs, USA) were used. Primers were synthesized by Sigma-Aldrich (USA), the sequence of a forward primer was 5´-CCTGCTCTGCCGCTTCACGC-3´ and the sequence of a reverse primer was 5´-TCCGGATAAAAACGTCGATGACATTTGC-3´. The cycling conditions of PCR were as follows: initial denaturation at 95°C for 120 s; 25 cycles of denaturation at 95 °C for 15 s, annealing at 64 °C 15 s, extension at 72 °C 45 s and a final extension at 72 °C for 5 min. Obtained DNA fragments (498 bp) were purified by MinElute PCR Purification Kit (Qiagen, Germany). DNA concentration was determined spectrophotometrically (Analytic Jena, Germany).

2.2 Platinum-based cytostatic drugs interaction with DNA

DNA fragments solution (100 μg/ml) was mixed with platinum-based cytostatic drugs at various concentrations in the rate 1:1 (v/v) in the environment of 10 mM $NaClO_4$. These cytostatic drugs were used: cisplatin (0.5 μg/ml; 1 μg/ml; 2 μg/ml; 4 μg/ml;), oxaliplatin (10 μg/ml; 20 μg/ml; 30 μg/ml) and carboplatin (100 μg/ml; 150 μg/ml; 200 μg/ml; 300 μg/ml). Solutions of DNA with drugs were incubated 24 hours at 37 °C. To remove the excess of platinum-based drug the dialysis by 0,025 μm membrane filter (Millipore, Ireland) for 24 hours at 6 °C was used.

2.3 Sequencing of platinated DNA

For sequencing reaction the DTCS Quick Start Kit (Beckman Coulter, USA) was used. The conditions of 30 cycle sequencing reaction were as follows: 96 °C for 20 s; 50 °C for 20 s and 60 °C for 4 min. A fluorescence-marked DNA fragments were purified by using magnetic particles CleanSEQ (Beckman Coulter). DNA sequencing was performed using Genetic Analysis System CEQ 8000 (Beckman Coulter). After denaturation at 90 °C for 2 min, the fluorescence-marked DNA fragments were separated in 33 cm capillary with 75 μm i.d. (Beckman Coulter), which was filled with a linear polyacrylamide denaturing gel (Beckman Coulter). The separation was run at capillary temperature of 50 °C and voltage of 4.2 kV for 85 min.

3 RESULTS AND DISCUSSION

The DNA fragment (498 bp) was amplified by PCR reaction and when the desired concentration is reached the incubation with selected cytostatic drugs was performed. The obtained adducts were sequenced by Sanger method enabling fluorescent labeling and

subsequently separated by capillary electrophoresis with laser-induced fluorescence detection. It was found that the signal intensity decreased with increasing concentration of the cytostatic drug. In Fig. 1, the analysis of carboplatinated DNA is shown. The three minute part (32.-35. minute of separation) of the electropherogram was taken for the analysis and the average signal intensity was in this range was used. The signal of non-platinated DNA (control) is taken as 100%. In Fig 1A, the signal of thymine was evaluated showing 50% decrease for 50 µg/ml of applied carboplatin. The signal decreased linearly with the concentration and it is shown that when 150 µg/ml of carboplatin is applied, the measured signal is only 6.3% of the control signal. Signal decrease was observed in case of all four bases; however the decrease was 36.5% (Fig. 1B), 31.4% (Fig. 1C) and 13.2% (Fig. 1D) in case of guanine, cytosine and adenine, respectively (when 50 µg/ml of carboplatin is applied).

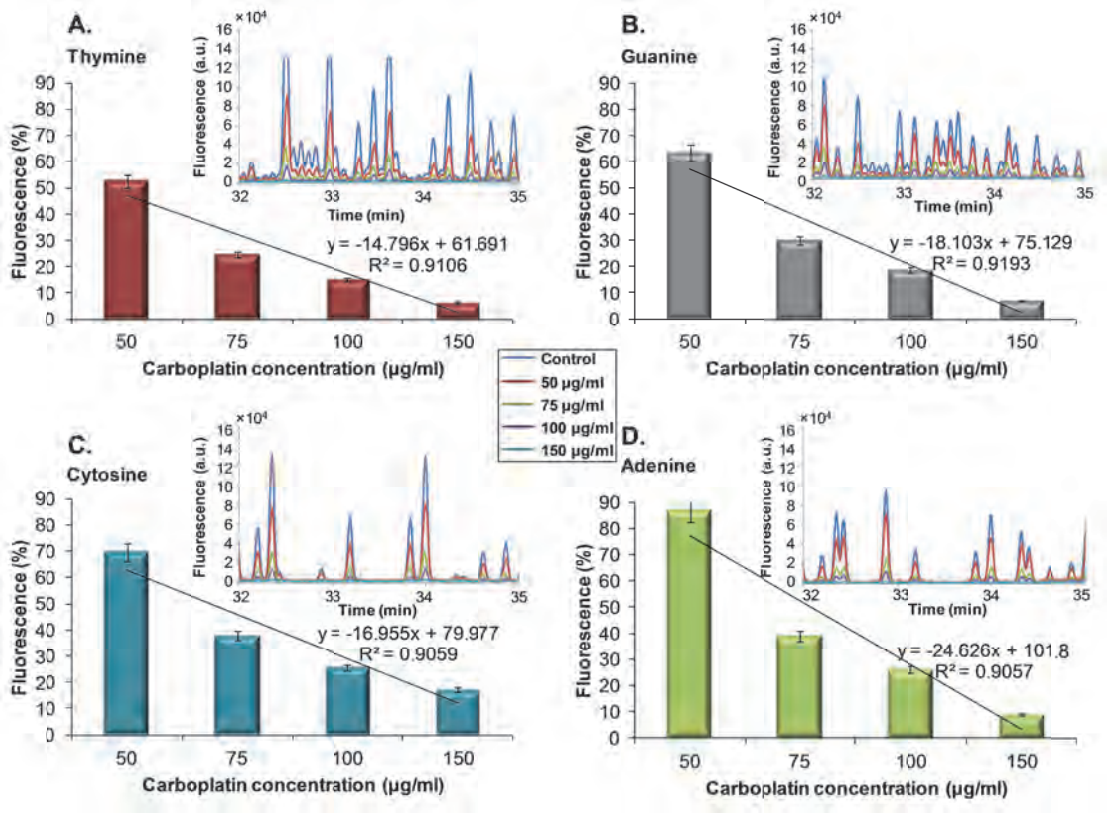

Fig. 1: The dependence of the signal intensity on the concentration of cytostatisc applied. 1A) The signal intensity dependence of tymine (inset: raw electrophoretic data used), 1B) The signal intensity dependence of guanine (inset: raw electrophoretic data used), 1C) The signal intensity dependence of cytosine (inset: raw electrophoretic data used), The signal intensity dependence of adenine (inset: raw electrophoretic data used).

From the results can be concluded that cytostatics bound to the DNA influence the LIF signal for all four bases the same way which suggests that it is not affecting the CE-LIF analysis but the labeling reaction and the fragment synthesis by polymerase. We believe that when the drug is bound to the DNA the polymerase stops the synthesis of the complementary fragment and therefore the signal decreases. Therefore the more of the drug is bound the less fragments is synthesized and the lower the signal.

To verify the hypothesis, DNA adducts with cisplatin and oxalipaltin were prepared and analyzed by the same means. We observed that the concentration of the drug causing the

same level of signal decrease differed for each type of cytostatic drug. To compare the results we calculated the concentration of the drug causing the decrease for 75% of the for control signal. It was found that for carboplatin 75 µg/ml is required. In case of oxalipaltin only 7 µg/ml is needed and finally only 0.3 µg/ml of cisplatin is causing such decrease.
From these results it can be concluded that different cytostatics have different abilities to form adducts with DNA. Our results were verified by electrochemical analysis to determine the amount of platinum present in each sample and as expected the highest amount was determined in the cisplatinated DNA followed by the oxalipaltinated and carbopaltinated DNA samples.

4 CONCLUSION

Using Sanger sequencing method, the influence of platinum-based cytostatics on DNA was investigated. The intensity of the signal decreased linearly with the amount of the cytostatics in the sample in case of all four DNA bases. Moreover it was found that different types of cytostatics have different behavior and influence on the sequencing reaction. These results may also suggest that each generation of the therapeutics has different mechanism of action and efficiency for cancer therapy.

ACKNOWLEDGEMENT

The financial support by NanoBioTECell GA ČR P102/11/1068 and IGA IP19/2012 is highly acknowledged.

LITERATURE

[1] Siegel, R., Naishadham, D., Jemal, A., *CA-Cancer J. Clin.* 2012, *62*, 10-29.
[2] Wang, D., Lippard, S. J., *Nat. Rev. Drug Discov.* 2005, *4*, 307-320.
[3] Rosenberg, B., Van Camp, L., Krigas, T., *Nature* 1965, *205*, 698-699.
[4] Go, R. S., Adjei, A. A., *J. Clin. Oncol.* 1999, *17*, 409-422.
[5] Adams, M., Kerby, I. J., Rocker, I., Evans, A.*, et al.*, *Acta Oncol.* 1989, *28*, 57-60.
[6] Holland, H. K., Dix, S. P., Geller, R. B., Devine, S. M.*, et al.*, *Journal of Clinical Oncology* 1996, *14*, 1156-1164.
[7] Grothey, A., Goldberg, R. M., *Expert Opin. Pharmaco.* 2004, *5*, 2159-2170.
[8] Silva, M. J., Costa, P., Dias, A., Valente, M.*, et al.*, *Environ. Mol. Mutagen.* 2005, *46*, 104-115.
[9] Shendure, J., Mitra, R. D., Varma, C., Church, G. M., *Nat. Rev. Genet.* 2004, *5*, 335-344.
[10] Sanger, F., Nicklen, S., Coulson, A. R., *Proc. Natl. Acad. Sci. U. S. A.* 1977, *74*, 5463-5467.
[11] Eid, J., Fehr, A., Gray, J., Luong, K.*, et al.*, *Science* 2009, *323*, 133-138.
[12] Guo, J., Xu, N., Li, Z. M., Zhang, S. L.*, et al.*, *Proc. Natl. Acad. Sci. U. S. A.* 2008, *105*, 9145-9150.
[13] Krizkova, S., Adam, V., Petrlova, J., Zitka, O.*, et al.*, *Electroanalysis* 2007, *19*, 331-338.
[14] Dospivova, D., Smerkova, K., Ryvolova, M., Hynek, D.*, et al.*, *Int. J. Electrochem. Sci.* 2012, *7*, 3072-3088.

P25 ANALYSIS OF DOXORUBICIN ENCAPSULATION IN APOFERRITIN CAGE BY CAPILLARY ELECTROPHORESIS WITH LASER-INDUCED FLUORESCENCE DETECTION

Maja Stanisavljevic[a], Marketa Ryvolova[a,b], Pavel Kopel[a,b], Vojtech Adam[a,b], Tomas Eckschlager[c], Rene Kizek[a,b]

[a]*Department of Chemistry and Biochemistry, Faculty of Agronomy, Mendel University in Brno, Zemedelska 1, CZ-613 00 Brno, European Union-Czech Republic*
[b]*Central European Institute of Technology, Brno University of Technology, Technicka 3058/10, CZ-616 00 Brno, European Union-Czech Republic*
[c]*Department of Paediatric Haematology and Oncology, 2nd Faculty of Medicine Charles University in Prague and University hospital Motol, Prague, European Union-Czech Republic*
kizek@sci.muni.cz

ABSTRACT

Doxorubicin is an effective cytostatic drug used for treatment of some leukemias and Hodgkin's lymphoma, as well as cancers of the bladder, breast, stomach, lung, ovaries, thyroid, soft tissue sarcoma and/or multiple myeloma. Even though this drug is effective for cancer treatment its toxicity, mainly cardiotoxicity, is limiting the use.
For this reason, encapsulation of the drug into the biocarriers, lowering the toxicity, is widely investigated. One of such carriers may be a protein called apoferritin, which is due to the cavity in its structure, able to incept the molecule of interest. Subsequent decrease of pH leads to the opening of the structure and release of the content.
The aim of this study is to investigate the behavior of the encapsulated doxorubicin using capillary electrophoresis with laser-induced fluorescence detection (CE-LIF).

Keywords: doxorubicin, apoferritin, capillary electrophoresis, cancer, cytostatic drug

1 INTRODUCTION

The ferritins/apoferritin are a family of proteins which in biological systems are used to store iron and prevent its toxic effect to the cells [1]. It is known that ferritin/apoferritin cages are stable in physiological conditions and applicable as a drug delivery system [2]. Drugs are loaded into the apoferritin cages using another characteristic of these proteins. They dissociate at low pH (pH 2) into 24 subunits, allowing loading of the drug and reassemble by changing pH to basic (pH 8.5) [3]. Chemotherapeutic drugs, like doxorubicin, which are used for cancer treatment, are highly toxic and due to the toxicity their usage is limited. Doxorubicin belongs to the anthracycline antibiotics group and it is known for his cardiotoxicity. Using apoferritin cages as carrier of doxorubicin there is possibility to reduce its toxicity and improve efficiency [4, 5].

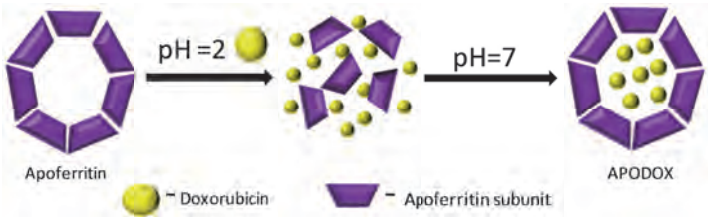

Fig. 1: Loading doxorubicin into apoferritin, by decreasing the pH to 2 causing disassemble of the apoferritin and increasing the pH to 7 to captive doxorubicin in the apoferritin cavity.

In this work we observed behavior of doxorubicin encapsulated in apoferritin using capillary electrophoresis with laser-induced fluorescence detection.

2 EXPERIMENTAL SECTION

Chemicals were purchased by Sigma Aldrich (Czech Republic) in ACS purity. Doxorubicin was purchased by TEVA Pharmaceuticals CR Ltd. (Czech Republic).

2.1 Capillary electrophoresis

Electrophoretic measurement was done using capillary electrophoresis system (Beckman P/ACE 5500) with laser-induced fluorescence detection (λ_{ex} = 488 nm, λ_{em} = 600 nm). Uncoated fused silica capillary (l_{tot} = 47 cm, l_{eff} = 40 cm and ID = 75 µm) was used. 50mMTris-HCl (pH 8.2) was used as background electrolyte. Separation was carried out at 20 kV with hydrodynamic injection for 20 s by 3.4 kPa. Injected sample volume was 0.1 µl. System GOLD was used as operating system for data processing. Sample of APODOX was prepared with doxorubicin concentrations of 0, 6.25, 12.5, 25, 100, 200 µg/ml, respectively by mixing it with apoferritin in concentration of 1 mg/ml. Procedure considered disassembling of apoferritin preformed by decreasing pH to 2 and than increasing pH to 7 to trap doxorubicin into cavity. APODOX was separated from the rest of the solution by dialysis. Under the previously written injection conditions with each injection we took 0.625, 1.25, 2.5, 10 and 20 ng of doxorubicin respectively.

2.2 Fluorimetric analysis

Fluorescence spectra were acquired by multifunctional microplate reader Tecan Infinite 200 PRO (TECAN, Switzerland). 480 nm was used as an excitation wavelength and the fluorescence scan was measured within the range from 510 to 850 nm per 5 nm steps. Each intensity value is an average of 5 measurements. The detector gain was set to 100. The absorbance was acquired within the range from 230 to 1000 nm with 5 nm steps as an average of 5 measurements per well. The sample (50 µl) and apoferritin (0 µg/ml of doxorubicine) as a blank probe (50µl) were placed in transparent 96 well microplate with flat bottom by Nunc (ThermoScientific, USA).

3 RESULTS AND DISCUSSION

Due to its structure doxorubicin exhibits intensive fluorescence and therefore selective optical methods such as fluorimetry and CE-LIF can be used for the analysis. In Fig. 2, emission spectra of doxorubicin encapsulated in apoferritin (APODOX) is shown. The emission maximum of APODOX is the same as the maximum of non-encapsulated doxorubicin - 600 nm and the dependence of the fluorescence on the doxorubicin concentration is linear.

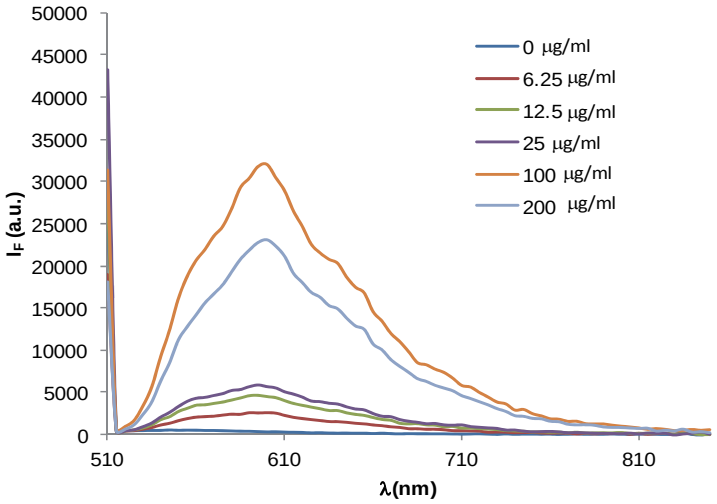

Fig. 2: Emission spectra of APODOX and its dependence on the concentration of encapsulated doxorubicin (0, 6.25, 12.5, 25, 100, 200 μg/ml). For fluorescence spectra excitation wavelength was 480 nm and fluorescence scan was measured in the range from 510 to 850 nm per 5 nm step.

Analysis of APODOX by CE-LIF shown, that two peaks with migration time 4.4 min (peak x) and 4.9 min (peak y) were present. As shown in Fig. 3 increasing concentration of doxorubicin in APODOX led to the increase of the peak heights. However the concentration of doxorubicin higher than 100 μg/ml led to the change in the shape of second peak (peak y).

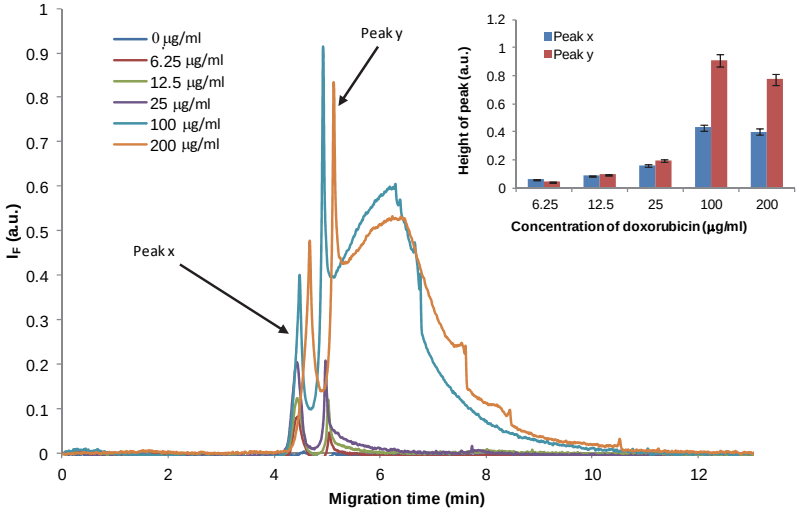

Fig. 3: CE-LIF of APODOX solutions with increasing concentraation of doxorubicin encapsulated in apoferritin, inset: dependence of the peah height on the concentration of doxorubicin in APODOX.

To identify the peaks in the electropherogram, the pH of the sample was decreased, which opened the structure and releases the doxorubicin into solution.

In Fig. 4, the electropherograms of the samples with different pH are shown. It can be seen that the height of peak x is increasing with the pH decrease. Based on this results we believe that peak x belongs to the free doxorubicin.

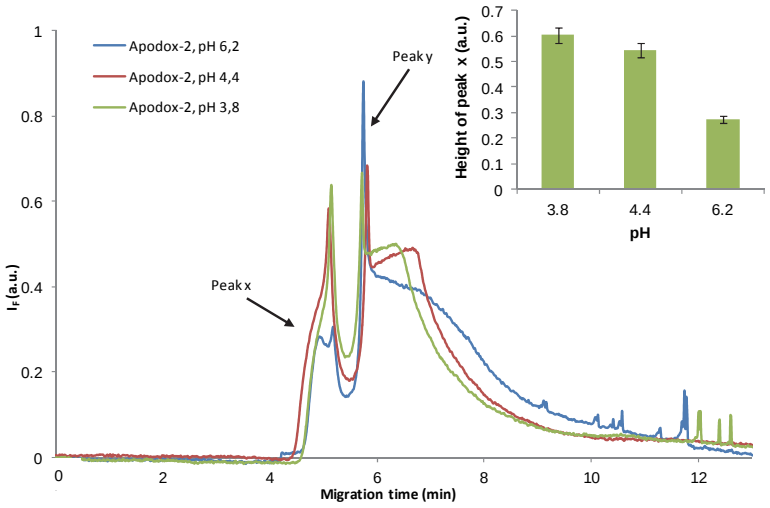

Fig. 4: CE-LIF of APODOX sample in different pH, inset: increase of the peak x height depending on the pH decrease.

4 CONCLUSION

It was found that apoferritin encapsulated doxorubicin is providing intensive fluorescence and its behavior can be investigated by CE-LIF. The structural changes of this nanocarrier under different conditions can be monitored by the peak shape changes. Based on the results can be concluded that complex processes are taking place during the structure opening and closing. This needs to be investigated in more details in the future.

ACKNOWLEDGEMENT

The financial support by CYTORES GA ČR P301/10/0356 and CEITEC CZ.1.05/1.1.00/02.0068 is highly acknowledged.

LITERATURE

[1] Zhao, Z., Malik, A., Lee, M. L., Watt, G. D., *Anal. Biochem.* 1994, *218*, 47-54.
[2] Dospivova, D., Hynek, D., Kopel, P., Bezdekova, A.*, et al.*, *Int. J. Electrochem. Sci.* 2012, *7*, 6378-6395.
[3] Ma-Ham, A. H., Wu, H., Wang, J., Kang, X. H.*, et al.*, *J. Mater. Chem.* 2011, *21*, 8700-8708.
[4] Tokarska-Schlattner, M., Wallimann, T., Schlattner, U., *Comptes Rendus Biologies* 2006, *329*, 657-668.
[5] Kizek, R., Adam, V., Hrabeta, J., Eckschlager, T.*, et al.*, *Pharmacol. Ther.* 2012, *133*, 26-39.

P26 VERY FAST ELECTROPHORETIC SEPARATION OF NEUROTRANSMITTERS ON COMMERCIAL INSTRUMENTS USING A COUPLED CAPILLARY

Petr Tůma[a], František Opekar[b], Eva Samcová[a]

[a] *Charles University in Prague, Third Faculty of Medicine, Institute of Biochemistry, Cell and Molecular Biology, Ruská 87, 100 00 Prague 10, Czech Republic, petr.tuma@lf3.cuni.cz*
[b] *Charles University in Prague, Faculty of Science, Department of Analytical Chemistry, Albertov 2030, 128 43 Prague 2, Czech Republic*

ABSTRACT

A capillary formed by connecting of two capillaries with different inner diameters (25 and 100 μm) was tested for electrophoretic separation at high electric field intensities. The laboratory made coupled capillary was directly placed into the cassette of Agilent CE apparatus and was tested for separation of dopamine, noradrenaline and adrenaline in a background electrolyte of 20 mM citric acid/NaOH, pH 3.2. An intensity of 2.7 kV cm^{-1} was attained in the separation part of the capillary, which is 2.9 times more than maximum intensity value attainable in the common capillary with the shortest possible length at maximum voltage +30 kV. At these high electric field intensities, the migration times were 12.3 s (dopamine), 12.8 s (noradrenaline), 13.3 s (adrenaline); and the attained separation efficiencies were between 2350 and 2760 plates s^{-1}.

Keywords: Coupled capillary; High-speed analysis; Neurotransmitters.

1 INTRODUCTION

At the present time, instruments are available on the market for capillary electrophoresis (CE), which are reliable and enable automatic analysis of a large number of samples. These instruments employ separation capillaries with lengths from 30 to 100 cm, with a maximum separation voltage of 30 kV. Under these conditions, the separation time is between 5 and 30 min [1, 2]. However, these times are too long for a number of applications.

The separation time can be substantially shortened to less than 100 s in commercial CE systems by a suitable modification of the separation program. This technique is termed high-speed CE [3]. These methods include primarily: shortening the effective length of the capillary by injecting the sample into the short end of the capillary – short-end injection [4, 5]; the acceleration of the movement of the analyte in the capillary under pressure (pressure-assisted CE) [6] or under electroosmotic flow using EOF modifiers [7]. However, when these techniques are used, the value of the effective voltage, U_{ef}, i.e. the voltage between the sample injection site and the detector, is shorter compared with the classical CE arrangement (at short-end injection) or, in the best case, is the same (for accelerated transport). This is disadvantageous, because the separation efficiency expressed in terms of the number of plates, N, is directly dependent on U_{ef} according to the relationship $N = \frac{u \cdot U_{ef}}{2D}$, where u is the electrophoretic mobility and D is the diffusion coefficient. Consequently, a technique must be used in which high N values are attained by utilizing most of the maximum voltage provided by the instrument for the actual separation.

This can be achieved using one BGE in a system formed of two connected capillaries with different internal diameters (*id*) [8]. The separation is performed in the part of the capillary with small *id*, in which the electric field intensity is greater than in the remaining part of the capillary with larger *id*. This principle was employed in the work [1], where the electric field intensity (E) of more than 3 kV cm^{-1} was attained in home-made CE instrument.

This article describes a system utilizing a combination of two capillaries with various *id* for fast separations on a standard CE system using the normally provided functions – hydrodynamic sample injection and UV detection.

2 EXPERIMENTAL

2.1 Connecting two capillaries with different internal diameters

The combined capillary was created using standard fused silica capillaries covered with polyimide with an outer diameter (*od*) of 363 µm (Composite Metal Services, UK). The separation part of the capillary, *id* 25 µm, length L_{25} = 9.7 cm, and the auxiliary capillary, *id* 100 µm, length L_{100} = 22.9 cm, were connected using thick-walled PVC tubes with *id* somewhat smaller than *od* of the connected capillaries. The tube with a length of 2 cm was first softened in chloroform so that it could be easily pulled over the pre-cut, ground and closely joined ends of the connected capillaries. Following evaporation of the chloroform, the tube shrinks and adheres closely to the surface of the capillary. For safety, the tube was glued at both ends to the surface of the capillary using fast-drying epoxide glue. This simple method was used to form a hydrodynamically sealed connection of the two separation capillaries – this system will be hereinafter termed a coupled capillary. A detection window was formed in the separation part of the capillary and the capillary was installed in a standard electrophoresis cassette so that, following installation in the CE apparatus, the separation part of the capillary is directed towards the terminal vessel (see Fig. 1).

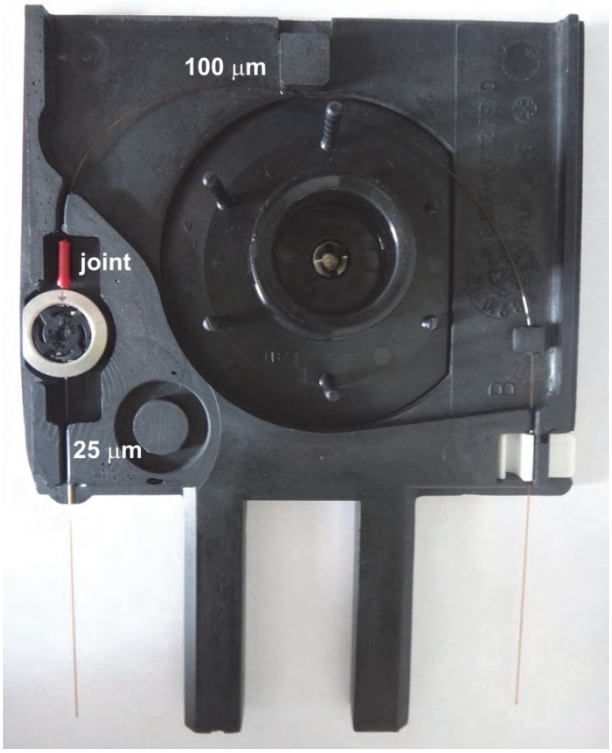

Fig. 1 Photograph of a coupled capillary inserted into a cassette.

2.2 CE experiments

Electrophoretic measurements were carried out using the HP^{3D}CE system (Agilent Technologies, Waldbronn Germany) with an in-built diode-array detector. The separations were performed in the short-end injection mode with an effective length of the coupled capillary of L_{ef} = 8.4 cm (distance from the injection end to the detector) and overall length of L = 32.6 cm. The sample was injected hydrodynamically at 200 mbar s. The separation in the coupled capillary was compared with the separation performed in a standard capillary with *id* 25 µm and the same effective and overall lengths. In this case, the sample was injected at a rate of 600 mbar s; under these conditions, the amount of sample injected is the same as for the coupled capillary. All the separations were performed under the following conditions: BGE, 20 mM citric acid/NaOH (pH 3.2), separation voltage, U = +30 kV, temperature of the cassette, 25 °C, UV detector, 200 nm. The inner surface of the capillaries was covered using INST coating solution (Biotaq, U.S.A.) to prevent electroosmotic flow. The tested sample was

a mixture of dopamine, noradrenaline and adrenaline with a concentration of 100 μM in water. All the chemicals used were of the p.a. purity.

3 RESULTS AND DISCUSSIONS

When the short-end injection method was used in the Agilent instrument, the minimum length of the separation part of the capillary was L_{25} = 9.7 cm for technical reasons; at a voltage of U = 30 kV and overall capillary length of L = 32.6 cm, this corresponds to an electric field intensity of E = 2.70 kV cm^{-1}. This value is 2.93 times higher than that in a capillary of the same length with uniform *id* (E = 30 kV/32.6 cm = 0.92 kV cm^{-1}).

The coupled capillary was tested for separation of a mixture of three neurotransmitters with similar chemical structures (dopamine, noradrenaline and adrenaline) that can be separated only using a system with high separation efficiency. The neurotransmitters are completely dissociated in the acidic BGE employed and move like cations in an electric field. Fig. 2 and Table 1 give the results obtained for the separation performed using the coupled capillary compared with the results for the comparative standard 25 μm capillary.

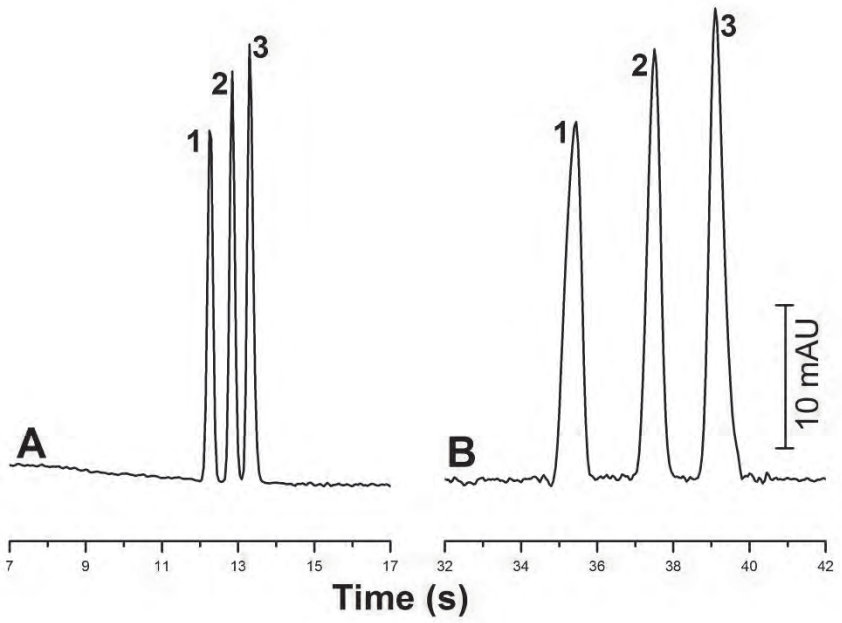

Fig. 2 Separation of 100 μM of a model mixture of dopamine (1), noradrenaline (2) and adrenaline (3) in the coupled capillary (A) and 25 μM capillary (B). BGE, 20 mM citric acid/NaOH, pH 3.2; voltage +30 kV, current 15.4 μA (A) and 5.3 μA (B).

Table 1 Parameters of CE separation of a mixture of neurotransmitters in a coupled capillary and standard 25 μm capillary.

	Coupled capillary					**25 μm capillary**				
	Time t_M (s)	Height (mAU)	Area (mAU.s)	N (10^3 m^{-1})	N/t_M (s^{-1})	Time t_M (s)	Height (mAU)	Area (mAU.s)	N (10^3 m^{-1})	N/t_M (s^{-1})
Dopamine	12.3	26.1	4.3	374	2560	35.3	26.2	12.1	383	910
Noradrenaline	12.8	28.8	4.6	422	2760	37.5	29.0	12.5	485	1090
Adrenaline	13.3	31.0	5.5	372	2350	39.2	34.3	15.0	396	850

The migration times, t_M, in the coupled capillary are 2.9 times lower compared with the migration times in the 25 μm capillary. This reduction in the migration time exactly corresponds to the calculated ratio of the intensities (E) in the two capillaries. The number of theoretical plates (N) and resolution (R) of neighbouring peaks, which are standardly

employed to characterize the efficiency of the separation process, are somewhat lower in the coupled capillary compared to the 25 μm capillary. For very fast separations, it is preferable to express the separation efficiency as the number of theoretical plates per unit time, $\frac{N}{t_M}$, which corresponds better to the requirement of separating a large number of substances in a short time [1]. The ratio of parameters $\frac{N}{t_M}$ in the coupled capillary and the 25 μm capillary is 2.5 to 2.8. This value is close to 2.9, corresponding to the ratio of E and U_{ef} in the coupled capillary and 25 μm capillary and demonstrated the importance of E for attaining high separation efficiency.

4 CONCLUSIONS

It is demonstrated in the work that advantageous separation in coupled capillaries can be simply performed in standard, commercially available electrophoretic systems. It is thus possible to separate substances at high electric field intensities, close to 3 kV cm^{-1}, which could so far be attained only on specialized laboratory equipment. High electric field intensity is localized in the capillary with small *id*, in which good removal of Joule heat is ensured. Thus, the preconditions are fulfilled for attaining critical migration times and high separation efficiencies.

For the separation of the tested neurotransmitters, the migration times were about 10 s and the separation efficiencies equalled 2000 to 3000 plates s^{-1}. It is apparent that the coupled capillary is an effective instrument for rapid analysis of extensive sets of samples. Coupled capillaries are not available on the market but can be prepared in very good quality by a simple method in the laboratory.

ACKNOWLEDGEMENTS

Financial support from the Grant Agency of the Czech Republic, grants No. P206/10/1231 and No. P206/11/0707; the Charles University in Prague, the Projects PRVOUK P31 and UNCE 204015/2012; the Ministry of Education, Youth and Sports, Czech Republic, Research Project No. MSM0021620857, is gratefully acknowledged.

LITERATURE

[1.] Monnig, C. A., Jorgenson, J. W., *Analytical Chemistry* 1991, *63*, 802-807.
[2.] Opekar, F., Coufal, P., Stulik, K., *Chemical Reviews* 2009, *109*, 4487-4499.
[3.] Altria, K. D., *Journal of Chromatography* 1993, *636*, 125-132.
[4.] Altria, K. D., Kelly, M. A., Clark, B. J., *Chromatographia* 1996, *43*, 153-158.
[5.] Tuma, P., Samcova, E., *Chemické Listy* 2009, *103*, 919-923.
[6.] Wan, H., Holmen, A., Nagard, M., Lindberg, W., *Journal of Chromatography A* 2002, *979*, 369-377.
[7.] Zemann, A. J., *Journal of Chromatography A* 1997, *787*, 243-251.
[8.] Nashabeh, W., El Rassi, Z., *Journal of Chromatography* 1993, *632*, 157-164.

P27 KINETIC AND THERMODYNAMIC PROPERTIES OF POROUS SHELL PARTICLES LC STATIONARY PHASES

Nikola Vaňková, Petr Česla, Jan Fischer

Department of Analytical Chemistry, Faculty of Chemical Technology, University of Pardubice, Studentská 573, 532 10 Pardubice, Czech Republic,
nikola.vankova@student.upce.cz

ABSTRACT

The aim of the work was to evaluate the efficiency and selectivity of selected columns for reversed-phase liquid chromatography packed with the porous shell particles. Kinetic properties of porous shell particles, dependent on band broadening of the solute, were evaluated using series of homologic alkylbenzenes. It is possible to express thermodynamic properties of separation by selectivity. Specific interactions contributing to the selectivity of separation of 23 phenol derivatives were evaluated using linear free energy relationship model (LFER) employing molecular structural descriptors. Similarities and differences between the columns were classified using multiple linear regressions of retention data and cluster analysis based on the similarity dendrograms. Two columns with the most different retention mechanism can be employed for orthogonal separations in two-dimensional system. The differences in selectivity are illustrated in separation with gradient elution of mixture of phenol derivatives.

Keywords: Porous shell particles, efficiency, phenol derivatives, selectivity, linear free energy relationship model

1 INTRODUCTION

Separation on the porous shell particles represents one of the recent trends in the modern liquid chromatography. Their advantage is in high efficiency, whose is comparable with efficiency of separation on the columns packed with fully porous particles, which size is under 2 µm. Columns packed with porous shell particles partially decrease the system pressure in comparison to fully porous particles[1,2]. In this study, we tested kinetic and thermodynamic properties of seven columns packed with the porous shell particles with different types of chemically bonded nonpolar (reversed-phase system) stationary phases. Kinetic properties were evaluated by the A, B and C-terms of the Van Deemter's equation, describing the contributions to the band broadening of the chromatographic zones. The thermodynamic properties, respectively separation selectivity, were expressed by linear free energy relationship (LFER) model.

In the linear free energy relationship model, the descriptors (solvation parameters) are used based on the molecular characteristics of the solutes. These descriptors are thermodynamic Gibbs energy related quantities and they are employed to describe Gibbs energy related data such as chromatographic retention. The correlation between logarithm of retention factor, log k, and solute descriptors can be characterized by equation:

$$\log k = c + rR_2 + s\pi_2^* + a\sum\alpha_2^H + b\sum\beta_2^H + vV_x \quad (1)$$

where R_2 is excess molar refraction, π_2^* is solute dipolarity/polarizability, $\sum\alpha_2^H$ is the overal hydrogen bond-donor acidity, $\sum\beta_2^H$ is the overal hydrogen bond-acceptor basicity, V_x is the McGowan characteristic volume and c is the intercept.[3,4]

In this work, the LFER model was applied to the set of retention data of phenolic compounds measured on seven different reversed-phase columns packed with porous shell particles. Parameters obtained by the multilinear regression analysis of the LFER model were

quantified with cluster analysis. Similarities between columns were evaluated by hierarchical clustering and can be graphically presented in a tree-form dendrogram. Terminal nodes at the bottom of the tree are the clusters containing all objects, the liquid chromatography columns, in this case.The root of the dendrogram is the single cluster containig all objects. The vertical axis represents similarity level. When the tree is cut parallely with horizontal axis, we can get amount of similarity expressed in percents.[5, 6]

2 EXPERIMENTAL

2.1 Chemicals and columns

Evaluation of kinetic a thermodynamic properties was performed on the series of the columns packed with porous sell particles (Table 1). The homologous series of n-alkylbenzenes were used for evaluation of kinetic properites. The standards of benzene, toluene, ethylbenzene, propylbenzene, butylbenzene and pentylbenzene were obtained from Sigma-Aldrich (Steinheim, Germany). Aqueous/acetonitrile mobile phases were prepared by mixing of appropriate amount of redistilled water and gradient grade acetonitrile. Standards of phenol derivatives (Table 2) purchased at Sigma-Aldrich were used to evaluate of the selectivity of columns. In this separations, the Formic acid was from Penta (Chrudim, Czech Republic).

Table 1: Columns used for study of kinetic and thermodynamic properties

Column	Stationary phase	Lenght (cm)	Diameter (mm)	Particle size (µm)	Porosity (Å)
Ascentis Express	C_{18}	15,00	3,00	2,70	90
Ascentis Express	C_8	15,00	3,00	2,70	90
Ascentis Express	F5	15,00	3,00	2,70	90
Ascentis Express	phenyl-hexyl	15,00	3,00	2,70	90
ACE 3	C_{18}-PFP	15,00	3,00	3,00	100
Agilent Poroshell 120	C_{18}	15,00	3,00	2,70	120
Kinetex	C_{18}	15,00	3,00	2,60	100

Table 2: Standards of phenol derivatives

Standards	pKa *	No.	Standards	pKa *	No.
3,4-dinitrophenol	5,42 ± 0,10	1	2,4-dinitro-6-chlorophenol	2,42 ± 0,44	12
2,3-dinitrophenol	5,01 ± 0,25	2	2,4,6-triiodphenol	6,47 ± 0,23	13
3-nitrophenol	8,34 ± 0,10	3	2,5-dimethylphenol	10,42 ± 0,1	14
2,5-dinitrophenol	5,35 ± 0,19	4	3,4-dimethylphenol	10,38 ± 0,18	15
2,6-dinitrophenol	3,49 ± 0,10	5	3,5-dimethylphenol	10,19 ± 0,10	16
2,4-dinitrophenol	4,04 ± 0,22	6	4-chlorophenol	9,47 ± 0,13	17
4-nitrophenol	7,23 ± 0,13	7	2-bromo-4-chlorophenol	7,98 ± 0,18	18
2-nitrophenol	7,14 ± 0,14	8	2-bromo-4-nitrophenol	5,36 ± 0,22	19
2,4,6-trinitrophenol	0,62 ± 0,10	9	2-bromophenol	8,43 ± 0,10	20
2-methylphenol	10,32 ± 0,10	10	4-bromo-2,6-dimethylphenol	10,10 ± 0,23	21
5-nitro-2-aminophenol	8,08 ± 0,19 1,24 ± 0,1	11	4-bromo-2-nitrophenol	6,28 ± 0,14	22
			4-bromophenol	9,34 ± 0,13	23

*Calculated using Advanced Chemistry Development (ACD/Labs) Software V11.02 (© 1994-2012 ACD/Labs)

2.2 APPARATUS AND METHODOLOGY

Liquid chromatography analyses were performed using Shimadzu liquid chromatograph equiped with degaser DGU $20A_5$, two high-pressure pumps LC - 30 AD (Shimadzu, Japan), Valco Vici high-pressure sample injector, termostated column compartment and UV/VIS detector SPD 20 A (all Shimadzu,Kyoto Japan). Analytes were monitored at wavelenght 254 nm.

The kinetic properties of the columns were characterized in water/acetonitrile mobile phases at concentrations of 70 %, 80 % and 90 % (v/v) acetonitrile using temperature of 40 °C, 50 °C and 60 °C. The flow rate of the mobile phase was set in the range from 0,05 ml/min to 1,5 ml/min. The hold-up volume of the columns was determined as elution volume of uracil.

The retention characteristic of phenol derivatives were measured in mobile phase consisting of redistilled water/acetonitrile and formic acid as an additive (3%, v/v). The concentration of acetonitrile in the water was from 35 to 90 %. The flow of mobile phase was 0,41 ml/min and the column temperature was 40 °C.

3 TABLES AND ILUSTRATIONS

The LFERs model was applied to find the differences between used columns. Based on the evaluation of the selectivity using dendrograms, the Poroshell C_{18} and Ascentis Expess columns have the most different retention mechanism compared to the columns Ascentis Express F5 and ACE 3 C_{18}-PFP (Figure 1), as the similarity of the clusters for these two pairs is the lowest.

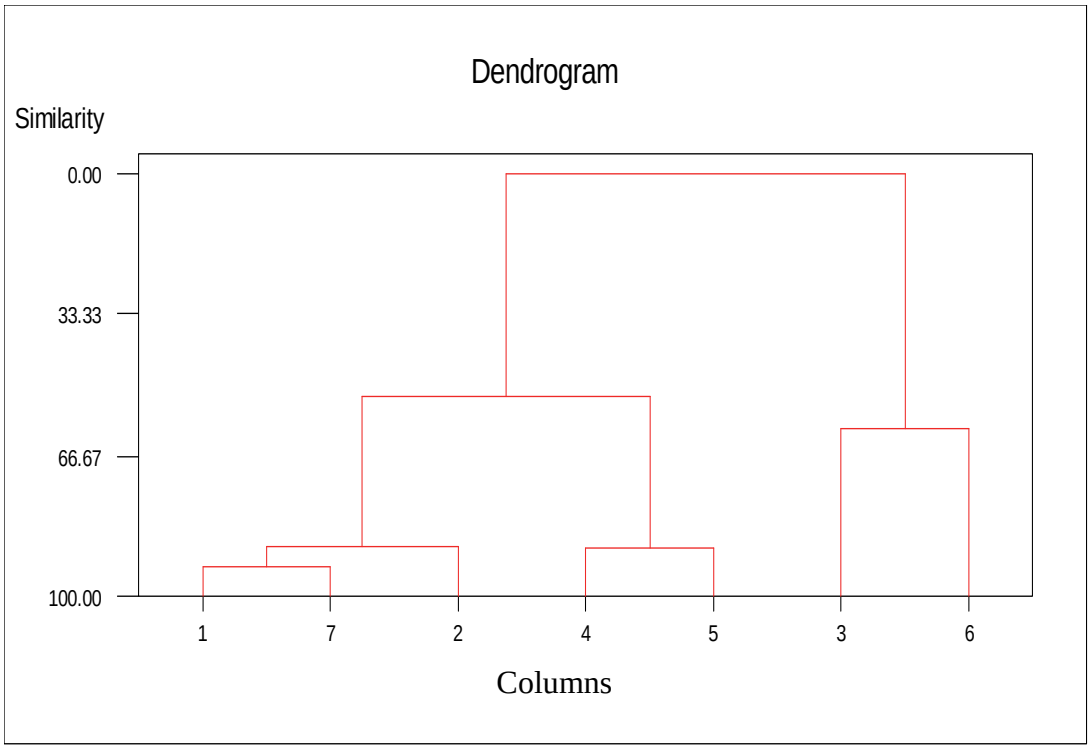

Fig. 1: 1-Ascentis Express C_8, 2-Ascentis Express C_{18}, 3-Ascentis Express F5, 4-Ascentis Express phenyl-hexyl, 5-Kinetex C_{18}, 6-ACE 3 C_{18}-PFP, 7-Poroshell C_{18}

The different retention mechanisms are illustrated by the gradient elution separation of the mixture of 23 phenol derivatives shown on the Figures 2 and 3. Althought the separation of all phenol derivatives is not complete, the high orthogonality of the selected combination of columns makes them ideal for application in two-dimensional liquid chromatography for separation of such complex mixture. Moreover, the application of porous

shell particles packed columns is highly suitable for the both, first and second dimension of the two-dimensional system, due to the fast analysis with high efficiency under moderate pressure generated.

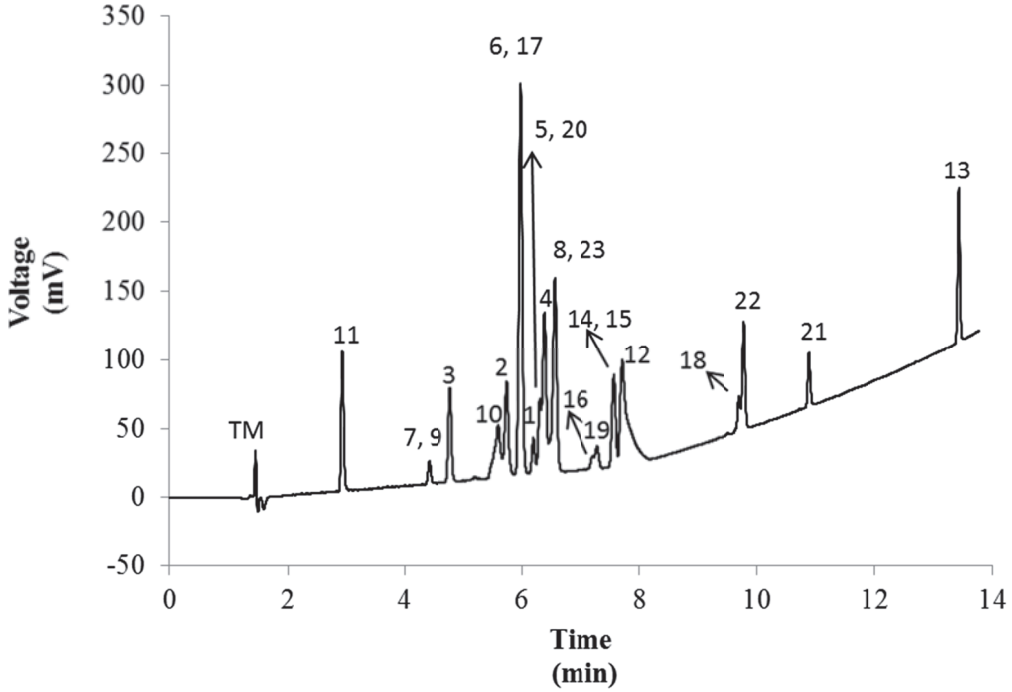

Fig. 2: Poroshell C_{18}: Gradient elution of mixture of phenol derivates, gradient 0,01 min-25% acetonitrile, 6,5 min-40% acetonitrile, 13,5 min-90% acetonitrile, mobile phase flow 0,41 ml/min, 40 °C. The numbers of the compounds corresponds to the table 2.

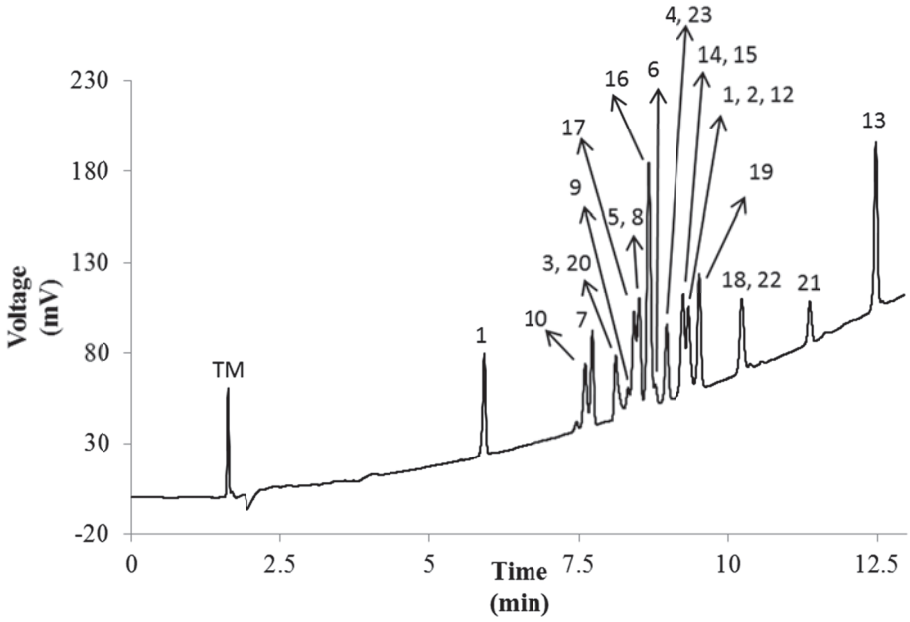

Fig. 3: Ascentis Express F5: Gradient elution of mixture of phenol derivates, gradient 0,01 min – 5% acetonitrile, 17 min – 90% acetonitrile, mobile phase flow 0,41 ml/min, 40 °C. The numbers of the compounds corresponds to the table 2.

4 CONCLUSION

In this work, the efficiency and selectivity of reversed-phase columns packed with the porous shell particles were evaluated. The optimal linear velocity of the mobile phase flow was selected using dependences of the height equivalent of the theoretical plate on the linear velocity for the set of homologous n-alkylbenzenes. Retention characteristics of 23 phenol derivatives used for calculation of contributions to the selectivity of separation by linear free energy relationship model (LFER). Similarities and differences between the columns were classified using multiple linear regression and by cluster analysis based on the similarity dendrograms, the combination of columns with highest degree of orthogonality was selected. The Poroshell C18 and Ascentis Express C8 columns in combination with Ascentis Express F5 and ACE 3 C18-PFP provided the highest differences in retention and separation selectivity of phenol derivatives. The differences in selectivity of separation were demonstrated by the gradient separation of mixture of phenol derivatives.

LITERATURE

[1.] McCalley V., D., *J. Chromatogr., A* 2011, *1218*, 2887–2897.
[2.] Guiochon, G.; Gritti, F, *J. Chromatogr., A* 2011, *1218*, 1915–1938.
[3.] Szepesy, L., *J.Sep.Sci*. 2003, *26*, 201–214.
[4.] Abraham M, H.; Rosés, M., *J. Phys. Org. Chem*. 1994, *7*, 672–684
[5.] Jandera, P.; Vyňuchalová, K.; Hájek, T.; Česla, P.; Vohralík, G., *J. Chemom*. 2008, *22*, 203–217.
[6.] Breretin G, R. Applied chemometrics for scientists; John Wiley & Sons, New York, 2007.

P28 INTEGRATED CHIP ELECTROPHORESIS AND MAGNETIC PARTICLE ISOLATION USED FOR DETECTION OF HEPATITIS B VIRUS OLIGONUCLEOTIDES

Jiří Vysloužil[a], Markéta Ryvolová[a,b], Vojtěch Adam[a,b], Jaromír Hubálek[b,c], René Kizek[a,b]

[a] *Department of Chemistry and Biochemistry, Faculty of Agronomy, Mendel University in Brno, Zemedelska 1, 613 00 Brno, Czech Republic*
[b] *Central European Institute of Technology, Brno University of Technology, Technicka 3058/10, CZ-616 00 Brno, European Union-Czech Republic*
[c] *Faculty of Electrical Engineering and Communication, Brno University of Technology, Technicka 3058/10, 616 00 Brno, Czech Republic*
kizek@sci.muni.cz

ABSTRACT

In this study, an integrated isolation of Hepatitis B virus (HBV) specific DNA fragment by magnetic nanoparticles (MNPs) and its immediate analysis by capillary gel electrophoresis was performed. Microfluidic CE chip was used to accommodate the complete process of DNA isolation by MNPs including hybridization and thermal denaturation followed by CE separation. For isolation on MNPs, specific streptavidin-biotin interaction was used to bind complementary HBV fragment to magnetic particles. The commercial CE chip was successfully used to perform a HBV fragment isolation and detection with low limit of detection.

Keywords: microfluidic chip, hepatitis B virus, chip electrophoresis, magnetic particle

1 INTRODUCTION

Hepatitis B virus caused worldwide several epidemics to the world's population. About a third of the world population has been infected in one point of their lives, including 350 million who are chronic carriers [1]. The global epidemic of hepatitis B and C is a serious public health problem. Hepatitis B and C are the major causes of chronic liver disease and liver cancer. Worldwide, liver cancer is the third most common cause of cancer mortality, with approximately 550,000 annual deaths [2]. Rapid and sensitive detection is therefore a key step to effectively diagnose and stop the virus to break out in global scale. For this purpose, there is a need for a quick and cheap method to identify the disease. Microfluidic devices, such as CE chip proved to be a suitable method to perform a quick and easy analysis of samples containing specific sequences of viral DNA [3]. In this work the commercially available chip CE platform dedicated for analysis of DNA, RNA and proteins was used to accommodate the isolation process carried by magnetic nanoparticles.

2 MATERIALS AND METHODS

2.1 Instrumentation

Chip electrophoresis station (Experion, Bio-rad, USA), DNA 1K chip + kit (Bio-rad, USA) was used to perform the experiment. Denaturation of DNA fragments in CE-chip was carried out by instrument, developed by Brno University of Technology. Electrochemical measurements were performed with AUTOLAB PGS30 Analyzer (EcoChemie, Netherlands) connected to VA-Stand 663 (Metrohm, Switzerland), using a standard cell with three electrodes.

2.2 Oligonucleotides

HBV and biotinylated HBV oligonucleotides with sequence were purchased from Sigma Aldrich (Czech Republic). The sequence of these HBV fragments is following: (5'-GGCAGAGGTGAAAAAGTTGC-3') and biotynylated sequence (3'CCGTCTCCACTTTTTCAACG-5'). DNA solutions needed for the experiment were prepared in ACS purity.

2.3 Magnetic particles

Streptavidin-coupled magnetic beads (Invitrogen, USA) were used to selectively isolate HBV fragments of DNA from the sample as shown in the scheme (Fig. 1).

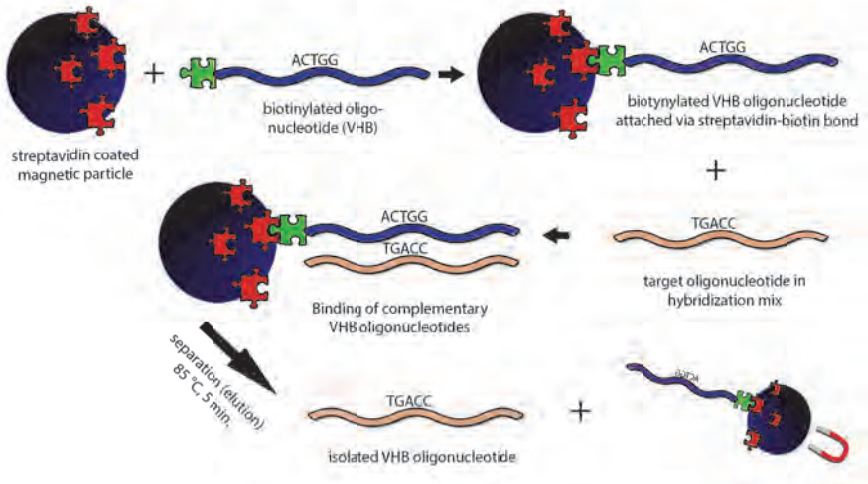

Fig. 1: Scheme of MNPs isolation.

The whole experiment took place inside of one CE chip and magnet was placed underneath the chip. Magnetic beads placed in the microwell of the chip can be easily manipulated by magnetic field caused by the magnet. After the isolation of desired HBV fragment, the chip was heated up to 85°C on a heating/cooling device with Peltier Thermo-Element, constructed for this purpose. After thermal denaturation, bounded HBV fragment was released from the magnetic beads and could be immediately analyzed by CE. To prevent preconcentration during evaporation of sample (denaturation), the sample was diluted to original volume. In next step, only 1 µl of sample was used (according to the instructions in Bio-rad DNA kit). The whole isolation process is briefly described on the following scheme (Fig. 2).

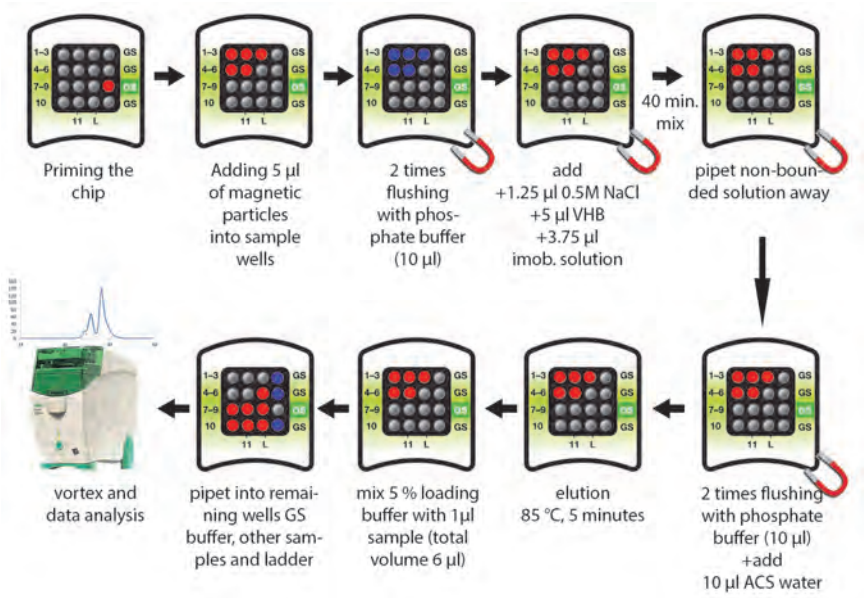

Fig. 2: Scheme of CE chip isolation.

3 RESULTS AND DISCUSSION

In first step, detection of single strand oligonucleotide HBV (ssODN HBV) fragment was carried out. Linear response of the chip-based CE to the concentration of ssODN HBV fragment was determined with correlation coefficient of R^2 = 0.9947. Limit of detection of 50 ng/ml was calculated (Fig. 3) with relative standard deviation (RSD) of migration time and peak height of 3.1% and 11.4%, respectively. These results were also compared to those obtained by square-wave voltammetry using hanging mercury drop electrode (HMDE). Correlation coefficient of the calibration curve was R^2 = 0.9993 and limit of detection was 31ng/ml (3 S/N).

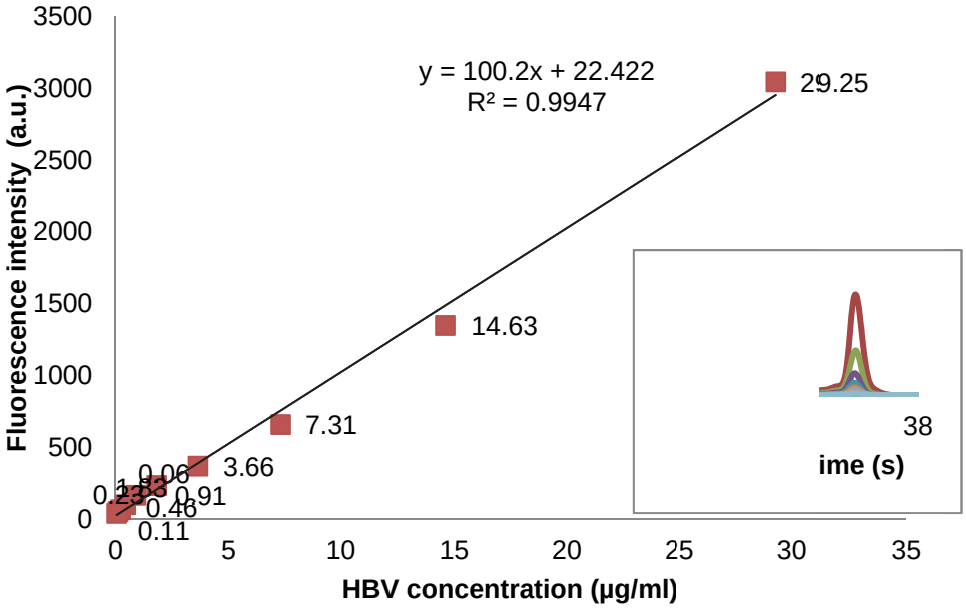

Fig. 3: ssODN HBV signal calibration on CE chip, concentrations: 29.25; 14.63; 7.31; 3.66; 1.83; 0.91; 0.46; 0.23; 0.11; 0.06 µg/ml. Sample volume: 1 µl. Chip analysis procedure according to the CE chip manufacturer instruction manual.

In following experiment, isolation by streptavidin-coated MPs was performed in the test tubes. Isolated HBV fragments were loaded on chip and successfully analyzed.

The final trial concerned complete isolation on MNPs in the chip wells, denaturation and analysis on Experion chip electrophoresis station.

It was found that magnetic nanoparticles used do not migrate through the channels of the chip when filled with supplied gel and therefore when the isolation is carried out in the chip well there is no need to remove the particles prior to the CE separation. Based on this knowledge, we carried out the isolation procedure by magnetic nanoparticles coated with streptavidin. These particles were surface modified with an oligonucleotide complementary to the HBV specific nucleotide.

Acquired peak in the electropherogram shows successful isolation and detection of desirable oligonucleotides (Fig. 4).

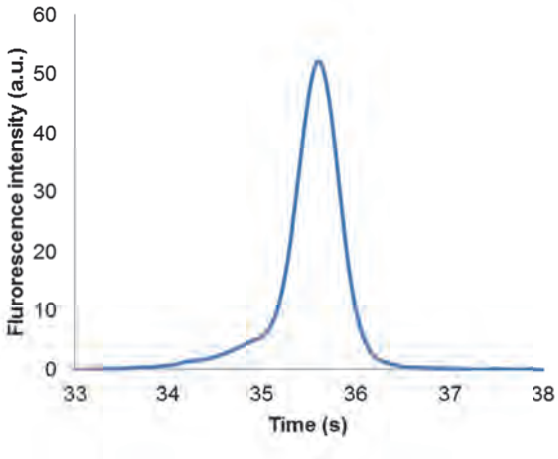

Fig. 4: Electropherogram acquired after complete process of ssODN HBV isolation, denaturation and detection on CE chip electrophoresis, Original concentration of ssODN HBV: 7.31 µg/ml, Sample volume: 1 µl. Chip handling: see figure 2.

Isolation of nucleic acids by magnetic nanoparticles and its automation was described before as very powerful tool for rapid analysis of DNA and RNA [4]. Patent of MNPs isolation of biological samples was approved in 2011 [5]. MNPs coupled with chip-based capillary

electrophoresis may even multiply advantages of this method and broaden the application potential.

4 CONCLUSION

Miniaturized analysis and integrated sample manipulation is the direction of current analytical research. Here proposed method of application of commercial CE chip for on-line integrated DNA isolation by streptavidin modified MNPs followed by CE separation of the isolated oligonucleotides demonstrated the benefits of such on-line coupling. Isolation of oligonucleotides by Chip electrophoresis is a very simple, quick and easy method to analyze small amount of sample and it is possible to perform it on the remote locations. CE chip electrophoresis, coupled with magnetic particle isolation can be easily integrated into one single small device and commercially produced. Laser induced fluorescence provides the sensitivity required for analysis of real biological samples (DNA molecules).

ACKNOWLEDGEMENTS

The financial support by SIX CZ.1.05/2.1.00/03.0072 and NanoBioTECell GA ČR P102/11/1068 is highly acknowledged.

LITERATURE

[1] Barker, L. F., Shulman, N. R., Roderick, M. D., Hirschman, R. J., Ratner, F., Diefenbach, W. C. L., Geller, H. M., *Jama-J Am Med Assoc* 1996, *276*, 841-844.

[2] Kuo, H. C., Wang, T. Y., Hsu, H. H., Lee, S. H., Chen, Y. M., Tsai, T. J., Ou, M. C., Ku, H. T., Lee, G. B., Chen, T. Y., *PLoS One* 2012, *7*.

[3] McGlynn, K. A., Tsao, L., Hsing, A. W., Devesa, S. S., Fraumeni, J. F., *Int. J. Cancer* 2001, *94*, 290-296.

[4] Huska, D., Hubalek, J., Adam, V., Vajtr, D., Horna, A., Trnkova, L., Havel, L., Kizek, R., *Talanta* 2009, *79*, 402-411.

[5] Kizek, R., in: Brno, U. o. T. (Ed.), Czech Republic 2012.

P29 FILTRATION MICROCARTRIDGE AND CAPILLARY ISOELECTRIC FOCUSING FOR THE ANALYSIS LOW NUMBER OF MICROORGANISMS IN REAL SAMPLES

Anna Kubesová[a], Marie Horká[a], Jiří Šalplachta[a], Jaroslav Horký[b]

[a] *Institute of Analytical Chemistry,Veveří 97, 602 00 Brno, Czech Republic*
kubesova@iach.cz
[b] *State Phytosanitary Administration, Division of Diagnostics, Šlechtitelů 23,77900 Olomouc, Czech Republic*

ABSTRACT

At present, detection and identification of microorganisms in real biological samples needs very sensitive methods for correct diagnosis and therapy in medical practice, biotechnology, agriculture, food safety and quality etc. Accordingly, it is essential to develop new cheap techniques for pathogen identification, particularly for pathogen in complex biological samples. Pre-concentration, separation, and sensitive detection of whole cells in one step are great potential and advantage for detection of pathogens in low concentration. Combination of filtration microcartridge and capillary isoelectric focusing was developed for pre-concentration

and pre-separation of microorganisms from real suspensions and the possibility its application to real samples was verified.

Keywords: capillary isoelectric focusing, pre-concentration of microorganisms, filtration microcartridge

1 INTRODUCTION

The number of microorganisms in biological suspension occurs in the range from tens to hundreds of cells per milliliter. That is one of the limiting factors for the detection of pathogens in real samples. Most procedures for detection and quantification of pathogens require a sample preparation step including rapid and robust methods for concentrating microorganisms from large sample volumes with high and reproducible efficiency [1]. Relatively few reports have been published dealing with online pre-concentration methods for the analysis of microorganisms [2-4]. In this study, we propose the possibility to use the pre-concentration and pre-separation of a low number of microorganisms from real samples in combination with filtration microcartridge and subsequent separation and identification by capillary isoelectric focusing with UV detection. As model microorganisms were selected spores of *Monilinia spp.* and of *Penicillium (P.) expansum*.

2 PLANT PATHOGENS

Pure cultures of *M. fructigena, M. laxa,* and *M. fructicola* were obtained from the collection of the Diagnostic Laboratory of the State Phytosanitary Administration in Olomouc. The strains of *M. fructigena and M. laxa* were isolated from samples originating in the Czech Republic. The strain of *M. fructicola* was received from a collection (Agroscope, Wädenswil, Switzerland). *P. expansum* was taken directly from the infected surface of an apple and was determined microscopically. Both *Monilinia spp. and P. expansum* belong to the same group of filamentous fungi as *Aspergillus spp*., *Fusarium solani,* and *P. chrysogenum*, previously separated by CE [5].

3 DESIGN AND PROCEDURES FOR THE PRE-CONCENTRATION AND CIEF SEPARATION

A sterile fiberglass filter prepared of hydrophilized polypropylene nonwoven fabric (PEGAS Nonwovens) was put into the silicone tube (3-mm outer diameter and 1-mm inner diameter; Agilent Technologies); see Fig. 1. The filtration cartridge was associated to a syringe or to the anolyte end of the separation fused-silica capillary with a silicon tube (1.5-mm outer 0.3-mm inner diameter). Fungal spores (200 µL to 2 mL) were resuspended in physiological saline solution with addition of 2% (w/v) PEG 1000 and were injected into the filtration cartridge by syringe. The spores retained on the filter cartridge surface were washed with 200 µL physiological saline solution and with 200 µL catholyte solution. The catholyte contained 3×10^{-2} mol L^{-1} sodium hydroxide, 3% (v/v) ethanol, and 3% (w/v) PEG 1000, that were dissolved also in anolyte 0.1 mol L^{-1} orthophosphoric acid. The segment of the spacers was firstly injected into the separation capillary. The cartridge with the retained spores was removed from the syringe and connected to the anolyte end of the separation capillary “as a sample segment.” Then the segment of carriers was injected hydrostatically, approximately 4 s. At the end, the cartridges were carefully washed with the anolyte solution.

4 ILLUSTRATIONS

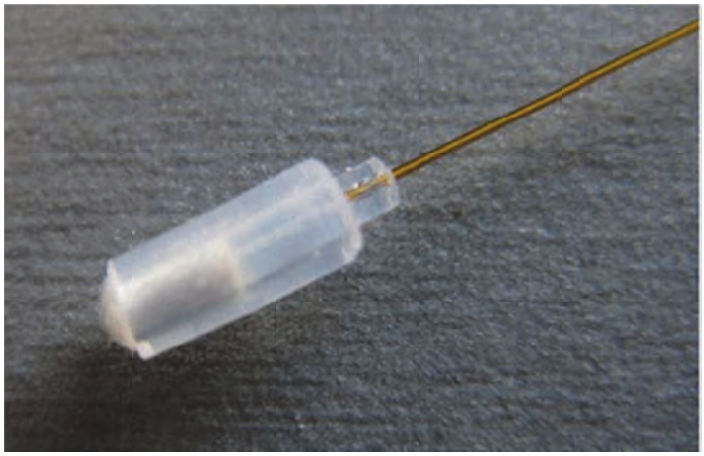

Fig. 1: Connection of the filtration cartridge to the anodic end of the fused-silica separation capillary.

5 CONCLUSIONS

Our results show that the proposed method can be used as an effective tool for pre-concentration and pre-separation of microorganisms from real suspensions. Coupling of the filtration cartridge with the separation capillary in isoelectric focusing can improve the detection limit of CIEF at least 4 orders of magnitude.

ACKNOWLEDGEMENTS

This work was supported by the Ministry of Education Youth and Sports of the CR - project Development of Multidisciplinary Research and Educational Centrum for Bioanalytical Technologies No.CZ.1.07/2.3.00/20.0182, by the grant of Ministry of the Interior of the Czech Republic no.VG20112015021 and by the Institutional Research Plan RVO: 68081715 of Institute of Analytical Chemistry, Academy of Sciences of the Czech Republic.

LITERATURE

[1.] Arai, F., Ichikawa, A., Ogawa, M., Fukuda, T., et al., Electrophoresis 2001, 22, 283-288.
[2.] Petr, J., Jiang, Ch., Sevcik, J., Tesarova, E., et al., Electrophoresis 2009, 30, 3870-3876.
[3.] Shen, Y., Berger, S.J., Smith, R.D., Analtical Chemistry 2000, 72, 4603-4607.
[4.] Yu, L., Li, S.F.Y., Journal of Chromatography A 2007, 1161, 308-313.
[5.] Horká, M., Růžička, F., Kubesová, A., Holá, V., et al., Analytical Chemistry 2009, 81, 39974004.

P30 HIGHLY SENSITIVE DETERMINATION OF CATIONIC PESTICIDES IN ORANGE JUICE BY CAPILLARY ISOTACHOPHORESIS - ELECTROSPRAY IONIZATION - MASS SPECTROMETRY WITH ADVANCED ELECTROLYTE TUNING

Zdena Malá, Pavla Pantůčková, Petr Gebauer, Petr Boček

Institute of Analytical Chemistry of the Academy of Sciences of the Czech Republic, v.v.i., Veveří 97, CZ-602 00 Brno, Czech Republic

ABSTRACT

We present the theory and experiments of a new approach how to increase the selectivity of capillary electrophoretic electrolyte systems compatible with electrospray ionization mass spectrometric (ESI-MS) detection, and how to considerably improve the sensitivity of the whole analysis. The approach is based on the model of extended isotachophoresis (ITP) which enables one to reach the selectivity of ITP stacking as high as needed. The theory and experiment are exemplified by using an ammonium acetate-acetic acid cationic ITP system extended by adding a controlled concentration of the leading ammonium to the terminating zone. This allows advanced selectivity tuning by controlling the velocity of the stacking ITP boundary through the composition of both the leading and terminating zones. The usefulness of this principle is demonstrated on the example of determination of carbendazim and thiabendazole with detection limits 5.10^{-10} M (95 ng/L) and 10^{-10} M (20 ng/L), respectively, and applied to analysis of orange juice without major pretreatment.

Keywords: ITP, ESI-MS, pesticides

1 INTRODUCTION

Capillary zone electrophoresis (CZE) with electrospray ionization mass spectrometric (ESI-MS) detection is a standard analytical electrophoretic technique [1,2]. Sensitivity problems are usually solved by offline analyte preconcentration or by online electrophoretic stacking from simple field amplification to transient ITP [3-5]. Full format ITP-MS has high on-line concentration potential but has been used only scarcely due to the very limited range of available ESI-compatible electrolyte systems [1,6,7]. This paper presents an application of our new extended ITP approach [8] that considerably increases the application range and selectivity of ITP-ESI-MS while maintaining its high sensitivity.

2 PRINCIPLE

In the present application, an extended ITP system is used based on the the ESI-compatible cationic system with ammonium as leader and acetic acid (H^+) as terminator, where a controlled amount of the leading substance is added to the terminating zone. Conditions of peak mode stacking of analyte X are

$$u_{X,T} > u_{ITP,T} \quad \text{and} \quad u_{ITP,L} > u_{X,L}$$

where $u_{X,j}$ is the effective mobility of X in zone j, L and T are the leading and terminating zones and $u_{ITP,j}$ is the mobility of the ITP boundary related to zone j, defined as

$$u_{ITP,j} = v_{ITP}\, \kappa_j / i$$

where v_{ITP}, κ_j and i are the velocity of the ITP boundary, conductivity of zone j and current density, respectively. The stacking conditions can be (for univalent weak bases) drawn in a

pK_{HX} vs. u_{HX} network, showing the area of the stacking window of the given system and allowing prediction of stacking/non-stacking in a given extended ITP system as shown in Fig. 1.

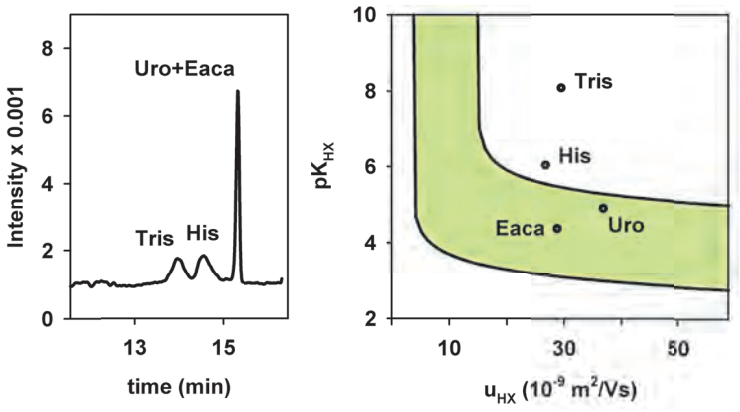

Fig. 1. : Right: Calculated stacking contours in an extended ITP system composed of 10 mM NH_4^+ + 12 mM acetic acid (HAc) (leading zone) and 2 mM NH_4^+ + 15.15 mM HAc (terminating zone), with marked points of model substances: Tris, histidine (His), hexa-methylene tetramine (Uro) and ε-amino-caproic acid (Eaca). Left: Experimental record (sum of single ion monitoring signals for *m/z* 122, 156, 141 and 132 for Tris, His, Uro and Eaca, respectively) of the model mixture. Sample: 10^{-4} M solution of Tris, His, Uro and Eaca in 10 mM HAc, injection by pressure, 30 mbar for 3 s, fragmentor 130.

3 ANALYSIS OF THIABENDAZOLE AND CARBENDAZIM

We applied the proposed extended acetate ITP system to the determination of carbendazim a thiabendazole, fungicides widely used for pre- and postharvest treatment of citrus fruits. Fig. 2 shows the records of ITP-MS analysis of thiabendazole (Tbz) in classical ITP (panel A) and an extended ITP system (panel B). The upper traces in panels A and B correspond to a model sample containing only the analyte, the middle traces show analyses of diluted orange juice spiked with the same analyte concentration and the lower traces correspond to non-spiked juice. When classical ITP was used (panel A), the single ion monitoring trace of the analyte for *m/z* 202 shows a pronounced signal for all three sample types at the time of arrival of the ITP boundary to the detector. Tbz determination was not possible due to another sample component/impurity from the juice that interfered by providing signal at just the same *m/z* value. To get rid of this interference, the terminating zone was modified by adding 1.5 mM ammonium to narrow the ITP stacking window. Here the interfering impurity did not migrate in stack and its broad peak (corresponding to zone electrophoretic migration in the leader) was well resolved from the sharp peak of the analyte (panel B). The estimated detection limit for standard samples was 10^{-10} M Tbz (approx. 20 ng/L) and two orders of magnitude better than published CZE-MS results [9]. The trace concentration of thiabendazole in real juice samples ($5x10^{-8}$ M) was sufficiently above the detection limit and the linearity of the calibration curve was confirmed up to 10^{-6} M.

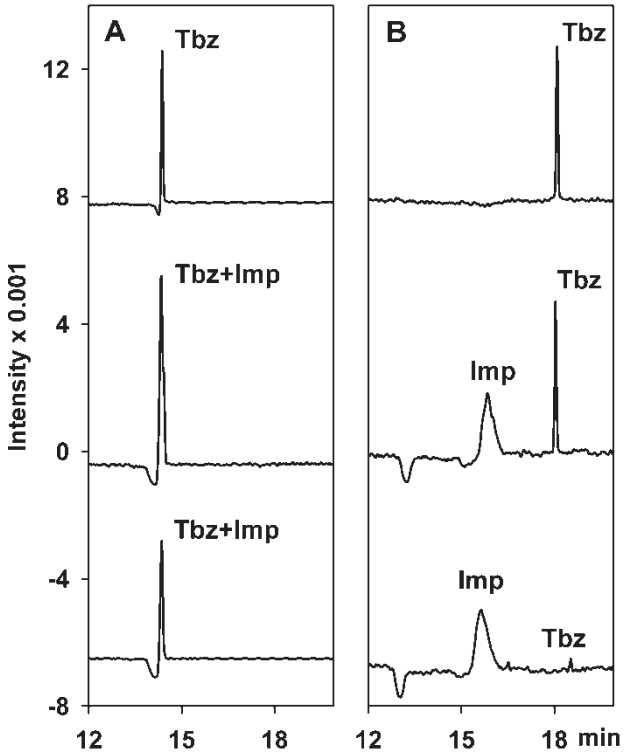

Fig. 2 : Single ion monitoring records of ITP-MS analyses of thiabendazol (*m/z* 202) using two electrolyte systems with leading zone composed of 10 mM NH_4^+ and 20 mM HAc and differing by NH_4^+ content in the terminating zone containing 20 mM HAc and 0 mM (A), and 1.5 mM (B) NH_4^+. The sample was 10^{-6} M Tbz in 5 mM HAc (top), 10^{-6} M Tbz in 10x diluted orange juice with 5 mM HAc (middle), and 10x diluted orange juice in 5 mM HAc (bottom). Sample injection by pressure 30 mbar for 10 s, fragmentor 90. "Imp" marks the unknown impurity.

Fig. 3 shows an experimental comparison of analyses of carbendazim in orange juice by CZE and classical and extended ITP. It is seen that ITP also in this case offers a considerable sensitivity improvement of approx. two orders of magnitude. In comparison with classical ITP, the extended system provided increased selectivity and thus better signal shape not distorted by impurities comigrating at the boundary (the detection limit of carbendazim in standard samples for the extended system was 5.10^{-10} M, *i.e.*, 95 ng/L).

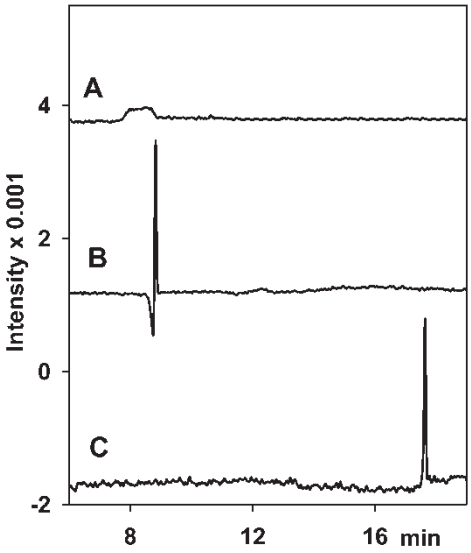

Fig. 3. : Single ion monitoring records of analyses of carbendazim (*m/z* 192) by CZE-ESI-MS and ITP-ESI-MS. The sample was 10^{-8} M carbendazim in 10x diluted orange juice with 5 mM HAc. (A) CZE in 10 mM NH_4^+ + 20 mM HAc; (B,C) ITP with 10 mM NH_4^+ + 20 mM HAc as leader and 20 mM HAc as terminator that contained 0 mM (B), and 1.5 mM (C) NH_4^+. Sample injection by pressure 30 mbar for 10 s, fragmentor 90.

The application of extended ITP systems to capillary ITP-ESI-MS offers a useful way to considerable enhancement of sensitivity and selectivity of capillary electrophoresis with ESI-MS detection, particularly for samples with difficult/complex matrix and only a few analytes of

interest. Easy tuning of both leading and terminating zones of ESI-compatible composition allows fast, sensitive and reproducible analyses employing the concentrating power of full ITP format.

ACKNOWLEDGMENTS

We gratefully acknowledge support by the Grant Agency of the Czech Republic (P206/10/1219) and by Institutional support RVO:68081715 of the Academy of Sciences of the Czech Republic.

LITERATURE

[1.] Pantůčková, P., Gebauer, P., Boček, P., Křivánková, L., *Electrophoresis* 2009, *30,* 203-214.
[2.] Pantůčková, P., Gebauer, P., Boček, P., Křivánková, L., *Electrophoresis* 2011, *32,* 43-51.
[3.] Gebauer, P., Boček, P., *Electrophoresis* 2009, *30*, S27-S33.
[4.] Malá, Z., Křivánková, L., Gebauer, P., Boček, P., *Electrophoresis* 2007, *28*, 243-253.
[5.] Gebauer, P., Malá, Z., Boček, P., *Electrophoresis* 2011, *32,* 83-89.
[6.] Udseth, H.R., Loo, J.A., Smith, R.D., *Anal. Chem.* 1989, *61*, 228-232.
[7.] Tomáš, R., Koval, M., Foret, F., *J. Chromatogr. A* 2010, *1217,* 4144-4149.
[8.] Malá, Z., Pantůčková, P., Gebauer, P., Boček, P., *Electrophoresis*, submitted (elps.201200533).
[9.] Juan-Garcia, A., Font, G., Picó, Y., *Electrophoresis* 2005, *26,* 1550-1561.

P31 DETERMINATION OF 2,4-DICHLOROPHENOXYACETIC ACID AND ITS METABOLITES BY IMMUNOAFFINITY CHROMATOGRAPHY IN PLANT MATRICES

Barbora Pařízková [a], Ondřej Novák [a], Jana Oklešťková [a], Luděk Eyer[b], Milan Fránek[b], Miroslav Strnad[a]

[a] *Laboratory of Growth Regulators, Palacký University & Institute of Experimental Botany ASCR, Šlechtitelů 11, CZ-783 71, Olomouc, Czech Republic*
[b] *Veterinary Research Institute, Hudcova 70, 621 00 Brno, Czech Republic*

ABSTRACT

Monoclonal antibodies against widely used herbicide 2,4-D were produced by hybridomas from fusion of murine myeloma cells and spleencells isolated from BALB/c mice immunized with hapten conjugated via the carboxyl group to thyroglobulin. The monoclonal antibodies was subsequently characterized by competitive ELISA employing rabbit anti-mouse immunoglobulin to capture antibody from the ascites fluid and the peroxidase conjugate as a detection component. The cross-reactivity of the antibodies was defined on the bases of competitive study with other 2,4-D structural analogs. The selected broad-specific monoclonal antibodies (E2/G2) were coupled to Affi-Gel® 10 and immunoaffinity columns were prepared. These columns were subsequently used for immunoaffinity isolation of 2,4-D and its metabolites from plant extracts.

Keywords: antibodies, 2,4-D, UHPLC-MS/MS.

1 INTRODUCTION

2,4-Dichlorophenoxyacetic acid (2,4-D, Fig.1) is a chlorinated phenoxy herbicide widely used in gardens and farming to control broadleaf weeds. Auxinic herbicides are structurally similar

to the natural plant hormone auxin, and induce several of the same physiological and biochemical responses at low concentration (Mithila et al. 2011). The molecular basis of mode of action is not entirely understood. It was assumed that they are uncouplers of the oxidative phoshorylation system and modify the stucture of thylakoidal membranes (Moreland 1980). Phenoxyacetic acid herbicides are relatively less persistent in soil and water and can accumulate in river and lake sediments. They show moderate toxicity, however, some chlorinated metabolites can be toxic to human and aquatic organisms. They can cause soft tissues carcinoma in man and show embryotoxicity in animals (Bovey et. Al. 1980, Lynge 1985). Due to their considerably practical importance, many efforts have been made to develop reliable and sensitive methods for analysing 2,4-D and its metabolites in various matrices.

Monoclonal antibodies against the 2,4-D were tested by enzyme-linked immunosorbent assay (ELISA) using a 2,4-D- peroxidase conjugate and then were used for preparation of an immunoaffinity chromatography (IAC).

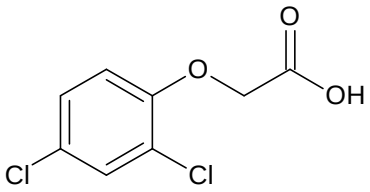

Fig.1.: Chemical structure of 2,4-dichlorophenoxyacetic acid

2 MATERIALS AND METHODS

2.1 Enzyme-linked immunosorbent assay (ELISA)

The microtiter plates (Nunc-Maxisorp) were coated with 200 μL of anti-mouse IgG antibody produced in rabbit (Sigma-Aldrich, 4μL/20mL 50mM $NaHCO_3/Na_2CO_3$, pH 9.6), incubated overnight at 4°C for binding, then washed twice with 300 μL of 1% PBS-TWEEN 20 buffer per well. The wells were then filled with 200 μL of E2/G2 monoclonal antibody (dilution 1:2000 in PBS; 50 mM Na_2HPO_4/ NaH_2PO_4 buffer, 0.15 M NaCl, pH 7.2), incubated at 4°C for 1 hour. The plates were then washed three times with of 1% PBS-TWEEN 20 buffer. After decanting, the wells were filled in the following sequence: 100μL of standard in PBS and 100μL of 2,4-D-HRP conjugate (dilution 1:2000 in 1% PBS-TWEEN 20 buffer) and the plates were incubated at 4°C for 1 hour. Unbound conjugate was removed by rinsing the plates three times with 1% PBS-$TWEEN_{20}$ buffer. Then the plates were filled with 200 μL of a 3,3',5,5'-tetramethylbenzidine as a substrate (1mg TMB, 500 μL CH_3COONa, 10 μL 16% H_2O_2 / 10mL H_2O). The reaction was stopped after 15 minutes incubation at 25°C by adding 50μL 2M H_2SO_4 and final absorbance measured at 450 nm (Titertek Multiscan® PLUS). Sigmoid curves for standards and cross-reacting compounds were linearized by the log-logit transformation: logit $B/B_0 = \ln\{(B/B_0)/(100-B/B_0)\}$.

Cross-reactivity

Percentage of cross-reactivity was calculated using the equation:

CR (%) = IC50(2,4-D)/IC50(cross-reactant) * 100.

The IC50 value represents the analyte concentrations obtained at 50% inhibition. It is the concentration at which 50% of the antibody is bound to the analyte.

2.2 Preparation and use of immunoaffinity columns

The mAbs were produced and purified in EXBIO company (Praha) into final amount 20 mg using the E2/G2 hybridoma clone, which was obtained previously (Franek et al. 1994).

The purified antibodies were coupled to N-hydroxysuccinimide-ester activated agarose (20mg IgG/mL Affi-Gel 10, Bio-Rad, USA). IAC columns were then created by dispensing 0.5 mL portions of the immunoaffinity gel (IAG) into 3 mL polypropylene columns and strored in PBS buffer (PBS; 50 mM NaH_2PO_4,15 mM NaCl, 0.1%NaN_3, pH 7.2) at 4°C. The capacity of the IAG was tested using standard solutions, in triplicate, containing 8 2,4-D standards in equal amounts at concentrations (per standard) ranging from 1 to 300 pmol in methanol:PBS buffer (5:95, v/v). Used gel was regenerated with a cycle of 3 mL portions of H_2O-MeOH-H_2O and finally re-conditioned by 3mL PBS. After elution, the samples were evaporated to dryness in a Speed-Vac concentrator (LabConco) and analyzed by UHPLC-MS/MS.

2.3 UHPLC-MS/MS

Acquity UPLC® System (Waters, USA) combined with Quattro micro API (Waters, UK) were used for analysis of 2,4-D, its metabolites and structure analogues. The samples (10µL) were injected onto a reversed-phase column (BEH C18, 2.1 x 50 mm, 1.7 µm; Waters) and eluted with an 8.0-min linear gradient of 35:65 A:B to 70:30 A:B (v/v) where A was aqueous 0.1% formic acid and B was 0.1% formic acid in methanol at a flow-rate of 0.25 $ml.min^{-1}$ and column temperature of 40°C. Optimal conditions for MRM experiments in negative electrospray mode were used - capillary voltage 4.0 kV, desolvation/source temperature 100/350 °C, dwell time 0.1-0.4 s and cone voltage (15-25 V) with collision energy (9-22 eV) in collision cell were optimized for each analyte.

3 CONCLUSIONS

1) New monoclonal antibodies against herbicide 2,4-D were developed.

2) Characteristics of antibodies were tested in enzyme-linked immunosorbent assay (ELISA). MAb E2/G2 exhibited high cross-reactivity with methyl ester 2,4-D (104.8 %), with MCPA13.8 % and with 2,4,5-T 9.5 %. Cross-reactivities with other structural analogs did not exceed 2.7 % *(see Table 1).*

3) These antibodies were used for preparation of immunoaffinity columns. The IAC capacity was estimated to be about 1.6 nmoL per mL of gel for 2,4-D. Different amounts of a mixture containing equal concentrations of 2,4-D and metabolites (ranging from 1 to 300 pmoL) of each of 8 standards (*Table 2*) were purified with 300 L IAC and eluates were analyzed by UHPLC-MS/MS.

4) A baseline chromatographic separation of eight analytes (2,4-D, its metabolites and structure analogues) on reversed-phase column Aquity UPLC® BEH C18 (1.7 µm, 2.1 x 50 mm) was obtained in 7.5 minutes (*Fig. 2*) and used testing the IAC capacity.

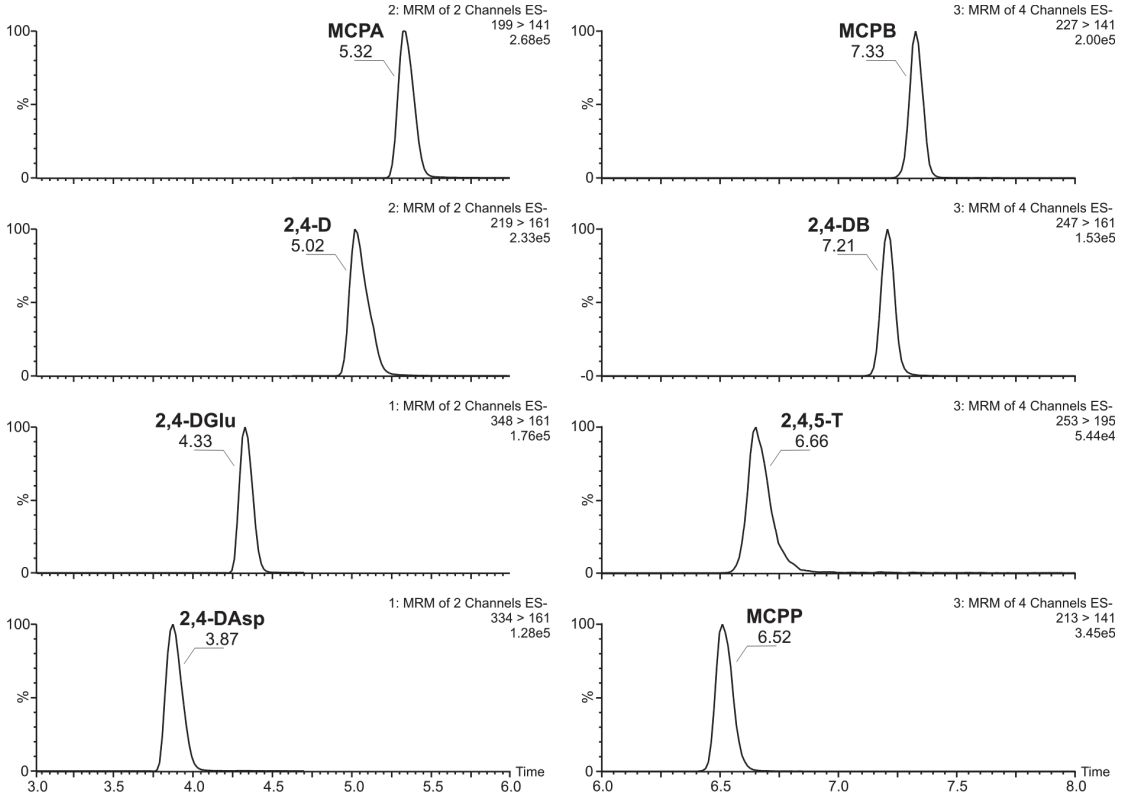

Fig.2.: Normalized multi-MRM chromatograms of 2,4-D and its structure analogues containing 50 pmol of each analyte per injection.

Table 1: Cross-reactivity of 2,4-D and related structures with MAbs against 2,4-D-thyroglobulin.

Coumpound	Cross-reactivity (%) - MAb E2/G2
2,4-Dichlorophenoxyacetic acid	100
2,4-D methylester (2,4-D-Me)	104.8
2-methyl-4-chlorphenoxyacetic acid (MCPA)	13.8
2,4,5-trichlorphenoxyacetic acid (2,4,5-T)	9.5
2- chlorphenoxyacetic acid	0.9
2- methylchlorphenoxyacetic acid	<0.2
2-methyl-4,6-dichlorphenoxyacetic acid	<0.2
2-methyl-6-chlorphenoxyacetic acid	<0.2
4-chlorphenoxyacetic acid	0.9
2,3-dichlorphenoxyacetic acid	1.6
3,4-dichlorphenoxyacetic acid	2.7
2-(2,4-dichlorphenoxy)propionic acid	0.4
4-(2,4-dichlorphenoxy)butyric acid (2,4-DB)	1.5
2-(2-methyl-4-chlorphenoxy)propionic acid (MCPP)	<0.2
4-(2-methyl-4-chlorphenoxy)butyric acid (MCPB)	0.9
2,4-dichlorphenol	1.6
2-methyl-4-chlorphenol	0.5
3,4-dimethylphenol	<0.2

pentachlorphenol	0.5
2,4-Dichlorophenoxyacetyl-L-aspartic acid (2,4-D-Asp)	57.5
2,4-Dichlorophenoxyacetyl-L- glutamic acid (2,4-D-Glu)	85.2

Table 2: Recovery (%) of 2,4-D and metabolites mixture (nd-not detected).

	1 pmol	**5 pmol**	**10pmol**	**50 pmol**	**100 pmol**	**300 pmol**
2,4-D	91.52	70.62	69.42	59.22	47.64	62.58
2,4-D-Asp	36.36	14.68	9.30	7.19	1.58	0.79
2,4-D-Glu	42.84	31.76	19.89	17.95	6.77	4.93
MCPA	32.36	20.25	15.33	13.83	3.96	1.88
MCPP	nd	nd	nd	nd	0.25	0.17
2,4,5-T	nd	nd	11.85	8.96	2.26	1.12
2,4-DB	nd	10.53	14.74	8.67	2.48	1.04
MCPB	nd	nd	nd	nd	nd	0.57

ACKNOWLEDGEMENTS

This research was supported by the Grant Agency of the Czech Academy of Sciences, Grants No. KAN200380801.

LITERATURE

[1.] J. Mithila, J.CH. Hall, et al., *Weed Science* 59, 2011, 445-457.
[2.] M.H. Moreland, *Ann. Rev. Plant Physiol*. 31, 1980, 597.
[3.] R.W. Bovey, A. Young, *The Science of 2,4-D and Associated Phenoxy Herbicides*, John Wiley, New York, 1980, 301.
[4.] E. Lynge, *Br.J.Cancer* 52, 1985, 259.
[5.] M. Fránek, V. Kolář, et al., *J.Agric. Food Chem*. 42, 1994, 1369-1374.

P32 UTILIZATION OF THE ANODIC ELECTRO-OSMOTIC FLOW FOR AN AMINO ACIDS PROFILING BY CAPILLARY ELECTROPHORESIS

Ales Madr, Katerina Svobodova, Jindra Musilova, Zdenek Glatz

Department of Biochemistry, Faculty of Science and CEITEC, Masaryk University, Kamenice 5, 625 00 Brno, Czech Republic
glatz@chemi.muni.cz

ABSTRACT

Amino acids profiling is sometimes considered to be a supplementary analysis for diagnostic purposes. Detection of amino acids by conventional spectrophotometric techniques is hindered by lack of chromophores in their structures, thus derivatization step in sample treatment protocol has to occur. However, amino acids in their native form can be detected by other detection techniques, *e.g.* mass spectrometry or capacitively coupled contactless conductivity detection (C^4D). C^4D is a non-specific detection technique suitable for detection

of ionic species. It can be easily coupled with capillary electrophoresis (CE) forming powerful combination of the non-specificity of the C^4D and a high selectivity of CE.

Keywords: amino acid profiling, capillary electrophoresis, conductivity detection

1 INTRODUCTION

Metabolomic profiling/fingerprinting is highly demanding scientific field on selectivity of methods employed. Using CE, one should use relatively long capillaries, electroosmotic flow (EOF) suppression for better precision and sensitive and non-specific detection to acquire as much information as possible/demanded. Amino acids analyses by CE-C^4D were thoroughly optimized both *in silico* by Peakmaster [1] and experimentally by Gas research group [2]. Published conditions were successfully applied with minor changes on different biological samples [3-5] with the common denominator the 80 cm long capillary. Long capillary is necessary to obtain completely resolved peaks of all proteinogenic amino acids at EOF suppressed conditions.

Effective separation length/time for analytes of interest can be altered by EOF modification. For amino acids in their cationic form, strong cathodic EOF (normal) causes faster analyses but resolution losses; au contraire, controlled anodic EOF (reversed) can prolong separation time and shorter capillaries can be used for complete separation of all amino acids. Advantages of the use of shorter capillaries are faster exchange of the inner capillary volume and the broader range of electric field intensities that can be applied.

The aim of our study was to explore behavior of EOF in an acidic electrolyte in bare fused silica capillaries and to modify EOF by an addition of alkylammonium salts commonly used for giving rise to the anodic EOF. Utilization of the alkylammonium salts for EOF modification in CE-C^4D system is discussed and future prospects are outlined.

2 EXPERIMENTAL

2.1 Material

There was used commercially available CE instrument Agilent G7100A (Agilent Technologies, Santa Clara, CA, USA) with integrated A/D converter. C^4D was in-house-assembled derived from the one presented by Gas *et al.* [6]. The C^4D was basically an in-cassette-built printed circuit fixed by bolts and nuts to a plastic cassette case. Two cylindrical metal electrodes were coaxially placed in close succession with 2 mm gap with fixed geometry supported by a grounded holder. A thin copper plate with a gap for a capillary was placed and grounded within electrodes to eliminate signal transmission by the air. The holder was firmly soldered to the printed circuit. There was used a high-frequency crystal oscillator of 1.84 MHz frequency.

All capillaries were purchased from Polymicro Technologies (Polymicro Technologies, Phoenix, AZ, USA). They were made of bare fused silica with 50 μm inner diameter, 375 μm of outer diameter with polyimide protective coating.

All chemicals were purchased from Sigma-Aldrich (Sigma-Aldrich Corporation, St. Louis, MO, USA) and were of analytical grade purity. Solution were prepared using deionized water purified by Direct-Q® 3 UV (EMD Millipore, Billerica, MA, USA). There were prepared stock solutions of dodecyltrimethylammonium bromide (DTAB), tetradecyltrimethylammonium bromide (TTAB) and hexadecyltrimetylammonium bromide (CTAB) of 100 mM, 25 mM, 25 mM concentrations, respectively. Dissolution was facilitated by a mild heating and the stock solutions were prepared at the day of need.

Background electrolytes (BGEs) were prepared by mixing water, acetic acid and the one of the mentioned alkylammonium salts giving final concentration of 16 % (v/v) of acetic acid and 0-10 mM CTAB/TTAB or 0-25 mM DTAB. Mixture was filtered through nylon membrane filters with 0.45μm porosity using syringe membrane filter devices (Thermo Fisher Scientific, Waltham, MA, USA) and degased for 10 minutes in an ultrasonic bath.

2.2 Methods

Since BGE composed of an acetic acid has high conductivity and strongly absorb at UV region of electromagnetic spectrum, water was used as marker of EOF for both C^4D and UV detections. Water was introduced into capillary by 25 mbar pressure gradient for 6 seconds thus form approx. 8 nl plug. There were used capillary of 50 μm of inner diameter, total length 32.0 cm. Cassette was tempered to 25 °C and there was applied 20 kV voltage in positive or negative polarity mode according to the direction of EOF. There were recorded signals both from C^4D and UV detectors and there were read times of the water peak (presented as negative peak) passing the detector cell. Distance from the inlet capillary end to the C^4D and UV detector cells were 17.6 cm and 23.5 cm, respectively.

Capillaries were dedicated to certain alkylammonium salt and before the first use they were treated by flushing by 1 M NaOH, 0.1 M NaOH and water for 10 minutes by the approx. 0.9 bar pressure gradient. Prior to each analysis, capillary was sequentially flushed by 0.1 M NaOH, water and BGE for 2 minutes, 1 minute and 3 minutes, respectively. After an analysis, capillary was flushed by the water for 1 minute.

3 RESULTS

Data recorded by C^4D were used for calculations of EOF mobilities at certain concentration and type of alkylammonium salt in the BGE. Each concentration was measured six-times in consecutive runs. Data were tested for outliers by Grubbs test and were fitted into a sigmoid function by OriginPro 8.6 software (OriginLab Corporation, Northampton, MA, USA) for graphical representation.

Figure 1 clearly shows that all alkylammonium salts reverse EOF in the acidic BGE. Length of the alkyl chain is inversely proportional to the concentration of the alkylammonium salts causing anodic EOF and is related to sigmoid curve steepness. From this point of view, CTAB and TTAB cause strong anodic EOF at low concentrations but it can be rather difficult to regulate EOF velocity by their concentration in BGE due to the steep change of EOF mobilities. On the other hand, there is observed significant noise increase in C^4D signal correlating with concentration of the alkylammonium salt. Similar dependence was observed when a sulfated-β-cyclodextrin was used for selectivity alteration (data not shown). Noise increase could be ascribed to a presence of larger ionic species in the BGE, *e.g.* micelles, which can create an ionic inhomogeneity. Application of the alkylammonium salts for the induction of the controlled anodic EOF is therefore hindered by the large noise increase. There should be tested physically attached cationic layers, *e.g.* polybrene, and the regulation of anodic EOF velocity by a viscosity or an ionic strength.

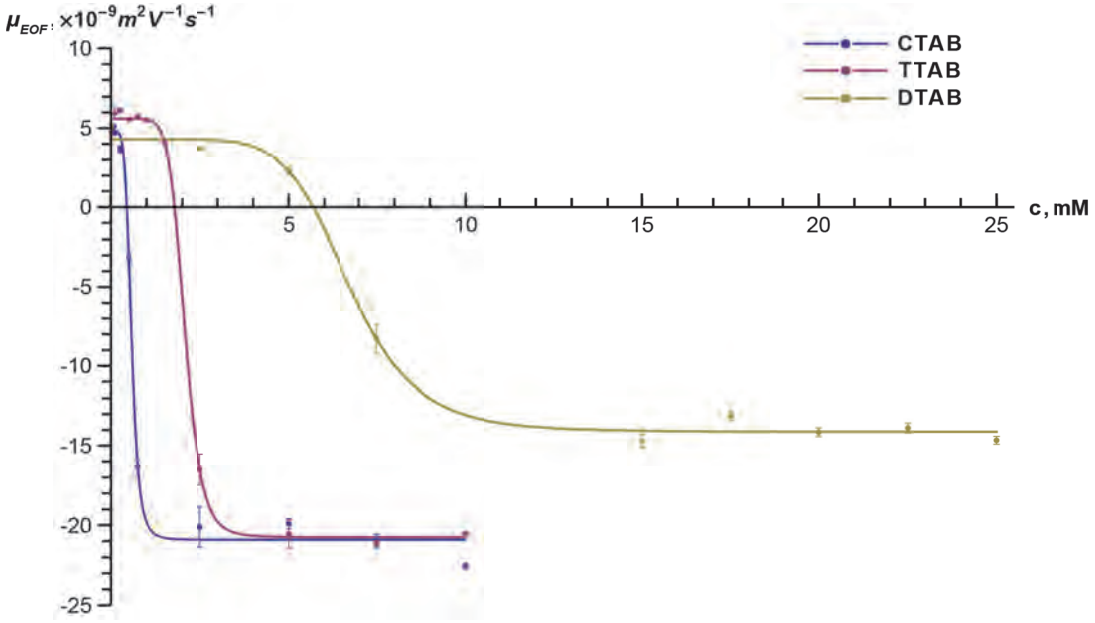

Fig. 1: Graph showing the dependence of EOF mobilities on concentration and alkylammonium salt used. Data were fitted into a sigmoid function using OriginPro 8.6 software and error bars indicate standard deviations of a sample. Each data point was measured six-times in consecutive runs. Presented values are related to an acidic BGE composed of 16 % (v/v) acetic acid and defined concentration of the alkylammonium salt. Data were measured at 25 °C, 20 kV using 50 µm inner diameter bare fused silica capillary of a total length 32.0 cm.

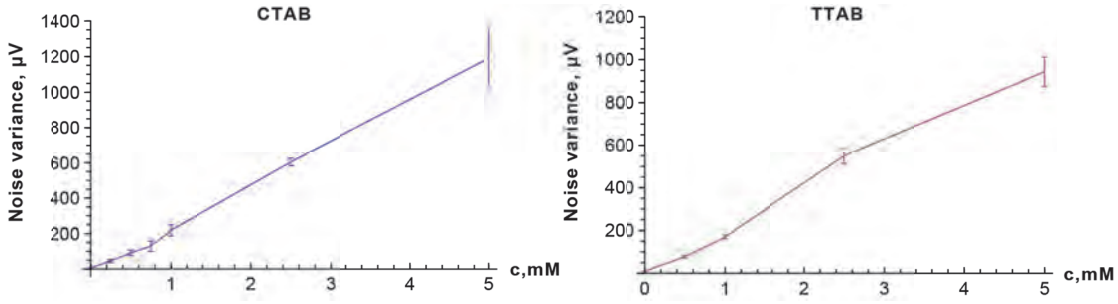

Fig. 2: Graph showing the dependence of noise increase represented as noise variation on concentration and alkylammonium salt used. Error bars indicate standard deviations of a sample for six readings of 1000 data points wide non-baseline-drifting region of the C^4D signal.

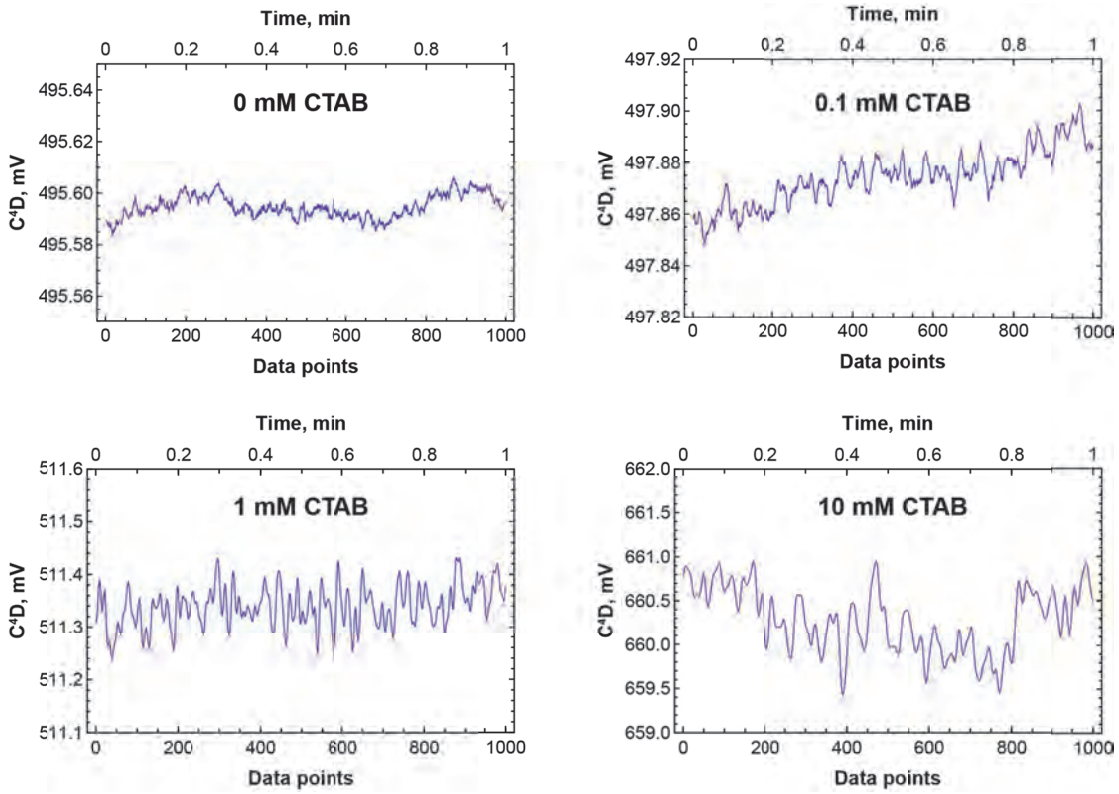

Fig. 3: Selection of representative noise samples observed at different concentrations of CTAB. The selections are of 1000 points range (sampling frequency 1000 min^{-1}) taken from non-baseline-drifting region of the C^4D signal. Graphs illustrate noise increase and its change from high-frequency into low-frequency wavy-like noise.

CONCLUSION

There were tested three alkylammonium salts, namely CTAB, TTAB and DTAB. All cause anodic EOF at acidic BGE but at different concentration. However, there were observed significant noise increases in the C^4D signal correlating with concentration of the alkylammonium salt used. In the light of this fact, utilization of the commonly used alkylammonium salts for giving rise of the anodic EOF is hindered. Physically attached cationic layers, *e.g.* polybrene coating, were proposed to overcome noise obstacles and will be tested in the near future.

ACKNOWLEDGEMENTS

Financial supports granted by the Czech Science Foundation are highly acknowledged (Projects P206/11/0009 and P206/12/G014).

LITERATURE

[1.] http://web.natur.cuni.cz/gas/
[2.] Coufal, P., Zuska, J., van de Goor, T., Smith, V., *et al.*, *Electrophoresis* 2003, *24*, 671-677.
[3.] Samcova, E., Tuma, P., *Electroanalysis* 2006, *18*, 152-157.
[4.] Tuma, P., Samcova, E., Andelova, K., *Journal of Chromatography B* 2006, *839*, 12-18.
[5.] Tuma, P., Samcova, E., Duska, F., *Journal of Separation Science* 2008, *31*, 2260-2264.
[6.] Gas, B., Zuska, J., Coufal, P., van de Goor, T., *Electrophoresis* 2002, *23*, 3520-3527.

P33 SACCHARIDES IN PM2.5 AEROSOLS IN BRNO

Kamil Křůmal[a], Nela Kubátková[a,b], Pavel Mikuška[a], Zbyněk Večeřa[a]

[a] *Institute of Analytical Chemistry of the ASCR, v.v.i., Veveří 97, 602 00 Brno, Czech Republic*
[b] *Faculty of Chemistry, Brno University of Technology, Purkyňova 464/118, 612 00 Brno, Czech Republic, krumal@iach.cz*

ABSTRACT

Contribution summarizes the concentrations of saccharides (monosaccharides, disaccharides and sugar alcohols) in PM2.5 aerosols in urban area during different seasons (winter, spring, summer and autumn 2010 and winter 2011). We optimized conditions for the extractions of saccharides from quartz filters.

Keywords: saccharides, urban aerosols

1 INTRODUCTION

Saccharides are the most abundant group of the natural molecules, produced in large quantities by photosynthesis by plants and microorganisms. They form also a major part of cellular structure of plants and animals [1]. Saccharides are sources of energy for living organisms and basic structural unit of plant tissues – cellulose (glucose) and hemicellulose (xylose, arabinose, mannose and galactose) [2]. Cellulose is the most abundant biopolymer, representing 40 – 50 % of dry weight of wood while hemicellulose represents 20 – 30 % of dry weight of wood. Another type of plant biopolymer is lignin which represent 20 – 30 % of dry weight of wood [3]. Saccharides could be emitted to the atmosphere during burning of biomass, resuspension of soil particles, wind abrasion of leaf surfaces [4] and they are present in biological aerosol particles (spores, pollens, fungi, algae, protozoa, bacteria, viruses and fragments of plants and animals) [5]. Microorganisms, plants and animals can release into the atmosphere primary saccharides (monosaccharides and disaccharides) while fungi, lichens and bacteria produce saccharidic polyols (sugar alcohols; arabitol, manitol and sorbitol) [6].

2 EXPERIMENTAL

2.1 Aerosol sampling

The concentrations of monosaccharides (fructose, glucose, mannose, galactose, xylose), disaccharides (maltose, sucrose, trehalose) and sugar alcohols (arabitol, sorbitol, manitol, myo-inositol) in the atmospheric aerosols were measured in Brno in the Czech Republic in spring, summer, autumn and winter of 2010 and in winter of 2011. The concentrations were measured in PM2.5 aerosol samples, over one week in each season.

2.2 Sample preparation, extraction and analysis

Analysis included extraction of filters with mixture methanol/dichloromethane (1:1) under ultrasonic agitation, evaporation to dryness under a stream of nitrogen, derivatization of extracts with mixture of MSTFA/TMCS, evaporation to dryness under a stream of nitrogen, redissolution in hexane and GC-MS analysis.

3 RESULTS

3.1 Optimalization of extraction

We evaluated the extraction efficiency and reproducibility of saccharides with different solvents: methanol (M), dichloromethane (D) and their mixtures 1:1, 1:2, 2:1 (v/v). The result of comparison is shown in **Fig. 1**. Dichlormethane was not effective for the extraction of saccharide compounds from the filters because its polarity is low to extract more polar compounds. By contrast, the high polarity of methanol caused extraction of huge amount of organic compounds resulting in poor reproducibility of the derivatization process. The mixture of D:M 1:1 (v/v) was used as an optimum solvent for the best extraction process of saccharides.

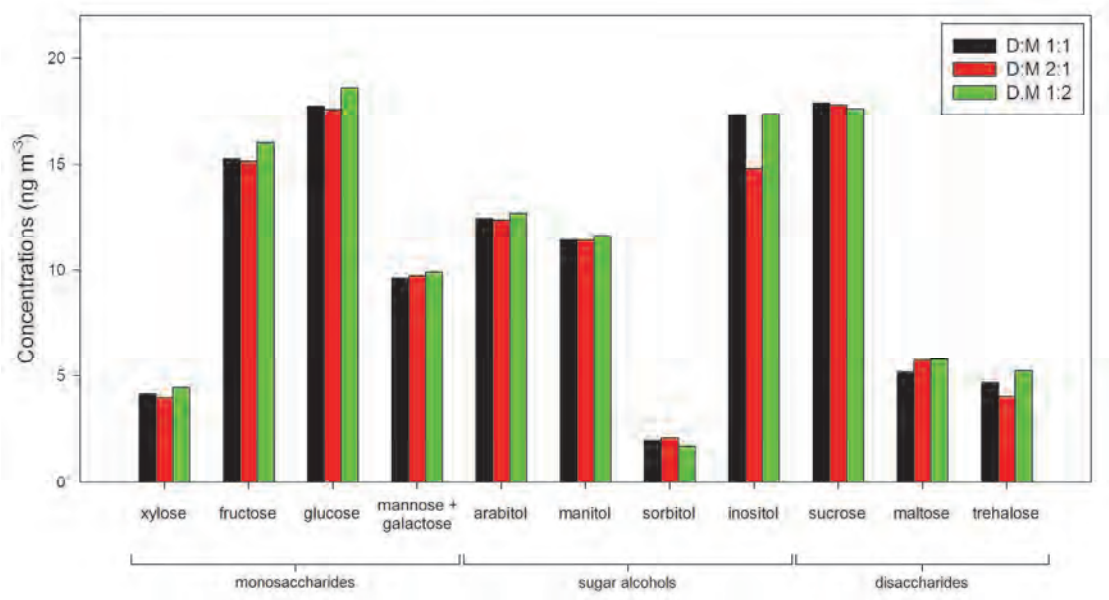

Fig. 1.: Extraction of saccharides with different solvents.

3.2 Concentrations of saccharides in PM2.5

The mean mass concentration of PM2.5 aerosols was in the range from 13.9 µg m^{-3} in spring 2010 to 39.3 µg m^{-3} in winter 2011. **Fig. 2** shows the mean concentrations of saccharide compounds in individual seasons. The highest concentrations of monosaccharides and sugar alcohols were in summer 2010 (27.4 ng m^{-3} and 67.4 ng m^{-3}) and autumn 2010 (32.2 ng m^{-3} and 74.4 ng m^{-3}) while the highest concentrations of disaccharides were in spring 2010 (91.9 ng m^{-3}). Sucrose as a dominant disaccharide was determined in the range from 7.7 ng m^{-3} (winter 2010) to 85.4 ng m^{-3} (spring 2010). Glucose was the most abundant monosaccharide in the range from 5.3 ng m^{-3} (winter 2010) to 11.4 ng m^{-3} (summer 2010). From the group of sugar alcohols, dominant myo-inositol was found in the range from 23.1 ng m^{-3} (spring 2010) to 55.9 ng m^{-3} (autumn 2010).

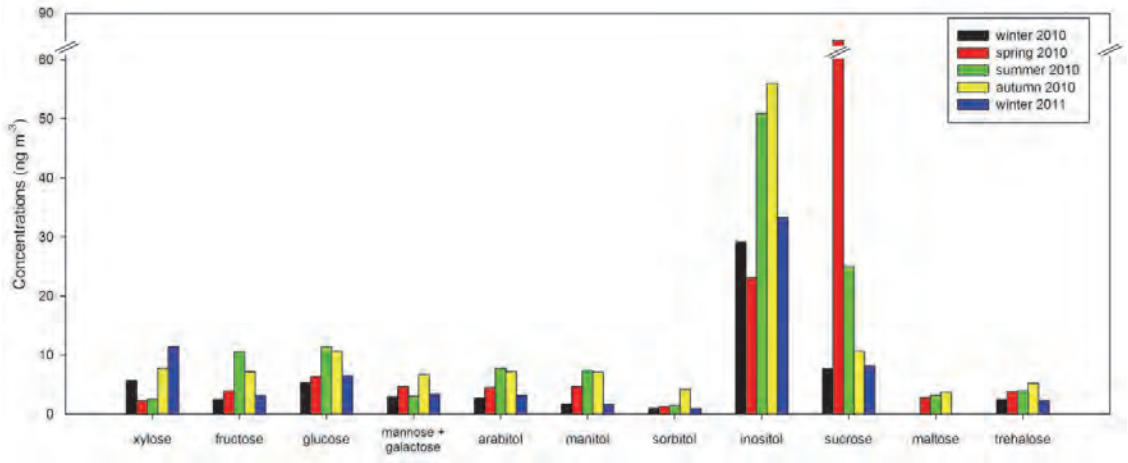

Fig. 2.: Comparison of concentrations of saccharides in different seasons.

ACKNOWLEDGEMENTS

This work was supported by Grant Agency of the CR under grant No. P503/11/2315 and by Institute of Analytical Chemistry of the ASCR, v.v.i. with institutional support RVO:68081715.

LITERATURE

[1.] Lindhorst, K., *Essentials of Carbohydrate Chemistry and Biochemistry*, Wiley-VCH, Weinheim 2007.

[2.] Ek, M., Gellerstedt, G., Henriksson, G., *Wood Chemistry and Biotechnolgy, vol. 1.*, Walter De Gruyter, Berlin 2009.

[3.] Simoneit, B. R. T., Schauer, J. J., Nolte, C. G., Oros, D. R., et al., *Atmospheric. Environment* 1999, *33*, 173-182.

[4.] Wan, E., Yu, J., *Environmental Science and Technology* 2007, *41*, 2459-2466.

[5.] Jia, J., Clements, A., Fraser, M., *Journal of Aerosol Science* 2010, *41*, 62-73.

[6.] Caseiro, A., Marr, I. L., Claeys, M., Kasper-Giebl, A., et al., *Journal of Chromatography A* 2007, *1171*, 37-45.

P34 DETERMINATION OF COPPER IN HUMAN URINE BY LIQUID CHROMATOGRAPHY WITH SPECTROPHOTOMETRIC DETECTION WITH USED MONOLITH COLUMN

Simona Čurmová[a], Radoslav Halko[a], Milan Hutta[a], Natália Bielčíková[a], Peter Božek[b]

[a] *Department of Analytical Chemistry, Faculty of Natural Sciences, Comenius University in Bratislava, Mlynská dolina CH2-312, 842 15 Bratislava, Slovakia, curmova@fns.uniba.sk*

[b] *MVSR, OKBH, NSP, 812 74 Bratislava, Slovakia*

ABSTRACT

This work is focused on developing a new method for the determination of trace concentration of copper in human urine. Copper can be determined in human urine as chelate by spectrophotometric detection, but the applied method must be highly sensitive and specific. This can be achieved by appropriate option of selective chelating reagents. In our work, we used 2,9-dimethyl-1,10-phenanthroline (neocuproine) in pre-column derivatization step. Developed method is based on the reaction of neocuproine with Cu^{+} which forms

orange-yellow hydrophobic chelate in a neutral or slightly acidic buffer solution (adjusted to pH = 5.9). Cu^{2+} was reduced to Cu^{+} ions by ascorbic acid as a weak reducing reagent. Considering that yellow-orange chelate product is formed, yellow components of human urine can greatly interfere in this spectrophotometric detection. Therefore we added a separation step for the aim to separate of copper^{+}-neocuproine chelate from other yellow urine components. The HPLC technique with monolithic analytical column, Chromolith Performance RP-8e (100 × 4.6 mm) at detection wavelength of 453 nm, was used for the solving of this problem. Gradient elution of the mobile phase composed of aqueous buffer and methanol was used to achieve a required separation of hydrophobic chelate within 9 minutes. This newly developed method was successfully applied to the determination of copper in human urine.

Keywords: HPLC, copper, urine

1 INTRODUCTION

Copper (Cu) is an essential trace element for humans. It plays an important role in many biological processes. In human body, even a small amount of copper affects various enzymes as a powerful catalyst. In the human organism, copper exists in two forms - the first and second oxidation form and most of the copper in the human organism is in the second form. The highest concentrations of copper are discovered in the brain and the liver. The central nervous system and the heart have high concentrations of copper as well. About 50% of copper content is stored in bones and muscles. The total copper content of the adult body is typically 70-80 mg [1.]. Copper enters the body by food consumption, inhalation of contaminated air and by direct contact with the skin. Metabolic processes in the human body create a variety of waste byproducts. Urine is an important way of removing these substances from the body. Moreover urine is most widely used as a biological matrix. Increased copper content in the human body is clearly seen in genetic diseases of metabolism like Wilson's disease. This disease is a rare inherited disorder that causes the body to retain copper. Normally liver releases excessive copper it into bile, a digestive fluid. With Wilson disease, this does not happen. Copper builds up in the liver and damages liver tissue. Over the time, the damage causes liver to release the copper directly into the bloodstream. The blood carries copper all over your body. Excessive concentration of copper can damage kidneys, liver, brain and eyes [2.]. Disease diagnosis is confirmed by low levels of the protein ceruloplasmin and increased excretion of copper in the urine. The measurement of copper in the urine is a better indicator since the excretion of copper in the urine is normally higher than 1.5 µmol per 24 hours. The excretion of copper in the urine for individuals infected by Wilson's disease is several times higher reaching a level of 5-7 µmol per 24 hours [3.].

The aim of this study was to develop an analytical method for the determination of trace concentrations of copper in human urine. For the realization of this aim, we used liquid chromatography with spectrophotometric detection in the visible spectrum (HPLC-VIS). In the proposed case, copper was separated as a hydrophobic chelate formed with reaction Cu^{+} with a selective chelating reagent 2,9-dimethyl-1,10-phenanthroline (neocuproine) in the pre-column derivatization step.

2 EXPERIMENTAL PART

2.1 Instrumentation

Study of the retention behavior copper^{+}:neocuproine (Cu^{+}:Nc) chelate in human urine was carried out by the UV-1800 spectrophotometer (Shimadzu Corporation, Japan) with software UV Probe Ver. 2.33. HPLC system Elite LaChrom (Merck-Hitachi, Darmstadt, Germany) consisting of L-2130 pump provided by quaternary low-pressure gradient with solvent degasser, L-2200 autosampler, L-2400 UV-Visible detector, organizer and PC data

station with software EZChrom Elite ver. 3.1.3. Other used instruments were: AR 0640 analytical balance (Ohaus, USA), Ultrasound UCM 9 (Ecoson, Nové Mesto nad Váhom, Slovakia), Automatic Pipettes Brand 100-1000 µL, 10-100 µL, 1-10 µL and pH meter WTW InoLab pH 730 (Weilheim, Germany).

2.2 Chemicals

The solvents methanol (Merck, Darmstadt, Germany) were of gradient grade purity. Water for gradient HPLC was prepared by Labconco Pro-PS unit (Labconco, Kansas City, USA). Ascorbic acid and ammonium acetate (Merck, Darmstadt, Germany) were used for preparation of buffer solutions. Neocuproine from Fluka was used as selective chelate reagent for Cu^{+}.

3 WORKING CONDITIONS

3.1 Pre-treatment of human urine sample

After collection, human urine sample was cooled to room temperature. The human urine was introduced into a 10 mL volumetric flask which included 2.84 mmol·L^{-1} ascorbic acid, 64.87 mmol·L^{-1} ammonium acetate and $1.38 \cdot 10^{-1}$ mmol·L^{-1} neocuproine chelate reagent. The solution was shaken and it was left at rest for 15 minutes. Some samples were spiked with predefined small volumes of a copper standard solution. Injection volume of sample into chromatographic system was 20 µL.

3.2 HPLC separation conditions

Mobile phase consisted of methanol-buffer (2.84 mmol·L^{-1} ascorbic acid, ammonium acetate 64.87 mmol·L^{-1}, pH = 5.9). Parameters of the applied gradient elution are shown in *Table 1*. Flow rate of mobile phase was 2.0 mL·min^{-1}. Analytical column was a Chromolith Performance RP-8e (100 x 4.6 mm) from company Merck (Darmstadt, Germany). Column temperature was 30 ± 0.1 °C. All measurements were carried out at a wavelength of 453 nm.

Table 1: Parameters of gradient elution

	Time [min]			
	0.0	**9.0**	**10.0**	**12.0**
Methanol	2	95	2	2
Buffer solution	98	5	98	98

4 RESULTS AND DISCUSSION

Neocuproine is white powder, which reacts with Cu^{+} and to form a yellow-orange chelate. It is insoluble in cold water, soluble in hot water, ethanol and chloroform. The reaction Cu^{+} with neocuproine is specific. Determination of copper affects the other elements. The molar absorptivity of this chelate in chloroform is 7.9×10^{3} L·mol^{-1}·cm^{-1} at 460 nm. The structure of neocuproine is shown in *Fig. 1*.

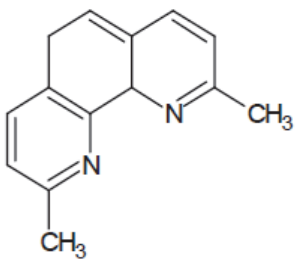

Fig. 1: Structure of neocuproine

The absorption spectrum of the Cu^+:Nc chelate in aqueous solution was studied over the wavelength range of 400-600 nm. This chelate exhibited absorption maxima at 453 nm *(Fig. 2)*.

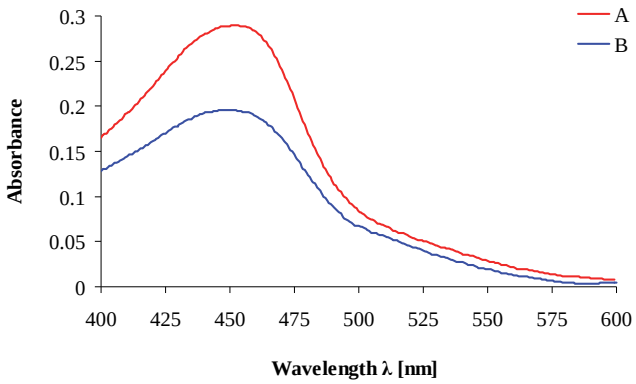

Fig. 2: VIS absorption spectra of the chelate; A - molar ratio (n_{Cu^+}:n_{Nc} - 1:3) B - molar ratio (n_{Cu^+}:n_{Nc} - 1:2); Experimental conditions: λ_{max} = 453 nm; 25 °C; pH = 5.9

4.1 Optimalization of conditions for the spectrophotometric determination of copper

In our work, we decided to monitor the effect of various factors on the spectrophotometric determination of copper as chelate. We studied effect of different molar ratios, temperature, pH and time on the absorbance of the chelate.

In the first step, we have studied the form and stability of Cu^+:Nc chelate. From the literature we know that the optimal molar ratio for the chelate is 1:2 [4.]. The molar-ratio method was applied to ascertain the stoichiometric composition of the chelate. Our results show that the optimal stoichiometric ratio of metal and chelate reagent is 1:3.

The effect of pH variation on the chelate Cu^+:Nc absorbance has been studied. It is well known that in the pH range of 3.0-10.0 the Cu^+ ions together with neocuproine form an orange water-insoluble complex which is completely extractable with n-amyl alcohol, iso-amyl alcohol or 1-hexanol and chloroform/ethanol by shaking [5.]. The effect of pH on the determination of copper in aqueous medium was investigated spectrophotometry. For this purpose, the solution containing Cu^+:Nc in a molar ratio 1:3 was measured in the pH range of 3.0-6.5 at 453 nm. The optimum pH in our case was 5.9.

To determine the effect of time, absorbance of the chelate was evaluated after different intervals of time. Maximum absorbance was observed after 15 minutes and then gradually decreased. Between 15 minutes - 10 hours a kinetically stable chelate was observed. After 24 hours the absorbance of chelate was immeasurable. This was probably caused by spontaneous change in the structure. The optimum temperature for the chelate development was 25 °C.

4.2 Optimalization of chromatographic separation

Yellow components of human urine could interfere with spectrophotometric detection of chelate. Consequently, another separation step was added, in order to separate chelate from other yellow components of human urine. As can be seen from the separation of real human urine, by our chromatographic conditions, we separated all potential interfering substances of human urine. The determination of copper in human urine has been successfully performed by the newly developed gradient HPLC-VIS method using pre-column derivatization step. *Figure 3* shows the chromatograms obtained from analysis. The concentration of copper was 1.44 $\mu mol \cdot L^{-1}$ for standard aqueous solution and for spiked healthy volunteer human urine was 1.64 $\mu mol \cdot L^{-1}$. In *Table 2* are results obtained by HPLC

analysis the above samples.

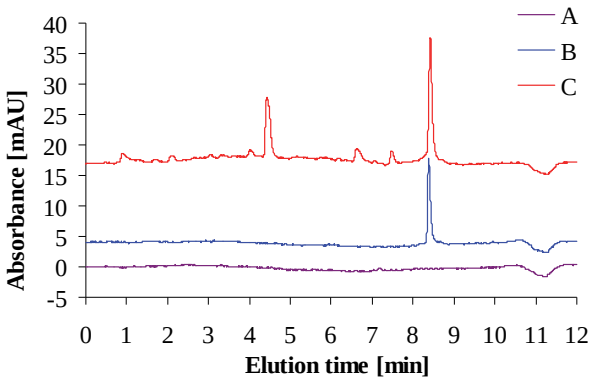

Fig. 3: A - blank B - standard aqueous solution of copper and C - spiked healthy volunteer human urine samples with copper after pre-column derivatization with neocuproine chelate reagent

Table 2: Retention time of Cu^{+}:Nc chelate, calibration curve parameters and limit of detection of copper obtained by HPLC analysis of spiked water samples and human urine samples

Sample	Elution time [min]	Calibration range [µmol·L^{-1}]	Linear regression equation	R^2	LOD
Water	8,42	0.72-5.75	y = 27116x + 15566	0.997	0.62
Human urine	8,41	0.72-11.50	y = 25232x + 34858	0.999	0.60

R^2 - Squared correlation coefficient

4.3 Analysis of standard reference materials

The developed method was applied to analysis of standard reference materials of human urine. Two standard reference materials of human urine, first Assayed Urine Control Level 2 (URN ASY CONTROL 2) with normal copper concentration (range 1.30-1.94 µmol·L^{-1}) and second Assayed Urine Control Level 3 (URN ASY CONTROL 3) with increased copper concentration (range 3.25-4.87 µmol·L^{-1}) were analyzed. The chromatograms of the analysis of both reference materials are presented on the *Fig. 4*. *Table 3* shows result from determination of copper in standard human urine solutions.

Table 3: Determination of copper in standard reference human urine solutions

Sample	Reference range [µmol·L^{-1}]	Target [µmol·L^{-1}]	Determined[a] [µmol·L^{-1}]
URN ASY Control 2	1.16-1.74	1.45	1.36 ± 0.11
URN ASY Control 3	2.76-4.14	3.45	3.10 ± 0.80

[a]Mean ± SD (n = 5)

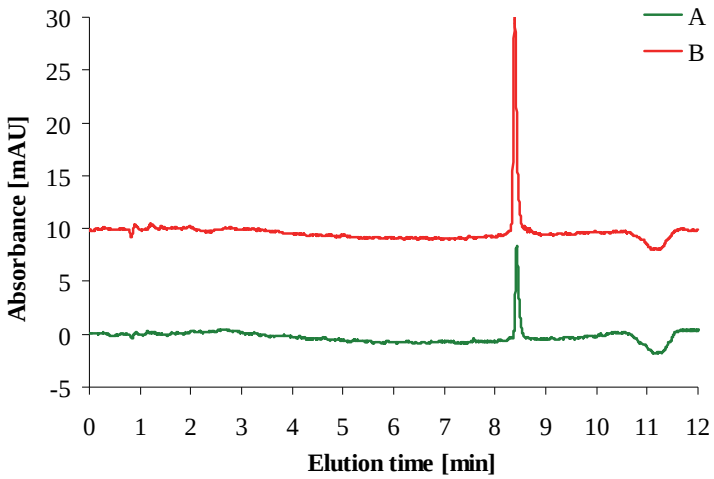

Fig. 4: Analysis of copper in standard reference materials by proposed HPLC-VIS method. A - URN ASY CONTROL 2 with normal copper concentration and B - URN ASY CONTROL 3 with increased copper concentration.

5 CONCLUSIONS

A novel, simple and environmentally friendly procedure for copper determination based on the formation of an ion associate of Cu^{+} with neocuproine was demonstrated. The results obtained in the analysis of human urine sample indicate that our proposed method of HPLC-VIS with pre-column derivatization can be used for rapid and satisfactory determination of copper in human urine. Cu^{+} ions form yellow-orange chelate, with the maximum absorption at 453 nm. This method is a good alternative to traditional techniques (e.g. atomic spectrometry) usually employed to determine copper in the human urine sample.

ACKNOWLEDGEMENTS

This work was generously supported by the grant of Scientific Grant Agency of the Ministry of Education of Slovak Republic and the Academy of Sciences - project VEGA 1/1349/12 and the grant of Slovak Research and Development Agency - project APVV-0583-11. This work is partially outcome of the project VVCE-0070-07 of Slovak Research and Development Agency solved in the period 2008-2011.

LITERATURE

[1.] http://www.diet.com/g/copper
[2.] http://www.nlm.nih.gov/medlineplus/wilsondisease.html
[3.] MAREČEK, Z. 2007. Současné možnosti diagnostiky a léčby Wilsonovy choroby. Praktický lékař. ISSN 0032-6739, roč. 87, č. 1, s. 17-22.
[4.] COLLINS A. G. 1975. Geochemistry of oilfield waters. 1rd. ed. New York: *American Elsevier publishing*, 1975. p. 95. ISBN 0-444-41183-6.
[5.] MALÁT, M. 1988. Extrakční spektrofotometrie kovů a nekov. 1. vyd. Praha: Nakladateľství technické literatúry, 1988. s. 182-190. DT 535.243:546.1/.3

P35 COMPARISON OF CONCENTRATION OF IONS IN PM1 AEROSOL SAMPLED ON NITRATE CELLULOSE AND TEFLON FILTERS

Alena Kořínková[a,b], Pavel Mikuška[b], Zbyněk Večeřa[b], Kamil Křůmal[b]

[a] *Brno University of Technology, Faculty of Chemistry, Purkyňova 118, 612 00 Brno, Czech Republic, korinkova@iach.cz*
[b] *Institute of Analytical Chemistry, Academy of Science of the Czech Republic, v .v. i., Veveří 97, 602 00 Brno, Czech Republic*

ABSTRACT

Atmospheric aerosols in the size fraction PM1 were sampled in Šlapanice and Brno in summer and winter periods in 2009 and 2010. Aerosols were analyzed on content of selected anions and cations.

Aerosols were sampled on nitrate cellulose filters by means of a high-volume sampler and, in parallel, on teflon filters using a low-volume sampler. An annular diffusion denuder was placed between cyclone inlet and teflon filter to eliminate interferences of gaseous co-pollutants.

Positive interferences of gaseous pollutants captured on aerosols that are collected on nitrate cellulose filters cause higher concentrations of anions and ammonium on nitrate cellulose filters than on teflon filters. These positive interferences of gaseous pollutants were eliminated during sampling of aerosols on teflon filters because of annular diffusion denuder placed upstream of a filter of low-volume sampler.

Keywords: aerosol, ions, nitrate cellulose and teflon filter

1 INTRODUCTION

Atmospheric aerosols play an important role in many environmental problems. During last years much attention has been paid to the study their impact on global climate [1] and human health [2]. The concentration and chemical composition of atmospheric aerosols is necessary to know to determine sources of atmospheric aerosols and their health risk.

Aerosols are usually sampled on filters, material and type of filters is chosen according to the compounds to be analyzed.

The contribution presents comparison of concentration of ions in atmospheric aerosol particles PM1 which were sampled in parallel on nitrate cellulose and teflon filters.

2. EXPERIMENTS

Atmospheric aerosols in the size fraction PM1 were sampled in Šlapanice in the garden of a family house (representing small town) and on a busy traffic street in the centre of Brno (representing large city). The samples were sampled for 24 hours during one week in summer and winter periods in 2009 and 2010.

The high-volume sampler (DHA-80, 30 m^3 /h, Digitel) was used for sampling of PM1 aerosols on nitrate cellulose filters (porosity 3 µm, diameter 150 mm, Sartorius). One half of nitrate cellulose filter was extracted with deionized water in ultrasonic bath and 6 selected anions (fluorides, chlorides, nitrites, nitrates, sulphates, and oxalates) and 5 selected cations (Na^+, K^+, NH_4^+, Ca^{2+} a Mg^{2+}) were determined in the extracts by ion chromatography (ICS-2100, Dionex).

In parallel, PM1 aerosol were sampled on teflon filters (porosity 1 µm, diameter 47 mm, type Zefluor, PALL) using the low-volume sampler (flow rate 1 m^3 /h). The annular diffusion denuder [3] placed between cyclone inlet (1 µm, URG) and the teflon filter eliminates interferences of gaseous pollutants (NO_2, HNO_3, HONO, SO_2, O_3, HCl, VOC, etc.). Teflon

filters were extracted with deionized water in ultrasonic bath and extracts were analyzed for the same anions and cations as nitrate cellulose filters.

3 RESULTS AND DISCUSSION

The concentrations of analyzed anions in PM1 aerosols during their parallel sampling on nitrate cellulose (NCF) and teflon (TF) filters during summer 2009 campaign in Brno and Šlapanice are shown in Fig. 1. Similar results were obtained in other campaigns.

Fig. 1: Mean concentrations of analyzed ions during summer campaigns 2009

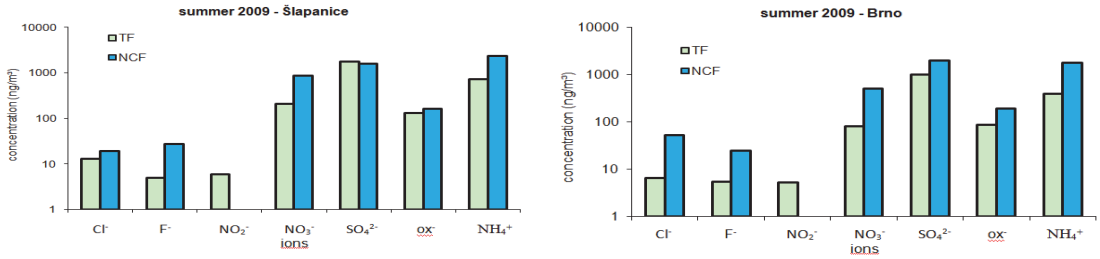

A comparison of concentrations of anions on teflon and nitrate cellulose filters in different season shows that fluorides (except winter 2009), chlorides, nitrates (except winter 2009) and oxalates had higher concentrations on nitrate cellulose filters than on teflon filters. Sulphate concentrations were higher on NC filters just in 2010. Nitrites weren´t detected on NC filters in summer 2009.

Ammonium cations had higher concentrations on NCF filters than on TF filters during all campaign in 2009 and 2010. Other selected cations (Na^+, K^+, Mg^{2+}, Ca^{2+}) had similar concentrations on nitrate cellulose and teflon filters during all campaigns.

Positive interferences of gaseous pollutants captured on aerosols that are collected on nitrate cellulose filters resulted in higher concentrations of anions and ammonium on NCF filters than on TF filters. These positive interferences of gaseous pollutants were eliminated during sampling of aerosols on teflon filters because of annular diffusion denuder placed upstream of a filter of low-volume sampler.

ACKNOWLEDGEMENTS

This work was supported by Institute of Analytical Chemistry of ASCR under an Institutional support by RVO: 68081715 and by Grant Agency of the Czech Republic under grant P503/11/2315 and P503/12/G147.

LITERATURE

[1.] Novakov, T., and C. E. Corrigan, *Geophysical Research Letter* 1996, *23*, 2141– 2144

[2.] Seinfeld, J.H., Pandis, S.N., *John Willey and Sons*, New York 1998

[3.] Mikuška, P., Večeřa, Z., Bartošíková, A., Maenhaut, W., *Analytica Chimica Acta* 2012, *714*, 68-75

P36 ANALYSIS OF THE ALTERED GLYCOSYLATION OF IGG IN DIFFERENT LUNG DISEASES

Nóra Rezsu, Csaba Váradi, András Guttman

Horváth Laboratory of Bioseparation Sciences, University of Debrecen, Hungary

ABSTRACT

The aim of this study was to investigate the changes in the relative amount of N-linked glycans of IgG in different lung diseases. We analyzed and compared the glycosylation pattern in Normal, Pneumonia, TBC and Lung cancer patients. IgG was isolated from the patient's samples using Protein A affinity pulldown and the N-glycans were released by peptide-N-glycanase F (PNGase F). The released glycans were then fluorescently labeled with aminopyrene-trisulfonate (APTS) and analyzed by capillary electrophoreiss with laser induced fluorescence detection. Kruskal-Wallis test was used to reveal disease associated differences between the groups examined.

Keywords: glycan analysis, biomarker discovery, IgG

1 INTRODUCTION

Glycosylation is one of the most important posttranslational modifications.Comprehensive analysis of glycans released from glycoproteins of interest holds the promise to identify biological markers for various diseaes. The N-glycosylation on human immunoglobulins, especially on IgG1, plays a critical role in the bioactivity of this goup of very important proteins. Significant differences have been reported in IgG glycosylation in pregnancy, aging and various diseases. The major glycans of IgG are biantennary-agalacto (FA2), biantennary-mongalacto (FA2(3)G1 and FA2(6)G1) and biantennary–digalacto (FA2G2) structures and their distribution can change in the above mentioned conditions.

2 ANALYSIS OF IGG N-GLYCANS

100 µL of human serum samples were used to capture the IgG molecules by Potein A affinity chromatography. After the elution, buffer exchange was performed with each sample by 10 kDa spinfilters because of the low pH of the elution buffer. The captured proteins were digested by N-glycanase (Prozyme, Hayward, CA) at 37 °C overnight and then precipitated by ice cold ethanol to separate them from the released glycans. 0.02 M APTS (Beckman Coulter, Brea, CA) in 15 % acetic acid was used to label the dry glycan samples and normal phase pipette tips (PhyNexus, San Jose, CA) tips to get rid off the salts and the free unreacted dye. For the capillary-gelelectrophoresis analysis of the labeled glycans, 60 cm NCHO coated capillary columns (Beckman Coulter) with 50 um inner diameter were used with the NCHO carbohydrate separation matrix (Beckman Coluter). All injection were accomplished by 1 psi for 5 sec and the separation voltage was 30 kV.

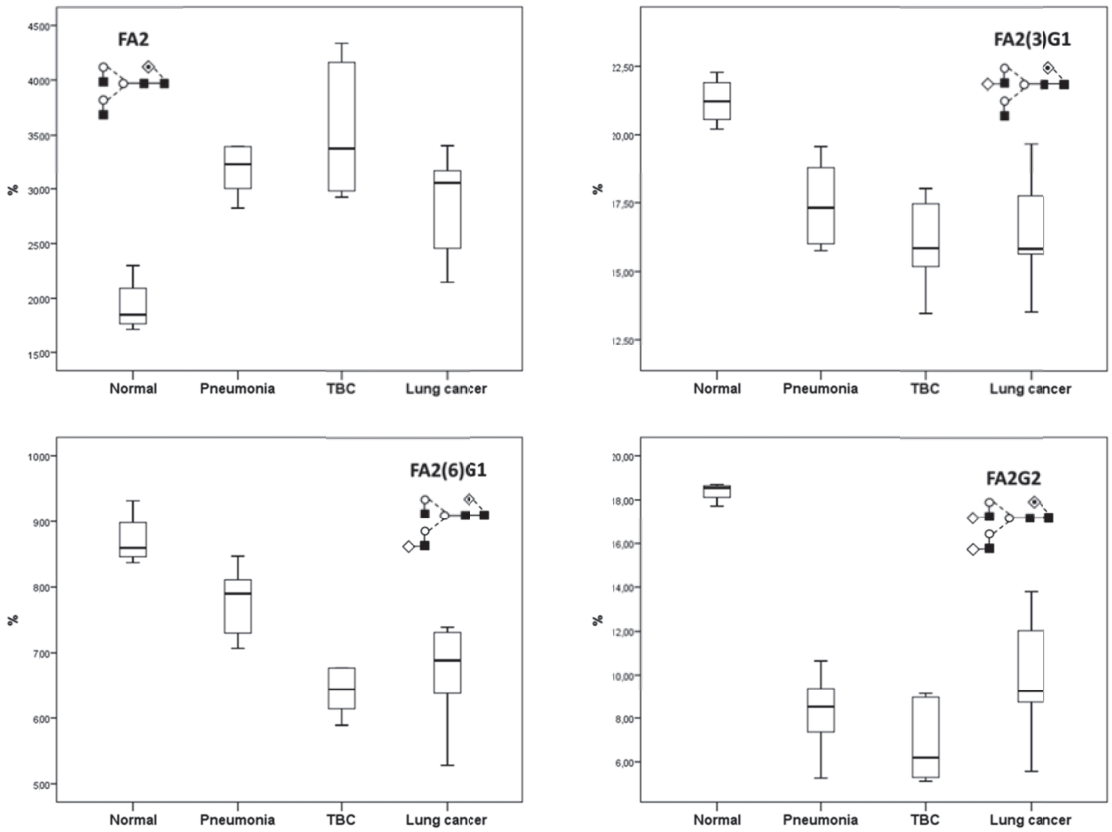

Figure 1. Boxplot comparison of the major IgG N-glycans in the diferent diseases compared to normal

3 RESULTS

Kruskal-Wallis test was used to find any significant differences between the examined grops. As shown in Figure 1 the level of FA2 was increased while FA2G2 was clearly decreased in each disease group compared to the control, suggesting that the level of IgG galactosylation was significantly altered in these diseases. The level of FA2(3)G1 and FA2(6)G1 also shown slight decrease in the disease groups. The observed results suggest that the altered galactosylation can be an interesting marker in these diseases.

ACKNOWLEDGEMENTS

This work was supported by the OTKA K-81839 grant of the Hungarian Government.

LITERATURE

[1.] Multiplexed Analytical Glycomics: Rapid and Confident IgG N-Glycan Structurall Elucidation Stefan Mittermayr, Jonathan Bones, Margaret Doherty, András Guttman, and Pauline M. Rudd J. Proteome Res. 2011, 10, 3820–3829.

P37 THE CONTENT OF SULPHUR DIFFERENT FRACTIONS IN SOIL FROM NOVÉ SADY LOCATION

Melánia Feszterová[a], Lýdia Jedlovská[b]

[a] *Department of Chemistry, Faculty of Natural Sciences, Constantine the Philosopher University, Tr. A. Hlinku 1, 949 74 Nitra, Slovakia, mfeszterova@ukf.sk*
[b] *Department of Environmental Science and Zoology, Faculty of Agrobiology and Food Resources, Slovak University of Agriculture, Tr. A. Hlinku 2, 949 76 Nitra, Slovakia*

ABSTRACT

The importance of sulphur content monitoring in soils increases not only with its effect on the quality of production but also from the environment protection point of view. Dominant part of soil sulphur is bounded in organic compounds, so the content of sulphur depends on the content of organic compounds in soil. Sulphur is essential for synthesis of certain amino acids in plants. Sulphur is one of the most abundant elements in the earth's crust. The aim of our work is to determine selected fractions of sulphur, and organic carbon in soil samples from the area of Nové Sady. We compared these characteristics in soil samples from different types, in different soil depths, during three years (2007 – 2009). Soil samples from the three probes (S1 - S3, Haplic Luvisols, Haplic Chernozems, Gleyic Phaeozems) were collected for this study. The average values of sulphate sulphur (SS) content were 427.13 $mg.kg^{-1}$, 316.40 $mg.kg^{-1}$, and 387.39 $mg.kg^{-1}$ in the probes S1, S2, and S3, respectively. The probe S2 had the lowest – sulphate sulphur content but also the lowest average content of chloride soluble sulphur (513.16 $mg.kg^{-1}$). The average contents of the chloride soluble sulphur (ClSS) in the probes S1 and S3 were 669.87 $mg.kg^{-1}$, and 609.73 $mg.kg^{-1}$, respectively. In the probe S1 was found the average content of the heat soluble sulphur (HSS) 194.2 $mg.kg^{-1}$, the probe S2 had 147.72 $mg.kg^{-1}$, and probe S3 had the lowest average value (133.29 $mg.kg^{-1}$). In the year 2007 (SS=378.00 $mg.kg^{-1}$, ClSS=604.28 $mg.kg^{-1}$, HSS=161.81 $mg.kg^{-1}$) average contents of selected sulphur fractions in soil types were higher than in the year 2008 (SS= 376.97 $mg.kg^{-1}$ $mg.kg^{-1}$ ClSS=602.10 $mg.kg^{-1}$, HSS=60.64 $mg.kg^{-1}$). The content of organic carbon in cultivated soil in all mould was relatively balanced as a result of regular cultivation. The highest content of humus (2.18 % Cox, in the depth 0.00-0.20 m) was found in the samples of the probe S3. The lowest content of humus in the depth 0.00-0.20 m from the analysed soil samples was found in the probe S2 (1.55 % Cox), where has been seen decrease of the organic carbon content in the depth of 0.3 m, with the significant decrease in the depth of 0.6 m. The medium content of humus was found in the probe S1 (1.75 % Cox).

Keywords: soil type, fractions of sulphur, sulphur dynamics

1 INTRODUCTION

Soil is one of the elemental components of environment with many functions. Chemical changes in soil composition have contributed largely to the knowledge of natural edaphic systems and their corresponding modification after the intrusion of agronomic management [2]. The origin and development of soil influences formation of its elementary attribute - fertility [15]. Fertility is the result of complex action of physical, chemical, and biological attributes and different processes in soil. The type of soil, class of soil, depth of soil and of mould, structure of soil, content of accessible nutrients, favourable water and thermal mode, the reaction of soil, content and quality of humus, biological activity, and content of harmful compounds in soil directly influence it. The index of fertility of soil is the quality and content of humus [29]. High content of quality humus is the conclusive assumption for stable soil fertility but it is not its guarantee, because for example, compression of soil, absence of nutrients and other factors may decrease the productive ability [16]. The missing nutrients in soil are filled-up by

fertilisation, for example we increase the intensity of mineralisation of sulphur organic fractions in soil. In the last decades, sulphur has become a frequent limiting nutrient deserving closer examination [3, 8, 9, 12, 13, 28, 32, 34, 37]. Correspondingly at present, scientists investigate more often S - cycling, S - requirement in plants and S - depletion from soil pools [6, 24, 27, 30].

Sulphur is a major inorganic element, essential for the entire biological kingdom because of its incorporation into amino acids, proteins, enzymes, vitamins, and other biomolecules [5, 18, 19, 22]. Unlike humans and monogastric animals, plants can use inorganic sulphur and synthesize sulphur-containing amino acids such as methionine and cysteine [4]. Mineralization of S in crop residues varied with type of crop residue and soil studied [31]. The content of sulphur in soil varies between 0.01 % and 1 %. Organic compounds are dominant and often form 90 % - 95 % of total amount of the sulphur in soil [31]. Disulphates as inorganic compounds form about 5 %, but elementary sulphur and disulphides form not more than 3 % [26]. One of the limiting factors for vegetal production is the deficit of sulphur. In many parts of the world, the soil concentration of sulphur is too low, resulting in reduced sulphur content of plant foodstuffs used by humans and animals [7]. In the consequence of global loss of organic and industrial manures, and mainly of manures with the content of sulphur [20], and because of the environment protection and ecological measures oriented to decreasing of discharged sulphur compounds, caused the fall of the supply of sulphur [23]. Monitoring some fractions of sulphur is important not only as far as the quality of production and produces is concerned but the care about environment, too.

The aim of our work is to determine selected fractions of sulphur, organic carbon in soil samples. We compared examined indicators in samples from different types, which were taken from the soils close to Nové Sady in different depths, during three years (2007 – 2009). The obtained results enabled us to characterise the soil conditions of the area.

2 MATERIAL AND METHODS

The village Nové Sady (geographical latitude 48° 25‘8´´, geographical longitude 17°59‘) is situated in the South Slovakia, 20 kilometres north-westwards from the town Nitra. (Fig. 1.) This climatic region is relatively hot, dry, folded and continental.

Three probes (S1 - S3) from different types of soil (*Haplic Luvisols, Haplic Chernozems, Gleyic Phaeozems*) were realised the intakes of soil samples for this study.

1. Probe S1 (*Haplic Luvisols*) was situated between the industrial court DEVIO and Šurianky in upright the road Nitra – Nové Sady.
2. Probe S2 (*Haplic Chernozems*) was taken between the villages Čáb and Nové Sady on the left side of the road from Nitra to Piešťany (60 m from the road).
3. Probe S3 (*Gleyic Phaeozems*) was located on the right bank of the stream Radošinka in front of the village Nové Sady (the underground water level on 1 m).

The soil samples were taken during sunny weather, from arable soil in many depths (0.00 – 0.20 m; 0.20 – 0.40 m; 0.40 – 0.70 m; 0.70 – 0.85 m; 0.85 – 1.10 m) in the cadastral area of Nové Sady.

2.1 Chemical analysis

1. pH was determined in 1:2,5 soil–water mixture (deionized water, 1 mol.L-^{1}KCl).
2. Chloride soluble sulphur (ClSS), sulphate sulphur (SS), heat soluble sulphur (HSS) were measured applying the Williams, Steinbergs method developed for this type of soils [36].
3. Isotachophoresis was used for determination of anion concentrations (nitrate, nitrite, sulphate) [38].
4. The content of the total organic carbon was determined using by the Tjurin method [16].

We determined the content of the sulphate sulphur, chloride soluble sulphur and heat soluble sulphur in samples after their drying and homogenisation.

Fig. 1.: The monitoring region - Nové Sady

3 RESULTS AND DISCUSSION

Sulphur is mainly incorporated in soil as primary minerals, sulphate being liberated during aging and soil forming processes [2]. The content of individual fractions of sulphur in the taken soil samples of individual probes was fairly different. The decrease of available sources of S has led to S deficiency symptoms in plants [30], favouring studies focusing on the distribution and availability of sulphur in soil. The results show that the content of the sulphate sulphur in soil was influenced by the depth of the soil samples' intake, by resorption by plants, pH of soil, and meteorological conditions. In the probe S1 there was the total average of the content of the sulphate sulphur 427.13 mg.kg^{-1}, in the probe S3 it was 387.39 mg.kg^{-1}, and in the probe S2 it was the lowest – 316.40 mg.kg^{-1}. The sulphate sulphur contain in the year 2007 was higher than in the year 2008. Higher content of the sulphate sulphur was in the depth 0.20 – 0.70 m (Table 1), except for the probe S3 (452.98 mg.kg^{-1} in the depth of 0.00 – 0.20 m). Higher content of the sulphate sulphurs in the depth of 0.20 – 0.60 m is correspondent with the results of other authors [35], who presented the possibility of accumulation of the sulphate sulphur.

Total average of the chloride soluble sulphur was 602.10 mg.kg^{-1} in 2008 and 604.28 mg.kg^{-1} in 2007. According to the results during the time of monitoring the degradation of the content of the chloride soluble sulphur fraction occurred, which could be caused except for the meteorological conditions also by resorption of sulphur by vegetables and washing out. In the probe S1, the content of the chloride soluble sulphur is decreasing with the depth. The same value is for the depth 0.20 – 0.40 m and for the depth 0.70 – 0.85 m (Table 1).

In the probe S2, there was the content of the chloride soluble sulphur fraction relatively equable, with slightly decreasing values. The probe S3 has the lowest content in the depth of 0.00 – 0.20 m (283.97 mg.kg^{-1}, Table 1). The changes in the content of this fraction in soil in monitored depths were influenced not only by processes of mineralisation, quality of humus, but also by the resorption of sulphur and its migration in the soil, too.

The higher average content of the heat soluble sulphur was in the year 2007 (161.81 mg.kg^{-1}) than 2008 (160.64 mg.kg^{-1}) in all monitored depths. According to the results during the monitored period the content of the heat soluble sulphur was decreased. The increased content of the heat soluble sulphur may be influenced by the fertilisation by mineral fertilisers and also by the supply of the sulphur from atmosphere.

Gradual decrease of the heat soluble sulphur in the year 2008 is in the probe S2. In the year 2008, in the probe S1 and in the probe S3, there was the highest contain in the depth of 0.40 – 0.70m (S1 – 225.00 mg.kg^{-1}, S3 – 162.06 mg.kg^{-1}) and the lowest in the depth 0.70 – 0.85 m (S1 – 175.00 mg.kg^{-1}, S3 – 139.12 mg.kg^{-1} , S3 – 105.00 mg.kg^{-1}).

Table 1: The changes of selected sulphur fractions – the year 2008

Sampling points	The depth	Sulphate sulphur	Chloride soluble sulphur	Heat soluble sulphur
	[m]	[mg.kg^{-1}]	[mg.kg^{-1}]	[mg.kg^{-1}]
Probe S1	0.00 – 0.20	244.00	810.08	190.06
	0.20 – 0.40	853.10	726.12	200.25
	0.40 – 0.70	371.65	590.36	225.00
	0.70 – 0.85	391.78	710.06	175.00
	0.85 – 1.10	361.21	621.45	182.61
	1.10 – 1.50	341.02	561.16	192.28
Probe S2	0.00 – 0.20	280.17	577.08	172.17
	0.20 – 0.40	317.02	565.71	145.30
	0.40 – 0.70	326.78	512.61	142.89
	0.70 – 0.85	328,97	487.56	139.12
	0.85 – 1.00	329.08	422.83	139.12
Probe S3	0.00 – 0.20	452.98	283.97	152.14
	0.20 – 0.40	253.00	737.88	144.05
	0.40 – 0.70	626.12	755.26	162.06
	0.70 – 0.85	306.66	647.99	105.00
	0.85 – 1.00	298.17	623.54	103.15

The fertilisation (ammonia disulphite) apparently influenced the rising amounts of particular fractions of sulphur in cultivated soil. The average amounts of particular fractions of sulphur varied between 77 and 860 mg.kg^{-1} of soil. The soils which contained less than 1000 mg.kg^{-1} Trocme classified as poor for sulphur [33]. The changes in the content of the heat soluble sulphur are influenced by migration, by the content of the organic mass and by soil reaction. Soil organic matter (SOM), together with biological activity are the most important factors affecting nutrient cycling modelling, soil fertility and their associated plant nutrition processes [1,10]. The content of organic carbon in cultivated soil in all mould was relatively balanced as a result of regular cultivation. The highest content of soil organic carbon (2.18 % C_{ox}) was from the soil samples in the probe S3, which is better evaluated as mould (*Haplic Chernozems).* It occurs largely in broad alluvial plans of Slovak rivers. It satisfies high assortment of plants, mainly because their soil profile is periodically moistened by underground water. The lowest content of humus from the analysed soil samples was found in the probe S2 (1.55 % Cox), where we could see the drop of the content of the organic carbon in the depth of 0.3 m, distinctive drop was observed in the depth of 0.6 m. The medium content of humus was in the probe S1 (1.75 % Cox). The soil reaction in selected soil types was slightly alkaline up to neutral in the probe S1 and slightly alkaline in the probe S2 and S3. The pH varied from 6.51 to 8.45.

4 CONCLUSION

Sulphur economy is mainly affected by type of soil, organic matter content, microbial community and redox conditions [24]. However, the maintenance of sufficient levels of sulphur in the biosphere involves the biogeochemical sulphur cycle [22]. The development of the knowledge about nutrition and fertilization served as a development impulse of fertilisation in agricultural practice. The fertilisation by artificial fertilisers increases the intensity of mineralisation of the organic sulphur fractions in soil, and therefore it is important to pay attention to the fertilisation with organic fertilisers, too. The content of organic acceptors for the resynthesis of the sulphur organic fractions in the soil is increasing and the washing out sulphur from the soil of is decreasing.

The immobilisation and mobilisation processes influence the availability of the sulphur for plants. The sulphur immobilisation positively correlates with the ratio of C : S in the substrate. After monitoring the dynamics of the changes of the content of the selected sulphur fractions it can be stated that in all soil profiles there is a change of sulphur content (sulphate sulphur, chloride soluble sulphur, heat soluble sulphur) and that there cannot be made conclusions of binding force. In various soil types the content of the sulphur changes differently with the depth of the soil samples. Soil carbon storage is sensitive to human management and disturbance [14]. In the comparison of various soil types there were presented differences in the values of total content of organic carbon. The soil organic matter, organic carbon and its fractions are soil components that we can be systematically changed; therefore it is important to monitor the above-mentioned agrochemical characteristics, especially in the regions with the influence of chemical industry and other producers of emissions [17, 25]. The carbon nutrient dynamics can be used as indicators of environmental change, specifically to show how land management, restoration strategies and climate change may be impacting the soil ecosystems [11]. Soil disturbance generally causes carbon losses by stimulating organic matter decomposition [21].

To reach sustainable production potential of soils it is inevitable to prevent large single or long-term decreases of the organic matter content in soil, as well as the decrease of its quality influenced by the changes of the amount of selected sulphur fractions. This is achievable only by systematic monitoring of soil organic matter content management and regulation of the input of organic and inorganic matters.

ACKNOWLEDGEMENT

This work has been supported by the CEEPUS programme (CIII-HU-0010-06-1112-M-52225).

LITERATURE

[1.] Aguilera, S.M., Borie, G., del Canto, P., Peirano, P. Contribucio´n del sistema conservacionista Cero-Labranza en los niveles de C, P y bioactividad de suelo Santa Ba´rbara. Agricultura Te´cnica, Chile 56 (1996) p. 250–254.

[2.] Aguilera, M., de la Luz Mora, M., Borie, G., Peirano, P., Zunino, H. Balance and distribution of sulphur in volcanic ash-derived soils in Chile. Soil Biology & Biochemistry, 34 (2002) p. 1355–1361.

[3.] Amelung, W., Zech, W., Zhang, X., Follett, R. F., Tiessen, H., Knox, E., Flach, K. W., Carbon, nitrogen, and sulfur pools in particle-size fractions as influenced by climate. Soil Science Society of America Journal, 62 (1998) p. 172–181.

[4.] Baker, D. H., Literature review on sulfur in nonruminant nutrition Grants-in-Aid Committee, National Feed Ingredients Association, Des Moines. 1977.

[5.] Castellano, S. D., Dick, R. P.Cropping and sulphur fertilization influence on sulphur transformations in soil. Soil Science Society of America Journal, 55, (1991) p. 114–121.

[6.] Chapman, S. J. Barley straw decomposition and S inmobilization. Soil Biology and Biochemistry, 29 (1997) p.109–114.

[7.] Chinoim, N., Lefroy, R. D. B., Blair, G. J. Effect of crop duration and soil type on the ability of soil sulfur tests to predict plant response to sulfur. Aust J Soil Res, 35 (1977) p. 1131.

[8.] Chowdhury, A. H., Kouno, K., Ando, T., Nagaoka, T. Microbial biomass, S mineralization and S uptake by African millet from soil amended with various composts. Soil Biology and Biochemistry, 32 (2000) p. 845–852.
[9.] Dail, D. B., Fitzgerald, J. W. S cycling in soil and stream sediments: influence of season and in situ concentrations of carbon, nitrogen and sulfur. Soil Biology and Biochemistry, 31 (1999) p. 1395–1404.
[10.] David, M. B., Mitchell, M. J., Nakas, J. P. Organic and inorganic sulfur constituents of a forest soil and their relationship to microbial activity. Soil Science Society of America Journal, 46 (1982) p. 847–852.
[11.] Eaton, W. D., Chassot, O. Characterization of soil ecosystems in Costa Rica using microbial community metrics. Tropical Ecology, 53, 2, (2012) pp. 185-195
[12.] Eriksen, J. Sulphur cycling in Danish agricultural soils: turnover in organic fractions. Soil Biology and Biochemistry, 29 (1997 a) p. 1371–1377.
[13.] Eriksen, J. Sulphur cycling in Danish agricultural soils: inorganic sulphate dynamics and plant uptake. Soil Biology and Biochemistry, 29 (1997 b) p. 1379–1385.
[14.] Gough, Ch. M., Elliott, H. L. Lawn soil carbon storage in abandoned residential properties: An examination of ecosystem structure and function following partial human-natural decoupling. J. of environ. management , Vol. 98, (2012) pp. 155-62.
[15.] Hanes, J. et al. Pedológia. 2.nd ed. Nitra: Vydavateľské a edičné stredisko SPU, 1997. p. 119. ISBN 80-7137-390-7.
[16.] Hanes, J., Antropogénne vplyvy na vlastnosti poľnohospodárskych pôd. Nitra: Vysoká škola poľnohospodárska, 1995. 89. p. ISBN 80-7137-238-2.
[17.] Hrnčiarová, T. Impact of changing environment to landscape diversity. European Landscapes in Transformation: Challenges for Landscape Ecology and Management. European IALE Conference 2009 : 70 years of Landscape Ecology in Europe. Bratislava : University of Salzburg : STU : Comenius University, 2009. p. 244. ISBN 978-80-227-3100-3.
[18.] Jedlovská, L., Feszterová, M. Dynamika zmien vybraných frakcií síry v rôznych pôdnych typoch. Aktuálne problémy riešené v agrokomplexe, zborník z X. roč.. medzinár. vedeckého seminára, Nitra, 19. 11. 2004, 14 s. ISBN 80-8069-477-8.
[19.] Johnson, D. W. Sulfur cycling in forests. Biochemistry, 1 (1984) p. 29-43.
[20.] Kalocsai, R., Schmidt, R., Földés, T., Szakal, P. Sulphur forms in soils, sulphur fertilization. Nõvénytermelés, 51, 2002, č. 6, s. 725. ISSN 0546-8191.
[21.] Kaye, J. P., McCulley, R. L., Burke I. C. Carbon fluxes, nitrogen cycling, and soil microbial communities in adjacent urban, native and agricultural ecosystems. Global Change Biology, 11 (2005) pp. 575–587.
[22.] Komarnisky, L. A., Christopherson, R. J., Basu, T. K. Sulfur: its clinical and toxicologic aspects. Nutrition, 19 (1) (2003) pp. 54–61. DOI: http://dx.doi.org/10.1016/S0899-9007(02)00833-X.
[23.] Ložek, O. 2004. Efektívnosť N-Mg-S hnojív vo výžive rastlín. In: "Efektívnosť hnojív obsahujúcich síru a horčík vo výžive rastlín." zborník z medzinárodného sympózia konaného 5. – 7.5.2003 v Šoporni. Nitra : SPU 2004. s. 18 – 19.
[24.] Miller, R., Donahue, R. Soils. An Introduction to Soils and Plant Growth, sixth ed, Prentice Hall, New Jersey, USA, 1990.
[25.] Prousek, J. Rizikové vlastnosti látok. Bratislava: Vydavateľstvo STU, 2001. s. 75 – 76. ISBN 80-227-1497-6
[26.] Schung, E. Sulphur nutritional status of european crops and consequences for agriculture. Sulphur in agriculture, 15 (2001) p. 7-12.
[27.] Sharma, P., Swarup, A. Comparison of pyrites varying in water-soluble sulfur with gypsum for the reclamation of alkali soils under a rice-wheat rotation. Biol Fertil Soils, 24 (1996) p. 96.
[28.] Sorensen, L. H. Carbon–nitrogen relationships during the humification of cellulose in soils containing different amounts of clay. Soil Biology and Biochemistry, 13 (1981) pp. 312–321.
[29.] Spychaj – Fabisiak, E. et al., The effect of differentiated nitrogen fertilisation on the total carbon and nitrogen content on the rate of microflora development in soil. Goent, S., Dębska, B., Zaujec, A. (Eds.) Proceedings z 5 th International Conference „Humic Substances as Factor of the Terrestrial and Aquatic Ecosystems“ Duszniki Zdrój, Bydgoszcz: University of Technology and Agriculture, 2003. p. 109 – 117. ISBN 83-919331-0-5.
[30.] Stevenson, F.J. Cycles of Soils. Carbon, Nitrogen, Phosphorus, Sulfur, Micronutrients, Wiley, New York. 1986.
[31.] Tabatabai, M. A., Importance of sulphur in crop production. Biogeochemistry, Vol. 1(2005), ISSN 1573-515X.
[32.] Tabatabai, M. A., Bremner, J. M., Forms of sulfur, and carbon, nitrogen and sulfur relationships, in Iowa soils. Soil Science, 114 (1972) pp. 380–386.
[33.] Trocme M. Tanaur an soufre des solad Europe. In: Intenational symposium sur le soufre en agriculture. Versailes. 3-4-12, 1970. s. 103-112.
[34.] Wander, M. M., Traina, S. J. Organic matter fraction from organically and, conventionally managed soils. I. Carbon and nitrogen distribution. Soil Science Society of America Journal, 60 (1996) pp. 1081–1087.
[35.] Whitehed, D. C. Soil and plant nutrition aspects of the sulphur cycle. Soil and Fert 227/1-8, 1964
[36.] Williams, C. H., Steinbergs, A. Soil sulphur fractions as chemical indices of available sulphur in some Australian soils. Australian Journal of Agricultural Research, 10 (3) (1958). pp. 340 – 352.
[37.] Zhou, W., Li, S.T., Wang, H., He, P., Lin, B. Mineralization of organic sulfur and its importance as a reservoir of plant-available sulfur in upland soils of north China. Biology and Fertility of Soils, 30 (1999) 245–250.

[38.] Prest, J. E., Fielden, P. R. The simultaneous determination of chloride, nitrate and sulphate by isotachophoresis using bromide as a leading ion. Talanta 75 (2008) 841-845.

P38 FAST ON-LINE TWO-DIMENSIONAL LCXCE USING FLOW AND VOLTAGE GATING INTERFACES

Petr Česla, Jan Fischer, Lenka Kovaříková

Department of Analytical Chemistry, Faculty of Chemical Technology, University of Pardubice, Studentská 573, 532 10 Pardubice, Czech Republic, Petr.Cesla@upce.cz

ABSTRACT

On-line two dimensional separation systems combining capillary liquid chromatography with capillary electrophoresis is presented, with special attention to the interface design. Two types of transparent interfaces have been fabricated in the poly methyl methacrylate, with different approaches to the transfer of the fractions from first dimension liquid chromatography separation to the second dimension micellar electrokinetic capillary chromatography separation. The interfaces used for the injection of the mobile phase effluent into the separation capillary are based either on the transverse flow of the background electrolyte, or on the voltage-switching in the tangentially connected channels. The application of both approaches for the separation of selected antioxidants is presented and merits of the interface designs are compared with the recently developed automated off-line two-dimensional LCxMEKC separation method.

Keywords: Two-dimensional separation, capillary liquid chromatography, capillary electrophoresis

1 INTRODUCTION

Separation of complex samples, which contain analytes with different physicochemical properties, can be greatly improved in the two-dimensional separation system. The prerequisite for the successful two-dimensional separation is at least two types of distributions presented in the sample (distribution of chemical composition, molar mass distribution), which can be utilized by the independent separation mechanisms of the coupled separation methods for improvement of the overall peak capacity and resolution of sample components. Combination of capillary electrophoresis or micellar electrokinetic capillary chromatography (MEKC) in the second dimension with reversed-phase liquid chromatography (RP-LC) in the first dimension provides highly orthogonal separations [1]. While RP-LC separates analytes according to the differences in hydrophobicity, MEKC is capable of resolution of both, ionized analytes on the basis of charge and size, as well as neutral compounds by partitioning in the micellar pseudostationary phases.

The optimization of two-dimensional LCxCE separation methods employs selection of suitable experimental setup. The off-line connection represents simpler approach, however, the reliability and reproducibility of the setup can be increased by automation of fraction collection [1]. The on-line approach introduced by Bushey and Jorgenson [2] utilizes computer-controlled six-port valve and second pump that flushes the loops containing effluent from conventional LC column directly into the anode end of the separation capillary. For the application of capillary microcolumns, the valve-based interface becomes essentially

impractical and can be successfully replaced by the transverse flow gating interface [3]. Major advantage of such flow gating interface is in lower extracolumn dilution due to the absence of storage loops and more efficient fraction transfer process, which results in approximately 8-fold improvement in sensitivity of the method. The another alternative of similar interface fabricated from clear polycarbonate plastic allows direct observation and routine manipulation with separation column and capillaries for the analysis of fluorescently labeled amino acids [4]. The transferring of the analytes between the LC column and CE capillary by high-voltage switching has not been yet reported, however, it can be used with two-dimensional CE in tangentially connected capillaries [5].

In the present work, we have developed and optimized the transverse flow and high-voltage switching interfaces for on-line connection of capillary liquid chromatography with micellar electrokinetic capillary chromatography. The interfaces were fabricated in poly methyl methacrylate and the suitability of this approach was demonstrated by fast MEKC second dimension separation of LC fractions containing natural antioxidants in range of several tens of seconds.

2 EXPERIMENTAL CONDITIONS

The standards of natural antioxidants, acetonitrile, boric acid, sodium tetraborate, sodium decylsulfate and sodium dodecyl sulfate were obtained from Sigma-Aldrich (Steinheim, Germany). The electrophoretic experiments were performed using in-laboratory assembled capillary electrophoresis, containing Spellman CZE30PN high voltage power supply (Spellman, New York, USA) and ATI Unicam Spectra 100 variable wavelength UV detector (ATI Unicam, Cambridge, UK). The non-coated fused silica capillaries obtained from Agilent (Palo Alto, CA, USA) were subsequently washed for 10 min with 1 mol/L sodium hydroxide, water and background electrolyte. Background electrolytes were prepared by dissolving the buffer components in distilled water and mixed in appropriate ratios. The pH of the background electrolytes was measured using an Orion 3 Star pH meter (Thermo Scientific, Waltham, MA, USA).

3 TABLES AND ILLUSTRATIONS

The precise design, fabrication and optimization of interface for on-line connection of capillary liquid chromatography and capillary electrophoresis are necessary. In our work, we have used two types of interfaces, with different positions of LC and CE separation capillaries (Fig. 1). Both interfaces were fabricated by drilling of the channels in the poly methyl methacrylate cylinder. The first approach (Fig. 1B) is the transverse flow gating interface, where the outlet capillary from the LC column is in one plane with the CE separation capillary with aligned longitudinal axes of both capillaries. The gating and transfer of appropriate fractions is provided by the flow of background electrolyte in perpendicular direction.

The voltage gating interface utilizes tangentially connected channels, where the outlet capillary from LC is in parallel plane to the CE separation capillary. The fractions are transferred between both channels by application of voltage on the opposite ends of the capillaries. The interfaces (inner diameter and distance between the used capillaries, transverse flow of the background electrolyte) were optimized using methylene blue solution to achieve fast and efficient transfer of the fractions with minimal contribution to the band broadening and thus increased sensitivity in comparison to the off-line two-dimensional LCxMEKC method [1].

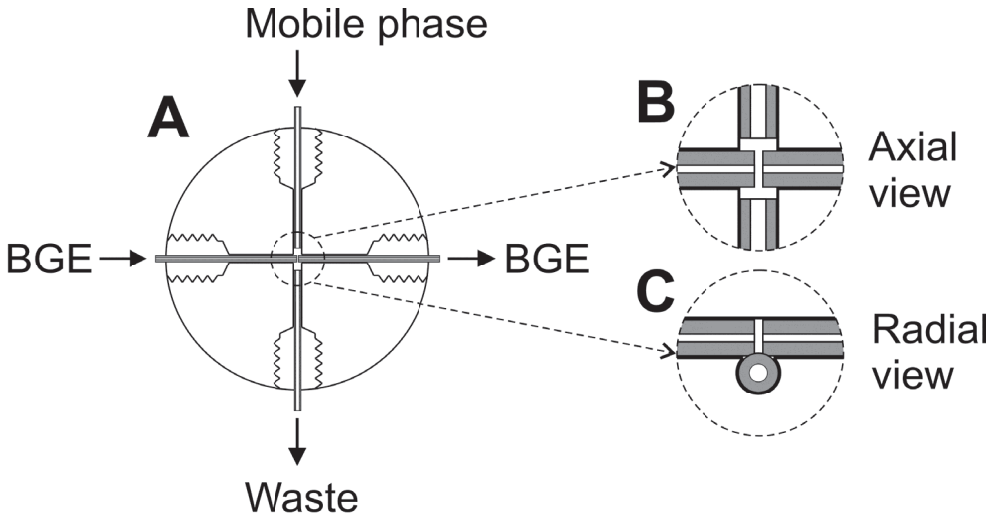

Fig. 1. : Schematic view of the LCxCE interfaces (A) with detailed scheme of the transverse flow (B) and voltage-gated interface (C). Both devices are fabricated from poly methyl methacrylate cylinder.

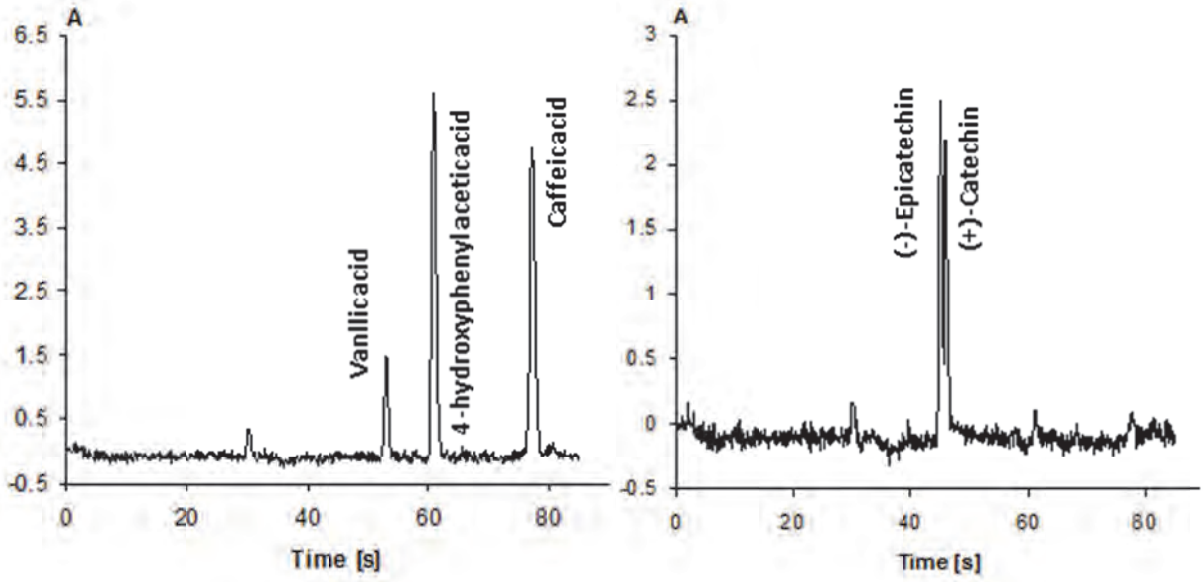

Fig. 2. : MEKC separation of selected fractions transferred from LC using flow gating interface in non-coated fused silica capillary, 50 μm i.d., 48 cm total length, 10 cm effective length. Background electrolyte 25 mmol/L borate buffer pH 9.05 with addition of 15 mmol/L sodium decyl sulfate, applied voltage 30 kV, detection UV at 254 nm.

The highly efficient and fast MEKC separations of the fractions transferred from LC were obtained using fabricated interfaces. The analysis time of MEKC separation in the second dimension was achieved in the range of several tens of seconds (Fig. 2). The on-line separation of standard mixture of natural antioxidants using developed interfaces provides significantly higher peak capacity and lower overall analysis time in comparison to the automated off-line LCxMEKC method [1].

ACKNOWLEDGEMENTS

The financial support by the Czech Science Foundation, project No. 206/12/0398 is gratefully acknowledged.

LITERATURE

[1.] Česla, P., Fischer, J., Jandera, P., *Electrophoresis* 2010, *31*, 2200-2210.
[2.] Bushey, M.M., Jorgenson, J.W., *Anal. Chem.* 1990, *62*, 978-984.
[3.] Lemmo, A.V., Jorgenson, J.W., *Anal. Chem.* 1993, *65*, 1576-1581.
[4.] Hooker, T.F., Jorgenson, J.W., *Anal. Chem.* 1997, *69*, 4134-4142.
[5.] Sahlin, E., *J. Chromatogr. A* 2007, *1154*, 454-459.

P39 DETERMINATION OF ENDOCANNABINOIDS 2-ARACHIDONOYLGLYCEROL AND ANANDAMIDE IN HUMAN SERUM

Jan Juřica[a], Žaneta Jurčková[b], Ondřej Zendulka[a]

[a] *Masaryk University, Faculty of Medicine, Department of Pharmacology and Central European Institute of Technology, Kamenice 5, 628 00, Brno, jurica@med.muni.cz*

ABSTRACT

Various cannabinoid receptor ligands are very promising group of drug candidates. In the research of endocannabinoid system there are utilized methods for determination of endocannabinoids, anandamide and 2-arachidonoylglycerol. Here we present an innovative, simple, rapid, and sufficiently sensitive method for determination of anandamide and 2-arachidonoylglycerol in human serum samples. Methanandamide was used as internal standard to ensure precision and accuracy of the method. Analytes were extracted into diethyl ether and derivatized at 60°C for 120 min. A reversed phase analytical column and a mobile phase composed of acetonitrile and water were used for the chromatographic separation with fluorescence detection. Limits of detection were assessed to be 7 and 12 nmol/L for anandamide and 2-arachidonoylglycerol. The overall extraction recovery for the analytes were above 68,9 %. Precision, the intra- and interday variation at three different concentrations in all analytes never exceeded 8.4 and 9.5 %, respectively.

Keywords: 2-arachidonoylglycerol; anandamide; HPLC

1 INTRODUCTION

Anandamide ((N-(2-Hydroxyethyl)-5Z,8Z,11Z,14Z-eicosatetraenamide) and 2-Arachidonoylglycerol (5Z,8Z,11Z,14Z)-5,8,11,14-Eicosatetraenoic acid, 2-hydroxy-1-(hydroxymethyl)ethyl ester) are endogenous lipid signalling molecules characterized as endocannabinoids (EC). EC play an important role in the regulation of many physiological and pathophysiological processes, e.g. cardiovascular function, satiety, reward pathways, immune

response, movement disorders and many others [1]. Artificial or natural substances affecting endocannabinoid system seem to become valuable drugs. Several cannabinoid derivatives or plant extracts have been recently registered as drugs for the treatment of anorexia, nausea and vomiting, multiple sclerosis, neuropathic pain (dronabinol, nabilon, standardized cannabis extract) [2]. Endogenous cannabinoid system is nowadays intensely investigated concerning its possible involvement in the pathophysiology and treatment of drug dependence, schizophrenia, movement disorders or cancer. In the research of abovementioned diseases, it is necessary to determine changes in the levels of endocannabinoids. 2-arachidonoylglycerol and anandamide is mostly determined by the mass spectrometry after chromatographic separation [3-5].

In the literature available, there are only few methods for simultaneous determination of both 2-AG and anandamide, even for use in practice – i.e. determination of these analytes in biological samples. There were also published methods for determination of anandamide by use of HPLC with fluorescence detection, after derivatization procedure with 4-(N,N-dimethylaminosulfonyl)-7-(N-chloroformylmethyl-N-methyl-amino)-2,1,3-benzoxadiazol (DBD-COCl) [6-7].

In our opinion, in the research of endocannabinoid system there is general need for rapid, simple, robust and accessible method for the determination of two major endocannabinoids: 2AG and anandamide in biological samples.

2 METHODS

2.1 Chemicals

Anandamide (ANA), methanandamide (MT ANA, (R)-N-(2-Hydroxy-1-methylethyl)-5Z,8Z,11Z,14Z-eicosatetraenamide) and arachidonoylglycerol (2AG) were purchased from Cayman chemical (San Diego, California, USA).4-(N,N-dimethylaminosulfonyl)-7-(N-chloroformylmethyl-N-methyl-amino)-2,1,3-benzoxadiazol (DBD-COCl) and phenylmethanesulfonylfluoride were purchased from Sigma-Aldrich (Darmstadt, Germany), diethylether and acetonitrile were of HPLC grade and were purchased from Scharlau Chemie S.A. (Madrid, Spain), water solutions were prepared with Ultrapure water (Elga Ultrapure water systems, ChromSpec, Czech Republic).

2.2 Equipment

The HPLC system consisted of a Shimadzu LC-10 series (Shimadzu, Kyoto, Japan), i.e. LC-10ADvp gradient pump with DGU-14A degasser, SIL10ADvp autosampler, CTO10ACvp column oven, fluorescence detector RX10 Avp and system controller SCL10Avp. Data from the detector was collected and analyzed using LabSolution 1.03 SP3 software (Shimadzu, Kyoto, Japan). A Gemini C18 reversed-phase chromatographic column (150 × 4,6 mm; 5µm) equipped with SecurityGuard™ C18 (8.0 x 3.0 mm I.D.; 5µm) (Phenomenex, Torrance, CA, USA) was used for the separation.

2.3 Sample extraction and derivatization

Blank serum samples were obtained from healthy volunteers and left at 25°C for 6 hours so as to decompose natural ANA and 2AG. The purity was chromatographically verified. Methanandamide, a synthetic ligand of endocannabinoid receptors (25 µl, 20 mM) was added as an internal standard to the fresh serum samples (500 µl). The samples were extracted with 4 ml of diethylether and vortexed for 10 minutes at 1400 /min. Organic fraction was decanted and evaporated at 30°C under gentle stream of nitrogen. The evaporated extracts were dissolved in 100 µl of acetonitrile and subsequently derivatized with 25 µl DBD-COCl (15 mM) and samples were heated at 60°C for 2 hours. The derivatization procedure was then stopped

by addition of (75 µl) cold water (4°C). The samples were subsequently injected into the HPLC system.

2.4 Chromatographic conditions

The analytes were eluted isocratically at 45°C, the composition of the mobile phase was acetonitrile:water (75:25, v/v), the flow was maintained at 1.5 ml/min and analytes were detected in the fluorescence detector (λex = 430 nm, λem = 540 nm).

3 RESULTS

The retention times of were 7.5 min, 8.7 min and 10.9 min for ANA, MT ANA and 2-AG, respectively. Figures 1 and 2 present typical chromatograms of analysis of solution of standards or real sample of human serum, respectively.

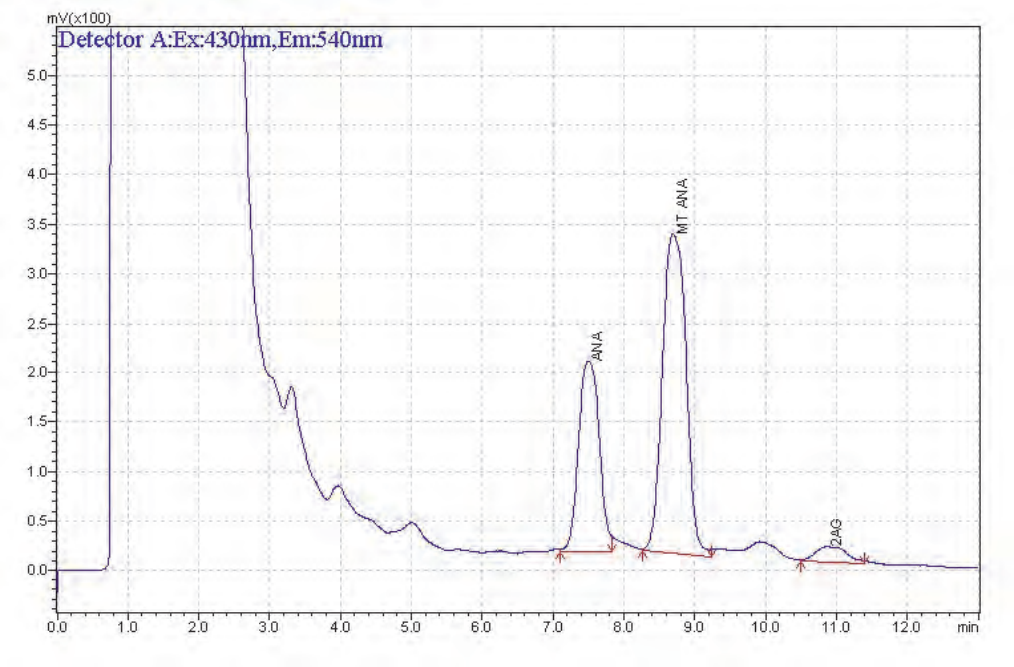

Fig 1: Typical chromatogram of blank human serum (left 6 hours at room temperature) spiked with standards of ANA, MT ANA (ISTD) and 2AG; chromatographic conditions described elsewhere.

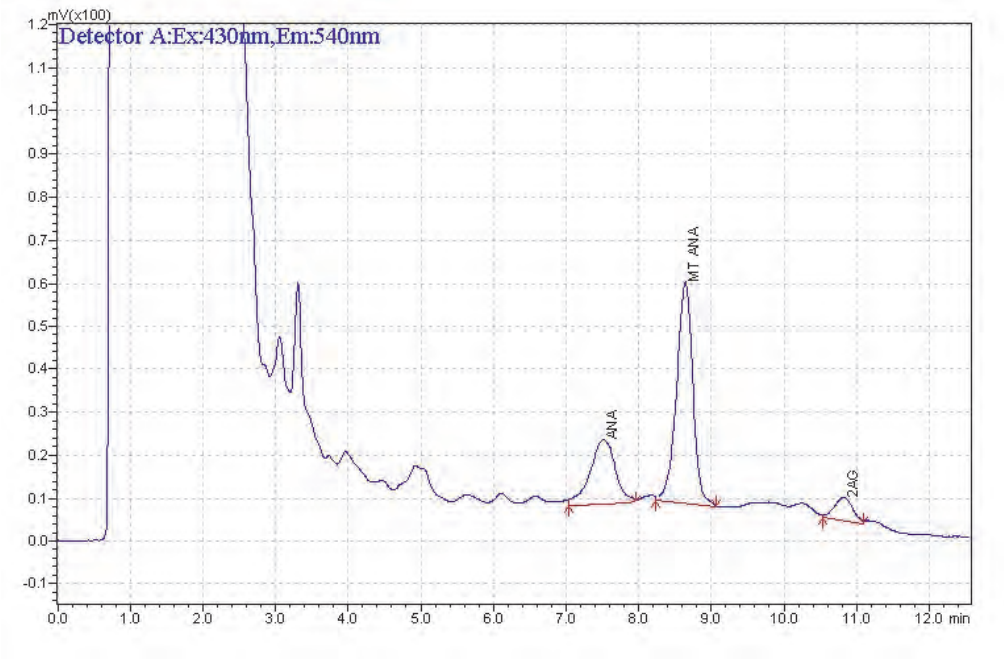

Fig. 2: Chromatogram of human serum with addition of internal standard; chromatographic conditions described elsewhere.

Linearity of detector response was investigated over the range 0.01–100 µmol/L for.ANA, over the range 0.05–200 µmol/L for 2AG and over the range 0.5-200 µmol/L for MT ANA. The extraction recovery was assessed as a ratio of peak areas of extracted samples of known concentration to the peak areas of standards in mobile phase (without extraction). The extraction recoveries were greater than 78,6 % for ANA, 68,9 for 2AG and 69,4 for MT ANA. The limit of detection (LOD, S/N > 3:1), were calculated from the analysis of the lowest concentration in the linearity verification. The LOD for ANA was found to be 7 nmol/L and for 2AG was found to be 12 nmol/L.

To determine the intra- and inter-day precision and accuracy of the assay, replicate sets (n = 10 and 6 consecutive days, respectively) of three concentrations of each analyte in blank serum were analyzed. Precision was calculated as intra- and inter-day RSD values and accuracy was expressed as mean relative error. The intra- and inter-day variations for the measured analytes were below 8.4 and 9.5 %, respectively.

4 CONCLUSION

Innovative HPLC-fluorescence method for simultaneous determination of anandamide and 2-arachidonoyl glycerol in human serum was developed. Derivatization procedure enables sensitive fluorescence detection. Method utilizes methanandamide as internal standard to ensure precision and accuracy. This method may be useful in preclinical research of various endocannabinoid system functions.

ACKNOWLEDGEMENTS

This work was supported by "CEITEC - Central European Institute of Technology" (CZ.1.05/1.1.00/02.0068) from European Regional Development Fund and the Grant Agency of Czech Republic (P206/10/0057). The authors report no financial or other relationship relevant to the subject of this article.

LITERATURE

[1.] Giuffrida, A., McMahon, L.R. *Prostaglandins Other Lipid Mediat.* 2010, 91(3-4), 90-103.
[2.] Micromedex T. Micromedex Healthcare series (2012). Available at: http://www.thomsonhc.com, (accessed: 02.10.2012).
[3.] Ghafouri, N., Ghafouri, B., Larsson, B., Turkina M.V. et al. *PLoS ONE* 2011, 6 (11): e272557
[4.] Brown, I., Wahle, K.W.J., Cascio, M.G., Smoum-Jaouni, R., Mechoulam R. *Prostaglandins Leukot Essent Fatty Acids* 2011, 85(6),305-310.
[5.] Palandra, J., Prusakiewicz, J., Ozer, J.S., Zhang, Y., Heath, T.G. J Chromatogr B Analyt Technol Biomed Life Sci. 2009, 877(22):2052-60.
[6.] Arai, Y., Fukushima, T., Shirao, M., Yang, X., Imai, K. Sensitive determination of anandamide in rat brain utilizing a coupled-column HPLC with fluorimetric detection. Biomed Chromatogr 2000, 14: 118-124.
[7.] Schmidt, A., Brune, K., Hinz, B. Determination of the endocannabinoid anandamide in human plasma by high-performance liquid chromatography. Biomed Chromatogr 2006, 20: 336-342.

P40 SYNTHESIS OF NEOGLYCOPROTEINS FOR CARBOHYDRATE SPECIFIC ANTIBODY GENERATION

Márta Kerékgyártó[a], Anikó Fekete[b], László Takács[c], István Kurucz[c], András Guttman[a]

[a] *Horváth Laboratory of Bioseparation Sciences, University of Debrecen, 98 Nagyerdei krt, H-4032 Debrecen, Hungary; kmarti1987@gmail.com*
[b] *Faculty of Sciences and Technology, University of Debrecen, 1 sqr Egyetem, H-4032 Debrecen, Hungary*
[c] *BioSystems International Kft., 98 Nagyerdei krt, H-4032 Debrecen, Hungary*

ABSTRACT

In this work, we report on the synthesis and analysis of carbohydrate specific antigens, namely neoglycoproteins that were used for immunization purposes. Firstly, maltose was linked to the ε-amino groups of the lysine residues in bovine serum albumin (BSA). A formyl-heptyl spacer [7-(1,3-dioxan-2-yl)-heptyl[1]] was utilized to conserve the intact annular disaccharide structure to promote the accessibility of the carbohydrate antigen during immunization. The degree of sugar incorporation in the carrier protein was determined by matrix-assisted laser desorption/ionization-time of flight mass spectrometry (MALDI-TOF MS). The newly synthesized carbohydrate antigens were utilized to immunize BALB/c mice. Ultimately, the specificity of the polyclonal antibody response was examined with enzyme-linked immunosorbent assay (ELISA).

Keywords: Carbohydrate antigen, Carbohydrate specific antibody, Immunization

1 INTRODUCTION

The study of glycoproteins and glycosylation itself became increasingly important in the past couple of years[2-4]. Naturally occurring and adaptive anti-glycan antibody development against carbohydrate antigens is of increasing importance since glycosylation is recognized as a significant player in biomarker research and discovery[5]. Therefore neoglycoproteins as sugar-specific antigens have been utilized in a wide variety of applications such as diagnostics markers e.g. the cancer-associated carbohydrate antigens as potential biomarkers[6].

2 SYNTHESIS OF THE CARBOHYDRATE SPECIFIC ANTIGENS AND ANALYSIS OF THE POLYCLONAL ANTIBODY RESPONSE WITH ELISA

For the proof of concept experiment, maltose was converted into maltose octaacetate and then the anomeric acetyl group was removed with hydrazine acetate to form the hemiacetal anomers as shown Figure 1, Panel A. The resulted hemiacetal was transformed to a trichloroacetimidate donor and then reacted with an formyl-heptyl spacer [7-(1,3-dioxan-2-yl)-heptan-1-ol][1] as shown Figure 1, Panel B. After removing the protecting acetyl and acetal groups, the resulting aldehyde was linked to the lysine ε-amino groups of bovine serum albumin as shown Figure 1, Panel C. The carbohydrate antigens possessing five different number of sugar residues were determined by MALDI-TOF MS. The synthesized carbohydrate antigens namely low (32 maltose units per BSA) and high (66 maltose units per BSA) sugar incorporated glycoprotein were immunized into BALB/c mice after that the polyclonal antibody responses were analyzed by ELISA tests.

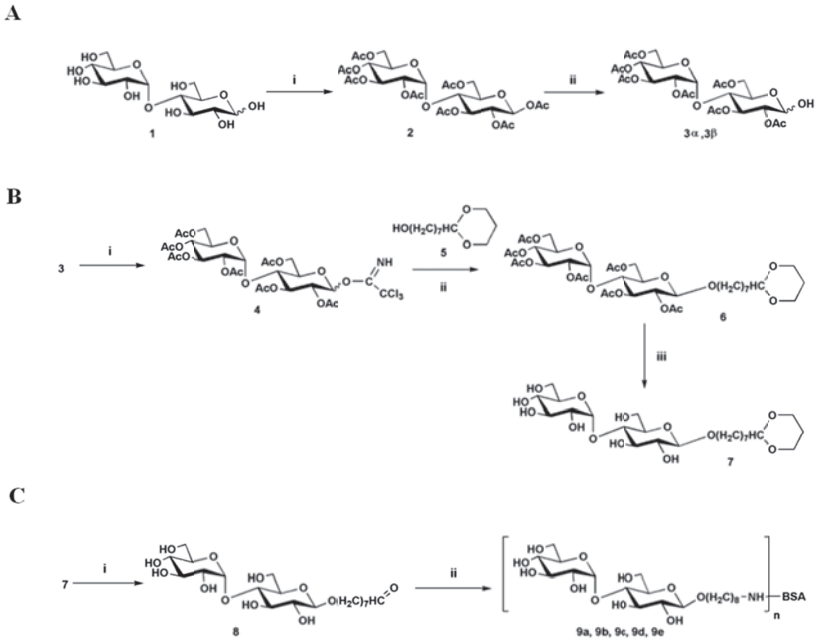

Figure 1. Schematic representation of the synthesis of carbohydrate antigens.

3 RESULTS

After the synthesis of carbohydrate antigens and following immunization, the polyclonal antibody response was analyzed against the neoglycoproteins with ELISA tests. It was found that the IgG response was more intense in the presence of high sugar incorporated neoglycoproteins (66 maltose units per BSA) in immunized BALB/c mice. On the other hand, weaker antibody response was observed against low sugar incorporated carbohydrate antigens (32 maltose units per BSA). Our result suggested that antibody populations specific for the synthesized neoglycoproteins were present in the mouse immune sera. Moreover, we tested the specificity of the polyclonal antibody response generated by immunization of BALB/c mice with BSA, low and high sugar incorporated carbohydrate antigens as well as maltose and other simple sugar as inhibitors. No IgG response was detected in the presence of glucose or maltose, isomaltose, lactose, galactose and maltodextrin. Meanwhile, anti-glycan antibody response was exhibited on both carbohydrate antigens using low and high sugar incorporated antigen inhibitors. These observations were confirmed in the presence of anti-glycan antibodies against neoglycoproteins in the mouse serum.

ACKNOWLEDGEMENT

This research was supported by the OTKA K-81839 grant of the Hungarian Government.

LITERATURE

[1.] Clausen, M., Madsen, R., *Carbohydr Res* 2004, *339*, 2159-2169.
[2.] Taylor, A. D., Hancock, W. S., Hincapie, M., Taniguchi, N., Hanash, S. M., *Genome Med* 2009, *1,* 57.
[3.] Varki, A., R. D. Cummings, Esko J. D., Freeze H. H., Stanley P., Bertozzi C. R., Hart G.W. and Etzler M. E., *Essentials of Glycobiology*. 2nd ed., Cold Spring Harbor (NY): Cold Spring Harbor Laboratory Press, 2009.
[4.] Dotan, N.; Altstock, R. T.; Schwarz, M.; Dukler, A., *Lupus* 2006, *15*, 442-450.
[5.] Heimburg-Molinaro, J., Rittenhouse-Olson, K., *Methods Mol Biol* 2009, *534*, 341-357.
[6.] Legendre, H., Decaestecker, C., Goris Gbenou, M., Nagy, N., Hendlisz, A., Andre, S., Pector, J. C., Kiss, R., Gabius, H. J., *Int J Oncol* 2004, 25, 269-276.

P41 THE EFFICIENT APPROACHES FOR ENZYMATIC DIGESTION OF PLANT PROTEINS

Filip Dyčka[a], Pavel Bobáľ[b], Janette Bobáľová[a]

[a] *Institute of Analytical Chemistry of the ASCR, v. v. i., Veveří 97, 602 00 Brno, Czech Republic*
[b] *Department of Chemical Drugs, Faculty of Pharmacy, University of Veterinary and Pharmaceutical Sciences Brno, Palackého tř. 1/3, 612 42 Brno*
dycka@iach.cz

ABSTRACT

In this work the fast and efficient methods applying ultrasound and infrared radiation were employed for in-gel digestion of proteins extracted from *Hordeum vulgare*. These techniques can be used instead of time consuming conventional protocol prior mass spectrometry analysis. The comparative study indicates that the examined protocols are able to enhance digestion efficiency and protein identification.

Keywords: ultrasonic, infrared, digestion

1 INTRODUCTION

The standard approach to identify proteins includes separation step by polyacrylamide gel electrophoresis (PAGE) and/or liquid chromatography followed by enzymatic digestion of protein and analysis of peptide solution by mass spectrometry (MS) which is time consuming procedure. Several alternative techniques have been used for rapid and highly efficient protein digestion. Modified trypsin can be used for the in-gel digestion of proteins instead of native trypsin [1]. Various water-miscible organic solvents were used for the in-solution digestion of proteins [2]. Researchers have shown that techniques using microwave, ultrasonic or infrared radiation energy during in-gel digestion can result both in high efficiency and accuracy in minutes, while the conventional method requires several hours [3]. In this study the rapid and efficient protein enzymatic digestion techniques using ultrasonic energy and infrared radiation were compared with time consuming conventional method.

2 EXPERIMENTAL

2.1 Protein Extraction

Barley malt (400 mg) was extracted in 2 ml of water. The extraction was carried out at room temperature in a shaker for 2 h. The extracts were then centrifuged, and proteins were precipitated in acetone with 10% trichloroacetic acid and 8 mM dithiothreitol (DTT) at –20 °C overnight. The precipitate was washed twice with acetone.

2.2 In-gel Digestion

Dried protein extracts from barley malt were dissolved in 150 µl Laemmli sample buffer (62.5 mM Tris-HCl, pH 6.8, 2% SDS, 25% glycerol, 0.01% bromophenol blue, 5% 2-mercaptoethanol). After briefly being boiled in a water bath (10 min, 95 °C), a 15 µl sample was applied onto the 12% 1-D SDS-PAGE gel. The visualization was carried out using Coomassie Brilliant Blue G-250 dye.
The protein bands separated by 1-D GE were excised, cut into pieces and in-gel digestion procedure was performed in the three different protocols outlined in Table 1.

Table 1.: In-gel digestion protocol using conventional, ultrasonic- and infrared-assisted methods

Protocol	Solution	Convent.	Ultrasound	Infrared light
Reduction	10 mM DTT	45 min	45 min	45 min
Alkylation	55 mM iodoacetamide	30 min	30 min	30 min
Washing	50% MeCN in 0.1 M NH_4HCO_3	30 min	30 min	30 min
Rehydration	12.5 ng/µl of trypsin in 50 mM NH_4HCO_3, 5 mM $CaCl_2$	45 min	45 min	45 min
Digestion	50 mM NH_4HCO_3, 5 mM $CaCl_2$	16 h	10 min	5 min
Extraction	0.1% TFA, 50% MeCN	30 min	30 min	30 min
Total time		~19 h	~3 h	~3 h

2.3 In-solution Digestion

Nanosep® Centrifugal Devices (Pall Corporation) were used to provide fractionation of the protein extract from *Hordeum vulgare*. In solution digestion was carried out with trypsin at 37 °C overnight, in an ultrasonic bath for 10 min and in an exposure to infrared radiation for 5 min, respectively.

2.4 Protein Identification

Obtained peptides were analyzed by MALDI-TOF/TOF 4700 Proteomic Analyzer (Applied Biosystems, Framingham, MA, USA) equipped with an ND:YAG laser (355 nm). For the MS analysis, α-cyano-4-hydroxycinnamic acid (CHCA) was used as a MALDI matrix.

3 RESULTS

The usefulness of combining the fast methods of applying ultrasound and infrared radiation for in-gel digestion with MALDI-TOF MS protein analysis was demonstrated in our comparative study [4]. In this work the rapid digestion techniques were applied to the extracted proteins from *Hordeum vulgare*. Three samples of investigated protein excised from

1-D SDS-PAGE gel were subjected to in-gel digestion with trypsin using tested methods. The fast methods that were used resulted in more matched peptides, a higher score and better coverage than the conventional method (Fig. 1.).

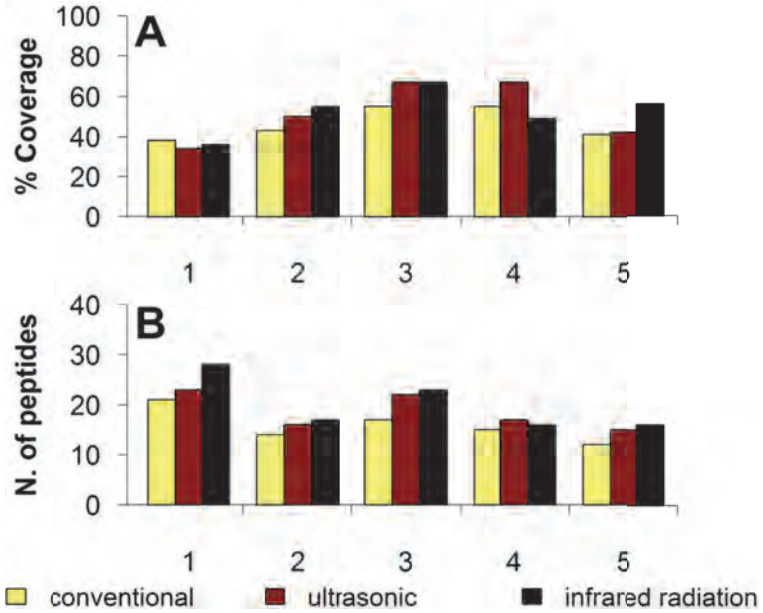

Fig. 1.: Comparative study of protein digestion using conventional, ultrasonic and infrared methodologies. A – sequence coverage, B – number of matched peptides.
1 – methionine synthase, 2 – fructose-bisphosphate aldolase, 3 – aldose reductase, 4 – peroxidase, 5 – triosephosphate isomerase. Aldose reductase (3) and peroxidase (4) were identified in the same spot as protein mixture.

The protein extract from barley grain was fractionated by Nanosep Centrifugal Devices. Subsequently, the tested approaches were employed to enhance the in-solution digestion of extracted proteins. The major protein lipid transfer protein 1 that participates in the formation and stabilization of beer foam was identified by MALDI-TOF MS/MS. Both alternative methodologies led to similar spectra with small differences. However, the methods using ultrasonic power and infrared radiation gave a higher score and better coverage than enzymatic digestion by the conventional method (Table 2.).

Table 2.: The number of matched peptides, the score and the coverage obtained from extract of barley grain by searching the peptide fragment masses against NCBInr sequence database using the MASCOT program.

Name of protein	Convent.		Ultrasound		Infrared light	
	Score/pept.	Cov.	Score/pept.	Cov.	Score/pept.	Cov.
Lipid transfer protein 1	96/3	38%	277/4	50%	324/4	50%

4 CONCLUSION

The results of this study demonstrate that the fast methods using ultrasonic energy and infrared radiation for in-gel or in-solution digestion with the MALDI-TOF MS measurement are a valuable tool for identification of plant proteins. The alternative approaches of protein digestion take only minutes, in contrast to several hours required by conventional method. More important, both studied proteolytic techniques led to more matched peptides, better score and higher sequence coverage compared to the conventional method. In forthcoming work, the hydrophobic proteins that remain a significant challenge for high-throughput proteomics will be characterized with the assistance of these methods.

ACKNOWLEDGEMENTS

This work was supported by Ministry of Education, Youth and Sports, Czech Republic (1M0570 and 1M06030), by the project No. CZ.1.07/2.3.00/20.0182, and the institutional support RVO: 68081715 of the Institute of Analytical Chemistry, Academy of Sciences of the Czech Republic.

LITERATURE

[1.] Havlis, J., Thomas, H., Sebela, M., Shevchenko, A., *Analytical Chemistry* 2003, *75*, 1300–1306.
[2.] Russell, W. K., Park, Z. Y., Russell, D. H., *Analytical Chemistry* 2001, *73*, 2682–2685.
[3.] Capelo, J. L., Carreira, R., Diniz, M., Fernandes, L., *et. al.*, *Analytica Chimica Acta 2009*, *650*, 151–159.
[4.] Dycka, F., Bobal, P., Mazanec, K., Bobalova, J., *Electrophoresis* 2012, *33*, 288–295.

P42 DIODE LASER THERMAL VAPORIZATION INDUCTIVELY COUPLED MASS SPECTROMETRY FOR DETERMINATION OF TRACE ELEMENTS IN MICROSAMPLES

Preisler Jan, Foltynová Pavla, Kanický Viktor

Central European Institute of Technology and Department of Chemistry, Faculty of Science, Masaryk University, 625 00 Brno, Czech Republic
preisler@chemi.muni.cz

ABSTRACT

A new technique for determination of trace elements in submicroliter sample volumes, diode laser thermal vaporization inductively coupled mass spectrometry (DLTV ICP MS) is presented. The technique employs low-cost components, such as a diode laser, a simple laboratory-built chamber and common filter paper as the sample carrier. Rapid and reproducible DLTV determination of Pb and Cd in whole blood is demonstrated. The advantages of LDTV are also very low consumption of sample solution, easy sample archiving and transportation and option of prearranged multi-elemental calibration sets.

Keywords: diode laser thermal vaporization, microsample, inductively coupled plasma mass spectrometry

1 INTRODUCTION

Diode laser thermal vaporization (DLTV) is a new technique for introduction of submicroliter sample volumes into inductively coupled mass spectrometry (ICP MS).[1] Common laser-based techniques for generation of sample aerosol use an expensive high-energy pulse laser, whereas DLTV employs a low-cost diode laser. Samples are deposited on a preprinted sheet of paper and the diode laser power is sufficient to induce pyrolysis and generate sample aerosol for ICP MS analysis. The limits of detection of Co, Ni, Zn, Mo, Cd, Sn and Pb deposited on the preprinted paper were found to be in the range of 4 – 300 pg. The technique was applied to determine lead in whole blood and tin in canned food without any sample treatment. In this contribution, a simple and inexpensive approach for determination of metals in small volumes of liquid samples based on DLTV ICP MS is demonstrated.

2 EXPERIMENTAL

2.1 Deposition

Patterns consisting of rectangles (2×1 mm) were printed with black ink (HP CB316E, Hewlett Packard, Ireland) using an inkjet printer (HP Photosmart C5380) onto filter paper (Munktell quant 389, Germany). Sample solution was then deposited on the preprinted paper as 200-nL or 300-nL droplets using a micropipette.

2.2 DLTV

The samples were vaporized in a laboratory-built chamber made of glass tube (i.d. 4 mm, o.d. 6 mm, length 170 mm) using 1.2 W, 808 nm diode laser (RLDH808-1200-5, Roithner LaserTechnik) and a syringe pump (NE-1010, New Era Pump Systems, USA) for the laser translation. The linear scan rate was set to 0.7 mm/s; the carrier strip accommodates 23 samples along the total travel path 102 mm.

2.3 ICP MS

Parameters of the employed quadrupole ICP MS (Agilent, model 7500CE) were: flows of carrier gas (He) 1.0 $L.min^{-1}$, auxiliary gas (Ar) 0.6 $L.min^{-1}$, collision cell (He) 2.5 $mL.min^{-1}$, and integration time 0.1 s/isotope. For other parameters, see ref. [1].

3 RESULTS

3.1 DLTV chamber

A new chamber has been designed and built (Fig. 1). The design of the prototype chamber is kept as simple as possible: it is made of a glass tube and equipped with the near infrared continuous-wave diode laser attached to a common syringe pump serving as a translational stage for fast line scanning along the paper strip. The minimal dead volume reduces turbulent flow and provides very fast wash-out. The prototype can hold up to 24 samples deposited on the paper strip; analysis time per sample ~ 8 s has been achieved.

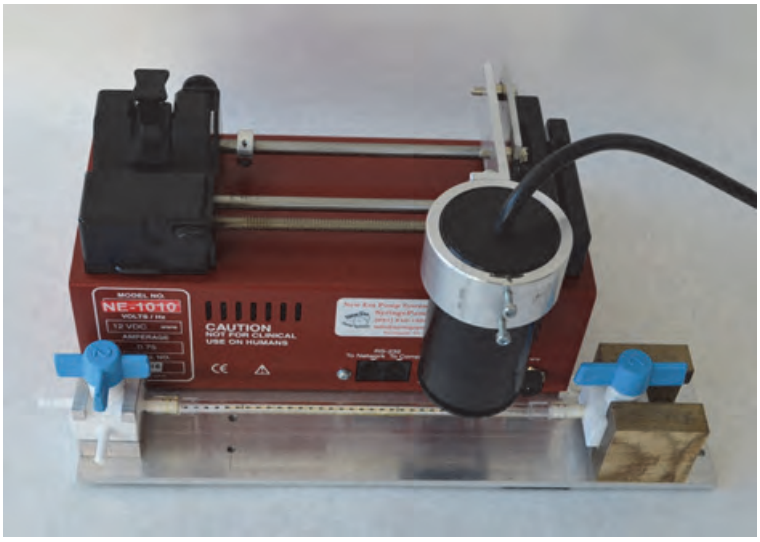

Fig. 1. Photograph of the device for DLTV with a tubular chamber and a syringe pump for diode laser advancement. A preprinted paper strip is inserted in the chamber.

3.2 Optimization of laser position and focusing

In order to choose the optimal experimental arrangement, the signal intensities of selected metals (ten 200-nL droplets of 100 μg.L^{-1} $Pb(NO_3)_2$ and $Cd(NO_3)_2$ standard) were measured at various combinations of vertical distance of the laser from the paper strip and laser focusing. Signal to noise ratio and RSD were evaluated and the most suitable laser position was at the distance 2.5 cm from the paper strip with the focal point ~1.5 mm above the paper strip.

3.3 Determination of metals in whole blood

To check the setup performance, a series of seven 200-nL droplets of 100 μg.L^{-1} standard $Pb(NO_3)_2$ solution were deposited on the paper strip. DLTV ICP MS signal generated during a laser scan along the strip is shown in Fig. 2. Linear scan across one sample was obtained during ~5 s and wash-out time was ~2 s.

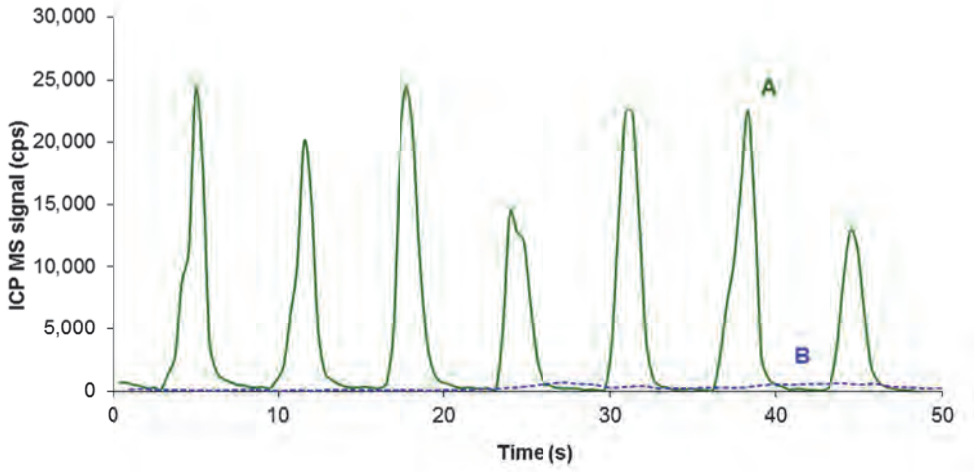

Fig. 2. DLTV ICP MS signal (m/z = 208) from seven rectangles with (A) 200 nL of 100 μg.L^{-1} standard $Pb(NO_3)_2$ solution and (B) control sample deposited on preprinted paper.

Certified reference material BCR-634 of human blood contained 46 ± 5 μg.L^{-1} of Pb and 1.4 ± 0.4 μg.L^{-1} of Cd. A prearranged multi-elemental calibration set was prepared by depositing of standard solution containing Pb and Cd at concentrations 10 and 100 μg.L^{-1} as 200-nL droplets in three replicates onto the pre-printed paper carrier. The whole blood was deposited as 300-nL droplets on all spots in calibration set without any pre-treatment. The standard addition technique was employed to eliminate matrix effect. Samples were analyzed under optimized instrumental conditions and the ion signals of one lead isotope ^{208}Pb and one cadmium isotope ^{111}Cd were recorded. The content of the metals was determined as 49 ± 9 μg.L^{-1} and 1.3 ± 0.2 μg.L^{-1}, respectively.

4 CONCLUSIONS

A new experimental arrangement employing a low-cost diode laser, simple laboratory-built chamber and common filter paper serving as the sample carrier were tested successfully for DLTV ICP MS analysis of lead and cadmium in whole blood. Using a multi-elemental calibration set prearranged on the carrier, LDTV ICP MS provided rapid (78 seconds for calibration, samples and control) and reproducible (~15 %) quantitative analysis and it presents an alternative to conventional nebulizer-based analysis of metals in liquid samples. Advantages are easy preparation, archiving and transportation of samples on the paper strip and high throughput due to minimization of memory effects.

ACKNOWLEDGEMENTS

Czech Science Foundation (P206/12/0538) and CEITEC - Central European Institute of Technology (CZ.1.05/1.1.00/02.0068).

LITERATURE

[1.] Foltynová, P., Kanický, V., Preisler, J., *Analytical Chemistry* 2012, *84*, 2268 – 2274.

P43 BIOANALYTICAL ICP-MS METHOD FOR QUANTIFICATION OF POTASSIUM IN THE CELLS AND SUPERNATANTS.

Inga Petry-Podgórska[a], Tomáš Matoušek[a], Tomáš Wald[b,c], Peter Šebo[b], Jiří Mašín[b], Jiří Dědina[a]

[a] *Institute of Analytical Chemistry of the ASCR, v.v.i., Veveri 97, 60200 Brno, Czech Republic, podgorska@iach.cz*

[b] *Laboratory of Molecular Biology of Bacterial Pathogens Cell and Molecular Microbiology Division, Institute of Microbiology of the ASCR, Videnska 1083, 142 20 Prague 4, Czech Republic, wald@biomed.cas.cz*

[c] *Department of Biochemistry and Microbiology, Faculty of Food and Biochemical Technology, Institute of Chemical Technology, Technicka 3,16628 Praha 6, Czech Republic*

ABSTRACT

Inductively Coupled Plasma Mass Spectrometry (ICP-MS) is a technique commonly used for determintation of concentrations of elements in biosamples to support the studies in the field of microbiology. The biggest advantage of this method is sensitivity and accuracy of the analysis.

The aim of this publication is to present a bioanalytical ICP-MS method applied to the quantification of changes of intracellular potassium concentration after action of the pore-forming adenylate cyclase toxin (CyaA) from the bacterium *Bordetella pertussis*. Several cell lines were treated with CyaA causing different degree of potassium release due to its interaction with target plasma membrane. The ICP-MS was employed to carry out kinetic studies monitoring the changes of the potassium concentration inside the cells and in the cell supernatants in different time-points. The quantification was realized using external calibration with potassium standards in the range 0-2 ppm prepared in water for the samples of lysed cells and in the reaction buffer for the supernatants. Scandium and yttrium were used as internal standards. In result the ICP-MS procedure provided a reliable and straightforward analytical approach enabling kinetic studies in the microsamples for biological studies.

Keywords: ICP-MS, Potasium, Adenylate cyclase

1 INTRODUCTION

By instantaneously disrupting bactericidal functions of host phagocytes, the adenylate cyclase toxin-hemolysin (CyaA) plays a major role in virulence of pathogenic *Bordetellae (Vojtova et al, 2006)*. The toxin rapidly paralyzes phagocytes by translocating across their cytoplasmic membrane an N-terminal adenylate cyclase enzyme domain that binds cytosolic calmodulin and converts ATP to a key signaling molecule, cAMP. In parallel, the multidomain1300 residues-long RTX (Repeat in ToXin) cytolysin moiety of CyaA acts independently as a pore-

forming leukotoxin and hemolysin. Study of Dunne et al (Dunne A., Ross P. et al,, J Immunology, 2010 showed that by eliciting K^+ efflux from CD11b –expressing dendritic cells, the pore-forming activity of CyaA contributes to activation of the NALP3 inflammasome and thereby to induction of innate IL-1β response, which supports the clearance of *Bordetella* bacteria at later stages of infection. The recent results showed that the capacity of CyaA to permeabilize cells for K^+ efflux depends on the capacity of the toxin to promote Ca^{2+} influx into cells and escape the rapid macropinocytic removal from target cell membrane of phagocytes (Fiser R., Masin J. et al, PloS Pathogens, 2012).

The ICP-MS is increasingly used to quantify the concentrations of elements in biomatrices as a competitive method to other commonly applied approaches. Here we present potassium amount measurements in samples treated with adenylate cyclase toxin in support of the microbiological studies. For the purpose of potassium release measurement, we used stably a transfected cell line CHO-CD11b/CD18 and as a control the not transfected CHO cells lacking the receptor.

Previously the measurement of potassium was carried out using PBFI-AM (Potassium-binding benzofuran isophthalate-acetoxymethyl ester) fluorescence, which displayed several disadvantages, such as:

- K_d of the probe: The potassium-sensitive dye PBFI is a selective ion indicator for the fluorometric determination of K^+ concentration. The K^+ dissociation constant of PBFI,, however, strongly dependeds on whether Na^+ is present. The K_d of PBFI for K^+ varies from about 100 mM to 10 mM in the presence and absence of Na^+ (CyaA toxin forms pores selective for monovalent ions, Na^+ concentration inside the cells is changing during the experiment).
- Sensitivity of the method: relatively poor – nonphysiological concentrations of CyaA had to be employed in order to observe any substantial decrease of cytosolic potassium concentration.
- Time needed for measurement. The whole procedure takes 2 days. Cells have to be seeded (attached) to the glass slip at least 12 hours before measurement. The fluorimeter can process only 1 glass per the whole time dependence.

2 EXPERIMENTAL

2.1 Measurements conditions

The measurements were carried out using Agilent 7700x inductively coupled plasma mass spectrometer (ICP-MS) with ASX-500 autsampler, equipped with a Micro-Mist concentric nebulizer and High Matrix Interface.
Potassium was detected at m/z 39, in a collision cell mode (He 4.8 ml/min). The torch position, gas flows and lens voltages were optimized to give maximum signal to noise ratio.
Other conditions of the measurements:

- Internal standard: 45Sc, 89Y;
- Standards for supernatant measurement: 0, 0.1, 0.2, 0.5, 1 mg/l K in HBSS 20 times diluted with deionized water.
- Standards for pellet measurements: 0, 0.09, 0.2, 0.5, 1 mg/l K in water.
- Sample preparation: The supernatants and the lyzed cells (pellets) were diluted 20x and 50x times respectively with deionized water prior to the ICP-MS analysis.
- The resulting values of the cps were recalculated into the potasium concentrations in the sample respectively to the standard curve.

2.2 Toxin treatment and cell preparation

The cells were transferred with EDTA-PBS from the plate into a 15 ml falcon tube. After centrifuging with 1300 rpm at 4°C the supernatant was removed and the cells were washed three times with 5ml of cold HBSS. The number of the cells was calculated in the Bürker

chamber.1x10E6 cells in 1 ml HBSS was incubated at 37 °C for 5 min in an Eppendorf tube. The reaction was started by adding diluted CyaA in TUC to the first reaction tube and TUC only (control) to the second one. The reaction was carried out for 0, 5, 15 and 30 minutes. The mixtures were centrifuged (3 min, 1300 rpm, 4 °C). The supernatants were separated from the cells and stored at -20 °C. The cells were washed four times with HBSS and lysed with 200 μl of distilled water. The lysed cells were centrifuged (20 min, 4 °C, 40000 g) to remove the membranes from the sample. The soluble part was stored at -20 °C.

3 RESULTS

The samples of the lyzed cells and the supernatants were diluted with deionized water and analyzed by ICP-MS. We can observe changes in the potassium concentration in particular samples (Table 1).

Table 1. The data obtained after ICP-MS measuremetents of the cells lysates.

Time of reaction	Treatment	Cell type	Calculated K ppm
0		**CHO-CD11b/CD18**	1,159
5 min.	CyaA	**CHO-CD11b/CD18**	0,426
15 min.	CyaA	**CHO-CD11b/CD18**	0,190
30 min.	CyaA	**CHO-CD11b/CD18**	0,188
15 min.	TUC	**CHO-CD11b/CD18**	0,642
30 min.	TUC	**CHO-CD11b/CD18**	0,399
30 min.	Blank	**CHO-CD11b/CD18**	0,609
0		**CHO**	0,284
15 min.	CyaA	**CHO**	0,152
30 min.	CyaA	**CHO**	0,124
15 min.	TUC	**CHO**	0,146
30 min.	TUC	**CHO**	0,129
30 min.	Blank	**CHO**	0,147

The limits of detection were as follows: LOD = 0,030 ppm (pellets), LOD = 0,014 ppm (supernatnats), and limits of quantification: LOQ= 0,100 ppm (pellets), LOQ = 0,047 ppm (supernatants).

The data obtained from the ICP-measurement have been recalculated and summarized. There was a significant difference in the response to the toxin treatment between CHO and CHO-CD11b/CD18 cells. The CHO-CD11b/CD18 cells released the potassium over time of incubation with the toxin, while the CHO cells resisted to potassium leakage (Fig. 1A).

A B

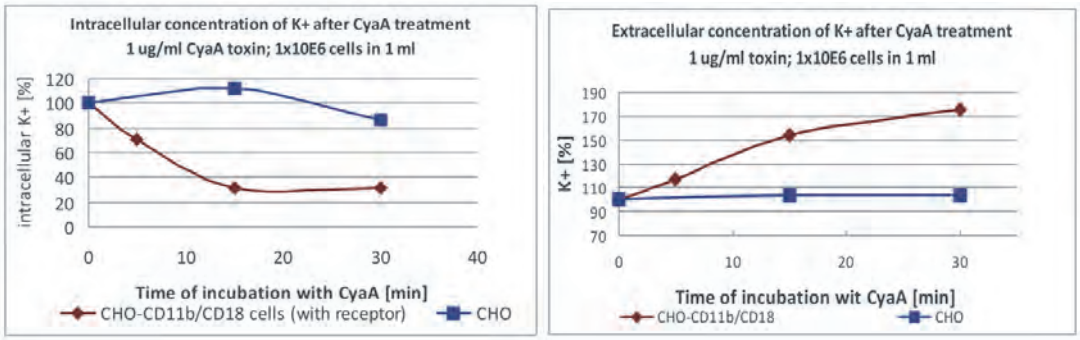

Fig. 1. The percentage of the potassium content remaining in : **A)** the CHO-CD11b/CD18 cells treated with the toxin versus the CHO cells; **B)** in the supernatants after treatment with toxin.

Confirmation of this observation is in the supernatant analysis, which showed an increase of the potassium content only for CHO-CD11b/CD18 supernatants (Fig. 1B).

Among many methods that could serve for the analysis of the potassium content in the samples after treatment with toxins, the ICP-MS provides a suitable and sensitive tool for elemental analysis of the biological samples.

ACKNOWLEDGEMENTS

This project was supported by Grant project P302/11/0580, P302/12/0460 and with institutional support RVO:68081715 and 61388971.

LITERATURE

[1.] Vojtova J, Kamanova J, Sebo P (2006) Bordetella adenylate cyclase toxin: a swift saboteur of host defense. Curr Opin Microbiol 9: 69–75.

[2.] Dunne A, Ross PJ, Pospisilova E, Masin J, Meaney A, et al. (2010) Inflammasome activation by adenylate cyclase toxin directs Th17 responses and protection against Bordetella pertussis. J Immunol 185: 1711–1719.

[3.] Fiser R, Masin J, Bumba L, Pospisilova E, Fayolle C, et al. (2012) Calcium Influx Rescues Adenylate Cyclase-Hemolysin from Rapid Cell Membrane Removal and Enables Phagocyte Permeabilization by Toxin Pores. PLoS Pathog 8(4): e1002580. doi:10.1371/journal.ppat.1002580

P44 ANALYSIS OF PHARMACEUTICAL SUBSTANCES BY ISOTACHOPHORESIS ON A CHIP

Marína Rudašová, Michaela Joanidisová, Zdenka Radičová, Róbert Bodor, Marián Masár

Department of Analytical Chemistry, Faculty of Natural Sciences, Comenius University in Bratislava, Mlynská dolina CH-2,842 15 Bratislava, Slovak Republic, rudasova@fns.uniba.sk

ABSTRACT

The development of new analytical methods that provide a rapid and accurate determination of active ingredients in various pharmaceutical preparations is desired currently. Miniaturized analytical systems in this respect meet all the requirements for fast monitoring and

concentration sensitivity in modern analytical approaches for pharmaceutical analysis. The aim of this work was to develop analytical methods realized on a chip for fast and precise determinations of the major component, N-acetylcysteine in mucolytic pharmaceutical preparations. Isotachophoretic separations were performed on a poly(methylmethacrylate) chip with a conductivity detection. External calibration and internal standard methods were used for results evaluation in this respect. The achieved values of the recoveries (97-106%) predetermine the proposed ITP method for high precision determination of N-acetylcysteine in the analyzed pharmaceuticals (Solmucol 200 and 90 and ACC Long).

Keywords: isotachophoresis; electrophoretic chip; N-acetylcysteine

1 INTRODUCTION

At present, capillary electrophoresis (CE) methods have an important role in chemical analyses, for example in the analysis of pharmaceuticals. A control of pharmaceutical preparations generally involves two approaches: (1) a determination of the main components (majority components) and (2) a determination of impurities (minority components) in preparation. In order to determine the main component, the analysis of pharmaceuticals demands a use of analytical method with high separation capacity. On the other hand, requirements for concentration sensitivity (limit of detection) are not so critical. One of the CE techniques that meets these requirements is isotachophoresis (ITP) used in this work.
N-acetylcysteine (Fig. 1) is an active ingredient in mucolytics, because of its sulfhydryl (-SH) group reacts with disulfide bonds in mucoproteins to split them into smaller units, whereby the viscosity of the mucus becomes reduced [1]. This process of cleavage of disulfide bonds also works at a reduction of abnormally thick mucus in patients with cystic fibrosis. Because of its antioxidant properties, N-acetylcysteine is known as an antiviral, anti-tumor and anti-inflammatory agent and also has been used in the treatment of acquired immune deficiency syndrome (AIDS) and hepatitis B, for the prevention of cancer, the treatment of oxidative stress of different origins and paracetamol overdose [2].

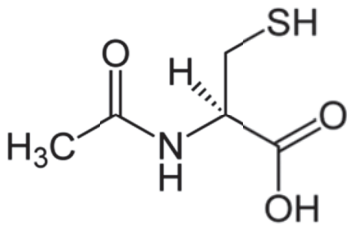

Fig. 1.: Structure of N-acetylcysteine

Microchip capillary electrophoresis (MCE) technology has been developed rapidly since 1992, when it was first introduced by Manz et al. [3]. MCE has many advantages beside conventional CE, such as high separation efficiency, low sample consumption, low financing costs and a wide range of applications. In recent years, researches in this area have focused on the development of new detection systems that provide adequate analytical performance and easy integration [4]. Although the conductivity detection is rarely used in conventional CE, the increased interest in this type of the detection in miniaturized CE systems occurred in recent years. This detection technique plays a key role in monitoring the ITP separations. It is a universal detection technique for ITP with high-resolution power, while fluctuations in response of the conductivity detector have no significant effect on the quantitative analysis (zone length of separated substances).
The aim of this work was to develop an ITP method for fast and precise determination of the main component, N-acetylcysteine in various pharmaceuticals, such as ACC Long and Solmucol performed on the chip with the conductivity detection.

2 EXPERIMENTAL

2.1 Chemicals and electrolyte solutions

Chemicals used for the preparation of electrolyte and model sample solutions were obtained from Merck (Darmstadt, Germany), Sigma-Aldrich (Seelze, Germany), Serva (Heidelberg, Germany) and Lachema (Brno, Czech Republic).

Water demineralized by a Pro-PS water purification system (Labconco, Kansas City, KS, USA) and kept highly demineralized by a circulation in a Simplicity deionization unit (Millipore) was used for the preparation of the electrolyte and sample solutions. Electrolyte solutions were filtered before the use through membrane filters with a pore diameter of 0.8 µm (Millipore).

Stock solutions of N-acetylcysteine and Anthralic acid (used as an internal standard) were prepared at 1000 mg/l concentrations.

Pharmaceutical preparations (Solmucol 200 and 90, Institut Biochimique SA, Switzerland, and ACC Long, Salutas Pharma GmbH, Germany) were bought in local pharmacy. They were dissolved in demineralized water and filtered through membrane filters (Millipore). No other sample pretreatment was used before the analysis.

2.2 Instrumentation

Poly(methylmethacrylate) (PMMA) chip with coupled separation channels (CC) and on-column conductivity detectors (Merck) used in this work was made by technological procedure described in detail in the literature [5]. Schematic drawing of the chip is shown in Fig. 2.

Fig. 2.: CC chip used in ITP separations
a) arrangement of channels and conductivity detection sensors on the PMMA chip; b) filling sequence of chip channels with leading (L) and terminating (T) electrolyte and sample (S) solutions (W = waste), the number in parenthesis indicates the step in the filling sequence; c) starting configuration of electrolyte and sample solutions before the application of the driving current. C3 = a non-separative part of the separation channel (9.8 µl); s = sample injection channel (900 nl volume); C1 = the first separation channel (4.5 µl volume; 59 mm separation path) with Pt conductivity sensor D1; C2 = second separation channel (4.3 µl volume; 56 mm separation path) with Pt conductivity sensor D2; BF = bifurcation section.

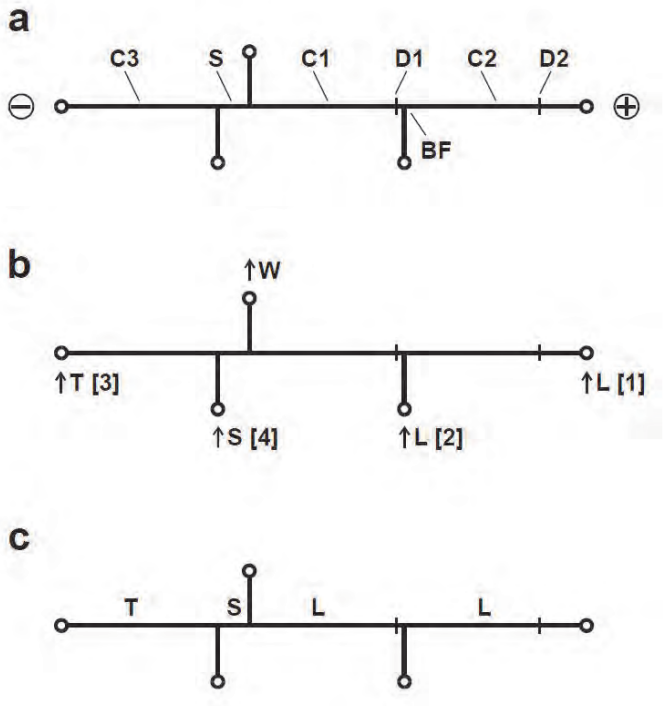

ITP separations on the chip were performed on a laboratory designed device consisted of two units: (1) an electrolyte and sample management unit (E&SMU, Fig. 3.) provided with peristaltic pumps (P1-P3 and PS) and membrane driving electrodes (E1, E2 and E3) and (2) an electronic and control unit (E&CU, Fig. 3.) drives peristaltic pumps of E&SMU during preparation for the run. Its control unit also interfaces the CE equipment to a PC [6].

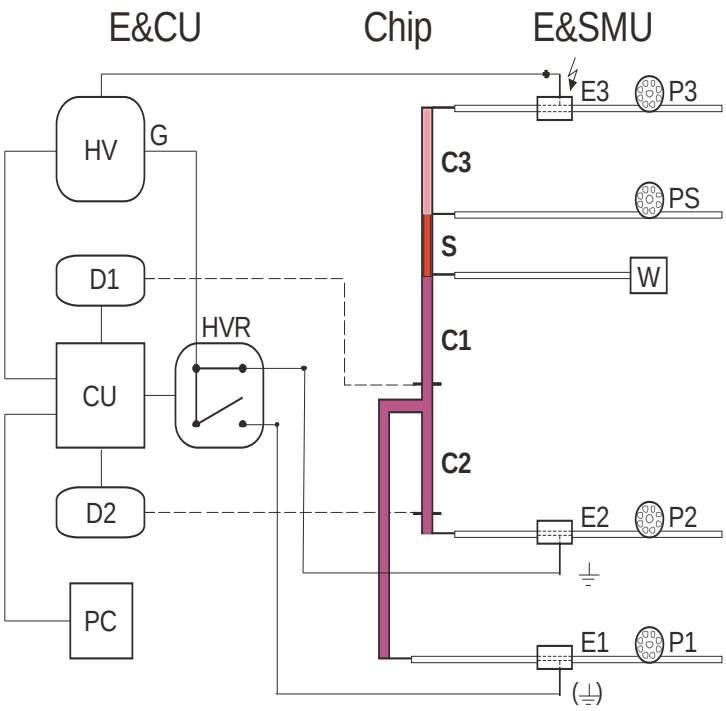

Fig. 3.: A scheme of the CE equipment used in ITP separations on the chip Electronic and control unit (E&CU): CU = control unit; HV = a high-voltage power permanently connected to the driving electrode E3; D1, D2 = conductivity detectors for the first and second separation channels; HVR = a high-voltage relay (moving reeds of the relay connect to the ground pole (G) either E1 or E2). Electrolyte and sample management unit (E&SMU): P1, P2, P3, PS = peristaltic pumps for filling the first (C1) and second (C2) separation channels and third - terminating (C3) and sample injection (S) channels with corresponding electrolyte and sample solutions; W = waste container; E1, E2 = driving electrodes for C1 and C2.

MicroCE Win software (version 2.4), written in the laboratory, controlled automated preparations of the runs (filling the chip channels with corresponding solutions in a required sequence), provided a time-programmed control of CE runs, acquired the data and provided their processing.

3 RESULTS AND DISCUSSION

Basic separation parameters for the fast and high-precision determination of N-acetylcysteine were optimized. Due to the pK_a values of N-acetylcysteine (pK_{a1} = 9.52 thiol group and pK_{a2} = 3.24 carboxylic group), the pH of leading electrolyte containing chloride as a leading anion was set to 6.0. Morpholino ethanesulfonate was chosen as a terminating anion. The total analysis time was less than 700 s, when the second conductivity detector on the chip (Fig. 3) was used for data evaluation.

Fig. 4 shows the isotachophoreogram from the analysis of Solmucol 200 sample containing 100 mg/l of N-acetylcysteine and 100 mg/l of Anthranilic acid used as an internal standard. Separations were carried out with a driving current of 20 µA.

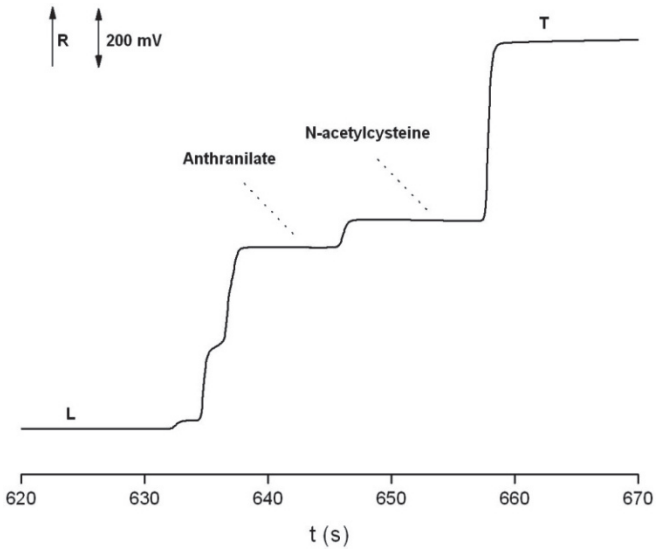

Fig. 4.: ITP separation of N-acetylcysteine in Solmucol 200 with Anthranilic acid used as the internal standard on the chip. L = leading electrolyte; T = terminating electrolyte; R = resistance.

ITP separations were performed in a hydrodynamically closed separation system with suppression of electroosmotic and hydrodynamic flow. Under these working conditions, the RSD values of the zone lengths of N-acetylcysteine were in the range 1-8%, independently of the used chip (Table 1). Repeatabilities of quantitative parameters for corrected zone lengths of N-acetylcysteine on internal standard (Anthranilic acid) improved approx. 2-4-fold while the ITP repeated measurements were performed on three chips (Table 1). The internal standard eliminates run-to-run fluctuations in injected sample volume.

Table 1: Repeatibilities of zone lengths of N-acetylcysteine

Concentration (mg/l)	Zone length (N-acetylcysteine)		Corrected zone length (N-acetylcysteine / anthranilate)		n
	Average	RSD (%)	Average	RSD (%)	
50 A	4.02	2.15	0.49	1.30	20
50 B	4.24	4.29	0.51	1.44	20
50 C	4.23	7.94	0.51	2.11	16
50 D	4.20	6.40	0.46	1.76	56
100 A	7.60	1.32	0.96	1.14	20
100 B	8.68	3.34	1.06	0.41	20
100 C	8.23	1.88	1.01	2.20	16
100 D	8.18	3.63	0.90	3.39	56
200 A	15.55	0.85	1.96	0.39	20
200 B	16.85	2.88	2.15	0.34	20
200 C	16.95	2.44	2.14	1.81	16
200 D	16.45	2.68	1.85	2.61	56

A, B, C = ITP measurements made in 1 day, on 1 chip (A, B, C) and at 1 MCE device; D = ITP measurements made during three days, on three chips (A, B, C); l = zone length; RSD = relative standard deviation; n = number of measurements. Concentration of anthranilate (internal standard) was approx 100 mg/l.

Table 2 summarized the parameters of the regression equation for N-acetylcysteine present in model samples in the concentration range 25-200 mg/l together with Anthranilic acid used as the internal standard. The concentration of Anthranilic acid was 100 mg/l. ITP measurements were performed in one day, on one chip and one MCE device. Parameters of the regression equation for calibration solutions were evaluated by methods of external calibration and internal standard.

Table 2: Parameters of the regression equation for N-acetylcysteine with Antranilic acid used as the internal standard

External calibration			Internal standard			n	Δc (mg/l)
Slope (s.l/mg)	Intercept (s)	r	Slope (s.l/mg)	Intercept (s)	r		
0.072	0.317	0.9995	0.0095	0.012	0.9997	19	25-200

ITP measurements performed in 1 day, on 1 chip and at 1 MCE device; Y = zone length of N-acetylcysteine (s); x = concentration of N-acetylcysteine in the sample (mg/l); r = correlation coefficient; n = number of measurements; Δc = concentration span. The concentration of Anthranilic acid (internal standard) in model samples was approx. 100 mg/l.

Developed ITP method for determination of N-acetylcysteine was applied for the analysis of this anionic component in pharmaceuticals, e.g. Solmucol 200 (Fig. 4.), Solmucol 90 and ACC Long. The contents of N-acetylcysteine in these pharmaceuticals were evaluated by methods of external calibration and internal standard (Table 3). External calibration method showed a higher dispersion of the content of N-acetylcysteine in the sample (about 10-fold higher RSD values).

Table 3: The contents of N-acetylcysteine in various pharmaceuticals calculated by methods of external calibration and internal standard

Sample	Content of N-acetylcysteine (mg/l)		
	Declared by producer	Determined	
		External calibration	Internal standard
Sol 200	200	211.9 ± 5.0	198.2 ± 0.4
Sol 90	90	100.8 ± 6.5	88.3 ± 0.6
ACC 600	600	615.4 ± 4.6	605.3 ± 0.7

The concentration of anthranilate (internal standard) in pharmaceuticals Solmucol and ACC Long was approx. 100 mg/l.

Recoveries of N-acetylcysteine in the analyzed samples were evaluated and ranged from 97 to 106%. These values predetermine the proposed ITP method for high-precision determination of N-acetylcysteine in different pharmaceuticals.

4 CONCLUSION

The work dealt with the determination of N-acetylcysteine, the active ingredient in various pharmaceutical preparations, Solmucol and ACC Long, using the ITP on the chip with the conductivity detection. Contents of N-acetylcysteine in pharmaceutical samples were evaluated by methods of external calibration and internal standard. The method of internal standard eliminated run-to-run fluctuations in the sample volume. RSD values of the contents of N-acetylcysteine in the preparation using internal standard method were less than 0.7%.

Developed ITP method on the chip can be used for rapid and precise analysis of the main compound in pharmaceuticals.

AKNOWLEDGEMENTS

This work was generously supported by the grant of Slovak Research and Development Agency (project APVV-0583-11), the Slovak Grant Agency for Science (VEGA 1/1149/12) and the Research & Development Operational Programme funded by the ERDF (CEGreenII, 26240120025). This work is partially outcome of the project VVCE-0070-07 of Slovak Research and Development Agency solved in the period 2008-2011.

LITERATURE

[1.] Tomkiewicz, R. P., App, E. M., De Sanctis, G.T., Coffiner, M., et al., *Pulmonary Pharmacology* 1995, *8*, 259-265.

[2.] Daly, F. F. S., Fountain, J. S., Murray, L., Graudins, A., et al., *The Medical Journal of Australia* 2008, *188*, 296-301.

[3.] Manz, A, Harrison, D.J., Verpoorte, E.M.J., Fettinger, J.C., et al., *Journal of Chromatography A* 1992, *593*, 253-258.

[4.] Zhao, J., Chen, Z., Li, X., Pan, J., *Talanta* 2011, 85, 2614-2619.

[5.] Grass, B., Neyer, A., Jöhnck, M., Siepe, D., et al., *Sensors and Actuators B* 2001, *72*, 249-258.

[6.] Masár, M., Poliaková, M., Danková, M., Kaniansky, D., et al., *Journal of Separation Science* 2005, *28*, 905-914.

P45 STUDY OF THE POSSIBILITY OF USING RP-HPLC WITH TANDEM MULTIDETECTION TO CHARACTERIZE SAMPLES OF PROTEIN SUPPLEMENTS WITH THERAPEUTIC EFFECT

Veronika Komorowska, Milan Hutta

Department of Analytical Chemistry, Faculty of Natural Sciences, Comenius University in Bratislava, Mlynská Dolina CH-2, SK-84215 Bratislava, Slovakia, komorowska@fns.uniba.sk

ABSTRACT

In the present work we focused on study of the separation process of proteins with enzyme nature contained in a model sample. The model sample was food supplement with therapeutic effect with trade name Wobenzym. Reversed-phase high-performance liquid chromatographic (RP-HPLC) method on LiChrospher® WP 300 RP-18 column was applied under the conditions of gradient elution with buffered water/acetonitrile eluents using tandem of spectrophotometric (DAD) and fluorimetric detection (FLD). We found it appropriate to use the gradient, in which the concentration of organic solvent increases slower, what resulted in better separation of analytes. Furthermore, to ensure the reproducibility of the HPLC analysis of a mixture of enzymes as natural substances a fresh sample solution should be prepared before each injection to the separation system. It is also good to abide with the same time from preparation the sample solution until the injection. In the last stage composition of a mixture of alternatively formic acid and acetic acid titrated with ammonium hydroxide (pH ranging from 2.5 to 5.1) was investigated with found optimum buffer values set around pH 3.5. Selection of buffer took into account also detection needs. The pH values were selected to avoid denaturation of enzymes, while the enzymes achieve minimum of enzymatic activity.

Keywords: Wobenzym enzymes, HPLC-UV(DAD) – FLD(3D), profiling

1 INTRODUCTION

With the latest advances in molecular biology, genomics, proteomics and bioinformatics increased number of biotechnology products with therapeutic effects, including macromolecular substances with enzymatic nature. Those substances are obtained either by isolation from animal and plant tissues or are produced by recombinant techniques. The need for analysis of protein samples is part of the quality control of commercially available products as well as fulfillment the requirements imposed on the quality of the proteins produced by recombinant techniques[1].

High performance liquid chromatography (HPLC) is one of the most widely used analytical techniques for the separation of proteins. From simple chromatographic techniques are used RP-HPLC[2, 3], ion exchange chromatography[4-6], affinity chromatography in different variations[7-9] and gel chromatography[10, 11]. Mentioned separation techniques are combined with suitable detectors for the detection of proteins on the principle of mass spectrometry with electrospray ionization (ESI-MS) or MALDI-MS[12]. Spectrophotometric[13-15] and fluorimetric[13-16] detection are useable too. The main problems analyst must fight with are:

- sample instability due to self biotransformation (proteolytic enzymes)
- thermal lability
- conformational changes induced by pH, ion strength, accompanying substances, etc.

The work is an introductory study to the problem of proteinaceous sample HPLC analysis, profiling and characterization aiming analytical chemistry approach, including detailed study of the variables that are part of validation protocols of analytical methods.

2 EXPERIMENTAL

2.1 Chemicals

Formic acid 98-100%, acetic acid 96%, aqueous ammonia 28-30% and acetonitrile (ACN) 99.9% were purchased from Merck (Darmstadt, Germany) all in analytical grade. Rutin was obtained from Sigma Aldrich (St. Louis, USA). Commercially availabled tablets Wobenzym (Mucos Pharma CZ, Průhonice, Czech Republic). All aqueous solutions were prepared with ultrapure water purified by Simplicity (Molsheim, France).

2.2 Preparation of mobile phase A

Mobile phase A at pH 2.50 consisted of formic acid diluted with water to a concentration 56 mmol L^{-1}. For other values of pH of mobile phase A buffer consisted from formic acid / ammonium formate (pH 2.90, 3.30, 3.75, 4.10, 4.67) and acetic acid / ammonium acetate (pH 5.10, 5.50). Preparation of both buffers was same. Acid was diluted to one liter of water to a concentration 56 mmol L^{-1}. Then was acid solution titrated with ammonia solution using a pH meter with a combined glass and silver / silver chloride electrode (WTW pH inoLab 730, Wellhelm, Germany) at the desired pH.

2.3 Preparation of mobile phase B

Mobile phase B consisted of ACN and water, the ratio 70/30. The mobile phase B was adjusted the volume of acid and ammonia, which was consumed for the preparation of mobile phase A with a given pH.

2.4 Sample preparation

From tablet Wobenzym was removed coating, which protect enzymes inside from the effect of low pH digestive juices. Then was the tablet crushed in a porcelain mortar. The powder was dissolved in a volumetric flask with water for the mass concentration 1 mg ml^{-1}. Prepared solution was mixed and kept for 16 min. in an ultrasonic bath (UCM9, ECOSON, Slovakia) at 20°C and 100% of the performance. Finally, to remove insoluble constituents (usually fillers) of the pill was centrifuged the sample solution for 10 min. (Eppendorf AG, Hamburg, Germany) at 13,400 rpm. Supernatant solution was injected onto the HPLC system.

2.5 Chromatography

All chromatographic separations were performed using RP-HPLC on LiChrospher ® WP 300 RP-18 (length 250 mm, 4 mm internal diameter, 5µm particle, pore size 30 nm) thermostated at 35 ± 0.1°C. The HPLC system (Agilent Technologies, Japan) consisted of the following modules: vacuum degasser mobile phases (G1379B), dual-channel high-pressure binary pump (G1312B), auto sampler (G1329B), column thermostat (G1316B), DAD (G1315) and FLD (G1321A). Wavelength range of DAD was set to 190–400 nm. Excitation wavelength FLD was set at 250 nm and emission wavelength at 300 nm. Agilent ChemStation was used for process chromatographic data.
Two different gradients were used by flow rate 1 ml min^{-1}: *Gradien 1* was set from 0-3 min isocratic 100% A, from 3-33 min linear increase from 0% B to 95% B in A, followed by 2 min isocratic elution 95% B in A, from 35-40 min linear decrease from 95% B in A to 100% A, followed by 5 min isocratic elution 100% A. *Gradient 2* was set from 0-3 min isocratic 100% A, from 3-40 min linear increase from 0% B to 70% B in A, followed by 5 min isocratic elution 70% B in A, from 45-49 min linear decrease from 70% B in A to 100% A, followed by 6 min isocratic elution 100% A.

3 RESULTS AND DISCUSSION

3.1 Effect of resting time of the sample solution on reproducibility of the HPLC analysis

From comparison of chromatograms, which were obtained by analyzing samples of Wobenzym pills after several hours, we found that the resting time of the sample solution affects the reproducibility of measurements. The time factor is manifested as loss, respectively obseravtion of new peaks in several areas of the chromatogram obtained until the 12th minute separation. Reproducibility of measurements decreased with increasing pH. The biggest changes have occurred on the chromatograms at pH close above four. Investigated sample contains four proteolytic enzymes (see Table 1), so it is in place to assume, that there may be between them proteolysis and autoproteolysis, respectively. To ensure the profile reproducibility a fresh sample solution should be prepared before each injection to the separation system.

Table 1. Enzymatic composition of the product Wobenzym and some physicochemical properties of involved enzymes

Name of enzyme	Amount[a] (mg)	Substrate specificity	pH optimum catalytic	Isoelectric point	The relative molar mass
amylase	10	polysaccharides	7[17]	6,34[18]	55 905[19]
bromelain	45	proteins, peptides, amides	4,5-7,5[20]	9,55[20]	28 500[21]
chymotrypsin	1	peptides, amides, esters	8[22]	8,8[23]	25 000[22]
lipase	10	triglycerides, fats and oils	7,7[24]	5,8[25]	45 000[26]
papain	60	proteins, peptides	4-7[27]	9,5[28]	23 453[29]
trypsin	24	peptides	7,5-8,5[30]	10,5[30]	23 500[31]
pancreatin[b]	100	-	-	-	-

[a] The amount of enzyme in 1 tablet declared by the manufacturer.

[b] Pancreatin is a mixture of pancreatic enzymes in mammals. It includes protease (trypsin and chymotrypsin) and exocrine pancreatic enzymes (α-amylase and lipase). Pancreatin also contains other enzymes and other substances without enzymatic activity[32].

3.2 Selection of an appropriate gradient for separation of components of the product Wobenzym

Gradient used for all subsequent experiments was selected from two gradients differing in their slopes. The chromatograms obtained by separation using the Gradient 1 show more visible peaks compared to chromatograms obtained by using the Gradient 2 (see Fig. 1). This trend was seen by both detectors. This fact we put into the context of complexity of the sample and the large signal dynamics of analytes. Gradient 1 is steeper than Gradient 2, there is a situation, where the peak capacity concentrated in a smaller space of separation column, as a result there may be counted small signals and creating multiplet peaks. At a slower increase of elution strength, there is a better separation and merger of separated peaks with zero line. From these reasons we used Gradient 2 for all next experiments.

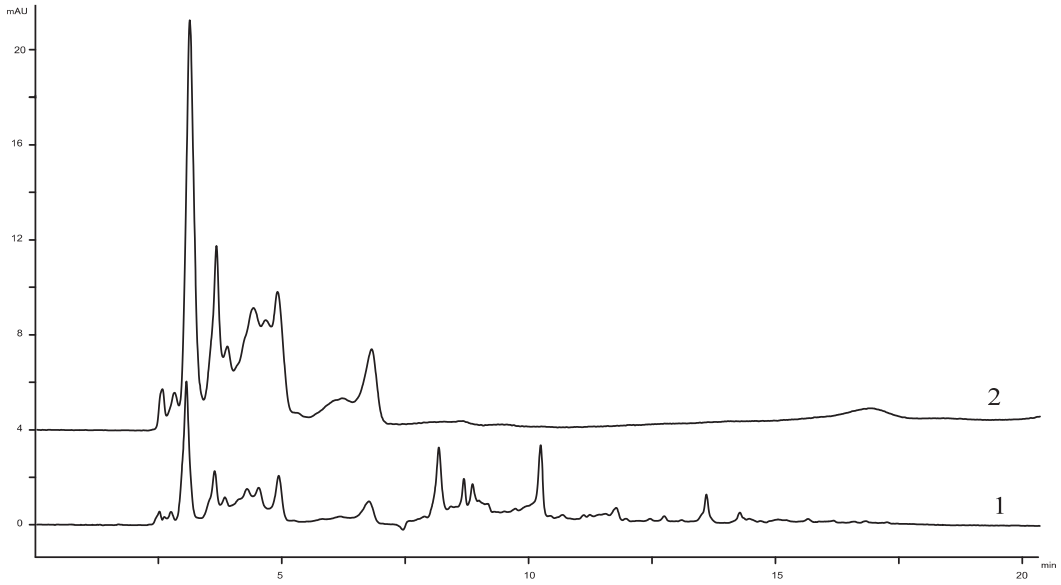

Fig. 1. : Chromatograms of sample solution Wobenzym obtained in two different gradients. Curve 1 - chromatogram obtained by using a Gradient 1, curve 2 - chromatogram obtained by using a Gradient 2. Chromatography column LiChrospher ® WP 300 RP-18 heated to working temperature 35°C, injected volume of sample solution 100µl, mobile phase A: pH 2.5 formic acid, mobile phase B: ACN, flow rate 1 ml min^{-1}, UV detection at 280 nm.

3.3 Time shift of detectors in tandem

To determine the time shift of FLD signals with respect to DAD signals was used a standard low molecular weight non-protein substance called rutin. Rutin was injected into HPLC system and analysed at same conditions as in the case of model sample. Dwell volume between DAD and FLD obtained by calculation was 40µl ± 1µl.

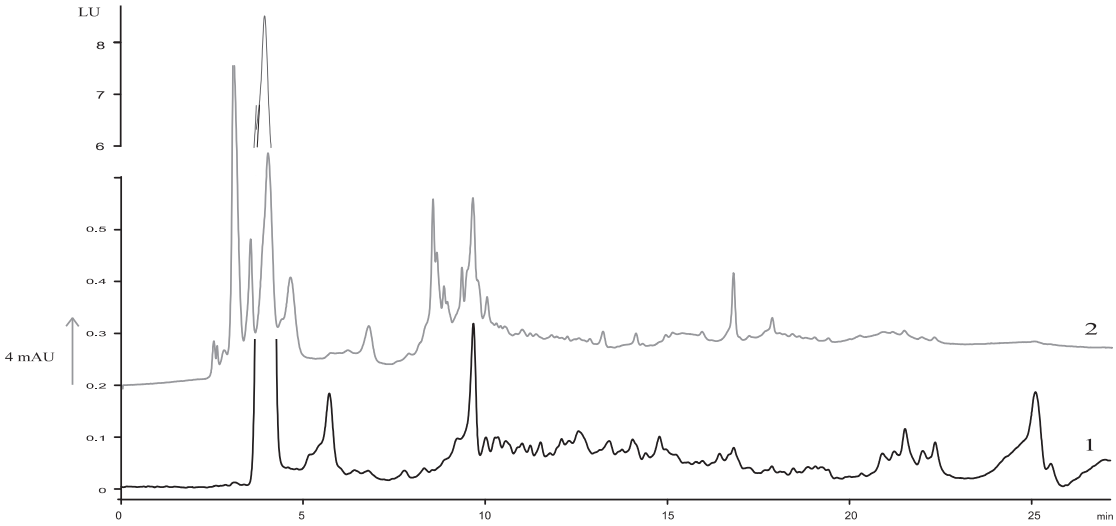

Fig. 2.: Chromatograms of the sample solution obtained by tandem of detectors. Curve 1 – chromatogram obtained by FLD: excitation wavelength 250 nm, emission wavelength 300nm, curve 2 – chromatogram obtained by DAD at 280 nm. Chromatography column LiChrospher ® WP 300 RP-18 heated to working temperature 35°C, injected volume of sample solution 100µl, mobile phase A: pH 3.3 formic acid/ammonium formate, B ACN/H2O 70/30 (v/v), Gradient 2 by flow rate 1ml min^{-1}.

3.4 Effect pH value of mobile phase for HPLC analysis of model protein sample Wobenzym

Given chromatograms (see Fig. 3) show that the pH of the mobile phase has a significant effect on the separation and shape of the chromatogram. The most striking feature is the difference of chromatogram obtained by separation with mobile phase of pH 2.5 from all other chromatograms. This chromatogram has fewer peaks and thus much poorer information compared to chromatograms obtained by higher pH values. That phenomenon can be related to denaturation of some analytes at such low pH value. This conclusion agrees with data in the literature, which states that chymotrypsin[22] and papain[27] denatures at pH lower than 3 respectively 2.8. Therefore, pH values lower than 3 are not appropriate for analysis of our sample.

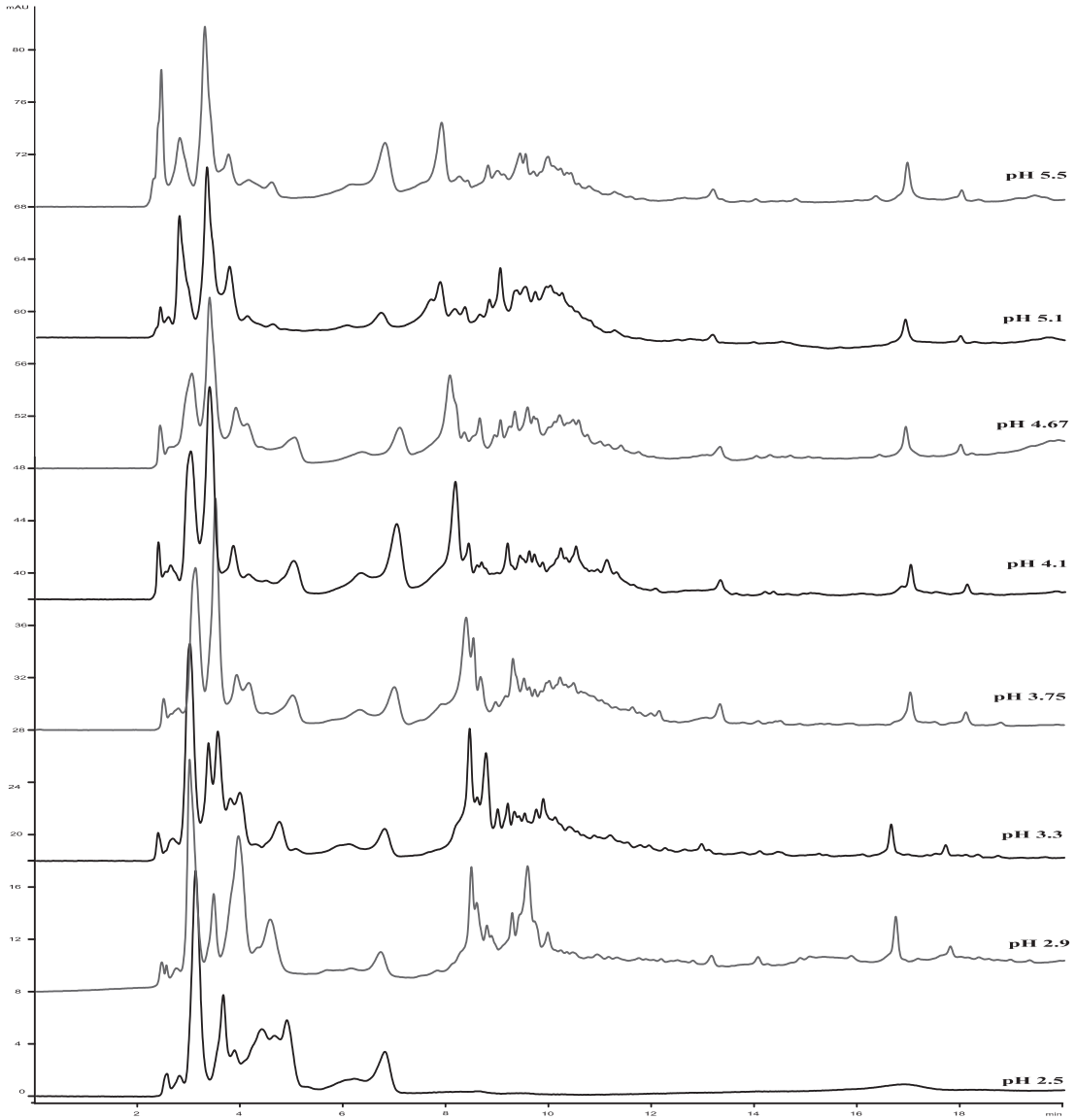

Fig. 3.: Chromatograms obtained at different pH values of mobile phase A. Chromatography column LiChrospher ® WP 300 RP-18 heated to working temperature 35°C, injected volume of sample solution 100µl, mobile phase A: pH 2.5 formic acid, mobile phase A: pH 2.9, pH 3.3, pH 3.75, pH 4.1 and pH 4.67 formic acid/ammonium formate, mobile phase A: pH 5.1, pH 5.5 acetic acid/ammonium acetate, mobile phase B: ACN/H2O 70/30 (v/v), Gradient 2 by flow rate 1 ml min^{-1}, UV detection at 280 nm.

For analytical process that aims a systematic study of separation and determination of enzymes it is disadvantageous, if pH in the system enters the values in which analytes are enzymatically active. The resolution is in use of an appropriate buffer. From measured chromatographic results and the information obtained from the literature, we concluded that for separation most of the sample components-proteins is suitable to use buffer with pH values ranging also from 3 to 4. By these pH values analytes-enzymes should not denaturate and enzymes should reach the minimum of their enzyme activity what is important in terms of reproducibility of the separation and detection.

ACKNOWLEDGEMENTS

This work was generously supported by the grant of Scientific Grant Agency of the Ministry of Education of Slovak Republic and the Academy of Sciences - project VEGA 1/1349/12 and the grant of Slovak Research and Development Agency - project APVV-0583-11. This work is partially outcome of the project VVCE-0070-07 of Slovak Research and Development Agency solved in the period 2008-2011.

LITERATURE

[1.] Korf U., Kohl T., Zandt H., *Proteomics* 2005, *5*, 3571.
[2.] Kanie Y., Enomoto A., Goto S., Kanie O., *Carbohydrate Res.* 2008, *343*, 758.
[3.] Thomä C., Krauseb I., Kulozi U., *Int. Dairy Journal* 2006, *16*, 285.
[4.] Regnier F. E., *Anal. Biochem.* 1982, *126*, 1.
[5.] Rűckert M., Wohlfarth M., Bringmann G., *J. Chromatogr. A* 1999, *840*, 131.
[6.] Adachi T., Takayanagi H., Sharpe A.D., *J. Chromatogr. A* 1997, *763*, 57.
[7.] Chaga G.S., *J. Biochem. Biophys. Methods* 2001, *49*, 313.
[8.] Burgess R. R., Thompson N. E., *Curr. Opin. Biotechnol.* 2002, *13*, 304.
[9.] Xiong L., Andrews D., Regnier F. E., *J. Proteome Res.* 2003, *2*, 618.
[10.] García M.C., *J. Chromatogr. B* 2005, *825*, 111.
[11.] Shi Y., Xiang R., Horváth C., Wilkins J. A., *J. Chromatogr. A* 2004, *1053*, 27.
[12.] Alomirah H.F., Alli I., Konishi Y., *J. Chromatogr. A* 2000, *893*, 1.
[13.] Heath T. G., Giordani A. B., *J. Chromatogr. A* 1993, *638*, 9.
[14.] Dziuba J., Nałęcz D., Minkiewicz P., *Anal. Chim. Acta* 2001, *449*, 243.
[15.] Julka S., Folkenroth J., Young S. A., *J. Chromatogr. B* 2011, *879*, 2057.
[16.] Ravindran G., Bryden W.L., *Food Chem.* 2005, *89*, 309.
[17.] http://www.worthington-biochem.com/AA/default.html, downloaded 30th April 2011.
[18.] Rosenmund H., Kaczmarek M. J., *Clin. Chim. Acta* 1976, *71*, 185.
[19.] http://www.pdb.org/pdb/explore/biologyAndChemistry.do?structureId=1XGZ, downloaded 30th April 2011.
[20.] http://www.biozym.de/datasheets/bromelain.php, downloaded 30th April 2011.
[21.] Wharton Ch. W., *Biochem. J.* 1974, *143*, 575.
[22.] http://www.biozym.de/datasheets/chymotrypsin.php, downloaded 30th April 2011.
[23.] Ghosh K. K., Verma S. K., *Indian J. Biochem. Biophys.* 2008, *45*, 350.
[24.] http://www.sigmaaldrich.com/etc/medialib/docs/Sigma/General_Information/lipase_olive_oil.Par.0001.Fle.dat/lipase_olive_oil.pdf, downloaded 30th April 2011.
[25.] Caro A. D., Figarella C., Amic J., Michel R., Guy O., *Biochim. Biophys. Acta* 1977, *490*, 411.
[26.] http://www.worthington-biochem.com/PL/default.html, downloaded 30th April 2011.
[27.] http://www.biozym.de/datasheets/papain.php, downloaded 30th April 2011.
[28.] Sangeetha K., Abraham T. E., *J. Molec. Catal. B: Enzymatic* 2006, *38*, 171.
[29.] http://www.pdb.org/pdb/explore/biologyAndChemistry.do?structureId=1PPN, downloaded 30th April 2011.
]30.] http://www.worthington-biochem.com/TRY/default.html, downloaded 30th April 2011.
[31.] Barman T. E., *Enzyme Handbook*, 2. volume. Springer, New York-Heidelberg-Tokyo 1985.
[32.] http://www.edukafarm.cz/clanek.php?id=227, downloaded 30th April 2011.

P46 FRACTIONATION OF HUMIC ACIDS BY PREPARATIVE ISOTACHOPHORESIS

Zdenka Radičová, Róbert Bodor, Róbert Góra, Andrea Pastierová, Michaela Joanidisová, Marína Rudášová, Milan Hutta, Marián Masár

Department of Analytical Chemistry, Faculty of Natural Sciences, Comenius University in Bratislava, Mlynská Dolina CH-2, 842 15 Bratislava, Slovakia
radicovaz@fns.uniba.sk

ABSTRACT

The present work dealt with a fractionation of humic acids (HAs) by preparative capillary isotachophoresis (CITP) in discontinuous mode as a sample pretreatment method for HPLC using 10-step gradient of N,N-dimethylformamide (DMF) in buffered (pH=3.00) aqueous mobile phase and wide-pore octadecylsilica column. CITP separations were carried out in electrolyte system at pH 10. Three discrete spacers (DSs), injected into the CITP column together with the HAs, were used to reach a spatial separation of HAs. A micropreparative valve, with a volume of 22 µl placed behind the conductivity detector in CITP column, was used for fractionation of HAs according to their effective mobilities into five fractions. Separately collected fractions were controlled toward the presence of corresponding DSs zones by analytical CITP with conductivity detection in the same electrolyte system as used for preparative CITP. Differences found in the chromatographic profiles of CITP fractions of HAs indicate that ionogenic components trapped in the individual fractions have different effective mobilities with different hydrophobicity and/or interaction with DMF.

Keywords: preparative isotachophoresis, reversed phase high performance liquid chromatography, humic acid

1 INTRODUCTION

Humic substances are one of the most spread environmental macromolecules of biological origin and they have direct influence on many processes playing significant role in a nature. Humic substances have a complex chemical structure of hydrophilic character and acid polyelectrolyte properties. Humic acids (HAs) are the major extractable component of soil humic substances that are not soluble in water under acidic conditions but they are soluble at higher pH [1].

Separation methods play an important role in the analysis of the HAs. The complexity of the problem that has to be solved with respect to HAs requires valuation and utilization of all possible combinations of basic operations and methods creating base for numerous individual approaches [2].

Mostly used RP-HPLC which uses organic solvents (methanol and acetonitrile) typical for separation of small molecules has only limited applications in the analysis of humic substances. RP sorbents with pore diameters of 6-12 nm were used, as well. The results were probably influenced also by the size exclusion phenomena, because estimated exclusion limit for typical bare silica having 10 nm average pore diameter was close to relative molecular mass around 5000 [3]. Unconventional RP-HPLC uses dimethylformamide (DMF) as an exceptional solvent of humic substances in stepwise gradient RP-HPLC with controlled pH of mobile phase [2, 4] and stationary phase with pore size of 30 nm. This chromatographic system allows an efficient mass transfer and a very good recovery for macromolecules, as one of the important prerequisites of robust RP-HPLC method for analysis of humic substances, their characterization and/or fractionation.

Capillary isotachophoresis (CITP), one of the basic modes of capillary electromigration methods, is very useful for micropreparative purposes. Preparative CITP as a discontinuous

fractionation technique can be realized by micropreparative valve placed at the end of the capillary. This technique allows physical isolation of micro amount of ionic analytes to the fractions which could be subsequently analyzed by different analytical methods [5, 6].
The aim of this work was a preliminary study of an off-line combination of preparative ITP and RP-HPLC. Potential of this approach is in acquirement of comprehensive information about HAs by various separation methods with different principles.

2 EXPERIMENTAL

2.1 Instrumentation

An electrophoretic analyzer EA-102 (Villa-Labeco, Spišská Nová Ves, Slovakia) working in a hydrodynamically closed one-column arrangement was used for the fractionation of the HAs. The column was provided with 1.5 mm i.d. of the capillary tube made of fluorinated ethylenepropylene (FEP) copolymer. The length of the capillary tube was 160 mm. The driving current was stabilized at 900 μA. The sample solutions were injected by injection valve with a volume of 150 μl. The micropreparative valve with a volume of 22 μl was placed at the end of column, behind a conductivity detector and used for isolation of the fractions under no current conditions.
An electrophoretic analyzer EA-101 (Villa-Labeco) working in a hydrodynamically closed one-column arrangement was used for the analytical CITP control of the fractions collected. The column was provided with FEP capillary tube (160 mm length and 0.3 mm i.d.) and conductivity detector. The driving current was stabilized at 50 μA. Fractions (5 μl) were injected by microsyringe (Hamilton, Bonaduz, Switzerland) via the septum.
RP-HPLC characterization of compounds in CITP fractions were carried out by the HPLC system LaChrom (Merck-Hitachi, Darmstadt, Germany) consisting of pump L-7100 provided by a quaternary low-pressure gradient, autosampler L-7200, column oven L-7300, diode-array detector L-7450, fluorescence detector L-7480 and on-line four channel solvent degasser. Separations were carried out using a LiChroCART column 250x4 mm filed by wide pore octadecylsilica LiChrospher WP 300 RP-18, 5 μm spherical particles, guarded by LiChroCART 4x4 mm pre-column filled by identical particles.

2.2 Stepwise gradient HPLC method

Separation conditions for optimized gradient elution of HAs were as follows. Mobile phase A composition was aqueous phosphate buffer (pH 3.00, 50 mmol/l) containing 1 % (v/v) dimethylformamide (DMF) and mobile phase B was 100 % DMF. Flow-rate was 0.5 ml/min. Gradient program was set from 0 to 3.6 min isocratic 0% (v/v) B in A. From 3.7 min, every 4 min isocratic step was added increasing content of B in A by 10% (v/v) up to the last step increased by 9% (v/v) ending in 99% (v/v) B in A, maintained till 55.0 min isocratic 99% (v/v) B in A, from 55.1 min to 60.0 min linear decrease from 99% (v/v) B in A to 0% (v/v) B in A and between runs 10 min re-equilibration was maintained. Fluorescence detection parameters were set to excitation wavelength 470 nm and emission wavelength 530 nm, photomultiplier gain medium was chosen.

2.3 ITP electrolyte system

Preparative and analytical CITP experiments were carried out using chloride anion at 10 mmol/l concentration as leading ion. Final pH of leading electrolyte was adjusted with ethanolamine as counter ion to 10.0. Hydroxyethylcellulose (HEC), as a suspensor of electroosmotic flow, present at 0.1% (v/v) in a leading electrolyte (LE) was used. Hydroxide anion was used as a terminating ion.

2.4 Samples

The stock solution of HAs was prepared at a 100 mg/l concentration. The stock solution of HAs with discrete spacers (HDS) consisted of a 100 mg/l concentration of HAs and 3.10^{-4} mmol/l of spacers (aspartic acid - ASP, 2-aminoadipic acid - AAD, taurin - TAU).
Samples for HPLC analysis: (1) standard of HAs prepared by mixing 160 µl of stock solution of HAs and 50 µl of deionized water (Labconco, Kansas City, KS, USA), (2) standard of HAs with added spacers (HDS) prepared by mixing 110 µl of stock solution of HDS and 50 µl of deionized water, (3) fractions obtained by preparative CITP prepared by mixing 50 µl of fractions (pooled from three fractionations) and 10 µl of deionized water.

3 RESULTS AND DISCUSSION

The preparative CITP in anionic mode of separation with suppressed EOF was employed. Separations were performed in alkaline electrolyte system (pH=10) due to the dissociation of acidic groups of HAs and, therefore, aggregations of these constituents should not be significant in the ITP separations. The use of suitable spacers in preparative ITP is very important for the following reasons: (1) the zones of DSs split the mobility interval between leading and terminating ion into well-defined subintervals, (2) HAs are spatially separated into an interzonal boundary layers of the DSs zone, (3) a very reproducible fractionation can be realized by micropreparative valve, because any fluctuation in migration is expressed only in changes of the DSs ratio in a fraction and not in analyt content. An appropriate mixture of twenty discrete spacers for CITP characterization of HAs was published by Nagyová and Kaniansky [7]. Based on the results of this work we chosen three spacers (ASP, AAD and TAU) distributing the HAs constituents into CITP zone boundaries relatively uniformly. Isotachopherogram from the separation of HAs with the used mixture of DSs, each at 0.3 mmol/l concentration, is shown in Fig. 1. Carbonates naturally present in the electrolyte solutions were served also as discrete spacer (Fig. 1). Length of carbonates zone was minimized by capturing carbon dioxide from the air with aid of cartridge filed with KOH lentils inserted into the hole of the cap of terminating electrolyte reservoir. A mixture of HAs and DSs after CITP separation was fractionated by micropreparative valve placed at the end of CITP column. Individual fractions were defined by migration position of DSs which spatially separated the sample constituents. In this way, constituents in the injected sample were distributed into five fractions based on different effective mobility subintervals. The mobility subintervals were defined by following couples of CITP zones: (1) chloride-carbonate, (2) carbonate-ASP, (3) ASP-AAD, (4) AAD-TAU, (5) TAU-OH^-. All fractions were isolated in one CITP run by re-filling of the micropreparative valve with LE after the collection of previous fraction and a subsequent electrophoretic transfer of the next fraction into the micropreparative valve.
Conductivity detection used for monitoring of CITP separations are not very convenient for detection of components migrating in “spike-mode” in the interzonal boundaries of regular CITP zones. Nevertheless, the correctness of fractionation procedure is possible to verify by means of presence of corresponding DSs zones on the isotachopherograms from the analytical CITP control of individual fractions. The isotachopherograms in Fig. 2 show the presence of DSs forming the boundaries of individual fractions.

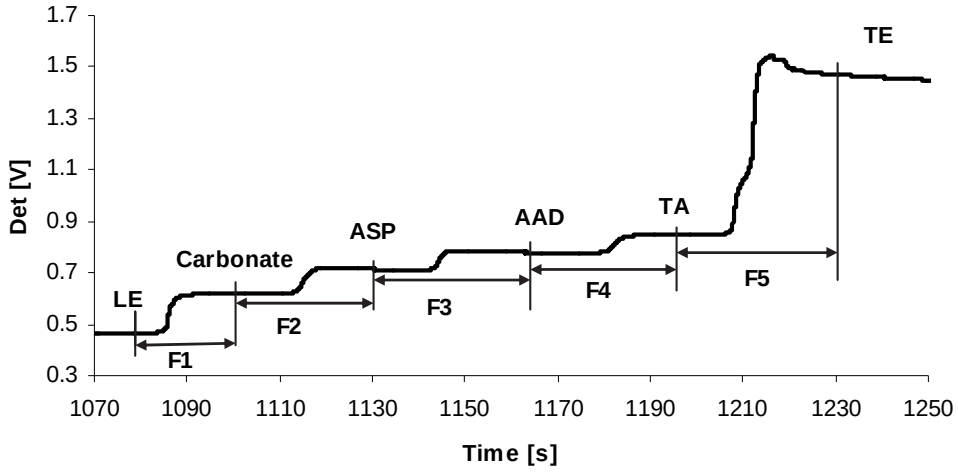

Fig. 1: Isotachopherogram of HAs with three added spacers derived from the conductivity detector. Arrow shows the selection of individual fractions. Injected sample: 100 mg/l HAs (Sigma-Aldrich) and spacers (ASP, AAD, TAU), each at 3.10^{-4} mol/l concentration. The separations were performed in the electrolyte system described in section 2.3 with 900 μA driving current.

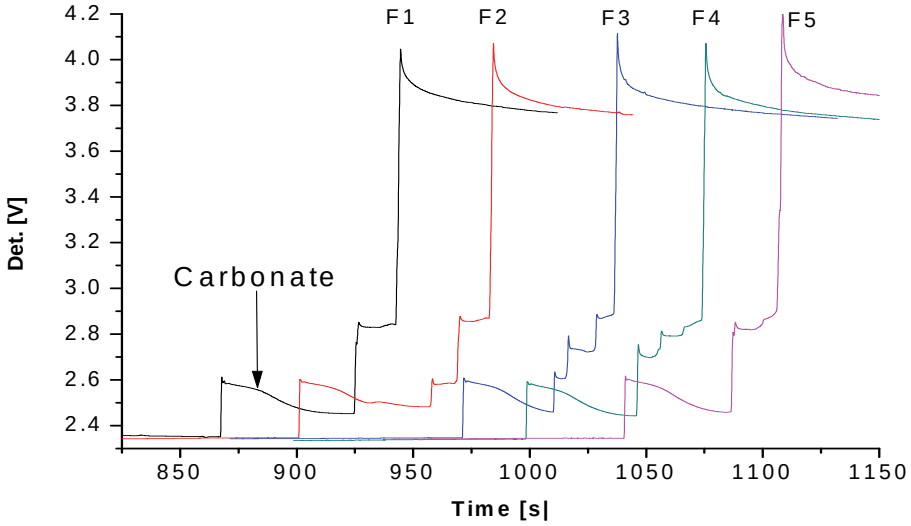

Fig. 2: Isotachopherograms of fractions of HAs from the conductivity detector of control CITP run. The separations were performed in the electrolyte system described in section 2.3 with 50 μA driving current.

The step-wise gradient chromatographic method [4] with fluorimetric detection (FLD) was used for characterization of HAs present in CITP fractions by their chromatographic properties from FLD response. Fig. 3 shows the background corrected profiles as resulted from analysis of standard solution of HAs and mixture of HAs with DSs. RP-HPLC profiles of fractions obtained from preparative CITP (Fig. 4) showed no presence of the peaks eluted before 15 min compared with chromatograms of HAs directly injected to RP-HPLC (Fig. 3) where several peaks with relatively high fluorescence response eluted in the region mentioned above. Observed phenomenon is probably related to CITP fractionations in which these components migrated out of the trapped mobility intervals. The chromatograms obtained from

the separation of CITP fractions normalized to the highest peak (Fig. 5) showed that the fractions 3-5 have very similar chromatographic profiles. Thus, proportional distribution of the compounds presented in these fractions based on the crucial properties for the chromatographic separation system is comparable. First and second CITP fractions have considerably various composition then those (fractions 3-5) discussed above.

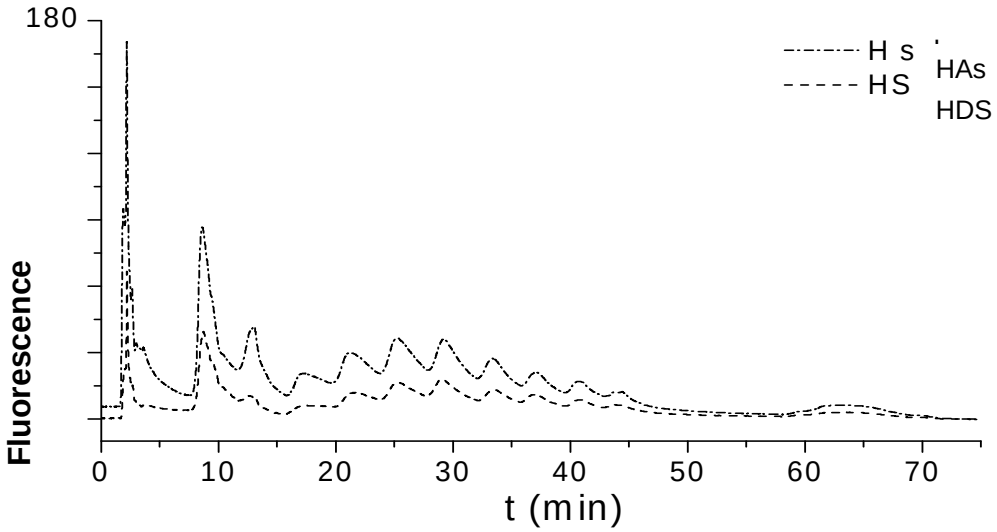

Fig. 3: RP-HPLC profiles of HAs obtained by stepwise gradient elution with fluorimetric detection (ex. 470 nm/em 530 nm). Injected volume was 100 µl of samples (HAs = humic acid, HDS = humic acid with added spacers). For other conditions see the section 2.

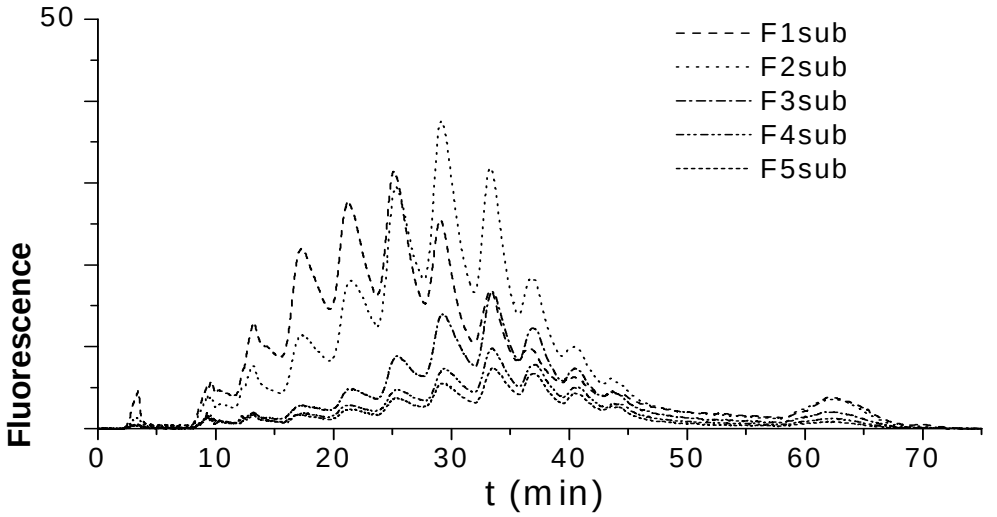

Fig. 4: RP-HPLC profiles of the CITP fractions of HAs obtained by stepwise gradient elution with fluorimetric detection (ex. 470 nm/em 530 nm). Injected volume was 50 µl of fractions. For other conditions see the section 2.

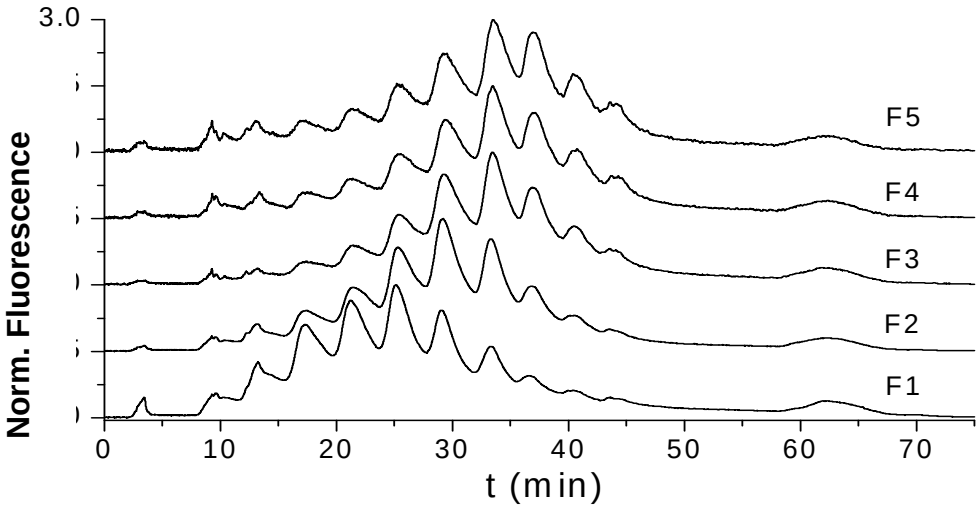

Fig. 5: Normalized RP-HPLC chromatograms of the CITP fractions of HAs obtained by stepwise gradient elution with fluorimetric detection (ex. 470 nm/em 530 nm). Injected volume was 50 µl of fractions. For other conditions see the section 2.

4 CONCLUSION

Differences between chromatographic profiles of the fractions acquired by preparative ITP suggested that individual CITP fractions contained different types of HAs compounds. Therefore, preparative ITP combined with step-wise gradient RP-HPLC should be considered as an alternative way for characterization of humic substances. However, verification of this approach by higher number of different HAs samples is needed, in future.

ACKNOWLEDGEMENTS

This work was generously supported by the grant of Slovak Research and Development Agency (project APVV-0583-11), the Slovak Grant Agency for Science (VEGA 1/1149/12) and the Research & Development Operational Programme funded by the ERDF (CEGreenII, 26240120025). This work is partially outcome of the project VVCE-0070-07 of Slovak Research and Development Agency solved in the period 2008-2011.

LITERATURE

[1.] Ghambour, G., Davies, E. A. (EDs.), *Humic Substances: Structures, Models and Functions,* Royal Society of Chemistry, Cambridge 2001.
[2.] Hutta, M., Góra, R., Halko, R., Chalányová, M., *Journal of Chromatography A* 2011, *1218*, 8946-8957.
[3.] Krauss, G. -J., Krauss, G., *Hochleistungs-Flussigchromatographie, Band 2,* Serva Praxishefte, Serva Feinbiochemica GmBH, Heidelberg 1986.
[4.] Hutta, M., Góra, R., *Journal of Chromatography A* 2003, *1012*, 67-79.
[5.] Madajová, V., Šimuničová, E., Kaniansky, D., Marák, J., et al., *Electrophoresis* 2005, *26*, 2664-2673.
[6.] Hutta, M., Kaniansky, D., Kovalčíková, E., Marák, J., et al., *Journal of Chromatography A* 1995, *689*, 123-133.
[7.] Nagyová, I., Kaniansky, D., *Journal of Chromatography A* 2001, *916*, 191-200.

P47 USE OF PHYSICAL-CHEMICAL METHODS TO ANALYSIS OF ORGANIC MICRO- AND NANOPARTICLES WITH ENCAPSULATED CAFFEINE

Petra Matoušková, Andrea Lichnová, Klára Patočková, Pavla Benešová, Jana Hurtová, Stanislav Obruča, Ivana Márová

Materials Research Centre, Faculty of Chemistry, Brno University of Technology, Purkynova 118, 612 00 Brno, Czech Republic
xcmatouskovap@fch.vutbr.cz

ABSTRACT

Caffeine is a bitter xanthine alkaloid that acts as a stimulant drug. It is the world's most widely consumed psychoactive drug, it is both legal and unregulated in nearly all parts of the world. Beverages containing caffeine enjoy great popularity. Caffeine is toxic at sufficiently high doses, but ordinary consumption poses few known health risks, even when carried on for years. There are some tendencies to regulated release of caffeine from beverages into human organism. One of this ways is encapsulation of caffeine into edible organic particles with controlled release. This study is focused on possibilities of encapsulation caffeine in micro- and nanoparticles. Five different methods were used for preparation of organic particles with encapsulated caffeine. Caffeine was packaged into liposomes and polysaccharide particles (chitosan/alginate or chitosan). Encapsulation's effectiveness was determined by HPLC/UV-VIS. Prepared particles were monitored for size and stability by dynamic light scattering. The particles were exposed to the artificial stomach and intestinal juices and bile acids. Analytical centrifugation was used to measurement of sedimentation velocity and stability of the prepared particles. Electron microscopy and light were used for particle size monitoring too.

Keywords: caffeine, nanoparticles, dynamic light scattering

1 INTRODUCTION

Micro-encapsulation is a process in which tiny particles or droplets are surrounded by a coating to give small capsules many useful properties. In a relatively simplistic form, a microcapsule is a small sphere with a uniform wall around it. The material inside the microcapsule is referred to as the core, internal phase, or fill, whereas the wall is sometimes called a shell, coating, or membrane. Most microcapsules have diameters between a few micrometers and a few millimeters [1,2].

The definition has been expanded, and includes most foods. Every class of food ingredient has been encapsulated; flavors are the most common. The technique of microencapsulation depends on the physical and chemical properties of the material to be encapsulated [1,2].

Caffeine is a bitter xanthine alkaloid that acts as a stimulant drug. Caffeine is found in varying quantities in the seeds, leaves, and fruit of some plants, where it acts as a natural pesticide that paralyzes and kills certain insects feeding on the plants. It is most commonly consumed by humans in infusions extracted from the seed of the coffee plant and the leaves of the tea bush, as well as from various foods and drinks containing products derived from the kola nut. Other sources include yerba maté, guarana berries, guayusa, and the yaupon holly. In humans, caffeine acts as a central nervous system stimulant, temporarily warding off drowsiness and restoring alertness. It is the world's most widely consumed psychoactive drug, but, unlike many other psychoactive substances, it is both legal and unregulated in nearly all parts of the world. Beverages containing caffeine, such as coffee, tea, soft drinks, and energy drinks, enjoy great popularity [3,4].

Caffeine is toxic at sufficiently high doses, but ordinary consumption poses few known health risks, even when carried on for years — there may be a modest protective effect against some diseases, including certain types of cancer. Some people experience sleep disruption if they consume caffeine, especially during the evening hours, but others show little disturbance and the effect of caffeine on sleep is highly variable. There are some tendencies to regulated release of caffeine from beverages into human organism. One of this ways is encapsulation of caffeine into edible organic micro- and nanoparticles with controlled release [3,4].

In this work caffeine was used as a model molecule for testing of encapsulation techniques.

2 METHODS

2.1 Encapsulation techniques

Caffeine was packaged into liposomes (ethanol injection, thin layer evaporation – TLE and thin layer evaporation on reverse phase - RP-TLE) and polysaccharide particles (chitosan/alginate and chitosan). Encapsulation efficiency was determined by HPLC/PDA using Agilent Eclipse Plus C18 (4,6 x 150 mm, 5 mm) column at 30°C and methanol + water + HAc (HCl:H2O 1:99) as mobile phase. Quantitative analysis was performed by external calibration.

2.2 Particle anaysis

Particle size and distribution were analyzed by dynamic light scattering and by light microscopy and electron microscopy, respectively. The unified particle size was set using membrane extruder. Analytical centrifugation was used to measurement of sedimentation velocity and stability of the prepared particles. The particles were exposed to model physiological conditions - artificial stomach and intestinal liquids and bile acids. After exposition, particles stability and amount of released caffeine was monitored. Finally, caffeine containing particles were added in several soft drinks to evaluate potential changes of sensory properties.

3 RESULTS AND DISCUSSION

In this work five different methods were used for preparation of organic particles with encapsulated caffeine. Caffeine was packaged into liposomes and polysaccharide particles (chitosan/alginate or chitosan). Encapsulation's effectiveness was determined by HPLC/UV-VIS.

As the best encapsulation method in terms of caffeine encapsulation efficiency ethanol injection was evaluated (83 %; Fig.1). Size of particles was analyzed by light and elektron microscopy (Figs. 2, 3) and verified by dynamic light scattering (Fig.5). Stability of the particles was measured using a zeta potential (Fig.4). All prepared particles exhibited relatively good stability (Table 1). As the less stable (-29 mV) chitosan-alginate particles were determined, while as the most stable – liposomes prepared by TLE were found (stability range: -30 mV to 30 mV). Only chitosane particles exhibites positive value of zeta potential (+42 mV) (Table 1).

The highest sedimentation stability was observed in polysaccharide particles (Fig.4). Oppositely, liposomes prepared by ethanol injection are relatively unstable. Chitosane particles exhibited relatively high encapsulation efficiency and also DLS stability; unstability was observed in model juices only.

Caffeine particles were exposed to model physiological conditions. The lowest stability was observed in the acidic environment of artificial stomach juice. The values of zeta potential decreased. The particles were partially disintegrated (TLE 58%; chitosan 10%) and

the release of caffeine was evaluated. In alkaline pH of intestinal juice particles were disintegrated to substantially lower degree.

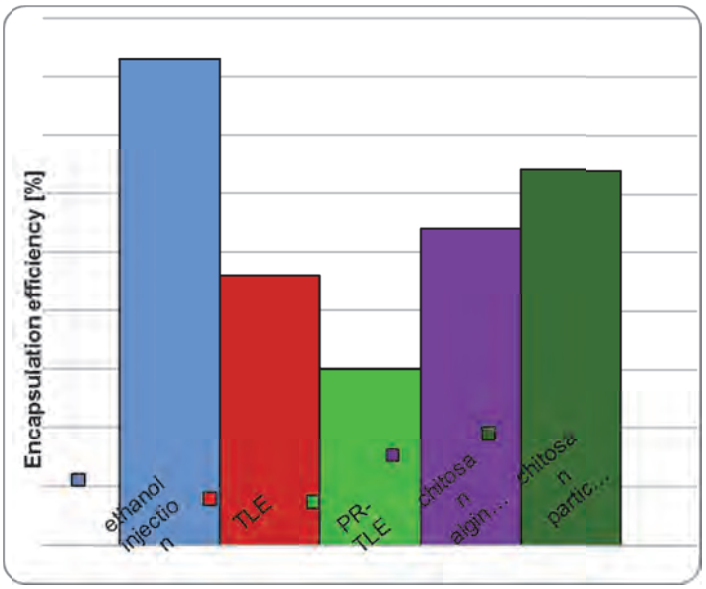

Fig.1: Comparison of the encapsulation efficiency of used encapsulation techniques

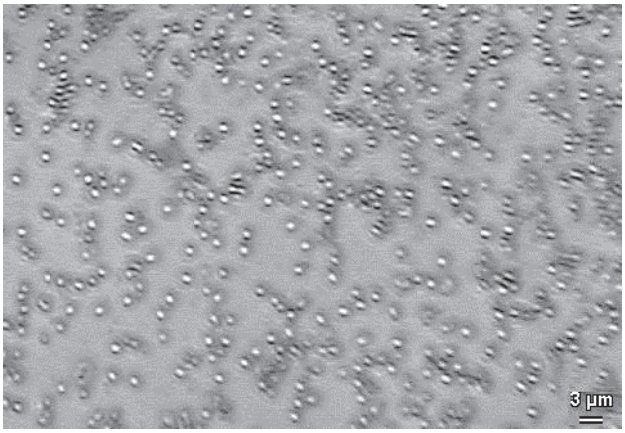

Fig.2: Light microscopy of TLE-liposomes, 640x.

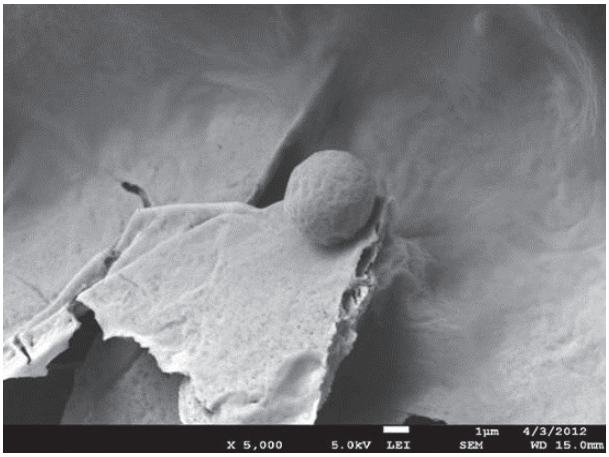

Fig.3: Electron microscopy of TLE-liposomes, 5 000x.

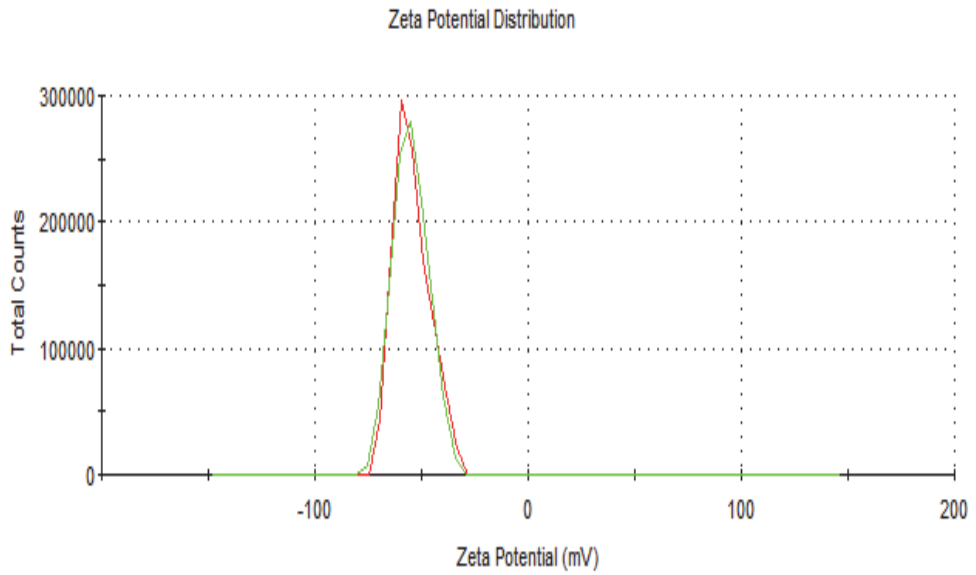

Fig.4: Zeta-potential of TLE-liposomes measured by dynamic light scattering.

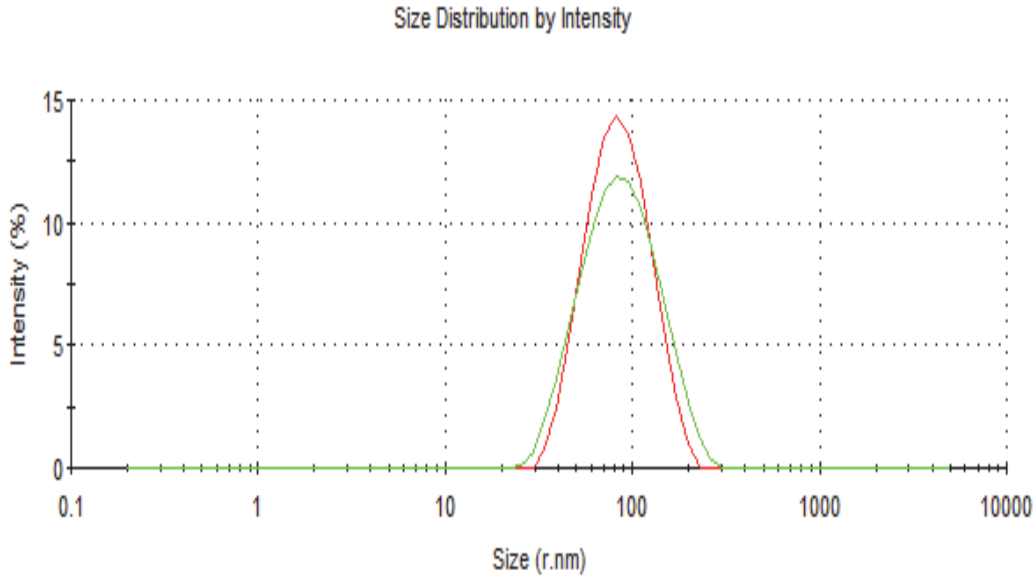

Fig.5: Particle size distribution of TLE-liposomes measured by dynamic light scattering

Table.1: Zeta-potential of particles measured by dynamic light scattering.

Encapsulation method	Particles without caffeine zeta potential [mV]	Particles with caffeine zeta potential [mV]
ethanol injection	- 46.0	- 45.1
TLE	- 51.9	- 54.5
RP- TLE	- 48.0	- 52.5
chitosan/alginate particles	- 29.6	- 29.2
chitosan particles	46.2	42,5

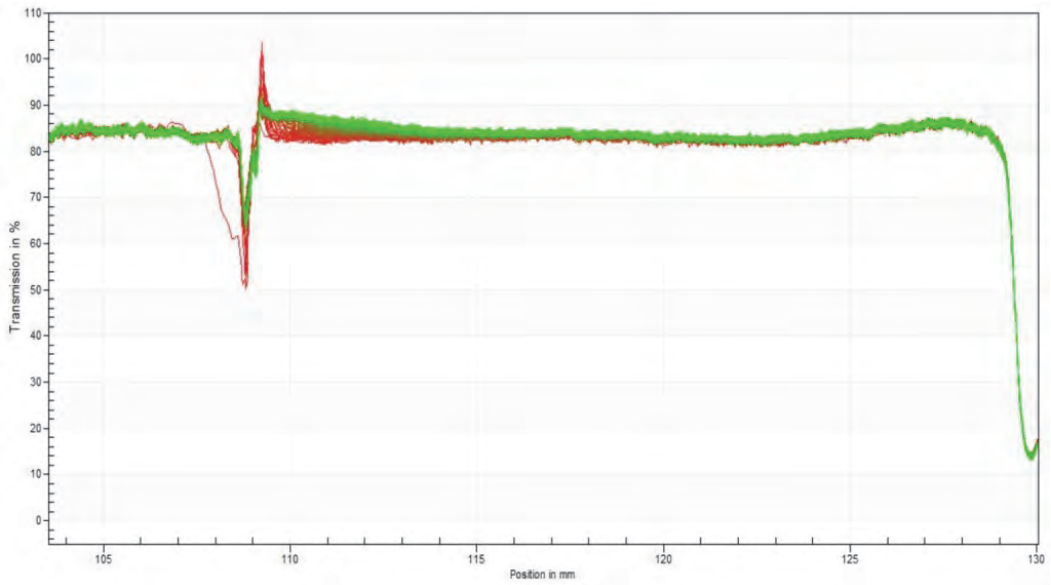

Fig.6: Sedimentation stability of chitosan particles measured by analytical centrifugation

Caffeine containing particles were added in several soft drinks to determine particles amount when turbidity occurred.

Similarly to pure caffeine also some natural extracts were encapsulated too. It can be concluded that some encapsulation procedures could be a suitable alternative for addition of caffeine into stimulation beverages. Encapsulated form of caffeine enables controlled release of caffeine in digestive system.

ACKNOWLEDGEMENTS

This work was supported by "Materials Research Centre at FCH BUT" Project No. CZ.1.05/2.1.00/01.0012 from ERDF (European Regional Development Fund), FP7 Framework Programme (PROETHANOL2G, Project no. 251151) and Regional Innovation Strategy 3. of the City of Brno.

LITERATURE

[1.] Nedović, V., Kalusevic, A., Manojlovic, V., Levic, S., et al., *Procedia Food Science* 2011, *1*, 1806-1815.

[2.] Zuidam, N. J., Nedović, V. A. (Eds.) *Encapsulation Technologies for Active Food Ingredients and Food Processing* Springer Science, 2010.

[3.] Michael J. Glade, *Nurition* 2010, *26,* 932-938.

[4.] Fisone. G., Borgkvist, A., Usiello, A., *Cellular and molecular life sciences* 2004, *61*, 857-872.

P48 SILICA-BASED MONOLITHIC CAPILLARY COLUMNS MODIFIED TO ZWITTERIONIC STATIONARY PHASE FOR HYDROPHILIC INTERACTION LIQUID CHROMATOGRAPHY

Dana Moravcová, Josef Planeta, Vladislav Kahle, Marie Horká, Michal Roth

Institute of Analytical Chemistry of the ASCR, v. v. i., Veveří 97, 602 00 Brno, Czech Republic, moravcova@iach.cz

ABSTRACT

Zwitterionic monolithic capillary columns intended for isocratic gradient hydrophilic interaction chromatography (HILIC) separations are introduced. Silica-based capillary columns (150 mm x 0.1 mm) were prepared by acidic hydrolysis of tetramethoxysilane in the presence of polyethylene glycol and urea. The modification by a 3-(trimethoxysilyl)propyl methacrylate and then by a zwitterionic [2-(methacryloyloxy)ethyl]-dimethyl-(3-sulfopropyl)-ammonium hydroxide to HILIC stationary phase bearing sulfoalkylbetaine groups on its surface followed. Prepared columns were characterized in HILIC separation mode employing mobile phase containing 10% (v/v) of 5 mM ammonium acetate pH = 4.5 in acetonitrile. Comparison with the commercially available ZIC-HILIC® column (Merck SeQuant®) under the same separation conditions using a mixture of aromatic carboxylic acids as a sample was done on the basis of separation efficiency of tested columns as well as retention factors and peak asymmetry of individual solutes.

Keywords: zwitterionic stationary phase, HILIC, phenolic acids

1 INTRODUCTION

Hydrophilic interaction chromatography has become very popular separation technique in the recent years due to its ability to separate polar and highly hydrophilic compounds. Zwitterionic stationary phases occupy a special position among the sorbents designed for HILIC separations. These phases contain two oppositely charged groups in molar ratio 1:1; thus, they can be classified as neutral. Polymer-based monolithic capillary columns bearing zwitterionic groups are prepared mainly using [2-(methacryloyloxy)ethyl]-dimethyl-(3-sulfopropyl)-ammonium hydroxide as a part of polymerization mixture [1-3]. However, there are only few papers describing the preparation and applications of zwitterionic silica-based monolithic capillary columns in HILIC separation mode [4, 5].

2 EXPERIMENTAL

HPLC syringe pump Isco 100 DM with D-series controller, an electrically actuated Valco E90-220 sampling valve with a 60 nL internal sample loop, a lab-made splitter, and an UV detector Spectra 100 were used for characterization of prepared columns. Commercially available analytical column ZIC®-HILIC (150 mm x 2.1 mm, 5 µm; Merck SeQuant®) was evaluated using the system Agilent 1100 HPLC. Capillary columns were prepared by acidic hydrolysis of tetramethoxysilane in the presence of polyethylene glycol PEG 10,000 and urea at our laboratory [6]. The skeleton of the silica-based monolith was modified to sulfoalkylbetaine stationary phase by a simple two-step reaction. In the first step, the prepared bare silica-based capillary columns were modified by 3-trimethoxysilylpropyl methacrylate and then the monolith was thermally grafted using solution of [2-(methacryloyloxy)ethyl]-dimethyl-(3-sulfopropyl)-ammonium hydroxide in a mixture of methanol and xylenes where azobisisobutyronitrile was employed as radical initiator.

3 RESULTS

Prepared silica-based monolithic columns were evaluated in HILIC system using mobile phases consisting of high-percentage of acetonitrile (90% (v/v)) and 5 mM ammonium acetate buffer (10% (v/v), pH = 4.5). The sample included 10 well soluble and under the separation conditions UV detectable aromatic carboxylic acids, see **Table 1**. Toluene was used as t_0 marker (void volume of the column) in all experiments. Considering that the prepared silica-based monolithic capillary columns were modified by zwitterionic ligand originating from [2-(methacryloyloxy)ethyl]-dimethyl-(3-sulfopropyl)-ammonium hydroxide, column properties similar to the commercially available analytical ZIC®-HILIC column were expected. Thus, obtained data were compared with this one.

The minimum plate height measured for synthesized capillary column equals 7.3 µm for toluene as unretained compound corresponding to 136,600 theoretical plates/m, 6.3 µm for cinnamic acid corresponding to 159,000 theoretical plates/m, and 6 µm for vanillic acid corresponding to 167,360 theoretical plates/m at 1 mm/sec mean linear velocity of mobile phase (0.5 µl/min), see **Table 1**. On the other hand, analytical ZIC®-HILIC column shown higher values of the minimum plate height - 46.1 µm for toluene corresponding to 21,690 theoretical plates/m, 52.7 µm for cinnamic acid corresponding to 18,980 theoretical plates/m, and 38.9 µm for vanillic acid corresponding to 25,700 theoretical plates/m at 1.2 mm/sec mean linear velocity of mobile phase (200 µl /min).

The analytical ZIC®-HILIC column provided higher retention factors for all tested compounds, e.g., cinnamic acid k = 0.342 or vanillic acid k = 1.256, when compared to capillary column where cinnamic acid had got k = 0.275 and vanilic acid k = 0.912. Peak asymmetry for tested compounds was close to 1 on ZIC®-HILIC column, e.g., cinnamic acid *As* = 1.267 or vanillic acid *As* = 1.273, while peak asymmetry for cinnamic acid was 0.474 and for vanillic acid 1.313 on synthesized capillary column, see **Table 1**.

Table 1: Separation efficiency, retention factors (*k*), and values of peak asymmetry (*As*) obtained for the tested compounds on the synthesized capillary column under isocratic conditions – 90% (v/v) ACN / 10% (v/v) 5mM ammonium acetate pH=4.5, flow rate 0.5 µl/min.

Analyte	Column efficiency*	*k*	*As*
4-butylbenzoic acid	134,070	0.081	0.500
Salicylic acid	81,586	0.124	0.273
2,4,6-trimethylbenzoic acid	86,561	0.230	0.579
Cinnamic acid	159,012	0.275	0.474
Benzoic acid	54,574	0.437	0.216
2-methoxybenzoic acid	129,078	0.503	0.455
Ferulic acid	163,022	0.589	1.583
Syringic acid	147,079	0.792	1.235
Vanillic acid	167,360	0.912	1.313
4-hydroxybenzoic acid	107,255	1.175	3.154

* theoretical plates/meter; Retention factor: $k=(t_R-t_0)/t_0$, where t_R is the analyte retention time and t_0 the retention time of toluene used as void volume marker.

Figures 1A and **1B** present HILIC separation of aromatic carboxylic acids on zwitterionic columns. All tested compounds are well separated on capillary monolithic column, see **Figure 1A**. However, coelution of toluene and 4-butylbenzoic acid, salicylic acid and 2,4,6-

trimethylbenzoic acid, and 2-methoxybenzoic acid with ferulic acid occurred on ZIC-HILIC® column, see **Figure 1B**, when the same mobile phase is used for separation.

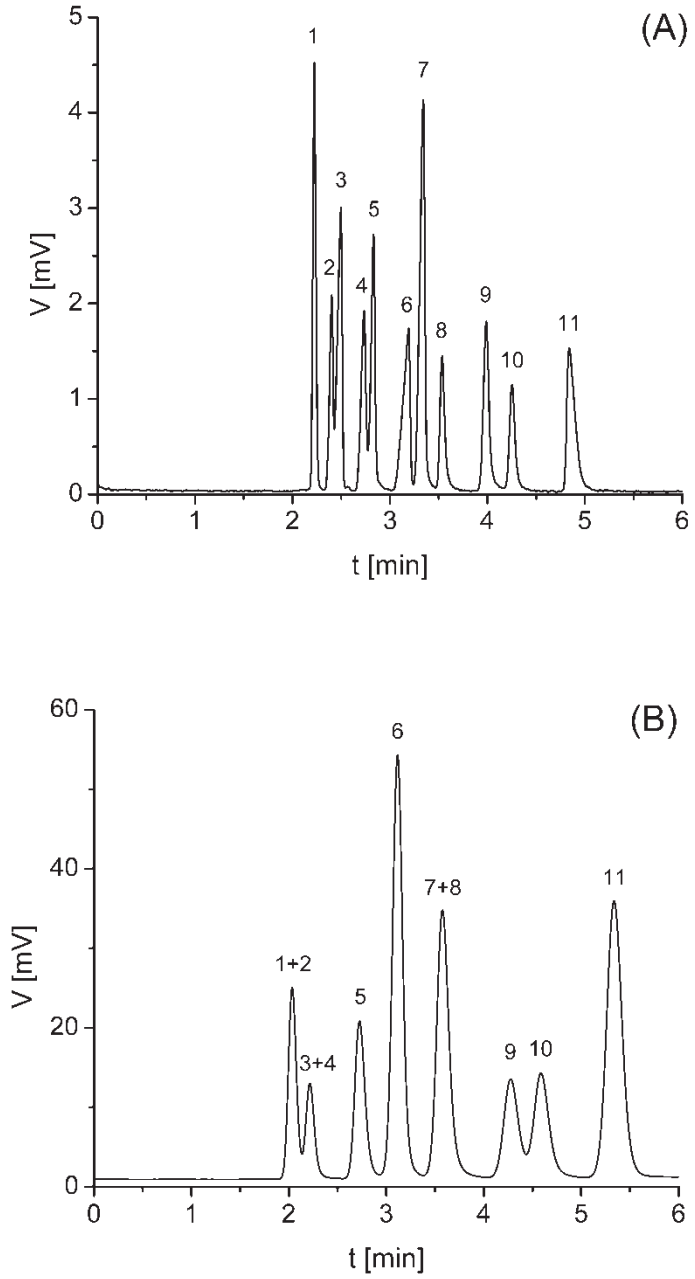

Fig. 1: HILIC separation of aromatic carboxylic acids on zwitterionic columns. Mobile phase: 90% (v/v) of acetonitrile with 10% (v/v) of 5 mM ammonium acetate, pH = 4.5. (A) synthesized monolithic capillary column (150 mm x 0.1 mm), flow rate 0.5 µl/min*; (B) ZIC-HILIC® column (150 mm × 2.1 mm), flow rate 200 µl/min*; UV detection 210 nm. Sample: toluene (1), 4-butylbenzoic acid (2), salicylic acid (3), 2,4,6-trimethoxybenzoic acid (4), cinnamic acid (5), benzoic acid (6), 2-methoxybenzoic acid (7), ferulic acid (8), syringic acid (9), vanillic acid (10), and 4-hydroxybenzoic acid (11). *mean linear velocity of the mobile phase is (A) 1 mm/sec and (B) 1.2 mm/sec.

4 CONCLUSIONS

The simple two-step modification of silica-based monolithic capillary columns has provided stable zwitterionic stationary phase suitable for separation of strongly polar aromatic acids. The high separation efficiency of original bare silica monolithic column was preserved even after modification by zwitterionic monomer. The elution order of tested compounds was the same as on the commercially available ZIC-HILIC® column. The retention of tested compounds was slightly lower on synthesized capillary column under the tested conditions, although the capillary column has got higher separation selectivity.

ACKNOWLEDGEMENTS

This work was supported by the Ministry of the Interior of the Czech Republic (Project No. VG20112015021), by the Czech Science Foundation (Projects No. P206/11/0138 and P106/12/0522), and by the Academy of Sciences of the Czech Republic (Institutional support RVO: 68081715).

LITERATURE

[1.] Jiang, Z., Smith, N. W., Ferguson, P. D., Taylor, M. R., *Anal. Chem.* 2007, *79*, 1243-1250.
[2.] Wang, X., Lin, X., Xie, Z., *Electrophoresis* 2009, *30*, 2702-2710.
[3.] Urban, J., Škeříková, V., Jandera, P., Kubíčková, R., Pospíšilová, M., *J. Sep. Sci.* 2009, *32*, 2530-2543.
[4.] Wohlgemuth, J., Karas, M., Jiang, W., Hendriks, R., Andrecht, S., *J. Sep. Sci.* 2010, *33*, 880-890.
[5.] Lin, H., Ou, J., Zhang, Z., Dong, J., Wu, M., Zou, H., *Anal. Chem.* 2012, *84*, 2721-2728.
[6.] Planeta, J., Moravcová, D., Roth, M., Karásek, P., Kahle, V., *J. Chromatogr. A* 2010, *1217*, 5737-5740.

P49 SENSOR BASED ON FÖRSTER RESONANCE ENERGY TRANSFER WITH QUANTUM DOT

Marcela Liskova[a,b]; Vladimira Datinska[a]; Karel Kleparnik[a]; Frantisek Foret[a]

[a] *Institute of Analytical Chemistry ASCR, v.v.i., Brno, Czech Republic*
[b] *Masaryk University, Faculty of Science, Centre for Syntheses at Sustainable Conditions and their Management, Brno, Czech Republic*

ABSTRACT

Förster resonance energy transfers (FRET) are based on the nonradiative transfer of energy between a donor and acceptor dye in the distance 1-10 nm. With respect to this, quantum dots (QDs) with a high absorbance can serve as suitable donors of energy in FRET. Here, we present architectures of two sensors based on QD conjugates useful in imaging and diagnostics of cancer. One sensor, based on an oligonucleotide conjugate, can be used for the detection of complementary oligonucletide chains. The other was designed for the detection of enzymes inside cells.

1 INTRODUCTION

1.1 QDs

The most successful application of quantum dots (QDs) is their implementation as highly fluorescent probes in molecular diagnostics [1.]. The most important manifestation of QDs electronic states is the sharp and symmetric and narrow emission spectra, broad excitation spectra and size-dependent emission wavelengths [2.]. In addition, QDs have a good

chemical stability with practically no photobleaching [3.]. QDs have extremely high extinction coefficients. Therefore, we decided to use them like energy donors in FRET.

1.2 FRET

The process of FRET is a photophysical phenomenon through which an energy absorbed bya fluorophore (the energy donor) is transfered nonradiatively by dipole-dipole interactions to the second fluorophore (the energy acceptor) [4., 5.]. The efficiency of energy transfer between the fluorophores is sensitive to their distance (1-10 nm).

1.3 Conjugation reactions

The spectroscopic and physicochemical properties of QDs are given by a material of their core, size and chemistry of surface layers and ligands. We focused on preparing CdTe QDs, which can be passivated by inorganic salts (CdS, ZnS). We have mastered the preparation of water soluble QD by addition of thiolated ligands, e.g., mercaptopropionic acid (MPA) [6.]. QDs can be cojugated with a variety of biomolecules by different techniques [7.], which can be divided into four main groups: (*i*) non-covalent electrostatic interactions, (*ii*) direct binding of thiolated compouds or polyhistidine residues to the metal atoms on the particle surface, (*iii*) covalent bonding by organic linker, (*iv*) conjugation *via* avidin-biotin system.
The most popular cojugation technique is the use of zero-length cross-liker, 1-ethyl-3-(3-dimethylaminopropyl) carboiimide hydrochloride (EDC), in a presence of hydrophilic active group, e.g. *N*-hydroxysulfosuccinimide (sulfo-NHS). It is a reaction between the carboxylic group on the QD surface and the primary amino group of molecule of interest by a forming of peptide bond [8.].

1.4 Application of sensors

QDs conjugated with biological molecules (proteins, peptides, DNA etc.) have a widespread applicability in areas ranging from in *vivo* imaging and diagnostics in medicine to environmental monitoring for public health. QD sensors have already been prototyped for detecting targets such as explosives, toxins, nucleic acids, peptides, drugs, carbohydrates, and enzymatic processes [1., 3.].

2 PROPOSAL OF SENSORS

2.1 Caspase 3 sensor

Caspase 3 a cysteine-aspartic acid protease, activated in the apoptotic pathway, is a key factor in apoptosis execution and is the active form of procaspase 3. Caspase 3 recognizes tetra-peptide sequences Asp-Glu-Val-Asp (DEVD). We designed sensor based on QD-DEVD-quencher conjugate. The principle of sensor based on quenching of fluorescence is irradiated with some source of light at given wavelength. This energy is transported nonradiatively *via* linker chain to quencher. The transported energy is quenched by a modified BHQ-2 quencher. However, after the cleavage of the bond between quencher and DEVD sequence by caspase 3 present in analyzed samples, there is no nonradiative transfer, quencher does not absorb and QD emits light at given wavelength (Fig. 1).

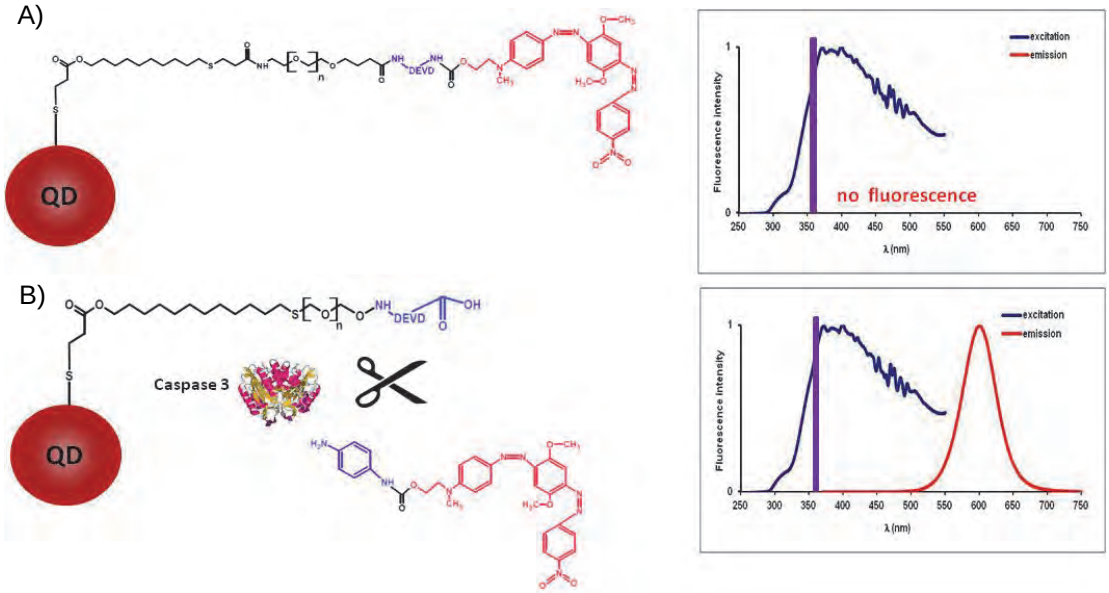

Fig. 1: A) Model of Caspase 3 sensor, with DEVD chain. Fluorescence emission of QD is quenched. B) Cleavage of the bond between DEVD and quencher. QD´s emmision is visible.

2.2 Oligonucleotide sensor

We have designed a new FRET sensor based on QD-oligonucleotide conjugate. A source of light should excite only QD, not the fluorophore dye. A green QD is proposed as donor of energy and rhodamine type dye as acceptor (Fig. 2). Associated complementary oligonucleotide chains can be detected as a reduction in the fluorescent quantum yield in emitted light of the donor, and a simultaneous increase in the fluorescent emission from the acceptor dye.

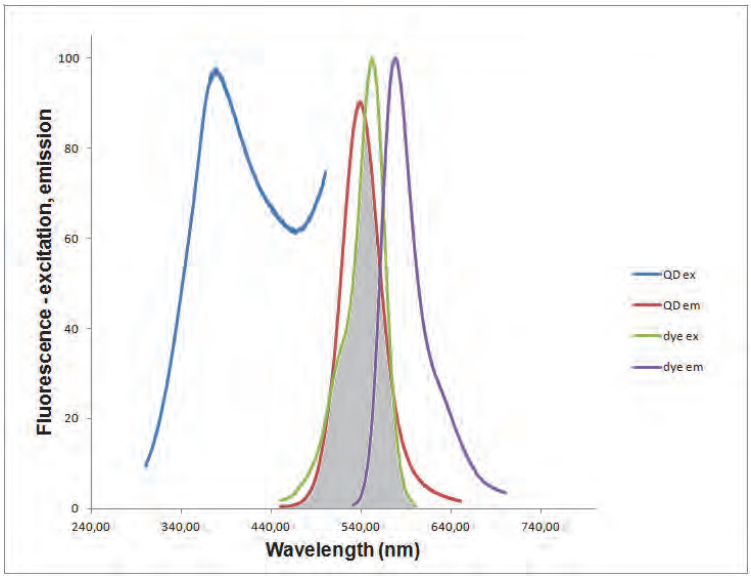

Fig. 2: Example of excitation and emission spectra of green QD and rhodamine dye (ROX). Spectral overlap is shown as the grey region.

Proposed sensor is based on the three oligonicleotides (Fig. 3): one oligonucleotide, probe of a length of 18 nt, is conjugated with QD. Another nucleotide, reporter (15 nt), is conjugated with a rhodamine dye. These two oligonucleotides are comlementary to a third oligonucleotide, target (33 nt).

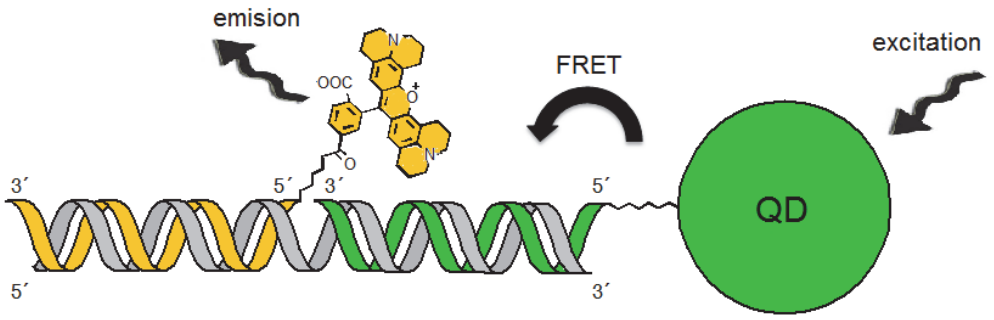

Fig. 3: Design of QD-FRET hybridization assay based on three oligonicleotices. Oligonucleotide conjugates with QD probe (green), ROX dye reporter (orange) and a complementary target (grey) are associated.

3 EXPERIMENTAL RESULTS

We used CdTe QDs with a maximum emmision wavelength of 600 nm and with mercaptopropionic acid as a surface ligand for synthesis of Caspase 3 sensor. For QDs preparation was used one-step synthesis described elsewhere [9.]. For organic quencher preparation was used synthesis described in US patent [10.]. As a linker chain were used 12-bromo-1-dodecanol and *O*-(3-Carboxypropyl)-*O′*-[2-(3-mercaptopropionylamino)ethyl]-polyethylene glycol (Sigma Aldrich). DEVD sequence was purchased from Sigma Aldrich as *N*-Acetyl-Asp-Glu-Val-Asp *p*-nitroanilide. All chemicals were used without further purification.

4 CONCLUSION

The potential of two sensors based on QD conjugates has been demonstrated. Both utilize FRET between quantum dot donors and fluorophore labeled acceptors for analysis of biomolecules, potentially applicable for imaging and diagnostic of cancer. The optimum Förster distance between QD and quencher for efficient FRET was determined theoretically and problems with QDs precipitation during synthesis solved.

ACKNOWLEDGEMENTS

This work was supported by The Grant Agency of the Czech Republic (GA203/08/1680, P301/11/2055 and P206/11/2377), Ministry of Industry and Trade (2A-1TP1/090), Ministry of Education, Youth and Sports (OP Education for Competitiveness-CZ. 1.07/2. 3 00/20. 0182) and institute research plan AV0Z40310501.

LITERATURE

[1.] Algar, W. R., Tavares, A. J., Krull, U. J., *Analytica Chimica Acta* 2010, *673*, 1-25.
[2.] Rajh, T., Micic, O. I., Nozik, A. J., *Journal of Physical Chemistry* 1993, *97*, 11999-12003.
[3.] Klostranec, J. M., Chan, W. C. W., *Advanced Materials* 2006, *18*, 1953-1964.
[4.] Forster, T., *Naturwissenschaften* 1946, *33*, 166-175.
[5.] Forster, T., *Annalen Der Physik* 1948, *2*, 55-75.
[6.] Liskova, M., Voracova, I., Kleparnik, K., *et al.*, *Analytical and Bioanalytical Chemistry* 2011, *400*, 369-379.
[7.] Medintz, I. L., Uyeda, H. T., Goldman, E. R., *et al.*, *Nature Materials* 2005, *4*, 435-446.
[8.] Hermanson, G., *Bioconjugate techniques*, Elsevier, San Diego 1996.
[9.] Duan, J., Song, L., Zhan, J., *Nano Res* 2009, *2*, 61-68.
[10.] Gharavi et al., patent US 7205347 B2 2007.

P50 OCCURRENCE OF LIGNANS IN ENVIRONMENTAL WATERS

Jan Tříska[a], Martin Moos[a], Iveta Marešová[b], Naděžda Vrchotová[a]

[a] *Laboratory of Metabolomics and Isotopic Analyses, Global Change Research Centre AS CR, Branišovská 31, 370 05 České Budějovice, Czech Republic, triska.j@czechglobe.cz*
[b] *Faculty of Agriculture, University of South Bohemia, Studentská 13, 370 05 České Budějovice, Czech Republic*

ABSTRACT

The content of lignans, especially hydroxymatairesinol (HMR) was investigated in different types of natural waters from the environment. Collected water samples were extracted with methyl tert.butylether, derivatized and analysed by means of GC-MS. HMR was found in different amount in all water samples beside the other lignans.

Keywords: waters, lignans, hydroxymatairesinol (HMR)

1 INTRODUCTION

Lipophilic and water soluble compounds occur in softwoods of the trees. Lipophilic compounds in the Norway spruce are composed mainly of fatty acids, resin acids, sterols, sterylesters and triglycerides. Beside lipophilic compounds there are also hydrophilic compounds, especially lignans which are phenolic compounds consisting of two phenylpropane units. Lignans form a major part of the water soluble substances which are releasing into waste water during mechanical pulping process. Örså and Holbom [1] found in the waters from thermo mechanical pulping (TMP) 20.3 mg/L of lignans in average, Jørgensen et al. [2] found lignans in the effluents from TMP plants in the range of 79 - 162 mg/L. In the sewage treatment plant in Turku the concentration of lignans in inflow water was the the following: 0.052 nM of HMR, 0.062 nM of hydroxyenterolactone, 0.097 nM of enterodiol and 4.10 nM of enterolactone [3]. The same authors have found almost the same amount of lignans in humic water. This is probably due to releasing of lignans from decaying plant material from living and/or dead plant and tree tissues, ranging from deciduous and coniferous trees growing in the water. Lignans are present in wood [4], especially in the knots [5] there is no data about presence of lignans in roots which could be the source of lignans in the environmental waters. The main goal of our contribution is to investigate the possibility of lignans occurrence in the wetlands with different tree population.

2 MATERIALS AND METHODS

2.1 Locality and sampling

The sampling localities were selected with regard to our hypothesis near the town of České Budějovice and Třeboň, Czech Republic (A: 48°58'19.606"N 14°24'51.401"E; B 48°59'47.669"N, 14°26'38.004"E; C 48°59'11.260"N, 14°50'49.536"E). The day of sampling was sunny without any rainfall in these localities.

2.2 Methodology of lignans determination

For all performed chromatographic analyses the ITQ 1100 instrument (Thermo Fisher Scientific, U.S.A.) equipped with the Trace GC Ultra (Thermo Fisher Scientific, U.S.A.) was used. For the HMR analysis the volume of 1 µl was injected splitless at 250°C (split after 30 s, 45 mL/min) to a 2-mm ID Siltek liner (Restek Corporation, Bellefonte, PA, USA). Separation of analytes was performed on a fused silica capilary column (ZB-5MS, 30 m × 0.25 × 0.25 µm, Phenomenex, Torrance, CA, USA). Helium was used as the carrier gas, at a constant column

flow rate 1 mL min-1 and the following temperature program: 150 °C , rate 40 °C min-1 to 230 °C, then 5 °C min-1 to 285 °C holding 8 min. Transfer line temperatute was 250 °C. The MS was operated in full scan mode and scanning range m/z 50-600. From the data files the peak area of TMS-HMR were derived using four specific fragments: m/z 297; 304; 500 and 590. Liquid-liquid extraction (LLE) was performed on 200 ml of water sample with pH to about 3.5 (adjusted by sulphuric acid) with 100 ml of tert.butyl methyl ether (MTBE). The extraction was repeated using 100 ml of MTBE. The pooled MTBE-extracts were evaporated to dryness in the rotary evaporator. Finally, the flask was rinsed four-times with 1 ml of toluene using ultrasonic bath and the sample was placed in the 4ml vial and put into the freezer. The extraction was performed in triplicate from all the samples. Trimethylsilyl (TMS) derivatization of HMR was achieved by adding 70 µl of N,O-bis(trimethylsilyl) trifluoroacetamide with 1% of trimethylchlorosilane (BSTFA, Fluka) and 50 µl of pyridine to 1 ml sample aliquots evaporated with stream of nitrogen. Mixture was held at 60°C, after 30 min was evaporated at 35°C to dryness by a stream of nitrogen, redissolved in 1 ml of hexane, stored at 4°C and analysed within 48 hours in order to minimize the decomposition of the TMS derivatives of HMR in the samples. Concentrations of HMR in the samples were calculated using an external standard (ArboNova, Turku, Finland).

3 RESULTS AND DISCUSSION

In the first part of our study we have studied the silylation procedure and analytical condition for the lignans determination. The detection limits calculated from calibration curve of HMR (see **Fig 1.**), were quantified according to Graham (X_D^{α} ; X_D^{β}) [6] and Miller (X_m) [7]. The results are shown in **Table 1.**

Table 1: Summary of calibration data for HMR

X_D^{α}	1.32 ug/ml
X_D^{β}	3.78 ug/ml
X_m	2.43 ug/ml
y = 2592965x-76907	

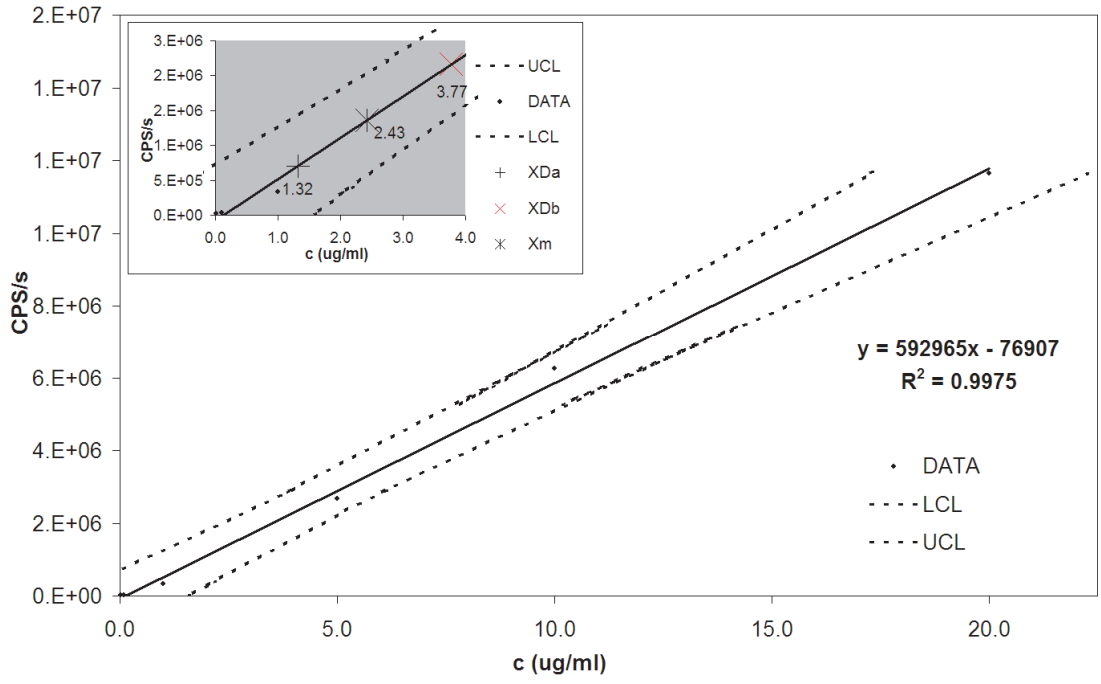

Fig. 1.: Calibration curve for HMR.

The detected contents of HMR is about several order of magnitude higher than published data in humic water (see **Table 2**), but lower than published data from paper mill effluents, which are in the range of tens milligrams of HMR in one litre of water. In the sample the other lignans were determined as it can be seen on the **Fig. 2**, where secoisolariciresinol and α-coninedrin are also present.

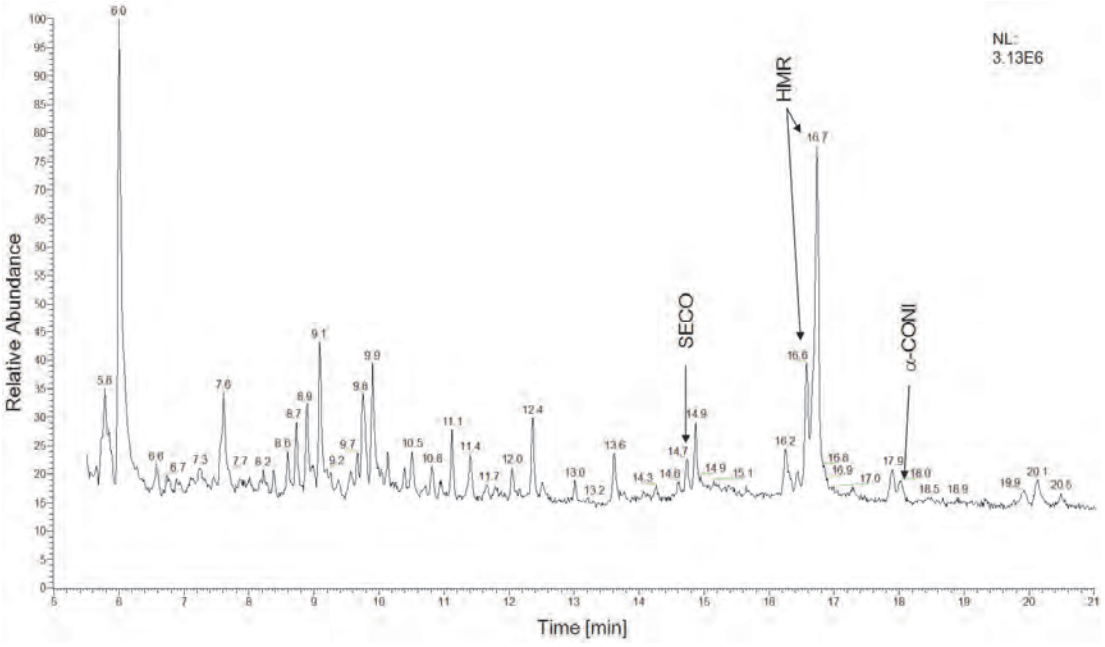

Fig. 2.: Chromatogram (TIC) of water sample C. Secoisolariciresinol (SECO), α-Conidendrin (α-CONI).

Table 2: Concentrations of HMR in water samples from investigated localities in comparison with published data [3].

Locality	HMR [ug/l]	α-CONI [ug/l]	SECO [ug/l]
A	27.1	D	D
B	206.6	D	D
C	64.9	D	D
Sea water	0.000049	-	ND
Tap water	0.157	-	ND
Humic water	0.071	-	0.0279

4 CONCLUSIONS

The developed analytical procedure based on extraction of natural waters using methyl tert.butyl ether is suitable for the extraction of polar compounds from water including lignans. In all water samples we have found the main lignans (HMR, α-coninedrin and secoisolariciresinol) and HMR was quantified in all samples. The calibration curve is linear in the range of 0.01-20 ug/ml, detection limit for HMR using above mentioned procedure is between 1.32 ug/ml to 3.78 ug/ml.

ACKNOWLEDGEMENTS

This study was supported by MŠMT COST project LD11016 and by the Project CzechGlobe – Centre for Global Climate Change Impacts Studies, reg. no. CZ.1.05/1.1.00/02.0073.

LITERATURE

[1.] Örså, F., Holmbom, B., A convenient method for the determination of wood extractives in papermaking process waters and effluents, Journal of Pulp and Paper Science 1994, *20*, J361-366.

[2.] Jørgensen G., Carlberg G.E., Hoel H., Lystad E., Lignans in TMP effluents: Fate and effects, Tappi Journal 1995, *78*, 171-176.

[3.] Smeds A.I., Willför S.M., Pietarinen S.P., Peltonen-Sainio P., Reunanen M.H.T., Occurence of "mammalian" lignans in plant and water sources, Planta 2007, *226*, 639-646.

[4.] Willför S.M., Hemming J., Reunanen M., Eckerman Ch., Holmbom B., Lignans and lipophilic extractives in Norway spruce knots and stemwoods, Holzforshung 2003, *57*, 27-36.

[5.] Holmbom B., Eckerman Ch., Eklund P., Hemming J., Nisula L., Reunanen M., Sjöholm R., Sundberg A., Sundberg K., Willför S.M., Knots in trees – A new rich source of lignans, Phytochemistry Review 2003, *2*, 331-340.

[6.] Graham: *Data Analysis for The Chemical Sciences*. VCH PUBL. INC, New York,1993

[7.] Miller J. N., Miller J. C.: *Statistics and Chemometrics for Analytical Chemistry*, Pearson Education Limited, 268 s., 2005, ISBN 0-13-129192-0

P51 MONOLITHIC COLUMNS FOR SEPARATION OF LOW-MOLECULAR COMPOUNDS

Magda Stankova, Pavel Jandera, Jiri Urban, Veronika Skerikova

Department of Analytical Chemistry, Faculty of Chemical Technology, University of Pardubice, Studentska 573, Pardubice, 532 10, Czech Republic
magda.stankova@student.upce.cz

ABSTRACT

Crosslinking monomers with various lengths of methylene or oxyethylene chains between two methacrylate units were applied for preparation of polymethacrylate monolithic columns suitable for isocratic separation of low-molecular compounds, using lauryl methacrylate as the functional monomer for reversed-phase chromatography. The crosslinking monomers included ethylene-, tetramethylene-, hexamethylene-, dioxyethylene-, trioxyethylene-, and tetraoxyethylene dimethacrylates. The replacement of generally used ethylene dimethacrylate as a crosslinking monomer by monomers with longer methylene and oxyethylene chain led to significant increase in the column efficiency. For example, a column prepared with tetraoxyethylene dimethacrylate shows the column efficiency of 71 000 theoretical plates per meter and offers fast isocratic separation of six low-molecular alkylbenzenes in 2 minutes. This confirms the significant effect of the length of the oxyethylene chain in the crosslinking monomer on the efficiency of polymethacrylate capillary columns.

Keywords: Organic polymer monoliths, Efficiency, Low-molecular compounds

1 INTRODUCTION

Miniaturization in micro-bore or capillary liquid chromatography allows lower volumes of mobile phases, and of samples to be used. Monolithic stationary phases formed by a single piece of highly porous material are very suitable for miniaturization.

Organic polymer monolithic columns in capillary or micro-bore format can be prepared by in-situ polymerization in a fused silica capillary. The polymerization mixture generally contains a crosslinking monomer, a functional monomer, porogen solvents and an initiator of radical polymerization [1]. Optimization of the polymerization mixture allows straightforward control of hydrodynamic and separation properties of columns such as porosity, efficiency, and selectivity.

Separation of low-molecular compounds on organic polymer monolithic columns has been not as easy to achieve as with silica gel monolithic columns because of different pore morfology causing relatively low efficiency of polymethacrylate or polystyrene monolithic columns prepared in traditional way. In our recent work, we compared monolithic capillary columns prepared from various functional monomers: butyl-, cyclohexyl-, ethylhexyl-, lauryl-, and stearyl methacrylate with ethylene dimethacrylate crosslinker [2]. The lauryl methacrylate monomer provided the columns with best separation properties, but the efficiency for low-molecular compounds was still rather low. The objective of the present work was increasing the efficiency of separation of low molecular compounds by varying the chemistry of crosslinking monomers with two methacrylate units.

2 EXPERIMENTAL PART

The generic polymerization mixture contained lauryl methacrylate as functional monomer with ethylene dimethacrylate as a crosslinking monomer. The crosslinker was replaced by dimethacrylates with longer alkyl or oxyethylene chains between the two end methacrylate units. These columns have been optimized for application in reversed-phase chromatography. Because the separation of highly polar compounds in reversed-phase chromatography is very difficult, hydrophobic lauryl methacrylate monomer was replaced by zwitterionic N,N-dimethyl-N-metacryloxyethyl-N-(3-sulfopropyl)ammonium betaine functional monomer for hydrophilic interaction chromatography, where polar compounds provide sufficient retention. The chemical structures of applied monomers are shown in **Fig. 1**.

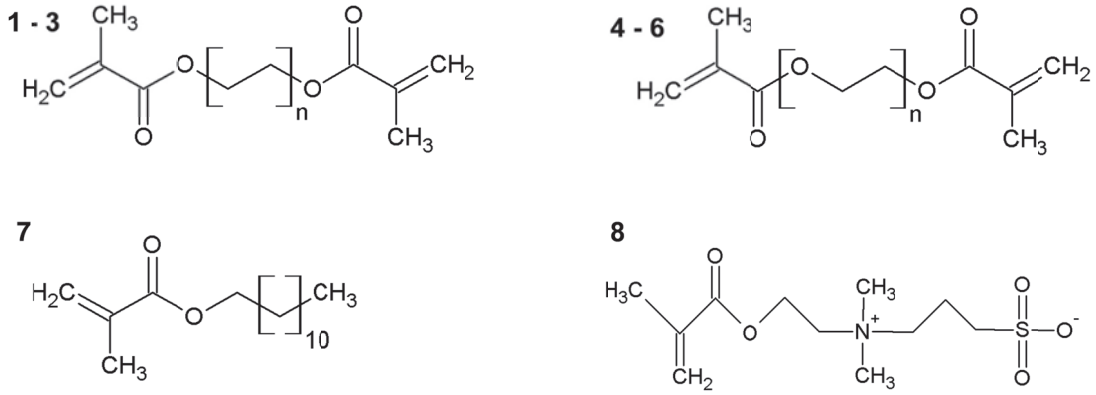

Fig. 1. Chemical structure of methacrylate monomers used in this study. (1) ethylene dimetacrylate, n = 1 (EDMA), (2) tetramethylene dimetacrylate, n = 2 (BUDMA), (3) hexamethylene dimetacrylate. n = 3 (HEDMA), (4) dioxyethylene dimetacrylate, n = 2 (DiEDMA), (5) trioxyethylene dimetacrylate, n = 3 (TriEDMA), (6) tetraoxyethylene dimetacrylate, n = 4 (TeEDMA), (7) lauryl metacrylate (LMA), and (8) N,N-dimethyl-N-metacryloxyethyl-N-(3-sulfopropyl)ammonium betaine.

3 RESULTS AND DISCUSSION

In the present study, we used the laurylmethacrylate (LMA) functional monomer in combination with various cross-linking agents to investigate the effects on the chromatographic properties of polymethacrylate monolithic capillary columns. **Fig. 1** shows the structures of the cross-linkers studied, which included a series with two (EDMA), four (BUDMA) and six (HEDMA) repeat methylene groups and a series with two (DiEDMA), three (TriEDMA) and four (TeEDMA) more polar oxyethylene groups.

In the series of columns prepared with (poly)methylene and (poly)oxyethylene dimethacrylate series, the plate height significantly decrease and the efficiency improves with increasing size of the crosslinker chain in both reversed-phase and hydrophilic interaction chromatography mode, respectively. The optimized columns afford very fast isocratic separation of low-molecular non-polar and polar compounds in less than two minutes and show efficiencies of 70 000 theoretical plates/meter (**Fig. 2**) [3].

The columns show very good repeatability of isocratic separations on individually prepared column batcher with average run-to run errors of 0.3% in retention volumes and of 1.1% (benzene) to 3.9% (butylbenzene) in the efficiency in terms of plate height**.** The repeatability of separation on nine columns prepared from three freshly prepared polymerization mixtures was approximately 2.5% in retention volumes and 7% in plate height for the alkylbenzene samples. These results prove reliability of preparation of monolithic polymethacrylate columns using the present approach.

The result of this work confirmed significant effect of the length and chemistry of the chain in the crosslinking monomer on the efficiency of polymethacrylate capillary columns and importance of its optimization to obtain suitable pore morphology enabling fast and efficient isocratic separations of low molecular compounds.

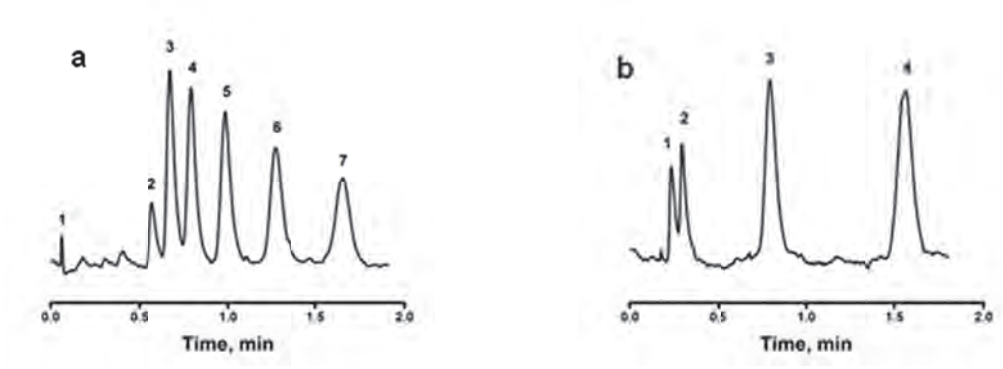

Fig. 2.: Examples of fast isocratic separations of low-molecular non-polar (a) and polar (b) compounds on columns optimized for separation in (a) reversed-phase and (b) hydrophilic interaction liquid chromatography. (a) Monolithic capillary column with tetraoxyethylene dimethacrylate and lauryl methacrylate, mobile phase: 70% acetonitrile, length 183 mm, flow-rate 40.6 µl/min, back pressure 20.3 MPa, UV detection at 214 nm. Samples: 1 – uracil, 2 – benzene, 3 – toluene, 4 – ethylbenzene, 5 – propylbenzene, 6 – butylbenzene, 7 – amylbenzene. (b) Monolithic capillary column with dioxyethylene dimethacrylate and sulfobetaine monomer, mobile phase: 95% acetonitrile, length 174 mm, flow-rate 48.2 µl/min, back pressure 21.6 MPa, UV detection at 214 nm. Samples: 1 – toluene, 2 – phenol, 3 – uracil, 4 – thiourea.

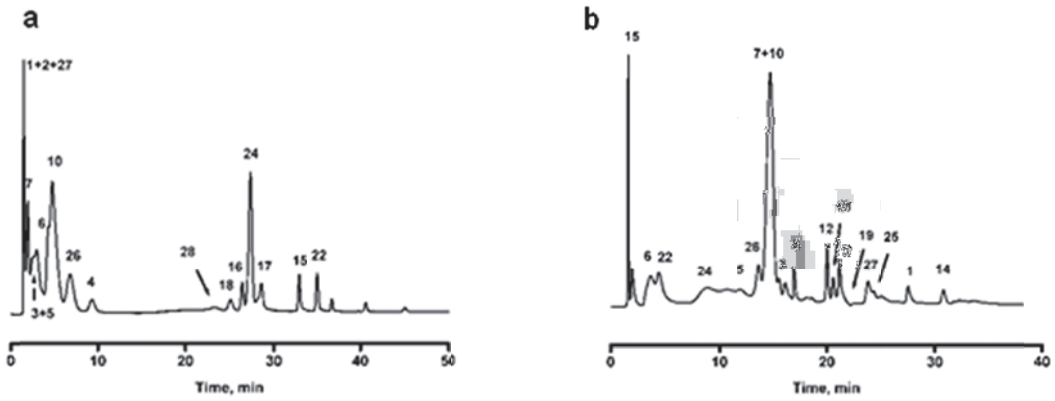

Fig. 3.: Examples of gradient separations of complex mixture of phenolic compounds on columns optimized for separation in (a) reversed-phase and (b) hydrophilic interaction liquid chromatography. (a) Monolithic capillary column with tetraoxyethylene dimethacrylate and lauryl methacrylate, mobile phase: 10 mM NH_4Ac and acetonitrile, length 170 mm, flow-rate 20 µl/min, temperature 80°C, gradient elution: 0 min – 0% acetonitrile, 10 min – 0% acetonitrile, 40 min – 60% acetonitrile. Samples: **Tab.1**. (b) Monolithic capillary column with dioxyethylene dimethacrylate and sulfobetaine monomer, mobile phase: 10 mM NH_4Ac and acetonitrile,length 170 mm, flow-rate 20 µl/min, temperature 60°C. Gradient elution: 0 min – 100% acetonitrile, 10 min – 100% acetonitrile, 40 min – 60% acetonitrile. Samples: **Tab.1**.

Table 1: Complex mixture of phenolic compounds

No.	Compounds	No.	Compounds	No.	Compounds
1	Gallic acid	11	Ferulic acid	21	Naringine
2	Protocatechuic acid	12	Chlorogenic acid	22	Biochanin A
3	p-Hydroxybenzoic acid	13	(-)-Epicatechine	23	Naringenine
4	Salicylic acid	14	(+)-Catechine	24	Hesperetine
5	Vanillic acid	15	Flavone	25	Hesperidine
6	Syringic acid	16	7-Hydroxyflavone	26	4-Hydroxycoumarine
7	4-Hydroxyphenylacetic acid	17	Apigenine	27	Esculine
8	Caffeic acid	18	Lutheoline	28	Morine
9	Sinapic acid	19	Quercetine	29	Vanillin
10	p-Coumaric acid	20	Rutine		

The optimized columns have been tested for reversed-phase and hydrophilic interaction separations of complex mixture of flavones and phenolic acids in one-dimensional (**Fig. 3.**) and comprehensive two-dimensional liquid chromatography.

ACKNOWLEDGEMENT

The financial support of GACR project P206/12/0398 is gratefully acknowledged.

LITERATURE

[1] Jandera, P., Urban, J., *J. Sep. Sci.* 2008, 31, 2251 - 2540.

[2] Urban, J., Langmaier, P., Jandera, P., *J. Sep. Sci.*, 2011, 34, 2054 - 2062.

[3] Jandera, P., Stankova, M., Skerikova, V., Urban, J., *J. Chromatogr. A*, 2012, submitted.

P52 BEHAVIOR OF SHEATHLESS AND ELECTRODELESS ELECTROSPRAY ELECTROPHORESIS DURING INORAGANIC ION SEPARATION

Anna Tarantová[a,b], František Foret [a]

[a] *Institute of Analytical Chemistry, Czech Academy of Sciences, Veveří 967/97, 602 00 Brno, Czech Republic*

[b] *Department of Chemistry, Faculty of Science, Masaryk University, Kotlářská 267/2, 61137 Brno, Czech Republic, tarantova@iach.cz*

ABSTRACT

This work is aimed at optimization of a separation process in a thin capillary for future application in mass spectrometry (CE-MS). The analysis of inorganic ions by capillary electrophoresis (CE) with contactless conductivity detection was studied for sheathless, electrodeless arrangement. In commonly used CE-MS interface the potential gradient is established by defining voltage between the entrance and the exit of the separation capillary. However, in the presented experimental design the voltage was applied only on the capillary entrance whereas the opposite end was sharpened into an electrospray tip and situated opposite to the grounded vacuum inlet electrode. This system is called a sheathless and electrodeless interface and brings several potential advantages especially in the instrumental design simplicity.

1 INTRODUCTION

A very sensitive analysis of complex samples is required in current analytical chemistry. Coupling capillary electrophoresis to a sensitive detector such as mass spectrometer can appear as an ideal approach. CE offers fast analysis without extensive sample pretreatment and high efficiency of separation with very low sample consumption. The use of a proper interface is critical for successful coupling.

Sheath flow interface employs so called sheath liquid, composed of water/organic solvents, enabling to reach stable signal. Unfortunately, this approach also leads to dilution of the sample and lower sensitivity. Other type of an interface, the sheathless arrangement, suppresses this disadvantage because no additional liquid is involved (Fig.1A). However, the electrospray electrode has to be integrated at the capillary exit, complicating the mechanical arrangement. Additionally the stability of the electrode, mostly created on the outside of the ESI tip is severely limitted[1]. Recently a new approach to the sheathless interface desing was published by Mazereeuw at all and is called sheathless and electrodeless interface (Fig.1,B)[2] . In comparison to the previous options it simplifies the application of the electric high voltage at the electrospray tip. In both previous cases the voltage was defined in the beginning as well as at the end of the capillary, while at the sheathless and electrodeless interface the voltage is applied only at the injection end of the separation capillary.

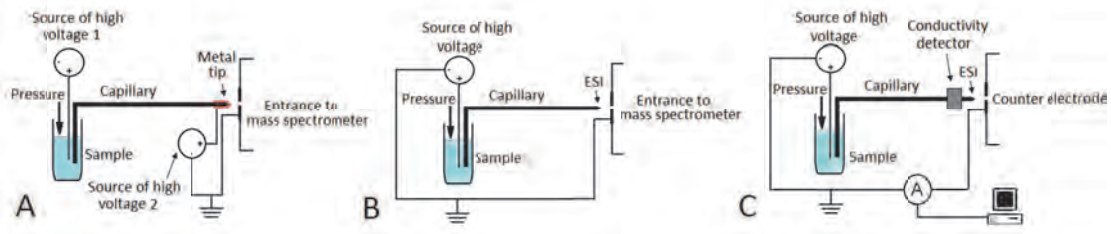

Fig. 1: A – an example of commonly used interface for CE-MS (sheathless interface with a metal tip), B – experimental design of sheathless and electrodeless interface which we are going to use in future work, C – our current instrumentation for optimization of sheathless and electrodeless interface.

The voltage in the separation channel is continuously reduced due to the resistance of the background electrolyte and potential gradient, which is crucial for separation, is created. In this design the applied voltage has to be sufficient for driving the electrophoretic separation and forming fine electrospray plume at the tip. Too low or too high voltage leads to unwanted phenomena (e.g. droplet pulsed mode or bifurcate mode)[3].
Although there is no direct control over potential in the capillary end it is possible to calculate it according to the equitation:

$$U_{ESI} = U_{APL} - \frac{U_{APL}}{I_{SEP}} * I_{ESI}$$

Where U_{ESI} is voltage on the electrospray tip, U_{APL} is voltage applied on the beginning of a capillary, I_{SEP} is current during electrophoretic separation and I_{ESI} is electrospray current.

2 MATERIAL AND METHODS

Experiments were carried out in a laboratory made instrumentation (Fig. 1,C). CE was performed in silica fused capillaries of 25 cm and I.D. of 10 μm or 50 μm with the end sharpened into a tip. Nine kV voltage was applied at the capillary inlet. Approximately 1 mm in front of the electrospray tip a ground electrode was situated. For detection of analyzed ions TradeDec Contactless Conductivity Detector was positioned 19 cm from the injection entrance of the capillary. Mixture of cations (Na^+, K^+, Zn^{2+}, Ca^{2+} and Li^+) was loaded from a gas pressurized chamber used also to assist the liquid flow inside the capillary during the experiments with electrospray.

3 RESULTS AND DISCUSSION

We have tested several improvements in comparison to the previous papers which dealt with this interface[2,4]. We have used thinner capillaries ended by grind tips (instead of pulled tips) and we have left out percentage of organic solvent in background electrolyte. All these improvements should bring higher separation efficiency and better reproducibility. For the purpose of optimization mass spectrometric detection has been replaced by a conductivity detector.

Fig. 2: Profile of electrospray tips. A – grind tip, B – etched tip, C – pulled tip

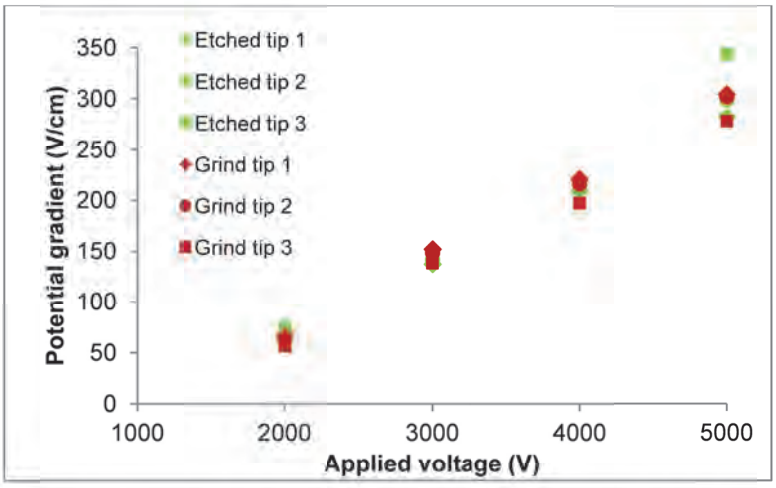

Fig. 3: Reproducibility of potential gradient within capillaries with either etched tip or grind tip. Electrolyte: 1% formic acid, capillary length: 15cm.

Electrospray tip is one of the most important parts of each interface. It is possible to prepare it by several methods including pulling in a flame, mechanical grinding or etching by hydrofluoric acid. Each of these techniques gives a unique tip profile (Fig. 2). Mazereeuw at all fabricated tips by pulling to reach the thinnest tip. Nevertheless, the width of the separation

channel became deformed therefore it is not suitable for online coupling of CE-MS. The narrowing of a separation channel poses high resistance and the potential gradient within the capillary became poor. We have suggested using either ground tips or etched tips, where the width of the separation channel remains constant. We have investigated potential gradient within six capillaries where three were ended by ground tips and three by etched tips. If one of fabrication process leads to lower tip resistance, there will be higher potential gradient and faster separation. However, Fig. 3 proves that both types give very similar results. If five kilovolts was applied on a capillary of 15 cm length, potential gradient approximately about 300 V/cm is reached. For further work ground tips have been chosen due to their easier and less time consuming preparation.

During the separation a zone of analyte is broadened by various contributions such as loading, detection cell, Joule heating, sorption, diffusion and/or hydrodynamic flow[5]. In our system contributions of electroosmosis and Joule heating are reduced to minimum, whereas hydrodynamic flow and diffusion have significant influences and are dependent on the capillary diameter. If a number of theoretical plates was calculated under condition that only hydrodynamic flow and diffusion are considered, the number of theoretical plates is five times higher for capillary with 10 μm I.D. than for capillary with 50 μm I.D. Moreover, if narrow capillary was used, sharper tip is easier fabricate. Thin electrospray tip enables fine electrospray plume formation and provides more effective ionization.

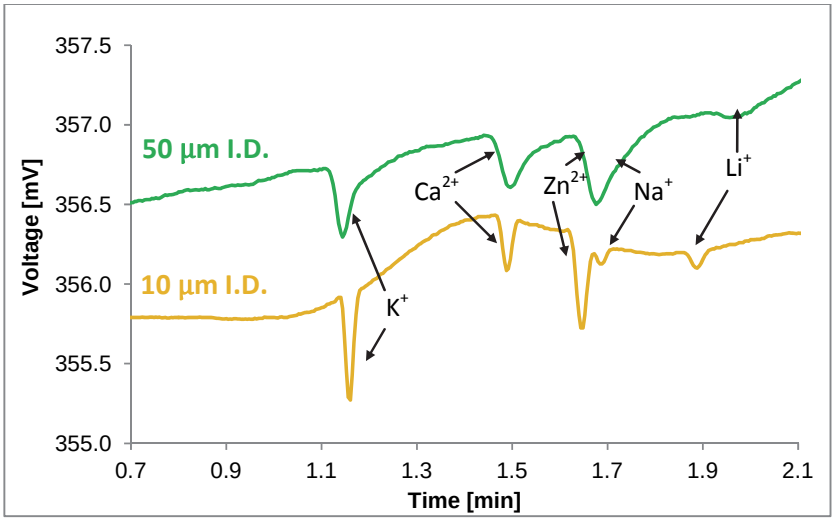

Fig. 4: Separation of inorganic cation mixture (K^+, Ca^{2+}, Na^+, Zn^{2+} and Li^+) with application of sheathless and electrodeless interface. Concentration: 10^{-5} mol/L , applied voltage: +9 kV, capillary I.D.: 10 μm or 50 μm, capillary length: 19/25 cm, BE: 1% formic acid, linear flow rate: $7 \cdot 10^{-4}$ m/s.

If we were about to spray an electrolyte without organic solvent it is indispensable to employ as thin electrospray tip as possible. Naturally, number of theoretical plates would be even more favorable for capillary with 5 μm I.D., however, resulting in excessively high pressures. There is also a strong tendency for clogging which makes the system with very narrow capillary less user-friendly.

We have carried out our experiment with all suggested improvements in capillary with I.D. of 10 μm as well as 50 μm to demonstrate importance of low theoretical plates. Separation of inorganic cations mixture with application of sheathless and electrodeless interface is in the Fig. 4. It is obvious that in 10 μm capillary much higher efficiency was obtained. There were all five cations detected whereas in 50 μm capillary peaks of sodium and zinc are not resolved properly and signal of lithium was nearly lost.

4 CONCLUSION

We have investigated main characteristics of sheathless and electrodeless interface and we have successfully used this interface for separation of inorganic cation mixtures. In further studies we are going to replace ground electrode for a mass spectrometer for analyses of larger molecules.

ACKNOWLEDGEMENT

The work has been supported by GACR P20612G014, P206-11-2377, P301-11-2055 and CZ.1.07/2.3.00/20.0182.

LITERATURE

[1] Sanz-Nebot, V.; Balaguer, E.; Benavente, F.; Barbosa, J. Electrophoresis 2005, 26, 1457.
[2] Mazereeuw, M.; Hofte, A. J. P.; Tjaden, U. R.; vanderGreef, J. Rapid Communications in Mass Spectrometry 1997, 11, 981.
[3] Valaskovic, G. A.; Murphy, J. P.; Lee, M. S. J. Am. Soc. Mass Spectrom. 2004, 15, 1201.
[4] Wu, Y. T.; Chen, Y. C. Rapid Communications in Mass Spectrometry 2006, 20, 1995.
[5] F. Foret, L. Křivánková, P. Boček, Capillary Zone Electrophoresis, 1993.

P53 THE USE OF AN INTERNAL STANDARD EXTENDS THE LINEAR RANGE OF THE SALDI MS ANALYSES

Iva Tomalová[a], Huan-Tsung Chang[b], Jan Preisler[a]

[a] CEITEC and Department of Chemistry, Faculty of Science, Masaryk University, 625 00 Brno, Czech Republic, iva.tomalova@gmail.com
[b] Department of Chemistry, National Taiwan University, 1, Section 4, Roosevelt Road, Taipei 10617, Taiwan, R.O.C.

ABSTRACT

Surface-assisted laser desorption/ionization mass spectrometry (SALDI MS) employing gold nanoparticles (Au NPs) has been presented as a useful method for the both qualitative and quantitative analysis of low molecular weight analytes. Besides the well-known benefitof improvement in the analysis precision, the use of an internal standard was also observed to extend the linear range of SALDI MS. Without the use of the internal standard, the linear range is presumably limited by the saturation of the Au NP surface where the desorption process takes place: at higher analyte concentration, an imperfect, multilayer assembly is formed leading to inefficient desorption and/or ionization and thus to reduced linearity and poor reproducibility. An internal standard can partially eliminate this limitation: as long as the Au NP surface is not fully saturated, the signal intensities of the analyte and the internal standard do not affect each other; with further increase of the analyte concentration, the signal intensity of the internal standard is gradually suppressed preserving the linearity of the analyte/internal standard ratio. Although quantitative analyses using SALDI MS without any internal standard were presented, based on our findings, the use of the internal standard for quantitative analysis is highly recommended. The limited Au NP surface as well as interfering components can have notable consequences in analyses of complex samples, especially if the nanoparticles are employed as extraction/concentration probes.

Keywords: nanoparticles, SALDI MS

1 INTRODUCTION

Gold nanoparticles (Au NPs) were presented as a useful substrate for analyses of small molecules by surface-assisted laser desorption/ionization mass spectrometry (SALDI MS). Compared to conventional organic matrixes, they are reported to offer many advantages, such as low MS background or high reproducibility. Moreover, they act as an efficient

extraction and/or concentration probes for analytes possessing thiol group, which can interact with the Au NP surface [1, 2].
Here, on the model of glutathione (GSH) and N-(2-mercaptopropionyl)glycine (MPG) as the internal standard, we demonstrate that in addition to the well-known benefit of the improvement in the analysis precision, the use of internal standard can also extend the SALDI MS linear range.

2 MATERIALS AND METHODS

Citrate-capped Au NPs (7.5 nM) were prepared by reaction of boiling sodium citrate (2 mM, 50 mL) with $Na[AuCl_4]$ (100 mM, 250 µL) and used as prepared.
The samples of GSH with MPG (Fig. 1) as the internal standard (1 µM) and Au NPs (0.75 nM) were prepared in ammonium citrate buffer (0.75 mM, pH 4). All samples were centrifuged (16 090 g, 10 min) and afterwards, the bottom fraction (20 µL) containing GSH-Au NPs/MPG-Au NPs was vortexed for 1 min. One µL of the mixture was loaded on the MALDI target and allowed to dry at the room temperature.
Mass spectra were acquired in the positive reflector mode by MALDI TOF MS (AutoflexSpeed, Bruker).

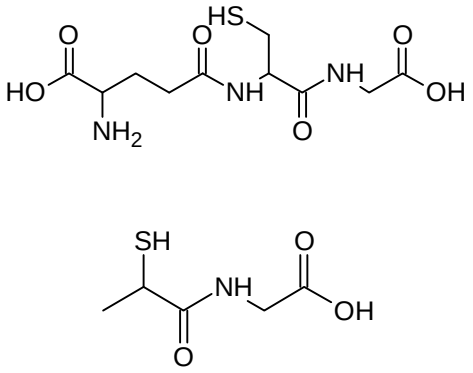

Fig. 1. : Structures of glutathione (GSH) and N-(2-mercaptopropionyl)glycine (MPG)

3 RESULTS

Fig. 2a shows the SALDI MS calibration curve of GSH. Without the internal standard, the SALDI MS linear range is limited by the nanoparticle surface. As soon as the NP surface becomes saturated with GSH (c ~ 0.4 µM), the signal intensity does not increase proportionally to the GSH concentration. The reasons may be inefficient capturing of the GSH molecules within the concentration process and/or formation of a multilayer assembly on the nanoparticle surface that leads to inefficient desorption and thus to reduced linearity and poor reproducibility [2].
The employment of the internal standard, MPG in this case, results not only in the improvement in the analysis precision, but also in the extension of the linear range as shown in Fig. 2b. This occurs due to the maintaining the ratio analyte/internal standard even at high analyte concentration despite of the inefficient concentration/desorption process.
This observation is supported by the Fig. 2c, which shows the gradual decrease in the MPG signal intensity while increasing the analyte concentration. At high analyte concentration, this signal suppression of the internal standard leads to its reduced S/N ratio (> 1 µM) and thus to increase of the RSD values of GSH determination.
Although quantitative analyses using SALDI MS without any internal standard were presented, based on our findings, the use of the internal standard for quantitative analysis is highly recommended. The limited Au NP surface as well as interfering components can have notable consequences in analyses of complex samples, especially if the nanoparticles are employed as extraction/concentration probes.

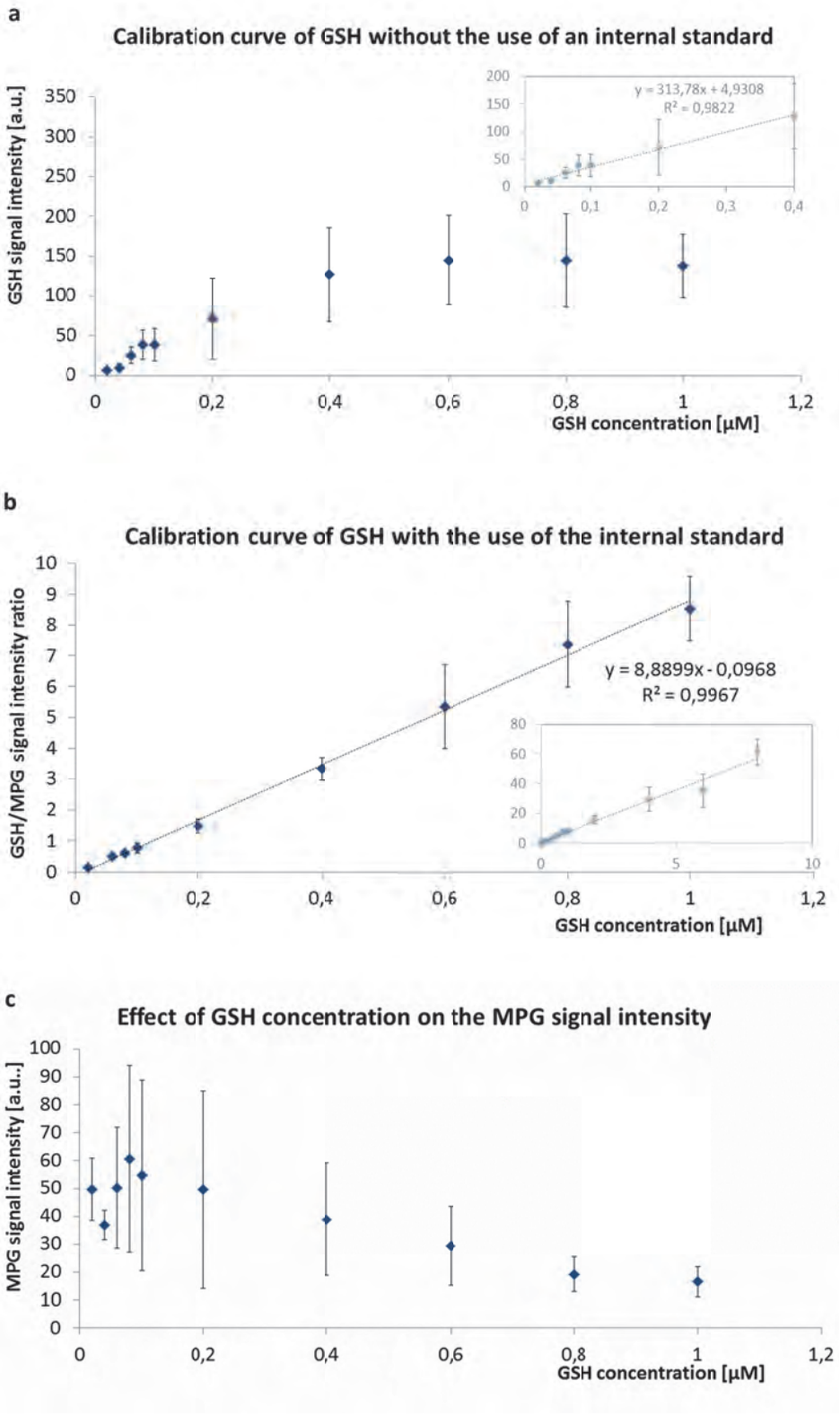

Fig. 2. : Calibration curve of GSH (3a) with and (3b) without the use of an internal standard and (3c) the effect of GSH concentration on the signal intensity of MPG.

4 CONCLUSIONS

Without an internal standard, the linear range of SALDI MS analyses is limited by the saturation of the Au NP surface. The use of an internal standard was observed to improve the analysis precision and extend the linear range from 0.02 – 0.4 µM (without an internal standard) to 0.02 – 8 µM (with the MPG internal standard).
The limited Au NP surface as well as interfering components can have significant consequences in analyses of complex samples, especially if the nanoparticles are employed as the extraction/concentration probes.

ACKNOWLEDGEMENTS

We thankfully acknowledge the Czech Science Foundation (P206/12/0538), CEITEC - Central European Institute of Technology (CZ.1.05/1.1.00/02.0068) and the National Science Council of Taiwan (NSC 99-2923-M-002-004-MY3). Iva Tomalová is supported by Brno City Municipality Scholarships for Talented Ph.D. Students.

LITERATURE

[1.] Chen, W.-T., Tomalová, I., Preisler, J., Chang, H.-T., *Journal of the Chinese Chemical Society* 2011**,** *58*, 769-778.

[2.] Chiang, C.-K., Lin, Y.-W., Chen, W.-T., Chang, H.-T., *Nanomedicine-Nanotechnology Biology and Medicine* 2010**,** *6*, 530-537.

P54 DEVELOPMENT AND VALIDATION OF UHPLC METHOD FOR THE DETECTION AND QUANTIFICATION OF ERECTILE DYSFUNCTION DRUGS

Ludovit Schreiber, Radoslav Halko, Milan Hutta, Anna Kabzanová, Soňa Lopuchová

Prírodovedecká Fakulta UK, Katedra analytickej chémie, Mlynská dolina, 842 15 Bratislava
schreiber@fns.uniba.sk

ABSTRACT

Erectile dysfunction (ED), inability to achieve a penile erection sufficient for satisfactory sexual performance is estimated to affect many men worldwide. ED is more common in advanced age and related to hypertension or diabetes mellitus or use of certain pharmacological agents e.g. antihypertensive. ED has been treated by the drugs that inhibit the enzyme phosphodiesterase type 5 (PDE5) activities. Tadalafil is a selective phosphodiesterase type 5 inhibitor, which is used to treat mild to severe ED in man. Drug testing is an integral part of pharmaceutical analysis and routine quality control monitoring of drug. Standard analytical method for Tadalafil impurities determination according to European Pharmacopoeia takes more than 60 minutes of HPLC analysis time. The speed and economic analysis is becoming increasingly important in many application areas of HPLC including pharmaceutical analysis in order to increase throughput and reduce costs. The latest UHPLC instrumentation and stationary phases chemistry allows to successfully reduce analysis time, increase detection and quantification limits. Ultrafast, robust and reliable 6 minutes HPLC method was developed and validated according to European Medicines Agency recommendations for validation of analytical methods.

ACKNOWLEDGEMENTS

This work was supported by Hermes Labsystems Slovakia and Zentiva a.s. Hlohovec and grant MŠ SR VEGA 1/1136/12 APVV-0595-07 and VVCE-0070-07.

P55 DYNAMIC HIGH-RESOLUTION COMPUTER SIMULATION OF ELECTROPHORETIC ENANTIOMER SEPARATIONS

Jitka Caslavska[a], Michael C. Breadmore[b], Hiu Ying Kwan[a], Wolfgang Thormann[a]

[a] *Clinical Pharmacology Laboratory, Institute for Infectious Diseases, University of Bern, Murtenstrasse 35, CH-3010 Bern, Switzerland*
[b] *Australian Centre for Research on Separation Science, School of Chemistry, University of Tasmania, Hobart, Tasmania, Australia*

ABSTRACT

GENTRANS, a comprehensive one-dimensional dynamic simulator for studying electrophoretic separations and transport, was extended for handling electrokinetic chiral separations. The code can be employed to study the 1:1 interaction of monovalent weak and strong acids and bases with a single monovalent weak or strong acid or base additive, including a neutral cyclodextrin, under real experimental conditions. For model systems with charged weak bases and neutral modified β-cyclodextrins at acidic pH, for which complexation constants, ionic mobilities and mobilities of selector-analyte complexes have been determined by capillary zone electrophoresis, simulated and experimentally determined electropherograms are shown to be in good agreement.

Keywords: electrokinetic chiral separation, simulation, complexation

1 INTRODUCTION

GENTRANS, a comprehensive one-dimensional dynamic simulator for electrophoretic separations and transport [1.,2.], was extended for handling electrokinetic chiral separations [3.]. The code can be employed to study the 1:1 interaction of monovalent weak and strong acids and bases with a single monovalent weak or strong acid or base additive, including a neutral cyclodextrin, under real experimental conditions. It is a tool to investigate the dynamics of chiral separations and to provide insight into the buffer systems used in chiral capillary zone electrophoresis and chiral capillary isotachophoresis. For evaluation of the new code, complexation constants and mobilities of protonated cationic model drugs in presence of neutral cyclodextrins were determined experimentally by capillary zone electrophoresis at low pH and simulated electropherograms for zone electrophoresis and isotachophoresis were compared to those obtained experimentally.

2 MATERIAL AND METHODS

All capillary zone electrophoresis measurements were performed on a BioFocus 3000 capillary electrophoresis system (Bio-Rad Laboratories, Hercules, CA, USA), equipped with a 50 µm id untreated fused-silica capillary (Polymicro Technologies, Phoenix, AZ, USA). The total length of the capillary was 50 cm (45.4 cm to the detector) and the applied voltage was 17 - 20 kV. The electrophoretic mobilities of the detected protonated bases and electroosmosis were determined as function of cyclodextrin concentration and complexation

constants and mobilities of the complexes were calculated as described in [3.]. The capillary isotachophoresis data were taken from Lanz et al. [4.] and were obtained on a Tachophor 2127 analyzer (LKB AB, Bromma, Sweden) with conductivity detection at the column end. Computer simulations were executed on Windows 7 based PC's featuring Intel Core i5 2.8 GHz processors.

3 RESULTS AND DISCUSSION

For model systems with charged weak bases and neutral modified β-cyclodextrins at acidic pH, for which complexation constants, ionic mobilities and mobilities of selector-analyte complexes have been determined by capillary zone electrophoresis, simulated and experimentally determined electropherograms were found to be in good agreement. This is shown with the capillary zone electrophoresis data of methadone, EDDP and codeine presented in Fig. 1. The buffer used was composed of 90 mM NaH_2PO_4 (adjusted to pH 2.3 with concentrated phosphoric acid), 10 % methanol and 1.8 mM heptakis(2,6-di-O-methyl)-β-cyclodextrin (DIMEB) as chiral selector.

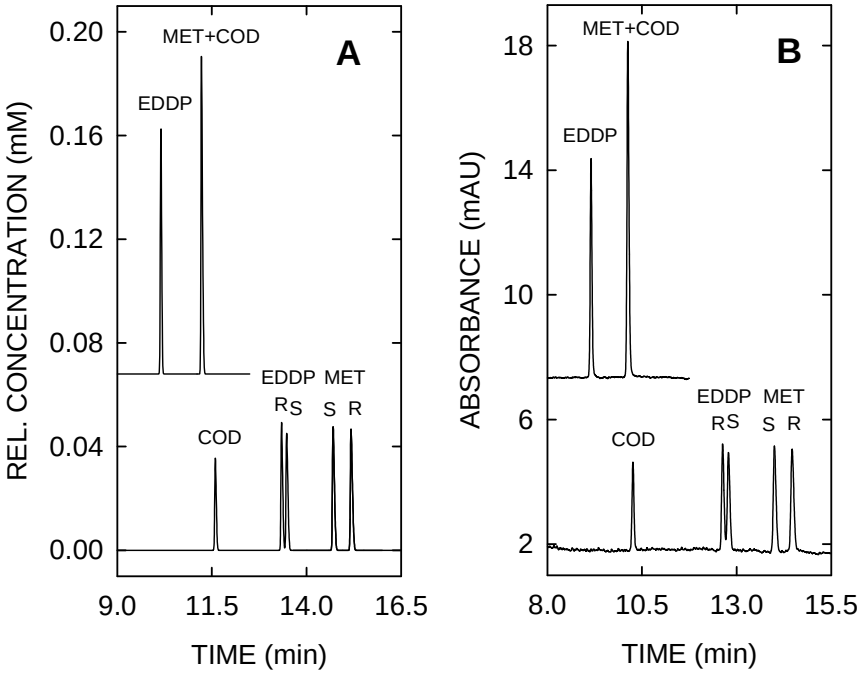

Fig.1: Simulation and experimental validation of the capillary zone electrophoretic enantiomer separation of weak bases in a 50 cm capillary with a detector placed at 45 cm. (A) Computer predicted detector responses at 6 Hz and (B) experimental data at 20 kV. Simulation was performed with a 4 µm mesh at constant current density of 32365.34 A/m^2. The pH 2.3 phosphate buffer contained 1.8 mM DIMEB. The sample was composed of methadone, EDDP and codeine in 10-fold diluted buffer without additive. pKa values for MET, EDDP and COD were 8.9, 9.6 and 8.2, respectively, and the free mobilities were 1.35, 1.55 and 1.35 x 10^{-8} m^2/Vs, respectively. Complexation constants for S-MET, R-MET, S-EDDP and R-EDDP were 473.9, 379.0, 366.6 and 344.5 L/mol, respectively. Mobilities of the complexes were 0.418, 0.402, 0.406 and 0.402 x 10^{-8} m^2/Vs, respectively. The upper graphs are data obtained in absence of the chiral selector. MET, EDDP and COD refer to methadone, 2-ethylidene-1,5-dimethyl-3,3-diphenylpyrrolidine and codeine, respectively. For details refer to [3.].

Using SIMUL5 in the newly extended complex version [5.] with the same input data provided identical results. The same was found to be the case for chiral isotachophoresis of

methadone [3.]. GENTRANS extended for handling the interaction of monovalent compounds with neutral cyclodextrins is demonstrated to be a valuable tool to investigate the dynamics of separations in chiral capillary zone electrophoresis and chiral isotachophoresis at power levels that are typically used in experiments. Dynamic simulation can be employed to study many aspects of buffer systems and analyte peaks for a given configuration, including (i) analyte stacking across conductivity and buffer additive gradients, (ii) changes of additive concentration, buffer component concentration, pH and conductivity across migrating sample zones and peaks, and (iii) the formation, shape and migration of system peaks. Thus, the two newly developed simulation codes provide insights into electrophoretic configurations in a hitherto inaccessible way.

LITERATURE

[1.] Thormann, W., Breadmore, M.C., Caslavska, J., Mosher, R.A., *Electrophoresis* 2010, *31*, 726-754.
[2.] Mosher, R.A., Breadmore, M.C., Thormann, W., *Electrophoresis* 2011, *32*, 532-541.
[3.] Breadmore, M.C., Kwan, H.Y., Caslavska, J., Thormann, W., *Electrophoresis* 2012, *33*, 958-969.
[4.] Lanz, M., Caslavska, J., Thormann, W., *Electrophoresis* 1998, *19*, 1081-1090.
[5.] Hruška, V., Beneš, M., Svobodová, J., Zusková, I., Gaš, B., *Electrophoresis* 2012, *33*, 938-947.

ACKNOWLEDGEMENTS

This work was supported by the Swiss NSF, the Australian Research Council and the University of Tasmania.

P56 ULTRA FAST HPLC METHOD FOR TADALAFIL ACCORDING TO PH.EUR. VALIDATION CRITERIA AND IDENTIFICATION OF IMPURITIES USING ACCURATE MASS MS

Ludovit Schreiber, Radoslav Halko, Milan Hutta, Anna Kabzanová, Soňa Lopuchová

Prírodovedecká Fakulta UK, Katedra analytickej chémie, Mlynská dolina, 842 15 Bratislava
schreiber@fns.uniba.sk

ABSTRACT

Erectile dysfunction (ED), inability to achieve a penile erection sufficient for satisfactory sexual performance is estimated to affect many men worldwide. ED is more common in advanced age and related to hypertension or diabetes mellitus or use of certain pharmacological agents e.g. antihypertensive. ED has been treated by the drugs that inhibit the enzyme phosphodiesterase type 5 (PDE5) activities. Tadalafil is a selective phosphodiesterase type 5 inhibitor, which is used to treat mild to severe ED in man. Drug testing is an integral part of pharmaceutical analysis and routine quality control monitoring of drug. Standard analytical method for Tadalafil impurities determination according to European Pharmacopoeia takes more than 60 minutes of HPLC analysis time. The speed and economic analysis is becoming increasingly important in many application areas of HPLC including pharmaceutical analysis in order to increase throughput and reduce costs. The latest UHPLC instrumentation and stationary phases chemistry allows to successfully reduce analysis time, increase detection and quantification limits. Ultrafast, robust and reliable 6 minutes HPLC method was developed and validated according to European Medicines Agency recommendations for validation of analytical methods. Known Tadalafil impurities were identified using accurate mass TOF instrument and qualified with novel metabolite ID software.

ACKNOWLEDGEMENTS

This work was generously supported by the grant of Scientific Grant Agency of the Ministry of ducation of Slovak Republic and the Academy of Sciences - project VEGA 1/1349/12 and the grant of Slovak Research and Development Agency - project APVV-0583-11. This work is partially outcome of the project VVCE-0070-07 of Slovak Research and Development Agency solved in the period 2008-2011 and Hermes Labsystems Slovakia and Zentiva a.s. Hlohovec.

P57 IDENTIFICATION AND ANTIMICROBIAL ACTIVITY OF *LACTOBACILLUS* STRAIN ISOLATED FROM INFANT FAECES

Kristýna Turková[a], Alena Španová[a], Bohuslav Rittich[a], Bojana Bogovič Matijašić[b]

[a] *Institute of Food Science and Biotechnology, Faculty of Chemistry, Brno University of Technology, Purkyňova 118, 61200 Brno, Czech Republic, xcturkovak@fch.vutbr.cz*
[b] *Institute of Dairy Science and Probiotics, Biotechnical Faculty, University of Ljubljana, Groblje 3, 1230 Domžale, Slovenia*

ABSTRACT

The strain RL22P isolated from infant faeces was identified using genus-specific polymerase chain reaction (PCR), species-specific PCRs and 16S rDNA gene sequencing as *Lactobacillus gasseri.* The strain RL22P was tested for the production of antimicrobial substances using agar-spot test and agar-diffusion test. The strain produced antimicrobial substances (organic acids, hydrogen peroxide and proteinaceous substances) against fifteen indicator strains. The most effective was against *Lactobacillus* and *Clostridium* indicator strains. Antimicrobial proteinaceous substances produced only against six *Lactobacillus* strains.

Keywords: Lactobacillus, identification, antimicrobial activity

1 INTRODUCTION

Lactobacillus strains have been widely used in food industry for centuries and are considered to be GRAS (Generaly Recognized As Safe) organisms. In recent years, antimicrobial proteinaceous substances produced by lactobacilli have been the subject of extensive studies, especially due to their prospective use as natural food preservatives (Gálvez, 2007). Inhibitory role may play antimicrobial compounds such as different organic acids, hydrogen peroxide, carbon dioxide or proteinaceous substances. The antimicrobial activity of lactobacilli against closely related species and a wide range of pathogenic microorganisms have been reported, including *Escherichia coli, Salmonella*, and *Staphylococcus aureus* (Pan, 2009; Hacin, 2008).

2 AIM OF WORK

The aim of the work was the identification of the strain RL22P isolated from infant faeces and characterization of antimicrobial substances produced by this strain.

3 MATERIALS AND METHODS

The strain RL22P isolated from breast-fed full-term infant faeces was collected in Czech Collection of Dairy Microorganisms (Tábor, Czech Republic). DNA of the strain RL22P was isolated by fenol extraction and ethanol purification. DNA of the strain RL22P was amplified using genus-specific PCR for *Lactobacillus* and eleven species-specific PCRs (*L. casei/paracasei, L. paracasei, L. plantarum, L. gasseri, L. johnsonii, L. fermentum, L. salivarius, L. delbrueckii, L. rhamnosus, L. zeae, L. acidophilus*). The confirmation of species identification was performed by sequence analysis of 16S rDNA gene.

The strain RL22P was screened for the antimicrobial activity against some Gram-positive and Gram-negative strains using agar-spot test (Jacobsen, 1999) and agar-diffusion test (Hacin, 2008). The strain RL22P was cultivated in MRS (de Mann, Rogosa and Sharpe) medium at 37°C for 24 hours aerobically. Strains selected at Biotechnical Faculty, University of Ljubljana, Slovenia were used as indicator strains. Proteolytic enzymes - proteinase K and trypsin (10 mg/ml) were used for the characterisation of proteinaceous antimicrobial substances produced by strain on agar plates. The neutralization by 1 M NaOH and treatment by proteinase K (1 mg/ml), trypsin (1 mg/ml) and catalase (1 mg/ml) were used for characterization of antimicrobial substances in supernatant.

4 RESULTS

The strain RL22P was identified as *Lactobacillus gasseri* using genus-specific and species-specific PCRs. The identification was confirmed by the sequencing of 16S rDNA gene.

In agar-spot test the strain RL22P produced different antimicrobial substances which were antagonistic against fifteen indicator strains from 20 tested. The most effective was against *Clostridium (C.) tyrobutyricum* IM104 (inhibition zone 10.0 mm), *C. perfringens* IM72 (10.0 mm), *L. delbrueckii* ssp. *delbrueckii* IM349 (6.3 mm), *L. delbrueckii* ssp. *bulgaricus* IM348 (6.3 mm), *L. johnsonii* IM345 (5.0 mm) and *L. sakei* IM398 (4.8 mm). Inhibition zones of six indicator strains were constricted by proteinase K and/or trypsin (Table 1).

In agar diffusion test it was confirmed that the inhibition of *Clostridium* strains was caused by organic acids. The inhibition of the growth of six *Lactobacillus* indicator strains (*L. salivarius* IM124, *L. fermentum* IM351, *L. gasseri* IM340, *L. johnsonii* IM345, *L. delbrueckii* ssp. *delbrueckii* IM349, *L. delbrueckii* ssp. *bulgaricus* IM348, *L. sakei* IM398) was observed by the neutralized and catalase-treated supernatants. The growth of these strains was inhibited by antimicrobial proteinaceous substances sensitive to proteinase K and trypsin. The results are shown in the Table 1.

Table 1: Antimicrobial activity of the strain RL22P against 20 tested indicator strains

Indicator strain	Agar-spot test (inhibition zone in mm)	Agar-diffusion test /treated by				
		NaOH	catalase	trypsin	proteinase K	Non-treated
Lactobacillus acidophilus IM304	0	-	-	-	-	-
Lactobacillus salivarius IM124	0.7	-	-	-	-	-
Lactobacillus fermentum IM351	2.9 PT	+	+	-	-	+
Lactobacillus gasseri IM340	4.2 P	+	+	-	-	+
Lactobacillus gasseri IM341	0	-	-	-	-	-
Lactobacillus johnsonii IM345	5.0 P	+	+	-	-	+
Lactobacillus delbrueckii ssp. *delbrueckii* IM349	6.3 PT	+	+	-	-	+
Lactobacillus delbrueckii ssp.	6.35 P	+	+	-	-	+

bulgaricus IM348						
Lactobacillus sakei IM398	4.8 P	+	+	-	-	+
Clostridium difficile IM66	4.0	-	+	+	+	+
Clostridium perfringens IM72	10.0	-	+	+	+	+
Clostridium perfringens IM83	4.0	-	+	+	+	+
Clostridium tyrobutyricum IM103	3.0	-	+	+	+	+
Clostridium tyrobutyricum IM104	10.0	-	+	+	+	+
Staphylococcus aureus IM353	5.2	-	+	+	+	+
Salmonella enterica ser. Typhimurium IM318	0.5	-	-	-	-	-
Enterococcus faecalis IM435	0	-	-	-	-	-
Enterococcus faecalis IM436	3.2	-	-	-	-	-
E.coli IM429	0	-	-	-	-	-
E.coli IM430	0	-	-	-	-	-

+: detection of inhibition zone

-: inhibition zone not detected

P: inhibition zone contricted by proteinase K (10 mg/ml)

T: inhibition zone constricted by trypsin (10 mg/ml)

5 DISSCUSION

The tested strain RL22P which was identified as *Lactobacillus gasseri* produced antimicrobial substances against fifteen indicator strains. The growth of six indicator strains was inhibited by antimicrobial substances sensitive to proteinase K and/or trypsin. Lactobacilli are known for their production of various antimicrobial compounds which can inhibit different food pathogens including *Escherichia coli, Salmonella*, and *Staphylococcus aureus* and against related bacteria species (Pan, 2009; Hacin, 2008). The proteinaceous compounds dependent activity was observed only against selected *Lactobacillus* representatives. Antimicrobial proteinaceous substances which were sensitive to proteolytic enzymes could be bacteriocins or bacteriocin–like substances (Nespolo, 2010).

6 CONCLUSION

Lactobacillus gasseri RL22P produced strain-specific antimicrobial substances inhibiting the growth of indicator strains. The inhibition was dependent on indicator strain. Production of antimicrobial proteinaceous substances was detected just only against indicator strains of *Lactobacillus* genus.

ACKNOWLEDGEMENTS

The financial support of the Ministry of Education, Youth and Sports of the Czech Republic, grant No. 2B08070 is gratefully acknowledged.

LITERATURE

[1.] Gálvez, A., Abriouel, H., López, R.L., Omar, N.B. *International Journal of Food Microbiology* 2007, 120, 51-70.

[2.] Hacin, B., Rogelj, I., Matijašić, B.B. Folia *Microbiologica* 2008, 53, 569-576.

[3.] Jacobsen, C.N., Rosenfeldt Nielsen, V., Hayford, A.E., Møller, P.L., Michaelsen, K.F., Pærregaard, A., Sandström, B., Tvede, M., Jakobsen, M. *Applied and Environmental Microbiology* 1999, 65, 4949-4956.

[4.] Nespolo, C.R., Brandelli, A. Brazilian *Journal of Microbiology* 2010, 41, 1009-1018.

[5.] Pan, X., Chen, F., Wu, T., Tang, H., Zhao, Z. *Food Control* 2009, 20, 598-602.

P58 CHIRAL ANALYSIS OF SELECTED GROUP OF PROFENS BY LIQUID CHROMATOGRAPHY

Veronika Vojtková, Mária Chalányová, Ivana Petránová, Milan Hutta

Department of Analytical Chemistry, Faculty of Natural Sciences, Comenius University, Mlynská dolina CH-2, 842 15 Bratislava, Slovakia, vojtkova@fns.uniba.sk

ABSTRACT

In this work we dealt with the study of chromatographic conditions of the selected group of profens such as naproxen, fenoprofen, flurbiprofen and ibuprofen. The influence mobile phase, flow rate and pH was studied.

The work is devoted to the study of enantiomeric separation of fenoprofen, flurbiprofen, and ibuprofen on the chiral stationary phase, Chiradex. The mobile phase consist of methanol:ammonium formate pH 3.0 (90:10, v/v), flow rate 1.0 ml/min. The chiral resolution of flurbiprofen enantiomers was 0.74 and ibuprofen 0.81. The separation was not achieved for fenoprofen. Partial enantiomeric separation was also attained in the commercially available drug with the active substances flurbiprofen in Flugalin tablets.

Keywords: profens, chiral separation, Flugalin

1 INTRODUCTION

The present paper deals with the study of chromatographic parameters (separation factor, pH, flow rate of mobil phase) for chiral separation of selected chiral drug from the group of profens (naproxen, fenoprofen, flurbiprofen and ibuprofen). Profens belong to a group of non-steroidal anti-inflammatory drugs. They are used to relieve pain in chronic and acute rheumatoid arthritis, osteoarthritis, and for other connective tissue disorders, for pain and fever. Chemically, they are derivatives of 2-methylarylpropionic acid. The most common is the separation of enantiomers and determination of this group of drugs in dosage forms. Problem of the preparation of pure enantiomers of the group of profens is interesting to their anti-inflammatory properties are observed only in the S-enantiomers. This need is necessitated for the social order, for the widest range of drugs available only with the active enantiomer, less side effects and better tolerance by the body [1, 2].

2 EXPERIMENTAL

2.1 Drugs and reagents

Fenoprofen, Flurbiprofen, Ibuprofen, Naproxen (Sigma Aldrich, St. Louis, USA)
Methanol gradient grade (Merck, Darmstadt, Germany)
Ultrapure water, Simplicity UV (Millipore S.A.S., France)
Formic acid 99,7% (Lachema, n.p. Brno)
Ammonia solution 28-30% (Merck, Darmstadt, Germany)
Studied analytes are on the Figure 1-4.

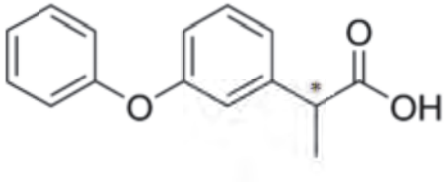

Fig. 1: Structure of fenoprofen

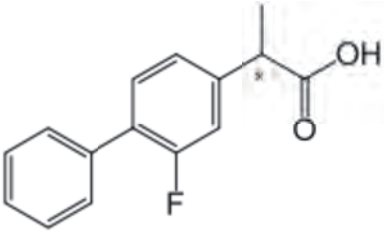

Fig. 2: Structure of flurbiprofen

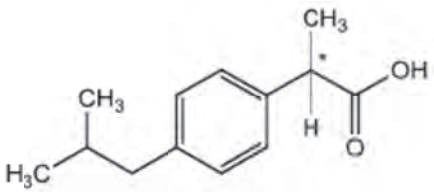

Fig. 3: Structure of ibuprofen

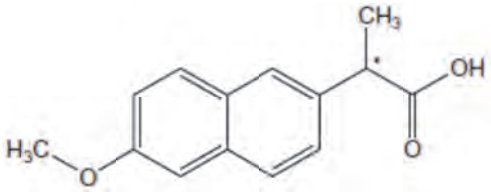

Fig. 4: Structure of naproxen

2.2 Instruments and columns

We used HPLC system from Agilent Technologies (Waldbronn, Germany), consisting of: mobile phase vacuum degasser (G1379B), dual-channel high-pressure binary pump (G1312B), auto sampler (G1329B), column thermostat (G1316B), DAD detector (G1315), ELSD detector (1200 Series). Chiral column: Chiradex (250 x 4) mm, 5 µm particals (Merck, Darmstadt, Germany) was used.

2.3 Solutions

Stock solutions with concentration were made up at 1000 µg/ml in 100% methanol. Working solutions were prepared from the stock solutions. Buffer preparation we proceed as follows to 1000 ml of water was added 5.9 ml of concentrated formic acid and pH was adjusted with ammonia to the desired value.

100 mg of the Flugalin drug was dissolved in 2 ml of 100% MeOH. 2.5 µl of drug solution was with microsyringe collected in 5 ml 80% MeOH: $HCOONH_4$ pH 3.0. Estimated concentration of Flugalin solution is 6.5 µg / ml.

3 RESULTS AND DISCUSSION

To study the separation of selected chiral drugs fenoprofen, flurbiprofen and ibuprofen from group of profens were used reverse-phase liquid chromatography RP-HPLC with spectrophotometric detection at 225, 230, 254 nm. The retention characteristic of profens to β-cyclodextrin chiral stationary phase Chiradex was studied. The mobile phase of methanol:ammonium formate was from 75% to 95%. The flow rate from 0.8 to 1.2 ml and pH 3.0, 5.0 and 7.0 was investigated. The optimal condition of chiral separation of flurbiprofen and ibuprofen was methanol:ammonium formate, pH 3.0 (90:10, v/v) with flow rate 1 ml/min. The resolution of the enantiomers of flurbiprofen 0.74 and 0.81 for the ibuprofen. Separations are shown on the Figure 5 and 6. The separation was not achieved for fenoprofen in range from 75% to 95% methanol content in the mobile phase.

Chromatographic analysis have been measured in series connection DAD and ELSD detectors.[3] The chromatohraphic separation of drug Flugalin on DAD and ELSD detector is shown on the Figure 7. ELSD detector did not provide the relevant signal of the concentration levels of Flugalin. Measurred data shown that Flugalin tablet with active substance flurbiprofen consists of both R- and S- racemates.

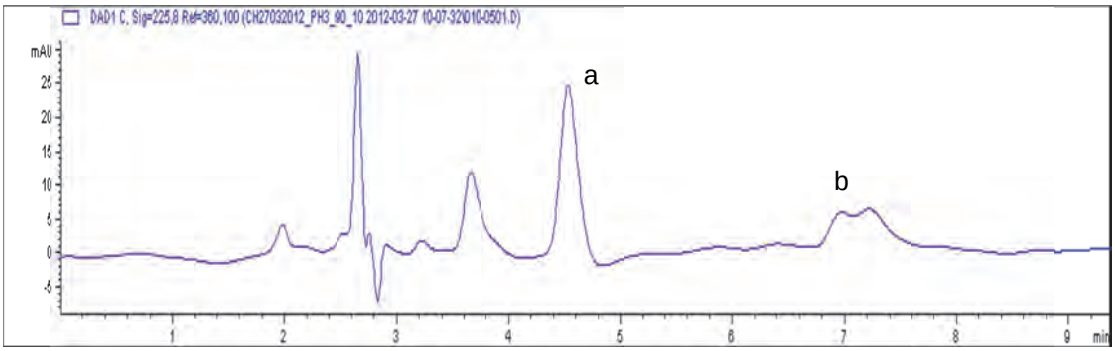

Fig. 5: Chromatographic separation of standards, concentration 10 µg/ml: **a)** fenoprofen; **b**) ibuprofen

Experimental condition: methanol:ammonium formate, pH 3.0 (90:10, v/v), flow rate 1 ml/min, UV detection at 225 nm of ibuprofen and fenoprofen.

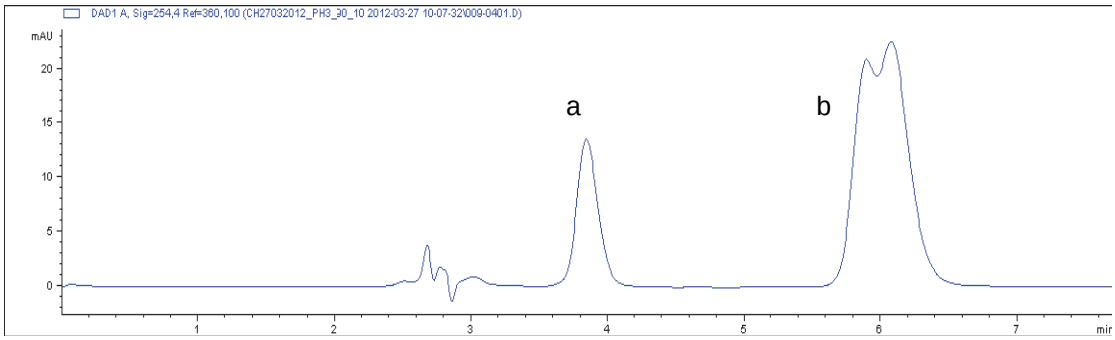

Fig. 6: Chromatographic separation of standards, concentration 10 µg/ml: **a)** naproxen; **b)** flurbiprofen

Experimental condition: methanol:ammonium formate, pH 3.0 (90:10, v/v), flow rate 1 ml/min, UV detection naproxen at 230 nm and flurbiprofen at 254 nm.

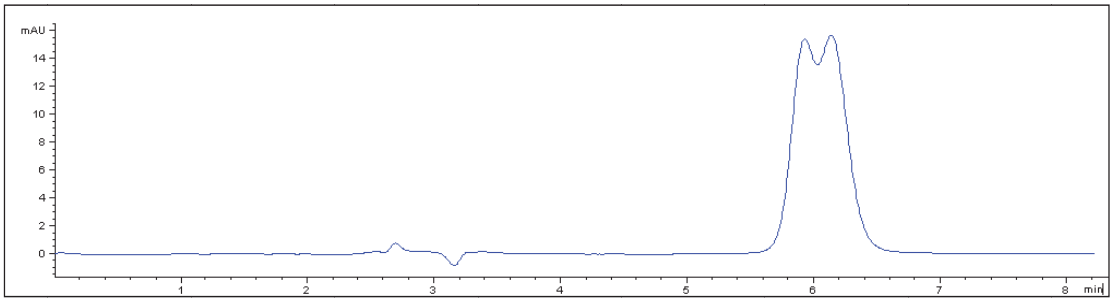

Fig. 7: Chromatographic separation of flurbiprofen in Flugalin tablets.

Experimental condition: methanol:ammonium formate, pH 3.0 (90:10, v/v), flow rate 1 ml/min, UV detection at 254 nm for flurbiprofen.

ACKNOWLEDGEMENTS

This work was generously supported by the grant of Scientific Grant Agency of the Ministry of Education of Slovak Republic and the Academy of Sciences - project VEGA 1/1349/12 and the grant of Slovak Research and Development Agency - project APVV-0583-11. This work is partially outcome of the project VVCE-0070-07 of Slovak Research and Development Agency solved in the period 2008-2011.

LITERATURE

[1.] GUBITZ, G. *et al.* 2001. Chiral separation by Chromatographic and electromigration techniques. In *Biopharmaceutics & Drug Disposition*. ISSN 0142-2782, 2001, vol. 22, p. 291-336.

[2.] CANCELLIERE, G., *et al.* 1999. Synthesis and applications of novel, highly efficient HPLC chiral stationary phases: a chiral dimension in drug research analysis. In *Pharmaceutical Science & Technology Today*. 1999, vol. 12.

[3.] WHELAN, M. *et al.* 2002. Simultaneous determination of ibuprofen and hydroxypropylmethylcellulose (HPMC) using HPLC and evaporative light scattering detection. In *Journal of Pharmaceutical and Biomedical Analysis*. ISSN 0731-7085, 2002, vol. 30, p. 1355-1359.

P59 THE COMPARISON OF ANTIOXIDANT PROPERTIES OF ORGANIC AND CONVENTIONAL DAIRY PRODUCTS

Jurgita Raudonytė, Lina Šimkevičiūtė, Jonas Damašius

Kaunas University of Technology, Department of Food Technology, Radvilenu pl. 19, Kaunas, LT 50254, Lithuania, jonas.damasius@ktu.lt

ABSTRACT

Dairy products can be classified as organic and conventional depending on the production. Organic dairy products have indirect benefits to animals and the environment, while many consumers believe that organic food is even healthier. Numerous studies have been published on the health effects of dairy products, which partly related with antioxidative properties. The present study compares antioxidant properties of organic and conventional dairy products obtained from the supermarkets. Freeze-dried water extracts of milk, yogurt and curd were prepared and measured using various methods (Folin-Ciocalteau method; $DPPH^{\bullet}$, $ABTS^{\bullet+}$ and FRAP). The obtained results indicate that significant differences were found on the antioxidant activity between organic and conventional dairy products. The total phenolics content was higher in organic dairy products, especially in yogurt samples. All analysed water extracts possessed ability to scavenge free radicals depending on the used extract concentration. From this preliminary study it can be concluded that use of organic dairy products can have an impact on human health.

Keywords: dairy products, antioxidant properties, organic milk

P60 CHARACTERIZATION OF ATMOSPHERIC PARTICULATE MATTER BY DIFFUSIVE GRADIENT IN THIN FILM (DGT) TECHNIQUE

Michaela Gregusova, Bohumil Docekal

Institute of Analytical Chemistry of the ASCR, v.v.i, Veveri 97, CZ-602 00 Brno, Czech Republic, gregusova@iach.cz

ABSTRACT

The increase of automobile emissions relates to the rapid growth of urbanization and industrialization. Toxicity of heavy metals associated with atmospheric particulate matter depends also on solubility, speciation and kinetics of metal release from solid phase. The diffusive gradients in thin films (DGT) technique is an in situ technique which can be used in measurement of kinetics of mobilization fluxes of metals.

In this study, characteristics of heavy metal contamination in road dust collected from urban area with heavy traffic in Brno, Czech Republic was investigated. The DGT probes were exposed in aqueous suspensions of particulate matter for different time periods to monitor responses of the sample matter. The road dust and DGT sorption gels were decomposed by microwave assisted extraction and analyzed by inductively coupled plasma mass spectrometry for estimation of trace metals contents.

The results revealed that the traffic appears to be responsible for the high levels of Cu, Pb, Ni and Sb and also that DGT technique, as alternative to conventional extraction procedures is a useful tool for characterization of metals mobility.

Keywords: DGT, particulate matter, metals

1 INTRODUCTION

Human exposures to particulate matter (PM) emitted from on-road motor vehicles include complex mixtures of metals from tires, brakes, parts wear and re-suspended road dust. Fine particulate material containing platinum group metals (PGM) is introduced into the environment due to utilization of three-way catalytic converters. The content of heavy metals in PM is significantly affected by vehicle volume and speed, type of engine and its operation conditions, road type, rush time periods, neighboring environment and meteorological conditions, etc. [1, 2].

Toxicity of heavy metals associated with atmospheric PM depends also on solubility [3], speciation and kinetics of metal release from the solid phase. The diffusive gradient in thin films (DGT) technique [4] accumulates metals in a resin after their diffusive transport through the well-defined hydrogel. DGT-sampling probe reduces metals concentration in the adjacent solution, so induces resupply of metals associated with the solid phase.

The scope of this study was to investigate the kinetics of metals resupply from a particulate matter into the aqueous phase by employing the DGT technique.

2 EXPERIMENTAL

The particulate matter was sampled on filters of an air-conditioning unit in the building of the IAC in Brno (at the heavy traffic area in Brno, Czech Republic). Mixture of 20 g particulate matter and 25 g water was equilibrated 24 h at a laboratory temperature of 23 °C. DGT probes with polyacrylamide diffusive gels and Chelex-100 resin gels were deployed in sample suspensions of particulate matter.

Resin gels and samples of PM were decomposed by acid-assisted microwave digestion in a mixture of 2 ml nitric acid and 0.5 ml chloride acid (Uniclever, Plazmatronika, Poland). Metals in digests were determined by ICP MS (Agilent 7700 Series).

3 EQUATIONS

DGT is able to measure directly a flux by accumulating a mass of ions (*M*) over time (*t*) through well-defined area (*A*):

$F_{DGT} = M / (tA)$

When ions are removed from solution by DGT, they may be resupplied from the particulate matter to the solution. Thus a flux from particulate matter to solution is induced by the DGT device and at the same time the response can be measured.

4 TABLES AND ILLUSTRATIONS

A Plot of DGT-measured lead uptake versus deployment time is presented as an example of results of DGT experiments. Similar data were obtained also for other monitored metals. DGT uptake sharply increases during a short deployment period of time. After few hours of deployment, the resupply rate from the solid phase to solution is too slow to sustain metals concentration in the aqueous phase, i.e. to follow the demand of the DGT probes. Consequently, the resupply of metals is predominantly by diffusion from solution in deeper zones of the PM suspension.

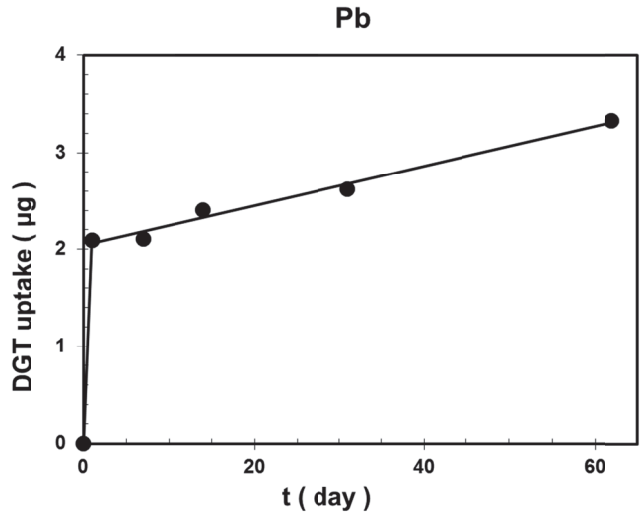

Fig. 1. : Influence of deployment time on lead uptake in Chelex 100 resin gel exposed in DGT probes with polyacrylamide diffusive gel to suspension of particulate matter.

ACKNOWLEDGEMENTS

This work was performed within the Institutional support RVO: 68081715, projects P503/10/2002, P503/11/2315 and P503/12/G147 of the Czech Science Foundation.

LITERATURE

[1.] E. Apeagyei, M. S. Bank, J.D. Spnegler. *Atmospheric Environment* 2011, 45, 2310.

[2.] B.A. Lesniewska, B. Godlewska-Zylkiewicz, B. Bocca. *Science of Total Environment* 2004, 321, 93.

[3.] M. Vojtesek, P. Mikuska, Z. Vecera. *International Journal of Environmental Analytical Chemistry* 2012, 92, 432.

[4.] H. Zhang, W. Davison. *Analytical Chemistry* 1995, 67, 3391.

P61 INVESTIGATION OF CHEMICAL COMPOSITION AND ANTIMICROBIAL ACTIVITIES OF ESSENTIAL OILS OF *LAVANDULA HYBRIDA L., CYMBOPOGON FLEXUOSUS L., MALALEUCA ALTERNIFOLIA L.*

Rūta Mickienė[a], Audrius Maruška[a], Ona Ragažinskienė[b]

[a] *Dept. of Biochemistry and Biotechnologies, Vytautas Magnus University, Vileikos str. 8, LT-44404 Kaunas, Lithuania.* mickiene@lva.lt
[b] *Kaunas Botanical Garden of Vytautas Magnus University, Ž.E. Žilibero 6, LT-46324 Kaunas, Lithuania*

ABSTRACT

The present research work describes the chemical composition and antimicrobial activity of the essential oils of the *Lavandula hybrida L., Cymbopogon flexuosus L., Malaleuca alternifolia* L.The essential oils were analyzed by gas chromatographic-mass spectrometric (GC-MS) analysis. Linalol (34.09%) and bergamiol (39.26%) were the main compounds of *Lavandula hybrida* L. essential oils; terpineol (45.77%) and terpinene (19.46%) of *Malaleuca alternifolia* L.; neral (33,92%) and geranial (43.76%) of *Cymbopogon flexuosus* L. This study used *Escherichia coli*, DSM-No. 10232 and *Aspergillus niger* DSM-No.1957. The antimicrobial activity of the essential oils was evaluated using the agar diffusion method. The essential oils exhibited antimicrobial activity to varying degrees against the tested strains. This study indicated, that the essential oils of *Lavandula hybrida L., Cymbopogon flexuosus L., Malaleuca alternifolia* L. possesses antimicrobial activities *in vitro* against tested microorganisms. Namely best activity show *Cymbopogon flexuosus L.,against Aspergillus niger* DSM-No.1957. inhibition halos 14.4 ± 2.5 mm, *Escherichia coli* DSM-No. 10232 inhibition halos 13.1± 2.5mm.

Keywords: essential oils, GC-MS, antimicrobial activity

1 INTRODUCTION

The plant essential oils as natural substances could represent a potential source of new antifungal and antibacterial agent. During the past years, a number of studies have been carried out concerning the application of essential oils as antimicrobial agents. Due to their bactericidal and fungicidal properties, pharmaceutical and food uses, the essential oils are more and more widespread as alternatives to synthetic chemical products to protect the ecological equilibrium. The extraction product can vary in quality, quantity and in composition according to climate, soil composition, plant organ, age and vegetative cycle stage [1, 2]. Essential oils and their components are gaining increasing interest because of their relatively safe status, wide acceptance by consumers, and their exploitation for potential multi-purpose functional use [3]. Essential oils are composed of many different volatile compounds. It is difficult to correlate the fungitoxic activity to a single compound or classes of compounds. In many cases the antimicrobial effects of essential oils are the result of many compounds acting synergistically. Most of the investigations on the antimicrobial activity of essential oils concern inhibition of microbial growth rather than lethal or antitoxic effects. Therefore, essential oils are one of the most promising groups of natural compounds for the development of safer antifungal agents [4]. This study was undertaken to investigate the inhibitory effects of *Lavandula hybrida L., Cymbopogon flexuosus L., Malaleuca alternifolia* L. essential oils against microorganisms.

2 MATERIALS AND METHODS

2.1 Essential oils

Essential oils of *Lavandula hybrida L., Cymbopogon flexuosus L., Malaleuca alternifolia* L. and were obtained from a commercial source (Oil manufacturer Sensient Essential Oils, GmbH, Germany), steam distillation method was used for the production of essential oils.

2.2 Microorganisms species

This study used *Escherichia coli*, DSM-No. 10232 and *Aspergillus niger* DSM-No.1957 Microorganisms species were obtained from the Deutsche Sammlung von Mikroorganismen und Zellkulturen GmbH (Germany). These germs are commonly used for the evaluation of disinfectant agents.

2.3 Essential oils determination of the antimicrobial activity by disc diffusion assay

The microorganisms were cultivated on Bloodagar-Base N. 2 (Oxoid, UK) and on DG-18 (Oxoid, UK) respectively for the mould. One colony of each microorganism was picked and diluted in sterile peptone-water (PW) (Oxoid, LTD, Basingstoke, Hampshire, UK) with reference to the McFarland standard to achieve an inoculum of approximately 10^5-10^6 colony-forming units per ml ($CFUml^{-1}$). 50 µl of this inoculum was uniformly plated onto the surface of Bloodagar-Base N. 2 (Oxoid, UK) (bacteria), Malt Extract Agar (Oxoid, UK) (yeast) and DG-18 (Oxoid, UK) (moulds) in Petri dishes. After one minute, sterile 6 mm diameter paper discs were placed on the plates and immediately immersed with 10µl portions of the 100 % concentration essential oils. Sterile PW was used as control. After allowing the essential oils to diffuse across the surface for 1h at room temperature, the plates with bacteria were incubated at 37ºC for 24 h. Moulds were cultivated on DG-18 at 25ºC for 7–10 days. At the end of the incubation period, the inhibition halo diameters were measured and expressed in millimetres. When the inhibition halo observed was equal or higher than 10 mm diameter, it was considered as a positive antimicrobial activity [5].The method was used to determine the minimum inhibitory concentration (MIC) according to the National Committee for Clinical Laboratory Standards. The minimum inhibitory concentration (MIC) is defined as the lowest concentration of the essential oil at which the microorganism does not demonstrate visible growth.

2.4 Gas chromatographic-mass spectrometric analysis

Quantitative and qualitative analyses of essential oils were carried out using gas chromatograph GC-2010 with mass spectrometric detector GCMS- QP 2010 (Shimadzu, Tokyo, Japan). MS was operated in the electron impact ionization mode at 70 eV. Spectra were registered within the mass range *m/z* 30-400. Compounds were separated using an RTX-5MS column (30m × 0.25 mm i.d. ×0.25 µm film thickness) (Restec, Bellefonte,PA, USA). Carrier gas, helium, was adjusted at 1.2 mL min^{-1} flow rate. For injection, a split mode was used at a ratio of 1:10; the injector temperature was 240 °C. The oven temperature was programmed as follows: initial temperature was maintained at 60°C (3 min), raised at 2 °C min^{-1} to 70°C (2 min), raised at 1 °C min^{-1} to 120 °C (2 min), raised at 20°C min^{-1} to 250 °C (5 min). For quantitative analysis, three replicates of each sample were run by GC-MS and the results were expressed as a mean.The compounds were identified by comparison of their linear retention indices (LRI) relative to C_8—C_{24} n-alkanes obtained on a non-polar DB-5 column with those provided in the database [6] and by matching their mass spectra to the data in NIST 05 library and to the results reported elsewhere [6, 7, 8, 9].

3 RESULTS AND DISCUSIONS

The qualitative and quantitative composition of *Lavandula hybrida L., Cymbopogon flexuosus L., Malaleuca alternifolia* L. essential oils is given in table 2. Essential oils were identified by GC-MS methods. Linalol (34.09%) and bergamiol (39.26%) were the main compounds of *Lavandula hybrida* L. essential oils; terpineol (45.77%) and terpinene (19.46%) of *Malaleuca alternifolia* L.; neral (33,92%) and geranial (43.76%) of *Cymbopogon flexuosus* L. The antimicrobial activity of various concentrations of essential oils is illustrated in table 1. The *Cymbopogon flexuosus* L. essential oils showed the largest antimicrobial activity against the used microorganisms strains: *As. Niger and E. coli*. According to these observations, it can be conclude that strong antimicrobial activity of - *Cymbopogon flexuosus* L. essential oil could be attributed to geranial itself or could be a result of synergism of other main components in the oil. Essential oils interact with the membrane causing leakage of cellular components, change fatty acid and phospholipid constituents, impair energy metabolism and influence genetic material synthesis [10].

Table 1: Antimicrobial activity of essential oils on moulds strains and microorganisms using the disc diffusion method (medium values of the inhibition halos (mm)).

ESSENTIAL OIL	FUNGI	BACTERIA
	Aspergillus niger	***Esherichia coli***
Lavandula hybrida L.	4.6 ± 0.85	4.3 ± 0.6
Cymbopogon flexuosus L.	14.4 ± 2.5	13.1 ± 2.5
Malaleuca alternifolia L.	12.8 ± 2.2	12.2 ± 2.5

Screening results for essential oils antimicrobial activity are shown in table 1. Most of the oils evaluated exhibited significant inhibitory activity against *Aspergillus niger* and *Escherichia coli* species tested. The results show the wide variation in the antimicrobial properties of plant essential oils. *Salvia sclarea L.* showed very slight inhibition against testet microorganisms, volatile compounds produced inhibition zones of 2.8 ± 0.3mm in mould strain *Aspergillus niger* and 4.2 ± 0.3 mm *Escherichia coli* strain cultures. Identic, very slight inhibitory activity presented *Lavandula hybrida L.* essential oil. In the plates with *Aspergillus niger* and *Escherichia coli* microorganisms strains the radius of inhibition was between 4.6 ± 0.85 and 4.3 ± 0.6 mm correspondingly.Strongest antimicrobial effect exhibited *Cymbopogon flexuosus L., Malaleuca alternifolia L.* – sterile filter paper discs soaked with of each essential oil presented inhibition halos between 12.8 ± 2.2 and 14.4 ± 2.5 mm.
Essential oils *Lavandula hybrida L.* presented to very low antimicrobial activy compare with *Cymbopogon flexuosus L., Malaleuca alternifolia L.*

Table 2: Qualitative and quantitative composition of *Lavandula hybrida* L., *Malaleuca alternifolia* L., *Cymbopogon flexuosus* L. essential oils (values are expressed as means of three determinations; standard deviation did not exceed 10%)

[a]LRI	[b]Identification	[c]Compound	[d]Peak Area	[e]Area %	Match (%)
LAVANDULA HYBRIDA L.					
1027	MS, LRI	eucalyptol	22.3	2.86	96
1044	MS, LRI	ocimene	11.3	1.43	94
1103	MS, LRI	linalol	271.2	34.09	94
1138	MS, LRI	camphor(+)-	36.0	4.53	97
1160	MS, LRI	borneol	22.0	2.77	83
1258	MS, LRI	bergamiol	312.3	39.26	97
1293	MS, LRI	lavandulol	13.8	1.75	95

1404	MS,LRI	caryophyllene	9.7	1.23	93
Total peak area (a.u.)[e]			**794.9**		
***MALALEUCA ALTERNIFOLIA* L.**					
932	MS, LRI	α-pinene	10.4	2.11	97
1015	MS, LRI	4-carene	44.9	9.08	96
1022	MS, LRI	o-cymene	11.4	2.30	97
1025	MS, LRI	β-pinene	8.3	1.68	91
1027	MS, LRI	1,8-eucalyptol	12.1	2.46	95
1055	MS, LRI	α-terpinene,	96.3	19.46	96
1087	MS, LRI	carvomenthene	15.8	3.21	96
1175	MS, LRI	4-terpineol	226.5	45.77	95
1188	MS, LRI	α-terpene alcohol	16.7	3.36	97
1428	MS, LRI	alloaromadendrene	5.0	1.01	94
1485	MS, LRI	(+)-ledene	8.6	1.76	94
1517	MS, LRI	β-cadinene	7.0	1.43	93
Total peak area (a.u.)			**494.9**		
CYMBOPOGON FLEXUOSUS L.					
945	MS, LRI	camphene	4.3	1.23	96
985	MS, LRI	methyl heptenone	6.4	1.81	96
1069	MS, LRI	propylamylketone	5.1	1.45	97
1100	MS, LRI	d-linalool	4.0	1.14	96
1182	MS, LRI	epoxycarane	3.6	1.01	93
1240	MS, LRI	neral	121.1	33.92	97
1255	MS, LRI	geraniol	19.0	5.33	96
1271	MS, LRI	geranial, citral	156.3	43.76	95
1386	MS, LRI	neral acetate	14.4	4.04	95
1408	MS,LRI	caryophyllene	4.3	1.22	94
1507	MS,LRI	naphthalene	4.1	1.16	97
Total peak area (a.u.)			**350,0**		

[a]LRI, linear retention index on RTX -5MS column, experimentally determined using homologous series of C6-C24 alkanes. [b]Identification method: MS, by comparison of the mass spectrum with those of the computer mass library Wiley 7 Nist; LRI,
by comparison of LRI with those reported in literature. [c]Compounds are listed in order of their elution from a RTX -5MS column. [d]Values expressed in GC peak area/10^6. [e]a.u., arbitrary units.

4 CONCLUSIONS

From this study it can be concluded that the essential oils of *Lavandula hybrida L., Cymbopogon flexuosus L., Malaleuca alternifolia* L. exhibited antimicrobial activity to varying degrees against microorganisms *A. niger* and *E. coli*. when used individually. Namely best activity show *Cymbopogon flexuosus L.,against Aspergillus niger* DSM-No.1957. inhibition halos 14.4 ± 2.5 mm, against *Escherichia coli* DSM-No. 10232 inhibition halos 13.1± 2.5mm.

ACKNOWLEDGEMENTS

The authors acknowledge postdoctoral research work fellowship is being funded by European Union Structural Funds project "Postdoctoral fellowship Implementation in Lithuania'' (VP1-3.1-ŠMM-01).

LITERATURE

[1.] Masotti, V., Juteau, F., Bessie're, J, M., Viano, J., Seasonal and phenological variations of the essential oil from the narrow endemic species Artemisia molinieri and its biological activities. *Journal of Agricultural and Food Chemistry* 2003, 51, 7115–7121.

[2.] Angioni, A., Barra, A., Coroneo, V., Dessi, S., Cabras, P.,Chemical composition, seasonal variability, and antifungal activity of *Lavandula stoechas* L. ssp. stoechas essential oils from stem/leaves and flowers. *Journal of Agricultural and Food Chemistry* 2006, 54, 4364–4370.

[3.] Ormancey, X., Sisalli, S., Coutiere, P., Formulation of essential oils in functional perfumery. *Parfums, Cosmetiques, Actualites* 2001, 157, 30 – 40.

[4.] Mishra, A, K., Dubey, N, K., Evaluation of some essential oils for their toxicity against fungi causing deterioration of stored food commodities. *Applied and Environmental Microbiology*1994, 60, 1101-1105.

[5.] Lima, E, O., Gompertz, O, F., Giesbrecht, A, M., Paulo, M,Q. In vitro antifungal activity of essential oils obtained from officinal plants against dermatophytes. *Mycoses* 1993, 36, 333-336.

[6.] Adams, R, P., Identification of essential oil components by gas chromatography/quadrupole mass spectroscopy. *Allured Publishing Corporation*, Illinois 2007.

[7.] Gazim, Z, C., Rezende, C, M., Fraga, S, R., Svizinski, T, I, E., Cortez, D, A, G., Antifungal activity of the essential oil from *Calendula officinalis* L. (Asteraceae) growing in Brazil. *Brazil Journal Microbiology* 2008, 39, 61-63.

[8.] Petrovic, L., Lepojevic, Ž., Sovilj, V., Adamovic, D., Tesevic, V., An investigation of CO2 extraction of marigold (*Calendula officinalis* L.). *Journal of the Serbian Chemical Society.* 2007, 72, 407-413.

[9.] Okoh , O, O., Sadimenko, A, P., Asekun, O, T., Afolayan, A., The effects of drying on the chemical components of essential oils of *Calendula officinalis* L. *African Journal of Biotechnology* 2008, 7,1500-1502.

[10.] Ceylan, E., Fung, D, Y, C., Antimicrobial activity of spices. *Journal Rapid Methods and Automation in Microbiology* 2004, 12, 1-55.

P62 ENVIRONMENTAL POLLUTION OF VINEYARDS BY POLYCYCLIC AROMATIC HYDROCARBONS ORIGINATING FROM MOTOR VEHICLES EMISSIONS

Helena Fišerová [a], Vladimír Šnajdr [a], Štěpán Zezulka [b], Jan Tříska [c], Rudolf Jílek [c]

[a] *Dep. of Plant Biology, Faculty of Agronomy, Mendel University, Zemědělská 1, 613 00 Brno, Czech Republik, hfiser@mendelu.cz, snajdr.vladimir@seznam.cz*

[b] *Dep. of Plant Physiology and Anatomy, Institute of Experimental Biology, Faculty of Science, Masaryk University, Kotlářská 2, 611 37 Brno, Czech Republic, zezulka@sci.muni.cz.*

[c] *Laboratory of Metabolomics and Isotopic Analyses, Global Change Research Centre AS CR, Branišovská 31, 370 05 České Budějovice, Czech Republic, triska.j@czechglobe.cz, rujil@czechglobe.cz*

ABSTRACT

Contents of polycyclic aromatic hydrocarbons (PAHs) were monitored in grapevine (*Vitis vinifera* L.) berries and leaves and also in soil beneath the plants. Samples were collected along the first class road No. I/54 with heavy traffic near the town of Kyjov (Czech Republic). All samplings were performed before the harvest of grapes on sites situated in the distance of 5 and 10 m from the road. Collected samples were lyophilised, extracted with a mixture hexane/acetone in the ultrasonic bath and analysed by means of GC-MS. Contents of PAHs in berry skins were compared with their levels in leaves and in pulp, where the lowest were found in the berry pulp and the highest in leaves. A comparison of PAHs contents in soil with hygienic limits showed above-limit loading especially in the distance up to 5 meters from the road.

Keywords: emissions, traffic, Vitis vinifera (L.)

1 INTRODUCTION

Polycyclic aromatic hydrocarbons (PAHs) are potential mutagenic and/or carcinogenic compounds polluting the environment and penetrating into the human body via respiration of polluted air [1] and/or intake of contaminated foodstuffs [2]. The most frequently monitored PAHs contain in their molecule 2 to 6 condensed benzene rings. The road transport and motor vehicles represent an important source of PAHs; these compounds are released into the environment with exhaust gases, from scratched and discarded tyres and/or in a form of the run-off from the asphalt surface of roads. In tyre treads, the most frequent PAHs are the following: fluoranthene, pyrene, benzo[ghi]perylene and coronene [3]. From the source of pollution, they can spread not only in the gaseous form but also adsorbed on small particles of ash and dust. At present, there is no Directive in European Union concerning mobile sources of PAHs and defining admissible levels of these compounds in emissions [4]. Within the framework of international trade, the safety of consumers is regulated by strict standards defined in Maximum Residue Limits (MRL). In the EU the lowest MRL in agricultural commodities is defined as ≤ 0.01 mg.kg-1 (EC) [5]. PAHs levels in crops grown along roads with intensive traffic were studied using sugar beet [6] and another species as passive samplers and the authors concluded that the established levels of PAHs like benzo[b]fluoranthene, benzo[a]pyrene and benzo[a]anthracene surpassed limits approved for foodstuffs. Dasgupta et al. [7] observed a surface PAHs contamination of *Vitis vinifera* grapes due to the content of lipophilic components. These substances can pass in non-reduced amounts also into the final product (i.e. wine). In the Czech Republic, there are only very scarce information available about the PAHs contamination of crops planted close to roads.

2 MATERIALS AND METHODS

2.1 Locality and sampling

The sampling locality was selected with regard to the estimation of PAHs occurrence [8] along the heavy frequented first class road No. I/54 near the town of Kyjov, Czech Republic (GPS location: 49°0'16.77"N, 17°5'12.546"E). On this road, the average frequency of traffic ranges from 5 to 7 thousand of motor vehicles per year [9]. Soil (beneath plants) and grapevine samples (leaves and berries in the stage of harvest ripeness) were taken in the distance of 5 and 10 m from the road on September 16th in 2009. The day of sampling was sunny and the last rainfall was recorded nearly two months ago in this locality.

2.2 Methodology of PAHs estimation

Concentrations of PAHs in the grapevine biomass and soil beneath plants were estimated by means of GC-MS with a mass detector ITQ 1100 (Thermo Scientific, USA) [10]. Lyophilised samples of leaves, berry skin, berry pulp and soil were extracted three times in 10 ml of hexane/acetone mixture (3:2); extractions were performed in an ultrasonic bath and lasted for 15 minutes. Combined extracts were dried with anhydrous sodium sulphate and thereafter evaporated in a rotary vacuum evaporator to the volume of approximately 5 ml; thereafter, the concentrated extract was evaporated to dryness under a stream of nitrogen. Evaporated total solids were thereafter dissolved in 500 µl of toluene and analysed. Concentrations of 16 PAHs (U.S. EPA) in samples were calculated using an external standard (Dr. Ehrenstorfer, Germany). Arithmetic means of two estimations are presented in Tab. 1.

3 RESULTS AND DISCUSSION

The detected contents of fluoranthene (FLT), naphtalene (NAP) and other compounds belonging to the group of PAHs in the samples of grapevine plants and vineyard soil (Fig. 1, Tab. 1) show the trend of decreasing concentrations of these substances with increasing distances from sources of pollution. Similar results were obtained also by other authors who

studied contents of FLT in various fruit and vegetables [10, 11, 12]. Higher levels of PAHs are usually found in leafy vegetables than in fruits. Camargo and Toledo [12] reported a FLT content of 0.00387 μg.g^{-1} for the grapevine; this level was 10-times lower than the amount of fluoranthene estimated in our study in berry skin but comparable with the content estimated in the pulp. Concentrations of fluoranthene in pulp of grapevine berries were lower than in their skin and/or in leaves.

Table 1: Concentrations of PAHs in samples of plants and soil from a vineyard situated near the road No. I/54 in the neighbourhood of Kyjov city (samples taken in the distances of 5 and 10 m from the road)

Contents of PAHs in samples[a] (μg.g^{-1} of dry material)	Berries – skin		Berries – pulp		Leaves		Soil	
Distance from the road (m)	5	10	5	10	5	10	5	10
Naphthalene	**0.0299**	**0.0202**	**0.0057**	**0.0106**	**0.0492**	**0.0286**	**0.1783**	**0.0840**
Acenaphtylene	0.0014	--	--	--	--	0.0021	0.0021	0.0040
Acenaphtene	0.0098	0.0070	0.0069	0.0016	0.0900	0.0821	0.0308	0.0262
Fluorene	0.0018	0.0046	--	--	--	0.0188	0.0311	0.0224
Fenanthrene	0.0780	0.0738	0.0082	0.0062	0.3404	0.1537	0.7575	0.6053
Contents of PAHs in samples[a] (μg.g^{-1} of dry material)	Berries – skin		Berries – pulp		Leaves		Soil	
Anthracene	n.d.	n.d.	0.0022	n.d.	n.d.	n.d.	0.0093	0.0089
Fluoranthene	**0.0155**	**0.0149**	**0.0043**	**0.0015**	**0.0380**	**0.0333**	**0.1644**	**0.0871**
Pyrene	0.0094	0.0100	0.0042	0.0013	0.0218	0.0133	0.1116	0.0579
Benzo[a]anthracene	0.0077	0.0028	0.0040	n.d.	0.0014	0.0044	0.0329	0.0166
Chrysene	0.0087	0.0037	0.0038	n.d.	0.0028	0.0060	0.0406	0.0210
Benzo[b]fluoranthene	n.d.	n.d.	n.d.	n.d.	n.d.	n.d.	0.0428	0.0160
Benzo[k]fluoranthene	n.d.	n.d.	n.d.	n.d.	n.d.	n.d.	0.0279	0.0125
Benzo[a]pyrene	n.d.	n.d.	n.d.	n.d.	n.d.	n.d.	0.0347	0.0132
Indeno[123cd]pyrene	0.0135	0.0038	0.0062	n.d.	0.0023	0.0097	0.0247	0.0104
Dibenzo[ah]anthracene	0.0098	0.0015	0.0024	n.d.	n.d.	0.0029	0.0052	0.0019
Benzo[ghi]perylene	0.0140	0.0047	0.0059	0.0001	0.0015	0.0062	0.0213	0.0083
Total PAHs	**0.1994**	**0.1468**	**0.0539**	**0.0214**	**0.5473**	**0.3610**	**1.5155**	**0.9956**

[a] Data represent mean of two estimations, “n.d.” stands for “below detection limit”. Detection limit for fluoranthene 0.001 ug.g^{-1} of dry material.

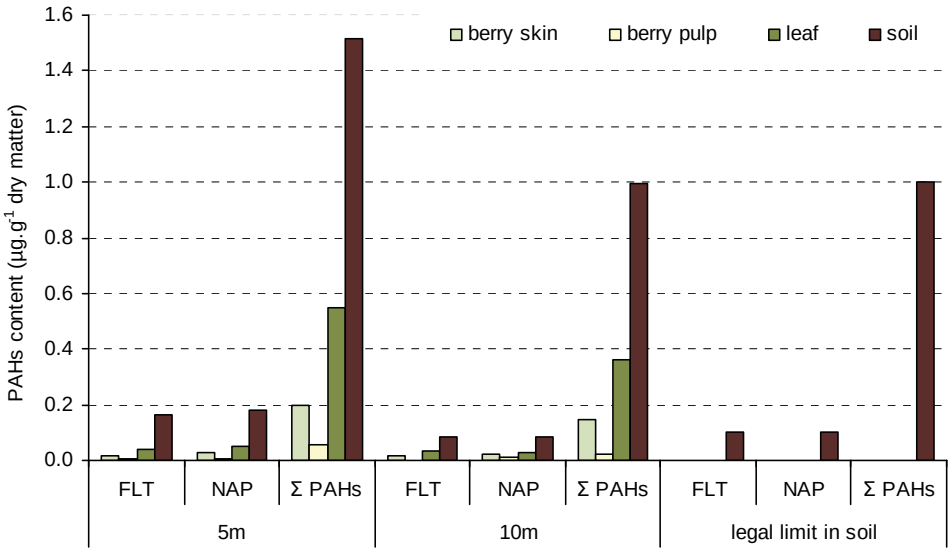

Fig. 1.: Contents of fluoranthene (FLT), naphtalene (NAP) and sums of PAHs (Σ PAHs) detected in grapevine berries, leaves and vineyard soil in the distance of 5 and 10 m from the road, supplemented with their approved legal limits for soil.

Surprisingly high contents of fluoranthene, naphtalene and total PAHs were found in soil samples taken at the distance of 5 m from the road (Fig. 1, Tab. 1). Levels were higher by more than one half than the legal limits in the Methodological Directive of the Czech Ministry of Environmental Protection [8].

4 CONCLUSIONS

It can be concluded that PAHs are adsorbed and accumulated mainly in leaves of grapevine plants. The highest levels of fluoranthene were detected in leaves. Its content in the skin of berries were up to three-times lower than in leaves and the lowest FLT level was found in the berry pulp (as much as ten-times lower than in berry skins). It is therefore evident, that the direct penetration of PAHs from berry skin into the pulp is limited. Whereas in the distance of 5 m from the road, the levels of fluoranthene, naphtalene and total PAHs in soil were above approved limits, In the distance of 10 m from the road, their contents were lower than legal limits and only the sum of PAHs was equal to the approved limit.

ACKNOWLEDGEMENTS

This study was supported by Czech Science Foundation project GAČR 522/09/0239 and by the Project CzechGlobe – Centre for Global Climate Change Impacts Studies, reg. no. CZ.1.05/1.1.00/02.0073.

LITERATURE

[1.] Phillips, D. H., Carcinogenesis 2002, 23, 1979-2004.
[2.] Cocco, P., Moore, P.S., Ennas, M.G., Tocci, M.G., *et al.*, Annals of Epidemiology 2007, 17, 1-8.
[3.] Larnesjö, P., Applications of source receptor models using air pollution data in Stockholm, Undergraduate Thesis, Department of Analytical Chemistry, Stockholm University 1999
[4.] Hailwood, M., King, D., Leoz, E., Maynard, R., *et al.*, In: Position Paper Annexes, Working Group On Polycyclic Aromatic Hydrocarbons, European Commission 2001.
[5.] Commission Regulation (EC) No 149/2008 of 29 January 2008 amending Regulation (EC) No 396/2005 of the European Parliament and of the Council by establishing Annexes II, III and IV setting maximum residue levels for products covered by Annex I thereto Official J. European Union 1.3.2008, L 58/1-L 58/398.
[6.] Loncar, E.S., Kolarov, L.A., Maltasa, R.V., Skrbic, B.D., Journal of Serbian Chemical Society 2005, 70, 1237-1242.

[7.] Dasgupta, S., Banerjee, K., Patil, S.H., Ghaste, M., *et al.*, Journal of Chromatography A 2010, 1217, 3881-3889.
[8.] Míšek, J., Výsledky sčítání dopravy, Ředitelství silnic a dálnic Brno 2005.
[9.] Adamec, V., Huzlík, J., Cigánek, M., Machala, M., DÚ 04 – Analýza toxických a genotoxických účinků reálných směsí emitovaných z dopravy, Centrum dopravního výzkumu, 2003.
[10.] Kummerová, M., Zezulka, Š., Krulová, J., Tříska, J., Lichenologist 2007, 39, 91-100.
[11.] Camargo M.C.R., Toledo M.C.F., Food Control 2003, 14, 49-53.
[12.] Larsson, B.K., Eriksson, A.T., Cervenka, M., Journal of the American Oil Chemists' Society, 1987, 64, 365-370.
[13.] Camargo, M.C.R., Toledo, M.C.F., Toxicology Letters 2005, 158, 193-193.

P63 SCREENING OF POTENCIAL USE OF THE CAPILLARY ZONE ELECTROPHORESIS METHOD WITH INDIRECT PHOTOMETRIC DETECTION FOR THE MONITORING OF SELECTED ORGANIC ACIDS IN FRUIT WINE, AND CULTURE MEDIA FOR MICROBIOLOGICAL AND BIOTECHNOLOGICAL PURPOSES

Miloš Dvořák, Milena Vespalcová, Bohuslav Rittich

Institute of Food Science and Biotechnology, Faculty of Chemistry, Brno University of Technology, Purkyňova 118, 61200 Brno, Czech Republic, mil.dvorak@seznam.cz

ABSTRACT

Determination of organic acids is an important control steps for biotechnological productions. To their determination can be electromigration methods used such as capillary zone electrophoresis method with indirect photometric detection. This paper describes development of the separation system for selected matrices (fruit must and culture media). We separated several basic organic acids with short chain and identified in real samples. Separation system contained 3,5-dinitrobenzoic acid and cationic surfactant (CTAB). Separation took place on uncoated fused silica capillary.

Keywords: organic acids, capillary zone electrophoresis (CZE)

1 INTRODUCTION

Monitoring of organic acids is important steps in biotechnology industry and an important tool for microbiological tests. Their composition and changes are an indicator of the state of the process, as an indicator of sensory and quality characteristics of the product. In particular, monitoring changes in the composition of the fermentation of the fruit must tell us about the properties of the resulting product, or the need to control the process [1]. At the beginning of the process gives information on the state of the raw material and its suitability for further processing. In the field of microbiology carboxylic acids are an important parameter that helps the taxonomy, or to monitor the impact of changes in conditions on the behavior of microorganisms. Both processes deals with the matrix characterized by short chain aliphatic carboxylic acids [2].

The need for monitoring of organic acids raises the requirements for their quick and easy and economical determination with sufficient efficiency. Such an alternative offer electromigration methods. In particular, capillary zone electrophoresis, and their arrangement is the most suitable principle for rapid analysis of biological samples containing organic acids. Possibility of its miniaturization and modifiable structure, as well as the possibility of routine analyzes make it one of the most perspective analytical methods [3].

2 AIM OF WORK

The aim was to select and test a simple separation system for determination of short chain carboxylic acids. Assess the capacity of separation and adequate detection limits with respect to the chosen matrix. Selected separation system was tested on real samples of fruit must and culture medium after cultivation.

3 MATERIALS AND METHODS

All reagents were of analytical grade (p.a). Standards of organic acids and cetyltrimethylamonium bromide (CTAB) were from Sigma-Aldrich, 3,5-dinitrobenzoic acid (3,5-DNB)from Penta. Standard stock solutions were prepared with purified water (Milli-Q). Capillary electrophoresis system was used PrinCE 460 (PrinCE Technologies B.V., Emmen, Neederland) with UV-VIS detector Spectra SYSTEM UV2000 (Thermo Separation Products Inc., San Jose, USA) and fused silica capillary, I.D 50 μm (MicroSolv Technology Corporation, Long Branch, NJ, USA).

All solutions were before used filtered through a 0,45 μm membrane. Backgound electrolyte (BGE) were prepared 10 mmol/l 3,5-dinitrobenzoic acid with 0,2 mmol/l CTAB. pH was set up at 3,6 (NaOH). Fused silica capillary had total length 125 cm, effective length 25 cm. Before first analysis capillary was conditioned with 1 mol/l NaOH (1200 mBar, 20 min), Milli-Q water (1200 mBar, 10 min), and BGE (1200 mBar, 10min) with elektrokinetic flush (+25 kV). Between analyses capillary was reconditioned BGE with elektrokinetic reflush (1200 mBar, +25 kV, 5 min). The electrophoretic system was operated with inverted polarity and constant voltage of -30 kV. Indirect photometric detection was at 254 nm. Temperature of all systems was constant at 25°C. All solution for analysis was diluted in the BGE.

4 RESULTS

Table 1 shows an overview of separated organic acids recovered in the chosen system. Effective mobilities were calculated for their identification of their content in real samples. Fig 1 shows real sample separation electrophoreogram culture medium after cultivation of bacteria of the genus *Clostridium*. Fig. 2 shows electrophoreogram of wine must. Limits of detection ranged from 50 to 100 mg/l.

Table 1: Selected organic acids separated of chosen system, their effective mobility, and identification of real sample.

Organic acids	**Effective mobility μ_{eff} /$m^2s^{-1}V^{-1}$/**	**Identification at Grape must / cultivation media**
Oxalic	$41{,}3.10^{-9}$	No / No
Formic	$32{,}5.10^{-9}$	No / Yes
Citric	$24{,}0.10^{-9}$	Yes / No
Acetic	$77{,}8.10^{-9}$	Yes / Yes
Propionic	$51{,}9.10^{-9}$	No / Yes
Lactic	$34{,}4.10^{-9}$	No / No
Tartaric	$28{,}8.10^{-9}$	Yes/ No
Malic	$25{,}0.10^{-9}$	Yes / No

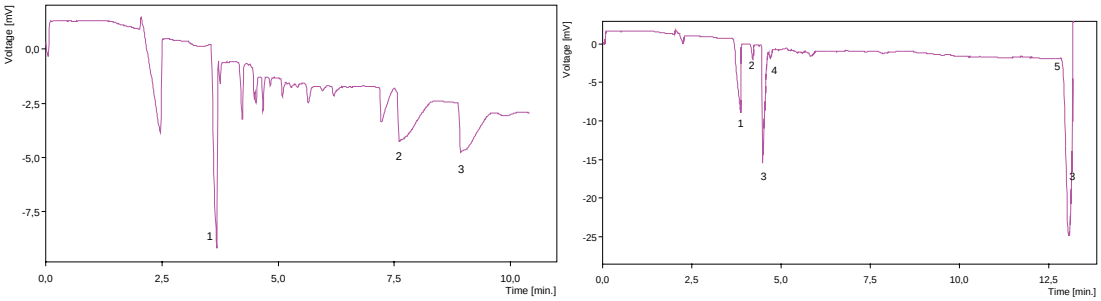

Fig. 1.(Left) : Electrophoretic separation of organic acids in the sample of cultivation media. Identification of peaks: 1 – Formic acid, 2 – Acetic acid, 3 – Propionic acid, others organic acid were not detected in this sample. Separation conditions: 25/125 cm fused silica capillary, separation voltage 30 kV (inverted polarity), 10 mM 3,5-DNB/0,2 mM CTAB, buffer pH=3,6.
Fig. 2.(Right) : Electrophoretic separation of organic acids in the sample of wine must. Identification of peaks : 1 – Acetic acid, 2 – Tartaric acid, 3 – Malic acid, 4 – Citric acid, 5 – Mesityloxide (marker electroosmotic flow), others organic acid were not detected in this sample). Separation conditions: 25/125 cm fused silica capillary, separation voltage 30 kV (inverted polarity), 10 mM 3,5-DNB/0,2 mM CTAB, buffer pH=3,6.

5 DISSCUSION

The separated analytes have sufficient resolution. An increased of the ionic strength of electrolyte improved resolution, but prolonged migration times. Oppositely, an increase of the concentration of CTAB decreased efficiency (number of theoretical plates). The best separation was achieved at a higher separation voltage (30 kV). The current level was about 4 µA. Real samples of grape must and cultivation media was necessary to dilute. This indicates sufficient sensitivity of method for this matrix. In addition, in real samples there were also other components which did not interfere with the monitored components [4].

6 CONCLUSION

Capillary zone electrophoresis with indirect photometric detection and chosen separation system is shown to be sufficiently effective for monitoring of the content of carboxylic acids in the tested matrices. Prepared method can be optimized and used for biotechnological and microbiological purposes. It is fast enough, economical and effective. It reflected a sufficiently reproducible.

ACKNOWLEDGEMENTS

The research was supported by a grant from program „Věda a výzkum pro život 2011“, from Nadace Tomáše Bati, Zlín

LITERATURE

[1.] Sádecká. J., Polonský. J., *Journal of Chromatography A*, 2000, Volume 880, Issues 1–2,2, 243-279,
[2.] Arellano. M., El Kaddouri. S., Roques. C., et. al., *Journal of Chromatography A*, 1997, Volume 781, Issues 1–2, 26, 497-501
[3.] Molnár-Perl. I., *Journal of Chromatography A*, 2000, Volume 891, Issue 1, 1, 1-32
[4.] Peres. R.G., Moraes. E.P., *et al.*, *Food Control*, 2009, Volume 20, Issue 6, 548-552

P64 CASPASE 3 CHEMILUMINESCENCE ACTIVITY DETERMINATION IN APOPTOTIC CELLS AND DESIGN OF CASPASE 3 SENSOR

Marcela Liskova[a,b], Karel Kleparnik[a], Pavel Pazdera[b], Frantisek Foret[a]

[a] *Institute of Analytical Chemistry ASCR, v.v.i., Brno, Czech Republic, liskova@iach.cz*
[b] *Masaryk University, Faculty of Science, Centre for Syntheses at Sustainable Conditions and their Management, Brno, Czech Republic*

ABSTRACT

Apoptosis, or programmed cell death, is an essential physiological process that plays a critical role in development of tumor or autoimmune disorders. In some instances knowledges of this pathway can be used for inhibit or prevent cancer development and other diseases. One of the earliest and most consistent observed features of apoptosis is the induction of a series of cytosolic proteases – caspases. Active caspases cleave numerous intracellular proteins and contribute to apoptotic cell death. Caspases recognize tetra-peptide sequences Asp-Glu-Val-Asp on their substrates and hydrolyze peptide bonds after aspartic acid residues. It is known from literature that in one apoptotic cell about 1.6×10^{-19} mol of caspase can be activated. Various techniques for the determination of caspase 3 in free cells or tissue samples are commercially available. Caspase 3 activity is usually assayed by a chemiluminescence reaction. The best commercial methods reach the limit o detection higher than 1 pg of caspase 3. We have developed a special device for the determination of caspases activity in apoptotic cells. The activity of caspase 3 is determined by the system based on Luciferin/Luciferase chemiluminescence (CL) reaction. The luciferin modified with tetrapeptide sequence (DEVD) specific to the recognition for caspase 3 is cleaved to form free luciferin, which immediately reacts with luciferase to produce light. Laboratory built luminometer is based on Sens-Tech P25 USB photomultiplier tube (PMT) working at digital photon counting mode. The sample is placed in a highly polished cell made of stainless steel. The sensitivity of the device proved to be by three orders of magnitude better than the commercially available technologies. The objective of this paper is the design of a fluorescent sensor based on Förster resonance energy transfer (FRET) for the determination of caspase 3 in cell nucleus or cytoplasm as a result of the apoptotic process. We designed two fluorescent caspase 3 sensors.

Keywords: Caspase 3, apoptosis, chemiluminescence, FRET

1 INTRODUCTION

A few ways to determine caspase 3 in apoptotic cells can be found in literature. Well-known is flow-cytometry method, a laser based biophysical technology, employed in cell counting, sorting, biomarker detection and protein engineering. Labeled cells suspended in a stream of fluid are detected when passing an electronic detector. Another example is the enzyme-linked immunosorbent assay (ELISA) which use antibody-antigen interactions to determine and quantify caspase 3 in complex matrices. These methods are commercially well-established and frequently used. Very sensitive is the monitoring of caspase 3 activity. This principal provides simple, fast and cheap detection methods with no need of consecutive washing steps and any immobilized agents. We have developed two special devices for caspase 3 activity measurement, an optical cell for the measurement of chemiluminescence induced by caspase 3 cleavage of modified luciferin and selective sensor for the detection of caspase 3 inside apoptotic cells designed for an immediate imaging analysis by fluorescence microscopy.

1.1 Apoptosis and caspases

The morphological features of apoptosis include changes in plasma membrane asymmetry and attachment, condensation of cytoplasm, nucleus and internucleosomal cleavage of DNA. In the final stage cell gets converted into “apoptotic bodies” which is rapidly eliminated by phagocytosis without eliciting inflammation in the surrounding areas.

The core component of the apoptotic machinery is a proteolytic system involving a family of proteases known as caspases. Caspases are essential in cells for apoptosis, one of the main types of programmed cell death, in development and most stages of adult life. Failure of apoptosis results in the tumor development and autoimmune disorders. However uncontrolled apoptosis occur in ischemia and Alzheimer´s disease. This has boomed interest in caspases as potential therapeutic targets. The caspases are cysteine proteases which cleave the peptide bond C-terminal to aspartic acid residues [1.]. There are 14 members of the caspase family classified: apoptosis activator (caspases 2,8,9,10), apoptosis executioner (caspases 3,6,7) and inflammatory mediator (caspases 1,4,5,11,12,13,14). Caspases are expressed widely almost in all the cells as zymogens. Procaspases contain a highly homologous protease domain subdivided into two subunits: a) large subunit of approximately 20 kDa and b) small subunit of approximately 10 kDa. Active caspase-1 and -3 consist of large and small subunits, which are released from the procaspase through proteolytic processing, and both subunits are required for the protease activity. The activated caspases initiate a death program by destroying key components of cellular infrastructure and activate factors, which damage the cell [1., 2.]. Caspase 3, a cysteine-aspartic acid protease activated in the apoptotic pathway, is a key factor in apoptosis execution and is the active form of procaspase 3. Caspase 3 recognizes tetra-peptide sequences Asp-Glu-Val-Asp (DEVD). Caspase 3 active site contains a cysteine residue (Cys-285) and histidine residue (His-237) that stabilize the peptide bond cleavage of a protein sequence to the carboxy-terminal side of an aspartic acid.

1.2 Measurement of caspase 3 activity

Determination of caspase 3 activity is based on a tetrapeptide corresponding to substrate. After cleavage of tetrapeptide sequence, the free colorimetric (*p*-nitroaniline) or fluorogenic (7-aminocoumarin or 7-amino-4-trifluoromethylcoumarin) group is released and measured by spectrophotometric or fluorometric methods. This measurement procedure of caspase 3 activity takes place in cell lysates.

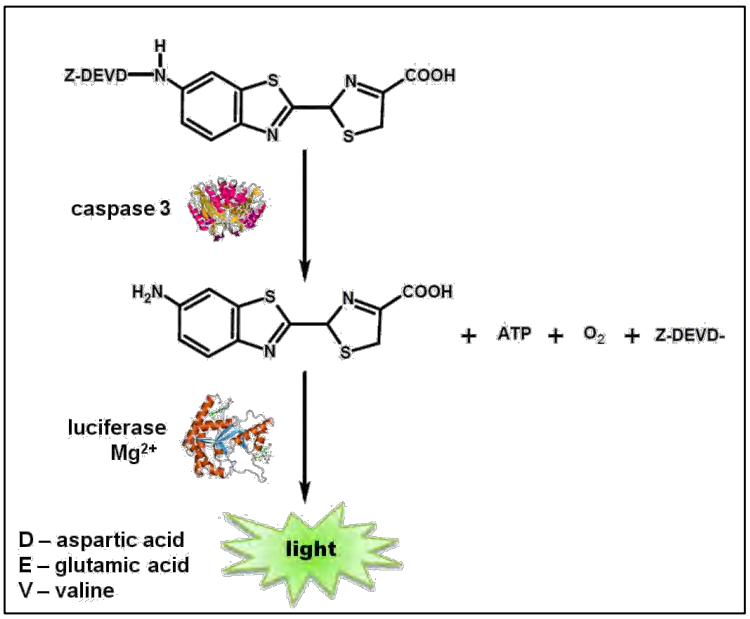

Fig. 1. : The biochemistry behind Caspase 3/7 activity measurement.

New method for very sensitive measurement of caspase 3 activity is using chemiluminescent system Caspase-Glo® 3/7 Assay (Fig. 1). This system provides a homogeneous chemiluminescent assay that measures caspase-3/7 activities. The assay provides a

proluminescent caspase-3/7 DEVD-aminoluciferin substrate and a proprietary thermostable luciferase in a reagent optimized for caspase 3/7 activity, luciferase activity and cell lysis. Adding the single Caspase-Glo® 3/7 Reagent in an "add-mix-measure" format results in cell lysis; followed by caspase cleavage of the substrate. This liberates free aminoluciferin, which is consumed by the luciferase, generating a "glow-type" chemiluminescent signal. The signal is proportional to caspase 3/7 activity. We used for caspase 3 activity determination laboratory built luminometer Sens-Tech P25 USB photomultiplier tube with digital mode (photon counting) see Experimental section.

1.3 Förster resonance energy transfer (FRET)

In this system, an energy absorbed by a chromophore (donor) is transferred non-radiatively to a fluorophore (acceptor) by dipole-dipole coupling through a linking chain (long-range 1-10 nm). The length of the chain determines the efficiency of the transfer. FRET is extensively exploited in biological research, in biomedicine diagnostics, biotechnological application, for distance determination studies, in vivo imaging [3, 4], probing the biological membrane organization and dynamics [5], examining of primary and secondary structure of DNA [6] etc. The nanoscale size and unique optical properties of semiconductor quantum dots (QDs) have made them attractive as central photoluminescent scaffolds for variety of biosensing platforms [4]. Modified QDs are very often used for FRET applications as a donor of transferred energy. Depending on the final application of sensor, different acceptors of transferred energy are used, fluorescent dyes (fluorophore), organic quenchers (chromophore) or gold nanoparticles. Principle of this method is very simple, QDs as a donor transfers absorbed energy at a given wavelength to an acceptor (chromophore, fluorophore) via linker chain. The transferred energy from QD can be quenched by some type of quencher (Au nanoparticles, organic dye) or emitted with different (longer) wavelength depending on the type of the used fluorescent dye.

2 EXPERIMENTAL SECTION

2.1 Chemiluminescence measurement

We have developed a special device for the determination of caspase 3 activity in apoptotic cells. Our detection device consists of a microfluidic chamber held inside a housing of photomultiplier tube (Sens-Tech P25 USB). A USB powered photodetector module includes a 25 mm diameter photomultiplier tube with a photocathode active from 280 to 630 nm. This photodetector module is operated in the photon counting mode. Photon Counting is the most sensitive method for measuring of ultra low light levels. The sample cells of volumes 5, 15 and 30 µl are made of highly polished stainless steel (Fig. 2). The sensitivity of the device proved to be by three orders of magnitude better than the commercially available technologies [7].

Fig. 2. : A) Laboratory built luminometer, B) highly polished sample cell made of stainless steel.

2.1.1 Reaction protocol

A portion of 15 µl of cell suspension with evaluated number of cells was well mixed with 15 µl of Caspase-Glo® 3/7 Assay (Promega, Madison, WI. A part of 20 µl of this mixture was injected into a specially designed chamber of a volume of 30 µl made of stainless steel. The highly polished inner surface and conical shape of the chamber are designed to reflect all the luminescence to PMT detection window. The CL emission was monitored immediately after mixing for a period of 1 h, sufficient to catch the steady-state plateau of the signal. The maximum signal was taken as a representative value proportional to the amount of caspase 3. After each experiment, the chamber was washed by acetonitrile and water [8]. We used mouse embrionic apoptotic cells treated by camptothecin for the determination of the peak of apoptosis process and for the determination of inhibitor *Z*-Asp(O-Me)-Glu(O-Me)-Val-Asp(O-Me) fluoromethyl ketone (FMK) efficiency to inhibit caspase 3 activity in apoptotic cells. FMK is a cell permeable, non-toxic inhibitor which can irreversibly bind to activated caspase 3 in apoptotic cells.

2.1.2 Sensor synthesis

We used CdTe QDs with maximum emmision wavelength 600 nm and with mercaptopropionic acid as a surface ligand. A one-step synthesis described elsewhere [9] was used for QDs preparation. For organic quencher preparation was used synthesis described in US patent [10]. As a linker chain were used 12-bromo-1-dodecanol (99%) and *O*-(3-Carboxypropyl)-*O'*-[2-(3-mercaptopropionylamino)ethyl]-polyethylene glycol (PEG) (M_w 3000). DEVD sequence was *N*-Acetyl-Asp-Glu-Val-Asp *p*-nitroanilide (97%) and this DEVD sequence was modified for further reaction in two ways. First *p*-nitroanilide end of DEVD sequence was reduced by moderate reduction agent $Na_2S_2O_4$ in $KHCO_3$. Second modification was deacetylation of terminal *N*-acetyl group via Penicillin amidase from Escherichia coli (M_r ~70000). Starting materials were purchased from Sigma-Aldrich (St. Luis, MO, USA) and were used without further purification.

3 RESULTS AND DISCUSSION

Peak of caspase 3 was successfully detected in experimental group and compared with control group. After 6 h of camptothecin treatment, content of caspase 3 in experimental and control group started to differentiate. Maximum presence of caspase 3 was achieved between 8- and 10-h intervals.

The efficiency of FMK inhibitor during long time cultivation of cells (camptothecin treatment with FMK) was constant for 48 h. The amount of caspase 3 was even determined lower than in control group (without treatment), because there are always some of apoptotic cells giving a slight caspase 3 positive signal in control group.

We designed two sensors based on FRET (Fig.3): sensor based on the change of wavelength of emitted light and sensor based on quenching of fluorescence. The principle of sensor based on quenching of fluorescence is irradiation of QD with some source of light at given wavelength. This energy is transported nonradiatively via linker chain to quencher. The transported energy is quenched by a modified BHQ-2 quencher. However, after the cleavage of the bond between quencher and DEVD sequence by caspase 3 present in analyzed samples, there is no non-radiative FRET transfer, quencher doesn´t absorb and QD emits light at given wavelength.

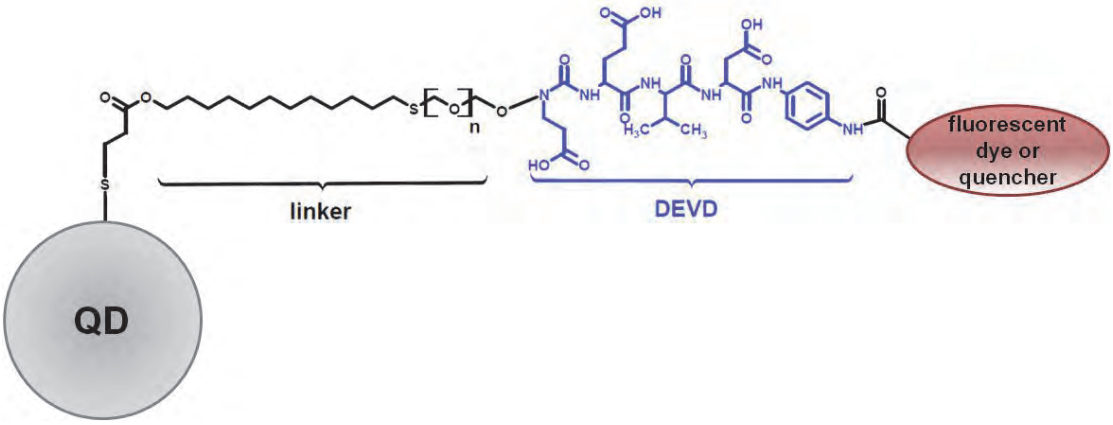

Fig. 3. : Model of caspase 3 sensor with DEVD sequence.

QDs were modified for DEVD bonding by long linker chains of 12-bromo-1-dodecanol and PEG. All reaction steps were checked by capillary zone electrophoresis with LIF detection. Quencher was successfully synthesized according US patent [10]. We have solved problems with QDs precipitation during synthesis and specified optimal Förster distance between QD and quencher for efficient FRET.

ACKNOWLEDGEMENTS

This work was supported by The Grant Agency of the Czech Republic (GA203/08/1680, P301/11/2055 and P206/11/2377), Ministry of Industry and Trade (2A-1TP1/090), Ministry of Education, Youth and Sports (OP Education for Competitiveness-CZ. 1.07/2. 3 00/20. 0182) and institute research plan AV0Z40310501.

LITERATURE

[1.] Rupinde, S. K., Gurpreet, A. K., Manjeet, S., *Vascular Pharmacology* 2011, 400, 369-379.
[2.] Fan, T. J., Han, L-H., Cong, R-S., Liang, J., *Acta Biochimica et Biophysica Sinica* 2005, 37, 719-727.
[3.] Hillisch, A., Lorenz, M., Diekmann, S., *Curr Opin Struc Biol* 2001, 11 ,201-207.
[4.] Prasuhn, D. E., Felt, A.,Menditz, L., et.al., *ACS Nano* 2010, 40, 5487-5497
[5.] Struck, D. K., Hoekstra, D., Pagano, R. E., *Biochemistry-Us* 1981, 20, 4093-4099.
[6.] Clegg, R. M., Murchie, A. I. H., Zechel, A., Lilley, D. M. J., *P Natl Acad Sci USA* 1993, 90, 2994-2998.
[7.] http://www.sens-tech.com/products/modules/usb-modules/
[8.] Chlastakova, I., Liskova, M., Kudelova, J., Dubska, L., Kleparmik,K., Matalova, E., *In Vitro Cellular and Development Biology- Animal*, Online FirsTM, DOI 10.1007/s11626-012-9542-8
[9.] Duan, J., Song, L., Zhan, J., *Nano Res* 2009, 2, 61-68.
[10.] Gharavi *et al.*, *US 7205347 B2* 2007

P65 IRON OXIDE NANOPARTICLE MODIFIED MONOLITHIC PIPETTE TIPS FOR SELECTIVE ENRICHMENT OF PHOSPHOPEPTIDES

Jana Krenkova, Frantisek Foret

Institute of Analytical Chemistry of the AS CR, v.v.i., Veveri 97, 602 00 Brno, Czech Republic, krenkova@iach.cz

ABSTRACT

We have developed iron oxide nanoparticle modified monolithic pipette tips for selective and efficient enrichment of phosphopeptides. Iron oxide nanoparticles were synthesized using a co-precipitation method and stabilized by citrate ions. A stable coating of nanoparticles was obtained via multivalent interactions of citrate ions on the nanoparticle surface with a quaternary amine functionalized surface of the methacrylate based monolithic tips. The performance of the developed and commercially available tips was demonstrated with the enrichment of phosphorylated peptides from tryptic digests of caseins followed by MALDI/MS detection.

Keywords: iron oxide nanoparticles; monolith; phosphopeptide enrichment

1 INTRODUCTION

Sample preparation represents a key step in phosphoproteomic analysis [1]. The selective enrichment of phosphopeptides is almost always required before their mass spectrometric analysis due to low ionization efficiency of phosphopeptides in the presence of non-phosphorylated counterpart. Several selective methods have been developed, mainly based on the immobilized metal ion affinity chromatography (IMAC) or metal oxide affinity chromatography (MOAC) [2].

Recently, we have developed the iron oxide nanoparticle coating of the monolithic capillary columns for protein separation and phosphopeptide enrichment [3, 4]. However, the capillary format is not very well suitable for routine use in proteomic laboratories. Therefore, the developed technologies were modified and transformed in the pipette tip format and used for selective and efficient enrichment of phosphopeptides.

2 PREPARATION AND CHARACTERIZATION OF IRON OXIDE NANOPARTICLE MODIFIED MONOLITHIC TIPS

A poly(hydroxyethyl methacrylate-co-ethylene dimethacrylate) monolith was prepared in 200-µL pipette tips by UV-initiated polymerization. The pore surface of the monolith was modified by [3-(methacryloylamino)propyl]trimethylammonium chloride using a two-step photografting method. In the final step, the 20-nm iron oxide nanoparticles synthesized by a co-precipitation method were attached to the monolithic surface via interactions of citrate ions on the nanoparticle surface with a quaternary amine functionalized surface of the methacrylate based monolithic tips. The multivalent interaction provides a very stable coating of iron oxide nanoparticles on the monolithic surface.

The monolithic tips were characterized by SEM/EDAX and the analysis confirmed the presence of carbon (65.4 wt%), oxygen (30.9 wt%), and iron (3.7 wt%). In contrast, the monolithic bed before the attachment of nanoparticles contained only carbon (57.8 wt%) and oxygen (42.2 wt%).

3 PHOSPHOPEPTIDE ENRICHMENT AND MASS SPECTROMETRIC ANAYSIS

Tryptic digests of β- and α-caseins were used to examine the selectivity of iron oxide nanoparticle modified monolithic tips to phosphorylated peptides. A solution of 1% acetic acid,

pH 2.7 containing 20 % acetonitrile was used as the binding/washing solution and phosphopeptides were eluted using a 10% solution of ammonium hydroxide.
β-casein contains five phosphorylation sites and its tryptic digest is expected to generate two phosphopeptides; however, more phosphorylated fragments containing miss cleavages are usually obtained. Although low intensity signals of three phosphopeptides were detected by direct MALDI/MS analysis, non-phosphorylated peptides dominate the spectrum (Fig. 1.). After enrichment using the iron oxide nanoparticle modified tip, the signals of non-phosphorylated peptides significantly decreased and 6 phosphopeptides were detected in the MS spectra. On the other hand, only 2 phosphopeptides were enriched using a titanium dioxide tip with a significantly larger number of non-phosphorylated peptides detected in the MS spectra in comparison to the nanoparticle modified monoliths.

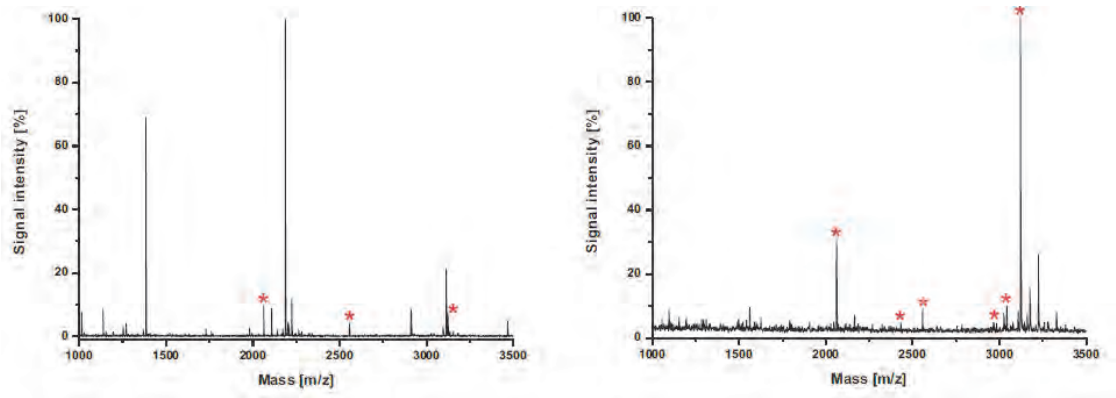

Fig. 1. MALDI/MS spectra of β-casein tryptic digest before (left) and after (right) phosphopeptide enrichment using the iron oxide nanoparticle modified tip. Peaks with an asterisk represent phosphorylated peptides.

To further evaluate the selectivity of the nanoparticle modified monolithic tips, a more complex tryptic digest of α-casein was enriched (Fig. 2.). When analyzed directly without enrichment, only 4 phosphopeptides of α-casein were observed in the MS spectra. However, 11 phosphopeptides were selectively isolated from the digest of α-casein using the iron oxide nanoparticle modified tip. As a control, a commercially available titanium dioxide tip was used for phosphopeptide enrichment and only 4 phosphopeptides were observed in the MS spectra and a significantly larger number of non-phosphorylated peptides were detected in comparison to the nanoparticle modified tips again.

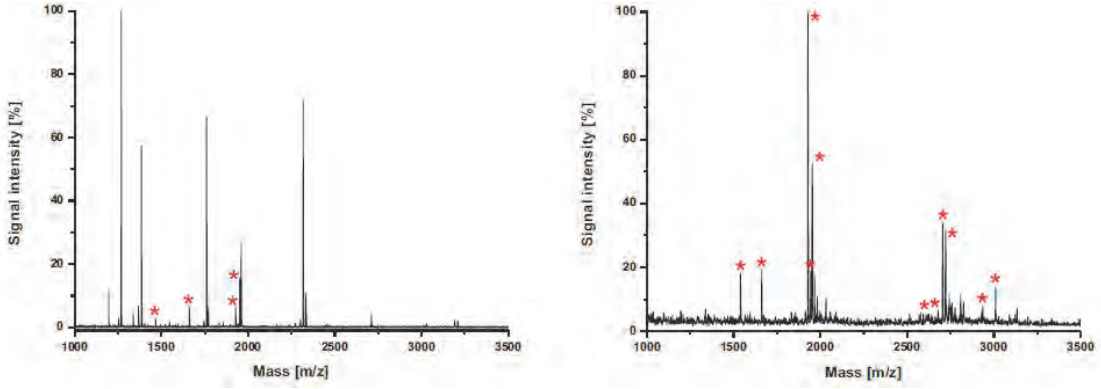

Fig. 2. MALDI/MS spectra of α-casein tryptic digest before (left) and after (right) phosphopeptide enrichment using the iron oxide nanoparticle modified tip. Peaks with an asterisk represent phosphorylated peptides.

In summary, we have developed the iron oxide nanoparticle modified monolithic bed in the pipette tips, which was successfully applied for selective enrichment of phosphopeptides. In comparison to the commercially available titanium dioxide tip, the nanoparticle modified monolith provides significantly better selectivity to phosphorylated peptides. Due to the ease of use, small sample and solvent consumption, and the possibility to process many samples simultaneously using robotic systems or multi-channel pipettes, the nanoparticle modified monoliths formed in the pipette tips represent a powerful tool for phosphoproteomic analysis.

ACKNOWLEDGEMENTS

The Project is funded from the SoMoPro programme. Research leading to these results has received a financial contribution from the European Community within the Seventh Framework Programme (FP/2007-2013) under Grant Agreement No. 229603. The research is also co-financed by the South Moravian Region. Additional financial support from the Grant Agency of the Czech Republic (P301/11/2055 and P206/12/G014) and the institutional research plan (RVO: 68081715) is also acknowledged.

LITERATURE

[1.] Thinghom, T. E., Jensen, O. N. and Larsen, M. R., *Proteomics* 2009, *9*, 1451-1468.
[2.] Leitner, A., *Trends in Analytical Chemistry* 2010, *29*, 177-185.
[3.] Krenkova, J., Lacher, N. A. and Svec, F., *Analytical Chemistry* 2010, *82*, 8335-8341.
[4.] Krenkova, J. and Foret, F., *Journal of Separation Science* 2011, *34*, 2106-2112.

P66 4-METHYLCOUMARINS AND THEIR IN VITRO PLATELET ANTIAGGREGATORY ACTIVITY

Jana Karlíčková[a], Přemysl Mladěnka[b], Kateřina Macáková[a], Zuzana Řeháková[a], Tomáš Filipský[b], Michal Říha[b], Ashok K. Prasad[c], Virinder S. Parmar[c] , Luděk Jahodář[a], Radomír Hrdina[b], Luciano Saso[d]

[a] *Department of Pharmaceutical Botany and Ecology, Faculty of Pharmacy, Charles University in Prague,Heyrovského 1203, 500 05 Hradec Králové, Czech Republic, jana.karlickova@faf.cuni.cz*

[b] *Department of Pharmacology and Toxicology, Faculty of Pharmacy in Hradec Králové, Charles University in Prague, Heyrovského 1203, 500 05 Hradec Králové, Czech Republic*

[c] *Bioorganic Laboratory, Department of Chemistry, University of Delhi, Delhi 110 007, India*

[d] *Department of Physiology and Pharmacology "Vittorio Erspamer", Sapienza University of Rome, Piazzale Aldo Moro 5, Rome, Italy*

ABSTRACT

Coumarins were documented to possess a row of potentially positive pharmacological activities. In particular, some coumarins are antiaggregants. However, there are marked differences among different studies. In this set of experiments, 18 different 4-methylcoumarins were tested for their antiplatelet activity.

5,7-Dihydroxymethylcoumarins were the most potent antiplatelet substances and reached the potency of acetylsalicylic acid. In addition, ethoxycarbonylmethyl and ethoxycarbonylethyl substitution appeared to increase the effect.

Keywords: coumarin, platelet, antiaggregatory

1 INTRODUCTION AND AIM OF THE STUDY

Coumarins are natural compounds sharing 1,2-benzopyrone structure. They were isolated from various plants, especially from Apiaceae, Rutaceae and Asteraceae families. Several studies suggested their positive pharmacological properties, e.g.antioxidant, anti-inflammatorory, antiagregant, hepatoprotective, lipid lowering and vasorelaxing effects. Such properties could be useful for the treatment and prevention of cardiovascular diseases [1].

The aim of this study was to test a series of simple natural and synthetic 4-methylcoumarins for their antiplatelet activity.

2 EXPERIMENTAL

2.1 Materials

Arachidonic acid (AA), adenosine diphosphate (ADP) and collagen were purchased from Chrono-Log Co. (Havertown, Pennsylvania, USA), and sodium citrate solution from Biotika (Slovenska Lupca, Slovakia). Scopoletin, umbelliferone and scopolin were earlier isolated from *Evolvulus alsinoides* at the Department of Pharmaceutical Botany and Ecology, Faculty of Pharmacy in Hradec Králové, Charles University in Prague, Czech Republic [2]. Dimethyl sulphoxide (DMSO), acetylsalicylic acid (ASA), dipyridamole and 4-hydroxycoumarin were purchased from Sigma-Aldrich (Germany). All other 4-methylcoumarins were synthesized at the Department of Chemistry, University of Delhi, India [3].

Blood samples from healthy non-smoking volunteers were collected by venipuncture into plastic disposable syringes containing 3.8% sodium citrate (1:9, V/V).

The study was performed under the supervision of the Ethical Committee of Charles University in Prague, Faculty of Pharmacy in Hradec Králové and conforms to the Declaration of Helsinki.

2.2 Methods

Platelet rich plasma (PRP) was obtained as a supernatant by centrifugation of the collected blood for 10 min at 500 g (centrifuge Boeco U-32R, rotor Hettich 1611, Germany). Platelet poor plasma (PPP) was prepared by centrifugation of the remaining blood for 10 min at 2 500 g. The platelet count was calculated using a BD Accuri C6 flow cytometer equipped with BD CFlow Software (BD Accuri Cytometers Inc., USA) and adjusted to 2.5 x 10^8 platelets/ml.

Platelet aggregation was determined by turbidimetry by means of a Chrono-log 500-Ca aggregometer with a computer (Aggro/Link software, Chrono-Log Co., USA) according to the previously published method [4]. Platelet aggregation was induced by the addition of either AA (final concentration 0.5 mM), ADP (10 mM) or collagen (2 mg/ml). The aggregation process was monitored for 5 min.

2.3 Statistical analysis

All data are presented as mean ± SD. Antiaggregation potencies of individual substances are expressed as IC_{50} values (concentration providing 50% inhibition of platelet aggregation). The effects of the substances were compared by ANOVA, followed by Dunnett's multiple comparison test (GraphPad Prism 5.0, GraphPad Software, San Diego, California, USA) at the level of statistical significance, $p < 0.05$.

3 RESULTS

5,7-Dihydroxy-4-methylcoumarins reached the activity of ASA on AA-induced aggregation and were as well the most active on collagen-induced aggregation. Their effect on AA-induced aggregation was comparable of that of ASA however their effect on collagen-based aggregation was rather low. Analogues containing the lipophilic side chain at C-3 (ethoxycarbonylmethyl or ethoxycarbonylethyl) appeared to increase the activity. Other substitutions including o-dihydroxycoumarins were apparently markedly less efficient.

None of the tested coumarins were able to substantially inhibit ADP-induced aggregation.

4 CONCLUSION

Ethoxycarbonylmethyl and ethoxycarbonylethyl derivatives of 5,7-dihydroxymethylcoumarins seem to be promising antiplatelet agents.

ACKNOWLEDGEMENTS

This study was supported by the grant from the Czech Science Foundation 130/11/1104.

LITERATURE

[1.] Fylaktakidou, K. C., Hadjipavlou-Litina, D. J., Litinas K.E., Nicolaides D. N., *Current pharmaceutical design* 2004, *10*, 3813-3833.

[2.] Cervenka, F., Koleckar, V., Rehakova, Z., *et al. Journal of Enzyme Inhibition and Medicinal Chemistry* 2008, *23*, 574-578.

[3.] Parmar, V. S., Singh, S., Boll, P. M., *Magnetic Resonance in Chemistry* 1988, *26*, 430-433.

[4.] Born, G. V., *Nature* 1962, *194*, 927-929.

P67 A SIMPLE DEVICE FOR QUANTITATION OF CASPASE 3 IN INDIVIDUAL APOPTOTIC EMBRYONIC CELLS

Jitka Hegrová[a], Karel Klepárník[a], Jan Přikryl[a], Marcela Lišková[a], Eva Matalová[b], František Foret[a]

[a]*Institute of Analytical Chemistry ASCR, v.v.i., Veveri 97, 60200 Brno, Czech Republic*
[b]*Institute of Animal Physiology and Genetics ASCR, v.v.i., Brno, Czech Republic*
klep@iach.cz

ABSTRACT

A newly developed system for the determination of Caspase 3 activity in individual apoptotic embryonic cells is described. Caspase 3, a cysteine-aspartic acid protease activated in the apoptotic pathway, plays an essential role in the programmed cell death. Moreover, failure of apoptosis is one of the main contributions to tumor development. It is known from literature and confirmed by our results that in one apoptotic cell about 1.6×10^{-19} mol of Caspase can be activated. The caspase activity is determined by the luminescent Caspase-Glo™ 3/7 assay system based on Luciferin/Luciferase chemiluminescence reaction. The luciferin modified with tetrapeptide sequence Asp-Glu-Val-Asp (DEVD) specific to the recognition for Caspase-3 is cleaved to form free luciferin, which immediately reacts with luciferase to produce light. The absence of photoexcitation, and therefore no interference of the scattered excitation light with the emission signal, represents the most important advantage of chemiluminescence for single-cell analysis.

Keywords: single cell, chemiluminiscence, Caspase 3

1 INTRODUCTION

Single-cell analysis (SCA) has been increasingly recognized as the key technology for the elucidation of cellular functions, which are not accessible from bulk measurements on the population level [1]. SCA let researchers track and catalogue this heterogeneity. They may be the only way to get at some fundamental questions, such as what makes individual cells different biochemically and functionally. How much is each cell influenced by its microenvironment, and what is the role of stochasticity random 'noise' in the behavior of cellular molecules? Many established techniques are being applied to single cells. Fluorescent tagging and microscopy can be used to analyze molecules that have already been characterized [2]. Analyses of individual cells or even the cell organelles can reveal an effect of cell-cycle, different life conditions, and surrounding environment on the genome, proteome, peptidome, metabolome, etc. The development of analytical techniques and methodology for SC metabolomics were reviewed by several authors. While the detection of chosen components in targeted analysis can rely on fluorescent probes, a comprehensive approach requires label-free methods like MS. Extremely high sensitivity of chemiluminiscence (CL) stems from several reasons. An interference of scattered excitation light, back-ground fluorescence of other species present in the sample, as well as any photobleaching can be excluded. Moreover, as low but long-lasting generation of photons is amenable to the application of the photon-counting detection regime, the most sensitive method for the quantitative measurement of light. Conventional photomultiplier tube (PMT) with nanosecond time resolution furnished with fast electronics enabling a gigahertz acquisition of the signal can be used as detection elements. Another advantage of this instrumentation is an easy processing of digital signal which can easily be discriminated from the dark signal and other interfering phenomena. Apoptosis is an essential physiological process whereby cells die in a controlled and regulated fashion. Central to the process of apoptosis, is a family of proteolytic enzymes known as caspases [3]. Fourteen members of

the caspase family of aspartate-specific thiol proteases have been identified [4]. Caspases 2, 3, 6, 7, 8, 9, 10, and 12 are involved in the process of apoptosis. Caspase-3 along with caspase-6 and caspase-7 belongs to a death trio of executioner proapoptotic caspases and is considered as the central caspase representing the point of no return [5]. Apoptosis is a major form of cell death, used to remove unwanted or excess cells [6]. Induction of apoptosis as an activity response to cell damage or stress response plays a role allowing recycling of monomers [7]. Caspase-3 is one of the important "executioner" caspase enzymes, triggering the cleavage of numerous proteins that lead to the ordered breakdown of the cell. The detection of caspase-3 activation is frequently used as a positive marker for apoptosis [8].

2 MATERIALS AND METHODS

The Eppendorf micromanipulator and Olympus microscope IX 71 were used for the micromanipulation and cell transfer. A series from 1 to 4 apoptotic cells were sucked into a capilary and transferred on a small piece of microscope slide (Fig.1A). The piece was inserted into the glass vial of a volume about 15 µl. A volume of 10 µl of Caspase-Glo™ 3/7 Assay (Promega, Madison, WI) reagent was added. Glass vial was fixed in a specially designed detection chamber. The highly polished inner surface and conical shape of the chamber are designed to reflect maximum of the luminescence to the PMT (P 25 USB, Sens-Tech, UK) with counting sensitivity at 400 nm. The chemiluminescence (CL) emission was monitored immediately after adding of assay for a period of forty minutes, sufficient to catch the plateau of the signal. The maximum signal was taken as a representative value proportional to the amount of caspase-3. After each experiment, the glass vial was consecutively washed by acetone and water and dried.

3 RESULTS AND DISCUSSION

The experimental design involved several steps. First, quantification of active caspase-3 was followed in the control group (without any treatment) and experimental group (camptothecin treatment) to detect the caspase-3 activation peak. Samples were collected and measured before initialization of the cultures, prior to addition of camptothecin and then in 1-h intervals. Caspase-3 activation peak was detected in the experimental group treated with camptothecin as compared with the control group without any treatment. The difference between control and experimental groups started to be clearly apparent 6 h after camptothecin treatment, and the peak was achieved and maintained between 8-h and 10-h intervals [9].

The second step, quantification of active caspase-3 was followed in the experimental groups (1-4 cells) treated by camptothecin. About fifteen repetition of each group were measured and statistically calculated. We can say that in one apoptotic cell treated with camptothecin is about 5 fg of caspase 3. Then other two types of apoptotic cells (cells of interdigital region and stem cells) were measured. In fig.1B is showed the differentiation between these types of cells. The cells of intermediate region take the smallest signal of caspase activation. These cells are naturally apoptotic, not treated with camtothecin. The signal to noise ratio is defined as: (mean signal - mean background)/standard deviation of the background. Detection limit of this method is four fg of Caspase 3. The limit of detection for a caspase assay can be defined as a signal-to-noise ratio of 3 (i.e. the amount of caspase activity giving a value at least 3 standard deviations above the background). Amount of Caspase 3 were determined from calibration curve. The calibration standards were prepared from human Caspase 3 Instand Elisa standard (Bender MedSystems GmbH, Austria). Maximum sensitivity is achieved once the caspase and luciferase activities reach steady state. Steady state, and thus maximum signal, is reached in approximately thirty minutes - one hour. The precise time to reach maximum signal will depend on the assay system and culturing conditions.

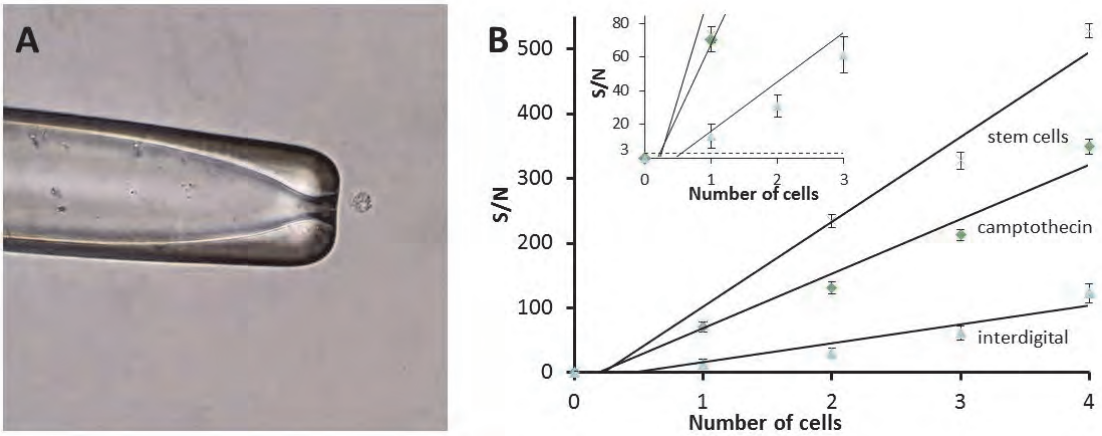

Fig.1: Manipulation with single embryonic cell (A) Dependency of S/N (signal to noise ratio) on number of cells.

ACKNOWLEDGEMENTS

This work was supported by The Grant Agency of the Czech Republic, grants # 206/11/2377, P301/11/2055 and P206/11/P002 and institutional support RVO: 68081715.

LITERATURE

[1] Fritzsch, F. S. O., Dusny, Ch., Frick, O., Schmidt, A., *Systems Biology, and Biocatalysis. Annual Review of Chemical and Biomolecular Engineering* 2012, 3, 129-155

[2] Schubert, Ch., *Nature* 2011, 480, 133-137

[3] Thornberry, N. A., Rano, T.A., Peterson, E. P., Rasper, D. M., Timkey, T., Garsia-Calvo, M., Houtyager, D. M., Roy, S., Vaillancourt, J. P., *et al.*, *J. Biol. Chem.* 1997, 272, 17907–17911

[4] Thornberry, N. A., Lazebnik, Y., *Caspases: Enemies within.Science* 1998, 28,11312–1316

[5] Kroemer, G., Galluzzi, L., Vandenabeele, P., Abrams, J., Alnemri, E. S., *et al.*, *Cell Death Differ*. 2009, *16(1),* 3–11

[6] Kohler, C., Gogvadze, V., Hakansson, A., Svanborg, C., Orrenius, S., Zhivotovsky, B., *Eur.J.Biochem*. 2001, *268,* 186-191

[7] Yao, T., Cohen, R. E., *Nature* 2002, 419(6905), 403-407.

[8] O´Brien, M. A., Daily, W. J., Hesselberth, P. E., Moravec, R. A., Scurria, M. A., Klaubert, D. H., Bulleit, R. F., Wood, K. V., *J Biomol Screen* 2005, 10, 137-148

[9] Chlastakova, I., Liskova, M., Kudelova, J., Dubska, L., Kleparnik, K., Matalova, E., *In Vitro Cell.Dev.Biol.—Animal*, 31 July 0122, DOI 10.1007/s11626-012-9 542-8

P68 HEXADECENAL ANALYSIS BY 5,5-DIMETHYLCYCLOHEXANEDIONE DERIVATIZATION FOR S1P LYASE ASSAY IN HPLC-FLUORESCENCE DETECTION

Kyong-Oh Shin, Cho-Hee seo, Yong-Moon Lee

College of Pharmacy, Chungbuk National University, Chongju 361-763, Korea,
ymleefn@hanmail.net

ABSTRACT

Sphingosine-1-phosphate (S1P) is a sphingolipid signaling molecule crucial for cell survival and proliferation. S1P lyase (S1PL) is the only known enzyme that irreversibly degrades sphingoid base-1-phosphates to phosphoethanolamine and the corresponding fatty

aldehydes. S1PL-mediated degradation of S1P results in the formation of (2E)-hexadecenal, whereas hexadecanal is the product of dihydrosphingosine-1-phosphate (DHS1P) degradation. We have devised an assay using a commercially available C17 DHS1P substrate. This substrate degrades pentadecanal and phosphoethanolamine. We have developed a simple, highly sensitive protocol for pentadecanal quantitation as a 5,5-dimethyl cyclohexanedione (5,5-dimethyl CHD) derivative by high performance liquid chromatography fluorescence detector (HPLC-FLD). We optimized derivative reaction as reaction time and reaction temperature and 5,5-dimethyl CHD, acetic acid, ammonium acetate concentration. The reaction is linear over 20 min and total protein concentrations of 10-50 µg. in this method SPL levels as low as 4 pmol/mg/min were readily detected. The SPL-catalyzed reaction is linear over a 30 min time period and yields a *K*m of 2.68 µM for C17 DHS1P.

To confirm our new methods, we assay the SPL level of different cell lines in F9-0, normal cell and F9-2 cell, S1PL knock down and F9-4 cell, S1PL overexpression. Furthermore, we treated F9-4 cells with different SPL inhibitor as FTY720 and 2-Acetyl-5-tetrahydroxybutyl Imidazole (THI), which competitively inhibits pyridoxal-5-phosphate (P5P), an essential cofactor for SPL activity, and observed a significant decrease in pentadecanal relative to the untreated cells.

In conclusion, we developed of the high sensitivity of HPLC-FLD and use of commercially available internal standard for pentadecanal quantification, heptadecanal, to develop a simple, sensitive protocol for characterization of S1PL activity in vitro.

Keywords: S1P lysase, 5,5-dimethylcyclohexanedione, HPLC-FLD

1 INTRODUCTION

The bioactive sphingolipid sphingosine 1-phosphate (S1P) regulates cellular processes such as cell proliferation, differentiation, migration and cell death. S1P signals through a family of five G protein-coupled membrane receptors(GPCRs) which regulate complex physiological processes such as vascular maturation and lymphocyte circulation. S1P levels in our body seem to be controlled three typical enzymes; S1P synthesis by sphingosine kinases (type I and II) and S1P degradations by S1P lyase and S1P phosphatase. S1P lyase is an ER membrane protein which catalyzes the irreversible cleavage of S1P at the C2-C3 carbon-carbon bond, resulting in reduction of S1P and yielding (E)-2-hexadecenal and ethanolamine phosphate. S1P lyase also can degrade dihydro-S1P (DHS1P) resulting in the formation of hexadecanal. The pharmacological inhibition of S1P lyase by THI produced lymphopenia in mice, which may be useful in the treatment of autoimmune diseases. Therefore, S1P lyase has emerged as a novel therapeutic target in a variety of immune-related diseases and thus studies in pharmaceutical modulation of S1P lyase activity could be useful in a therapeutic context. S1P lyase activity has been measured using radioactive, fluorescent substrates. In initial study, the incubation of enzyme with [4,5-3H] DHS1P yields its radioactive aldehyde which was separated by thin-layer chromatography and then quantified by radiometric facility. However, the use of radioactive substrate requires multiple cumbrous separation steps such as phase separation and a scraping the tritium-labeled reaction products from thin layer chromatographic plate. The fluorescent substrates such as 7-nitrobenz-2-oxa-1,3-diazol S1P (NBD-S1P), 4,4-difluoro-4-bora-3a,4a-diaza-s-indacene S1P (BODIPY-S1P) and coumarinic DHS1P analogue were employed to enhance the detectability by fluorescent monitoring of S1P lyase products. However, the use of fluorescent substrates, the appearance of multiple fluorescent byproducts or higher Km value becomes a main disadvantage of each method. Recently, to overcome these disadvantage, chemical derivatization method specific for aldehyde product was introduced which producing strong fluorophores such as semicarbazone, 2-diphenylacetyl-1,3-indandion-1-hydrazone (DAIH) and perfluorobenzyloxime (PFBO) derivatives. Here, we introduce a new fluorogenic derivatization method applying 5,5-dimethylchclohexane-1,3-dione (dimedone) derivatization for selectively detecting an aldehyde product by S1P lyase. To avoid possible interference by endogenous

fatty aldehydes, we used C17-dihydrosphingosine 1-phosphate (C17-DHS1P) as a substrate disintegrated into phosphoethanolamine and pentadecanal by S1P lyase. Heptadecanal as an internal standard which having odd number of carbon atoms and separated well from pentadecanal on a chromatogram was used. For high sensitive quantification, dimedone derivatization products of pentadecanal and heptadecanal were analyzed by HPLC equipped fluorescence detector holding excitation wavelength at 366 nm and emission wavelength at 455 nm.

2 RESULTS AND DISCUSSION

Statical data of variety concentrations of quality control samples of pentadecanal (n=4) determined by HPLC-FLD using C18 reverse phase column. S1PL activity as a function of substrate concentration. The S1PL reaction was performed for 20 min with variable amounts of C_{17} Sa1P and 50 µg of cell lysates protein. The reaction was stopped by 200 µL of ethanol and 5,5-dimethyl CHD solution with the addition of 100 pmol of heptadecanal as the internal standard. K_m (2.68 µM) and V_{max} (182.43 pmol / mg protein / min) values were calculated from the Michaelis menten equation. Aldehyde-5,5-dimethyl CHD was extracted with solid phase extraction and analyzed using C18 reversed-phase HPLC. The data represent means ± SD of triplicate analyses.

Table 1: . Statical data of variety concentrations of quality control samples of pentadecanal (n=4) determined by HPLC-FLD using C18 reverse phase column.

	Back calculation of pentadecanal								
pmol	2.5	5	10	25	50	100	250	500	1000
Ratio Ave.	0.02	0.04	0.06	0.08	0.14	0.24	0.49	0.96	1.9
Ratio S.D.	0	0	0	0	0	0	0	0.01	0.03
Mean	2.34	4.76	10.71	26.58	53.77	107.7	243.56	487.8	983
S.D.	0.03	0.04	0.11	0.23	0.68	0.34	1.32	3.45	5.85
Accuracy (%)	93.60	95.29	107.10	106.34	107.54	107.70	97.43	97.56	98.3
precision (%)	1.28	0.84	1.03	0.87	1.26	0.32	0.54	0.71	0.60

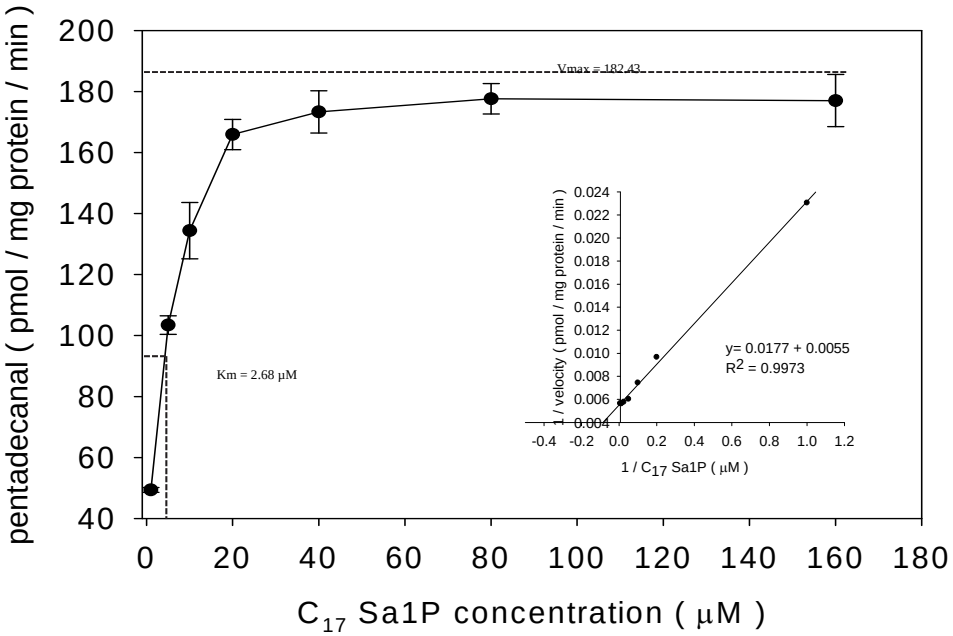

Fig. 1. : S1PL activity as a function of substrate concentration.

ACKNOWLEDGEMENTS

This study was supported by a research grant from the Chungbuk National University 2009 and by the NRF grants (MRC,2012-0029483; NRF-2012-0008046).

LITERATURE

[1] Saba, J.*, and T. Hla.* 2004*. Point-counterpoint of sphingosine 1-phosphate metabolism.* Circ. Res. 94**:** 724–*734.*

[2] Spiegel, S.*, and S. Milstien.* 2003*. Sphingosine-1-phosphate: an enigmatic signalling lipid.* Nat. Rev. Mol. Cell Biol. 4**:** 397–*407.*

[3] Hla, T. 2001*. Sphingosine 1-phosphate receptors.* Prostaglandins Other Lipid Mediat. 64**:** 135–*142.*

P69 SEPARATION OF CLINICALLY SIGNIFICANT MICROORGANISMS FROM CEREBROSPINAL FLUID BY CIEF WITH UV DETECTION AND MALDI-TOF MS

Marie Horká[a], Jiří Šalplachta[a], Anna Kubesová[a], Filip Růžička[b], Karel Šlais[a]

[a] Institute of Analytical Chemistry Academy of Sciences of the Czech Republic, v. v. i., Veveří 97, 602 00 Brno, Czech Republic

[b] Department of Microbiology, Faculty of Medicine, Masaryk University Brno, Pekařská 53, 656 91 Brno, Czech Republic

ABSTRACT

The identification of most of the clinically significant species by the conventional laboratory methods is still time-consuming and often insufficient for ensuring early targeted therapy. This is especially important in the case of the nosocomial infections where the number of

microorganisms in the cerebrospinal fluid is often ranging from units up to hundreds of cells per milliliter during bacterial infections of the central nervous system. The electrophoretic techniques with UV-detection reach the detection limit of intact cells approximately from 10^7 cells mL^{-1}. The coupling of the filtration cartridge with the capillary isoelectric focusing can improve the detection limit by four orders of magnitude. In order to improve the detection limit the red non-ionogenic surfactant 1-[[4-(phenylazo)phenyl]azo]-2-hydroxy-3-naphthoic acid polyethylene glycol ester, PAPAN 1000, has been prepared and used at the dynamic labeling of bioanalytes before filtration of the sample with a concentration modulation in the analysis of microorganisms. Minimum detectable amounts were lower than hundred of labeled cells. The introduced method, filtration of cerebrospinal fluid spiked with microorganisms and labeling with PAPAN, facilitates rapid CIEF separation of microorganisms in the pH gradient pH range 2 – 5 at their clinically important level 10^1 – 10^2 cells mL^{-1}.

Keywords: capillary isoelectric focusing, labeled microorganisms, pre-concentration

1 INTRODUCTION

Microbial meningitis, e.g., pyogenic bacterial, viral, tuberculous or fungal, is a severe infection of the central nervous system (CNS) and is an important cause of mortality and morbidity or permanent serious neurologic sequelae in all countries [1., 2.]. Simultaneously, the studies and diagnostic methods identifying virulent microbial strains, i.e., strains with a capacity for slime production and consequent biofilm formation, are necessary to develop effective strategies for biofilm control and improvement of patient care. Rapid and sensitive detection and identification of etiological agents is crucial for effective therapy and is a first-ranking priority in these infectious diseases area. Problem is that only limited amount of CSF (1-2 ml) can be withdrawn by the lumbar puncture for laboratory testing. Therefore highly sensitive method for detection of the microorganisms in CSF is required [1.]. Conventional laboratory diagnosis of bacterial meningitis based on microscopy followed by culture is time-consuming which takes more than 24 hours to obtain results, and has only moderate sensitivity.

1.1 OBJECTIVES

Capillary isoelectric focusing and capillary electrophoresis [3.,4.] are appropriate tools for the efficient separation and characterization of the phenotypically similar microorganisms according to their isoelectric points, p*I*'s, or mobilities. Simultaneously, the analysis of low number of microorganisms from real biological samples requires sample preparation step including a concentrating of microorganisms from large sample volumes with the high and reproducible efficiency. The electrophoretic techniques have a great potential to include the pre-concentration, separation and detection of the whole cells and therefore they can rapidly indicate a presence of risk pathogens.

2 METHODS

2.1 CIEF

The laboratory-made apparatus at constant voltage (-) 20 kV was used on the side of the detector supplied by high voltage unit Spellman CZE 1000 R (Plainview, NY, USA). The whole lengths of the fused silica capillaries (FS), 0.1 mm I.D. and 0.25 mm O.D. was 350 mm, 200 mm to the detector. The on-column UV-Vis detector LCD 2082 (Ecom, Prague, Czech Republic) was connected to the detection cell by optical fibers (Polymicro Technologies, Phoenix, AZ, USA). The light absorption (optical density) of the microbial suspensions was measured using a DU series 520 UV/Vis spectrophotometer (Beckmann Instruments, Palo Alto, CA, USA) at 550 nm. The clusters of the microorganisms were disrupted by the sonication of the microbial suspension in the ultrasound bath Sonorex (Bandelin electronic,

Berlin, Germany) before the injection of the cells into the capillary. Between the separation runs the sample suspensions were vortexed. The detector signals were acquired and processed with the Chromatography data station Clarity (DataApex, Prague, Czech Republic).

In the catholyte, 0.04 mol L^{-1} NaOH, and the anolyte, 0.1 mol L^{-1} H_3PO_4, the aditives, 0.08 %(w/v) PAPAN (515 nm, labeled bioanalytes) or 1 %(v/v) EtOH and 1 %(w/v) PEG 4000 (280 nm, native bioanalytes), were dissolved. The segmental injection of the sample pulse was used [5.]. The sample pulse was composed of a segment of spacers dissolved in the catholyte, segment of carrier ampholytes, 5 %(w/v) of synthetic carrier ampholytes, Biolyte, pH 3 – 10, ampholyte pH 3 – 4.5 and pH 2 – 4 (1 : 2 : 5) and p*I* markers, p*I,* 2.0, 2.7, 3.23, 3.9, 4.25, 4.71. Sample segments of microorganisms were resuspended in 0.015 mol L^{-1} NaCl, 0.01 %(w/v) and labeling reagent (515 nm) or 3 %(v/v) EtOH and 0.5 %(w/v) PEG 4000 (280 nm).

2.2 MALDI-TOF MS

Twenty microlitres of particular microbial suspension were mixed with 20 µL of sinapinic acid (SA) solution (16 mL^{-1} in acetonitrile/0.1% trifluoroacetic acid, 3:2, v/v) just before mass spectrometric analysis. Resulting mixture was applied on the sample plate and allowed to dry at room temperature. Each sample spot was next overlaid with the SA solution and allowed to dry at room temperature again. MS experiments were performed on 4700 Proteomics Analyzer (Applied Biosystems, Framingham, MA, USA) equipped with linear detector and a 200 Hz Nd:YAG laser operating at 355 nm. Accelerating voltage was set at 20 kV. Mass spectra were acquired in linear positive ion mode. Recorded mass spectra were processed using Data Explorer (ver. 4.6).

3. RESULTS

In our experiments common etiological agents of CNS and nosocomial infections, *Candida* species, *Staphylococcus epidermidis*, *Echerichia coli*, *Staphylococcus aureus,* were selected as model bioparticles. All microorganisms icluding biofilm-positive and biofilm-negative strains of *Candida* species were separated according to their p*I*'s, see **Fig. 1**. The coupling of the filtration cartridge [6.] with the separation capillary improved the detection limit of the isoelectric focusing with the UV/Vis-detection by at least five orders of magnitude down to tens detected cells in 1 ml of the real biological sample. In order to support CIEF results, MALDI-TOF MS was performed.

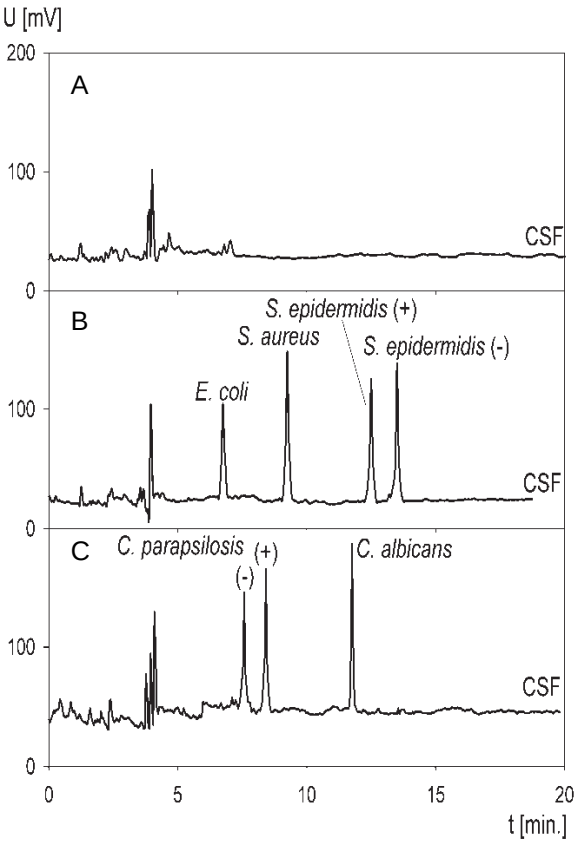

Fig. 1.: CIEF with UV/Vis detection of labeled samples, CSF (A) and CSF spiked with microorganisms (B,C), by PAPAN at 515 nm in the pH gradient pH range 2-4.

ACKNOWLEDGEMENTS

This work was supported by the Grant of Ministry of Interior No. VG20102015023 and by the institutional support RVO: 68081715.

LITERATURE

[1.] Roche, S., Gabelle, A., Lehmann, S., *Proteomics Clin. Appl.* 2008, *2,* 428-436.
[2.] Calvano, T. P., Hospenthal, D. R., Renz, E. M., Wolf, S. E., Murray, C. K., *Burns* 2010, *36,* 688-691.
[3.] Subirats, X., Blaze, D., Kenndler, E., *Electrophoresis* 2011, *32*, 1579-1590.
[4.] Petr, J., Maier, V., *Trends Anal. Chem.* 2012, *31*, 9-22.
[5.] Horká, M., Růžička, F., Holá, V., Šlais, K., *Anal. Bioanal. Chem*. 2006, *385*, 840-846.
[6.] Horká, M., Horký, J., Kubesová, A., Zapletalová, E., Šlais, K., *Anal. Bioanal. Chem*. 2011, *400*, 3133-3140.

P70 IMPROVED GENETICALLY ENCODED CALCIUM INDICATORS FOR TWO-PHOTON POLARIZATION MICROSCOPY

Valentyna Kuznetsova

Faculty of Science, University of South Bohemia in České Budějovice, Czech Republic,
kuznetsovav@nh.cas.cz

ABSTRACT

Our recent work (Lazar et al., 2011) has shown that two-photon polarization microscopy (2PPM) can yield insights into membrane protein structure and function, in living cells and organisms. The realization of 2PPM consists of illumination of sample with two distinct polarizations (vertically polarized light and horizontally polarized light) of the two-photon laser beam and comparison of the resulting images. Differences in absorption of light with distinct polarizations, or linear dichroism (LD) can be observed even when only a small orientation bias of fluorescent moieties is present. Changes in LD can report on molecular processes.

Genetically encoded calcium indicators (GECIs) allow researchers to measure calcium dynamics in specific targeted locations within living cells. We observed a GECI termed lynD3cpV (originally developed for FRET; Palmer A.E., Tsien R.Y., 2006) by 2PPM. Our results show that in resting state cells, the yellow fluorescent protein (cpVenus) present in lynD3cpV is in an almost randomly oriented state. Upon increasing intracellular calcium concentration, the cpVenus orientation becomes more fixed, as is reflected by an increase in LD. Thus, 2PPM allows observing changes in intracellular calcium concentration using the lynD3cpV sensor.

We have now designed new genetically encoded calcium sensors based on lynD3cpV, with improved sensitivity of LD to changes in intracellular calcium concentration. Our results demonstrate that even small changes in LD can be reproducibly observed, quantified and used to infer both structural and functional information.

LITERATURE

[1.] Lazar J., Bondar A., Timr S. and Firestein S.J. Two-photon polarization microscopy reveals protein structure and function. *Nature Methods*, 2011; 8(8):684-90.
[2.] Palmer A.E., Tsien R.Y. Measuring calcium signaling using genetically targetable fluorescent indicators. *Nature Protocols.* Vol.1, NO.3. 2006: 1057-1065.

P71 IMUNOTURBIDIMETRIC DETERMINATION OF NGAL IN THE URINE OF HEALTHY CHILDREN

Radka Šigutová[a,b,c], Michal Hladík[b,d], František Všianský[b,a], Tomáš Karlík[a], Pavlína Kušnierová[b,a], Zdeněk Švagera[b,a]

[a] *Department of Clinical Biochemistry, Institute of Laboratory Diagnostics, Faculty Hospital Ostrava, 17.listopadu 1790, 708 52, Ostrava, Czech Republic, radka.sigutova@fno.cz*
[b] *Faculty of Medicine, University of Ostrava, Ostrava, Czech Republic*
[c] *Department of Biochemistry, Faculty of Medicine, Masaryk University, Brno, Czech Republic*
[d] *Department of pediatrics, Faculty Hospital Ostrava, Ostrava, Czech Republic*

ABSTRACT

NGAL (neutrophil gelatinase-associated lipocalin) belongs to lipocalin family and within acute medicine, namely acute kidney injury (AKI) it is often regarded as “troponin of the kidney“. NGAL concentration increases considerably with toxic and ischemic kidney diseases, in connection with which it has been identified as one of the most frequent indicators (1). NGAL thus differs significantly from other markers, such as cystatin C and creatinine, used to monitor the functions of kidneys. These markers are produced in high concentrations in a long-term interval after the action of pathological stimulus and they only reflect acute kidney disease. Therefore, the determination of NGAL is regarded to be more convenient for its fast response to the stimulus and considerable increase in its values against its basal level.
Present studies carried out with adult patients consider favourable the determination of NGAL values in urine since NGAL determination in plasma may be influenced by some tumor diseases, infections, inflammatory states, chronic hypertension and other diseases (2).
The importance of this study consists in the determination of “normal“ NGAL values in the urine of healthy children and their evaluation with regard to the concentration of creatinine in urine. No physiological NGAL and NGAL/creatinine values have so far been known in pediatry.

Keywords: NGAL, NGAL in urine of healthy children, AKI

1 NGAL STRUCTURE AND FUNCTION

Human NGAL is a relatively small protein consisting of a polypeptide chain of 178 amino acid residues, the molecular mass of which has been determined to 22 kDA. Glycosylation subsequently increases its molecular mass to 25 kDa. X-ray crystalography studies have shown that NGAL is represented in neutrophils and urine mainly as a monomer, to a small extent also as a dimer and trimer. Also, it occurs covalently linked to matrix metalloproteinase-9 (MMP9, 92 kDa) known also as gelatinase B(1). In physiological conditions, NGAL is produced in low concentration by human tissue cells, particularly of kidney, bone marrow, prostate, and gastrointestinal and respiratory tracts. NGAL is released into urine via cell secretion of the ascendent arm of Henley´s loop. Apart from the recyclation of iron complexes by means of endocytosis, NGAL also participates in the chelatation of Fe-siderophores complexes and plays an important role in the protective function of kidney tubular cells (4).

2 NGAL, BIOMARKER AKI

In contemporary clinical practice, the diagnosis of acute kidney injury (AKI) is most often revealed by means of the determination of serum creatinine concentration and the calculation of the estimate of glomerular filtration rate. This diagnostic procedure is insufficient especially in acute modifications of glomerular filtration during which the increase in serum creatinine

concentration fails to reflect the real function of kidneys and is c. 2-3 days delayed after the insult (3). Therefore, the use of NGAL proves to be convenient as it appears in urine in high concentrations as early as 2 hours after ischemia reperfusion injuries or nephrotoxic and other changes. For this reason, NGAL is determined with patients after serious surgical interventions (mainly after cardiosurgical operations, major vessel operations and kidney transplantation), exposure to nephrotoxic action of contrast substances, aminoglycosides or cytostatics and also with patients that come in critical state to urgent and intensive units.

3 METHODOLOGY OF NGAL DETERMINATION

Three most known sets are used in order to determine NGAL, namely CMIA (Chemiluminescent Microparticle Immunoassay, Abott), ELISA (enzyme-linked immunosorbent assay, BioPorto) and imunoturbidimetric method set (IT, BioPorto).
This study made use of turbidimetric immunoassay test based on the reaction of mouse monoclonal antibodies to NGAL immobilized on polystyrene microparticles with antigene, i.e. NGAL protein present in biological sample. The resulting turbidity is directly proportional to the amount of NGAL in the sample and at the same time it is directly proportional to the amount of absorbed light. NGAL concentration is determined by the interpolation on an established 6-point calibration curve. The test is designated for quantitative determination of NGAL in urine and EDTA plasma on automated clinical chemistry analyzers.

4 REFERENCE RANGE

64 samples coming from preschool-age (3-7 years old) children were used for the analysis of physiological NGAL values in urine. 23 of the children were girls and 41 boys. NGAL values were determined in 2 hours after the sampling and centrifuged before the very analysis. The reference range was determined from obtained NGAL values in urine and NGAL values related to creatinine concentration in urine.

4.1 Data evaluation

Before the reference range calculation, regression analysis was used in order to verify the independence of NGAL values in children on their age. Also, no statistically significant difference between girls and boys was found by means of the t-test and Mann-Whitney U test. The reference range calculation therefore encompassed both male and female children. Obtained data were not normally distributed; hence, exponential transformation of the obtained values was performed. Using these data, reference values were calculated by means of a direct method (parametric calculation) and then back-transformed. The reference range was also calculated by means of an indirect method (nonparametric calculation of the reference range). The same calculation method was used in the case of NGAL values related to creatinine, in which the distribution of values was clearly abnormal, strongly skewed towards higher values. Gender differences of NGAL/creatinine values were also not found. Detailed results are shown in Tables 1 and 2.

Table 1: NGAL reference range.

Quantile	Direct method		Indirect method	
	Ref.range ($\mu g.l^{-1}$)	90% CI	Ref.range ($\mu g.l^{-1}$)	90% CI
2.5 %	11.56	9.85-13.52	12.40	11.61-13.20
97.5 %	50.88	42.68-60.38	52.1029	42.68-61.52

Table 2: NGAL/crea reference range.

Quantile	Direct method		Indirect method	
	Ref.range ($mg.mol^{-1}$)	90% CI	Ref.range ($mg.mol^{-1}$)	90% CI
2.5 %	1.27	1.09-1.50	1.20	0.97-1.43
97.5 %	37.69	19.42-74.97	39.61	23.12-56.10

5 CONCLUSION

Reference range of NGAL concentration in the morning urine for the above-mentioned group of children of the age of 3-7 years, obtained by means of the parametric method, was 11.56 to 50.88 $\mu g.l^{-1}$ (significance level α=5 %). This range of reference values was also confirmed by the nonparametric method of reference range calculation, although it failed to fulfill the criteria of a required amount of tested data necessary for the analysis (at least 120 values are required).

The reference range of NGAL/creatinine obtained by the parametric calculation method for the above-mentioned group of children is from 1.27 to 37.69 $mg.mol^{-1}$. The reference range calculation by the nonparametric method confirms the accuracy of this reference interval determination.

No study dealing with the acquisition of the reference range in children is so far known. Compared to the published NGAL values in the urine of adults in the paper of Delanay (the interquantile range is 15.4 – 52.8 $\mu g.l^{-1}$) (5), the interquantile range 17.5 – 32.85 $\mu g.l^{-1}$ in the children group presented in this study is characterized by the decrease in the upper reference limit. In order to obtain more precise reference values in children, older children need to be included in the reference group.

ACKNOWLEDGEMENTS

This study was supported by the Ministry of Health of the Czech Republic (01549/2012/RRC).

LITERATURE

[1.] Lippi, G., Plebani, M., Neutrophil gelatinase-associated lipocalin (NGAL): the laboratory perspective, *Clin Chem Lab Med* 2012; 50(9): 1483-1487.

[2.] Lavery, A., Meinzen-Derr, J., Anderson, E., *et al.*, Urinary NGAL in premature infants. *Pediatr Res*, 2008, 64, 423-428.

[3.] Han, W., Waikar, S., Johnson, A., *et al.*, Urinary biomarkers in the early diagnosis of acute kidney injury. *Kidney Int*, 2008, 73, 863–869.

[4.] Bennet, M., Dent, C., Ma, Q., *et al.*, Urine NGAL predicts severity of acute kidney injury after cardiac surgery: a prospective study. *Clin J Am Soc Nephrol* 2008, 3, 665– 673.

[5.] Delanaye, P., Rozet, E., Krzesinski, J.M., Cavalier, E., Urinary NGAL measurement: biological variatio and ratio to creatinine. *Clin Chim. Acta* 2011, 412, 3-4, 390.

P72 OCCURRENCE OF RISK METALS IN SMALL MAMMALS IN THE EASTERN TATRAS

Silvia Jakabová[a], Imrich Jakab[b], Ivan Baláž[b]

[a] *Department of Chemistry,* [b] *Department of Ecology and Environmental Science, Faculty of Natural Sciences, Constantine the Philosopher University in Nitra, Tr. A. Hlinku 1, 949 74 Nitra, Slovakia, sjakabova@ukf.sk*

ABSTRACT

The content of accumulative metals cadmium and lead was investigated in liver of small terrestrial mammals (*Apodemus flavicollis, Clethrionomys glareolus, Pitymys tatricus,* and *Microtus agrestis*), originated from The Eastern Tatras. ET-AAS method was used for the analysis of total content of the risk elements. In general, the mean contents of Pb and Cd in liver were higher in the locality Zadné Meďodoly, compared to levels found in the samples from Tatranská Javorina. The highest accumulation was observed in the tissues of bank vole.

Keywords: cadmium, lead, free living small mammals

1 INTRODUCTION

Small mammals are important components of ecosystems, occupying a variety of niches. They have been suggested to be effective biomonitors because of their abundance, widespread distribution, short migration distances, generalized food habits, short life span, high reproductive rate, and susceptibility to capture [1]. Free-living wild rodents and insectivores are often used for biomonitoring purposes due to their sensitivity to heavy metals [2,3]. Good evidence for monitoring and evaluation of pollution impact provides bioaccumulation ability of organisms [4].

Cadmium and lead are common risk elements in the environment. Cadmium (Cd) is a nonessential element with high migration ability in a food chain [5]. It belongs to accumulative poisons and its content in organism increases during the life [6]. The main exposure ways of Cd intake are inhalation from air and intake from food. Distribution of Cd in tissues of small terrestrial mammals was in order: kidneys > liver >> muscles [7]. Cd shows cancerogenous effects, high exposure affects hypertensis and decalcification of bones. Epidemiologic approach uses the Cd analysis of hair, which is the proposed test for the Cd exposure [8].

Lead (Pb) is the most common heavy metal, which is markedly accumulated in sediments, sludges, moreover in microorganisms and plants [8]. Humans can absorb Pb mostly via air, fewer via food and skin [9]. The highest Pb concentration in animals was found in liver, kidneys, spleen, bones, bone marrow and in muscles. Over 90 % of absorbed Pb is transported to bones [10]. Pb has neurotoxic effect on the organism and becomes a potential carcinogen [6].

The aim of our study was to determine concentrations of lead and cadmium in liver of small free-living mammals trapped in two sites The Eastern Tatas in Slovakia. These accumulative metals were investigated in liver of four herbivorous species (*Apodemus flavicolis, Clethrionomys glareolus, Microtus agrestis and Pitymys tatricus*) and determination was performed by the ET-AAS method. Concentration levels can be used for estimation of pollution of the area.

2 EXPERIMENTAL

2.1 Samples and sample preparation

Small terrestrial mammals – four herbivorous species (*Apodemus flavicolis*, *Cletrionomys glareolus , Pitymys tatricus, and Microtus agrestis)* species were obtained by means of

standard theriological methods and procedures [11] in the period September 2010 – March 2011. All animals were adult males and females, which appeared to be in good physical conditions.
Samples of liver were air dried and weighted directly into teflon vessels. The tissues were wet digested at 140°C in a mixture of HNO_3 (67%, analpur) and H_2O_2 (30%, p.a.) in high-pressure for 120 min. Final solutions were diluted to 25 ml volume by deionized water.

2.2 Apparatus

Determination was done by atomic absorption spectrometry with electrothermal atomization technique (ET-AAS) on a SpectrAA-200 apparatus. For the technique, cadmium and lead hollow cathode lamps operate at a wavelength of 228.8 nm and 217.0 nm, respectively. Atomizing environment was a graphite tube heated to 2600 °C, a flow solution was HNO_3 (1 %) and a modifier was ortophosphoric acid 0.1 %. All standards and solvents used were of analytical grade and solutions were prepared in deionized water.
The method used was optimized and several validation characteristics were determined. The results of validation showed that limits of detection (LOD) were 4.5 µg Cd .kg^{-1} and 4.6 µg Pb .kg^{-1} and limits of quantitation (LOQ) were 10.7 µg Cd .kg^{-1} and 13.8 µg Pb .kg^{-1}.

3 RESULTS AND DISCUSSION

Samples originated from the two trapping sites. The results of the study are shown in Table 1. The mean content of Pb in liver of herbivorous species did not exceed 1 mg.kg^{-1} in the area of Tatranská Javorina, however the individuals of bank vole and field vole from the site of Zadné Meďodoly (trapping site was near the wood bears) showed higher Pb levels. In Tatranská Javorina the content of cadmium varied in the range from levels below the LOD to 0.42 mg.kg^{-1}.

Table 1: Contents of kadmium and lead in liver (expressed on dry weight basis)

Lokality	Species	n	Pb [mg/kg]			Cd [mg/kg]		
			min.	mean	max.	min.	mean	max.
Tatranská Javorina	*Apodemus flavicollis*	4	0.28	0.38	0.47	0.10	0.24	0.42
	Clethrionomys glareolus	3	0.65	0.80	0.96	3.64	3.77	3.89
	Microtus agrestis	3	0.23	0.32	0.41	<LOD	0.20	0.42
Zadné Meďodoly	*Clethrionomys glareolus*	5	0.63	1.10	2.06	1.02	2.81	6.00
	Microtus agrestis	3	1.20	1.57	1.89	1.28	1.28	1.45
	Pitymys tatricus	6	0.21	0.57	1.14	0.04	0.31	0.64

Notes: n – number of samples, <LOD - below LOD

The highest mean accumulation of cadmium showed bank voles (3.77 and 2.81 mg.kg^{-1}). Yellow-necked mouse (*A. flavicollis*) and field vole (*M. agrestis*) showed similar tendency in accumulation of Pb and Cd in liver. Samples from Tatra pine voles (*P. tatricus*) did not reached as high values as in the case of bank and field voles, trapped in the same site.

4 CONCLUSION

Results of this study showed that trapping site in Zadné Meďodoly located on uphill of The Eastern Tatras is loaded by heavy metals even more than area in the valley (like in the case of Tatranská Javorina).
Our results confirmed the correlation between contamination by heavy metals and occurrence of the metals in parenchyma tissues; moreover we could see the different contamination in species. Seeing that the small terrestrial mammals present wide spread group of animals, which could be used in estimation of environmental pollution by contaminants.

ACKNOWLEDGEMENTS

The work was supported by the grant FCVV (Grant no.2012/6).

LITERATURE

[1] Levengood JM, Heske EJ, Science of the Total Environment 2008, *389,* 320-328.
[2] Martiniaková M, Omelka R, Grosskopf B, Jančová A., *Acta Veterinaria Scandinavica* 2010, *52*, 58.
[3] Rautio A, Kunnasranta M, Valtonen A, Ikonen M, Hyvarinen H, Holopainen I, Kukkonen J., *Archives of Environmental Contamination and Toxicology,* 2010, *59*, 642-651
[4] Jakabová S, Baláž I, Jakab I., *Occurence of risk elements cadmium and lead in small terrestrial mammals in upper Nitra region*, 2010. In: Mladí vedci 2010. Nitra : UKF, 2010, 347-351.
[5] Hunter BA, Johnson MS & Thompson DJ. , *Journal of Applied Ecology* 1987, *24*, 601-614.
[6] Toman, R., Golian, J., Massányi, P. *Toxikológia potravín*, SPU, Nitra 2003.
[7] Lodenius M, Soltanpour-Gargari A, Tulisalo E & Henttonen H., *Journal of Environmental Quality* 2002, *31*, 188–192.
[8] Prousek J. *Rizikové vlastnosti látok*. STU, Bratislava 2005.
[9] Makovníková J, Barančíková G, Dlapa P, Dercová K. *Chem listy* 2006, *100*,424-432.
[10] Ma WC., *Archives of Environmental Contamination and Toxicology* 1989,*18*, 617-622.
[11] Jančová A, Massányi P, Naď P, Koréneková B, Skalická B, Drábeková J, Baláž I., *Ecology* 2006, *25*,19-26.

P73 APPLICATION OF ON-LINE CAPILLARY ELECTROPHORESIS COUPLED TO MASS SPECTROMETRY FOR IDENTIFICATION OF CYTOCHROME P450 2C9 ISOFORM METABOLISM PRODUCTS

Monika Langmajerová, Roman Řemínek, Marta Zeisbergerová, Zdeněk Glatz

Department of Biochemistry, Faculty of Science and CEITEC – Central European Institute of Technology, Masaryk University, Kamenice 5, 625 00 Brno, Czech Republic

ABSTRACT

Drug biotransformation mediated by cytochrome P450 enzymes (CYP) is a pivotal factor in the early developmental stages of new drugs. Metabolism appraisal of every hit thus constitutes the inseparable part of ADME/tox screenings. Capillary electrophoresis (CE) represents a promising technique in the field of enzyme assays due to miniscule sample consumption and high-throughput by automation. Moreover, CE coupled to mass spectrometry (MS) combines the advantages of both techniques so that CYP metabolism products can be identified on the bases of migration time, molecular weight and fragmentation. A new CE-MS method enabling identification of reaction products provided by clinically important CYP2C9 isoform is thus introduced.

Keywords: Drug metabolism; Capillary electrophoresis; Mass spectrometry

1 INTRODUCTION

Cytochrome P450 enzymes (CYP) play a key role in metabolism of 75 % commonly prescribed drugs in the human body [1]. For this reason, studies of metabolism and the affinity of a candidate compound to this group of enzymes represent an important part of a new drug development process [2]. Since large compound libraries undergo the testing, there is ongoing trend towards the miniaturization and throughput enhancement of screening assays in order to economize and expedite the whole development process. Capillary electrophoresis (CE) is a promising technique in this field due to its rapid highly effective

separations, miniscule sample consumption, high throughput by automation and easy electrospray ionization (ESI) interfacing with mass spectrometric detection (MS). A CE assay typically constitutes a two-step (off-line) procedure when a reaction mixture is incubated in a vial prior to CE analysis. Conversely, in on-line CE analyses, a fused silica capillary is used not only as a separation column but also as a reaction chamber, creating a nanoliter-scale reactor. Incubation of the enzymatic reaction, separation of reaction mixture and detection of reaction products is integrated into a single fully automated analysis increasing the throughput of the assay and also minimizing the possibility of experimental error and consumption of reactants. The goal of this study was to introduce a new generic on-line CE-ESI-MS method allowing identification of drug metabolism products. The reaction of cytochrome P450 2C9 isoform (CYP2C9) with diclofenac was chosen as a model system. Whereas, CYP2C9 represents one of the most important human CYP's, forming approximately 20 % of all CYP in human liver and metabolizing over 10 % of commonly prescribed drugs [3], diclofenac is a nonsteroidal anti-inflammatory drug which acts as a potent inhibitor of prostaglandin endoperoxidase synthase [4].

2 EXPERIMENTAL

2.1 Capillary electrophoresis

All the experiments were conducted on the Agilent 7100 CE System. An uncoated fused silica capillary (75 cm; 75 µm) was thermostated at 37 °C. Separations were accomplished by application of 30 kV, (positive polarity, 50 µA current limit). Additional pressure of 50 mbar was applied after 8 min from the start of separation. 30 mM ammonium acetate (pH 9.20) was used as a BGE.

2.2 In-capillary reaction

All reactants were prepared in incubation buffer consisting of 50 mM phosphate (pH 7.40). Injection procedure was as follows: 2 s of diclofenac and NADPH solution, 2 s CYP2C9 solution, 2 s diclofenac and NADPH solution by pressure of 15 mbar. Enzymatic reactions were incubated for 15 min. Method optimization and validation was performed using solutions containing 200 µM diclofenac and 6 mM NADPH; and 333 nM CYP2C9.

2.3 MS detection

All experiments were carried out on the Bruker maXis impact ESI-Qq-TOF MS system enabling tandem MS in space analyses. CE-ESI-MS coupling was carried out with sheath liquid interface. Sheath liquid consisted of 0.1 % acetic acid and 2.5 mM ammonium acetate dissolved in methanol/water solution (50/50). The flow rate of sheath liquid was set on 4 µL/min. Nebulizing gas pressure was 0.4 bar. Drying gas was thermostated at 200 °C and its flow rate was 5 L/min. Voltage of -4 kV was applied on ESI needle.

3 RESULTS

The method optimization started by selecting an appropriate incubation buffer and subsequent separation conditions. Off-line reactions of CYP2C9 with diclofenac prepared in 50 mM phosphate (pH 7.4) containing either 0.1 M KCl and 5.1 mM $MgCl_2$, 50 mM phosphate (pH 7.4), 50 mM Tris-HCl (pH 7.5) or 10 mM ammonium acetate (pH 7.5) were carried out and the production of 4'-hydroxydiclofenac in each sample was determined. The reactions were incubated in triplicate for each incubation buffer and every sample was analyzed twice. On the basis of obtained results, 50 mM phosphate (pH 7.4) was chosen as the incubation buffer. Utilization of volatile BGE formed by 30 mM ammonium acetate (pH 9.20) represents a certain trade-off between sufficient resolution of analyte and short analysis time since

utilization of higher BGE concentrations increases the resolution as well as migration time of 4'-hydroxydiclofenac. Low BGE conductivity allowed application of maximal configurable separation voltage of 30 kV (positive polarity).

As was mentioned above, extensive numbers of candidates are tested within early stages of a new drug development process. For this reason, the generic procedure of transverse diffusion of laminar flow profiles (TDLFP) enabling reactants mixing inside the narrow capillary presented by Krylov et al. was employed [6]. In principle, solutions of CYP2C9 and diclofenac and NADPH are injected by relatively high hydrodynamic pressure as a series of consecutive plugs with parabolic profiles due to laminar nature of the flow inside the capillary (Fig. 1A). The plugs of reactants merge over the large longitudinal interfaces after injection. Beyond generic, TDLFP is also fast considering the molecules diffuse through the distance of the capillary radius at the most (1B). Reaction is stopped by application of voltage and separation of CYP2C9 and diclofenac (1C). Reaction products are then identified on the bases of their migration times, molecular weight and fragmentation.

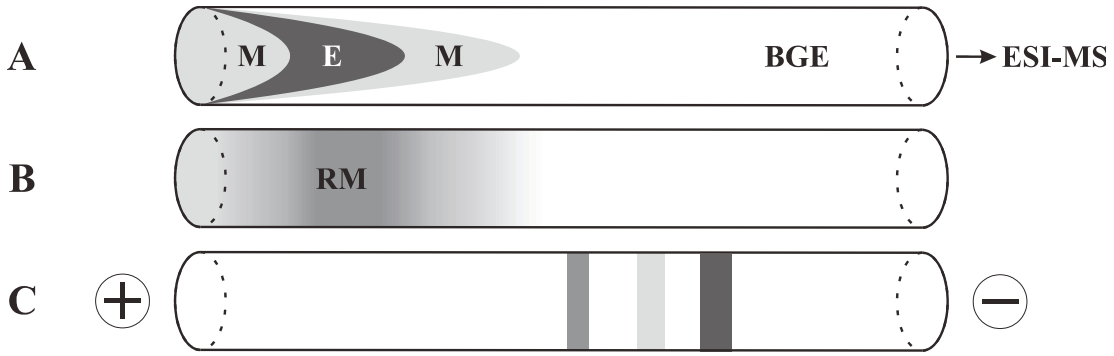

Fig. 1 : Principle of TDLFP-based mixing. (A) At the beginning of the analysis, the solutions of CYP2C9 (E) and diclofenac and NADPH (M) are injected as a series of consecutive plugs with parabolic profiles due to laminar flow inside the capillary. (B) After injection, the reactants are mixed by transverse diffusion. (C) The reaction is stopped and reaction products are separated by application voltage. See text for further details.

Using optimized method, model substrate diclofenac and its metabolite 4'-hydroxydiclofenac were detected in m/z range of 50 – 1600. Mass spectrum of 4'-hydroxydiclofenac showing specific pattern with fragments 231; 294; and 266 is depicted in Figure 2.

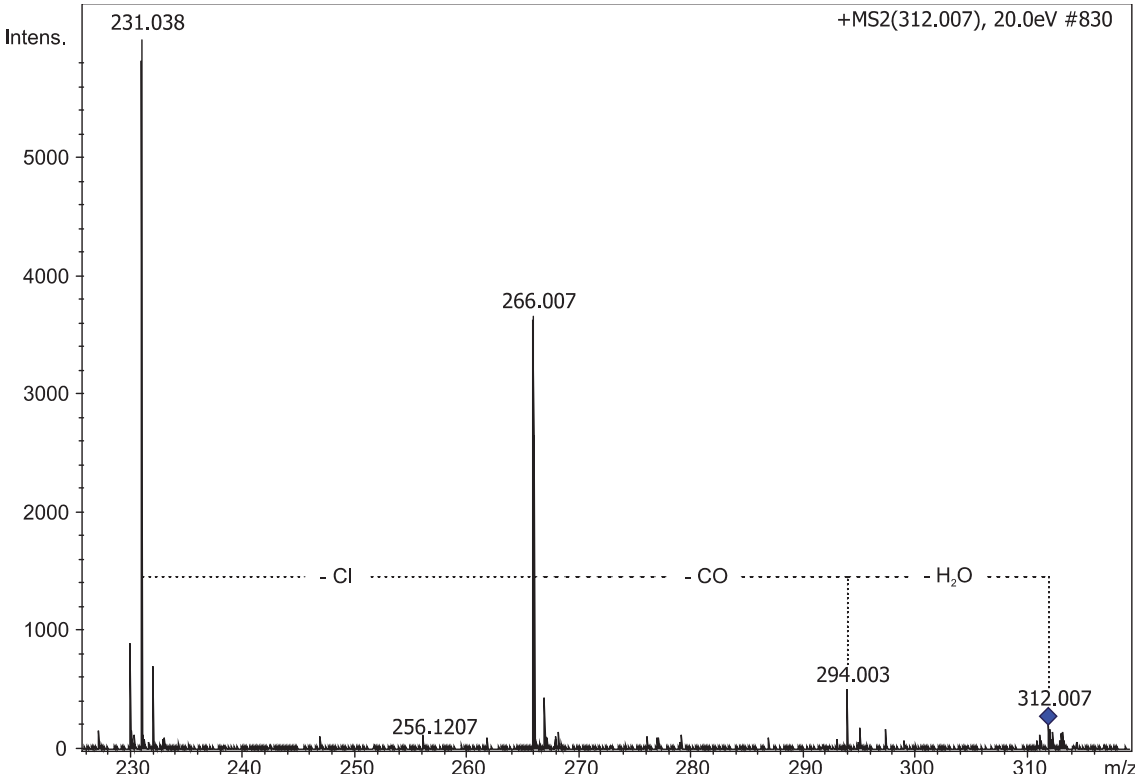

Fig. 2 : Mass spectrum of 4'-hydroxydiclofenac obtained after in-capillary reaction.

4 CONCLUSION

A new method integrating all processes of CYP2C9 assay from incubation of reaction mixture to identification of reaction products within single run was introduced. Principle of reactant's mixing inside capillary based on TDLFP and employment of tandem MS detection guarantee its generic applicability. After adaptation of incubation and separation conditions, method is thus conceptually applicable for on-line screenings of any CYP and its substrates.

ACKNOWLEDGEMENTS

This work was supported by grant No. P206/10/0057 and P206/12/G014 both from the Grant Agency of the Czech Republic.

LITERATURE

[1] Guengerich, F.P., *Chemical Research in Toxicology* 2008, *21*, 70-83.
[2] Lin, J.H., Lu, A.Y.H., *Pharmacological Reviews* 1997, *49*, 403-449.
[3] Rettie, A.E., Jones, J.P., *Annual Review of Pharmacology and Toxicology* 2005, *45*, 477-494.
[4] Brogden, R.N., Heel, R.C., Pakes, G.E., Speight, T.M., Avery, G.S., *Drugs* 1980, *20*, 24-48.
[5] Okhonin, V., Liu, X., Krylov, S.N., *Analytical Chemistry* 2005, *77*, 5925-5929.

P74 IMUNOTURBIDIMETRIC DETERMINATION OF NGAL IN THE URINE OF HEALTHY CHILDREN

Radka Šigutová[a,b,c], Michal Hladík[b,d], František Všianský[a,b], Tomáš Karlík[a], Pavlína Kušnierová[a,b], Zdeněk Švagera[a,b]

[a] *Department of Clinical Biochemistry, Institute of Laboratory Diagnostics, Faculty Hospital Ostrava, 17.listopadu 1790, 708 52, Ostrava, Czech Republic, radka.sigutova@fno.cz*
[b] *Faculty of Medicine, University of Ostrava, Ostrava, Czech Republic*
[c] *Department of Biochemistry, Faculty of Medicine, Masaryk University, Brno, Czech Republic*
[d] *Department of pediatrics, Faculty Hospital Ostrava, Ostrava, Czech Republic*

ABSTRACT

NGAL (neutrophil gelatinase-associated lipocalin) belongs to lipocalin family and within acute medicine, namely acute kidney injury (AKI) it is often regarded as “troponin of the kidney“. NGAL concentration increases considerably with toxic and ischemic kidney diseases, in connection with which it has been identified as one of the most frequent indicators (1). NGAL thus differs significantly from other markers, such as cystatin C and creatinine, used to monitor the functions of kidneys. These markers are produced in high concentrations in a long-term interval after the action of pathological stimulus and they only reflect acute kidney disease. Therefore, the determination of NGAL is regarded to be more convenient for its fast response to the stimulus and considerable increase in its values against its basal level. Present studies carried out with adult patients consider favourable the determination of NGAL values in urine since NGAL determination in plasma may be influenced by some tumor diseases, infections, inflammatory states, chronic hypertension and other diseases (2). The importance of this study consists in the determination of “normal“ NGAL values in the urine of healthy children and their evaluation with regard to the concentration of creatinine in urine. No physiological NGAL and NGAL/creatinine values have so far been known in pediatry.

Keywords: NGAL, NGAL in urine of healthy children, AKI

1 NGAL STRUCTURE AND FUNCTION

Human NGAL is a relatively small protein consisting of a polypeptide chain of 178 amino acid residues, the molecular mass of which has been determined to 22 kDA. Glycosylation subsequently increases its molecular mass to 25 kDa. X-ray crystalography studies have shown that NGAL is represented in neutrophils and urine mainly as a monomer, to a small extent also as a dimer and trimer. Also, it occurs covalently linked to matrix metalloproteinase-9 (MMP9, 92 kDa) known also as gelatinase B(1). In physiological conditions, NGAL is produced in low concentration by human tissue cells, particularly of kidney, bone marrow, prostate, and gastrointestinal and respiratory tracts. NGAL is released into urine via cell secretion of the ascendent arm of Henley´s loop. Apart from the recyclation of iron complexes by means of endocytosis, NGAL also participates in the chelatation of Fe-siderophores complexes and plays an important role in the protective function of kidney tubular cells (4).

2 NGAL, BIOMARKER AKI

In contemporary clinical practice, the diagnosis of acute kidney injury (AKI) is most often revealed by means of the determination of serum creatinine concentration and the calculation of the estimate of glomerular filtration rate. This diagnostic procedure is insufficient especially in acute modifications of glomerular filtration during which the increase in serum creatinine concentration fails to reflect the real function of kidneys and is c. 2-3 days delayed after the insult (3). Therefore, the use of NGAL proves to be convenient as it appears in urine in high

concentrations as early as 2 hours after ischemia reperfusion injuries or nephrotoxic and other changes. For this reason, NGAL is determined with patients after serious surgical interventions (mainly after cardiosurgical operations, major vessel operations and kidney transplantation), exposure to nephrotoxic action of contrast substances, aminoglycosides or cytostatics and also with patients that come in critical state to urgent and intensive units.

3 METHODOLOGY OF NGAL DETERMINATION

Three most known sets are used in order to determine NGAL, namely CMIA (Chemiluminescent Microparticle Immunoassay, Abott), ELISA (enzyme-linked immunosorbent assay, BioPorto) and imunoturbidimetric method set (IT, BioPorto).
This study made use of turbidimetric immunoassay test based on the reaction of mouse monoclonal antibodies to NGAL immobilized on polystyrene microparticles with antigene, i.e. NGAL protein present in biological sample. The resulting turbidity is directly proportional to the amount of NGAL in the sample and at the same time it is directly proportional to the amount of absorbed light. NGAL concentration is determined by the interpolation on an established 6-point calibration curve. The test is designated for quantitative determination of NGAL in urine and EDTA plasma on automated clinical chemistry analyzers.

4 REFERENCE RANGE

64 samples coming from preschool-age (3-7 years old) children were used for the analysis of physiological NGAL values in urine. 23 of the children were girls and 41 boys. NGAL values were determined in 2 hours after the sampling and centrifuged before the very analysis. The reference range was determined from obtained NGAL values in urine and NGAL values related to creatinine concentration in urine.

4.1 Data evaluation

Before the reference range calculation, regression analysis was used in order to verify the independence of NGAL values in children on their age. Also, no statistically significant difference between girls and boys was found by means of the t-test and Mann-Whitney U test. The reference range calculation therefore encompassed both male and female children. Obtained data were not normally distributed; hence, exponential transformation of the obtained values was performed. Using these data, reference values were calculated by means of a direct method (parametric calculation) and then back-transformed. The reference range was also calculated by means of an indirect method (nonparametric calculation of the reference range). The same calculation method was used in the case of NGAL values related to creatinine, in which the distribution of values was clearly abnormal, strongly skewed towards higher values. Gender differences of NGAL/creatinine values were also not found. Detailed results are shown in Tables 1 and 2.

Table 1: NGAL reference range.

Quantile	Direct method		Indirect method	
	Ref.range ($\mu g.l^{-1}$)	90% CI	Ref.range ($\mu g.l^{-1}$)	90% CI
2.5 %	11.56	9.85-13.52	12.40	11.61-13.20
97.5 %	50.88	42.68-60.38	52.1029	42.68-61.52

Table 2: NGAL/crea reference range.

Quantile	Direct method		Indirect method	
	Ref.range ($mg.mol^{-1}$)	90% CI	Ref.range ($mg.mol^{-1}$)	90% CI
2.5 %	1.27	1.09-1.50	1.20	0.97-1.43
97.5 %	37.69	19.42-74.97	39.61	23.12-56.10

5 CONCLUSION

Reference range of NGAL concentration in the morning urine for the above-mentioned group of children of the age of 3-7 years, obtained by means of the parametric method, was 11.56 to 50.88 $\mu g.l^{-1}$ (significance level α=5 %). This range of reference values was also confirmed by the nonparametric method of reference range calculation, although it failed to fulfill the criteria of a required amount of tested data necessary for the analysis (at least 120 values are required).

The reference range of NGAL/creatinine obtained by the parametric calculation method for the above-mentioned group of children is from 1.27 to 37.69 $mg.mol^{-1}$. The reference range calculation by the nonparametric method confirms the accuracy of this reference interval determination.

No study dealing with the acquisition of the reference range in children is so far known. Compared to the published NGAL values in the urine of adults in the paper of Delanay (the interquantile range is 15.4 – 52.8 $\mu g.l^{-1}$) (5), the interquantile range 17.5 – 32.85 $\mu g.l^{-1}$ in the children group presented in this study is characterized by the decrease in the upper reference limit. In order to obtain more precise reference values in children, older children need to be included in the reference group.

ACKNOWLEDGEMENTS

The study has been funded by the research grant of the Moravian-Silesian region (Support of science and research), MSK FNO 99/OVZ/12/011-Dot, (number of project 01549/2012/RRC).

LITERATURE

[1.] Lippi, G., Plebani, M., Neutrophil gelatinase-associated lipocalin (NGAL): the laboratory perspective, *Clin Chem Lab Med* 2012; 50(9): 1483-1487.

[2.] Lavery, A., Meinzen-Derr, J., Anderson, E., *et al.*, Urinary NGAL in premature infants. *Pediatr Res*, 2008, 64, 423-428.

[3.] Han, W., Waikar, S., Johnson, A., *et al.*, Urinary biomarkers in the early diagnosis of acute kidney injury. *Kidney Int,* 2008, 73, 863–869.

[4.] Bennet, M., Dent, C., Ma, Q., *et al.*, Urine NGAL predicts severity of acute kidney injury after cardiac surgery: a prospective study. *Clin J Am Soc Nephrol* 2008, 3, 665– 673.

[5.] Delanaye, P., Rozet, E., Krzesinski, J.M., Cavalier, E., Urinary NGAL measurement: biological variatio and ratio to creatinine. *Clin Chim. Acta* 2011, 412, 3-4, 390.

P75 THE USE OF REAL TIME PCR METHOD FOR EVALUATION OF MAGNETIC MICROSPHERES

ŠtepánkaTrachtová [a], Bohuslav Rittich [a], Daniel Horák[b], Alena Španová [a]

[a] Brno University of Technology, Faculty of Chemistry, Institute of Food Chemistry and Biotechnology, Purkyňova 118, CZ-612 00 Brno, Czech Republic, trachtova@fch.vutbr.cz

[b] Institute of Macromolecular Chemistry AS CR, v.v.i., Heyrovský Sq. 2, CZ-162 06 Prague, Czech Republic

ABSTRACT

The real-time quantitative PCR (qPCR) was used for the evaluation of non-porous HEMA-based magnetic microspheres on the PCR course (PCR sensitivity). It was shown that 1-10 µl

microsphere suspensions (2 mg/ml) in PCR mixtures do not interfere in the PCR. It can be assumed that the magnetic nuclei were covered with polymer layer.

Keywords: magnetic microspheres, real time PCR

1 INTRODUCTION

One of the modern methods to speed up and facilitate the DNA separation and purification from complex samples are magnetic driven separation techniques. Magnetic particles for these applications are mostly based on magnetic irons oxide core covered by polymer shell. Different methods of magnetic particles preparation are accompanied with some disturbing problems. 0 These are mainly associated with incomplete encapsulation of the magnetic core with polymer; as a result, some free cores remain uncovered. In previously published papers it was shown that not only incomplete encapsulation and free cores but also some components used in preparation of magnetic particles can significantly reduce the sensitivity of PCR detection. 0-0

Real-time quantitative PCR can be used for the detection of PCR inhibitors in samples on the basis of comparison of the amplification efficiency of unknown DNA samples with purified DNA standard. 0-0 The amplification efficiency of qPCR can fluctuate due to the presence of co-extracted amplification inhibitors. The increasing inhibitors concentration decreases the amplification efficiency and thus the reaction curve slope decreases. 0, 0 The attention was focused on the magnetic particles whose were used for the isolation of DNA from various complex samples containing PCR inhibitors (such as probiotic dairy products, food supplements). 0, 0-0

The aim of this study was to evaluate the influence of carboxyl-functionalized magnetic non-porous poly(2-hydroxyethyl methacrylate-co-ethylene dimethacrylate) (P(HEMA-*co*-EDMA)) and poly(2-hydroxyethyl methacrylate-co-glycidyl methacrylate) - P(HEMA-*co*-GMA) microspheres on the efficiency of DNA amplification by real-time quantitative PCR (qPCR).

2 METHODS

2.1 Chemical and equipment

The PCR primers were synthesized by Generi Biotech (Hradec Králové, Czech Republic), PCR was performed using SybrGreen – qPCR kit by Top-Bio (Prague, Czech Republic). DNA marker (100–1500 bp long DNA fragments) for gel electrophoresis was from Malamité (Moravské Prusy, Czech Republic). Agarose was purchased from Serva (Heidelberg, Germany), commercially supplied ordinary chemicals and solvents were of analytical grade. The bacterial strain *Lactobacillus gasseri* K7 was obtained from a culture collection of the Chair of Dairy Science, Biotechnical Faculty, University of Ljubljana, Slovenia.

DNA was amplified in the DNA thermal cycler Rotorgene 6000 (Corbett Research, Mortlake, Australia). Agarose gel electrophoreses were carried out using a standard electrophoresis unit (Bio-Rad, Richmond, USA). The PCR products were visualized on the UltraLum EB-20E UV transilluminator (Paramount, USA) at 305 nm and photographed with a digital camera. The DNA concentration was measured using the UV/Vis NanoPhotometer (Implen, München, Germany).

2.2 Magnetic microspheres

Different types of magnetic nonporous hydrophilic microspheres poly(2-hydroxyethyl methacrylate-co-ethylene dimethacrylate) (P(HEMA-*co*-EDMA)) and poly(2-hydroxyethyl methacrylate-co-glycidyl methacrylate) (P(HEMA-*co*-GMA)) were prepared by single step dispersion polymerization in the presence of sterically or electrostatically stabilized colloidal magnetite or magnetite and were used in the study (Table 1). 0-0, 0

Table 1: Characterization of magnetic particles.

Polymer	Fe content (%hm)	-COOH content (mM/g)	Diameter (μm)	PDI*
P(HEMA-*co*-GMA)	10.00	0.76	2.20	1.09
P(HEMA-*co*-EDMA)	6.55	0.85	1.50	1.07

**PDI* – polydispersity index (ratio of weight to number–average particle diameter)

Particle size distribution was characterized by the polydispersity index PDI (PDI = Dw/Dn, where Dw is the weight-average particle diameter and Dn is the number-average particle diameter). 0 The hydroxyl groups of the microspheres were oxidized with a 2% aqueous solution of potassium permanganate under acidic conditions (2 M sulphuric acid). 00 The content of carboxyl groups in the microspheres was determined by titration using 0.1 M NaOH on a 799 GPT Titrino (Metrohm, Herrisau, Switzerland) after ion exchange with a 10% aqueous solution of $BaCl_2$. 0

2.3 DNA isolation

DNA was isolated from bacterial cells of the strain *Lactobacillus gasseri* K7 using phenol and precipitated by ethanol. 0 The concentration and the purity of isolated DNA were estimated spectrophotometricaly at 260 nm. The concentration of isolated DNA was adjusted at 10 ng/μl. The integrity of nucleic acid was confirmed by gel electrophoresis (0.8 % agarose) in 0.5 x TBE buffer (45 mM boric acid, 45 mM Tris-base, 1 mM EDTA, pH 8.0). The DNA was stained with ethidium bromide (0.5 ng/μl), decolorized in water and observed on a UV transilluminator.

2.4 Real-time PCR

The DNA isolated from *Lactobacillus gasseri* K7 was used as template in real-time PCR. Amplification was performed with initial step of 95 ºC for 5 min, 30 cycles of 95 ºC for 30 s, 55 ºC for 30 s, and 72 ºC for 30 s. The last step of extension at 72 ºC was prolonged to 5 min. The amplification step was followed by a melting curve analysis from 50 to 99 ºC (held 1 s in the 1st step and 5 s in the next steps). Fluorescence measurements were performed in real time at the end of each cycle. The amplification was carried out with primers Feub and Reub specific to the *Bacteria* domain. 0 The PCR inhibition was analyzed in 25 μl amplification reactions consisting of 12.5 μl of the mixture supplied, 1 μl of each primer, 1 μl of template DNA (10 ng/μl) and corresponding volume of tested magnetic particles and PCR-grade water. The dilution method was used for the study of the influence of the magnetic particles on amplification efficiency. The PCR mixture contained DNA (1 μl DNA (10 ng/μl)/25 μl PCR mixture) and particles (0-10 μl microsphere suspensions (2 mg/ml)/25 μl of PCR mixture). The software supplied with the Rotorgene 6000 cycler (version 1.7.87) was used for the statistical evaluation of the data. The robustness of the amplification was estimated from the correlation coefficient of the linear regression (R^2). The reaction efficiency (r. e.) was calculated using linear regression from the slope (M) of plot Ct versus log of nucleic acid concentration using the equation:

$$r.e. = 10^{\left(-\frac{1}{M}\right)} - 1$$

The results of real-time PCR were verified by detection of specific PCR products using gel electrophoresis and by Melt analysis of PCR products.

3 RESULTS AND DISCUSSION

Rapid and sophisticated DNA isolation strategies are based on the utilization of solid phase systems selectively or non-selectively adsorbing genomic DNA on magnetic particles. Methods for confirmation of PCR inhibition used in this work utilize indirect verification effect of magnetic particles on PCR amplification. For this purpose, model experiments were proposed, which enabled the estimation of inhibitory effect of tested magnetic microspheres on the course of qPCR.

The values of the reaction efficiency (r.e.) were calculated according to Eq. 1. The results of linear regression analysis are presented in Table 2.

Table 2: The influence of magnetic microspheres on the efficiency of amplification on real-time PCR (linear regression analysis)

Type of particles	**Particles suspension** (µl[a])/25 µl PCR mixture**)**	**M**	**r.e. (%)**	**R^2**	**c.v. (%)**
P(HEMA-*co*-GMA)	0	-3.3	100	0.9998	1.2 – 9.4
	1	-3.3	101	0.9999	0.3 – 1.9
	5	-3.3	102	0.9981	3.3 – 22.7
	10	-3.2	103	0.9932	6.3 – 38.5
P(HEMA-*co*-EDMA)	0	-3.3	100	0.9998	1.1 – 8.7
	1	-3.3	100	0.9997	1.4 – 10.9
	5	-3.3	102	0.9991	2.2 – 16.3
	10	-3.3	102	0.9985	2.9 – 20.5

M – slope of regression curve, r. e. – reaction efficiency, R^2 – correlation coefficient, c. v. – coefficient of variance ,[a] 2 mg/ml, cDNA = 10 ng/µl

The acquired values of these parameters were compared with recommended criteria. 0 If the efficiency of PCR is 100%, the slope of the curve will be M = -3.33. The efficiency of qPCR between 80 to 110% is considered acceptable (-3.9 > slope >-3.0). The PCR efficiency is dependent on the assay, the mater mix performance and sample quality. Critical parameter for evaluating of PCR efficiency is R^2. If R^2 is 1 then the value of quantity can be predicted. An R^2 value > 0.99 provides good confidence in correlating two values.

Two types of tested microspheres (0-10 µl particle suspensions/25 µl of PCR mixture) do none inhibit PCR. The reaction efficiencies in the presence of P(HEMA-*co*-GMA) and P(HEMA-*co*-EDMA) microspheres were approximately the same as for the DNA standards without particles In the presence of these two types of particles correlation coefficient R^2 value were higher than 0.99 (Table 2). Both types of tested microspheres particles do not interfere with PCR in tested amount. From this reason, it can be assumed that the magnetic nuclei are well covered with polymer layer.

4 CONCLUSIONS

Model experiments which enabled the estimation of inhibitory effect of magnetic polymer particles on the qPCR course were proposed. It was confirmed that the qPCR can be used for the study of compatibility of magnetic particles applied in DNA analysis.

LITERATURE

[1.] Horak, D., *Journal of Polymer Science – Polymer Chemistry Edition* 2001, 39, 3707-3715.

[2.] Trachtova, S., Kaman, O., Spanova, A., Veverka, A., et.al. *Journal of Separation Science* 2011, 34, 3077-3082.

[3.] Spanova, A., Rittich, B., Benes, M. J., Horak, D., *Journal of Chromatography A* 2005, 1080, 93-98.

[4.] Kontanis, E. J., Floyd, F. A., *Journal of Forensic Science* 2006, 51, 795-804.

[5.] Schneider, S., Enkerli, J., Widmer, F., *Journal of Microbiological Methods* 2009, 778, 351-353.

[6.] Huggett, J. F., Novak, T., Garson, J. A., Green, C., et.al. *BMC Research Notes* 2008, 1, 70-79.
[7.] Horak, D., Rittich, B., Spanova, A., *Journal of Magnetism and Magnetic Materials* 2007, 311, 249-254.
[8.] Rittich, B., Spanova, A., Salek, P., et.al. *Journal of Magnetism and Magnetic Materials* 2009, 321, 1667-1670.
[9.] Horak, D., Babic, M., Mackova, H., Benes, M. J., *Journal of Separation Science* 2007, 30, 1751-1772.
[10.] Horak, S., Semenyuk, N., Lednicky, F., *Journal of Polymer Science Part A: Polymer Chemistry* 2003, 41, 1848-1863.
[11.] Krizova, J., Špánova, A., Rittich, B., Horak, D.,*Journal of Chromatography A* 2005, 1064, 247-253.
[12.] Dautzenberg, H., Philipp, B., *Faserforsch. Textiltechn.* 1974, 25, 469.
[13.] Sambrook, J., Russel, D. W., *Molecular Cloning (3rd ed.),* Cold Spring Harbor Laboratory Press, New York 2001.
[14.] Haarman, M., Knol, J., *Applied of Environmental Microbiology* 2006, 72, 2359-2365.
[15.] Bustin, S. A., Benes, V., Garson, J. A., et.al. Clinical Chemistry 2009, 55, 611-622.

P76 INFLUENCE OF THE O-PHOSPHORYLATION OF SERINE, THREONINE AND TYROSINE IN PROTEINS ON THE AMIDIC ^{15}N CHEMICAL SHIELDING ANISOTROPY TENSORS

Jiří Emmer[a], Andrea Vavrinská[b], Vladimír Sychrovský[c], Ladislav Benda[c], Zdeněk Kříž[d], Jaroslav Koča[d], Rolf Boelens[b], Vladimír Sklenář[d], Lukáš Trantírek[b]

[a] Biology Centre, Academy of Science of the Czech Republic and University of South Bohemia, Branisovska 31, 370 05 Ceske Budejovice, Czech Republic
[b] Bijvoet Centre for Biomolecular Research, Utrecht University, 3584 CH Utrecht, The Netherlands
[c] Institute of Organic Chemistry and Biochemistry, v.v.i., Academy of Science of the Czech Republic, Flemingovo nam. 2, 166 10, Prague, Czech Republic
[d] National Centre for Biomolecular Research and CEITEC, Masaryk University, Kamenice 5, 602 00 Brno, Czech Republic

ABSTRACT

Density functional theory was employed to study the influence of O-phosphorylation of serine, threonine, and tyrosine on the amidic ^{15}N chemical shielding anisotropy (CSA) tensor in the context of the complex chemical environments of protein structures.

1 MOTIVATION

Anisotropy of the chemical shielding (CSA) tensor of amidic nitrogen is used to characterize the relative orientations of segments of membrane proteins with respect to the membrane, to characterize the secondary structure of proteins, and as orientational restraints in the refinement of protein structures. Quantitative analysis of ^{15}N relaxation rates, which depend on the ^{15}N CSA, is widely used for the characterization of protein dynamics. In addition, the interference between ^{15}N CSA and ^{1}H-^{15}N dipolar relaxation mechanisms form the basis for the TROSY experiment, a broadly used technique used to increase the resolution of large proteins and protein complexes. Despite the importance of O-phosphorylation in protein biology, there has been no information on the amidic ^{15}N CSA tensor for O-phosphorylated amino acids.

Aim of the project is to estimate the extent to which the amidic ^{15}N CSA tensor of serine, threonine and tyrosine is affected by O-phosphorylation in the context of protein structure using density functional theory calculations.

2 RESULTS

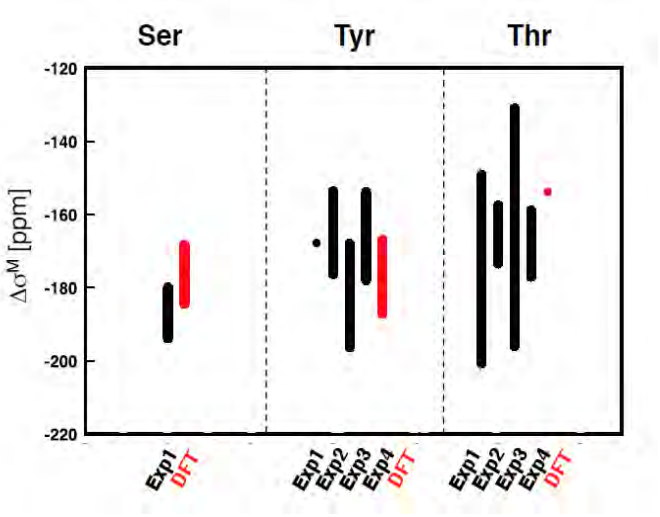

FIGURE 2. Comparison of the calculated $\Delta\sigma$ values for the non-phosphorylated residues in our model structures with experimental data available in the literature (Damberg et al. 2005; Wilye et al. 2006; Hall and Fushman 2006; Yao et al. 2010).

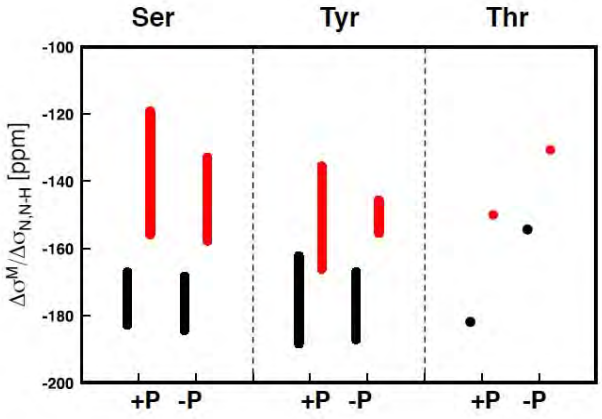

FIGURE 3. comparison of the ranges of the $\Delta\sigma$ (**IN BLACK**) and $\Delta\sigma_{N,N-H}$ (**IN RED**) values calculated separately for the phosphorylated and non-phosphorylated model peptides.

Table 1. The magnitudes (Δs), asymmetries (η), and orientations ($|\cos\theta_{ii}|$) of the amidic ^{15}N CSA tensors calculated for the model structures with non-phosphorylated (-P) and phosphorylated (+P) **serine** residues.
Pairs I, II, III, IV, and V correspond to the phosphorylated/non-phosphorylated pairs of proteins respectively identified with the following PDB numbers: 2AK7/1MU4, 2FWN/1BFD, 2BZI/2BZH, 3CY3/3CXW, and 3EXH/3EXE.

Pair no.		Δσ [ppm]	η	$\|\cos\theta_{zz}\|$ [°]	$\|\cos\theta_{xx}\|$ [°]	$\|\cos\theta_{yy}\|$ [°]	$\Delta\sigma_{N,N-H}$ [ppm]
I	+P	-175.42	0.08	0.96	0.16	0.25	-152.45
	-P	-184.41	0.07	0.95	0.09	0.31	-155.77
II	+P	-174.76	0.21	0.95	0.02	0.31	-147.91
	-P	-180.57	0.32	0.96	0.05	0.27	-157.34
III	+P	-177.14	0.19	0.92	0.20	0.34	-134.60
	-P	-171.54	0.22	0.94	0.11	0.32	-140.05
IV	+P	-182.86	0.16	0.95	0.03	0.30	-155.90
	-P	-168.32	0.38	0.94	0.23	0.27	-136.62
V	+P	-167.13	0.12	0.90	0.34	0.27	-119.92
	-P	-176.05	0.18	0.92	0.15	0.37	-132.97

Table 2. The magnitudes (Δs), asymmetries (η), and orientations ($|\cos\theta_{ii}|$) of the amidic ^{15}N CSA tensors calculated for the model structures with non-phosphorylated (-P) and phosphorylated (+P) **tyrosine** residues.
Pairs VI, VII, VIII, and IX correspond to the phosphorylated/non-phosphorylated pairs of proteins respectively identified with the following PDB numbers: 2QO7/2QO9, 2X2M/2IVS, 3CD3/3CBL, and 3CI5/1NM1

Pair no.		Δσ [ppm]	η	$\|\cos\theta_{zz}\|$ [°]	$\|\cos\theta_{xx}\|$ [°]	$\|\cos\theta_{yy}\|$ [°]	$\Delta\sigma_{N,N-H}$ [ppm]
VI	+P	-188.38	0.35	0.96	0.05	0.26	-166.14
	-P	-187.11	0.39	0.95	0.07	0.31	-155.49
VII	+P	-172.87	0.31	0.96	0.00	0.28	-150.54
	-P	-180.96	0.20	0.96	0.06	0.29	-156.49
VIII	+P	-173.58	0.22	0.96	0.09	0.25	-154.01
	-P	-167.07	0.29	0.96	0.09	0.26	-147.41
IX	+P	-162.28	0.13	0.95	0.09	0.31	-135.61
	-P	-178.26	0.18	0.94	0.08	0.34	-145.72

Table 3. The magnitudes (Δs), asymmetries (η), and orientations ($|\cos\theta_{ii}|$) of the amidic ^{15}N CSA tensors calculated for the model structures with non-phosphorylated (-P) and phosphorylated (+P) **threonine** residues. The calculations were performed with the use of the implicit PCM model only as in corresponding crystal structures no explicit solvent molecules could be identified in vicinity of the phosphorylated residue.
Pair X corresponds to the phosphorylated/non-phosphorylated pair of proteins identified with the PDB number: 3D5W/3D5U.

Pair no.		$\Delta\sigma$ [ppm]	η	$\lvert\cos\theta_{zz}\rvert$ [°]	$\lvert\cos\theta_{xx}\rvert$ [°]	$\lvert\cos\theta_{yy}\rvert$ [°]	$\Delta\sigma_{N,N\text{-}H}$ [ppm]
X	+P	-181.91	0.13	0.94	0.13	0.31	-150.05
	-P	-154.4	0.19	0.95	0.24	0.22	-130.71

3 CONCLUSIONS

The amidic CSA tensor sensitively responds to both the introduction of the phosphate group and the phosphorylation-promoted rearrangement of solvent molecules and the hydrogen-bonding network in the vicinity of the phosphorylated site.

The extent of changes in the amidic nitrogen CSA tensor due to introduction of the phosphate group appears to depend on both local structure at the phosphorylated site and identity of adjoining amino acids.

The calculated ^{15}N CSA tensor magnitudes and orientations in phosphorylated and solvated model peptides were in range of values experimentally observed for non-phosphorylated proteins. This suggests that the amidic ^{15}N CSA tensor in phosphorylated proteins could be reasonably well approximated with averaged CSA tensor values experimentally determined for non-phosphorylated amino acids in practical NMR applications, where chemical surrounding of the phosphorylated site is not known a priori.

Our calculations provide estimates of relative errors to be associated with the averaged CSA tensor values in interpretations of NMR data from phosphorylated proteins.

ACKNOWLEDGEMENTS

This work was supported by a VIDI career development grant by the Netherlands Organization for Scientific Research (NWO) and by the project "CEITEC - Central European Institute of Technology" (CZ.1.05/1.1.00/02.0068) from European Regional Development Fund.

The access to computing and storage facilities provided by the National Grid Infrastructure MetaCentrum, provided under the program "Projects of Large Infrastructure for Research, Development, and Innovations" (LM2010005) is highly appreciated.

LITERATURE

[1] Damberg P, Jarvet J, Graslund A (2005) Limited variations in 15N CSA magnitudes and orientations in ubiquitin are revealed by joint analysis of longitudinal and transverse NMR relaxation. J Am Chem Soc 127:1995-2005.

[2] Wylie BJ, Franks WT, Rienstra CM (2006) Determinations of 15N chemical shift anisotropy magnitudes in a uniformly 15N,13C-labeled microcrystalline protein by three-dimensional magic-angle spinning nuclear magnetic resonance spectroscopy. J Phys Chem 110:10926-10936.

[3] Hall JB, Fushman D (2006) Variability of the 15N chemical shielding tensors in the B3 domain of protein G from 15N relaxation measurements at several fields. Implications for backbone order parameters. J Am Chem Soc 128:7855-70.

[4] Yao L, Grishaev A, Cornilescu G, Bax A (2010) Site-specific backbone amide (15)N chemical shift anisotropy tensors in a small protein from liquid crystal and cross-correlated relaxation measurements. J Am Chem Soc 132:4295-4309.

P77 CHEMICAL COMPOSITION AND VOLATILITY OF ESSENTIAL OILS INVESTIGATED IN FRAME OF STUDY: SAVING OF CULTURE HERITAGE ON PAPER

Nela Kubátková[a,b], Kamil Křůmal[a], Zbyněk Večeřa[a], Pavel Mikuška[a]

[a] *Institute of Analytical Chemistry, Veveří 967/97, 602 00 Brno, Czech Republic*
[b] *Faculty of Chemistry, BUT Brno, Purkyňova 118, 612 00 Brno, Czech Republic*
kubatkova@iach.cz

ABSTRACT

Every of six investigated essential oils had 1 3 main components. Eucalyptol and α-Pinene were found as the main components of Myrtus communis (38.0 % and 36.5 % respectively). α-Pinene was identified as the primary component also in essential oil Juniperus communis (54.1 %). The principal components of Citrus aurantifolia and Cymbopogon nardus were limonene (52.9 %) and citronellal (40.4 %) respectively. Cinnamaldehyde was the main component of Cinnamomum zeylancium (62.0 %) and linalool was the basic component of Lavandula species (51.4 %). Concentrations of volatile components in gas phase with increasing course of time were also investigated.

Keywords: essential oils, volatility, composition

1 INTRODUCTION

Essential oils (EOs) are described as mixtures of volatile, strongly smelling compounds of oily consistency and lipophilic character [1]. Essential oils are products of secondary metabolism of higher plants. They are obtained from them mainly by the extraction. At present, about 3000 kinds of essential oils are known. One essence usually consists of 20-60 compounds and analysis of such complex sample is not an easy task. Chemical analysis of essential oils is mostly performed by gas chromatography and liquid chromatography, both coupled with mass spectrometry.

2 EXPERIMENTS

2.1 Chemical composition

Chemical identification and quantification of components of six EOs was carried out by GC-MS (Agilent. 7890A. 5975C). The GC was equipped with a capillary column HP5-MS (1 µm film thickness, 0.32 mm i.d., 30 m length). A sample volume of 4 µL was injected into a split/splitless injector operated in the splitless mode at temperature of 260 °C. Helium was used as a carrier gas at a flow rate of 4 mL/min. The temperature program started at 50 °C and this temperature was held for 2 min, after that a gradient of 5 °C/min was applied up to 280 °C and this temperature was held for 2 min. Mass spectrometer was operated in electron ionization (EI) and fullscan mode (m/z 20 - 500). Identification of components was performed by comparison of their retention time and mass spectra with those of standards. Identified components of essential oils are listed in Table 1.

2.2 Volatility of essential oils

Volatility of individual components of essential oils was also studied. The essential oils were placed in a diffusion cell, held at the constant temperature (20 °C). Occurred vapors of components were taken away from the diffusion cell by stream of nitrogen at the flow rate of 15 mL/min. The stream of nitrogen was then diluted by mixing with a clean air to the total flow rate of 500 mL/min. During passing of the mixture through a cylindrical wet effluent diffusion denuder [2], the vapors of studied oil components were captured into a thin film of n-heptane used as absorption liquid. Samples in n heptane were taken in specific time intervals, after 5 minutes, 60 minutes, and 20 hours from beginning of the experiment. The analyses of n-heptane samples were performed by GC-MS (Fig. 1.).

Table 1: Components of studied EOs

Lavandula species	Cymbopogon nardus	Citrus aurantifolia	Juniperus communis	Myrtus communis	Cinnamomum zeylancium
Linalool (51.4 %)	Citronellal (40.4 %)	Limonene (52.9 %)	α-Pinene (54.1 %)	Eucalyptol (38.0 %)	Cinnamaldehyde (62.0 %)
Linalyl acetate (26.6 %)	Geraniol (17.1 %)	γ-Terpinene (11.2 %)	β-Pinene (17.7 %)	α-Pinene (36.5 %)	Cinnamyl acetate (7.50 %)
Camphor (4.17 %)	Citronellol (10.1 %)	Terpinolen (11.2 %)	Limonene (13.1 %)	Limonene (14.5 %)	Eugenol (4.14 %)
Eucalyptol (2.88 %)	Limonene (3.78)	α-Terpineol (8.95 %)	Camphene (0.59 %)	α-Terpineol (3.89 %)	Eucalyptol (2.99 %)
Borneol (2.11 %)	Geranyl acetate (2.63 %)	β-Pinene (2.30)	α-Terpineol (0.33 %)	Linalool (3.48 %)	Linalool (2.96 %)
Myrcen (1.60 %)	Linalool (0.83 %)	1,4-Cineole (2.19 %)	Terpinolene (0.17 %)	Myrtenyl acetate (2.23%)	R-α-Phellandrene (1.98 %)

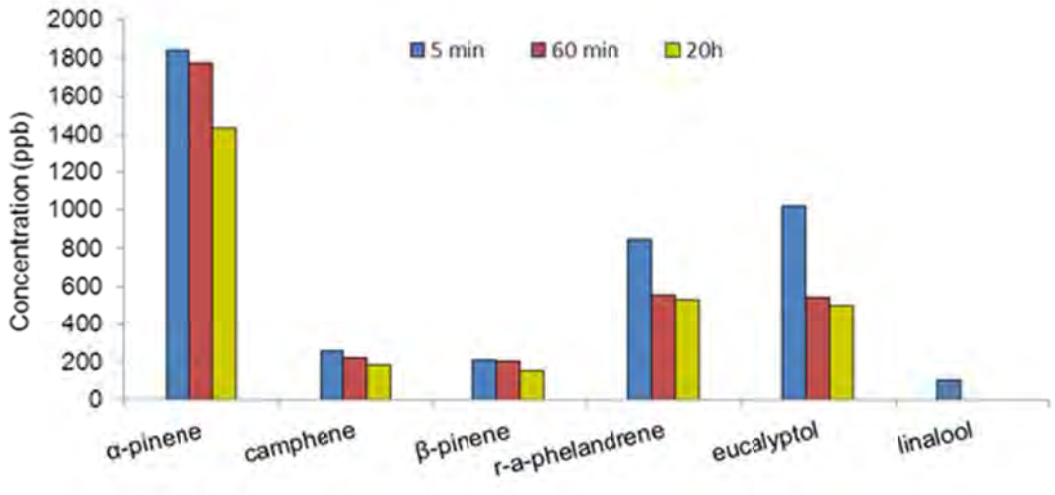

Fig. 1: Example of concentration course of volatile components of Cinnamomum zeylancium.

ACKNOWLEDGEMENTS

This work was supported by NAKI DF11P01OVV028 (Ministry of Culture of the Czech Republic).

LITERATURE

[1] Bakkali, F., Averbeck, S., et al., Food Chemistry and Toxicology 2008, *46*, 446-475.
[2] Zdráhal, Z., Mikuška, P., Večeřa, Z., Analytical Chemistry 1995, *67*, 2763-2766.

List of Poster Presentations

P01 METHOD DEVELOPMENT OF AMINO ACIDS PROFILING FOR PYRIDOXIN DEPENDENT EPILEPTIC SEIZURES DIAGNOSIS
Andrea Cela, Ales Madr, Jindra Musilova, Marta Zeisbergerova, Zdenek Glatz

P02 DIFFERENCES IN FINGERPRINTS OF BIOFILM-POSITIVE AND BIOFILMNEGATIVE *CANDIDA* STRAINS EXPLOITABLE FOR CLINICAL PRACTICE
Marie Vykydalová, Marie Horká, Jiří Šalplachta, Filip Růžička, Vladislav Kahle

P03 NANO COLUMN GRADIENT SEPARATIONS: IMPLEMENTATION OF SIMPLE SPLITLESS GRADIENT GENERATOR WITH INTEGRATED SAMPLE DELIVERY
Jozef Šesták, Filip Duša, Dana Moravcová, Vladislav Kahle

P04 MICROPREPARATIVE SOLUTION ISOELECTRIC FOCUSING OF PEPTIDES AND PROTEINS IN NONWOVEN STRIP
Filip Duša, Karel Šlais

P05 POTENTIAL OF EXHALED BREATH CONDENSATE ANALYSIS IN POINT OF CARE DIGNOSTICS
Petr Kubáň, Eeva-Gerda Kobrin, Mihkel Kaljurand

P06 SEASONAL VARIATIONS OF METALS AND IONS IN PM1 AEROSOL IN BRNO AND ŠLAPANICE
Pavel Mikuška, Kamil Křůmal, Martin Vojtěšek, Nela Kubátková, Zbyněk Večeřa

P07 METHOD FOR ON-LINE PRE-CONCENTRATION AND ANALYSIS OF HEAVY METALS USING LIGAND STEP GRADIENT FOCUSING IN COMBINATION WITH ITP
Eliška Glovinová, Jan Pospíchal

P08 A SIMPLE SAMPLE PRETREATMENT DEVICE WITH SUPPORTED LIQUID MEMBRANE FOR DIRECT INJECTION OF UNTREATED BODY FLUIDS AND IN-LINE COUPLING TO A COMMERCIAL CAPILLARY ELECTROPHORESIS INSTRUMENT
Pavla Pantůčková, Pavel Kubáň, Petr Boček

P09 A SENSITIVE GRADIENT LIQUID CHROMATOGRAPHY METHOD FOR ANALYSIS AMINO ACIDS IN DEGRADATION PRODUCTS OF HUMIC SUBSTANCES
Natália Bielčíková, Róbert Góra, Milan Hutta, Simona Čurmová

P10 PROTEOMIC EVALUATION OF MCF-7 HUMAN BREAST CANCER CELLS AFTER TREATMENT WITH RETINOIC ACID ISOMERS: PRELIMINARY INSIGHTS
Dana Flodrová, Dagmar Benkovská, Dana Macejová, Lucia Bialešová, Július Brtko, Janette Bobálová

P11 PREPARATION OF HYPERCROSSLINKED MONOLITHIC COLUMN FOR SEPARATION OF POLAR COMPOUNS
Veronika Skerikova, Jiri Urban, Pavel Jandera, Magda Stankova

P12 RP-HPLC SEPARATION OF THREE SELECTED CHIRAL PESTICIDES USING COLUMN-SWITCHING TECHNIQUES
Mária Chalányová, Ivana Petránová, Veronika Vojtková, Milan Hutta

P13 NEW MODIFICATION OF DIFFUSIVE GRADIENT IN THIN FILM TECHNIQUE (DGT) FOR DETERMINATION OF METALS IN SEDIMENTS
Michaela Gregusova, Bohumil Docekal

P14 PROFILING OF SOIL AND PEAT HUMIC SUBSTANCES BY ANION-EXCHANGE CHROMATOGRAPHY
Janka Ráczová, Milan Hutta, Veronika Komorowská

P15 DETERMINATION OF SELECTED ACIDS IN HUMAN URINE BY COMBINATION OF CAPILLARY ISOTACHOPHORESIS AND CAPILLARY ZONE ELECTROPHORESIS
Michaela Joanidisová, Róbert Bodor, Zdenka Radičová, Marína Rudašová, Marián Masár

P16 MULTIVARIATE STATISTICS FOR THE DIFFERENTIATION OF ERYTHROPOIETIN PREPARATIONS BASED ON INTACT GLYCOFORMS DETERMINED BY CE-MS
Christian Neusüß, Angelina Taichrib, Markus Pioch, Sabine Neuberger

P17 ANALYSIS OF SPECIFIC METABOLITES FORMED IN RED YEAST CELLS CULTIVATED ON PRETREATED WHEAT STRAW MATERIALS
Siniša Petrik, Andrea Hároniková, Zsófia Kádár, Ivana Márová

P18 ACHIRAL AND CHIRAL SEPERATIONS OF UNDERIVATIZED AMINOACIDS ON ELECTROPHORETIC CHIP
Katarína Uhlárová, Róbert Bodor, Marián Masár

P19 ANALYSIS OF GFP AND AHP5-GFP FUSION PROTEIN IN THE PLANT EXTRACT USING CE-LIF
Lenka Michalcová, Radka Dopitová, Jan Hejátko, Martina Válková, Jan Preisler

P20 DGGE ANALYSIS OF ARTIFICIAL *CLOSTRIDIUM* CONSORTIA
Barbora Gregušová, Alena Španová, Bohuslav Rittich

P21 OPTIMIZATION OF MEKC SEPARATION SELECTIVITY OF PHENOLIC COMPOUNDS USING HOMOLOGICAL SERIES OF ANIONIC SURFACTANTS
Jana Váňová, Petr Česla, Jan Fischer, Pavel Jandera

P22 PHOTOLITHOGRAPHIC TECHNIQUE FOR CONTROLLED FABRICATION OF METAL STRUCTURES
Petra Jusková, Jitka Hegrová, František Foret

P23 MALDI-TOF MS OF *DICKEYA* AND *PECTOBACTERIUM* SPECIES – CHARACTERIZATION OF PLANT PATHOGENIC BACTERIA
Jiří Šalplachta, Anna Kubesová, Jaroslav Horký, Marie Horká

P24 INVESTIGATION OF PLATINUM-BASED CYTOSTATIC DRUGS INTERACTIONS WITH DNA BY SANGER SEQUENCING
Kristýna Šmerková, Simona Dostálová, Markéta Ryvolová, Helena Škutková, Vojtěch Adam, Ivo Provazník, René Kizek

P25 ANALYSIS OF DOXORUBICIN ENCAPSULATION IN APOFERRITIN CAGE BY CAPILLARY ELECTROPHORESIS WITH LASER-INDUCED FLUORESCENCE DETECTION
Maja Stanisavljevic, Marketa Ryvolova, Pavel Kopel, Vojtech Adam, Tomas Eckschlager, Rene Kizek

P26 VERY FAST ELECTROPHORETIC SEPARATION OF NEUROTRANSMITTERS ON COMMERCIAL INSTRUMENTS USING A COUPLED CAPILLARY
Petr Tůma, František Opekar, Eva Samcová

P27 KINETIC AND THERMODYNAMIC PROPERTIES OF POROUS SHELL PARTICLES LC STATIONARY PHASES
Nikola Vaňková, Petr Česla, Jan Fischer

P28 INTEGRATED CHIP ELECTROPHORESIS AND MAGNETIC PARTICLE ISOLATION USED FOR DETECTION OF HEPATITIS B VIRUS OLIGONUCLEOTIDES
Jiří Vysloužil, Markéta Ryvolová, Vojtěch Adam, Jaromír Hubálek, René Kizek

P29 FILTRATION MICROCARTRIDGE AND CAPILLARY ISOELECTRIC FOCUSING FOR THE ANALYSIS LOW NUMBER OF MICROORGANISMS IN REAL SAMPLES
Anna Kubesová, Marie Horká, Jiří Šalplachta, Jaroslav Horký

P30 HIGHLY SENSITIVE DETERMINATION OF CATIONIC PESTICIDES IN ORANGE JUICE BY CAPILLARY ISOTACHOPHORESIS-ELECTROSPRAY IONIZATION-MASS SPECTROMETRY WITH ADVANCED ELECTROLYTE TUNING
Zdena Malá, Pavla Pantůčková, Petr Gebauer, Petr Boček

P31 DETERMINATION OF 2,4-DICHLOROPHENOXYACETIC ACID AND ITS METABOLITES BY IMMUNOAFFINITY CHROMATOGRAPHY IN PLANT MATRICES
Barbora Pařízková, Ondřej Novák, Jana Oklešťková, Luděk Eyer, Milan Fránek, Miroslav Strnad

P32 UTILIZATION OF THE ANODIC ELECTRO-OSMOTIC FLOW FOR AN AMINO ACIDS PROFILING BY CAPILLARY ELECTROPHORESIS
Ales Madr, Katerina Svobodova, Jindra Musilova, Zdenek Glatz

P33 SACCHARIDES IN PM2.5 AEROSOLS IN BRNO
Kamil Křůmal, Nela Kubátková, Pavel Mikuška, Zbyněk Večeřa

P34 DETERMINATION OF COPPER IN HUMAN URINE BY LIQUID CHROMATOGRAPHY WITH SPECTROPHOTOMETRIC DETECTION WITH USED MONOLITH COLUMN
Simona Čurmová, Radoslav Halko, Milan Hutta, Natália Bielčíková, Peter Božek

P35 COMPARISON OF CONCENTRATION OF IONS IN PM1 AEROSOL SAMPLED ON NITRATE CELLULOSE AND TEFLON FILTERS
Alena Kořínková, Pavel Mikuška, Zbyněk Večeřa, Kamil Křůmal

P36 ANALYSIS OF THE ALTERED GLYCOSYLATION OF IGG IN DIFFERENT LUNG DISEASES
Nóra Rezsu, Csaba Váradi, András Guttman

P37 THE CONTENT OF SULPHUR DIFFERENT FRACTIONS IN SOIL FROM NOVÉ SADY LOCATION
Melánia Feszterová, Lýdia Jedlovská

P38 FAST ON-LINE TWO-DIMENSIONAL LCXCE USING FLOW AND VOLTAGE GATING INTERFACES
Petr Česla, Jan Fischer, Lenka Kovaříková

P39 DETERMINATION OF ENDOCANNABINOIDS 2-ARACHIDONOYLGLYCEROL AND ANANDAMIDE IN HUMAN SERUM
Jan Juřica, Žaneta Jurčková, Ondřej Zendulka

P40 SYNTHESIS OF NEOGLYCOPROTEINS FOR CARBOHYDRATE SPECIFIC ANTIBODY GENERATION
Márta Kerékgyártó, Anikó Fekete, László Takács, István Kurucz, András Guttman

P41 THE EFFICIENT APPROACHES FOR ENZYMATIC DIGESTION OF PLANT PROTEINS
Filip Dyčka, Pavel Bobáľ, Janette Bobáľová

P42 DIODE LASER THERMAL VAPORIZATION INDUCTIVELY COUPLED MASS SPECTROMETRY FOR DETERMINATION OF TRACE ELEMENTS IN MICROSAMPLES
Preisler Jan, Foltynová Pavla, Kanický Viktor

P43 BIOANALYTICAL ICP-MS METHOD FOR QUANTIFICATION OF POTASSIUM IN THE CELLS AND SUPERNATANTS
Inga Petry-Podgórska, Tomáš Matoušek, Tomáš Wald, Peter Šebo, Jiří Mašín, Jiří Dědina

P44 ANALYSIS OF PHARMACEUTICAL SUBSTANCES BY ISOTACHOPHORESIS ON A CHIP
Marína Rudašová, Michaela Joanidisová, Zdenka Radičová, Róbert Bodor, Marián Masár

P45 STUDY OF THE POSSIBILITY OF USING RP-HPLC WITH TANDEM MULTIDETECTION TO CHARACTERIZE SAMPLES OF PROTEIN SUPPLEMENTS WITH THERAPEUTIC EFFECT
Veronika Komorowska, Milan Hutta

P46 FRACTIONATION OF HUMIC ACIDS BY PREPARATIVE ISOTACHOPHORESIS
Zdenka Radičová, Róbert Bodor, Róbert Góra, Andrea Pastierová, Michaela Joanidisová, Marína Rudášová, Milan Hutta, Marián Masár

P47 USE OF PHYSICAL-CHEMICAL METHODS TO ANALYSIS OF ORGANIC MICRO- AND NANOPARTICLES WITH ENCAPSULATED CAFFEINE
Petra Matoušková, Andrea Lichnová, Klára Patočková, Pavla Benešová, Jana Hurtová, Stanislav Obruča, Ivana Márová

P48 SILICA-BASED MONOLITHIC CAPILLARY COLUMNS MODIFIED TO ZWITTERIONIC STATIONARY PHASE FOR HYDROPHILIC INTERACTION LIQUID CHROMATOGRAPHY
Dana Moravcová, Josef Planeta, Vladislav Kahle, Marie Horká, Michal Roth

P49 SENSOR BASED ON FÖRSTER RESONANCE ENERGY TRANSFER WITH QUANTUM DOT
Marcela Liskova; Vladimira Datinska; Karel Kleparnik; Frantisek Foret

P50 OCCURRENCE OF LIGNANS IN ENVIRONMENTAL WATERS
Jan Tříska, Martin Moos, Iveta Marešová, Naděžda Vrchotová

P51 MONOLITHIC COLUMNS FOR SEPARATION OF LOW-MOLECULAR COMPOUNDS
Magda Stankova, Pavel Jandera, Jiri Urban, Veronika Skerikova

P52 BEHAVIOR OF SHEATHLESS AND ELECTRODELESS ELECTROSPRAY ELECTROPHORESIS DURING INORAGANIC ION SEPARATION
Anna Tarantová, František Foret

P53 THE USE OF AN INTERNAL STANDARD EXTENDS THE LINEAR RANGE OF THE SALDI MS ANALYSES
Iva Tomalová, Huan-Tsung Chang, Jan Preisler

P54 DEVELOPMENT AND VALIDATION OF UHPLC METHOD FOR THE DETECTION AND QUANTIFICATION OF ERECTILE DYSFUNCTION DRUGS
Ludovit Schreiber, Radoslav Halko, Milan Hutta, Anna Kabzanová, Soňa Lopuchová

P55 DYNAMIC HIGH-RESOLUTION COMPUTER SIMULATION OF ELECTROPHORETIC ENANTIOMER SEPARATIONS
Jitka Caslavska, Michael C. Breadmore, Hiu Ying Kwan, Wolfgang Thormann

P56 TALK-ULTRA FAST HPLC METHOD FOR TADALAFIL ACCORDING TO PH.EUR. VALIDATION CRITERIA AND IDENTIFICATION OF IMPURITIES USING ACCURATE MASS MS
Ludovit Schreiber, Radoslav Halko, Milan Hutta, Anna Kabzanová, Soňa Lopuchová

P57 IDENTIFICATION AND ANTIMICROBIAL ACTIVITY OF *LACTOBACILLUS* STRAIN ISOLATED FROM INFANT FAECES
Kristýna Turková, Alena Španová, Bohuslav Rittich, Bojana Bogovič Matijašić

P58 CHIRAL ANALYSIS OF SELECTED GROUP OF PROFENS BY LIQUID CHROMATOGRAPHY
Veronika Vojtková, Mária Chalányová, Ivana Petránová, Milan Hutta

P59 THE COMPARISON OF ANTIOXIDANT PROPERTIES OF ORGANIC AND CONVENTIONAL DAIRY PRODUCTS
Jurgita Raudonytė, Lina Šimkevičiūtė, Jonas Damašius

P60 CHARACTERIZATION OF ATMOSPHERIC PARTICULATE MATTER BY DIFFUSIVE GRADIENT IN THIN FILM (DGT) TECHNIQUE
Michaela Gregusova, Bohumil Docekal

P61 INVESTIGATION OF CHEMICAL COMPOSITION AND ANTIMICROBIAL ACTIVITIES OF ESSENTIAL OILS OF *LAVANDULA HYBRIDA L., CYMBOPOGON FLEXUOSUS L., MALALEUCA ALTERNIFOLIA L.*
Rūta Mickienė, Audrius Maruška, Ona Ragažinskienė

P62 ENVIRONMENTAL POLLUTION OF VINEYARDS BY POLYCYCLIC AROMATIC HYDROCARBONS ORIGINATING FROM MOTOR VEHICLES EMISSIONS
Helena Fišerová, Vladimír Šnajdr, Štěpán Zezulka, Jan Tříska, Rudolf Jílek

P63 SCREENING OF POTENCIAL USE OF THE CAPILLARY ZONE ELECTROPHORESIS METHOD WITH INDIRECT PHOTOMETRIC DETECTION FOR THE MONITORING OF SELECTED ORGANIC ACIDS IN FRUIT WINE, AND CULTURE MEDIA FOR MICROBIOLOGICAL AND BIOTECHNOLOGICAL PURPOSES
Miloš Dvořák, Milena Vespalcová, Bohuslav Rittich

P64 CASPASE 3 CHEMILUMINESCENCE ACTIVITY DETERMINATION IN APOPTOTIC CELLS AND DESIGN OF CASPASE 3 SENSOR
Marcela Liskova, Karel Kleparnik, Pavel Pazdera, Frantisek Foret

P65 IRON OXIDE NANOPARTICLE MODIFIED MONOLITHIC PIPETTE TIPS FOR SELECTIVE ENRICHMENT OF PHOSPHOPEPTIDES
Jana Krenkova, Frantisek Foret

P66 4-METHYLCOUMARINS AND THEIR IN VITRO PLATELET ANTIAGGREGATORY ACTIVITY
Jana Karlíčková, Přemysl Mladěnka, Kateřina Macáková, Zuzana Řeháková, Tomáš Filipský, Michal Říha, Ashok K. Prasad, Virinder S. Parmar, Luděk Jahodář, Radomír Hrdina, Luciano Saso

P67 A SIMPLE DEVICE FOR QUANTITATION OF CASPASE 3 IN INDIVIDUAL APOPTOTIC EMBRYONIC CELLS
Jitka Hegrová, Karel Klepárník, Jan Přikryl, Marcela Lišková, Eva Matalová, František Foret

P68 HEXADECENAL ANALYSIS BY 5,5-DIMETHYLCYCLOHEXANEDIONE DERIVATIZATION FOR S1P LYASE ASSAY IN HPLC-FLUORESCENCE DETECTION
Kyong-Oh Shin, Cho-Hee seo, Yong-Moon Lee

P69 SEPARATION OF CLINICALLY SIGNIFICANT MICROORGANISMS FROM CEREBROSPINAL FLUID BY CIEF WITH UV DETECTION AND MALDI-TOF MS
Marie Horká, Jiří Šalplachta, Anna Kubesová, Filip Růžička, Karel Šlais

P70 IMPROVED GENETICALLY ENCODED CALCIUM INDICATORS FOR TWO-PHOTON POLARIZATION MICROSCOPY
Valentyna Kuznetsova

P71 IMUNOTURBIDIMETRIC DETERMINATION OF NGAL IN THE URINE OF HEALTHY CHILDREN
Radka Šigutová, Michal Hladík, František Všianský, Tomáš Karlík, Pavlína Kušnierová, Zdeněk Švagera

P72 OCCURRENCE OF RISK METALS IN SMALL MAMMALS IN THE EASTERN TATRAS
Silvia Jakabová, Imrich Jakab, Ivan Baláž

P73 APPLICATION OF ON-LINE CAPILLARY ELECTROPHORESIS COUPLED TO MASS SPECTROMETRY FOR IDENTIFICATION OF CYTOCHROME P450 2C9 ISOFORM METABOLISM PRODUCTS
Monika Langmajerová, Roman Řemínek, Marta Zeisbergerová, Zdeněk Glatz

P74 IMUNOTURBIDIMETRIC DETERMINATION OF NGAL IN THE URINE OF HEALTHY CHILDREN
Radka Šigutová, Michal Hladík, František Všianský, Tomáš Karlík, Pavlína Kušnierová, Zdeněk Švagera

P75 THE USE OF REAL TIME PCR METHOD FOR EVALUATION OF MAGNETIC MICROSPHERES
Štepánka Trachtová, Bohuslav Rittich, Daniel Horák, Alena Španová

P76 INFLUENCE OF THE O-PHOSPHORYLATION OF SERINE, THREONINE AND TYROSINE IN PROTEINS ON THE AMIDIC ^{15}N CHEMICAL SHIELDING ANISOTROPY TENSORS
Jiří Emmer, Andrea Vavrinská, Vladimír Sychrovský, Ladislav Benda, Zdeněk Kříž, Jaroslav Koča, Rolf Boelens, Vladimír Sklenář, Lukáš Trantírek

P77 CHEMICAL COMPOSITION AND VOLATILITY OF ESSENTIAL OILS INVESTIGATED IN FRAME OF STUDY: SAVING OF CULTURE HERITAGE ON PAPER
Nela Kubátková, Kamil Křůmal, Zbyněk Večeřa, Pavel Mikuška

Notes